NEW APPROACHES TO CATALYST DESIGN AND IMMOBILIZATION

Irina Sagamanova

ADVERTIMENT. L'accés als continguts d'aquesta tesi doctoral i la seva utilització ha de respectar els drets de la persona autora. Pot ser utilitzada per a consulta o estudi personal, així com en activitats o materials d'investigació i docència en els termes establerts a l'art. 32 del Text Refós de la Llei de Propietat Intel·lectual (RDL 1/1996). Per altres utilitzacions es requereix l'autorització prèvia i expressa de la persona autora. En qualsevol cas, en la utilització dels seus continguts caldrà indicar de forma clara el nom i cognoms de la persona autora i el títol de la tesi doctoral. No s'autoritza la seva reproducció o altres formes d'explotació efectuades amb finalitats de lucre ni la seva comunicació pública des d'un lloc aliè al servei TDX. Tampoc s'autoritza la presentació del seu contingut en una finestra o marc aliè a TDX (framing). Aquesta reserva de drets afecta tant als continguts de la tesi com als seus resums i índexs.

ADVERTENCIA. El acceso a los contenidos de esta tesis doctoral y su utilización debe respetar los derechos de la persona autora. Puede ser utilizada para consulta o estudio personal, así como en actividades o materiales de investigación y docencia en los términos establecidos en el art. 32 del Texto Refundido de la Ley de Propiedad Intelectual (RDL 1/1996). Para otros usos se requiere la autorización previa y expresa de la persona autora. En cualquier caso, en la utilización de sus contenidos se deberá indicar de forma clara el nombre y apellidos de la persona autora y el título de la tesis doctoral. No se autoriza su reproducción u otras formas de explotación efectuadas con fines lucrativos ni su comunicación pública desde un sitio ajeno al servicio TDR. Tampoco se autoriza la presentación de su contenido en una ventana o marco ajeno a TDR (framing). Esta reserva de derechos afecta tanto al contenido de la tesis como a sus resúmenes e índices.

WARNING. Access to the contents of this doctoral thesis and its use must respect the rights of the author. It can be used for reference or private study, as well as research and learning activities or materials in the terms established by the 32nd article of the Spanish Consolidated Copyright Act (RDL 1/1996). Express and previous authorization of the author is required for any other uses. In any case, when using its content, full name of the author and title of the thesis must be clearly indicated. Reproduction or other forms of for profit use or public communication from outside TDX service is not allowed. Presentation of its content in a window or frame external to TDX (framing) is not authorized either. These rights affect both the content of the thesis and its abstracts and indexes.

ICIQ
Institut Català d'Investigació Química

UNIVERSITAT ROVIRA i VIRGILI

New Approaches to Catalyst Design and Immobilization

PhD Thesis presented by:

Irina Sagamanova

Developed under the supervision of:

Prof. Miquel A. Pericàs, Dr. Carles Rodríguez Escrich and Dr. M. Sonia Sayalero Sanz

Department of Analytical and Organic Chemistry (URV)
and Institute of Chemical Research of Catalonia (ICIQ)

TARRAGONA, 2015

UNIVERSITAT ROVIRA I VIRGILI
NEW APPROACHES TO CATALYST DESIGN AND IMMOBILIZATION
Irina Sagamanova

UNIVERSITAT ROVIRA I VIRGILI

DEPARTAMENT DE QUIMICA ANALITICA I QUIMICA ORGANICA

C/ Marcel.lí Domingo s/n
Campus Sescelades
43007 Tarragona
Tel. 34 977 55 97 69
Fax 34 977 55 84 46
e-mail: secqaqo@urv.net

ICIQ
Institut Català d'Investigació Química

Prof. Miquel A. Pericàs Brondo, Group Leader and Director of the Institute of Chemical Research of Catalonia (ICIQ) and,

Dr. Carles Rodríguez Escrich, Researcher and Group Coordinator in the Pericàs Research Group (ICIQ),

Dr. M. Sonia Sayalero Sanz, Researcher and Group Coordinator in the Pericàs Research Group (ICIQ),

CERTIFY that the present Doctoral Thesis entitled: ***New Approaches to Catalyst Design and Immobilization***, presented by IRINA SAGAMANOVA to receive the degree of Doctor, has been carried out under our supervision, in the Institute of Chemical Research of Catalonia (ICIQ) and fulfills all the requirements to be awarded with the "Doctor International" Mention.

Tarragona, 2nd November, 2015

Doctoral Thesis Supervisor/s

PhD Thesis Supervisor	PhD Thesis Co-supervisor	PhD Thesis Co-supervisor
Prof. Miquel A. Pericàs Brondo	Dr. Carles Rodríguez Escrich	Dr. M. Sonia Sayalero Sanz

UNIVERSITAT ROVIRA I VIRGILI
NEW APPROACHES TO CATALYST DESIGN AND IMMOBILIZATION
Irina Sagamanova

Acknowledgements

I have been thinking for some time how to choose the right words to express my thanks to all those who, in any way, helped me adapt to this country and to the Pericàs group. I am very grateful for having had the chance to meet so many great people during my post-graduate studies.

Honestly, it is very hard to describe how many wonderful moments I had since I began my post-graduate studies at the ICIQ. Nevertheless, I will try to summarize some of the important points.

First of all, I would like to express my gratitude to Miquel for the chance to become a member of his group; for his constant support and direction during the entire time of my studies and for the opportunities that he offered me. The first time I joined this group was during the summer period (Summer Fellowship), which was an amazing experience, followed by work in this group during the Master and PhD studies.

I am also grateful to the thesis committee for their time, care and consideration.

I would also like to give special thanks to my co-supervisors Dr. Sonia Sayalero and Dr. Carles Rodríguez for their support and assistant during this Thesis. Sonia Sayalero has ALWAYS taken the time to support me during all the period of my stay in ICIQ, starting from first moment I arrived. Carles Rodríguez helped a lot with his critical reading of this Thesis and his positive comments and suggestions, and for this I am really appreciate his patience with me and his time. Without their help and encouragement this thesis would have never reached its current state.

I would like to particularly express my thanks to Prof. Patrick J. Walsh for giving me the opportunity to work in his group, which provided me new experiences. The part of the work which was done in collaboration with the Walsh group is summarized in Chapter V and VI of this thesis. Special thanks to the group members for their friendship and support during my stay in the USA. I am especially thankful to Tiezheng, Mengnan, and Carol – it was really nice to work with you, as well as Jacque and Minyan for the time we spent together.

I would really like to give thanks to all of the current and former members of the Pericàs group: Andrea, Carles A., Carles L., Carles R., Carmen, Carolina, Ciril, Christian, Corina, Dina, Erhan, Erik, Estefanía, Esther, Evgeny,

Francesca, Gretchen (Upenn), Jagjit, Javi, Jerome (Upenn), Julien, Laura, Lidia, Lluís, Luca, Marta M., Marta R., Mercè, Míriam, Pablo, Rafa, Paola, Patri, Pedro, Pinar, Rocío, Santiago, Sara G., Sara R., Shoulei, Sonia, Soumi, Toni, Xinyuan. Thanks to everyone, who made my experience within this group a fun and stimulating one, and who shared the lab with me over the years.

In addition, I would like to thank all the co-workers, technical support and administrative staff in ICIQ. Special thanks to Mercè, Sara G. and Marta M. for all the help with the paperwork – it would have been so difficult to solve this without you.

I would like to take this opportunity to thank all those friends who cared and supported me in this amazing time. This support is much more precious and important.

Finally, thanks to my family and all my friends outside chemistry, particularly my friend Tatiana and her family, who treated me like part of their family since I am so far from my hometown. I also would like to thank my friend Maria in Moscow for keeping in touch during all the period I stayed abroad.

Above all, I would like to thank my family for their endless patience and constant support during all my life. They ALWAYS trusted me and supported me with every decision I made and also every time they tried to help me as much as they could.

Probably, it is impossible to count how many times I am grateful to everybody for this period time that I spent in Tarragona. Thank you very much to all of you.

The work developed in the present doctoral thesis has been possible thanks to the funding received from ICIQ Foundation (ICIQ grant 2011-2014) as well as from the following projects:

Consolider Ingenio 2010, Intecat (CSD2006-0003, MICINN), SICAM (2009SGR623, AGAUR), SMARTCAT (CTQ2008-00947/BGU, MICINN), CATFLOW (CTQ2012-38594- C02-01, MINECO), and Severo Ochoa Excellence Accreditation 2014-2018 (SEV-2013-0319).

UNIVERSITAT ROVIRA I VIRGILI
NEW APPROACHES TO CATALYST DESIGN AND IMMOBILIZATION
Irina Sagamanova

List of Acronyms and Abbreviations

In this document the abbreviations and acronyms most commonly used in organic chemistry have been used, according to the recommendations of the ACS "Guidelines for authors":

http://pubs.acs.org/paragonplus/submission/joceah/joceah_abbreviations.pdf

dba	dibenzylideneacetone
DBAD	dibenzylazodicarboxylate
DET	diethyl tartrate
DiMePEG	poly(ethylene glycol) dimethyl ether
DIPEA	*N*,*N*-diisopropylethylamine
DVB	1,4-divinylbenzene
f	level of functionalization
f_{max}	theoretical maximal level of functionalization
NB	norbornene
PS	polystyrene
^{t}Am	*tert*-amyl
TOF	turnover frequency
TON	turnover number

UNIVERSITAT ROVIRA I VIRGILI
NEW APPROACHES TO CATALYST DESIGN AND IMMOBILIZATION
Irina Sagamanova

Table of Contents

UNIVERSITAT ROVIRA I VIRGILI
NEW APPROACHES TO CATALYST DESIGN AND IMMOBILIZATION
Irina Sagamanova

To my family

UNIVERSITAT ROVIRA I VIRGILI
NEW APPROACHES TO CATALYST DESIGN AND IMMOBILIZATION
Irina Sagamanova

CHAPTER I

General Introduction

UNIVERSITAT ROVIRA I VIRGILI
NEW APPROACHES TO CATALYST DESIGN AND IMMOBILIZATION
Irina Sagamanova

CHAPTER I

General Introduction

"No subject so pervades modern chemistry as that of catalysis"
Ron Breslow, Chemistry Today and Tomorrow:
The Central, Useful, and Creative Science

I.1. Asymmetric catalysis.

The term enantioselective (asymmetric) catalysis refers to a chemical process in which a single molecule of chiral catalyst is able to mediate the formation of several molecules of stereisomeric product in unequal amount (i.e. favouring the formation of one enantiomer over the other). Enantiomerically pure compounds are produced in nature by chirality transfer from enzymatic catalysts, but they are difficult to make in the laboratory.

Different enantiomers or diastereomers of a molecule often have different biological activity. Therefore, enantioselective synthesis is a key process in modern chemistry and is particularly important in the field of pharmaceuticals. It was only recently that enantioselective approaches were employed in organic synthesis.

The area of asymmetric catalysis spans the last 50 years, with an impressive amount of publications and activities in the well-studied fields of organometallic[1] and bioorganic [2] catalysis. Recently, a third area named organocatalysis has also appeared.[3] Asymmetric catalysis is desirable for both cost and environmental reasons, as chiral catalysts favour the formation of one particular stereoisomer among all the possibilities. During this process the chiral catalysts are not consumed, which is beneficial when compared to stoichiometric reagents, improving the efficiency of the process. They enable alternative reactions with better atom economy and therefore reduced waste to be used.

---

[1] Metal catalysis: a) Noyori, R. *Asymmetric Catalysis in Organic Synthesis*, Wiley, New York, **1994**; b) *Comprehensive Asymmetric Catalysis* (Eds.: Jacobsen, E. N.; Pfaltz, A.; Yamamoto, H.), Springer, Berlin, **1999**; c) *Catalytic Asymmetric Synthesis, 2nd ed.* (Ed.: Ojima, I.), Wiley-VCH, New York, **2000**.
[2] Biocatalysis: a) Gröger, H.; Wilken*, J. Angew. Chem. Int. Ed.* **2001**, *40*, 529-53; b) *Biocatalysts for Fine Chemicals Synthesis* (Ed.: Roberts, S. M.), Wiley-VCH, New York, **1999**; c) *Enzyme Catalysis in Organic Synthesis*, 2nd ed. (Eds.: Drauz, K.; Waldmann, H.), Wiley-VCH, Weinheim, **2002**; d) Bommarius, A. S.; Riebel, B. R. *Biocatalysis*, Wiley-VCH, Weinheim, **2004**.
[3] a) Berkessel, A.; Gröger, H. *Asymmetric Organocatalysis: From Biomimetic Concepts to Applications in Asymmetric Synthesis*, Wiley-VCH, Weinheim, **2005**; b) Dalko, P. I. *Enantioselective Organocatalysis: reactions and experimental procedures* (Ed.: Dalko, P. I.), Wiley-VCH, Weinheim, **2007**, *Ch. 1*, 1-17; c) *Organocatalysis* (Eds.: Reetz, M. T.; List, B.; Jaroch, S.; Weinmann, H.), Springer, Verlag, Berlin, **2008**.

Chapter I

The catalytic asymmetric cyclopropanation of olefins, using a chiral Schiff base-copper complex as the catalyst, reported by Noyori *et al.* in 1966, is considered the starting point of metal enantioselective catalysis (**Scheme I.1**).[4] Since then, new concepts and new types of chiral catalysts have been continuously created and applied to various enantioselective reactions.

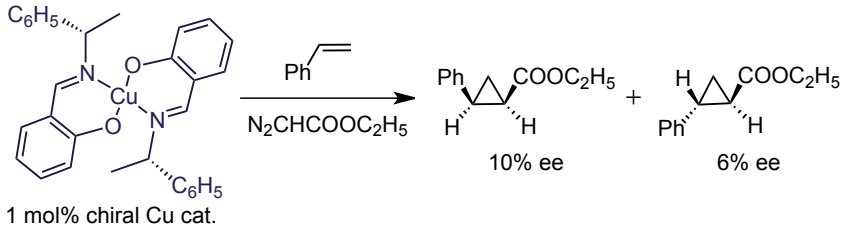

Scheme I.1. Discovery of asymmetric reaction by means of a chiral organometallic catalyst.

Nowadays, the appropriate combination of suitable chiral catalyst and reaction parameters becomes increasingly convenient to achieve a useful level of enantioselectivity (>90% ee) for the synthesis of chiral products. These successful results were evidenced by the Nobel Prize in Chemistry awarded to Knowles, Noyori and Sharpless for their contribution to chiral metal catalysis in 2001.[5]

I.1.1. Organocatalysis.

Organocatalysis is defined as the branch of catalysis that deals with the use of small organic molecules, containing C, O, N, S, P atoms, which are responsible for accelerating chemical reactions. It is currently recognized as an independent approach to asymmetric catalysis, which has been historically dominated by metal and bio-catalysis.[1,2] Since the year 2000, the research area of asymmetric organocatalysis has grown rapidly to become one of the most exciting fields in organic chemistry.[3] The synthesis of complex molecules is still an active challenge in organocatalysis, but several examples where organocatalyzed reactions play a crucial role[6] have been reported.

Organocatalysts present several advantages, since they are metal free, usually non-toxic and less expensive than chiral transition metal catalysts; they are readily available and often very robust. The rapid growth of organocatalysis can be also

---

[4] Nozaki, H.; Moriuti, S.; Takaya, H.; Noyori, R. *Tetrahedron Lett.* **1966**, *7*, 5239-5244.
[5] The Nobel Lectures: a) Knowles, W. S. *Angew. Chem. Int. Ed.* **2002**, *41*, 1998-2007; b) Noyori, R. *Angew. Chem. Int. Ed.* **2002**, *41*, 2008-2022; c) Sharpless, K. B. *Angew. Chem. Int. Ed.* **2002**, *41*, 2024-2032.
[6] a) Austin, J. F.; Kim, S.-G.; Sinz, C. J.; Xiao, W.-J.; MacMillan, D. W. C. *Proc. Natl. Acad. Sci. USA* **2004**, *101,* 5482-5487; b) Simmons, B.; Walji, A. M.; MacMillan, D. W. C. *Angew. Chem. Int. Ed.* **2009**, *48*, 4349-4353; c) Grondal, C.; Jeanty, M.; Enders, D. *Nature* **2010**, *2*, 167-168.

attributed to its tolerance towards moisture and oxygen which leads to user-friendly protocols. Indeed, demanding reaction conditions, such as inert atmosphere, low temperature, dry or degassed solvents, etc. are often not required. Furthermore, the presence of water is often beneficial to the rate and selectivity of the reaction.

Recently, there has been considerable interest towards the replacing of metal-based reactions due to several aspects, concerning the sustainability of the catalyst and the environmental impact. For this reason, asymmetric organocatalytic reactions seem to be attracting more interest nowadays from an industrial point of view (see **Chapter 1.4**). [3a,7]

The different approaches to the development of more sustainable chemical production are well summarized in the "twelve principles of Green Chemistry", described by Anastas and Kirchhoff.[8] This tendency is defined as the design of chemical products and processes that reduce or eliminate the use or generation of hazardous substances and/or waste products.

The first principle describes the basic idea of green chemistry – protecting the environment from pollution. The remaining principles are focused on issues such as atom economy, toxicity and solvent. It also aims to use the waste product of one system as the raw material for other systems. Less energy is consumed by reducing the operation temperature and pressure for the process, which is good for the environment.

The number of chiral, non-racemic pharmaceuticals on the market has increased during the past few decades, and several enantiopure compounds have been prepared by resolution of a racemic mixture. To minimize the losses derived from this approach, enantioselective methods are becoming more important to prepare these compounds.

According to this concept, organocatalysis appears very attractive for green chemistry. It involves low levels of chemical waste, which entails savings in time and energy; also, the cost is reduced because organocatalysts tend to be relatively inexpensive when compared with organometallic species. In addition, organocatalysts are relatively less toxic than transition metals; there is no risk of metal leaching, and therefore no expensive recovery process is required for waste treatment.

---

[7] Breuer, M.; Ditrich, K.; Habicher, T.; Hauer, M.; Keβeler, M.; Stürmer, R.; Zelinski, T. *Angew. Chem. Int. Ed.* **2004***, 43*, 788-824.

[8] a) Anastas, P. T.; Warner, J. C. *Green Chemistry: Theory and Practice*, Oxford Univ. Press: New York, **1998**, 30-48; b) Anastas, P. T.; Zimmerman, J. B. *Environ. Sci. Tech.* **2003,** *37*, 94A-101A; c) Jiménez-González, C.; Poechlauer, P.; Broxterman, Q. B.; Yang, B.-S.; am Ende, D.; Baird, J.; Bertsch, C.; Hannah, R. E.; Dell'Orco, P.; Noorman, H.; Yee, S.; Reintjens, R.; Wells, A.; Massonneau, V.; Manley, L. *Org. Process Res. Dev.* **2011**, *15*, 900-911.

Chapter I

The historic origins of organocatalysis go back to the use of low molecular weight compounds in an attempt both to understand and to mimic the catalytic activity and selectivity of enzymes. Despite the fact that the name was first used in the year 2000, organocatalysis has a rich background; starting in 1928 Wolfgang Langenbeck published "Analogies in the catalytic action of enzymes and definite organic substances".[9] Later, in 1932, the same author coined the term "Organic Catalysts",[9b] although J. Von Liebig described the first organocatalytic reaction in the middle of the 19th century.[10] Accidentally he found that cyanogen is transformed into oxamide in the presence of an aqueous solution of acetaldehyde (**Scheme I.2**).

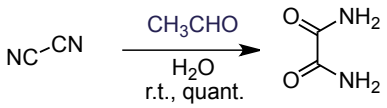

Scheme I.2. Organocatalytic oxamide synthesis.

However, one century after that, the first organocatalyzed metal-free reaction with an acceptable level of enantioselectivity was reported by H. Pracejus.[11] Using 1 mol% of a cinchona derivative (*O*-acetylquinine) as catalyst in the addition of methanol to a ketene, they obtained quite a remarkable 74% ee of the desired ester (**Scheme I.3**).

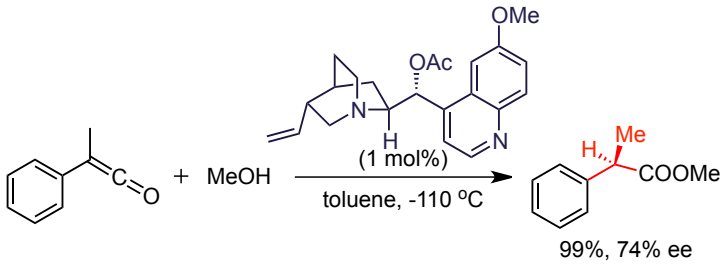

Scheme I.3. First example of practical organocatalytic asymmetric reaction.

Further challenges to perform reactions with high enantioselectivity were achieved in the early 1970s. In 1971, two groups, Hajos and Parrish[12] as well as Eder, Sauer and Wiechert [13] discovered that L-proline is capable of catalyzing the intramolecular asymmetric Robinson annulation of an achiral triketone. Indeed, this simple amino acid gave rise to the so-called Hajos-Parrish and Wieland-Miescher

---

[9] a) Langenbeck, W. *Angew. Chem.* **1928**, *41*, 740-745; b) Langenbeck, W. *Angew. Chem.* **1932**, *45*, 97-99.
[10] Von Liebig, J. *Ann. Chem. Pharm.* **1860**, *113, 2*, 246-247.
[11] Pracejus, H. *Justus Liebigs Ann. Chem.* **1960**, *634*, 9-22.
[12] a) Hajos, Z. G.; Parrish, D. R. *DE 2102623*, **1971**; b) Hajos, Z. G.; Parrish D. R. *J. Org. Chem.* **1974**, *39*, 1615-1621.
[13] Eder, U.; Sauer, G.; Wiechert, R. *Angew. Chem. Int. Ed.* **1971**, *10*, 496-497.

ketones, which are important intermediates in steroid synthesis, in excellent enantioselectivities (**Scheme I.4**).[14]

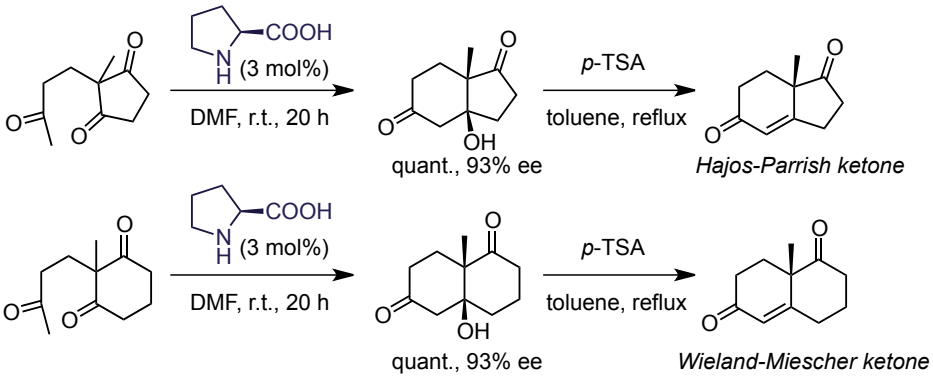

Scheme I.4. The Hajos-Parrish-Eder-Sauer-Wiechert reaction.

Despite the fact that several studies were carried out regarding the mechanism (although they were later proved wrong), the catalytic potential of proline in asymmetric aldol reactions went unexplored for almost 30 years.[15] The modern era of organocatalysis started with the works of List and Barbas[16] in enamine chemistry and MacMillan[17] in iminium ion chemistry in 2000.

List *et al.* reported pioneering studies on intermolecular aldol reactions with L-proline as the catalyst.[16b] Under these conditions, acetone could be added to a variety of aldehydes, affording the corresponding aldols in excellent yields and enantiomeric purity. An example with *iso*-butyraldehyde as acceptor is shown in **Scheme I.5**, the aldol adduct being obtained in 97% yield and 96% ee.[16b] The *in situ* generation of the enamine as an enolate surrogate is currently known as ”enamine catalysis”. Considering the remarkable chemo- and enantioselectivity observed by List *et al.*, further research in L-proline-catalyzed aldol, Mannich, Michael and related reactions started.

---

[14] For Hajos-Parrish ketone, see some examples in Total Synthesis: a) Deng, W.; Jensen, M. S.; Overman, L. E.; Rucker, P. V.; Vionnet, J.-P. *J. Org. Chem.* **1996**, *61*, 6760-6761; b) Peixoto, P. A.; Jean, A.; Maddaluno, J.; De Paolis, M. *Angew. Chem.* **2013**, *125*, 7109-7111; for Wieland-Miescher ketone, see review: c) Bradshaw, B.; Bonjoch J. *Synlett* **2012**, *23*, 337-356.

[15] For aldol and retro-aldol reactions that are catalyzed by achiral primary amines, see: a) Pollack, R. M.; Ritterstein, S. *J. Am. Chem. Soc.* **1972**, *94*, 5064-5069; b) Koshechkina, L. P.; Mel’nichenko, I. V. *Ukr. Khim. Zh.* **1974**, *40*, 172-174.

[16] a) List, B.; Lerner, R. A.; Barbas III, C. F. *Org. Lett.* **1999**, *1*, 59-61; b) List, B.; Lerner, R. A.; Barbas III, C. F. *J. Am. Chem. Soc.* **2000**, *122*, 2395-2396; c) Sakthivel, K.; Notz, W.; Bui, T.; Barbas III, C. F. *J. Am. Chem. Soc.* **2001**, *123*, 5260-5267; d) List, B. *Synlett* **2001**, 1675-1686; e) List. B. *Chem.Rev.* **2007**, *107*, 5413-5883.

[17] a) Ahrendt, K. A.; Borths, C. J.; MacMillan, D. W. C. *J. Am. Chem. Soc.* **2000**, *122*, 4243-4244; b) Jen, W. S.; Wiener, J. J. M.; MacMillan, D. W. C. *J. Am. Chem. Soc.* **2000**, *122*, 9874-9875; c) Austin, J. F.; MacMillan, D. W. C. *J. Am. Chem. Soc.* **2002**, *124*, 1172-1173; c) MacMillan, D. W. C. *Nature* **2008**, *455*, 304-308.

Chapter I

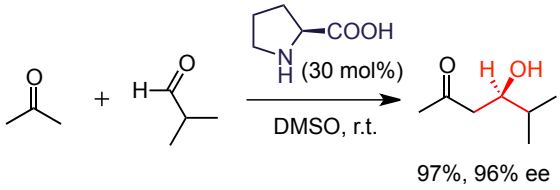

Scheme I.5. L-Proline-catalyzed intermolecular asymmetric aldol reaction.

In the same year, MacMillan *et al.* reported that a phenylalanine-derived imidazolidinone catalyzes the Diels-Alder reaction of α,β-unsaturated aldehydes with enantioselectivities up to 93% (**Scheme I.6**).[17a] This initial report by MacMillan *et al.* was followed by numerous applications of this catalyst and related secondary amines.[17]

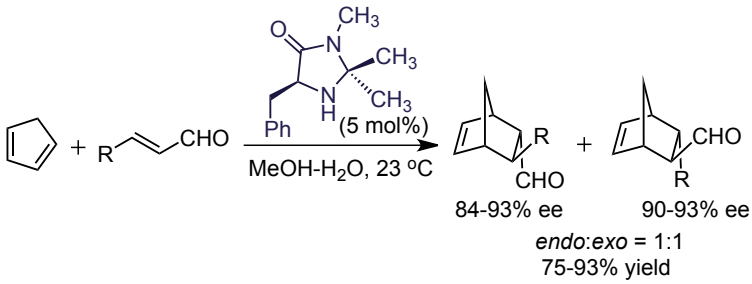

Scheme I.6. Asymmetric Diels-Alder reaction using MacMillan catalyst.

Triggered by the pioneering work of List, Barbas, MacMillan and others in the early 2000s, the last fifteen years have seen an exponential growth of this field. Consequently, it has become a very powerful, practical, and broadly applicable third methodological approach in catalytic asymmetric synthesis.[18]

The molecular structures of the mentioned organocatalysts and some additional representative ones are shown in **Figure I.1**.[19] New small organic catalysts were discovered and pared the way for new opportunities in the synthesis of chiral compounds with high efficiency for a wide variety of asymmetric processes.

---

[18] For reviews on aminocatalysis, see: a) Melchiorre, P.; Marigo, M.; Carlone, A.; Bartoli, G. *Angew. Chem. Int. Ed.* **2008**, *47,* 6138-6171; b) Bertelsen, S.; Jørgensen, K. A. *Chem. Soc. Rev.* **2009**, *38*, 2178-2189; c) Panday, S. K. *Tetrahedron: Asymmetry* **2011**, *22*, 1817-1847; d) Nielsen, M.; Worgull, D.; Zweifel, T.; Gschwend, B.; Bertelsen, S.; Jørgensen, K. A. *Chem. Commun.* **2011**, *47,* 632-649.

[19] *Multicatalyst system in asymmetric catalysis* (Ed.: Zhou, J.), John Wiley & Sons Inc., Hoboken, NJ, USA, **2014**.

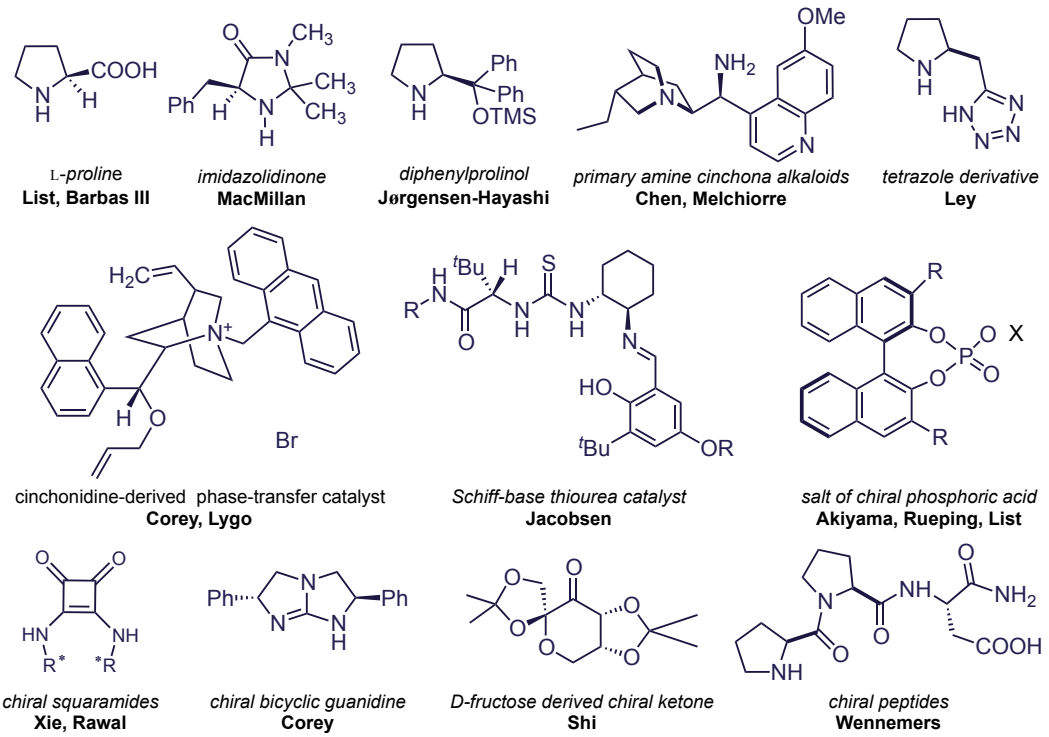

Figure I.1. Molecular structure of some representative organocatalysts.

Important contributions had been described by the beginning of the 21th century, such as the first examples of hydrogen-bonding catalysis, developed by Jacobsen and Corey for the asymmetric variant of the Strecker reactions.[20] Pioneering works on cinchona alkaloids catalysts, developed by Pracejus for the first time,[11] were rediscovered by Chen and Melchiorre groups. [21] Also bifunctional catalysts were developed.[22] Therefore, a new organocatalysts classification was developed in a short time, providing an overview of general aspects regarding organocatalysis and activation modes.

I.1.2. Organocatalysts classification.

Most research efforts have focused on the development of novel organocatalysts, new reactivities and asymmetric methodologies. In order to give an overview of this field of research, different catalysis concepts have to be considered.

---

[20] a) Corey, E. J.; Grogan M. J. *Org. Lett.* **1999**, *1*, 157-160; b) Wenzel, A. G.; Jacobsen, E. N. *J. Am. Chem. Soc.* **2002**, *124*, 12964-12965.
[21] a) Xie, J.-W.; Chen, W.; Li, R.; Zeng, M.; Du, W.; Yue, L.; Chen, Y.-C.; Wu, Y.; Zhu, J.; Deng, J.-G. *Angew. Chem. Int. Ed.* **2007**, *46*, 389-392; b) Bartoli, G.; Bosco, M.; Carlone, A.; Pesciaioli, F.; Sambri, L., Melchiorre, P. *Org. Lett.* **2007**, *9*, 1403-1405.
[22] a) Akiyama, T.; Itoh, J.; Yokota, K.; Fuchube, K. *Angew. Chem. Int. Ed.* **2004**, *43*, 1566-1568; b) Malerich, J. O.; Hagihara, K.; Rawal, V. H. *J. Am. Chem. Soc.* **2008**, *130*, 14416-14417.

Chapter I

A general classification of substrate activation modes can be made according to the catalyst-substrate interaction. In this way, they can be divided in two classes: covalent and non-covalent organocatalysis[3a,23] (**Fig. I.2**).

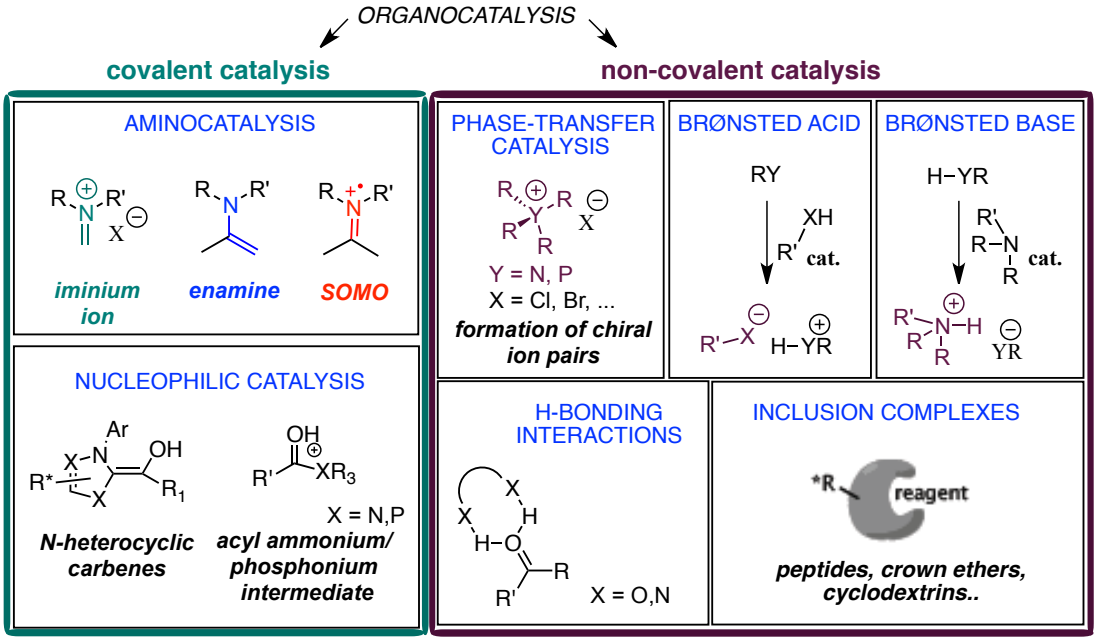

Figure I.2. Organocatalysis classification according to the catalyst-substrate interaction.

In the first one, a new covalent bond between the catalyst and the substrate is formed, as in the case of aminocatalysis[18] and carbenes,[24] leading to strong interactions that have to be, nevertheless, reversible.

On the other hand, in non-covalent organocatalysis the activation of the substrate occurs via weak binding exemplified by hydrogen bonding[25] or ionic interaction as in the case of phase transfer catalysis (PTC).[26]

List *et al.* introduced another way of differentiating the organocatalyst based on the mechanism of catalysis.[27] Most of them can be classified into four areas: Lewis bases, Lewis acids, Brønsted bases, and Brønsted acids. The corresponding (simplified) catalytic cycles and examples are shown in **Figure I.3**.

---

[23] a) Gaunt, M. J.; Johansson, C. C. C.; McNally, A.; Vo, N. T. *Drug Discovery Today* **2007**, *12*, 8-27; b) Lelais, G.; MacMillan, D. W. C. *New Frontiers in Asymmetric Catalysis* (Eds.: Mikami, K.; Lautens, M.), John Wiley & Sons Inc., Hoboken, NJ, USA, **2007**, *Ch. 11*, 313-358.
[24] For reviews on carbene organocatalysis, see: a) Enders, D.; Balensiefer, T. *Acc. Chem. Res.* **2004**, *37*, 534-541; b) Johnson, J. S. *Angew. Chem. Int. Ed.* **2004**, *43*, 1326-1328.
[25] a) Taylor, M. S.; Jacobsen, E. N. *Angew. Chem. Int. Ed.* **2006**, *45*, 1520-1543; b) Pihko, P. M. *Hydrogen Bonding in Organic Synthesis*, Wiley-VCH, Weinheim, **2009**.
[26] For reviews on asymmetric phase-transfer catalysis, see: a) Lygo, B.; Andrews, B. I. *Accounts of Chemical Research,* **2004**, *37*, 518-525; b) *Asymmetric Phase Transfer Catalysis* (Ed.: Maruoka, K.), Wiley-VCH, Weinheim, **2008**; c) Ooi, T.; Maruoka, K. *Angew. Chem. Int. Ed.* **2007**, *46*, 4222-4266; d) Shirakawa, S.; Maruoka, K. *Angew. Chem. Int. Ed.* **2013**, *52*, 4312-4348.
[27] Seayad, J.; List, B. *Org. Biomol. Chem.* **2005**, *3,* 719-724.

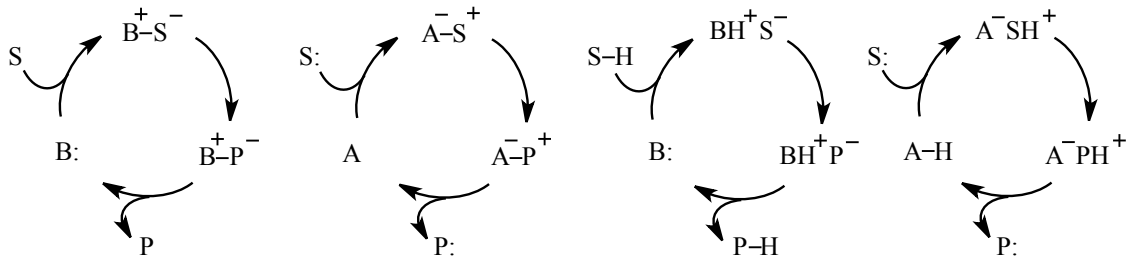

Lewis Bases: (B:) *iminium ion catalysis enamine catalysis NHC catalyst*

Lewis Acids: (A) *phase transfer catalyst ketone catalyzed epoxidation*

Brønsted Bases: (B:) *cinchona alkaloid catalyzed alcoholysis of anhydride*

Brønsted Acids: (A) *small molecules H-bond catalyst*

Figure I.3. Organocatalytic cycles according to the organocatalysts acid/base reactivity classification (B = base; A = acid; S = substrate; P = product).

Mechanistically, the catalytic cycles work in the following manner:[27]

-In Lewis base catalysis nucleophilic addition of B: to the substrate (S) initiates the cycle. The reaction takes place on this complex and, finally, the product (P) is formed and the catalyst (B:) is released.

-The cycle proceeds in a similar fashion in the case of Lewis acid catalysts (A) by addition of activate nucleophilic substrates (S:).

-Catalytic cycles in the case of Brønsted base and acids take place through (partial) deprotonation or protonation, respectively.

Covalent organocatalysts can be further divided according to the activation mode in HOMO (enamine),[28] LUMO (iminium ion)[29] and SOMO[30] activation to engage carbonyl compounds in catalysis (**Figure I.4**). This concept is perfectly applicable to amine-based organocatalysts (aminocatalysts). Conveniently, the same organocatalyst may promote reactions based on different activation modes depending on the reaction conditions or even in the same flask in a domino sequence.

[28] For reviews on enamine catalysis, see: a) Mukherjee, S.; Yang, J. W.; Hoffmann, S.; List, B. *Chem. Rev.* **2007**, *107*, 5471-5569; b) Pihko, M. P.; Majander, O.; Erkkilä, A. *Top Curr Chem.* **2010**, *291*, 29-75.
[29] For reviews on iminium ion catalysis, see: Erkkilä, A.; Majander, I.; Pihko, P. M. *Chem. Rev.* **2007**, *107*, 5416-5470.
[30] Pioneering SOMO catalysis applications: a) Beeson, T. D.; Mastracchio, A.; Hong J.-B.; Ashton, K.; MacMillan, D. W. C. *Science* **2007**, *316*, 582-585; b) Abbasov, M. E.; Romo, D. *Nat. Prod. Rep.* **2014**, *31*, 1318-1327.

Chapter I

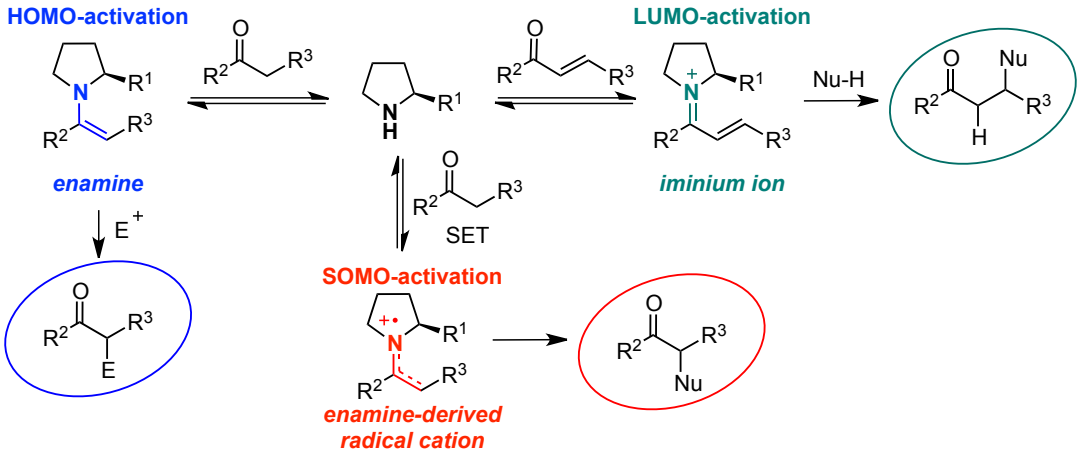

Figure I.4. Classical activation concepts in aminocatalysis.

Since most of the work in this thesis is based on pyrrolidine derivatives via enamine/iminium activation mode, the following discussion will give a brief introduction of these classical activation concepts,[18] in particular, focusing on enamine and iminium ion catalysis.

I.1.2.1. Enamine Catalysis.

Enamine catalysis[16,28] formally involves the highest occupied molecular orbital (HOMO)-raising activation of enols, the tautomeric form of aldehydes and ketones. This activation concept is based on the reversible condensation of an amine catalyst with a simple carbonyl compound to form an iminium ion intermediate. After deprotonation, this generates an enamine species that can be subsequently trapped by an appropriate electrophile (**Figure I.5**). These olefins have sufficient π-electron density to participate in nucleophilic addition with a variety of carbon-, nitrogen-, oxygen-, sulphur- and halogen-centered electrophiles.

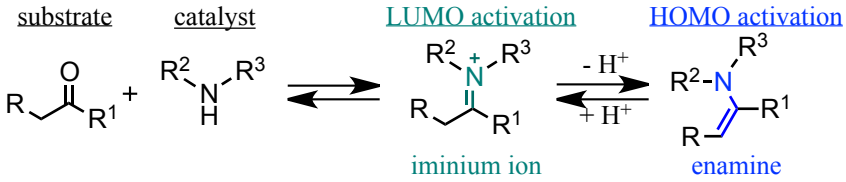

Figure I.5. Enamine catalysis intermediates.

The first example of asymmetric enamine catalysis is the abovementioned Hajos-Parrish-Eder-Sauer-Wiechert reaction, an intramolecular aldol reaction catalyzed by proline. Many mechanistic studies and computational work had been done to understand this catalytic process, before the work by List and co-workers led

to a better understanding and to the discovery of new enamine-based catalytic cycles.[31]

Initially, only limited mechanistic information was available on the proline-catalyzed intramolecular aldol reaction. Several groups suggested an enamine mechanism already in the 1970s and 1980s. However, there was some debate over several mechanistic aspects of the reaction, and a number of different transition state models were proposed (**Figure I.6**). An early example regarding these models was proposed by Hajos *et al.*, in which he suggests that the proline is attached to one of the two ketones on the cyclopentane ring. In this manner an intermediate is formed, which conformation is held by means of hydrogen bonding (**A**).[12b] Jung questioned the accuracy of this model soon after its proposal.[32] In 1986 Agami *et al.* observed a modest nonlinear effect in the asymmetric catalysis and a concentration-dependent enantioselectivity,[33] and their studies led to the view that two proline molecules could be involved in the transition state of the intramolecular aldol reaction (**B**). In 1999 Swaminathan *et al.* proposed a heterogeneous aldolization mechanism on the surface of crystalline proline (**C**) despite the fact that many proline-catalyzed aldolizations are completely homogeneous.[34]

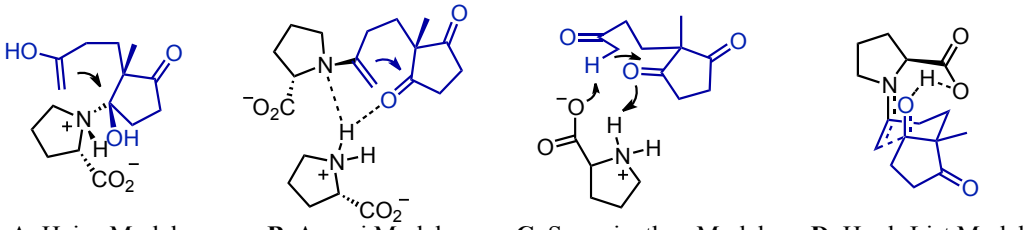

A. Hajos Model **B.** Agami Model **C.** Swaminathan Model **D.** Houk-List Model

Figure I.6. Proposed transition states for the proline-catalyzed Robinson annulation.

Agami's two-proline mechanism[33] was recently challenged when further studies by List *et al.* proposed a homogeneous one-proline enamine mechanism for the intermolecular variant.[16b-c] Also independent modelling studies by the Houk group proposed a very similar mechanism to the List proposal for intramolecular variants (**D**), based on density functional theory calculations.[35] Later, it was found that proline-

---

[31] List, B. *Acc. Chem. Res.* **2004**, *37*, 548-557.
[32] a) Jung, M. E. *Tetrahedron* **1976**, *32*, 3-31; b) Brown, K. L.; Damm, L.; Dunitz, J. D.; Eschenmoser, A.; Hobi, R.; Kratky, C. *Helv. Chim. Acta* **1978**, *61*, 3108-3135.
[33] a) Agami, C.; Meynier, F.; Puchot, C.; Guilhem, J.; Pascard, C. *Tetrahedron* **1984**, *40*, 1031-1038; b) Agami, C.; Puchot, C.; Sevestre. H. *Tetrahedron Lett.* **1986**, *27*, 1501-1504; c) Puchot, C.; Samuel, O.; Duñach, E., Zhao, S.; Agami, C.; Kagan, H. B. *J. Am. Chem. Soc.* **1986**, 108, 2353-2357; d) Agami, C.; Puchot, C. J. *Mol. Catal.* **1986**, *38*, 341-343; e) Agami, C. *Bull. Soc. Chem. Fr.* **1988**, *3*, 499-507.
[34] Rajagopal, D.; Moni, M. S.; Subramanian, S.; Swaminathan, S. *Tetrahedron: Asymmetry* **1999**, *10*, 1631-1634.
[35] a) Bahmanyar, S.; Houk, K. N. *J. Am. Chem. Soc.* **2001**, *123*, 9922-9923; b) Bahmanyar, S.; Houk, K. N. *J. Am. Chem. Soc.* **2001**, *123*, 11273-11283; c) Bahmanyar, S.; Houk, K. N.; Martin, H. J.; List, B. *J.*

catalyzed aldol reactions do not show any nonlinear effects[36] in contrast with earlier proposals.[33c]

Mechanistically, the aldol reaction (**Scheme I.7**) involves carbinolamine (**I.2**), iminium ion (**I.3**) and enamine (**I.4**) intermediates. The adjacent carboxylic acid group of the enamine intermediate then directs the approach of the electrophile by formation of a specific hydrogen bond in the transition state structure (**I.5**). Transition state **I.5** was supported experimentally by the absence of nonlinear effects in the intermolecular aldol reaction[16c-d] and by density functional theory calculations.[36] This provides both pre-organisation of the substrates and stabilization of the transition state. After the reaction, the resulting iminium ion (**I.6**) is hydrolyzed to release the product and the proline catalyst (**I.1**), which can proceed to repeat the cycle.

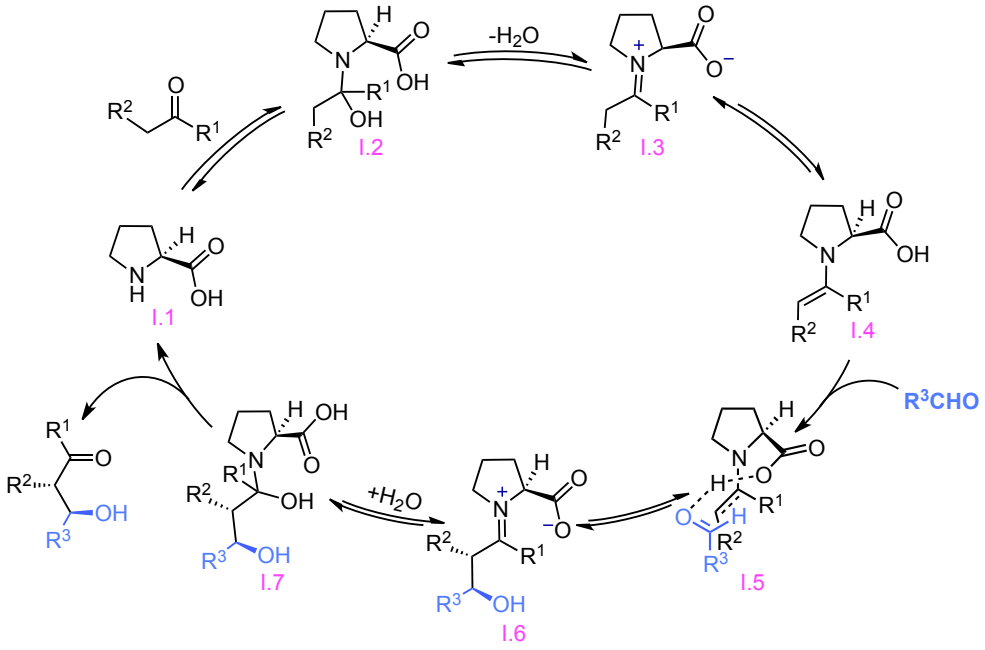

Scheme I.7. Proposed mechanism for the proline-catalyzed intermolecular aldol reaction.

Analogous reaction mechanisms can be proposed for other chiral amines (**Scheme I.8**).[28] Accordingly, the enamine which is generated upon condensation with the carbonyl compound via iminium ion formation, can react with an electrophile via nucleophilic addition (or substitution) to give an α-modified iminium ion and, upon hydrolysis, the α-modified carbonyl product.

Am. Chem. Soc. **2003**, *125*, 2475-2479; d) Clemente, F. R.; Houk, K. N. *Angew. Chem.* **2004**, *116*, 5890-5892.

[36] a) Hoang, L.; Bahmanyar, S.; Houk, K. N.; List, B. *J. Am. Chem. Soc.* **2003**, *125*, 16-17; b) Klussmann, M.; Iwamura, H.; Mathew, S. P.; Wells, D. H.; Pandya, U.; Armstrong, A.; Blackmond, D. G. *Nature* **2006**, *441*, 621-623.

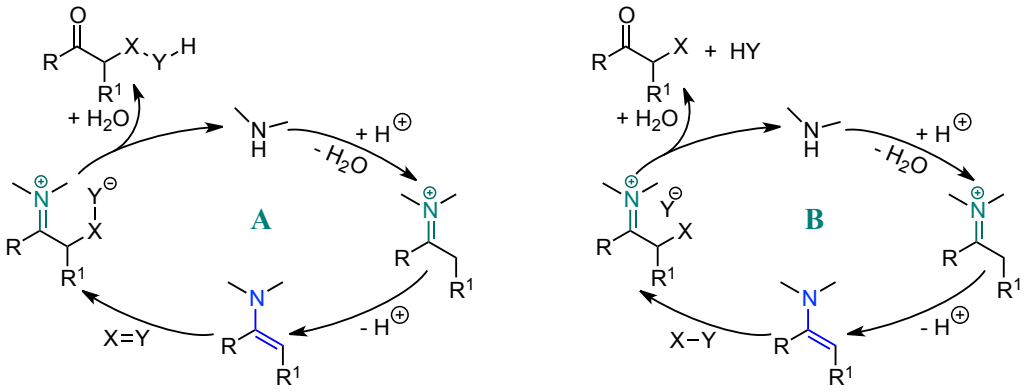

Scheme I.8. Catalytic cycles for the enamine catalysis of nucleophilic additions (A) and substitution (B) reactions.

This HOMO-rising methodology has successfully been utilized in the aldol, Mannich, Michael, and Baylis-Hillman reaction, as well as in α-functionalization of aldehydes and ketones such as amination, hydroxylation, alkylation or halogenation.[28]

Dienamine or trienamine modes of activation have been achieved using this strategy with enolizable α,β-unsaturated carbonyls or poly-conjugated carbonyls.[37]

I.1.2.2. Iminium ion catalysis.

MacMillan reported the first example of iminium ion catalysis using an imidazolidinonium salt to generate iminium ion intermediates. This opened up a new metal-free catalytic strategy for the activation of α,β-unsaturated carbonyl compounds towards cycloaddition (**Scheme I.6**).[17a] More recently, conjugate additions have been reported using the same catalyst.[17c]

Iminium ion catalysis is based on the ability of chiral amines to function as enantioselective catalysts for several transformations that traditionally use Lewis acid catalysts (**Figure I.7**). This concept was founded on the mechanistic hypothesis that α,β-unsaturated aldehydes and chiral amines react reversibly to form iminium ions. This LUMO lowering is analogous to what happens in Lewis acid catalysis. Indeed, iminium ions present equilibrium dynamics and π-orbital interactions similar to those of carbonyl groups activated Lewis acid.[17a,29,38] This approach enabled the asymmetric introduction of several nucleophiles to the β-position of unsaturated aldehydes and ketones.

---

[37] a) Jensen, K. L.; Dickmeiss, G.; Jiang, H.; Albrecht, Ł.; Jørgensen, K. A. *Acc. Chem. Res.* **2012**, *45*, 248-264; b) Arceo, E.; Melchiorre, P. *Angew. Chem. Int. Ed.* **2012**, *51*, 5290-5292.
[38] Watson, A. J. B.; MacMillan, D. W. C.; Wang, Y.; Deng, L.; Shirakawa, S.; Maruoka. K. *Asymmetric Organocatalysis, in Catalytic Asymmetric Synthesis*, 3rd edn (ed.: Ojima, I.), John Wiley & Sons Inc., Hoboken, NJ, USA, **2010**, 37-117.

Chapter I

Figure I.7. Iminium catalysis intermediate.

The proposed catalytic cycle involves three main steps: iminium ion formation, key bond formation reaction (for example, cycloaddition or conjugate addition), and iminium ion hydrolysis (**Scheme I.9**).

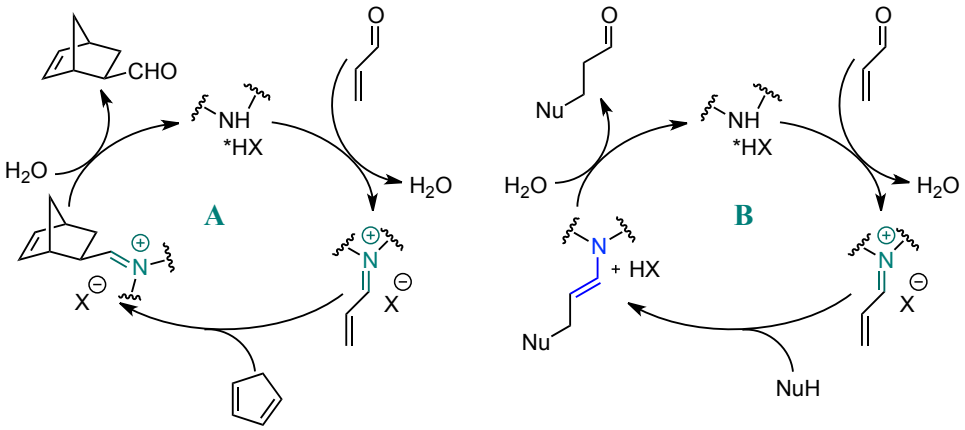

Scheme I.9. Catalytic cycles for the iminium ion mediated Diels-Alder **(A)** and conjugate addition **(B)** reactions.

Using the LUMO-lowering strategy, excellent results have been obtained in cycloaddition, Diels-Alder, Friedel-Crafts alkylation, Michael reaction of α,β-unsaturated ketones, Mukaiyama-Michael reactions or cyclopropanation.[39]

I.1.2.3. SOMO Activation.

We have just shown how chiral amines such as imidazolidinone **I.8** catalyze the enantioselective transformation of aldehydes or ketones by two activation modes (**Figure I.8**).[16,17b] Simple condensation leads to the electrophilic iminium ion **I.9**, whereas deprotonation of iminium ion **I.9** furnishes a nucleophilic enamine species **I.10**. Due to the fact that enamine and iminium ions are rapidly interconverted via a protonation/deprotonation process, MacMillan *et al.* proposed that it may be possible to interrupt this equilibrium by carrying out a one-electron oxidation of the electron-rich enamine.[30a] This 3-π-electron radical cation **I.11** should be accessible using single-

[39] For some examples, see: a) Northrup, A. B.; MacMillan, D. W. C. *J. Am. Chem. Soc.* **2002**, *124*, 6798-6799; b) Paras, N. A.; MacMillan, D. W. C. *J. Am. Chem. Soc.* **2002**, *124*, 7894-7895; c) Brown, S. P.; Goodwin, N. C.; MacMillan, D. W. C. *J. Am. Chem. Soc.* **2003**, *125*, 1192-1194; c) Robichaud, J.; Tremblay, F. *Org. Lett.* **2006**, *8*, 597-600.

electron-transfer (SET) oxidants (in this case, cerium ammonium nitrate, CAN) such as metal salts. The limitation of the existing enamine catalysis in direct catalytic alkylations was the motivation to find alternative reactivity patterns.

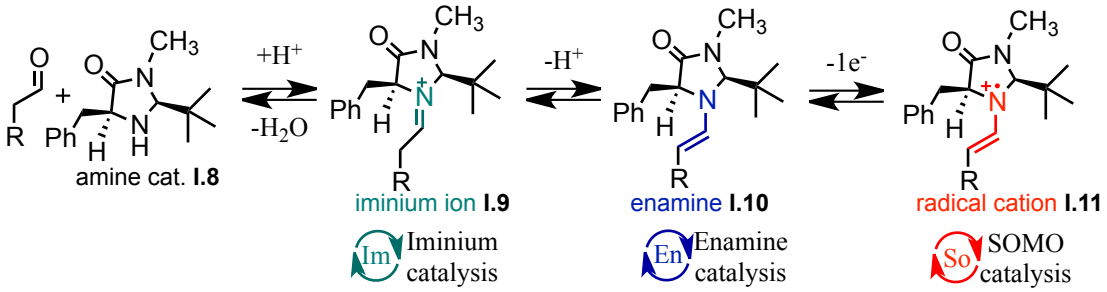

Figure I.8. Organocatalytic activation modes in chiral amine catalysis.

In their initial studies, MacMillan *et al.* found that different aldehydes in a presence of the chiral secondary amine catalyst reacted with an allyltrimethylsilane derivative by using 2 equiv. of ceric ammonium nitrate (CAN), as the stoichiometric oxidant (**Scheme I.10**).[30a]

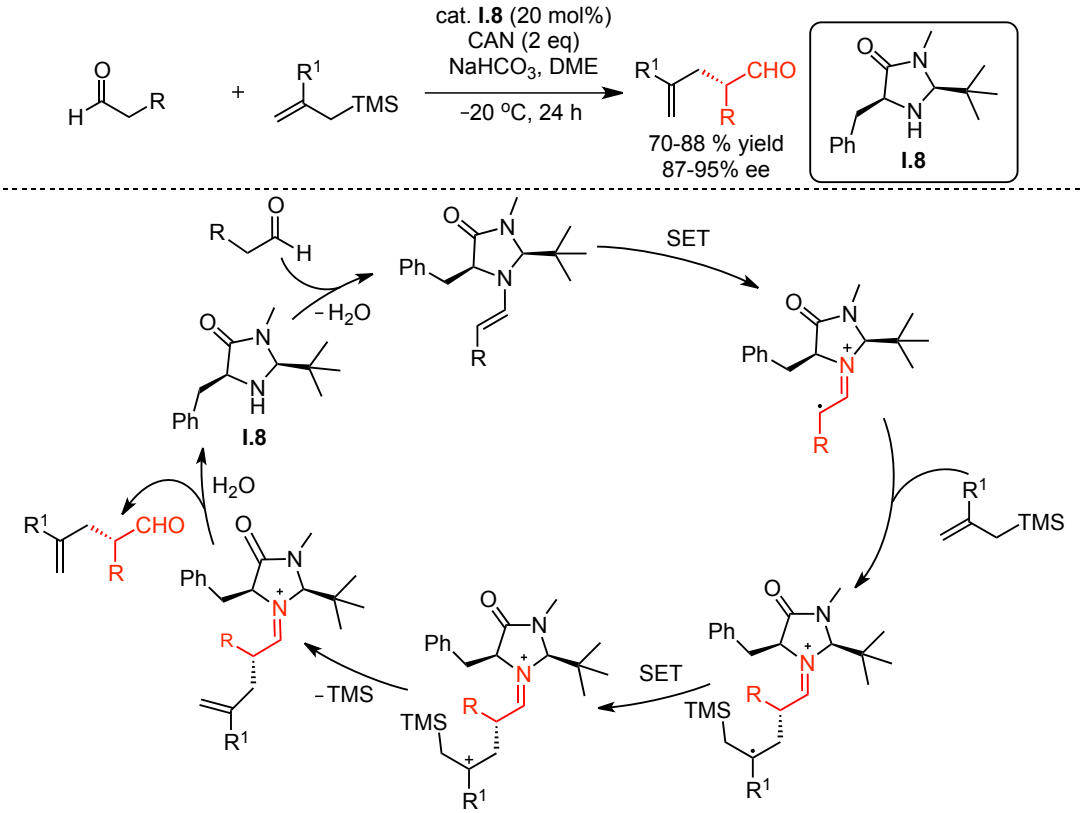

Scheme I.10. SOMO-activation for the stereoselective α-allylation of aldehydes.

In the general mechanism, the radical cation obtained after SET oxidation of the enamine reacts with the allyltrimethylsilane derivative, and then is oxidized again by the SET oxidant. In the next step TMS elimination provides the iminium ion, which is subsequently hydrolysed to the α-functionalized aldehyde and the catalyst **I.8**.

SOMO catalysis is one of the most recently discovered activation modes but it has been already used in a variety of enantioselective transformations that complement those developed with enamine catalysis (**Figure I.9**).[30,40]

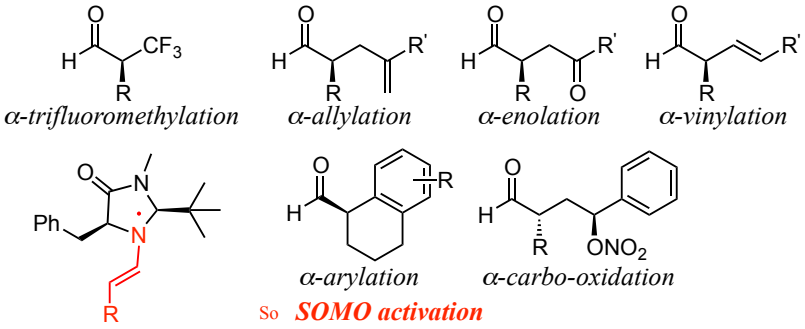

Figure I.9. Some of the applications of SOMO activation

I.1.2.4. Hydrogen-bonding catalysis.

In the 1980s, it was suggested that hydrogen-bonding interactions could be enough to fix a transition state in the desired conformation, leading to good enantioselectivities; however, these cases were considered to be exceptions.[41] The breakthrough was made by the Jacobsen group[42] in 1998, when they published the first real example of hydrogen-bonding asymmetric catalysis in the Strecker reaction (**Scheme I.11.A**),[42a] followed by other notable contributions in this area. Nowadays, Jacobsen's ureas and thioureas are still among the most efficient and broadly used scaffolds.[25] But not only ureas and thioureas structures were able to participate in double H-bonding interaction. Roughly at the same time, Corey and Grogan discovered that a guanidinium analogue such as a chiral bicyclic guanidine can mediate asymmetric the Strecker reaction of *N*-diphenylmethyl imines (**Scheme I.11.B**),[20a] although a single H-bond interaction was proposed. In addition, new concepts towards bifunctional hydrogen-bonding catalysts can be generated by

---

[40] For some examples, see: a) Ibrahem, I.; Córdova, A. *Angew. Chem. Int. Ed.* **2006**, *45*, 1952-1956; b) Jang, H.; Hong, J.; MacMillan, D. W. C. *J. Am. Chem. Soc.* **2007**, *129*, 7004-7005; c) Kim, H.; MacMillan, D. W. C. *J. Am. Chem. Soc.* **2008**, *130*, 398-399; d) Graham, T. H.; Jones, C. M.; Jui, N. T.; MacMillan, D. W. C. *J. Am. Chem. Soc.* **2008**, *130*, 16494-16495; e) García-Fortanet, J.; Buchwald, S. L. *Angew. Chem. Int. Ed.* **2008**, *47*, 8108-8111; f) Mastracchio, A.; Warkentin, A. A.; Walji, A. M.; MacMillan, D. W. C. *Proc. Natl. Acad. Sci. USA*, **2010**, *107*, 20648-20651.

[41] a) Hiemstra, H.; Wynberg, H. *J. Am. Chem. Soc.* **1981**, *103*, 417–430; b) Oku, J.-I.; Inoue, S. *J. Chem. Soc. Chem. Commun.* **1981**, 229–230; c) Dolling, U. H.; Davis, P.; Grabowski, E. J. J. *J. Am. Chem. Soc.* **1984**, *106*, 446–447.

[42] a) Sigman, M. S.; Jacobsen, E. N. *J. Am. Chem. Soc.* **1998**, *120*, 4901-4902; b) Vachal, P.; Jacobsen, E. N. *Org. Lett.* **2000**, *2*, 867-870; c) Sigman, M. S.; Vachal, P.; Jacobsen, E. N. *J. Angew. Chem. Int. Ed.* **2000**, *39*, 1279-1281; d) Vachal, P.; Jacobsen, E. N. *J. Am. Chem. Soc.* **2002**, *124*, 10012-10014.

introduction of other functional groups, such as Lewis bases, arenes, or even other hydrogen-bonding sites, which can provide additional stabilization.[25]

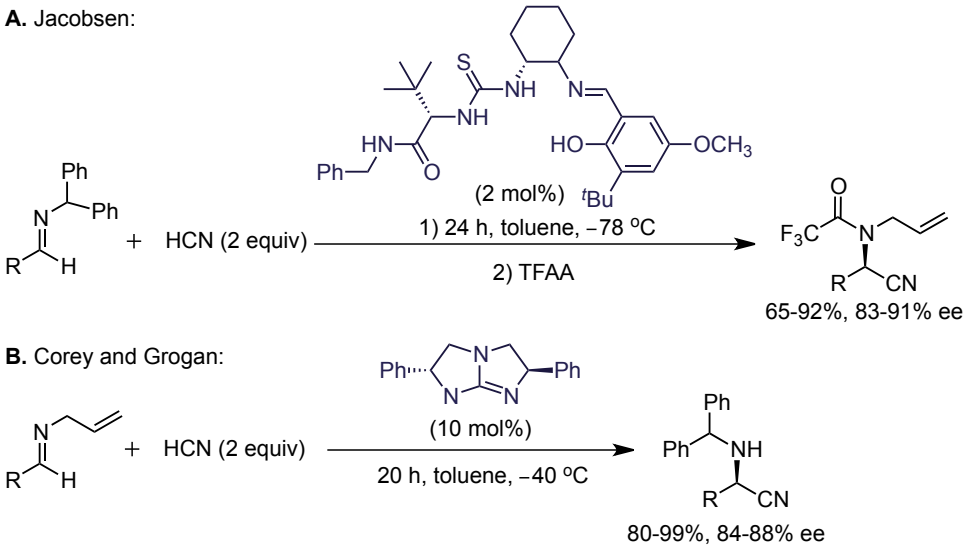

Scheme I.11. Enantioselective Strecker reaction.

These catalysts have been successfully employed to facilitate transformations such as aldol, nitro aldol, Strecker, Diels-Alder, aza Baylis-Hillman reactions or Claisen rearrangements.[43]

It is always difficult to distinguish between H-bond catalysis and Brønsted acid catalysis (**Scheme I.12**). Whereas the latter involves protonation (for Brønsted acid, **Scheme 1.3**), hydrogen bond catalysis is defined as "LUMO-lowering activation by the simultaneous sharing of a hydrogen atom by the substrate (acceptor) and the catalyst (donor)".[23b] The main role of this interaction is fixing the conformation of the substrate and directing the approach of the attacking nucleophile.

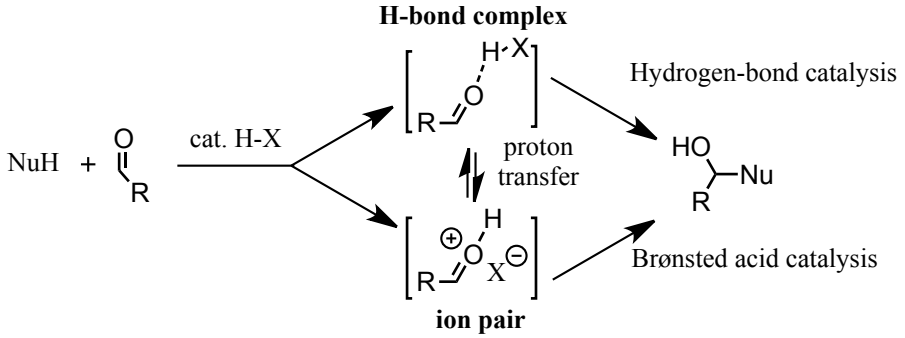

Scheme I.12. Hydrogen-bond catalysis versus Brønsted-acid catalysis.

[43] For examples, see: a) Vicario, J. L.; Carrillo, L. *Angew. Chem. Int. Ed.* **2012**, *124*, 4180; b) Zuend, S. J.; Coughlin, M. P.; Lalonde, M. P.; Jacobsen, E. N. *Nature* **2009**, *461,* 968-970; c) Raheem, I. T.; Jacobsen, E. N. *Adv. Synth. Catal.* ***2005, 347,*** 1701-1708.

I.1.2.5. Counter-ion directed catalysis.

The Jacobsen group developed a novel form of organocatalytic activation, which directs highly enantioselective additions via *in-situ* generated *N*-acyl-iminium ions and oxocarbenium ions (**Scheme I.13**).[44] In this work, chiral thiourea catalysts such as **I.12** generate an ion pair via binding by electrostatic effects and ionizing the weak carbon-chlorine bonds of chloroamides and chloroacetals. This chiral counter-ion directs the approach of nucleophiles to one of the enantiotopic faces of the transient α-heteroatom stabilized cationic species.

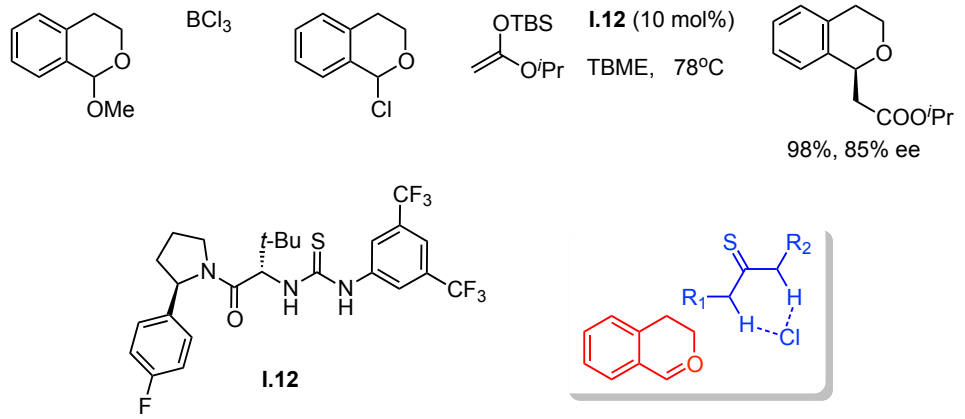

Scheme I.13. Counter-ion catalysis.

Phase transfer catalysis (PTC) is another example of counter-ion catalysis.[26] This involves the use of PTCs to facilitate the transfer of a molecule or ion from one reaction phase to another, where the reaction occurs. A Merck research group leaded by Grabowski conducted the first successful example of the use of cinchona alkaloid derivatives for chiral phase-transfer catalysis in 1984 (**Scheme I.14**).[41c] They could achieve the highly enantioselective methylation of phenylindanone derivative, which is an important intermediate in the synthesis of (+)-indacrinone (**I.14**), under organic-aqueous biphasic conditions in the presence of *N*-alkylated cinchonine **I.13**.

[44] a) Raheem, I.; Thiara, P. S.; Peterson, E. A.; Jacobsen, E. N. *J. Am. Chem. Soc.* **2007**, *129*, 13404-13405; b) Reisman, S. E.; Doyle, A. G.; Jacobsen, E. N. *J. Am. Chem. Soc.* **2008**, *130*, 7198-7199.

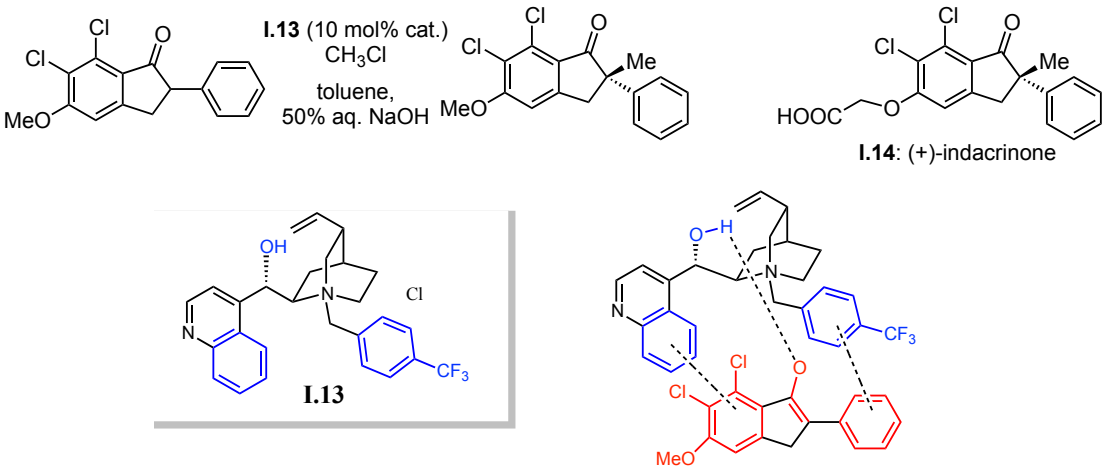

Scheme I.14. Alkylation of enolates via phase-transfer catalysis.

Five years later, O'Donnell employed successfully this type of catalyst for the asymmetric synthesis of α-amino acids, using *tert*-butyl glycinate benzophenone imine **I.15** as a key substrate (**scheme I.15**).[45] By simply switching the catalyst from the cinchonine **I.16a** to the cinchonidine-derivative **I.16b**, the opposite enantiomer (*S*)-**I.17** could be obtained with a similar degree of enantioselectivity.

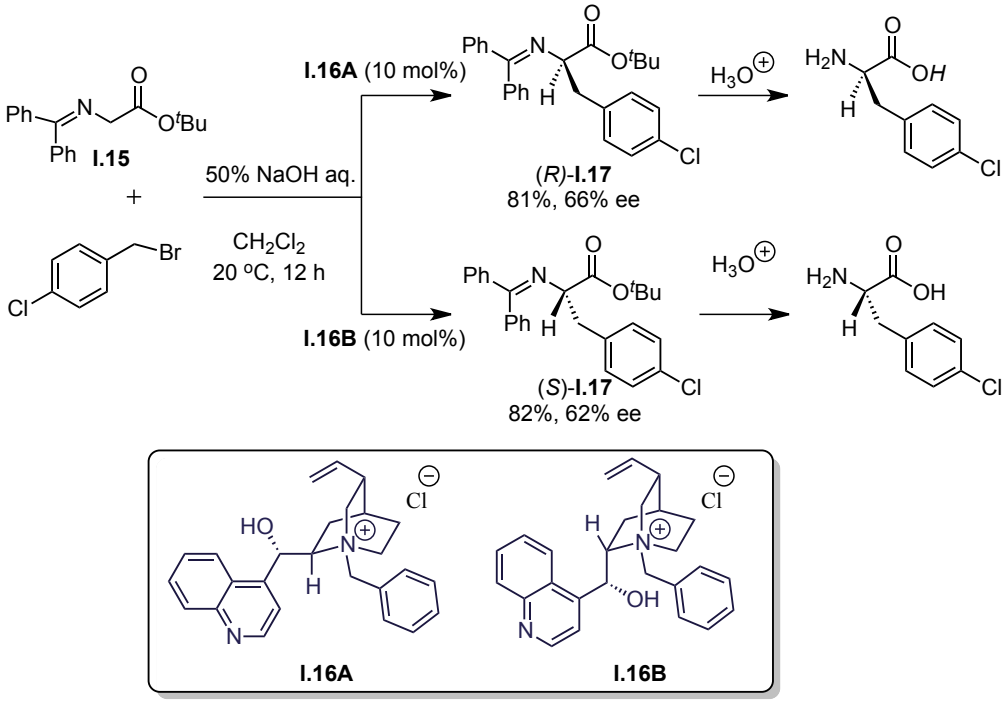

Scheme I.15. Early examples of phase transfer catalysis.

[45] a) O'Donnell, M. J.; Bennett, W. D.; Wu, S. *J. Am. Chem. Soc.* **1989**, *111*, 2353-2355; b) Lipkowitz, K. B.; Cavanaugh, M. W.; Baker, B.; O'Donnell, M. J. *J. Org. Chem.* **1991**, *56*, 5181-5196; c) Esikova, I. A.; Nahreini, T. S.; O'Donnell, M. J. *Phase-Transfer Reactions. ACS Symp. Ser.* (Ed.: Halperm, M. E.), Washington, DC, ***1997,*** *Vol. 659, Ch. 7,* 89-96.

Screening of the alternative *N*-protected groups in the catalyst design in order to optimize the conditions successfully provided a more practical and valuable protocol through the design of *N*-anthracenylmethylammonium salts (**Scheme 2.6**).[46] Their application in the asymmetric phase transfer alkylation of **I.15** provided chiral α-amino acids with much higher enantioselectivity.

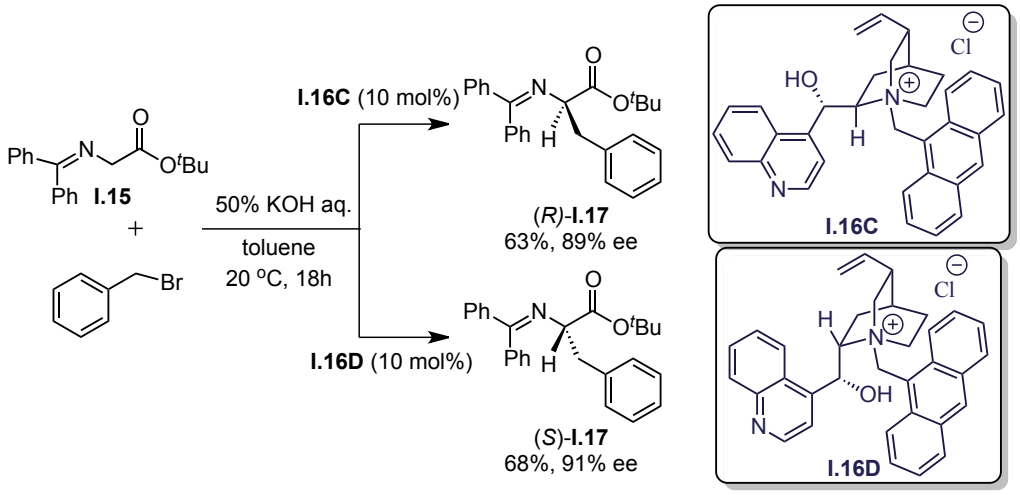

Scheme I.16. *N*-anthracenylmethylammonium salts in the phase transfer catalysis.

In fact, the development of chiral quaternary ammonium salts has increased significantly in asymmetric catalysis and found a myriad of applications since the pioneering example of Dolling *et al*.[47]

I.1.3. Polymeric supports for the immobilization of catalysts.

Asymmetric catalysis, especially in heterogeneous phase has become a key technology for the production of enantiomerically pure compounds in the industry, because of the demand and limited of natural resources. Homogeneous catalysts were established in the second half of the 20th century, proving their importance in many industrial applications.[48] The chemists involved in the pioneering breakthroughs were awarded the Nobel Prize in 2001.[5] William S. Knowles and Ryoji Noyori received the

[46] a) Lygo, B.; Wainwright, P. G. *Tetrahedron Lett.* **1997**, *38*, 8595-8598; b) Lygo, B.; Crosby, J.; Lowdon, T. R.; Wainwright, P. G. *Tetrahedron* **2001**, *57*, 2391-2402; c) Lygo, B.; Crosby, J.; Lowdon, T. R.; Peterson, J. A.; Wainwright, P. G. *Tetrahedron* **2001**, *57*, 2403-2409.
[47] For some examples, see: a) Wang, Y.-G.; Maruoka, K. *Org. Process Res. Dev.* **2007**, *11*, 628-632; b) Kitamura, M.; Arimura, Y.; Shirakawa, S.; Maruoka, K. *Tetrahedron Lett.* **2008**, *49*, 2026-2030; c) Kitamura, M.; Shirakawa, S.; Arimura, Y.; Wang, X.; Maruoka, K. *Chem. Asian J.* **2008**, *3*, 1702-1714; d) Moss, T. A.; Alonso, B.; Fenwick, D. R.; Dixon, D. J. *Angew. Chem. Int. Ed.* **2010**, *49*, 568-571; e) Matoba, K.; Kawai, H.; Furukawa, T.; Kusuda, A.; Tokunaga, E.; Nakamura, S.; Shiro, M.; Shibata, N. *Angew. Chem. Int. Ed.* **2010**, *49*, 5762-5766.
[48] Blaser, H. U.; Spindler, F.; Studer, M. *Appl. Catal. A: General* **2001**, *221*, 119-143.

prize for their work on chirally catalyzed hydrogenation reactions, and K. Barry Sharpless for his work on chirally catalyzed oxidation reactions.

Nevertheless, the efficiency of these processes can be improved even further through the employment of the corresponding heterogeneous catalysts that are derived from their homogeneous counterpart by immobilization.[49] The chemical industry is continuously looking for new processes which are environmentally friendly and allow to lower the cost and the time needed for commercialization. Consequently, heterogeneous catalysis has been receiving high attention in the last decades.

Catalyst modification can be defined as the modification of a homogeneous catalyst in to a heterogeneous one. In this manner, the catalyst can be separated from the reaction mixture and, ideally, be reused multiple times.[50] An important issue to take into account is the mechanism of the asymmetric reaction for rational design of recoverable organocatalysts. Most obvious loss of catalytic activity comes from catalyst decomposition, irreversible reaction with some of the components during the catalytic cycle or catalyst leaching.[51]

Furthermore, if the catalysts are robust enough and the kinetics are favorable, they can also be used under continuous flow operation. In case of expensive or not readily available enantiomerically pure catalysts, as well as for catalytic species employed in relatively large amounts, immobilized catalysts represent an environmentally friendly and cost effective solution. Overall, catalyst immobilization is a clearly convenient alternative. However, in order to use an immobilized chiral catalyst for a given chemical process, it is often necessary to make a critical evaluation in terms of its activity, productivity, enantioselectivity, stability, ease of recovery and reusability.

As a matter of principle, it is expected that the heterogenized catalyst will present less reactivity compared with its homogeneous counterpart. This is usually attributed to the increase in steric hindrance caused by the support, which makes the active sites less accessible, but it is not always the case.[42a,42c,52] If the immobilized

---

[49] For reviews, see: a) De Vos, D. E.; Vankelecom, I. F. J.; Jacobs, P. A. *Chiral catalyst immobilization and recycling* (Eds.: De Vos, D. E.; Vankelecom, I. F. J.; Jacobs, P. A.), Wiley-VCH, Weinheim, **2001**; b) Sheldon, R. A.; van Bekkum, H. *Fine Chemicals Through Heterogeneous Catalysis*, Wiley-VCH, Weinheim, **2001**; c) Heitbaum, M.; Glorius, F.; Escher, I. *Angew. Chem. Int. Ed.* **2006***, 45*, 4732-4762; d) Jimeno, C.; Sayalero, S.; Pericàs, M. A. In *Heterogenized Homogeneous Catalysts, for Fine Chemicals Production Catalysis by Metal Complexes*, (Eds.: P. Barbaro, F. Liguori), Springer, Heidelberg **2010**, Vol. 33, *Ch.4*, 123-170.

[50] Wang, Z.; Ding, K.; Uozumi, Y. *Handbook of Asymmetric Heterogeneous Catalysis* (Eds.: Ding, K.; Uozumi, Y.), Wiley-VCH, Verlag, Weinheim, **2008**, *Ch.1*, 1-24.

[51] Gladysz, J. A. *Recoverable and recyclable catalysts* (Ed.: Benaglia, M.), John Wiley & Sons Ltd., Chichester, UK, **2009**, *Ch. 1*, 1-14.

[52] For some reported examples where the immobilized catalyst has better performance than the non-supported one, see: a) Annunziata, R.; Benaglia, M.; Cinquini, M., Cozzi F.; Tocco, G. *Org. Lett.* **2000***, 2*,

organocatalyst has been designed to minimize the interaction between catalytic cycle and support, the catalytic process can take place in the same way as in the homogeneous environment.[49d]

Figure I.10 summarizes the most important approaches to immobilize or hererogenize soluble catalysts.[53] A differentiation is drawn between different types of catalyst precursor and support interactions: covalent binding, adsorption (van der Waals forces), electrostatic or ionic interactions, and entrapment.

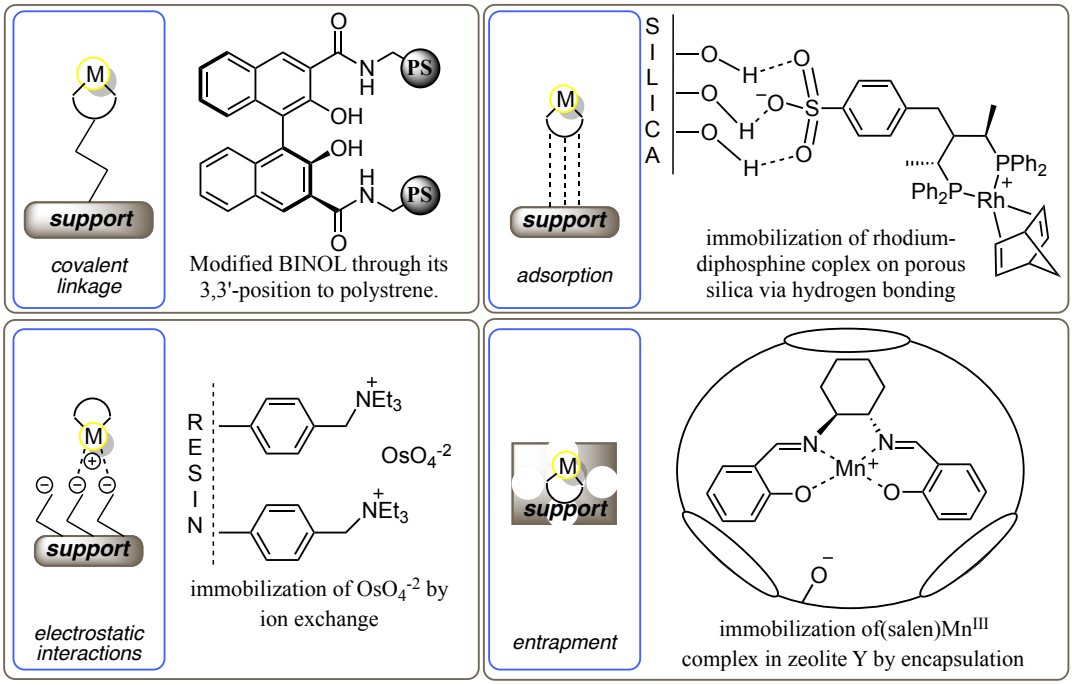

Figure I.10. Schematic representation (and example) of the strategies for immobilizing homogeneous chiral catalysts onto solid supports.

Covalent binding provides broad applicability due to the robustness of the resulting catalytic material in many reactions and work-up conditions. It can be immobilized via copolymerization with a monomer, or its covalent linkage to a suitable support, such as functionalized polymers, inorganic oxides, or nanotubes.

In some cases, the covalent binding method is relatively inconvenient for large-scale preparation, and immobilization via electrostatic or ionic interactions has been more practical from this point of view. This method involves ionic bonding between oppositely charged ions, also called immobilization by ion exchange. In addition, only

---

1737-1739; b) Selkälä, S. A.; Tois, J.; Pihko. P. M.; Koskinen, A. M. P. *Adv. Synth. Catal.* **2002**, *344*, 941-945.

[53] For some examples, see: a) Fan, Q.-H.; Wang, R.; Chan, A. S. C. *Bioorg. Med. Chem. Lett.* **2002**, *12*, 1867-1871; b) Bianchini, C.; Barbaro, P.; Dal Santo, V.; Gobette, R.; Meli, A.; Oberhauser, W.; Psaro, R.; Vizza, F. *Adv. Synth. Catal.* **2001**, *343*, 41-45; c) Choudary, B. M.; Karangula, J.; Madhi, S.; Kantam, M. L. *Adv. Synth. Catal.* **2003**, *345*, 1190-1192; d) Sabatier, M. J.; Corma, A.; Domenech, A.; Fornés, V.; García, H. *Chem. Commun.* **1997**, 1285-1286.

in this case the direct immobilization of the metal itself is possible,[49c] which can be important in the case of expensive or very toxic metal derivatives such as osmium tetroxide.[53c,54]

Immobilization of catalysts through adsorption is simple, but the weak nature of these interactions (such as van der Waals interactions) makes the resulting catalysts less robust (prone to leaching) and with a limited applicability. However, this method is very common for enzyme immobilization onto mesoporous materials (OMMs).[55] In addition, this method can be improved by modification of the catalyst via hydrogen-bonding interactions, therefore minimizing the leaching during use.

Heterogenization via entrapment or "ship in a bottle" can be done via two different preparation strategies. The first one is based on building up catalysts in well-defined cages of porous supports; the other approach consists in building up an inorganic sol gel or organic polymeric network around a preformed catalyst.[56] However, entrapment is limited basically due to issues with substrates and product diffusion.

In this thesis we will focus on covalent immobilization of chiral homogeneous catalysts, which is the most common strategy.

In the case of covalent immobilization many additional parameters such as type of support, solvent, spacer length and flexibility, or degree of surface coverage have to be optimized to obtain an acceptable catalytic performance.[57] A schematic representation of a supported catalytic species appears in **Figure I.11**.

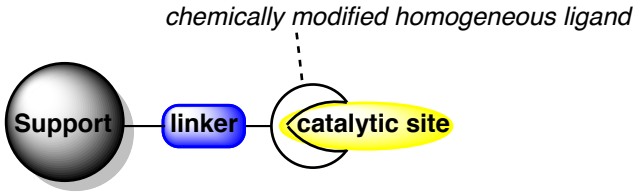

Figure I.11. Schematic representation of a supported catalytic species.

The choice of a suitable support plays a crucial role because its properties can have an influence in the catalyst behavior. The most used supports are inorganic oxides as silica or zeolites, different classes of nanostructured materials such as

[54] For some example, see: a) Choudary, B. M.; Chowdari, N. S.; Kantam, M. L.; Raghavan, K. V. *J. Am. Chem. Soc.* **2001**, *123*, 9220-9221; b) Choudary, B. M.; Chowdari, N. S.; Jyothi, K.; Kantam, M. L. *J. Am. Chem. Soc.* **2002**, *124*, 5341-5349.
[55] Hartmann, M.; Kostrov, X. *Chem. Soc. Rev.* **2013**, *42*, 6277-6289.
[56] a) De Vos, D. E.; Thibault-Starzyk, F.; Knops-Gerrits, P. P.; Parton, R. F.; Jacobs, P. A. *Macromol. Symp.* **1994**, *80*, 157-184; b) Blum, J.; Avnir, D.; Schumann, H. *Chemtech.* **1999**, *29*, 32-38;
[57] Hodge, P. *Chem. Soc. Rev.* **1997**, *26*, 417-424.

nanotubes or nanoparticles and organic polymers.[58] Considering the nature of the reaction mixture (homogeneous or heterogeneous) there are two main types of polymeric supports:

- Soluble supports, such as non-cross linked polystyrene resins or polyethylene glycol (PEG)-type polymers like $MeOPEG_{5000}$.
- Insoluble supports, such as cross-linked polystyrene resins, some polynorbornenes and polyacrylates.

The linker or spacer also plays an important role solving problems of reactivity because it can create a microenvironment around the active site of the catalyst more beneficial to reactivity than the one provided only by the support.[59] They are used to render more accessible catalytic sites and to modify the properties of the polymeric matrix (e.g. swelling characteristics). In most cases, higher swellability of the resin in some solvents can increase the performance of reaction to make it as fast as in homogeneous media.

In the present thesis, the catalytic species to be immobilized will be pyrrolidine derivatives ultimately ansing from L-proline derivatives, mainly because of our interest in aldol type, Michael and related reactions.

I.1.4. Click chemistry for covalent immobilization of catalytic units.

Click chemistry can be defined as “modular synthetic approach towards the assembly of new molecular entities”.[60] By applying this concept, construction of carbon-heteroatom bonds can be generated from relatively simple building blocks, providing remarkable modularity and diversity. The term “click chemistry” was introduced by Sharpless *et al*.[61a] Further development of this concept opened the door for preparation

---

[58] a) Lu, J.; Toy, P. H. *Chem. Rev.* **2009**, *109*, 815-838; b) Altava, B.; Burguete, I.; Luis, S. V. in *The power of functional resins in organic synthesis* (Eds. Tulla-Puche, J.; Albericio, F.), Wiley, Weinheim, 2008, *10*, 245-308.

[59] For the first publication demonstrating the importance of the spacer in polymer supported catalysis, see: Anelli, P. L.; Czech, B.; Montarani, F.; Quici, S. *J. Am. Chem. Soc.* **1984**, *106*, 861-869.

[60] a) Angell, Y. L.; Burgess, K. *Chem. Soc. Rev.* **2007**, *36*, 1674-1689; b) Moses, J. E.; Moorhouse, A. D. *Chem. Soc. Rev.* **2007**, *36*, 1249-1262; c) Kappe, C. O.; Van der Eycken, E. *Chem. Soc. Rev.* **2010**, *39*, 1280-1290; d) Lallana, E.; Riguera, R.; Fernandez-Megia, E. *Angew. Chem. Int. Ed.* **2011**, *50*, 8794-8804; e) Lau, Y. H.; Rutledge, P. J.; Watkinson, M.; Todd, M. H. *Chem. Soc. Rev.* **2011**, *40*, 2848-2866; f) Muller, T.; Bräse, S. *Angew. Chem. Int. Ed.* **2011**, *50*, 11844-11845; g) Sletten, E. M.; Bertozzi, C. R. *Acc. Chem. Res.* **2011**, 44, 666-676; h) Thirumurugan, P.; Matosiuk, D.; Jozwiak, K. *Chem. Rev.* **2013**, *113*, 4905-4979.

[61] a) Kolb, H. C; Finn, M. G.; Sharpless, K. B. *Angew. Chem. Int. Ed.* **2001**, *40*, 2004-2021; b) Rostovtsev, V. V.; Green, L. G.; Fokin, V. V.; Sharpless, K. B. *Angew. Chem. Int. Ed.* **2002**, *41*, 2596-2599.

of new types of triazoles with application in different topics, such as material science, drug discovery or biological studies (bioconjugation, proteins, nucleotides).[60,61]

The most popular click reaction is the Copper(I)-catalyzed azide-alkyne Huisgen cycloaddition[62] (CuAAC) that gives regioselectively only 1,4-disubstituted-1,2,3-triazoles.[63] CuAAC reaction works at room temperature, but it can also be accelerated by microwave heating.[64] In the absence of metal catalysts, the reaction can take place also by thermal activation, but this mostly results in a mixture of 1,4 and 1,5 regioisomers. The purely thermal transformation has a more limited scope and needs relatively high reaction temperatures. When it is catalyzed by Ru(II) (RuAAC) it proceeds with both terminal and internal alkynes and gives 1,5-disubstituted and fully 1,4,5-trisubstituted-1,2,3-triazoles (**Scheme I.17**).[65] In general, copper or ruthenium catalysts dramatically change the mechanism and the outcome of the reaction.

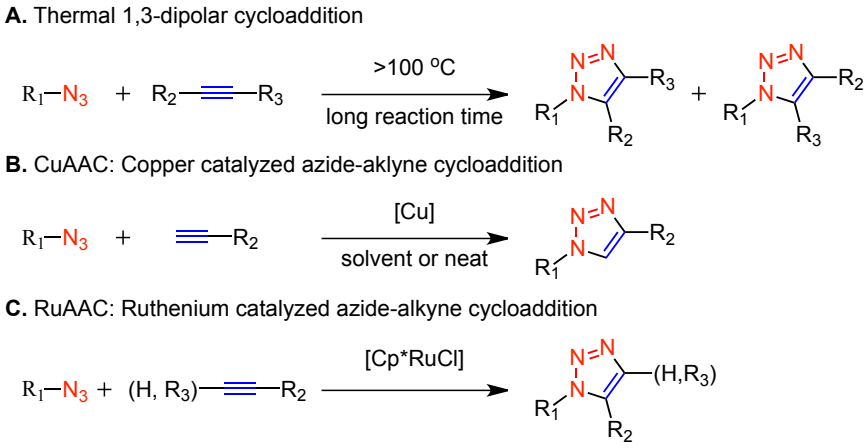

Scheme I.17. 1,3-dipolar cycloadditions to form different substituted triazole rings.

A mechanism for the copper-catalyzed reaction was proposed by Sharpless and Fokin in 2002.[61a] According to their model, the key C-N bond-forming event takes place between the nucleophilic vinylidene-like β-carbon of the copper(I) acetylide and the electrophilic terminal nitrogen of the coordinated organic azide (**Scheme I.18**). Complexation forms the metallacycle, which is then transformed to the triazole-copper derivative. Finally, the triazole is released from Cu upon protonation of the terminal carbon, and the catalyst is recovered.

---

[62] a) Huisgen, R. "Centenary Lecture - 1,3-Dipolar Cycloadditions", *Proc. Chem. Soc. London* **1961**, 357-369; b) Huisgen, R. *Angew. Chem.* **1963**, *75*, 604-637; c) Huisgen, R.; Szeimies, G, Möbius, L. *Chem. Ber.* **1967**, *100*, 2494-2507; d) Huisgen, R. *1,3-Dipolar Cycloaddition Chemistry* (Ed.: A. Padwa), John Wiley & Sons Inc., New York, **1984**, *Vol. 1*, 3-27.
[63] a) Meldal, M.; Tornøe, C. W. *Chem. Rev.* **2008**, *108*, 2952-3015; b) Fokin, V. V.; Hein, J. E. *Chem. Soc. Rev.* **2010**, *39*, 1302-1315.
[64] Appukkuttan, P.; Dehaen, W.; Fokin, V. V.; Van der Eycken, E. *Org. Lett.* **2004**, *6*, 4223-4225.
[65] a) Zhang, L.; Chen, X.; Xue, P.; Sun. H. H. Y.; Williams, I. D.; Sharpless, K. B.; Fokin, V. V.; Jia, G. *J. Am. Chem. Soc.* **2005**, *107*, 15998-15999; b) Rasmussen L. K.; Boren, B. C.; Fokin, V. V. *Org. Lett.* **2007**, *9*, 5337-5339.

Chapter I

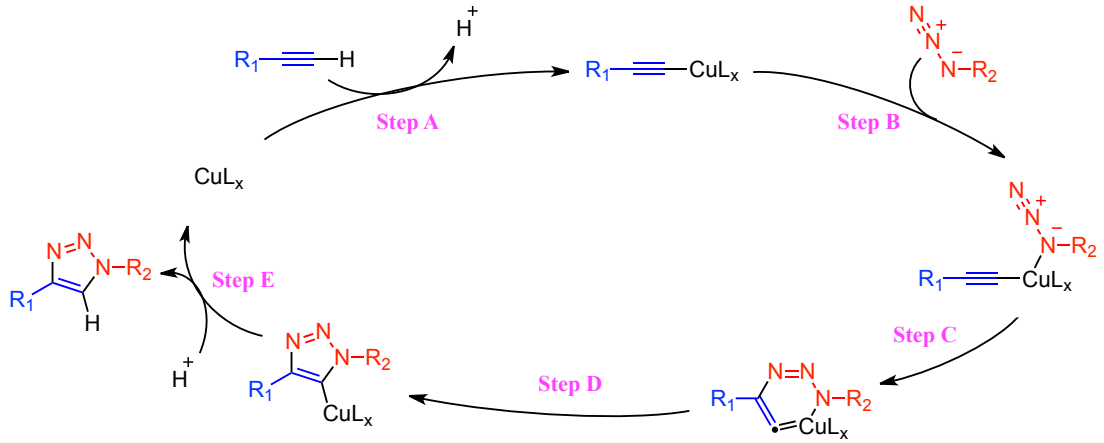

Scheme I.18. Mechanism of 1,3-dipolar cycloaddition CuAAC.

However, this mechanism is not fully accepted, and several studies toward of the clarification of the mechanism of the CuAAC with terminal alkynes have been reported.[66] The explanation of the activation of the azide and alkyne by different metal centers was suggested, involving compound **I.18**. This proposal was based on some experimental evidence of the possible involvement of polynuclear copper(I) intermediates,[67] also supported by theoretical studies.[68] Regarding the identification of nuclearity of the species involved in catalysis, this fact has not been established yet (**Scheme I.19**).

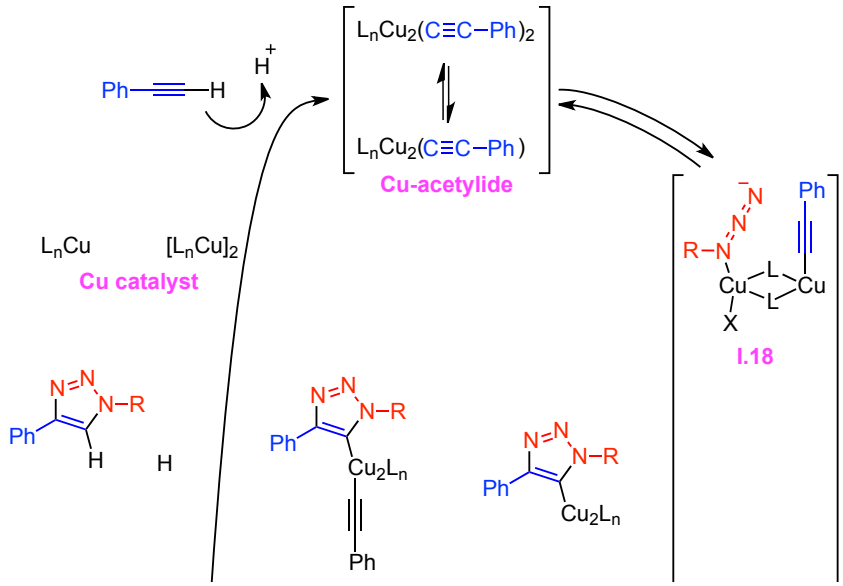

[66] a) Rodionov, V. O.; Fokin, V.V.; Finn, M. G. *Angew. Chem., Int. Ed.* **2005**, *44*, 2210-2215; b) Himo, F.; Lovell, T.; Hilgraf, R.; Rostovtsev, V.V.; Noodleman, L.; Sharpless, K. B.; Fokin, V. V. *J. Am. Chem. Soc.* **2005**, *127*, 210-216; c) Worrell, B. T.; Malik, J. A.; Fokin, V. V. *Science* **2013**, *340*, 457-460.
[67] a) Rodionov, V. O.; Presolski, S. I.; Díaz, D. D.; Fokin, V. V.; Finn, M. G. *J. Am. Chem. Soc.* **2007**, *129*, 12705-12712; b) Kuang, G.-C, Guha, P. M.; Brotherton, W. S.; Simmons, J. T.; Stankee, L. A.; Nguyen, B. T.; Clark. R. J.; Zhu, L. *J. Am. Chem. Soc.* **2011**, *133*, 13984-14001.
[68] a) Staub, B. F. *Chem. Commun.* **2007**, 3868-3870; b) Ahlquist, M.; Fokin, V. V. *Organometallics* **2007**, *26*, 4389-4391.

Scheme I.19. Catalytic cycle based on kinetic studies.

In 2013 "copper isotope labeling" mass studies provided more details regarding the mechanism and this research confirmed that in the cycloaddition step a binuclear copper species is responsible for carbon-nitrogen bond formation (**Scheme I.20**).[66c] The proposed dinuclear copper intermediate should be formed via triazolide ring (highlighted in **Scheme I.20**) according to the isotopic experiments.

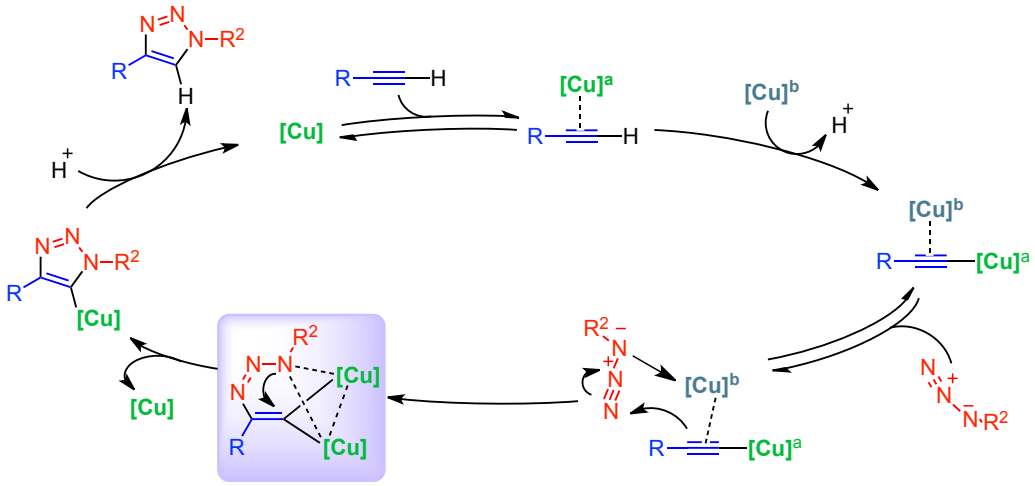

Scheme I.20. Proposed binuclear copper intermediate in the catalytic cycle by isotope labeling.

Recent studies carried out by several groups have confirmed that a dinuclear complex is involved in the kinetically favored pathway;[69] however the mono- and bis-copper pathways are active in the CuAAC reaction.[69b] Despite several evidences that the mononuclear pathway is incompatible with some experimental results, mononuclear copper acetylide intermediates were still considered in a recent theoretical study.[70]

The use of CuAAC is a very convenient strategy for catalyst immobilization because of its operational ease, mild reaction conditions and easy monitoring of the reaction by IR.

In our research group this methodology has been successfully applied to the preparation of different polystyrene (PS)-supported organocatalysts. The molecular structures of some of them are shown in **Figure I.12.**[71]

---

[69] a) Makarem, A.; Berg, R.; Rominger, F.; Straub, B. F. *Angew. Chem. Int. Ed.* **2015**, *54*, 7431-7435; b) Jin, L.; Tolentino, D. R.; Melaimi, M.; Bertrand, G. *Sci. Adv.* **2015**, *5*, 1-5.

[70] Díaz Velázquez, H.; García, Y. R.; Vandichel, M.; Madder, A.; Verpoort, F. *Org. Biomol. Chem.* **2014**, *12*, 9350-9356.

[71] For catalyst **I.19**, see: a) Font, D.; Jimeno, C.; Pericàs, M. A. *Org. Lett.* **2006**, *8*, 4653-4655; b) Font, D.; Bastero, A.; Sayalero, S.; Jimeno C.; Pericàs, M. A. *Org. Lett.* **2007**, *9*, 1943-1946; c) Alza, E.; Rodríguez-Escrich, C.; Sayalero, S.; Bastero, A; Pericàs, M. A. *Chem.-Eur. J.* **2009**, *15*, 10167-10172; d) Cambeiro,

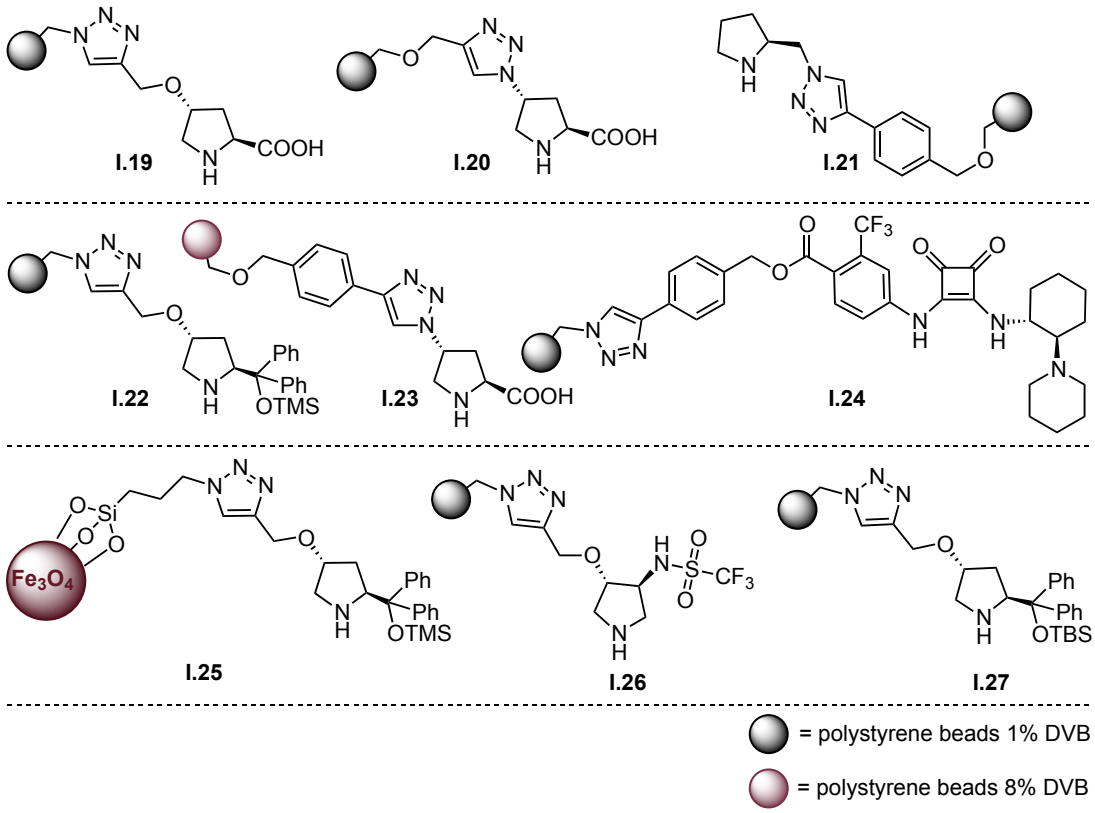

Figure I.12. Some polystyrene-supported organocatalysts reported by our group.

One of the most interesting features of these immobilized catalysts is the possibility of implementing them in continuous flow operations.

I.1.5. Organocatalysis in the Pharmaceutical and Chemical Industry.

Many metabolic processes involve chiral reactants and enzymes; therefore, chirality as a natural phenomenon, can be considered a crucial factor.[72] However, due to the lack of methods for the selective generation of stereocenters, the importance of this biological phenomenon was not taken into account. As a consequence, during the

---

X. C.; Martín-Rapún, R.; Miranda, P. O.; Sayalero, S.; Alza, E.; Llanes, P.; Pericàs, M. A. *Beilstein J. Org. Chem.* **2011**, *7*, 1486-1493; For catalyst **I.20**, see: e) Alza, E.; Cambeiro, X. C.; Jimeno, C.; Pericàs, M.A. *Org. Lett.* **2007**, *9*, 3717-3720; For catalyst **I.21**, see: f) Font, D.; Sayalero, S.; Bastero, A.; Jimeno, C.; Pericàs, M. A. *Org. Lett.* **2008**, *10*, 337-340; For catalyst **I.22**, see: g) Alza, E.; Pericàs, M. A. *Adv. Synth. Catal.* **2009**, *351*, 3051-3056; h) Alza, E.; Sayalero, S.; Cambeiro, X. C.; Martín-Rapún, R.; Miranda, P. O.; Pericàs, M. A. *Synlett* **2011**, *4*, 464-468 i) Alza, E.; Sayalero, S.; Kasaplar, P.; Almasi, D.; Pericàs, M. A. *Chem. Eur. J.* **2011**, *17*, 11585-11595; For catalyst **I.23**, see: j) Ayats, C.; Henseler, A. H.; Pericàs, M. A. *ChemSusChem* **2012**, *5*, 320-325; For catalyst **I.24**, see: k) Kasaplar, P.; Riente, P.; Hartmann, C; Pericàs, M. A. *Adv. Synth. Cat.* **2012**, *354*, 2905-2910; l) Kasaplar, P.; Rodríguez-Escrich, C.; Pericàs, M. A. *Org. Lett.* **2013**, *15*, 3498-3501; For catalyst **I.25**, see: m) Riente, P.; Mendoza, C.; Pericàs, M. A. *J. Mat. Chem.* **2011**, *21*, 7350-7355; For catalyst **I.26**, see: n) Martín-Rapún, R.; Sayalero, S.; Pericàs, M. A. *Green Chem.* **2013**, *15*, 3295-3301; For catalyst **I.27**, see: o) Fan, X.; Sayalero, S.; Pericàs, M. A. *Adv. Synth. Catal.* **2012**, *354*, 2971-2976.

[72] Riehl, J. P. Mirror-image asymmetry: an introduction to the origin and consequence of chirality, Wiley & Sons Inc.: Hoboken, **2010**.

early years of pharmaceutical development, drugs were produced and tested only in racemic form (**Figure I.13**).

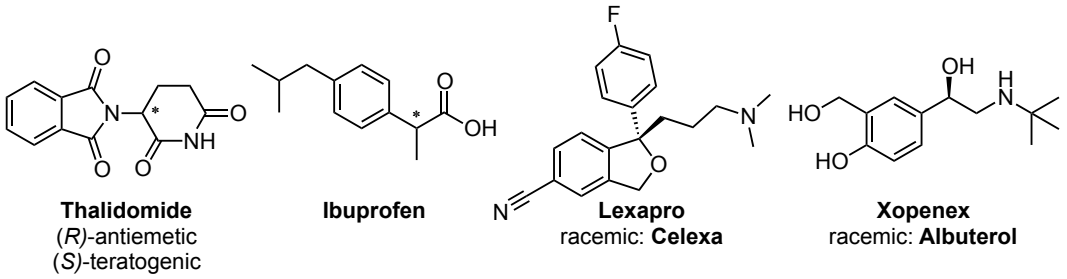

Figure I.13. Pharmaceuticals marketed as racemic mixtures.

One of the well-known examples is Thalidomide,[72,73] used to treat morning sickness, which appeared in the market in the early 1960's, and caused well over 10.000 cases of birth defects. Later, it was discovered that only the (*S*)-enantiomer of the drug is mutagenic. However, even with pure (*R*)-enantiomer the problem would persist, as Thalidomide racemizes *in vivo*. This example shows the importance of chirality in drug development, and it has been considered by testing the new drugs for toxicological and pharmacokinetic studies. In the case of Ibuprofen, it has been shown that the (*S*)-enantiomer produces the pain relief effect, whereas (*R*) is inactive. In addition, it also racemizes in the body, for this reason it can be sold in the racemic form.[72,74] These and other examples have shown that all pharmaceuticals have some degree of undesirable side effects, which can arise from one of the enantiomers in the case of racemates. Therefore, new methods for inducing asymmetric transformations have been studied in the last decades.[3a, 75]

Traditionally, industrial applications of enantioselective catalysis have been dominated by metal-catalyzed and bio-catalytic procedures.[76] It is also widely recognized that during the industrial large-scale production of chemicals the removal of impurities related to toxic catalysts from the waste steam can often have a huge financial impact. The advent of organocatalysts brought the prospect of non-toxic and environmentally friendly molecules, with the potential for saving cost, time and energy, while simplifying the experimental procedures, and reducing chemical waste. In principle, the economics of organocatalyzed reactions could be improved by recovery

[73] Brynner, R.; Stephens, T. *Dark remedy: the impact of Thalidomide and its revival as a vital medicine*, Perseus Publishing, Cambridge MA, **2001**.
[74] a) Hutt, A. J.; Caldwell, J. *Clin. Pharmacokin.* **1984**, *9*, 317-373; b) Caldwell, J.; Hutt, A. J.; Fasnel-Gigleux, Y. *Biochem. Pharmacol.* **1988**, *37*, 105-114.
[75] a) *Industrial Applications of Asymmetric Synthesis in Comprehensive Chirality* (Eds.: Carreira, E. M.; Yamamoto, H.), Elsevier, **2012**, Vol. 9, 1-506; b) Ricci, A. *ISRN Org. Chem.* **2014**, *2014*, 1-29.
[76] *Asymmetric Catalysis on Industrial Scale: Challenges, Approaches and Solutions* (Ed. Blaser, H.-U.; Federsel, H.-J.), Wiley-VCH: Weinheim, **2010**.

and reuse of the catalyst. This has made the field of organocatalysis very interesting from the industrial point of view.

To develop a robust, scalable catalytic asymmetric process generally takes time and resources, precious commodities for any company. Despite the risk of failure, catalytic synthesis is being increasingly embraced by industry. It is quite significant that Hajos, Parrish and Eder *et al.*, both teams from pharmaceutical companies (Hoffmann-la-Roche and Schering), described the first efficient organocatalyzed asymmetric process and implemented this reaction to manufacture steroids on multi-kilogram scales in the early 1970s (**Scheme I.4**).[12,13] Further large-scale industrial application of enamine catalysis has not been reported.

One of the most employed organocatalytic procedures at industrial scale is phase transfer catalysis.[77] As already mentioned, in 1984 Dolling *et al.* at Merck reported that indanone could be methylated in 95% yield and 92% ee (**Scheme I.14**). This process was developed with the objective of synthesizing (+)-indacrinone, at a time when industrial synthesis was dominated by the use of stoichiometric chiral auxiliaries.

The Merck synthesis was the first example of an efficient enantioselective PTC alkylation on large scale, and also one of the first practical methods for catalytic enantioselective synthesis in general.[41c] The enantioselective variant was found to be significantly more cost-effective, than the previous route to this target, involving a racemic alkylation followed by low-yielding classical resolution.[78]

A few decades later, a Merck research group employed the asymmetric PTC alkylation of substituted indanone derivatives for preparing kilogram quantities of a substrate-selective estrogen receptor β-selective agonist, using the same technique (**Scheme I.21**).[79]

---

[77] Halpern, M. E. *Process Chemistry in the Pharmaceutical Industry* (Ed.: Gadamasetti, K.), **1999**, Taylor & Francis, New York, 283-289.
[78] DeSolms, S. J.; Woltersdorf, O. W.; Cragoe, E. J.; Watson, L. S.; Fanelli, G. M. *J. Med. Chem.* **1978***, 21*, 437-443.
[79] Scott, J. P.; Ashwood, M. S.; Brands, K. M. J.; Brewer, S. E.; Cowden, C. J.; Dolling, U.-H.; Emerson, K. E.; Gibb, A. D.; Goodyear, A.; Oliver, S. F.; Stewart, G. W.; Wallace, D. J. *Org. Process Res. Dev.* **2008***, 12*, 723-730.

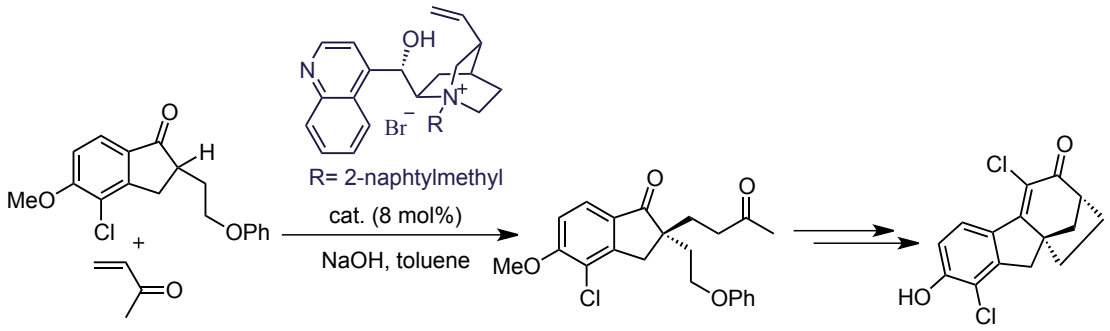

Scheme I.21. Synthesis of an estrogen receptor β-selective agonist.

Another example utilized with commercial purposes at Rhodia ChiRex company is an asymmetric organocatalytic Strecker reaction for the synthesis of optically active α-amino acids. The Jacobsen group developed excellent organocatalysts, namely urea or thiourea derivatives, for this transformation (**Scheme I.9**).[42] In addition, it was discovered that the immobilized urea derivative can be recycled and re-used very efficiently in an industrial manner (**Scheme I.22**).[42d]

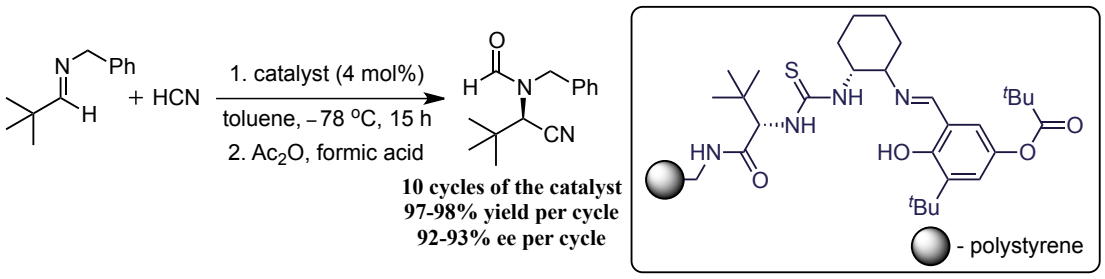

Scheme I.22. *Rhodia ChiRex concept.*

The first large-scale application of asymmetric iminium ion catalysis has been reported by Xu *et al.* at Merck as a key step in an improved process for the synthesis of Telcagepant.[80] The previous route provided intermediate caprolactam **I.30** in 12% overall yield, involving diastereoselective hydrogenation of **I.28•HX**, followed by correction of the C-3 configuration via epimerization (**Scheme I.23**).

[80] Xu, F.; Zacuto, M.; Yoshikawa, N.; Desmond, R.; Hoerrner, S.; Itoh, T.; Journet, M.; Humphrey, R.; Cowden, C.; Strotman, N; Devine, P. *J. Org. Chem.* **2010**, *75*, 7829-7841.

Chapter I

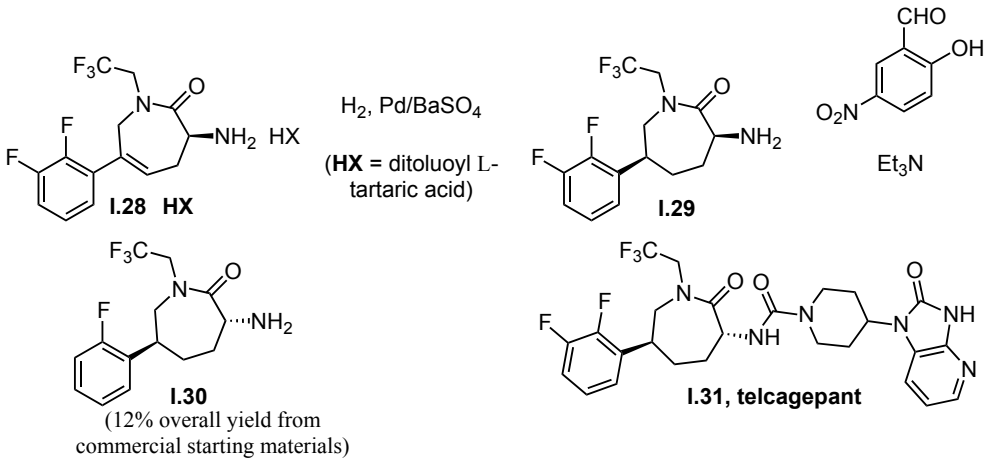

Scheme I.23. First-generation route to Telcagepant **31**.

Therefore, a more practical approach was desired for the synthesis of Telcagepant, and the Merck research group employed an organocatalyzed asymmetric 1,4-addition of nitromethane to an α,β-unsaturated aldehyde. Whit this route, the desired caprolactam **I.30•HCl** was obtained in 35% overall yield (**Scheme I.24**).[80] Thus, the organocatalytic asymmetric synthesis of this molecule has been developed, resulting in substantial low cost and environmental benefits over the previous production of Telcagepant **I.31**.

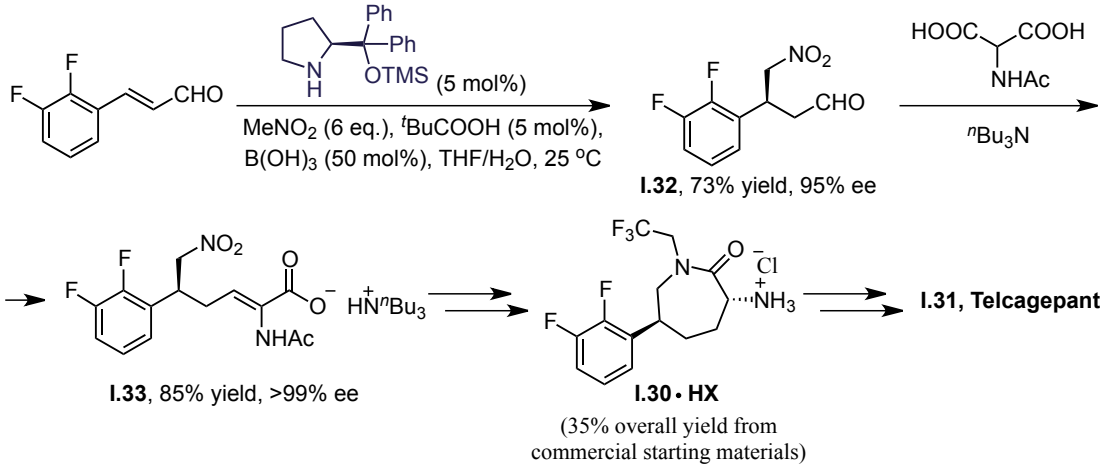

Scheme I.24. Organocatalysis-based second-generation route to Telcagepant **I.31**.

Several other examples in the field of organocatalysis, which will not be described in more detail in this contribution, have been reported as well.[81]

---

[81] The focus is primarily on reactions on "large-scale" see some examples: a) Keen. S. P.; Cowden, C. J.; Bishop, B. C.; Brands, K. M. J.; Davies, A. J.; Dolling, Ulf.-H.; Lieberman, D. R.; Stewart, G. W. *J. Org. Chem.* **2005**, *70*, 1771-1779; b) Yue, T.-Y.; McLeod, D. D.; Albertson, K. B.; Beck, S. R.; Deerberg, J.; Fortunak, J. M.; Nugent, W. A.; Radesca. L. A.; Tang, L.; Xiang, C. D. *Org. Process Res. Dev.* **2006**, *10*, 262-271; c) Ager, D. J.; Anderson, K.; Oblinger, E.; Shi, Y.; VanderRoest, J. *Org. Process Res. Dev.* **2007**, *11*, 44-51; d) Ishii, Y.; Fujimoto, R.; Mikami, M.; Murakami, S.; Miki, Y.; Furukawa, Y. *Org. Process Res. Dev.* **2007**, *11*, 609-615.

The examples highlighted here demonstrate that organocatalysis can become a powerful tool for solutions on industrial scale also. Albeit the number of publications from pharmaceutical companies using large-scale application of enantioselective organocatalysis is still limited, further development is expected to fully unlock the potential of this field in industrial environments.

It is clear that organocatalysis will become much more widely used on scale in the years to come.[82] Organocatalysts are often cheaper than metal-based catalysts, so they can be used in larger quantities for the same price. However, several drawbacks such as the relatively high catalyst loading, the long reaction time and also the difficult recyclability of the organocatalysts still remain. The possibility of recycling a catalyst has an important impact on catalyst costs, so various approaches for immobilization can be considered. Significant advances have been reported in recent times using polymer-supported organocatalysts[83] that can be easily recovered by filtration after the reaction has taken place. New applications, such as continuous flow, can be considered in the future for the improvement of large-scale transformations.

I.1.6. Continuous flow chemistry.

Flow chemistry involves the continuous introduction of a steam of chemical reactants into a flow or microreactor to yield a desired reaction product on a continuous basis.

In 2001, Paul Watts suggested using microreactors in order to synthesize organic molecules.[84a] Since then, a huge growth in the use of flow chemistry has been observed by creating new well-established procedures for performing chemical transformations.[84,85] Indeed, compared to the batch reactors traditionally applied in

---

[82] a) H. Gröger in *Organocatalysis* (Eds.: Reetz, M. T.; List, B.; Jaroch, S.; Weinmann, H.), Springer, Verlag, Berlin, **2008**, *Vol. 2*, 141-158; b) Busacca, C. A.; Fandrick, D. R.; Song, J. J.; Senanayake, C. H. *Adv. Synth. Catal.* **2011**, *353*, 1825-1864.

[83] For review on solid-supported enantioselective organocatalysts, see: a) Cozzi, F. *Adv. Synth. Catal.* **2006**, *348*, 1367-1390; c) Benaglia, M. *New J. Chem.* **2006**, *30*, 1525-1533; d) Gruttadauria, M.; Giacalone, F.; Noto, R. *Chem. Soc. Rev.* **2008**, *37*, 1666-1688; e) Kristensen, T. E.; Hansen, T. *Eur. J. Org. Chem.* **2010**, 3179-3204; f) Gruttadauria, M.; Giacalone, F.; Noto, R. *Polymeric Chiral Catalyst Design and Chiral Polymer Synthesis* (Ed.: Itsuno, S.), John Wiley & Sons Inc., Hoboken, NJ, USA, **2011**, *Ch. 3*, 63-89.

[84] a) Haswell, S. J.; Middleton, R. J.; O'Sullivan, B.; Skelton, V.; Watts, P. *Chem. Commun.* **2001**, 391-398; b) Watts, P.; Wiles, C. *Org. Biochem. Chem.* **2007**, *5*, 727-732; c) Wiles, C.; Watts, P. *Eur. J. Org. Chem.* **2008**, *10*, 1655-1671; d) Wiles, C.; Watts, P. *Green. Chem.* **2012**, *14*, 38-54.

[85] For relevant reviews on continuous flow process, see: a) Kirschning, K.; Solodenko, W.; Mennecke, K. *Chem. Eur. J.* **2006**, *12*, 5972-5990; b) Mason, B. P.; Price, K. E.; Steinbacher, J. L.; Bogdan, A. R.; McQuade, D. T. *Chem. Rev.* **2007**, *107*, 2300-2318; c) Kirschning, A. *Beilstein J. Org. Chem.* **2009**, *5*, 15; d) Luis, S. V.; García-Verdugo, E. *Chemical Reactions and Processes Under Flow Conditions,* RSC, Cambridge, **2010**; e) Wegner, J.; Ceylan, S.; Kirschning, A. *Chem. Commun.* **2011**, *47*, 4583-4592.

laboratory and industrial scale, this approach has many advantages, especially in terms of productivity, heat and mixing efficiency, safety, and reproducibility.[84,86]

In batch conditions mass and heat transport must be carefully controlled, and small changes in vessel geometry or stirring conditions can influence mixing efficiency. In addition, poor heat transfer can be observed. Rapid and homogeneous mixing can be achieved by continuous flow microreactors, where the desired temperature can be reached fast thanks to their high surface-to-volume rations. Another advantage is the increase in safety, offered by the small volumes of the microreactors. Thus, reactions of highly reactive species (for example, high-energy nitration reaction, or diazo ring expansions) can be performed safely in this manner.[87] In addition, by using immobilized reagents or catalysts, continuous flow processes can be further improved by techniques with parallelizing fixed bed reactors.[88]

Due to its numerous benefits, continuous flow chemistry has also been studied in our research group, in both metal catalysis and organocatalytic applications. In the present chapter, particular attention will be devoted to combining flow processes with solid-supported chiral organocatalysts to render them stereoselective.

Several advantages can be considered in the case of immobilized organocatalysts. The anchoring of a chiral organic catalyst onto a solid support provides separation of the products from the catalytic species and allows to extend the life cycle of the catalyst. In addition, the use of metal-free processes avoids the contamination of final products due to metal leaching; thus, use of immobilized organocatalysts for continuous flow chemistry is desirable.

Cinchona alkaloid derivatives were the first relevant example to demonstrate the great potential of chiral immobilized catalysts in continuous flow applications. Lectka *et al.* described a multistep continuous synthesis of enantiopure β-lactams by using a series of reaction columns, containing immobilized reagents and the organocatalyst, a quinine derivative, anchored to a Wang resin through an appropriate spacer (**Scheme I.25**).[89] An acid chloride was converted to the corresponding ketene with a polymer-supported phosphazene base (BEMP). The addition of this ketene to a sulfonylimine, catalyzed by a polymer supported cinchona alkaloid derivative, provided

---

[86] a) Ley, S. V.; Baxendale, I. R. *Nature Rev. Drug Discov*. **2002**, *1*, 573–586; b) Geyer, K.; Codeé, J. D. C.; Seeberger, P. H. *Chem. Eur. J.* **2006**, *12*, 8434-8442; c) Hartman, R. L.; McMullen, J. P.; Jensen, K. F. *Angew. Chem. Int. Ed.* **2011**, *50*, 7502-7519.
[87] Zhang, X.; Stefanick, S.; Villani, F. J. *Org. Proc. Res. Dev.*. **2004**, *8*, 455–460.
[88] For reviews on supported organocatalysts in enantioselective flow processes, see: a) Kristensen, T.E.; Hansen, T. *Eur. J. Org. Chem.* **2010**, *17*, 3179-3204; b) Puglisi, A.; Benaglia, M.; Chiroli, V. *Green Chem.* **2013**, *15*, 1790-1813; c) Rodríguez-Escrich, C.; Pericàs, M.A. *Eur. J. Org. Chem.* **2015**, 1173-1188.
[89] Hafez, A. M.; Taggi, A. E.; Dudding, T.; Lectka, T. *J. Am. Chem. Soc*. **2001**, *123*, 10853-10859.

the corresponding β-lactam. Subsequently, the product was purified using a supported scavenger in order to capture the unreacted ketene and imine within the same setup.

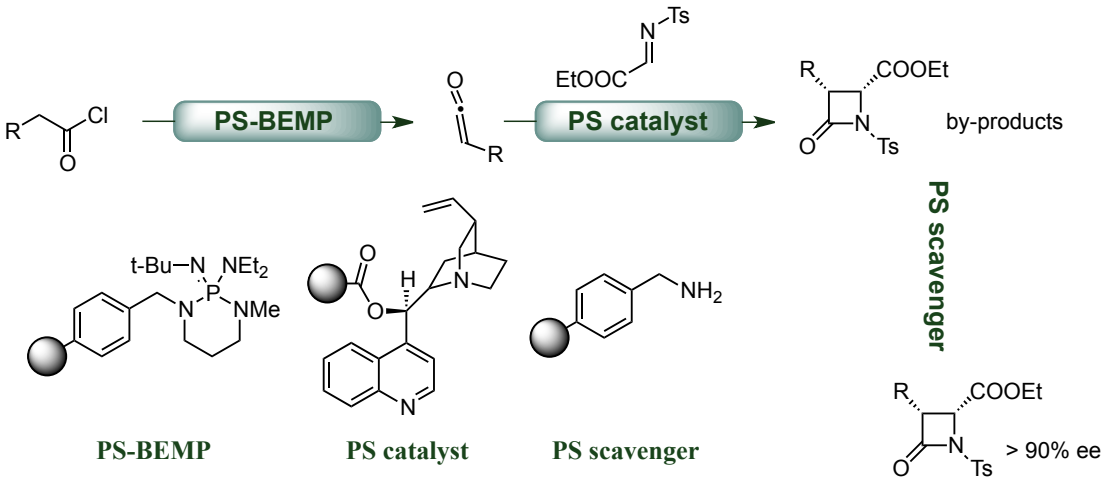

Scheme I.25. Preparation of enantioenriched β-lactams in flow.

Several enantioselective reactions under continuous flow conditions have been successfully accomplished with a series of different immobilized catalysts in our group. We have studied the use of polymer-supported proline[71b,c] and prolinol[71i,71h] derivatives in flow reactors. Several strategies towards catalyst immobilization have been developed, mostly using 1,2,3-triazole linkers with polystyrene beads as solid supports for catalyst immobilizations (**Figure I.12**).[71] Recently, our group reported the first example of solid-supported chiral phosphoric acid used in flow. Alternative organocatalysts such as primary amino acid derivative **I.35** and cinchona alkaloid **I.36** has also been developed for flow applications (**Figure I.14**).[90]

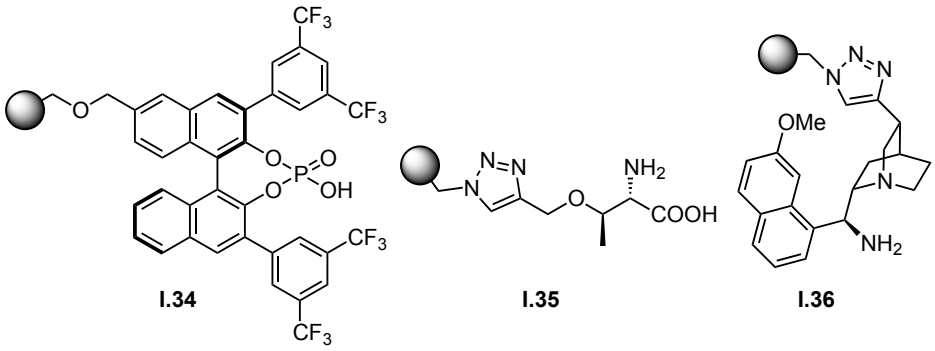

Figure I.14. Recent examples of polymer-supported catalysts used in flow in our group.

[90] For catalyst **(I.34)**, see: a) Osorio-Planes, L.; Rodríguez-Escrich, C.; Pericàs, M. A. *Chem. - Eur. J.*, **2014**, *20*, 2367–2372; for catalyst **(I.35)**, see: b) Ayats, C.; Henseler, A. H.; Dibello, E.; Pericàs, M. A. *ACS Catal.* **2014**, *4*, 3027-3033; for catalyst **(I.36)**, see: c) Izquierdo, J.; Ayats, C.; Henseler, A. H.; Pericàs, M. A. *Org. Biomol. Chem.* **2015**, *13*, 4204-4209.

Compounds, obtained by organocatalytic flow reactions, are presented in **Figure I.15**.[71,90]

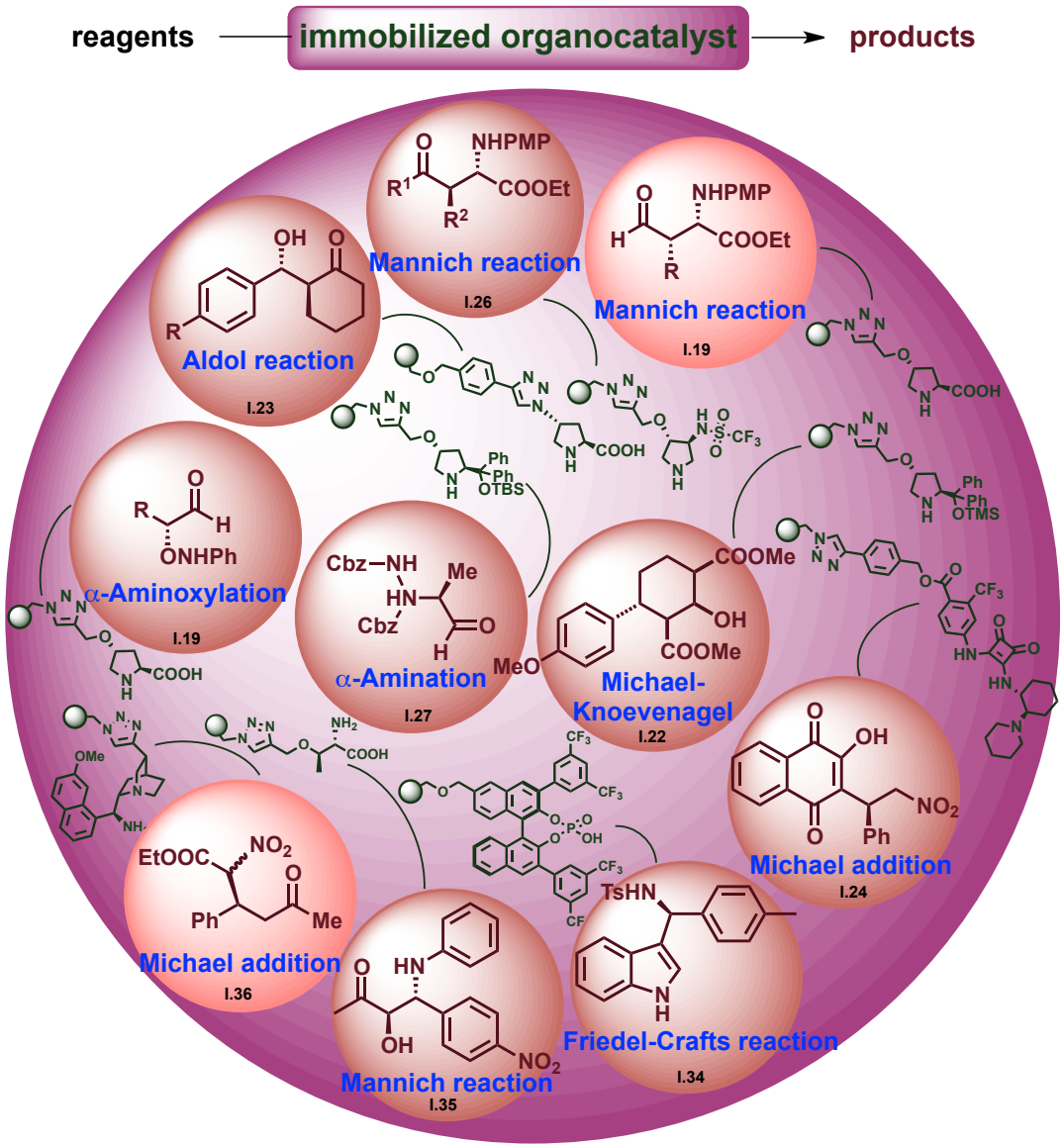

Figure I.15. Organocatalyzed flow reactions in our laboratories.

I.2. Introduction to the chemistry of sulfenates.

I.2.1. Metal-mediated catalysis.

The Nobel Prize has been awarded three times to researchers for their work in the area of transition metal catalysis (**Scheme I.26**). In 2001 Knowles, Noyori, and Sharpless were honoured for their research in asymmetric hydrogenation and oxidation reactions.[5] Only four years later, in 2005, Schrock, Grubbs and Chauvin received this prestigious award for their contribution in the development of the ruthenium- and molybdenum-catalyzed olefin metathesis.[91] Finally, in 2010 the Nobel Prize for chemistry was awarded to Heck, Negishi and Suzuki for their research within the area of carbon-carbon bond forming palladium-catalyzed cross-coupling reactions.[92]

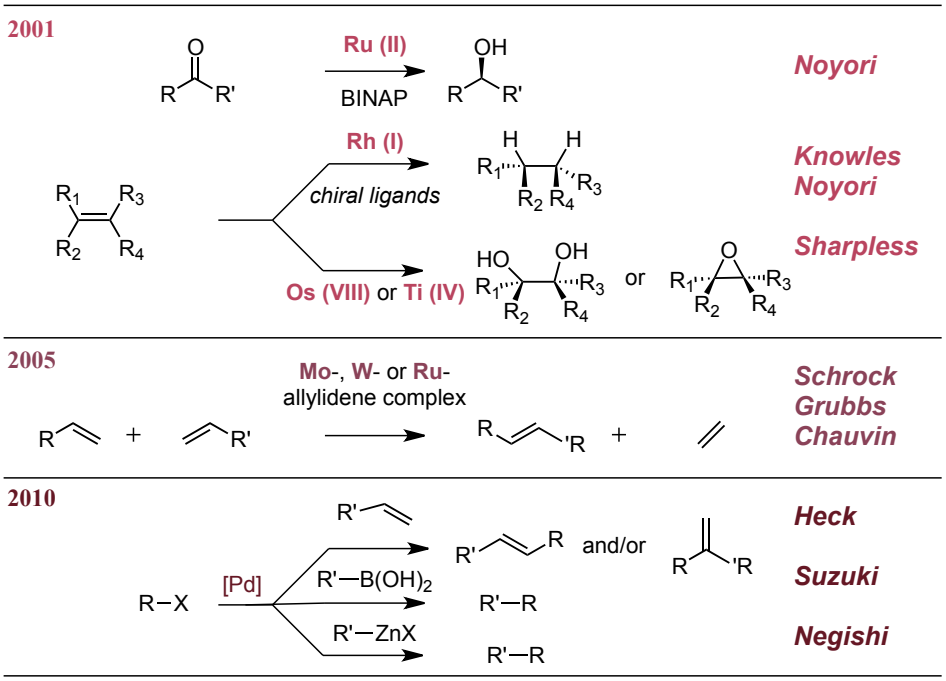

Scheme I.26. Nobel prizes in 2001, 2005 and 2010.

If we rank C-C bond formation methodologies in terms of the number of scientific publications, patents and industrial applications, Suzuki coupling (also called Suzuki-Miyaura) is by far the largest, followed by Heck (also called the Mizoroki-Heck), Sonogashira and Stille coupling.[93]

---

[91] a) Chauvin, Y. *Angew. Chem. Int. Ed.* **2006**, *45*, 3740-3747; b) Schrock, R. R. *Angew. Chem. Int. Ed.* **2006**, *45*, 3748-3759; c) Grubbs, R. H. *Angew. Chem. Int. Ed.* **2006**, *45*, 3760-3765.
[92] a) Suzuki, A. *Angew. Chem. Int. Ed.* **2011**, *50*, 6722-6737; a) Negishi, E.-I. *Angew. Chem. Int. Ed.* **2011**, *50*, 6738-6764.
[93] a) Colacot, T. J. *Platinum Met. Rev.* **2011**, *55*, 84-90; b) Johansson Seechurn, C. C. C.; Kitching, M. O.; Colacot, T. J.; Snieckus, V. *Angew. Chem. Int. Ed.* **2012**, *51*, 5062-5085.

The generally accepted mechanisms for these palladium-catalysed cross-coupling reactions are shown in **Scheme I.26**.[94] The first step is the oxidative addition of the aryl halide (or pseudohalide) to the catalytically active organopalladium species (L_nPd^0) to generate a Pd^{II} intermediate. This initiates the catalytic cycle for both types of coupling reaction.

After this stage, in the Mizoroki-Heck coupling the reaction progresses by co-ordination of an alkene to the Pd^{II} species, followed by its *syn* migratory insertion. The regioselectivity of this insertion depends on the nature of the alkene, the catalyst, and the reaction conditions employed. The newly generated organopalladium species then undergoes *syn* β-hydride elimination to form the alkene product. Subsequently, base-assisted elimination of H-X from $[L_nPd(H)(X)]$ occurs to regenerate the L_nPd^0 catalyst (n = 2 typically).

Alternatively, in the Negishi and Suzuki-Miyaura reactions (and the related Corriu-Kumada, Stille, and Hiyama coupling processes), the oxidative addition is followed by transmetalation of an organometallic species to generate a Pd^{II} intermediate bearing the two organic coupling partner fragments. Subsequent reductive elimination results in C-C bond formation with the regeneration of Pd^0 species to re-enter into the catalytic cycle.

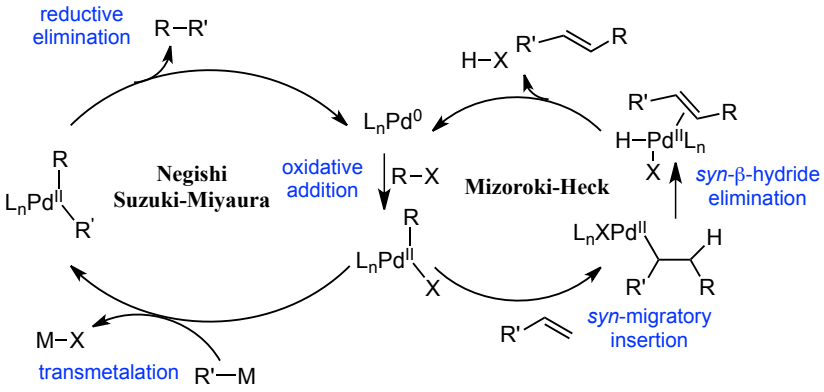

Scheme I.27. General catalytic cycles for Heck-Mizoroki, Negishi, and Suzuki-Miyaura reactions.

Most cross-coupling reactions are catalyzed by palladium, but nickel or copper catalysts are also common. An overview of cross-coupling reactions is presented in **Scheme I.28**.

[94] a) Negishi, E.-L. *Handbook of Organopalladium Chemistry for Organic Synthesis* (Eds.: Negishi, E.-I.), John Wiley & Sons Inc., New York, USA **2002**, *Ch. 11*, 127-145; b) Echavarren, A. M.; Cárdenas, D. J. *Metal-Catalyzed Cross-Coupling Reactions* (Eds.: de Meijere, A.; Diederich, F.), Wiley-VCH, Weinheim, **2004**, *Ch.1*, 1-40.

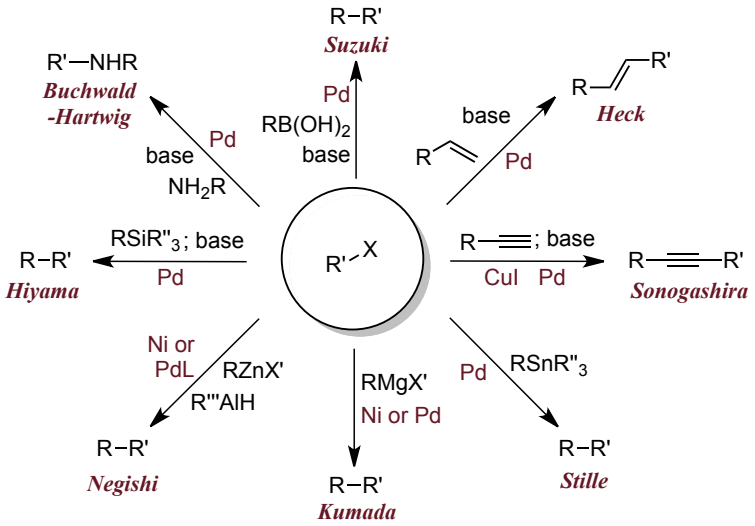

Scheme I.28. A variety of cross-coupling reactions.

In the last years many types of coupling reactions were studied, and the role of the ligands was reconsidered as important in the reaction course. They are not only providing solubility to the organometallic catalyst in organic solvents and preventing degradation pathways of this catalyst, but also they show a dramatic influence in all transformations, influencing selectivity (e.g., enantioselectivity, diastereoselectivity, regioselectivity and chemoselectivity).[95]

The continuous development of new ligands with different steric and electronic properties has allowed to generate more efficient catalytic systems.[96] Furthermore, these powerful ligands have ultimately led to the discovery of new cross-coupling reactions generating other bonds (e.g. C-N, C-O, C-P, C-S, C-B). In general, catalytic pathways for the formation of C-X bonds involve steps related to the one just described for C-C bond formation. Nevertheless, depending on the nature of the electrophile, nucleophile and the ligands on palladium, significant differences can be observed for these processes with regard to the rate-determining step(s).

I.2.2. Sulfoxides.

Research in the group of Prof. Walsh[97] covers the field of catalysis with the goal of achieving new catalytic asymmetric transformations for the synthesis of building blocks.

---

[95] For some example, see: a) Engle, K. M.; Yu, J.-Q. *J. Org. Chem*. **2013**, *78*, 8927-8955.
[96] For some review on phosphine ligands, see: Clarke, M. L.; Frew, J. J. R. *Organomet. Chem.* **2009**, *35*, 19-46.
[97] The Walsh group page: https://sites.google.com/site/titaniumupenn/.

Chapter I

One of the important topics of their research are palladium-catalyzed homogeneous reactions. In particular, they are interested in the synthesis and development of sulfur chemistry and sulfoxides derivatives. These are widely occurring molecules in organic chemistry, medicinal chemistry, and drug metabolism.[98] They often perform a major function as therapeutic agents such as anti-ulcer (proton pump inhibitor), antibacterial, antifungal, anti-atherosclerotic, antihypertensive and cardiotonic agents. Some important structural motifs in marketed therapeutics drugs are presented in **Figure I.16**, for example, esomeprazole (Nexium) or modafinil (Provigil).[99]

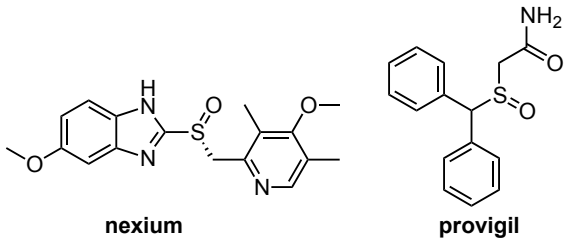

Figure I.16. Some examples of representative sulfoxides.

Furthermore, sulfoxides have attracted interest in the past three decades due to their use as chiral auxiliaries in a broad range of synthetic reactions.[100] The chirality in sulfoxides arises from their approximately pyramidal structure (**Figure I.17**); when the R groups are different, two possible enantiomers exist.

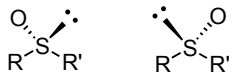

Figure I.17. Two enantiomeric forms of a sulfoxide.

In the present thesis, we will concentrate on recent advances in the synthesis of diaryl sulfoxides. There are two classical routes to generate diaryl sulfoxides: i) oxidation of sulfides[100b,101] and ii) nucleophilic substitution of electrophilic sulfinamides

---

[98] a) Andersen, K. K. *Sulphones and Sulphoxides* (Eds.: Patai, S.; Rappoport, Z.; Stirling, C.), **1988**, John Wiley & Sons Ltd, Chichester, UK, *Ch. 3*, 55-94; b) Organosulfur Chemistry II (Ed.: Page, P. C. B.), **1999**, Springer, Berlin, Germany; c) Suwanborirux, K.; Charupant, K.; Amnuoypol, S.; Pummangura, S.; Kubo, A.; Saito, N. *J. Nat. Prod.* **2002**, *65*, 935-937; d) Rinehart, K. L.; Sakai, R. *US2004/59112 A1*, **2004**; e) ACHAOGEN, Inc. *WO2009/13713O A2*, **2009**; f) Amira Pharmaceuticals, Inc. *US/2010/4331 A1*, **2010**; g) Hutchinson, J. H.; Seiders, T. J.; Arruda, J. M.; Roppe, J. R. Amira Pharmaceuticals, Inc. *WO2010/42652 A2*, **2010**; h) CombinatoRx (Singapore) Pte. Ltd. *US2010/9970 A1*, **2010**.

[99] a) Lindberg, P.; Weidolf, L. Astra Aktiebolag, US5877192 A, **1998**; b) Lafon, L. Laboratoire L. Lafon, *US4927855A*, **1990**.

[100] a) Solladié, G. *Synthesis* **1981**, 185-196; b) Drabowicz, J.; Kiełbasinski, P.; Mikołajczyk, M. *Sulphones and Sulphoxides* (Eds.: Patai, S.; Rappoport, Z.; Stirling, C.), **1988**, John Wiley & Sons Ltd, Chichester, UK, *Ch. 8*, 233-378; c) Senanayake, C. H.; Krishnamurthy, D.; Lu, Z.-H.; Han Z.; Gallou, I. *Aldrichimica Acta* **2005**, *38*, 93-103; d) Pellisier, H. *Tetrahedron*, **2006**, *62*, 5559-5601; e) Mellah, M.; Voituriez, A.; Schulz, E. *Chem. Rev.* **2007**, *107*, 5133-5209; f) Carreño, M. C.; G. Hernández-Torres, G.; Ribagorda, M.; Urbano, A. *Chem. Commun.* **2009**, 6129-6144.

[101] Bolm, C. *Coord. Chem. Rev.* **2003**, *237*, 245-256

or sulfenate esters[102] (**Scheme I.29**). The oxidation approach is the most popular because of its versatility, since the same route can be used to oxidise many sulfides. However both of them suffer from limited functional group tolerance because either strong oxidizing agents or reactive organolithium or Grignard reagents are employed. Therefore, rapid synthesis of diversified diaryl sulfoxides remains challenging in organic chemistry.

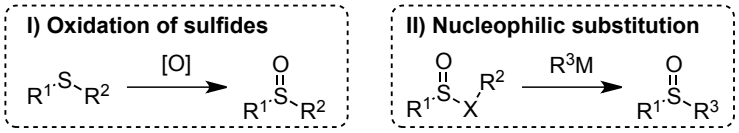

R1, R2, R3 = alkyl, aryl; **X**: heteroatom, such as O, N; **M**: lithium or magnesium.

Scheme I.29. Previous synthetic approaches to sulfoxides.

I.2.3. α-Arylation of carbonyl compounds, sulfones, and sulfoxides.

The oxidation of sulfides is the most common method for sulfoxide synthesis, and numerous reagents and oxidative procedures have been reported to date,[101] although many of them provide overoxidation to sulfones. Several factors such as limited availability of sulfide derivatives, or the use of strongly oxidant or reactive organolithium and Grignard reagents, highlight the need for an alternative synthetic methodology. Therefore, metal-catalyzed reactions can be the best alternative to overcome most of the restrictions for the efficient synthesis of sulfoxide derivatives.

Transition metal-catalyzed cross-coupling reactions to form C-C bonds are very powerful synthetic methods. Among these, new methods for the α-arylation have been recently disclosed (**Scheme I.30**).[103]

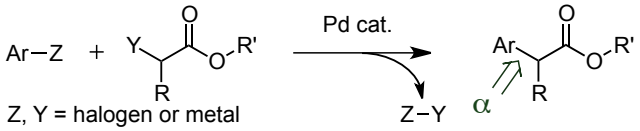

Scheme I.30. α-Arylated esters and amino acids (R = NH_2) by formation of Ar-C_α bond.

However, only a few reactions involving cross-coupling of enolates with aryl or vinyl halides are known, and they typically occur with modest yields and involve zinc[104]

[102] Han, Z.; Krishnamurthy, D.; Grover, P.; Fang, Q. K.; Su, X.; Wilkinson, H. S.; Lu, Z.-H.; Magiera, D.; Senanayake, C. H. *Tetrahedron* **2005**, *61*, 6386-6408.
[103] For some reviews, see: a) Lloyd-Jones, G. C. *Angew. Chem. Int. Ed.* **2002**, *41*, 953-956; b) Culkin, D. A.; Hartwig, J. F. *Acc. Chem. Res.* **2003**, *36*, 234-245; c) Johansson, C. C. C.; Colacot, T. J. *Angew. Chem. Int. Ed.* **2010**, *49*, 676-707.
[104] Fauvarque, J. F.; Jutand, A. *J. Organomet. Chem.* **1979**, *177*, 273-281.

or tin enolates.[105] Metal-mediated coupling of enolates has been achieved initially with stoichiometric quantities of nickel complexes.[106]

In 1997, Hartwig, Buchwald and Miura reported concurrently the palladium-catalyzed direct coupling of ketones with aryl bromides (**Scheme I.31**).[107] In their initial studies, the more reactive aryl iodides or aryl bromides were utilized as the coupling partners for C-C bond formation with ketone. Slightly different catalysts were employed in this transformation, but in all cases the reaction started by deprotonation of the acidic α-carbon. This method displayed a high degree of regioselectivity and functional group tolerance.

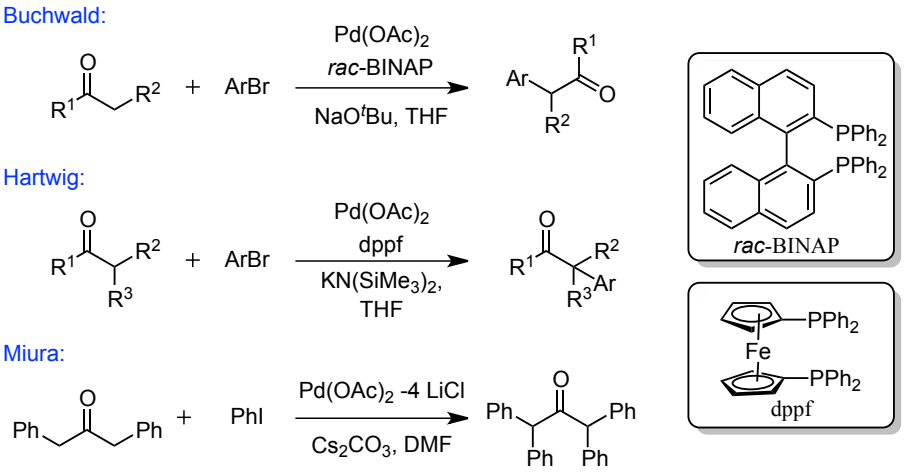

Scheme I.31. Palladium catalyzed α-arylation of ketones and aldehydes.

A plausible catalytic cycle for the palladium-catalyzed addition of enolates to aryl halides is shown in **Scheme I.32**.[103b, 108] Oxidative addition of an aryl halide to a Pd^0 complex would form an arylpalladium (II) halide complex (**I.28**). Substitution of the coordinated halide by an enolate nucleophile and reductive elimination from the resulting palladium enolate complex (**I.29a** or **I.29b**) would form the α-aryl ketone, ester, or amide and regenerate the Pd^0 complex that started the cycle.

[105] a) Kosugi, M.; Hagiwara, I.; Sumiya, T.; Migita, T. *Bull. Chem. Soc. Jpn.* **1984**, *57*, 242-246; b) Kuwajima, I.; Nakamura, E.-I. *Acc. Chem. Res.* **1985**, *18*, 181-187; c) Kosugi, M.; Negishi, Y.; Kameyama, M.; Migita, T. *Bull. Chem. Soc. Jpn*. **1985**, *58*, 3383-3384; d) Galarini, R.; Musco, A.; Pontellini, R.; Santi, R. *J. Mol. Catal.* **1992**, *72*, L11-L13.
[106] a) Semmelhack, M. F.; Stauffer, R. D.; Rogerson, T. D. *Tetrahedron Lett.* **1973**, *14*, 4519-4522; b) Millard, A. A.; Rathke, M. W. *J. Am. Soc. Chem.*, **1977**, *99*, 4833-4835.
[107] a) Hamann, B. C.; Hartwig, J. F. *J. Am. Chem. Soc.* **1997**, *119*, 12382-12383; b) Palucki, M.; Buchwald, S. L. *J. Am. Chem. Soc.* **1997**, *119*, 11108-11109; c) Satoh, T.; Kawamura, Y.; Miura, M.; Nomura, M. *Angew. Chem. Int. Ed.* **1997**, *36*, 1740-1742.
[108] Fox, J. M.; Huang, X.; Chieffi, A.; Buchwald, S. L. *J. Am. Soc. Chem.*, **2000**, *122*, 1360-1370.

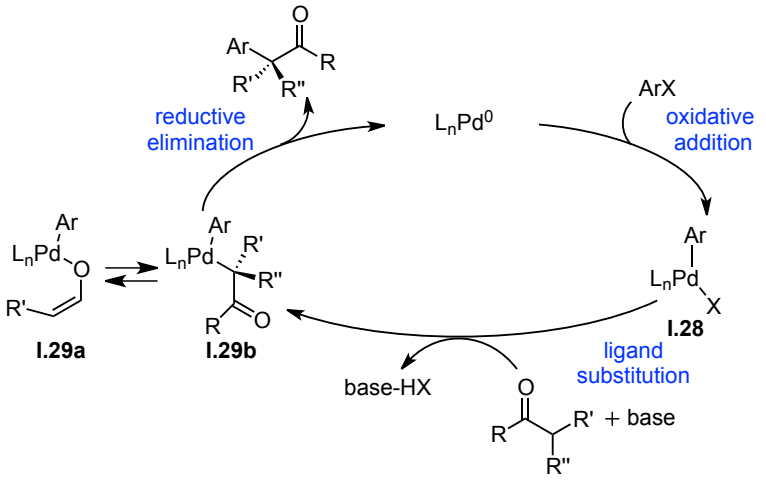

Scheme I.32. Palladium-catalyzed addition of enolates to aryl halides.

This methodology, reported by the Hartwig and Buchwald groups, has been extended to palladium-catalyzed α-arylation of esters (**Scheme I.33**).[109] This process takes place in high yields, under simple conditions with readily available substrates and reagents.

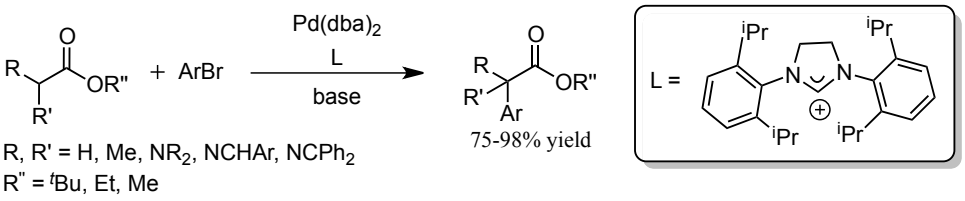

Scheme I.33. Palladium-catalyzed α-arylation of esters.

Despite the aldol condensation of aldehydes takes place under basic conditions, Miura *et al.* introduced α-arylation of aldehydes with aryl bromides under palladium catalysis (**Scheme I.34A**).[110] High temperature and high catalyst loadings were required for this transformation, but modest yields of desired compounds were obtained.

Later, more valuable protocols for α-arylation of aldehydes have been developed by several groups.[111] Martín and Buchwald improved these results with broad scope, involving mostly electron-poor aryl halides (**Scheme I.34B**).[111a] Later, this method was extended to electron-poor and electron-neutral aryl bromides[111b] and

[109] a) Lee, S.; Beare, N. A.; Hartwig, J. F. *J. Am. Soc. Chem.* **2001**, *123*, 8410-8411; b) Moradi, W. A.; Buchwald, S. L. *J. Am. Soc. Chem.* **2001**, *123*, 7996-8002.
[110] Terao, Y.; Fukuoka, Y.; Satoh, T.; Miura, M.; Nomura, M. *Tetrahedron Lett.* **2002**, *43*, 101-104.
[111] a) Martín. R.; Buchwald, S. L. *Angew. Chem. Int. Ed.* **2007**, *46*, 7236-7239; b) Vo, G. D.; Hartwig, J. F. *Angew. Chem. Int. Ed.* **2008**, *47*, 2127-2130; c) Martín. R.; Buchwald, S. L. *Org. Lett.* **2008**, *10*, 4561-4564.

electron-rich aryl halides.[111c] In general, α-arylation of aldehydes and ketones has become a useful and valuable chemical tools since the first reports in this area.

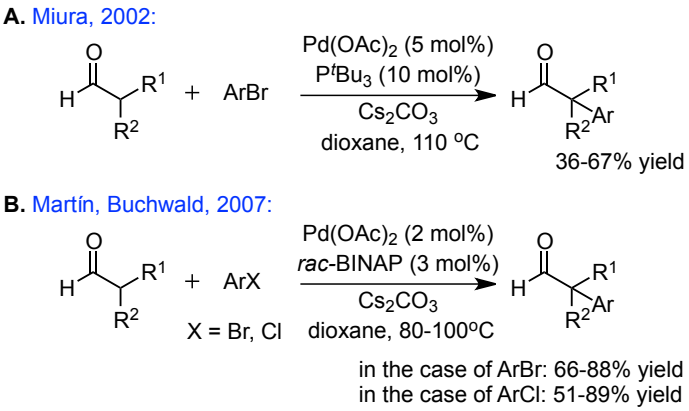

Scheme I.34. Palladium catalyzed α-arylation of aldehydes.

However, regarding the analogues methyl sulfoxides or methyl sulfones, there was only one example of α-arylation until the first report by Walsh group. Beletskaya *et al.* reported a similar protocol for the first example of α-arylation of activated sulfones using a Pd/PPh_3-derived catalyst (**Scheme I.35A**).[112] Later, in 2013, the group of Walsh developed the first direct α-arylation of unactivated alkyl and aryl methyl sulfoxides with aryl halides (**Scheme I.35.B**).[113]

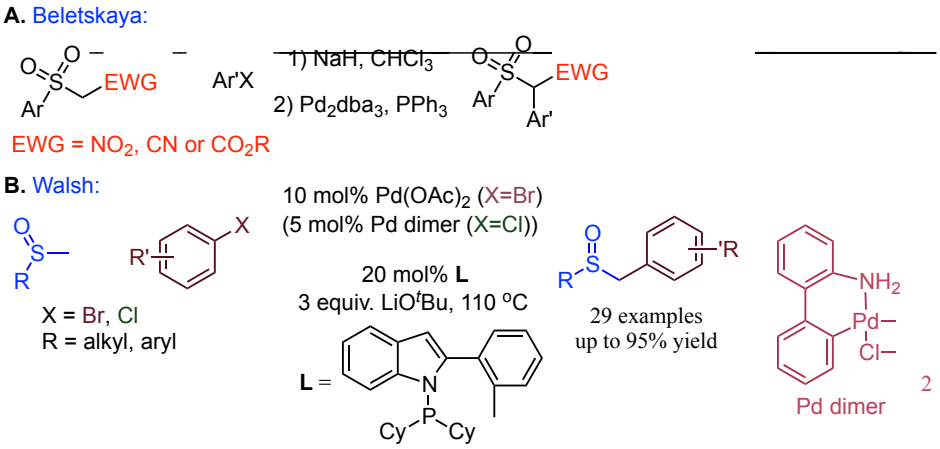

Scheme I.35. Palladium catalyzed α-arylation sulfones and methyl phenyl sulfoxides.

One year later they presented a novel approach to produce diaryl sulfoxides from aryl benzyl sulfoxides and aryl bromides, involving sulfoxide α-arylation, C-S bond cleavage and C-S bond formation (**Scheme I.36**).[114]

[112] Kashin, A. N.; Mitin, A. V.; Beletskaya, I. P.; Wife, R. *Tetrahedron Lett.* **2002**, *43*, 2539-2542.
[113] Jia, T.; Bellomo, A.; El Baina, K.; Dreher, S. D.; Walsh, P. J. *J. Am. Chem. Soc.* **2013**, *135*, 3740-3743.
[114] Jia, T.; Bellomo, A.; Montel, S.; Zhang, M.; El Baina, K.; Zheng, B.; Walsh, P. J. *Angew. Chem. Int. Ed.* **2014**, *53*, 260-264.

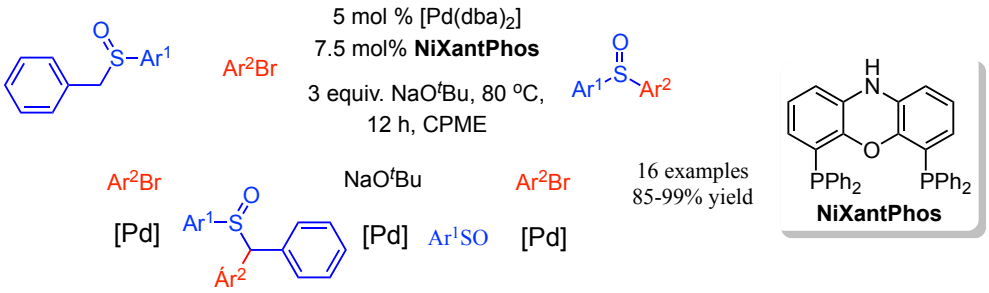

Scheme I.36. Palladium-catalyzed triple relay process.

More challenging coupling partners, such as aryl chlorides, could not be employed in this transformation. This catalytic reaction, via triple relay process, is the reaction object of study in the **Chapter V** of the present Thesis, where it will be commented in more detail.

I.2.3. Sulfenate anions.

Sulfenic acids are the simplest organosulfur oxyacids. They are important in biological and synthetic chemistry, frequently acting as reactive intermediates,[115] or playing a key role in enzymatic catalysis.[116] Sulfenic acids are also key intermediates in the preparation of sulfoxides because, given the electronic nature of their S-O bond they can be involved in various reactions.[115c] In contrast, the interest towards their conjugated sulfenate anions, has remained rather low.

These species have been rarely isolated and are created *in situ* for further functionalization. Sulfenate anions can be described by two valence bond structures that well explain the ambident nature of these anions: they are able to react with electrophiles at the sulphur or at oxygen. (**Figure I.18**).

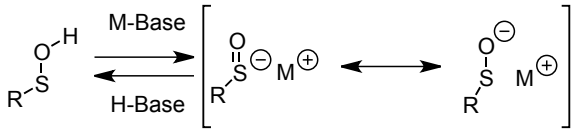

Figure I.18. Sulfenic acid and its conjugate base, the sulfenate anion.

As already mentioned, sulfenate anions are unstable species. Therefore, manipulation under inert atmosphere and/or at low temperature is required in order to

[115] For some review, see: a) Hogg, D. R. *The Chemistry of Sulphenic Acids and their Derivatives*, (Ed.: Patai, S.), **1990**, John Wiley & Sons Ltd, Vol.9, 361-402; b) O'Donnell, J. S.; Schwan, A. L. *J. Sulfur Chem.* **2004**, *25*, 183-211; c) Aversa, M. C.; Bonaccorsi, P.; Madec, D.; Prestat, G.; Poli, G. *Innovative Catalysis in Organic Synthesis: Oxidation, Hydrogenation, and C-X Bond Forming Reactions* (Ed.: Andersson, P. G.), **2012**, John Wiley & Sons Ltd, *Vol.3*, 47-76.
[116] For a review, see: a) Hall, A.; Karplus, P. A.; Poole, L.B. *FEBS J.*, **2009**, *276*, 2469–2477; b) Poole, L. B.; Karplus, P. A.; Claiborne, A. *Annu. Rev. Pharmacol. Toxicol.* **2004**, *44*, 325–347.

avoid side reactions such as oxidation to the corresponding sulfinate anion (RSO_2^-) or disproportionation to thiolate (RS^-) and sulfinate anions. If protic solvents are used, protonation to sulfenic acids and conversion into thiosulfinates [RSS(O)R] can also be observed (**Scheme I.37**).[115c]

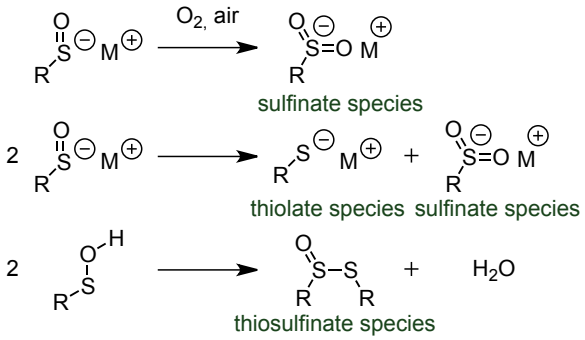

Scheme I.37. Possible decomposition pathways of sulfenate anions.

Sulfenate anions can be obtained via different strategies such as cleavage of sulfenate esters (I), oxidation of thiolates (II), β-elimination route (III), addition-elimination sequences (IV), or oxidative addition of alkynyl or allyl sulfoxides to Pd^0 species (V and VI) (**Figure I.19**).[115c]

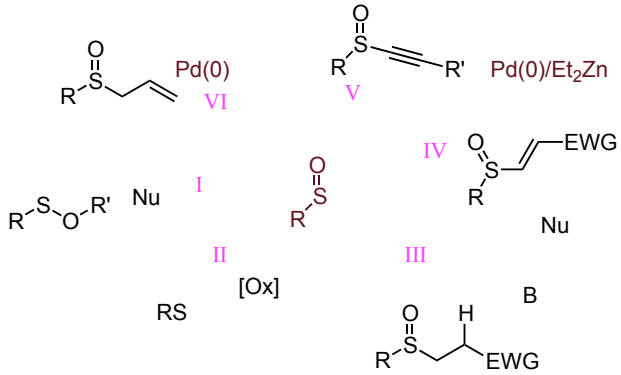

Figure I.19. Strategies towards sulfenate generation.

Different approaches to sulfoxide synthesis, complementary to sulfide oxidation protocols, can be provided via sulfenate chemistry. In recent years, these compounds have been employed as important intermediates in biological and synthetic chemistry, especially in the following contributions:

I) Employment of transient sulfenic acids in the synthesis of sulfoxides and disulfides.[117]

[117] For some examples, see: a) Caupène, C.; Boudou, C.; Perrio, S.; Metzner, P. *J. Org. Chem.* **2005**, *70*, 2812-2815; b) O'Donnell, J. S.; Schwan, A. L. *Tetrahedron Lett.* **2003**, *44*, 6293-6296; c) Singh, S. P.; O'Donnell, J. S.; Schwan, A. L. *Org. Biomol. Chem.* **2010**, *8*, 1712-1717; d) Schwan, A.L.; Verdu, M. J.; Singh, S. P.; O'Donnell, J. S.; Ahmadi, A. N. *J. Org. Chem.* **2009**, *74*, 6851-6854.

II) Application of sulfenate anions in palladium-catalyzed allylations and arylations to generate allyl and aryl sulfoxides.[118]

III) Development of an enantioselective version of palladium-catalyzed allylations and arylation reactions.[117d, 119]

IV) Use of sulfenate anions in different *pseudodomino* palladium-catalyzed transformations.[120]

However, the use of sulfenate anions as organocatalysts had not been previously reported, when Walsh *et al.* described the conversion of benzyl halides to symmetrically substituted stilbenes. This transformation presented, for the first time, the use of sulfenate anions as metal-free catalysts (**Scheme I.38**).[121]

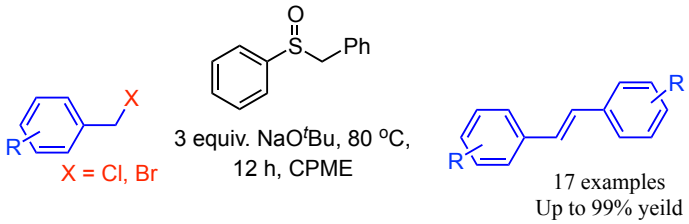

Scheme I.38. Conversion of benzyl halides to stilbenes.

[118] For some examples, see: a) Maezaki, N.; Yoshigami, R.; Maeda, J.; Tanaka, T. *Org. Lett.* **2001**, *3*, 3627–3629; b) Maitro, G.; Prestat, G.; Madec, D.; Poli, G. *J. Org. Chem*. **2006**, *71*, 7449-7454.
[119] For selected works on the use of sulfenate anions in enantioselective approaches, see: a) Kobayashi, M.; Manabe, K.; Umemura, K.; Matsuyama, H. *Sulfur Lett.* **1987**, *6*, 19-24; b) Drabowicz, J.; Łyzwa, P.; Mikołajczyk, M. *Phosphorus Sulfur* **1983**, *16*, 267-270.
[120] For some examples, see: a) Poli, G.; Giambastiani, G. *J. Org. Chem.* **2002**, *67*, 9456-9459; b) Bernoud, E.; Le Duc, G.; Bantreil, X.; Prestat, G.; Madec, D.; Poli, G. *Org. Lett.* **2010**, *12*, 320-323.
[121] Zhang, M.; Jia, T.; Yin, H.; Carroll, P. J.; Schelter, E. J.; Walsh, P. J. *Angew. Chem. Int. Ed.* **2014**, *53*, 10755-10758.

UNIVERSITAT ROVIRA I VIRGILI
NEW APPROACHES TO CATALYST DESIGN AND IMMOBILIZATION
Irina Sagamanova

CHAPTER II

Asymmetric Organocatalysts Supported on Vinyl Addition Polynorbornenes for Work in Aqueous Media

UNIVERSITAT ROVIRA I VIRGILI
NEW APPROACHES TO CATALYST DESIGN AND IMMOBILIZATION
Irina Sagamanova

CHAPTER II

Asymmetric Organocatalysts Supported on Vinyl Addition Polynorbornenes for Work in Aqueous Media

2.1 Introduction.

Our laboratory has a longstanding interest in the development of polymer-supported organocatalysts that may be applied in a wide range of asymmetric transformations. In this chapter, we will introduce the use of vinylic (or vinyl) addition polynorbornenes as insoluble polymeric supports for organocatalysts. These two species will be bound by a linker that contains a 1,2,3-triazole unit generated in a Copper(I)-Catalyzed Alkyne-Azide Cycloaddition (CuAAC) reaction, usually referred to as "click-chemistry".[60,61]

The interest in polymers of cyclic olefins such as norbornene (NB, **II.1**) (bicyclo-[2.2.1]hept-2-ene) has been driven by their dielectric and mechanical properties highly appreciated for technical applications.[122] Thus, several authors have studied their synthesis via different pathways during the past decades.[123] The norbornene copolymer features a high glass-transition temperature, excellent transparency, thermal stability and chemical resistance. Alternative routes to achieve the goal of an "all alicyclic backbone" are shown in **Figure II.1**. These include ring-opening metathesis polymerization (ROMP),[124] metal-catalyzed vinylic polymerization,[125] and radical-promoted vinylic polymerization.[126] All these synthetic routes lead to their own polymer type, each having different properties and structure.[127]

---

[122] a) Haselwander, T. F. A.; Heitz, W.; Krügel, S. T.; Wendorff, J. H. *Macromol. Chem. Phys.* **1996**, *197*, 3435-3453; b) Grove, N. R.; Kohl. P. A.; Allen, S. A. B.; Jayaraman, S.; Shick, R. *J. Polym. Sci.: Par B: Polym. Phys.* **1999**, *37*, 3003-3010.
[123] a) Nelkenbaum, E.; Kapon, M.; Eisen, M. S. *Organometallics* **2005**, *24*, 2645-2659; b) Ma, R.; Hou, Y.; Gao, J.; Bao, F. *Polym. Rev.* **2009**, *49*, 3, 249-287; c) Blank, F.; Janiak, C. *Coord. Chem. Rev*. **2009**, *253*, 827-861.
[124] a) Mathew, J. P.; Reinmuth, A.; Melia, J.; Swords, N.; Risse, W. *Macromolecules* **1996**, *29*, 2755-2763; b) Safir, A. L.; Novak, B. M. *Macromolecules* **1995**, *28*, 5396-5398.
[125] a) Cherndron, H.; Brekner, M.-J.; Osan F. *Angew. Makromol. Chem.* **1994**, *223*, 121-133; b) Kaminsky, W. *Angew. Makromol. Chem.* **1994**, *223*, 101-120; c) Rush, S.; Reinmuth, A.; Risse, W. *Macromolecules* **1997**, *30*, 7375-7385
[126] Crivello, J. C.; Shim, S.Y. *Chem. Mater.* **1996**, *8*, 376-381.
[127] Janiak, C.; Lassahn, P. G. *J. Mol. Catal. A: Chem.* **2001**, *166*, 193-209.

Chapter II

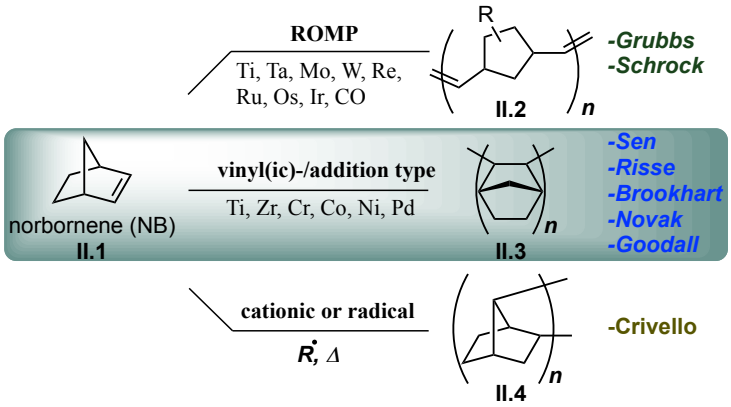

Figure II.1. Schematic representation of available routes to alicyclic backbone polymers.

The first synthetic approach is the well-known polymerization of norbornene, which is technically applied in the Norsorex® process.[128] Typical ROMP catalysts include late transition metals such as tungsten and molybdenum, ruthenium, etc. Polymer **II.2** is obtained with double bonds in the backbone and can be cross-linked or vulcanized, making it less stable thermodinamically. Based on Chauvin's proposal,[129] a general mechanism for ROMP reaction is illustrated in **Figure II.2**. Initiation begins with coordination of the cyclic olefin onto a transition metal alkylidene complex, followed by [2+2]-cycloaddition to form a four-membered metallacyclobutane intermediate. Finally, this intermediate undergoes a cycloreversion reaction to afford a new metal alkylidene. Then, this metal alkylidene can re-enter the catalytic cycle during the propagation stage until polymerization ceases (e.g. all monomer is consumed, a reaction equilibrium is reached or the reaction is terminated). This mechanism can proceed in the opposite direction, as well.[130]

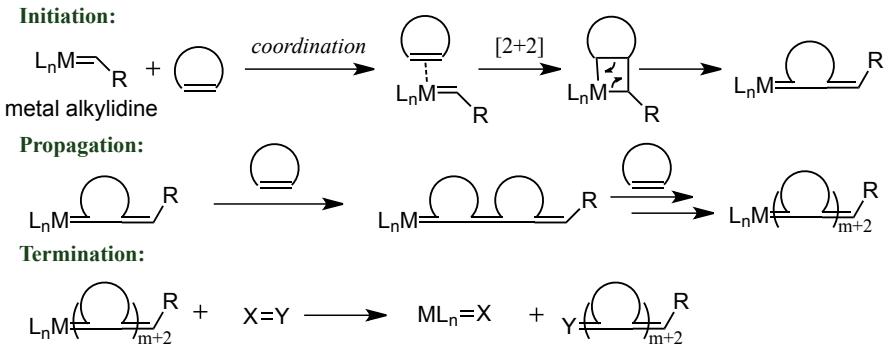

Figure II.2. A general mechanism to a typical ROMP reaction.

[128] For a review about industrial applications of olefin metathesis, see: Mol, J. C. *J. Mol. Catal.* **2004**, *213*, 39-45.
[129] Hérisson, J.-L.; Chauvin, Y. *Macromol. Chem.* **1970**, *141*, 161-176.
[130] Review for ROMP, see: Bielawski, C. W.; Grubbs, R. H. *Prog. Polym. Sci.* **2007**, *32*, 1-29.

One of the most widely employed reactions for the synthesis of polymers in the industrial and laboratory scale is radical polymerization. In the case of norbornene derivatives, two possible structures may be considered for a saturated polynorbornene (**II.3** and **II.4**, **Figure I.1**). Vinylic polymer structure **II.3** with 2,3-connectivity can be obtained in the presence of transition metal catalysts, while the cationic and "radical" polymers provide the 2,7-connectivity, which gives rearranged norbornanediyl units in the backbone.[131] The latter method, first described in 1967,[131a] is initiated by ethylaluminum dichloride ($EtAlCl_2$) or by free radicals (for example, azobisisobutyronitrile (AIBN), *tert*-butyl peracetate or *tert*-butyl perpivalate), providing oligomeric material **II.4**.

Vinyl addition polymerization of norbornene was first reported with $TiCl_4/AlR_3$ in the early 1960s.[132] This is an alternative way to prepare polynorbornenes via opening the double bond of the structure, and this approach is less developed than ROMP. However, the difference between their thermal properties, have made vinylic addition polymers highly attractive. Indeed, they exhibit high stability and transparency, which make them ideal for many electronic, optical, and other applications.

However, polynorbornenes with polar groups have been produced only with poor to modest yields when using functionalized monomers.[133] The absence of polar groups in the polymer leads to drawbacks in their use for the construction of devices due to the low adherence. In most cases, in the presence of a polar substituent group (such as an ester, alcohol) early transition metal catalysts are deactivated.[132a] Also, low polymer yield can be obtained in the presence of late transition metal complexes such as Ni or Pd derivatives.[134]

To avoid the problems of classical polymerization, a new attractive synthetic approach was developed by the group of Espinet and Albéniz, using vinylic addition polynorbornenes with polar functionalities.[135] Preparation of copolymers was done, using a *trans*-diaryl nickel complex,[136] via copolymerization of norbornene **II.5** and norbornene derivatives with a halogen group **II.6**. These were in turn generated by a

---

[131] a) Kennedy, J. P.; Makowski, H. S. *Macromol. Sci. Chem. A1* **1967**, *3*, 345-370; b) Gaylond, N. G.; Mandal, B. M.; Martan, M. *J. Polym. Sci. B Polym. Lett. Ed*. **1976**, *14*, 555-559.
[132] Sartori, G.; Ciampelli, F. C.; Cameli, N. *Chim. Ind.* **1963**, *45*, 1478-1482.
[133] a) Wendt, A. R.; Fink, G. *Macromol. Chem. Phys*. **2000***, 201*, 1365-1376; b) Liu, S.; Borkar, S.; Newsham, D.; Yennawar, H.; Sen, A. *Organometallics* **2007***, 26,* 210-216.
[134] For some examples, see: a) Jung, I. G.; Seo, J.; Chung, Y. K.; Shin, D. M.; Chun, S.-H.; Son, S. U. *J. Polym. Sci., A: Polym. Chem.* **2007**, *45*, 3042-3052; b) Liu, B; Li, Y.; Shin, B.-G.; Yoon, D. Y.; Kim, I.; Zhang, L.; Yan, W. *J. Polym. Sci., A: Polym. Chem.* **2007**, *45*, 3391-3399.
[135] a) Martínez-Arranz, S.; Albéniz, A. C.; Espinet, P. *Macromolecules* **2010**, *43*, 7482-7487, b) Albéniz, A. C.; Martínez-Arranz, S.; Espinet, P. *ES P201000273*, **2010**.
[136] Casares, J. A.; Espinet, P.; Martín-Alvarez, J. M.; Martínez-Ilarduya, J. M.; Salas, G. *Eur. J. Org. Chem.* **2005**, *19*, 3825-3831.

Diels-Alder reaction of cyclopentadiene and terminal 1-bromoalkenes. Finally, polynorbornenes with pendant functional groups can be obtained via subsequent halogen substitution in the Br-functionalized polymer (**Scheme II.1**).[135a] This method provides access to substituted polynorbornenes, which cannot be prepared by direct vinylic addition.[137]

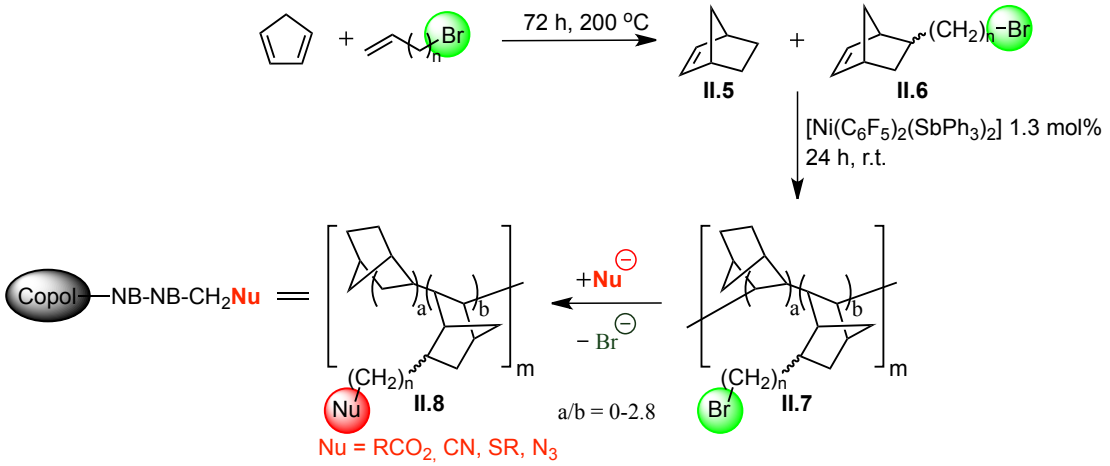

Scheme II.1. Functionalized vinylic addition polynorbornenes.

Reaction of the azido derivative Copol-NB-NBCH$_2$N$_3$ with an alkyne provides a new polynorbornene, bearing a triazole moiety (**Scheme II.2**).

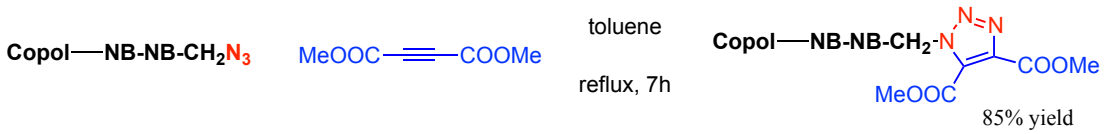

Scheme II.2. Synthesis of polynorbornene with pendant triazole groups.

Click chemistry has been previously used to attach catalysts onto polystyrene resins through a triazole linker.[71] We envisaged that these new polynorbornene copolymers could be very good supports to be used in organocatalytic applications.

Interestingly, to the best of our knowledge, the use of polynorbornene supports in organocatalytic transformations has not been previously reported.[58]

2.2. Immobilized proline and proline derivatives.

Since the discovery of L-proline-catalyzed reactions, this amino acid has been extensively studied as an organocatalyst.[138] There are several reasons why proline has

[137] For instance, substituted polynorbornene with cyano group: Park, K. H.; Twieg, R. J.; Ravikiran, R.; Rhodes, L. F.; Shick, R. A.; Yankelevich, D.; Knoesen, A. *Macromolecules* **2004**, *37*, 5163-5178.
[138] List, B. *Tetrahedron* **2002**, *58*, 5573-5590.

become an important chiral promoter in asymmetric catalysis. It is one example of abundant chiral molecule, inexpensive and that can be found in both enantiomeric forms. It is also non-toxic and soluble in water. Although proline is a versatile organocatalyst for different enantioselective transformations, it has some potential drawbacks, such as: a) proline has a low solubility in non-polar solvents which limits its reactivity; b) it can give possible side reactions; c) it is very often used in high catalyst loadings 10-30%, which can contaminate the final product.

The use of proline as organocatalyst, in spite of its effectiveness in the Hajos-Parrish-Eder-Sauer-Wiechert reaction[12-13] in the 1970s, has only recently received full attention in synthetic applications.[16] In addition, L-proline has been used in various type of reactions such as aldol,[16] Mannich,[139] Michael addition,[140] α-aminooxylation,[141] α-amination,[142] etc. Some reported examples are highlighted in **Scheme II.3**.

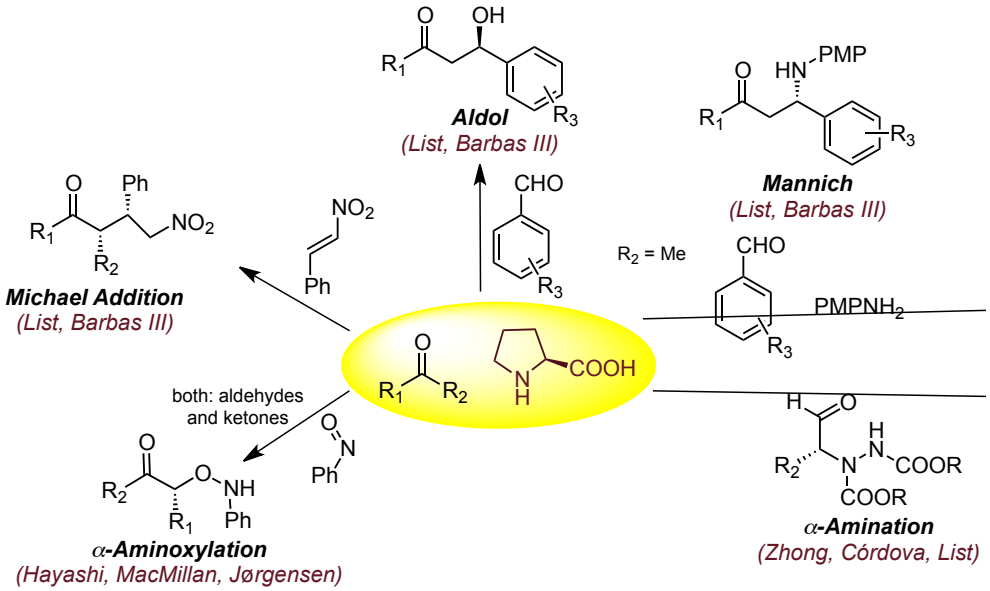

Scheme II.3. Representative examples of pioneer proline-catalyzed asymmetric reactions.

In the last years, numerous L-proline derivatives immobilized onto different supports using covalent or non-covalent immobilization techniques[71,83] have been reported. A few important aspects for proline immobilization have to be considered.

---

[139] a) List, B. *J. Am. Chem. Soc.* **2000**, *122*, 9336-9337; b) List, B.; Pojarliev, P.; Biller, W. T.; Martin, H. J. *J. Am. Chem. Soc.* **2002**, *124*, 827-833; c) Notz, W.; Sakthivel, K.; Bui, T.; Zhong, G.; Barbas III, C. F. *Tetrahedron Lett.* **2001**, *42*, 199-201.
[140] List, B.; Pojarliev P.; Martin, H. J. *Org. Lett.* **2001**, *3*, 2423-2425; b) Betancort, J. M.; Sakthivel, K.; Thyumanavan, R.; Barbas III, C. F. *Tetrahedron Lett.* **2001**, *42*, 4441-4444.
[141] a) Hayashi Y.; Yamaguchi, J.; Hibino, K.; Shoji M. *Tetrahedron Lett.* **2003**, *44*, 8293-8296; b) Hayashi, Y.; Yamaguchi, J.; Sumiya, T.; Shoji, M. *Angew. Chem. Int. Ed.* **2004**, *43*, 1112-1115; c) Brown, S. P.; Brochu, M.P.; Sinz, C.J.; MacMillan, D.W.C. *J. Am. Chem. Soc.* **2003**, *125*, 10808–10809; d) Zhong, G. *Angew. Chem. Int. Ed.* **2003**, *42*, 4247-4250; e) Bøgevig, A.; Sundén, H.; Córdova, A. *Angew. Chem. Int. Ed.* **2004**, *43*, 1109-1112.
[142] a) Bøgevig, A.; Juhl, K.; Kumaragurubaran, N.; Zhuang, W.; Jørgensen, K. A. *Angew. Chem. Int. Ed.* **2002**, *41*, 1790-1793; b) List, B. *J. Am. Chem. Soc.* **2002**, *124*, 5656-5657.

Chapter II

The first one is that proline is used in large catalyst loading (up to 30 mol%). Immobilization of proline may enhance its catalytic turnover through recycle and re-use. Moreover, supported proline derivatives can be used in different solvents, which facilitates the exploration of new solubility profiles for the reaction being considered. Finally, it introduces the possibility to test modifications of the properties of the supported catalysts by employing specific characteristics of each different support. In addition, more expensive organocatalyst derivatives may be applied, and their recovery and re-use will increase the greenness of the process.

Here, we would like to focus our attention mainly on the aldol reaction. This is a key carbon-carbon bond forming reaction, which creates a β-hydroxy carbonyl structural unit found in many natural products and drugs. In nature, type I and II aldolases catalyze this reaction in water with perfect control of the enantioselectivity.[143] Proline can catalyze direct aldol reactions in polar organic solvents with high enantioselectivity,[13,14,16b] but it affords the racemic compound in water.[144] In contrast with L-proline, some immobilized proline derivatives can be used in aqueous media.

An important breakthrough was made by Hayashi[145] and Barbas[146] for the preparation of aldol products in aqueous media with significantly higher stereoselectivities. They demonstrated independently that the incorporation of large hydrophobic groups into the catalytic structure improved the performance of the catalyst in the presence of water due to beneficial hydrophobic interaction in the aqueous microenvironment (**Figure II.3**, A).

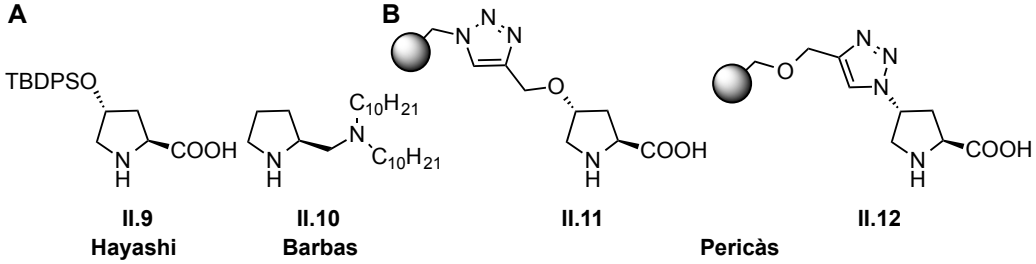

Figure II.3. Proline derivatives reported by Hayashi, Barbas and Pericàs.

[143] Machajewski, T. D.; Wong, C.-H. . *Angew. Chem. Int. Ed.* **2000**, *39*, 1352-1374.
[144] Córdova, A.; Nitz, W.; Barbas III, C. F. *Chem. Commun.* **2002**, 3024-3025.
[145] Hayashi, Y.; Sumiya, T.; Takahashi, J.; Gotoh, H.; Urushima, T.; Shoji, M. *Angew. Chem. Int. Ed.* **2006**, *45*, 958-961.
[146] Mase, N.; Nakai, Y.; Ohara, N.; Yoda, H.; Takabe, K.; Tanaka, F.; Barbas, C. F., III. *J. Am. Chem. Soc.* **2006**, *128*, 734-735.

In our research group, immobilized organocatalysts[71a-c] based on proline have been successfully applied to the direct aldol reaction in water with similar or even better performance than their monomeric counterparts[144-147] (**Scheme II.4**).

Our group has also demonstrated the beneficial effect of a triazole linker in polymer-supported proline-derived catalysts (**Figure I.3**, B).[71a-e,j] In this context, catalyst **II.11** provided better results than **II.12** in water, because it contains a 1,2,3-triazole moiety close to the catalytic site, which provides a hydrogen bond-based aqueous microphase around the hydrophobic polymer. This is probably correlated with water gelation in the presence of these catalysts and with aldol reactions taking place at a higher rate and improved stereoselectivity in the resulting aqueous environment (**Scheme II.4**).[71f]

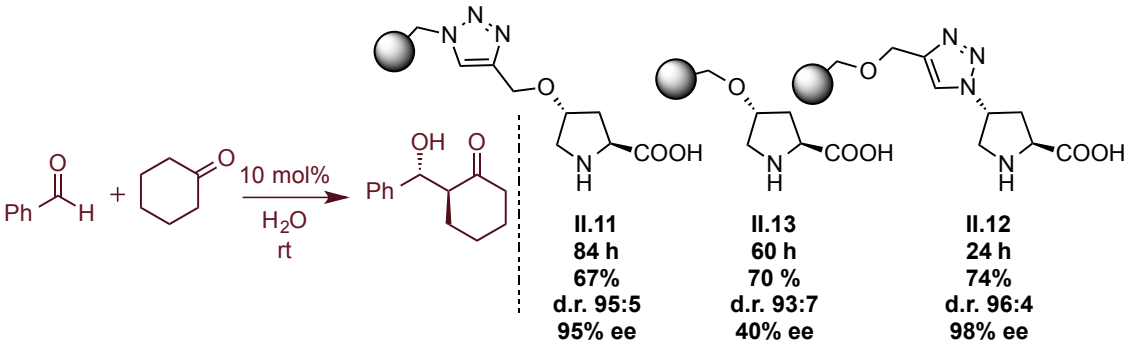

Scheme II.4. Influence of the triazole linker on the catalytic performance.

These PS-supported proline derivatives can be recovered by simple filtration, recycled and re-used. In addition, they have been efficiently employed in continuous flow processing.[71d]

[147] Hayashi, Y.; Aratake, S.; Okano, T.; Takahashi, J.; Sumiya, T.; Shoji, M. *Angew. Chem. Int. Ed.* **2006**, *45*, 5527-5529.

Chapter II

2.3. Aim of the project.

The experience of our group in the development of polymeric catalysts for sustainable chemical processes led to the idea of anchoring adaptable proline derivatives onto versatile polynorbornene supports to obtain multipurpose and robust insoluble polymer-supported organocatalysts for asymmetric transformations.

Following the approach introduced by our group, we will study the optimal anchoring strategy to the polynorbornene support. Two different approaches will be tested to obtain new polymeric families analogues to the polystyrene-based catalytic materials, previously reported in our group.

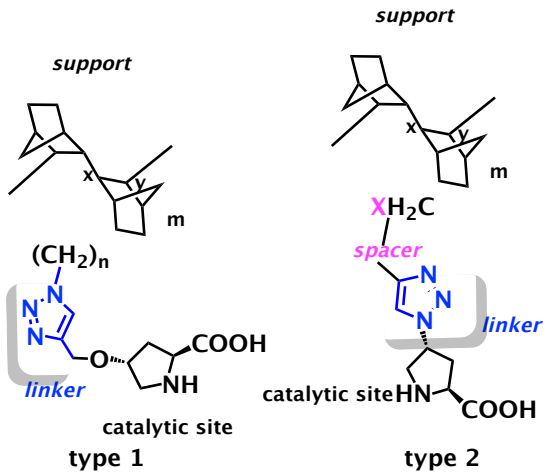

In the present project, we wish to establish the performance of polynorbornene-supported catalysts in asymmetric processes that take place in aqueous media.

To this end, the aldol reaction of aldehydes to ketones in aqueous media will be selected.

First of all, we will study the anchoring of L-proline derivatives onto the polynorbornene backbone, using the Cu-catalyzed azide-alkyne 1,3-dipolar cycloaddition.

Catalysis Science & Technology

PAPER

View Article Online
View Journal | View Issue

Published on 04 November 2014. Downloaded by Universitat Rovira I Virgili on 04/02/2015 08:21:23.

Cite this: *Catal. Sci. Technol.*, 2015, **5**, 754

Asymmetric organocatalysts supported on vinyl addition polynorbornenes for work in aqueous media†

Irina K. Sagamanova,[a] Sonia Sayalero,[a] Sheila Martínez-Arranz,[b] Ana C. Albéniz*[b] and Miquel A. Pericàs*[ac]

Received 15th October 2014,
Accepted 3rd November 2014

DOI: 10.1039/c4cy01344a

www.rsc.org/catalysis

In an effort to identify novel polymer architectures suitable for a covalent support for catalysts, L-proline derivatives have been immobilized onto rationally designed vinyl addition polynorbornene (VA-PNB) resins through copper-catalyzed azide–alkyne cycloaddition (CuAAC) reactions. These fully saturated resins have been found to be optimal catalyst supports, the resulting proline-functionalized resins behave as very active, easily recoverable and highly reusable organocatalysts for the asymmetric direct aldol reaction of benzaldehydes with ketones in aqueous media. The results show that, the combination of modular VA-PNB resins with proline derivatives and triazole linkers represents a promising strategy for the immobilization of organocatalytic species.

Introduction

With increasing concerns on sustainable characteristics of chemical processes, the use of polymer-supported catalysts in synthetic chemistry has considerably increased in recent years.[1] The covalent immobilization of catalytic species offers important advantages.[2] The catalytic activity of polymer-supported species is importantly determined by the accessibility of the catalytic sites to the reactants, and is modulated by mass transfer limitations. In this respect, various features of polymeric supports, such as the solubility/swellability profile, degree of functionalization and the possible involvement of the polymer backbone in the catalytic reaction, need to be considered.[3] Therefore, the choice of polymeric support is an essential issue because its structure and properties can importantly influence the course of chemical reactions mediated by catalysts immobilized onto it. As a matter of fact, no single polymer structure would be optimal for every conceivable synthetic application.[4] Despite this, a vast majority of applications reported to date rely on the use of polystyrenes as supports.[1] Recently, we have developed a straightforward route to functionalize vinyl addition (VA) polynorbornenes (PNBs).[5] In this approach, haloalkyl substituted norbornenes, which are prepared by Diels–Alder reactions of cyclopentadiene and terminal 1-haloalkenes, are co-polymerized with norbornene in the presence of $[Ni(C_6F_5)_2(SbPh_3)_2]$, and an intermediate ω-bromoalkyl substituted VA-PNBs are finally converted into the functional VA-PNBs by nucleophilic substitution (Scheme 1).[5]

In sharp contrast with polynorbornenes prepared by ring-opening metathesis polymerization (ROMP), VA-PNBs do not contain carbon–carbon double bonds in their skeletons. For this reason, the possibility of uncontrolled side reactions triggered by these skeletal functional groups, which could occur on ROMP-PNBs, is completely avoided in VA-PNBs (Fig. 1).

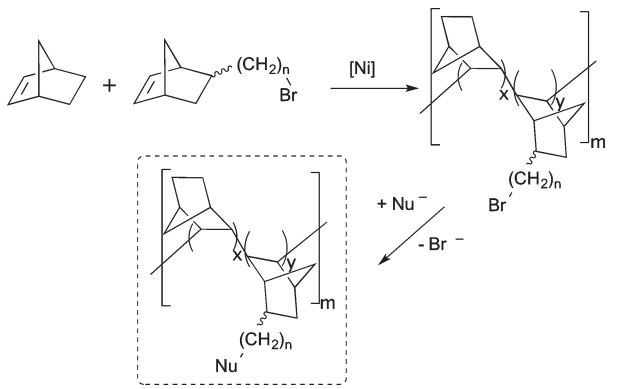

Scheme 1 Synthesis of functionalized VA-PNB polymers.

[a] *Institute of Chemical Research of Catalonia (ICIQ), Av. Països Catalans 16, 43007 Tarragona, Spain. E-mail: mapericas@iciq.es; Fax: (+34)977920244*
[b] *IU CINQUIMA/Química Inorgánica, Universidad de Valladolid, 47071 Valladolid, Spain. E-mail: albeniz@qi.uva.es*
[c] *Departament de Química Orgànica, Universitat de Barcelona, 08028 Barcelona, Spain*

† Electronic supplementary information (ESI) available: Preparation of compound **5**, screening of additives and solvent and temperature effects on the aldol reaction between **9a** and **10a**, recycling experiments, spectroscopic and chromatographic data of the aldol products, and characterization of the polymers are provided. See DOI: 10.1039/c4cy01344a

This journal is © The Royal Society of Chemistry 2015

UNIVERSITAT ROVIRA I VIRGILI
NEW APPROACHES TO CATALYST DESIGN AND IMMOBILIZATION
Irina Sagamanova

Chapter II

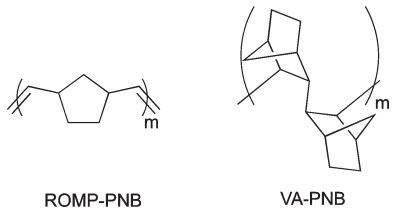

Fig. 1 General structures of ROMP-PNB and VA-PNB polymers.

Despite this potential limitation, ROMP-PNBs have been used as supports for the immobilization of reagents and catalysts.[4] In contrary, the chemically inert and fully saturated VA-PNB resins have not been evaluated, to date, for these applications.[6] Our previous experience in the development of polymer-supported, easily recyclable organocatalysts for chemical processes with improved sustainability characteristics[7] led to the idea of anchoring suitably functionalized proline derivatives onto VA-PNBs with the twin goal of assessing the suitability of these versatile polymers as inert supports for catalyst immobilization and developing new robust, efficient and recyclable organocatalysts for asymmetric transformations. Herein, we report the successful achievement of these goals through the application of novel functional polymers **1**–**2** (Fig. 2) as reusable catalysts for a highly stereoselective direct asymmetric aldol reaction in water.[8] The reported strategy opens up new path for supporting multiple-function catalytic systems onto fully saturated VA-PNB supports.

Results and discussion

Synthesis and characterization of the polynorbornene-supported catalysts

Previous studies on the covalent immobilization of proline derivatives onto polystyrene (PS) resins through 1,2,3-triazole linkers have shown that the triazole units appear to play an active and synergistic role in catalytic processes mediated by these species in aqueous solvents.[8c]

For similar immobilization approaches to be used in the present instance, first, either alkyne- or azide-functionalized VA-PNBs should be prepared. This has been carried out as illustrated in Scheme 2.

First, ω-bromoalkyl functionalized VA-PNBs (**3a**–**d**) were prepared by Ni-catalyzed copolymerization of norbornene and ω-bromoalkylnorbornenes, according to our previously reported procedure.[5] Two different lengths of the bromoalkyl chain (n = 1 and 4) were used to study the effect on the catalytic behavior of increased separations between the functional units and the polymer chain. For each bromoalkyl chain length, two levels of functionalization were studied. Interestingly, the functionalization level can be adjusted by varying the relative amounts of norbornene and ω-bromoalkylnorbornene used in the copolymerization. When a one-carbon spacer was used, the x/y ratio varied between 1.1 and 1.6. This corresponds in both cases to rather heavily functionalized resins. With the long spacer, in turn, the x/y composition ranged from 1.3 to 24.1, thus covering a broad range of functionalization. The composition of the copolymers (x/y ratio) was determined in all the cases by the analysis of the bromine content in the polymer. From the stereochemical point of view, the different ω-bromoalkylnorbornenes used for the preparation of the

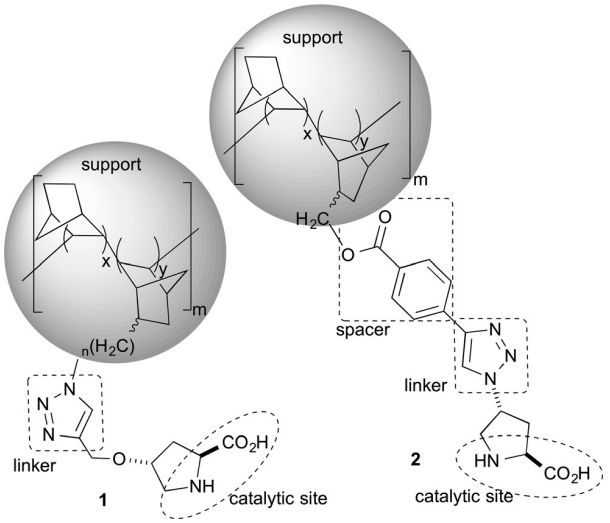

Fig. 2 Schematic design of the polynorbornene-supported prolines developed in this work.

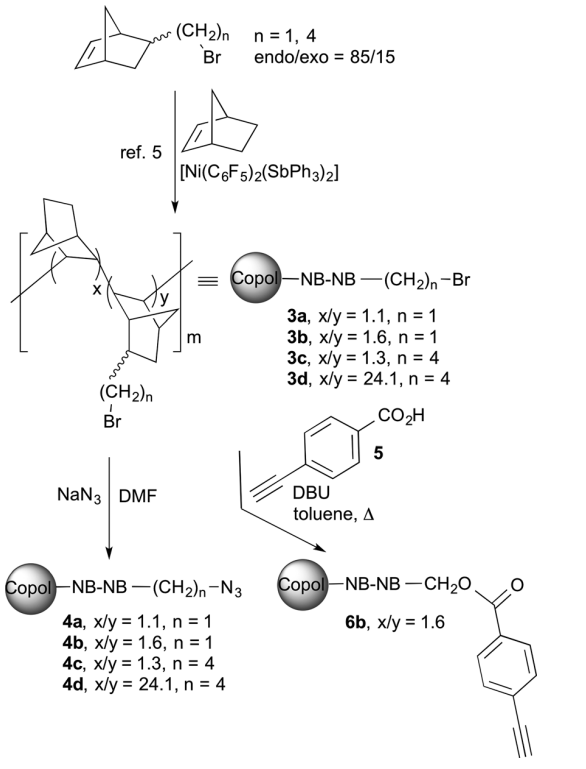

Scheme 2 Ready-to-click functional polymers employed in this study.

Published on 04 November 2014. Downloaded by Universitat Rovira I Virgili on 04/02/2015 08:21:23.

UNIVERSITAT ROVIRA I VIRGILI
NEW APPROACHES TO CATALYST DESIGN AND IMMOBILIZATION
Irina Sagamanova

Published on 04 November 2014. Downloaded by Universitat Rovira I Virgili on 04/02/2015 08:21:23.

copolymers are mixtures of *endo* (major) and *exo* (minor) stereoisomers in a ratio close to *endo* : *exo* = 85 : 15.

The azide functional group was introduced on these copolymers through nucleophilic substitution by treatment with sodium azide in DMF.[5] In this manner, ω-azidoalkyl VA-PNBs **4a–d** were readily prepared. On the other hand, the intermediate bromoalkyl VA-PNBs **3b** (x/y = 1.6; n = 1) was treated with *p*-ethynylbenzoic acid (**5**) and DBU in toluene under reflux to afford the alkynyl-functionalized resin **6b**. While the substitution of bromide by azide was essentially completed during the preparation of **4a–d**, the corresponding substitution by *p*-ethynylbenzoate leading to **6b** resulted in 31% unreacted bromomethyl groups present in **3b**. In any case, this was not problematic for the catalytic use of resins arising from **6b** because these residual $-CH_2Br$ groups turned out to be completely unreactive. The incorporation of the functional unit in polymer **6b** was monitored spectroscopically. Thus, the characteristic IR absorption bands for the ester and 4-ethynylphenyl groups became more intense as the reaction proceeded, while the C–Br absorption at 638 cm^{-1} was almost absent at the end of the process. Raman experiments also confirmed the presence of the alkyne (2109 cm^{-1}) and remaining Br (638 cm^{-1}) in the polymer. In addition, the ^{13}C NMR spectrum of the polymer confirmed the presence of 4-ethynylphenyl group.

For the preparation of the catalytic resins **1a–d**, diastereo- and enantiomerically pure (2*S*,4*R*)-*N*-Boc-4-propargyloxyproline **7** (ref. 7*b*) was used as the partner for resins **4a–d** in copper-catalyzed alkyne–azide cycloaddition (CuAAC) reactions (Scheme 3, left).[9] After deprotection with trifluoroacetic acid in dichloromethane, the target prolines immobilized onto VA-PNB supports **1a–d** were obtained.

Catalyst **2**, was readily prepared from copolymer **6b** (Scheme 3, right). First, the alkynyl functionalized polymer was transformed into a fully protected form of the organocatalyst by a CuAAC reaction with the diastereo- and enantiomerically pure azido derivative **8**.[8c] Then, deprotection with trifluoroacetic acid (TFA) in dichloromethane of *N*-Boc and *t*-butyl ester groups led to the ready-to-act catalytic resin **2**.

It is interesting to note that, while VA-PNBs **6b** is a white solid, soluble in common aprotic solvents of medium polarity, the copolymer **2** generated in the click reaction is completely insoluble in the above mentioned media. This change in properties is of particular interest in connection with the recovery and reuse of the immobilized catalyst **2**. A similar behavior was observed during the preparation of ω-azidoalkyl VA-PNBs from the corresponding ω-bromoalkyl precursors.[5] In addition to the structural changes introduced by the new substituent, a modification of the conformational behavior of the rigid bicyclic units in the polymer backbone during the cycloaddition and deprotection processes could also contribute to this change in solubility behavior.[10]

The incorporation of the functional proline derivatives onto the copolymers *via* the formation of a 1,2,3-triazole linker could be easily followed by IR spectroscopy. For catalysts **1a–d**, the characteristic IR absorption bands for the *N*-Boc and *t*-butyl ester groups (*ca.* 1737, 1699; *ca.* 1392, 1365 cm^{-1}) were present after the click reaction, whereas the stretching band of the azido group (*ca.* 2091 cm^{-1}) had completely disappeared. The presence of the free amino acid after the deprotection step was also confirmed spectroscopically (1615–1631 cm^{-1}). In case of catalyst **2**, the characteristic IR absorption bands for the *t*-butyl groups (*ca.* 1392,

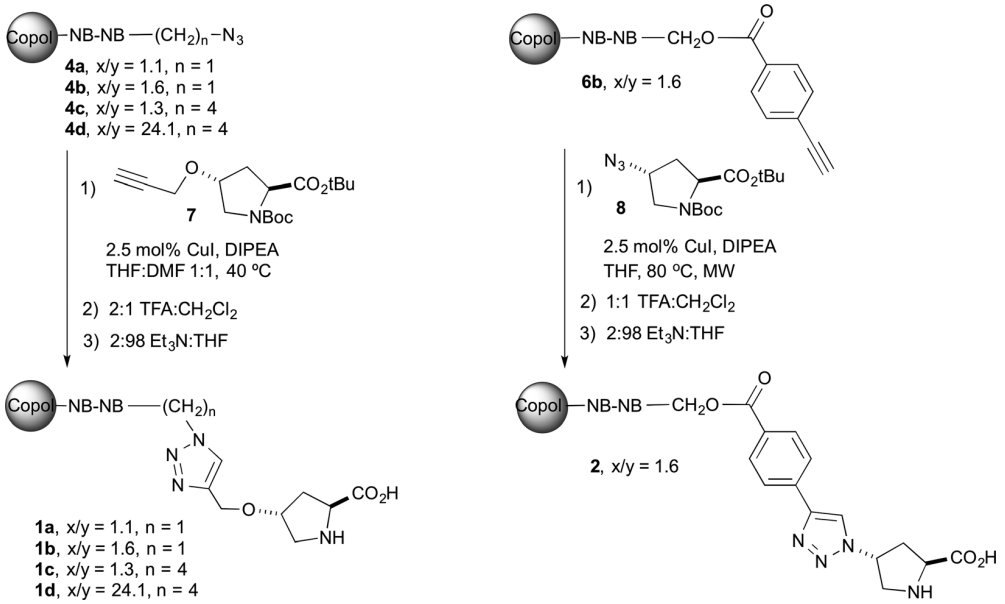

Scheme 3 Preparation of the VA-PNB immobilized catalysts **1a–d** and **2**.

This journal is © The Royal Society of Chemistry 2015

View Article Online

Published on 04 November 2014. Downloaded by Universitat Rovira I Virgili on 04/02/2015 08:21:23.

1365 cm^{-1}) and the ester group in the *p*-ethynylbenzoate fragment (C═O, 1709 cm^{-1}) were present after the click reaction.

Table 1 summarizes the preparation of the copolymer-supported organocatalysts **1a–d** and **2**, as well as the composition, functionalization (f),[11,12a] yield[12b] and equilibrium swelling ratio (SR).[13] As a general trend, the overall yield for the click reaction and deprotection steps in the preparation of **1a–d** was determined to be in the range of 83–95%. Surprisingly, the more intensely functionalized copolymers (**1a** and **1c**) lead to the highest incorporation of catalytic unit (yield column). On the other hand, the modification of the length of the alkyl spacer connecting the polymer backbone with the functional units (n = 1 or 4) had a little effect on the final functionalization yields (compare entries 1–2 and 3–4). In any case, and as we will see later, **1b** presented optimal characteristics in catalysis.

The preparation of catalyst **2**, in which the complementary click approach was used (alkyne on resin plus soluble azide), was slightly less efficient. As already discussed, the incorporation of *p*-ethynylbenzoate fragment to the bromomethyl substituted VA-PNB **3b** is not complete (*ca.* 69%). In addition, the click reaction and deprotection process required for the incorporation of the catalytic units also has slight low efficiency, and the functionalization of the final resin indicates overall yields of 49% (from **3b**) or 75% (from **6b**). The occurrence of some solvolytic ester cleavage during the final deprotection step could explain the decrease in yield for **6b**. Solvent uptake data, using different solvents, (water, dimethyl sulfoxide and dichloromethane) indicate the swelling ability of the copolymers. The equilibrium swelling ratio (SR) measured for each solvent shows that copolymers **1** and **2** swelled better in dichloromethane than in water, while dimethyl sulfoxide afforded an intermediate result. These data correlate well with the experimental results described in the following section.

Taking into account the close relationship between physical surface properties of supported catalysts and its catalytic performance, the surface morphology of the new polymers was examined by SEM microscopy. Very interestingly, VA-PNBs supported catalysts **1a–c** with a high functionalization level (x/y = 1.1–1.6) show a more porous surface compared to catalyst **1d** (Fig. 3). Similarly, polymer **2** shows a porous surface comparable to that of **1b** (Fig. 4).

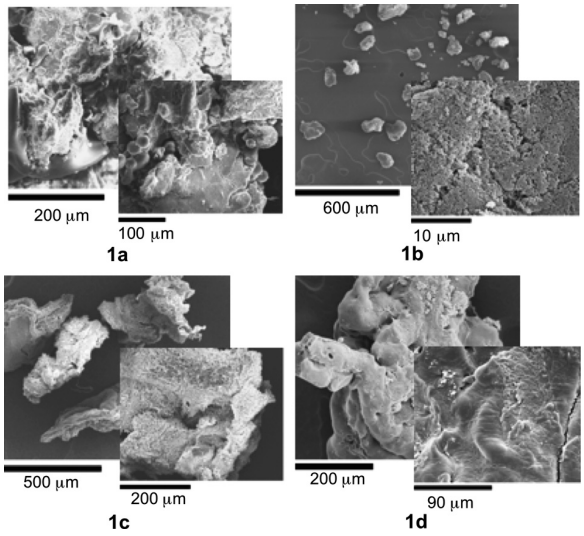

Fig. 3 SEM images of VA-PNB supported organocatalysts **1a–d**.

Asymmetric aldol reaction mediated by catalysts 1a–d

For the optimization of reaction conditions, we centered our attention on the use of benign reaction media (DMSO, water, and their binary mixtures) and on work under neat conditions with catalysts **1a** and **1b**. The reactions were performed at room temperature with a 10 mol% catalyst loading. The results of this study are summarized in Table 2. A complete information of the solvent optimization studies performed can be found in the ESI.†

With both the catalysts, optimal performance regarding yield (97–99%) and stereoselectivity (89 : 11 to 91 : 9 *anti* : *syn* ratio, 90–91% ee) was achieved in DMSO/water 83 : 17 mixtures (entries 4 and 9). Reactions in pure DMSO (entries 1 and 6) or in pure water (entries 2 and 7) led to decreased conversions and enantioselectivities, as the use of higher amounts of water also showed the same result (entries 3 and 8). This behavior is similar to that of organocatalytic aldol reactions mediated by PS-proline immobilized through triazole linkers.[8b] Moreover, in that case, the use of binary mixtures of polar aprotic solvents and water had positive effects,[14] importantly increasing both the reaction rate and enantioselectivity.[7c,8]

Similarly, the optimal solvent composition (DMSO/water 83 : 17) represents an optimal balance between ability for

Table 1 Characterization of polynorbornene-supported organocatalysts **1–2**

Entry	Cat.	x/y[a]	n[b]	f_0[c,d] (mmol g^{-1})	f_{max}[e] (mmol g^{-1})	f[d] (mmol g^{-1})	Yield[e] (%)	SR[f] (%)		
								H_2O	DMSO	CH_2Cl_2
1	**1a**	1.1	1	3.08	2.02	1.80	90	270	370	490
2	**1b**	1.6	1	2.37	1.69	1.47	87	290	430	600
3	**1c**	1.3	4	2.96	1.97	1.88	95	360	440	590
4	**1d**	24.1	4	0.48	0.44	0.37	83	170	280	370
5	**2**	1.6	1	2.98[g]	1.79	0.87	49	210	410	590

[a] x/y = NB/NB$(CH_2)_n$X ratio in the starting copolymer. [b] Chain length of the alkyl spacer in the functional norbornene monomer (NB$(CH_2)_n$X). [c] Functionalization of the starting copolymer (**4a–d** for **1a–d**, and **3b** for **2**). [d] Calculated from the results of elemental analysis. See ref. 11. [e] Calculated with the formula given in ref. 12. [f] Determined gravimetrically. See ref. 13 and ESI. [g] Determined by quantitative analysis of bromine in **3b**. See ref. 11.

View Article Online

Published on 04 November 2014. Downloaded by Universitat Rovira I Virgili on 04/02/2015 08:21:23.

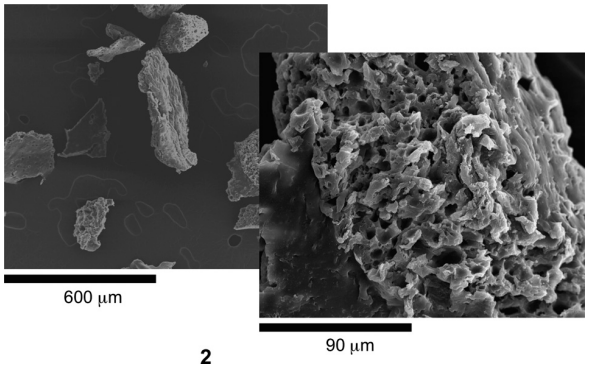

Fig. 4 SEM images of VA-PNB supported organocatalyst **2**.

establishing a hydrogen bond network and VA-PNB swelling.[8c] The combination of **1b** and this solvent mixture (entry 9) exhibited a slightly better profile and, for this reason, its use in combination with acidic additives (entries 10 and 11) was also studied. The best result (96 : 4 *anti* : *syn* ratio, 96% ee, entry 11) was achieved with trifluoroacetic acid (10 mol%), and attempts to further accelerate the reaction at higher temperatures (see ESI†) did not lead to any practical improvement.

When the reaction was performed under solvent free conditions, very low conversion and moderate stereoselectivity were observed (entries 5 and 12). However, performing the reaction in a ball-mill,[15] with the use of *p*-nitrobenzaldehyde and cyclohexanone in essentially stoichiometric amounts, resulted in significantly better conversion after a notably short reaction time, although the recorded stereoselectivity continued to be only moderate (entry 13).

It is apparent from these optimization studies that the best reaction conditions was using 10 mol% of the catalyst in combination with 10 mol% of TFA as an additive, a mixture of DMSO : H_2O (87 : 13) as solvent and performing the reactions at room temperature. Next, the transferability of these conditions was checked by performing the reaction of **9a** with **10a** under catalysis by **1a–d** (Table 3). Catalysts **1a**, **1b** and **1c** showed similar behavior in terms of conversion, diastereo- and enantioselectivity (entries 1–3). Copolymer **1d**, in turn, led to considerably lower conversion and decreased stereoselectivity (entry 4). This provides a clear indication that the

Table 3 Benchmarking of VA-PNB supported catalysts **1a–d** in the aldol reaction of cyclohexanone with *p*-nitrobenzaldehyde[a]

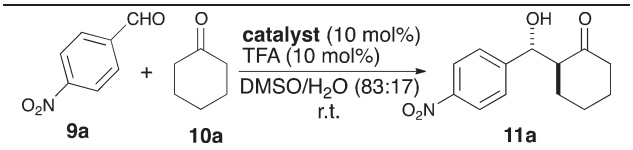

Entry	Cat.	Time (h)	Conv.[b] (%)	Yield[c] (%)	*anti* : *syn*[b]	ee *anti*[d] (%)
1	**1a**	23	95	88	96 : 4	96
2	**1b**	23	96	90	96 : 4	96
3	**1c**	23	93	80	96 : 4	96
4	**1d**	23	43	38	89 : 11	85
5	**1b**[e]	42	73	64	96 : 4	96
6	**1b**[f]	13	95	91	96 : 4	96

[a] Reactions were performed with resin **1** (0.015 mmol), **9a** (0.15 mmol), **10a** (0.75 mmol) in DMSO/water (83 : 17, 54 μL). [b] By ^{1}H NMR on the reaction crude. [c] Combined yield of isolated *anti* : *syn* diastereomers. [d] By chiral HPLC. [e] 5 mol% catalyst used. [f] 20 mol% catalyst used.

Table 2 Solvent effect on the aldol reaction of cyclohexanone with *p*-nitrobenzaldehyde catalyzed by polymers **1a–b**[a]

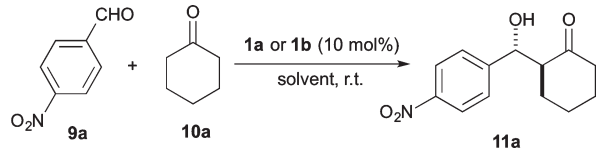

Entry	Cat.	Solvent	Time (h)	Conv.[b,c]	*anti* : *syn*[b]	ee *anti*[d] (%)
1	**1a**	DMSO	21	61	74 : 26	91
2	**1a**	H_2O	21	74	71 : 29	73
3	**1a**	DMSO/H_2O (50/50)	21	94	81 : 19	85
4	**1a**	DMSO/H_2O (83/17)	16	100 (97)	89 : 11	90
5	**1a**	Neat	21	10	77 : 23	76
6	**1b**	DMSO	21	82	76 : 24	92
7	**1b**	H_2O	21	81	79 : 21	78
8	**1b**	DMSO/H_2O (50/50)	21	96	86 : 14	93
9	**1b**	DMSO/H_2O (83/17)	19	100 (98)	91 : 9	91
10	**1b**	DMSO/H_2O (83/17)[e]	21	100 (97)	92 : 8	93
11	**1b**	DMSO/H_2O (83/17)[f]	21	99 (90)	96 : 4	96
12	**1b**	Neat	21	17	77 : 23	75
13	**1b**	Neat[g]	6.5	94	78 : 22	76

[a] Reactions were performed with **1a** or **1b** (0.015 mmol), *p*-nitrobenzaldehyde (**9a**, 0.15 mmol) and cyclohexanone (**10a**, 0.75 mmol) in the indicated solvents (54 μL). [b] By ^{1}H NMR on the reaction crude. [c] The combined yield of isolated diastereomers is given in parentheses. [d] By chiral HPLC. [e] *p*-Nitrobenzoic acid (0.022 mmol) was used as an additive. [f] Trifluoroacetic acid (0.015 mmol). [g] Reaction performed in a ball-mill: **9a** (89 mg, 0.59 mmol), **10a** (67 μL, 0.65 mmol), **1b** (40 mg, 0.059 mmol) and 60 zirconium oxide balls, rotation speed of 250–400 rpm.

This journal is © The Royal Society of Chemistry 2015

Published on 04 November 2014. Downloaded by Universitat Rovira I Virgili on 04/02/2015 08:21:23.

functionalization level of the catalytic polymers (**1d** is considerably less functionalized than **1a–c**) has a significant influence on their performance. An examination of the effect of the amount of catalyst **1b** (entries 5–6) showed that catalyst loading could be reduced to 5 mol%, but at the expense of increased reaction times. Thus, after 42 h the conversion was only 73%, while diastereoselectivity and enantioselectivity were maintained at the same level (entry 5). Conversely, when 20 mol% of the catalyst was used (entry 6), a considerable increase in reaction rate was observed, the process was essentially completed in only 13 h.

Then, we explored the applicability of **1b** with respect to the aldehyde reaction partners. As it can be seen in Scheme 4, a wide range of aromatic aldehydes can effectively participate in this reaction, affording the *anti*-aldol products in very high yields and with both high diastereo- and enantioselectivity. As a general trend, the reactions performed in the absence of TFA additive required slightly longer reaction times. Although higher yields were normally achieved in the absence of TFA, stereoselectivity was slightly eroded in these experiments (**11a, f–g, i–j**); therefore, the convenience of using this additive has to be evaluated in each particular case.

These results show that VA-PNB supported proline **1b** works in close parallelism to other amphiphilic polymeric proline derivatives, which have proven to be efficient catalysts for the asymmetric aldol reactions of ketones and benzaldehydes in aqueous reaction conditions,[7c,8b,c,16] and even outperforms the first reported monomeric proline derivative exhibiting aldolase-like behavior.[17]

Asymmetric aldol reaction mediated by catalyst 2

Catalyst **2** was designed with the goal of increasing the catalytic activity and stereoselectivity depicted by **1a–c**. We anticipated that the structural changes introduced in **2** would modify the hydrophobic/hydrophilic balance in the amphiphilic catalyst, leading to a higher catalytic activity in water and to higher levels of stereocontrol in this reaction media.[8,18]

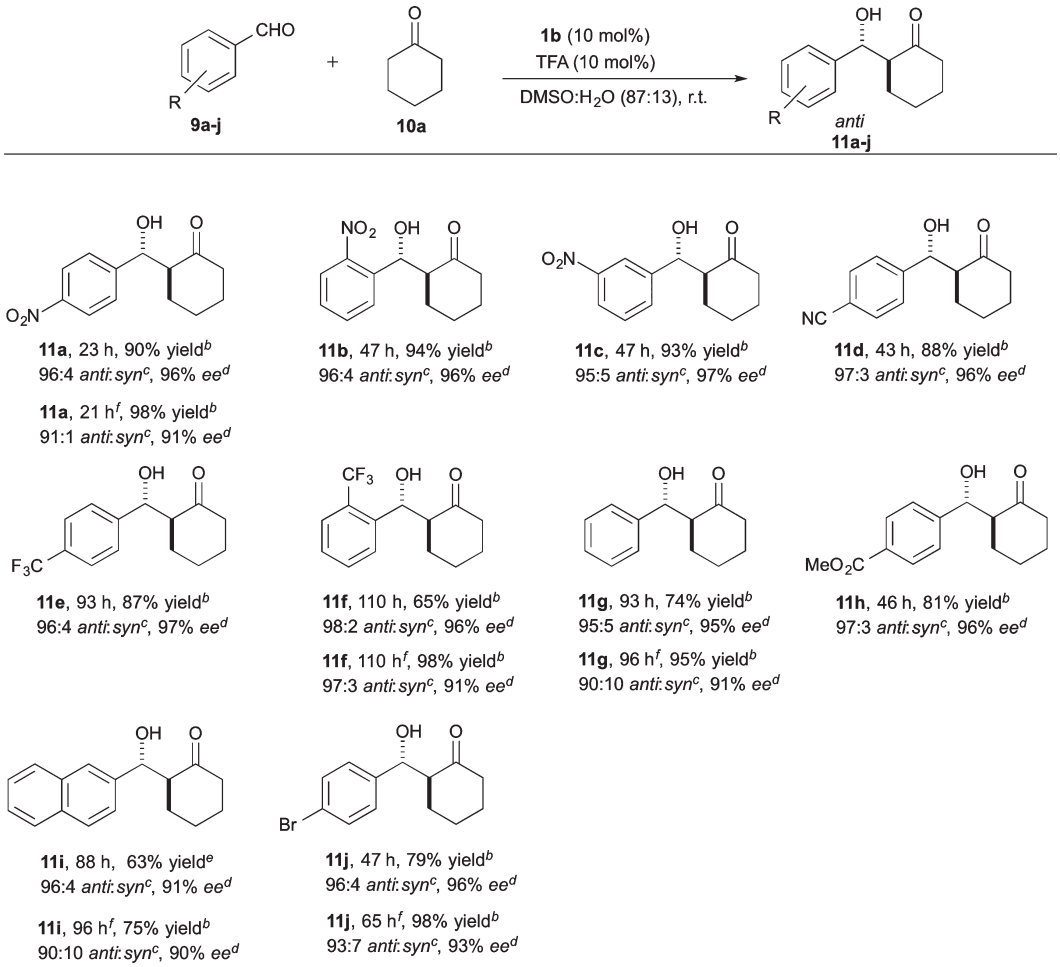

Scheme 4 Substrate scope of the aldol reaction catalyzed by 1b. [a]Reaction conditions: aldehyde (0.15 mmol), **10a** (0.75 mmol), **1b** (10.2 mg, 0.015 mmol), TFA (0.015 mmol) in DMSO : H_2O (83 : 17, 54 μL) at room temperature. [b]Combined yield of the isolated diastereomers. [c]By ^{1}H NMR on the reaction crude. [d]By chiral HPLC of **11**. [e]Isolated yield of *anti* isomer. [f]Without TFA additive.

UNIVERSITAT ROVIRA I VIRGILI
NEW APPROACHES TO CATALYST DESIGN AND IMMOBILIZATION
Irina Sagamanova

Published on 04 November 2014. Downloaded by Universitat Rovira I Virgili on 04/02/2015 08:21:23.

As a common characteristic, proline and pyrrolidine derivatives, which were able to catalyze aldol reactions in aqueous media, display a well differentiated molecular regions with hydrophobic and hydrophilic characters, as it is known for type-I aldolases. In polymer-supported prolines, the extended polymer backbone efficiently mimics the hydrophobic pocket of the natural enzymes, while the functional units provide the hydrophilic environment, in which the reaction takes place. The same behavior could be expected in case of copolymer **2**. According to precedents,[8c] the triazole unit could play the role of grafting the proline unit onto the polymer and allowing the formation of a hydrogen bond network connecting the linker with the amino and carboxy groups in the catalytic unit. In addition, the *p*-phenylene spacer present in **2** could also improve the catalyst activity and stereoselectivity because of the increased separation between the hydrophilic, catalytically active moiety and the hydrophobic polymer backbone, as previously noted with polystyrene-supported prolines.[7c] The study of the catalytic behavior of **2** in water was initiated using *p*-nitrobenzaldehyde (**9a**) and cyclohexanone (**10a**) as model substrates in the aldol addition (see ESI† for details). Pleasingly, the reaction nicely proceeded in water, affording aldol **11a** in 22 h with excellent yield (90%) and stereoselectivity (95 : 5 *anti* : *syn* ratio, 96% ee). Identical stereoselectivity was recorded when the reaction was conducted in DMSO : H_2O (50 : 50) or DMF : H_2O (50 : 50) mixtures. In these solvent mixtures, a slightly improved yield (95%) was recorded. In practice, a (50 : 50) mixture of DMF and water was the solvent of choice for these reactions. In this media, the reactions catalyzed by **2** provided the aldol adducts **11a–l** with excellent yield and stereoselectivity, in shorter reaction times compared with catalyst **1b** and without the need of acid (Scheme 5). Thus, it appears that the combination of the polynorbornene skeleton, the *p*-phenylenecarboxylate spacer and the triazole linker leads to a significant improvement in the catalytic activity of the proline unit in aqueous media. Reactions involving cyclopentanone (**10b**) and 4-pyranone (**10c**) as pronucleophiles were remarkably fast, providing the corresponding *anti*-aldol products **11k–l** in very high yield and good stereoselectivity.[15b,16d,19] In general, the products **11** were obtained in high purity after a simple filtration (to recover **2**), extraction with dichloromethane followed by evaporation, with no further purification being required. On the negative side, when **2** was used in the aldol reactions of *p*-nitrobenzaldehyde (**9a**) with acyclic ketones, such as acetone and hydroxyacetone, under the optimized conditions as shown in Scheme 5, very low conversions (<5%) were recorded after 48 h.

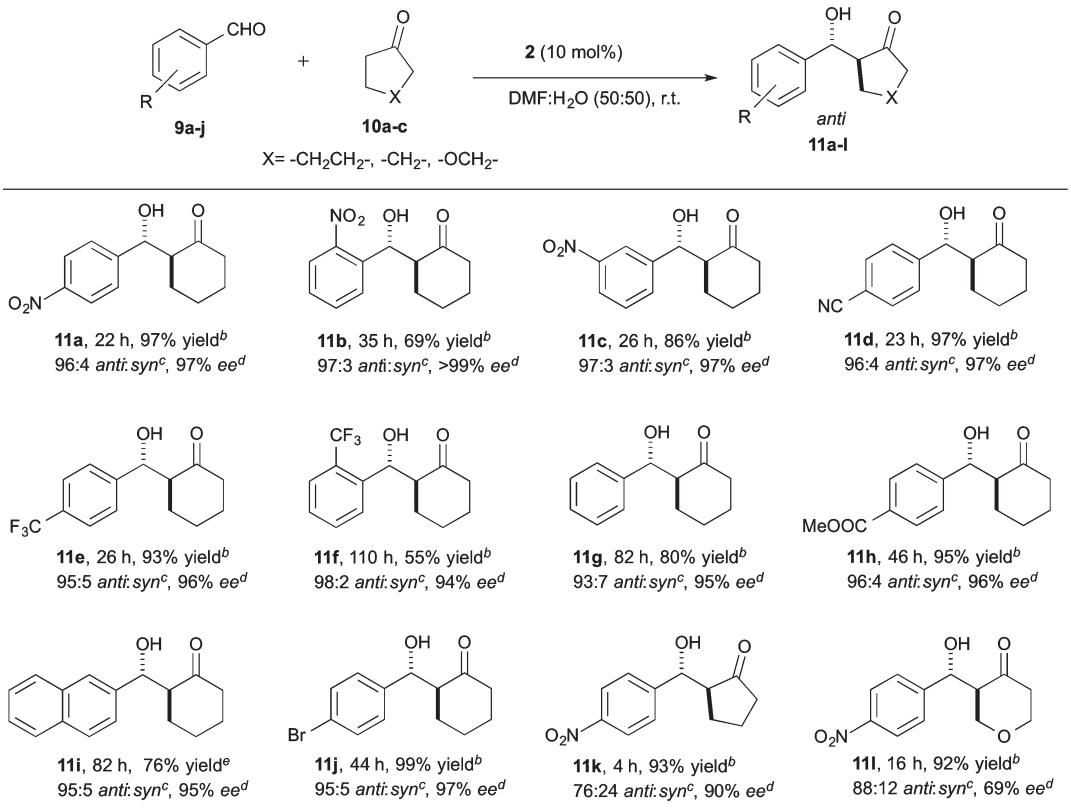

Scheme 5 Substrate scope of the aldol reaction catalyzed by **2**. [a]Reaction conditions: **9a–j** (0.15 mmol), **10a–c** (0.75 mmol), and **2** (17 mg, 0.015 mmol) in DMF : H_2O (50 : 50, 54 μL) at room temperature. [b]Combined yield of the isolated diastereomers after flash chromatography. [c]By ^1H NMR on the reaction crude. [d]By chiral HPLC of **11**. [e]Isolated yield of *anti* isomer.

This journal is © The Royal Society of Chemistry 2015

Published on 04 November 2014. Downloaded by Universitat Rovira I Virgili on 04/02/2015 08:21:23.

Catalysts recycling and reuse

To show the recyclability of the polymers **1b** and **2**, two series of experiments were planned, in which single samples of these catalytic copolymers were repeatedly used at a constant reaction time to mediate the aldol addition of cyclohexanone (**10a**) to *p*-nitrobenzaldehyde (**9a**) leading to **11a**. The results of these studies are summarized in Fig. 5. The insoluble nature of the polymer allows the catalyst recovery by performing a simple filtration. Thus, after each run, the catalyst was readily recovered from the reaction mixture, washed and reused in the next reaction cycle (see ESI†).

Copolymer **1b** was recycled seven times affording the aldol product with constant stereoselectivity and only a marginal decrease of catalytic activity in every cycle was observed. IR analysis of the catalyst after recycling did not show any difference with the initial polymer. In an attempt to understand the origin of the observed decrease in catalytic activity, SEM studies were performed to monitor the changes in the catalyst surface morphology. Compared with fresh catalyst **1b**, a very similar surface morphology was observed after the seventh run. This observation indicates that **1b** does not experience structural collapse with repeated use. On the other hand, it was found that the %N determined by elemental analysis decreased after recycling, which was indicative that leaching of catalytic proline units from the copolymer backbone takes place to some extent. Catalyst **2**, on the contrary, could be recycled and reused for at least seven runs *without any appreciable loss in yield or in stereoselectivity*. The polymer presented similar IR spectra and the same surface morphology before and after recycling.

Furthermore, it was observed that the %N determined by elemental analysis remained unchanged after recycling (see ESI†). Thus, it is clear that the presence of the *p*-phenylenecarboxylate spacer has a notable and very positive effect on the chemical stability of the polynorbornene-supported organocatalyst.

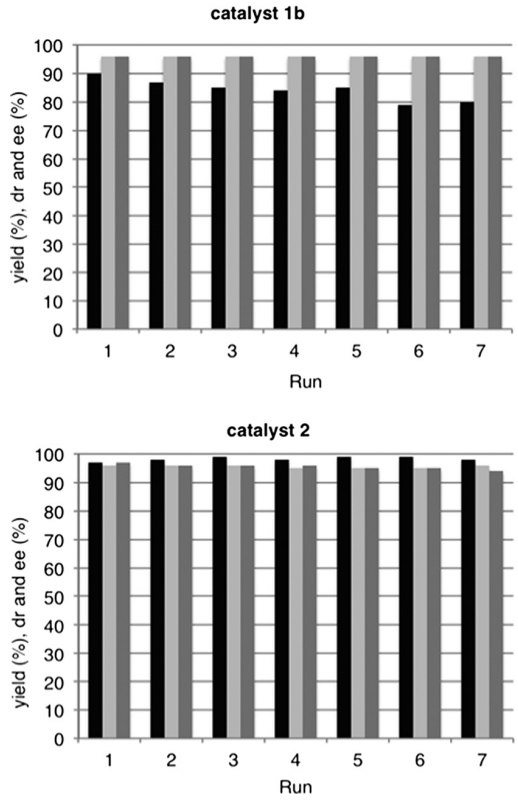

Fig. 5 Catalyst recycling experiments in the aldol addition of cyclohexanone (**10a**) to *p*-nitrobenzaldehyde (**9a**) leading to **11a** under optimized conditions with catalysts **1b** and **2**. Black bars: yield (%); pale gray bars: dr; gray bars: ee (%).

Conclusions

In summary, we have successfully developed a family of modified prolines anchored onto VA-PNBs through two complementary alkyne–azide click reactions. The versatility of these species as organocatalysts has been also illustrated by their application in asymmetric aldol additions of ketone pronucleophiles to aromatic aldehydes under a variety of reaction conditions. Polynorbornene-supported proline has shown excellent performance in this particular aldol transformation in an aqueous environment, and the robustness of the new polymeric catalysts has been demonstrated by the possibility of extending its use to seven cycles in the aldol reaction of cyclohexanone and *p*-nitrobenzaldehyde. These results show that VA-PNBs can be considered as viable alternatives to well-established polystyrene resins as supports for the immobilization of catalysts. In addition, the absence of unsaturation in the polymer backbone of VA-PNBs should make these polymers transparent to UV light, and therefore could greatly facilitate the use of catalysts supported on these resins in photocatalytic processes. Furthermore, the applications of VA-PNBs as catalyst supports, dictated by the structural characteristics of these copolymers, are now in progress in our laboratories.

Experimental section

Synthesis of catalysts 1a–d

1a. *t*-Butyl (2*S*,4*R*)-*N*-Boc-4-propargyloxyprolinate **7** (600 mg, 1.84 mmol), *N*,*N*-diisopropylethylamine (2.5 mL, 14.20 mmol) and copper(I) iodide (6.7 mg, 0.035 mmol) were added to a suspension of copolymer **4a** (Copol–NB–$NBCH_2N_3$ x/y = 1.1 : 1, n = 1; 460 mg, f = 3.084 mmol g^{-1}) in a DMF : THF 1 : 1 mixture was (9 mL) placed in a flask under N_2. The reaction mixture was shaken at 40 °C for 24 h, the reaction progress was monitored by FTIR. When the IR band of the azido group had completely disappeared, the polymer was collected by filtration, sequentially washed with H_2O (40 mL), THF (40 mL), THF–MeOH (40 mL), MeOH (40 mL), THF (40 mL) and CH_2Cl_2 (50 mL) and dried under reduced pressure at 40 °C for 24 h. The intermediate polynorbornene-supported *t*-butyl prolinate, which was obtained as a white solid (892 mg,

Published on 04 November 2014. Downloaded by Universitat Rovira I Virgili on 04/02/2015 08:21:23.

97% yield) [FTIR (ATR, neat): ν 2941, 2868, 1738 (C═O), 1699 (C═O), 1476, 1453, 1393 (*t*-butyl), 1393 (*t*-butyl), 1254, 1366 cm^{-1}. Elemental analysis (%): calcd.: N, 8.63. Found: N, 8.51; f = 1.52 mmol g^{-1}], was directly submitted to the deprotection process. To this end, the prolinate (870 mg) was swollen in CH_2Cl_2 (10 mL), after 10 min TFA was added (20 mL) and the mixture was shaken at room temperature. When the IR bands of the *t*-butyl and carbonyl moieties in the protecting groups had completely disappeared, the reaction mixture was filtered off and the polymer was sequentially washed with THF (with 2% of Et_3N, 50 mL), H_2O (50 mL), THF (50 mL), THF–MeOH 1 : 1 (50 mL), MeOH (50 mL), THF (50 mL) and CH_2Cl_2 (50 mL). The solid was dried under reduced pressure at 40 °C for 24 h (648 mg, 98% yield). FTIR (ATR, neat): ν 3409 (COOH), 2942, 2866, 1622 (C═O), 1450, 1371, 1317, 1219, 1154 cm^{-1}. Elemental analysis (%): calcd.: N, 11.37; found: N, 10.06; f = 1.80 mmol g^{-1}. Catalysts **1b**, **1c** and **1d** were synthesized in the same manner, starting from the corresponding azido-copolymer.

1b. The intermediate polynorbornene-supported *t*-butyl prolinate (a white solid) was obtained from 7 (1.0 g, 3.08 mmol), *N*,*N*-diisopropylethylamine (4.2 mL, 23.70 mmol), copper(I) iodide (10 mg, 0.059 mmol) and copolymer **4b** (Copol–NB–$NBCH_2N_3$ x/y = 1.6 : 1, n = 1; 1.0 g, f = 2.37 mmol g^{-1}) in DMF : THF 1 : 1 (12 mL) after 22 h reaction in 95% yield (1.69 g). [FTIR (ATR, neat): ν 2943, 2867, 1737 (C═O), 1699 (C═O), 1476, 1453, 1392 (*t*-butyl), 1365 (*t*-butyl), 1255, 1217 cm^{-1}. Elemental analysis (%): calcd.: N, 7.50. Found: N, 7.67; f = 1.37 mmol g^{-1}]. Then final catalytic polymer **1b** (1.18 g, 99% yield) was obtained by shaking the intermediate prolinate (1.50 g) in CH_2Cl_2 (15 mL) with TFA (30 mL). FTIR (ATR, neat): ν 3430 (COOH), 2942, 2867, 1631 (C═O) cm^{-1}. Elemental analysis (%): calcd.: N, 9.47. Found: N, 8.26; f = 1.47 mmol g^{-1}.

1c. The polynorbornene-supported *t*-butyl prolinate (a white solid) was obtained from 7 (292 mg, 0.89 mmol), *N*,*N*-diisopropylethylamine (1.2 mL, 6.90 mmol), copper(I) iodide (3.3 mg, 0.017 mmol) and copolymer **4c** (Copol–NB–$NBCH_2N_3$ x/y = 1.3 : 1, n = 1; 233 mg, f = 2.96 mmol g^{-1}) in DMF : THF 1 : 1 (6 mL) after 23 h reaction in 98% yield (464 mg). [FTIR (ATR, neat): ν 2934, 2865, 1738 (C═O), 1698 (C═O), 1476, 1454, 1393 (*t*-butyl), 1365 (*t*-butyl), 1255, 1218 cm^{-1}. Elemental analysis (%): calcd.: N, 8.46. Found: N, 8.75; f = 1.56 mmol g^{-1}]. Then final catalytic polymer **1c** (365 mg, 98% yield) was obtained by shaking the intermediate prolinate (440 mg) in CH_2Cl_2 (4 mL) with TFA (8 mL). FTIR (ATR, neat): ν 3416 (COOH), 2933, 2863, 1625 (C═O) cm^{-1}. Elemental analysis (%): calcd.: N, 11.04. Found: N, 10.56; f = 1.88 mmol g^{-1}.

1d. The polynorbornene-supported *t*-butyl prolinate (a white solid) was obtained from 7 (61 mg, 0.19 mmol), *N*,*N*-diisopropylethylamine (250 mL, 1.43 mmol), copper(I) iodide (1 mg, 5.74 mmol) and copolymer **4d** (Copol–NB–NB-$(CH_2)_4N_3$ x/y = 24.1 : 1, n = 4; 300 mg, f = 0.478 mmol g^{-1}) in DMF : THF 1 : 1 (2 mL) after 24 h reaction in 92% yield (320 mg). [FTIR (ATR, neat): ν 2940, 2865, 1743 (C═O), 1707 (C═O), 1451, 1392 (*t*-butyl), 1366 (*t*-butyl), 1255, 1218 cm^{-1}. Elemental analysis (%): calcd.: N, 2.31. Found: N, 1.91; f = 0.34 mmol g^{-1}]. Then, final catalytic polymer **1d** (280 mg, 98% yield) was obtained by shaking the intermediate prolinate (300 mg) in CH_2Cl_2 (4 mL) with TFA (8 mL). FTIR (ATR, neat): ν 2940, 2864, 1620 (C═O) cm^{-1}. Elemental analysis (%): calcd.: N, 2.48. Found: N, 2.09; f = 0.37 mmol g^{-1}.

Synthesis of polymer 6b

Bromoalkyl polynorbornene **3b** (Copol–NB–$NBCH_2Br$, x/y = 1.6 : 1, 330 mg, f = 2.98 mmol g^{-1}), toluene (21 mL), *p*-ethynylbenzoic acid (**5**, 393 mg, 2.69 mmol) and DBU (0.41 mL, 2.69 mmol) were mixed in a flask under N_2, and the mixture was heated under reflux for 22 h. The solvent was evaporated and MeOH was added (30 mL). A solid appeared, which was stirred for 30 min, filtered, washed with MeOH (2 × 30 mL) and dried under reduced pressure at 40 °C for 24 h. Compound **6b** was obtained as a white solid (375 mg) soluble in dichloromethane or THF, which contained 73.3 mg of Br per g of copolymer, indicating that the substitution level has been of 69%. ^{13}C NMR (gel-phase, 126 MHz, $CDCl_3$): δ 166.3 (C═O), 132.2, 130.6, 129.6, 126.9, 83.0 (C═C), 80.2 (C═C), 56–52.8 (br), 52.2–50.2 (br), 47.9–45.9 (br), 43.7–41.6 (br), 40.2–38.6 (br), 36.8–34.4 (br), 32.2–31.0, 30.6–29.0 (br), 28.7–28.3 (br) ppm. Raman: ν 2100 (C═C), 1720, 1600, 638 (C–Br) cm^{-1}. FTIR (ATR, neat): ν 3301 (═CH), 2942, 2866, 1719 (C═O), 1607, 1266 (C–O), 1173, 1094, 857, 768 cm^{-1}.

Synthesis of catalyst 2

(2*S*,4*R*)-*N*-Boc-4-azido-L-proline *tert*-butyl ester **8** (151 mg, 0.48 mmol), *N*,*N*-diisopropylethylamine (650 mL, 3.72 mmol) and copper(I) iodide (2 mg, 9.3 mmol) were added to a solution of 4-ethynylphenyl-polynorbornene copolymer **6b** (220 mg) in THF (1.5 mL) placed in a flask under N_2. The reaction mixture was shaken at 40 °C for 24 h, the reaction progress being monitored by FTIR. When the IR band of the alkynyl group had completely disappeared, the polymer was collected by filtration, sequentially washed with H_2O (20 mL), THF (20 mL), THF–MeOH (20 mL), MeOH (20 mL), THF (20 mL) and CH_2Cl_2 (20 mL) and dried under reduced pressure at 40 °C for 24 h. The polynorbornene-supported prolinate was obtained as an insoluble white solid (320 mg). [FTIR (ATR, neat): ν 2942, 2867, 1709 (C═O), 1614 (C═O), 1392 (*t*-butyl), 1367 (*t*-butyl), 1266 (C–O) cm^{-1}. Elemental analysis (%): found: N, 5.05; f = 0.90 mmol g^{-1}]. Then polymer **2** (250 mg) was obtained by shaken the prolinate (200 mg) in CH_2Cl_2 (1.5 mL) with TFA (1.5 mL). When the IR bands of the *t*-butyl and carbonyl moieties in the protecting groups had completely disappeared, the reaction mixture was filtered off and the polymer was sequentially washed with THF (with 2% of Et_3N, 20 mL), H_2O (20 mL), THF (20 mL), THF–MeOH 1 : 1 (20 mL), MeOH (20 mL), THF (20 mL) and CH_2Cl_2 (20 mL). The solid was dried under reduced pressure at 40 °C for 24 h. FTIR (ATR, neat): ν 3431 (COOH), 2943,

This journal is © The Royal Society of Chemistry 2015

UNIVERSITAT ROVIRA I VIRGILI
NEW APPROACHES TO CATALYST DESIGN AND IMMOBILIZATION
Irina Sagamanova

Published on 04 November 2014. Downloaded by Universitat Rovira I Virgili on 04/02/2015 08:21:23.

2865, 1717 (C═O), 1615 (C═O), 1449, 1267 (C–O), 1177, 1100, 771 cm^{-1}. Elemental analysis (%): found.: N, 4.89; f = 0.87 mmol g^{-1}.

General procedure for the asymmetric aldol reaction catalyzed by polymers 1a–d

Polynorbornene-supported proline **1** (0.015 mmol) was swollen in 54 mL of a DMSO/H_2O (87 : 13) mixture containing TFA (0.015 mmol). The corresponding aldehyde **9a–j** (0.15 mmol) and cyclohexanone (0.75 mmol) were added and the reaction mixture was shaken at room temperature. When the reaction was completed (see Table 3 and Scheme 4), dichloromethane (1 mL) was added and the polymer was filtered off, washed with water (2 mL) and dichloromethane (2 mL) and air-dried. The aqueous filtrate was separated by decantation and extracted with dichloromethane (3 × 10 mL). The combined organic phases were washed with brine, dried ($MgSO_4$) and concentrated under reduced pressure.

Purification by flash column chromatography (ethyl acetate/hexanes, 9 : 1 to 4 : 1) obtained the aldol products **11a–j** as mixtures of *anti* and *syn* diastereomers. Conversion and diastereomeric ratio were determined by ^{1}H NMR spectroscopy on the crude samples after polymer removal. The enantiomeric excess was determined by HPLC on a chiral stationary phase after purification by flash column chromatography on silica gel.

General procedure for the asymmetric aldol reaction catalyzed by polymer 2

Polynorbornene-supported proline **2** (0.015 mmol) was swollen in a mixture of DMF/H_2O (50 : 50, 54 μL). The corresponding aldehyde **9a–j** (0.15 mmol) and ketone **10a–c** (0.75 mmol) were added and the reaction mixture was stirred at room temperature (see Scheme 5). After the indicated time, dichloromethane (1 mL) was added and the polymer was filtered off, washed with water (2 mL) and dichloromethane (2 mL) and air-dried. The aqueous filtrate was separated by decantation and extracted with dichloromethane (3 × 10 mL). The combined organic phases were washed with brine, dried ($MgSO_4$) and concentrated under reduced pressure. When required, purification by flash column chromatography (ethyl acetate/hexanes, 9 : 1 to 4 : 1) was performed to give the aldol products **11a–l** as mixtures of *anti* and *syn* diastereomers. Conversion and diastereomeric ratio were determined by ^{1}H NMR spectroscopy on the crude samples after polymer removal. The enantiomeric excess was determined by HPLC on a chiral stationary phase after purification by flash column chromatography on silica gel.

Acknowledgements

Financial support from Institute of Chemical Research of Catalonia (ICIQ) Foundation, the Spanish MINECO (DGI, grants CTQ2013-48406-P and CTQ2012-38594-C02-01), DEC- Generalitat de Catalunya (grant 2014SGR827) and the Junta de Castilla y León (grant VA373A11-2) is gratefully acknowledged. We also thank MINECO for support through Severo Ochoa Excellence Accreditation 2014–2018 (SEV-2013-0319). The authors thank Dr. Carles Lizandara for valuable support in the characterization of polymers.

Notes and references

1 For reviews about polymer-supported catalysts, see: (*a*) *Handbook of Green Chemistry & Technology*, ed. J. Clark and D. Mcquarrie, Blackwell Publ., London, 2002; (*b*) N. E. Leadbeater and M. Marco, *Chem. Rev.*, 2002, **102**, 3217; (*c*) C. A. McNamara, M. J. Dixon and M. Bradley, *Chem. Rev.*, 2002, **102**, 3275; (*d*) *Polymeric materials in organic synthesis and catalysis*, ed. M. R. Buchmeiser, Wiley-VCH, Weinheim, 2003; (*e*) M. Benaglia, A. Puglisi and F. Cozzi, *Chem. Rev.*, 2003, **103**, 3401; (*f*) R. Haag and S. Roller, *Immobilized Catalysts in: Topics in Current Chemistry*, ed. A. Kirsching, Springer, Heidelberg, 2004; (*g*) *Polymer-Supported Reagents and Catalysts: Increasingly Important Tools for Organic Synthesis*, ed. P. H. Toy and M. Shi, Tetrahedron, 2005, vol. 61, p. 12025; (*h*) B. M. L. Dioos, I. F. J. Vankelecom and P. A. Jacobs, *Adv. Synth. Catal.*, 2006, **348**, 1413; (*i*) S. Itsuno and N. Haraguchi, *Heterogeneous Enantioselective Catalysis Using Organic Polymeric Supports in Handbook of Asymmetric Heterogeneous Catalysis*, ed. K. Ding and Y. Uozumi, Wiley-VCH, Weinheim, 2008; (*j*) *Recoverable and Recyclable Catalysts*, ed. M. Benaglia, John Wiley & Sons, Chichester, 2009; (*k*) K. E. Kristensen and T. Hansen, *Eur. J. Org. Chem.*, 2010, 3179.

2 C. Jimeno, S. Sayalero and M. A. Pericàs, Covalent Heterogenization of Asymmetric Catalysts on Polymers and Nanoparticles, in *Heterogenized Homogeneous Catalysts for Fine Chemicals Production. Catalysis by Metal Complexes*, ed. P. Barbaro and F. Liguari, Springer, Heidelberg, 2010, ch. 4, vol. 33, pp. 123–170.

3 F. Cozzi, *Adv. Synth. Catal.*, 2006, **348**, 1367.

4 J. Lu and P. H. Toy, *Chem. Rev.*, 2009, **109**, 815.

5 (*a*) S. Martínez-Arranz, A. C. Albéniz and P. Espinet, *Macromolecules*, 2010, **43**, 7482; (*b*) A. C. Albéniz, S. Martínez-Arranz and P. Espinet, ES2364781A1.

6 For examples of the use of tin reagents supported on vinyl addition polynorbornes in the Stille reaction see: (*a*) S. Martínez-Arranz, N. Carrera, A. C. Albéniz, P. Espinet and A. Vidal-Moya, *Adv. Synth. Catal.*, 2012, **354**, 3551; (*b*) I. Meana, A. C. Albéniz and P. Espinet, *Adv. Synth. Catal.*, 2010, **352**, 2887; (*c*) N. Carrera, E. Gutierrez, R. Benavente, M. M. Villavieja, A. C. Albéniz and P. Espinet, *Chem. – Eur. J.*, 2008, **14**, 10141.

7 For recent examples see: (*a*) E. Alza, S. Sayalero, X. C. Cambeiro, R. Martín-Rapún, P. O. Miranda and M. A. Pericàs, *Synlett*, 2011, 464; (*b*) X. C. Cambeiro, R. Martín-Rapún, P. O. Miranda, S. Sayalero, E. Alza, P. Llanes and M. A. Pericàs, *Beilstein J. Org. Chem.*, 2011, **7**, 1486; (*c*) C. Ayats, A. H. Henseler and M. A. Pericàs, *ChemSusChem*, 2012, **5**, 320; (*d*) X. Fan, S. Sayalero and

UNIVERSITAT ROVIRA I VIRGILI
NEW APPROACHES TO CATALYST DESIGN AND IMMOBILIZATION
Irina Sagamanova

Published on 04 November 2014. Downloaded by Universitat Rovira I Virgili on 04/02/2015 08:21:23.

M. A. Pericàs, *Adv. Synth. Catal.*, 2012, **354**, 2971; (*e*) P. Kasaplar, C. Rodríguez-Escrich and M. A. Pericàs, *Org. Lett.*, 2013, **15**, 3498; (*f*) R. Martín-Rapún, S. Sayalero and M. A. Pericàs, *Green Chem.*, 2013, **15**, 3295; (*g*) X. Fan, C. Rodríguez-Escrich, S. Sayalero and M. A. Pericàs, *Chem. – Eur. J.*, 2013, **19**, 10814; (*h*) L. Osorio-Planes, C. Rodríguez-Escrich and M. A. Pericàs, *Chem. – Eur. J.*, 2014, **20**, 2397.

8 (*a*) *Modern Aldol Reactions*, ed. R. Mahrwald, Wiley-VCH, Weinheim, 2004For selected examples see: (*b*) D. Font, C. Jimeno and M. A. Pericàs, *Org. Lett.*, 2006, **8**, 4653; (*c*) D. Font, S. Sayalero, C. Jimeno and M. A. Pericàs, *Org. Lett.*, 2008, **10**, 337.

9 (*a*) R. Huisgen, Centenary Lecture - 1,3-Dipolar Cycloadditions, *Proc. Chem. Soc., London*, 1961, 357; (*b*) R. Huisgen, *1,3-Dipolar Cycloaddition Chemistry*, ed. A. Padwa, Wiley, New York, 1984; (*c*) M. Meldal and C. W. Tornøe, *Chem. Rev.*, 2008, **108**, 2952.

10 P. P. Chu, W.-J. Huang, F.-C. Chang and S. Y. Fan, *Polymer*, 2000, **41**, 401.

11 The functionalization of a given resin can be calculated from the results of elemental analysis with the formulae: for nitrogen containing functional resins: f (mmol g^{-1}) = 0.714(%N)/n_N, (%N) representing the weight percentage of nitrogen determined by elemental analysis and n_N representing the number of nitrogen atoms in the functional unit; for bromine containing functional resins: f (mmol g^{-1}) = 0.125(%Br)/n_{Br}, (%Br) representing the weight percentage of bromine determined by elemental analysis and n_{Br} representing the number of bromine atoms in the functional unit.

12 (*a*) The maximal functionalization (f_{max}) of a given resin can be calculated from the functionalization of a precursor resin (f_0) by means of the following formula: f_{max} (mmol g^{-1}) = $f_0/(1 + f_0(\Delta M_W/1000)$, where ΔM_W represents the variation in molecular mass of the functional unit along the considered transformation(s); (*b*) Yield in reactions involving functional resins is not related to mass recovery, which is generally complete, but rather to the ratio between actual functionalization (f) and maximal functionalization (f_{max}) for the resin undergoing the considered process: yield (%) = 100(f/f_{max}).

13 The equilibrium swelling ratio (SR) in each solvent was determined gravimetrically with the formula: swelling ratio (SR, %) = 100($W_s - W_{dry}$)/W_{dry}, where W_s is the weight of swollen samples after the certain time and W_{dry} is the weight of dried samples.

14 P. M. Pinko, K. M. Laurikainen, A. Usano, A. I. Nyberg and J. A. Kaavi, *Tetrahedron*, 2006, **62**, 317.

15 For the role of concentration effect in solvent-free aldol reactions, see: (*a*) B. Rodríguez, T. Rantanen and C. Bolm, *Angew. Chem., Int. Ed.*, 2006, **45**, 6924; (*b*) B. Rodríguez, A. Bruckmann and C. Bolm, *Chem. – Eur. J.*, 2007, **13**, 4710.

16 For linear supports, see: (*a*) Y.-X. Liu, Y.-N. Sun, H.-H. Tan, W. Liu and J.-C. Tao, *Tetrahedron: Asymmetry*, 2007, **18**, 2649; (*b*) Y.-X. Liu, Y.-N. Sun, H.-H. Tan and J.-C. Tao, *Catal. Lett.*, 2008, **120**, 281For cross-linked supports, see (*c*) F. Giacalone, M. Gruttadauria, A. M. Marculescu and R. Noto, *Tetrahedron Lett.*, 2007, **48**, 255; (*d*) M. Gruttadauria, F. Giacalone, A. M. Marculescu, P. Lo Meo, S. Riela and R. Noto, *Eur. J. Org. Chem.*, 2007, 4688For acrylic polymers, see (*e*) T. E. Kristensen, K. Vestli, K. A. Fredriksen, F. K. Hansen and T. Hansen, *Org. Lett.*, 2009, **11**, 2968; (*f*) T. E. Kristensen, K. Vestli, M. G. Jakobsen, F. K. Hansen and T. Hansen, *J. Org. Chem.*, 2010, **75**, 1620.

17 Y. Hayashi, T. Sumiya, J. Takahashi, H. Gotoh, T. Urushima and M. Shoji, *Angew. Chem., Int. Ed.*, 2006, **45**, 958.

18 (*a*) M. Gruttadauria, F. Giacalone and R. Noto, *Adv. Synth. Catal.*, 2009, **351**, 33; (*b*) J. Paradowska, M. Stodulski and J. Mlynarski, *Angew. Chem., Int. Ed.*, 2009, **48**, 4288; (*c*) M. Raj and V. K. Singh, *Chem. Commun.*, 2009, 6687.

19 K. Sakthivel, W. Notz, T. Bui and C. F. Barbas III, *J. Am. Chem. Soc.*, 2001, **123**, 5260.

This journal is © The Royal Society of Chemistry 2015

Chapter II

2.6. Conclusions and Outlook.

We have successfully developed a general method for the preparation of polynorbornene-supported proline. A new family of immobilized catalysts has been prepared by Huisgen 1,3-dipolar cycloaddition between azido-copolymers and a propargyloxyproline derivative (**type 1**) or, alternatively between alkynyl-functionalized copolymers and an azido-prolinate (**type 2**).

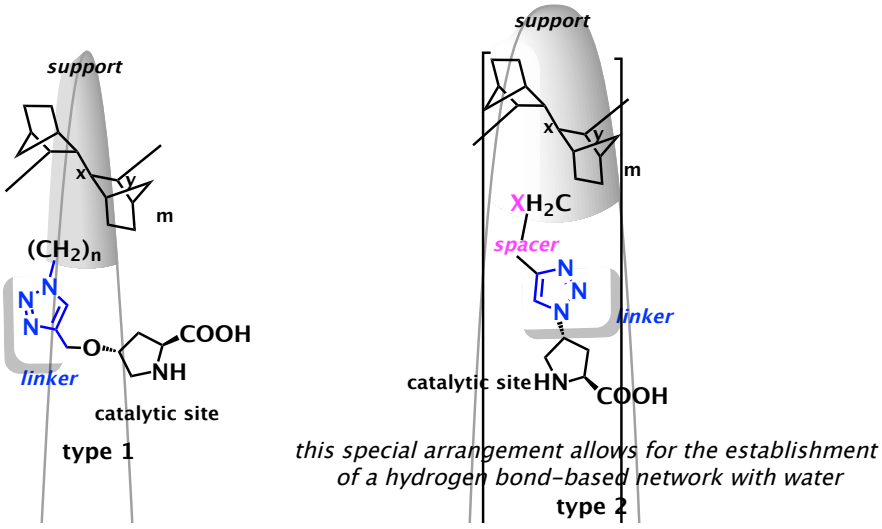

The versatility of these catalysts has also been illustrated by their application in the asymmetric aldol reaction of cyclohexanone and *p*-nitrobenzaldehyde under different reaction conditions. Furthermore, polynorbornene-supported proline has shown excellent performance in this particular aldol transformation in an aqueous environment. Especially, this behaviour has been observed for the **type 2**, which is analogous to the polystyrene-derivatives, developed in our group.

The robustness of the polynorbornene-supported catalysts has been illustrated by the possibility of extending their use for up to seven cycles in the aldol reaction of cyclohexanone and *p*-nitrobenzaldehyde.

Finally, we have explored the generality of catalysts **1** and **2** in the aldol reaction with respect to benzaldehyde reaction partners.

However, given the excellent results obtained in asymmetric aldol reaction in an aqueous environment, further studies should be devoted to the development of other proline-catalyzed reactions. In particular, application of this type of polymers in photocatalytic applications can be interesting due to their transparency to UV light in the case of the first family, which is unsaturated and lacks aromatic rings.

In addition, investigation towards the implementation of a continuous flow process involving these catalysts would greatly improve their significance.

Electronic Supplementary Material (ESI) for Catalysis Science & Technology.
This journal is © The Royal Society of Chemistry 2014

Supporting Information for

Asymmetric Organocatalysts Supported on Vinyl Addition Polynorbornenes for Work in Aqueous Media

Irina K. Sagamanova,[†] Sonia Sayalero,[†] Sheila Martínez-Arranz,[‡] Ana C. Albéniz,*[,‡] and Miquel A. Pericàs*[,†,§]

[†]*Institute of Chemical Research of Catalonia (ICIQ), Av. Països Catalans, 16, 43007 Tarragona, Spain.* [‡]*IU CINQUIMA/Química Inorgánica, Universidad de Valladolid, 47071 Valladolid, Spain.* [§]*Departament de Química Orgànica, Universitat de Barcelona (UB), 08028 Barcelona, Spain*

mapericas@iciq.es, albeniz@qi.uva.es

Chapter II

General Information

Unless otherwise stated, all commercial reagents were used as received. The aldehydes were vacuum distilled before use. Solvents were dried using a solvent purification system (SPS). Reactions requiring anhydrous conditions were performed under nitrogen using standard Schlenk line techniques. Thin layer chromatography was carried out using Merck TLC Silicagel 60 F254 aluminium sheets. Components were visualized by UV light (λ = 254 nm) or by staining with *p*-anisaldehyde solution. Flash chromatography separations were carried out using 60-mesh silicagel and dry-packed columns. NMR spectra were acquired on Bruker Avance Ultrashield spectrometers in $CDCl_3$ at room temperature, operating at 400 or 500 MHz (^1H) and 100 or 126 MHz ($^{13}C\{^1H\}$). TMS was used as internal standard for ^1H NMR and $CDCl_3$ for ^{13}C NMR. Chemical shifts are reported in ppm referred to TMS. ATR-FTIR spectra were recorded on a Bruker Tensor 27 FT-IR spectrometer. FT-Raman spectra were measured on a Via Raman spectrometer with laser excitation in 785 nm, equipped with a Leica microscope and Peltiercooled CCD detectors (-70 ^{0}C). Elemental analyses were performed on a LECO CHNS 932 micro-analyzer at the Universidad Complutense de Madrid, Spain. The halogen content in the polymers was determined by oxygen-flask combustion of a sample and analysis of the residue by mercurimetric titration of the chloride.[S1] Scanning Electron Microscopy (SEM) was performed on a JSM-6400 scanning microscope at the Microscopy Unit of the Universitat Rovira i Virgili, Spain. High performance liquid chromatography (HPLC) was performed on an Agilent Technologies chromatograph (1200 Series), using Chiralcel OD-H, Chiralpak AD-H and Chiralpak AS-H columns and guard columns. Racemic standards of reaction products were prepared using DL-proline as catalyst according to reported procedures in order to establish HPLC conditions.

Solvent absorption measurements were performed by gravimetric analysis according to common practice.[S2] Dried samples (30-32 mg) were weighed and then immersed in an excess of the swelling solvent (0.4 mL) at room temperature. At regular time intervals, the samples were taken out, wiped of excessive solvent with filter paper, weighed, and returned to the swelling medium. The experiment was continued until a constant weight of the samples was achieved. The equilibrium swelling ratio (SR) in each solvent was determined

gravimetrically with the formula: Swelling Ratio (SR, %) = $100(W_s-W_{dry})/W_{dry}$, where W_s is the weight of swollen samples after the certain time and Wdry is the weight of dried samples.

Preparation and characterization of 4-ethynylbenzoic acid (**5**)

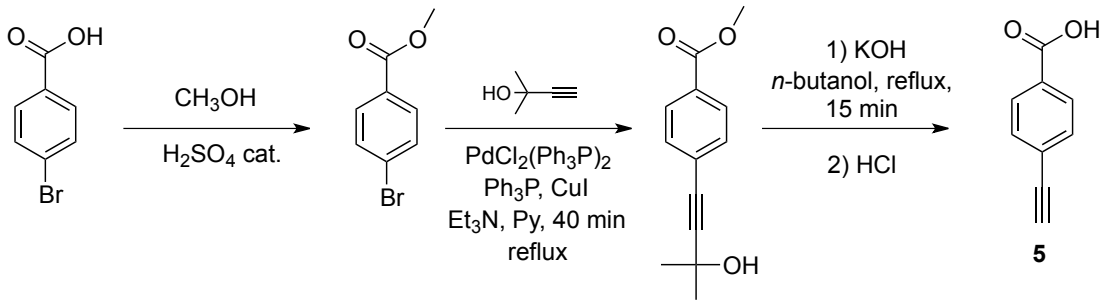

a) Synthesis of methyl *p*-bromobenzoate. Methyl *p*-bromobenzoate was prepared quantitatively (10.6 g, 99% yield) by refluxing *p*-bromobenzoic acid (10 g, 49.7 mmol) with an excess of methanol (60 mL, 1.54 mmol) and a catalytic amount of sulfuric acid (0.66 mL, 12.4 mmol).

b) Synthesis of 4-(4-(methoxycarbonyl))-phenyl-2-methyl-3-butyn-2-ol. To a solution of Ph_3P (67 mg, 0.011 mmol), CuI (18 mg, 0.093 mmol), methyl *p*-bromobenzoate (5.0 g, 23.25 mmol) and 2-methyl-3-butyn-2-ol (2.33 g, 27.7 mmol) in Et_3N (32 mL) and pyridine (18 mL) was added dichloro-*bis*(triphenylphosphine)palladium (20 mg, 0.0028 mmol) under N_2 and the mixture was refluxed for 40 min. After cooling to room temperature, the reaction mixture was filtered to remove the insoluble triethylamine hydrobromide formed. The salt was washed with triethylamine and ethyl ether until the ether washings were clear. The combined filtrates were reduced to dryness under reduced pressure. The obtained solid was stirred twice with H_2O (40 mL) and then with 3% HCl (40 mL) and again twice with H_2O (40 mL). 4-(4-(Methoxycarbonyl)-phenyl-2-methyl-3-butyn-2-ol was isolated as a slightly tan solid after filtration and drying under reduced pressure (4.32 g, 85% yield).

c) Synthesis of *p*-Ethynylbenzoic acid (**5**). 4-(4-(Methoxycarbonyl)-phenyl-2-methyl-3-butyn-2-ol (1 g, 4.58 mmol) was dissolved in a refluxing solution of KOH (1 g, 18.33 mmol) in *n*-butanol (30 mL). After refluxing for 15 min, the mixture was cooled with an ice-bath, acidified with 1 M HCl to pH 2 and extracted with ethyl acetate (3 × 40 mL). The combined organic layers were dried ($MgSO_4$) and concentrated under reduced pressure to

give *p*-ethynylbenzoic acid as yellow solid (630 mg, 94% yield). All the spectroscopic data of the product matched with those reported in the literature.[S3]

Solvent effects on the aldol reaction of cyclohexanone with *p*-nitrobenzaldehyde catalyzed by polymers **1a,b**

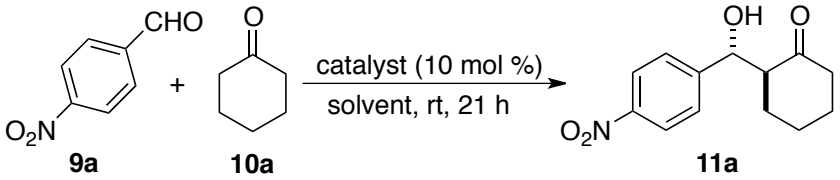

Table SI-1. Solvent effects on the aldol reaction of cyclohexanone with *p*-nitrobenzaldehyde catalyzed by polymers **1a,b**.[a]

entry	catalyst	solvent	conversion (%)[b,c]	*anti:syn*[b]	ee *anti*[d] (%)
1	**1a**	CH_2Cl_2[e]	80 (17)	82:18	90
2	**1a**	DMF[e]	50 (4)	75:25	84
3	**1a**	DMSO[e]	61 (6)	74:26	91
4	**1a**	H_2O	74 (8)	71:29	73
5	**1a**	CH_2Cl_2/H_2O (50:50)	57 (16)	80:20	73
6	**1a**	IPA/H_2O (50:50)	65 (17)	71:29	54
7	**1a**	THF/H_2O (50:50)	68 (3)	72:28	62
8	**1a**	DMF/H_2O (50:50)	88 (4)	78:22	78
9	**1a**	DMSO/H_2O (50:50)	94	81:19	85
10	**1a**	DMSO/H_2O (83:17)	100[f] (97)[g]	89:11	90
11	**1a**	DMSO/H_2O (91:9)	100[f] (95)[g]	88:12	91
12	**1a**	neat	10	77:23	76
13	**1b**	DMSO[e]	82	76:24	92
14	**1b**	H_2O	81	79:21	78
15	**1b**	DMSO/H_2O (50:50)	96	86:14	93
16	**1b**	DMSO/H_2O (83:17)	100[h] (98)[g]	91:9	91
17	**1b**	DMSO/H_2O (91:9)	100[h] (96)[g]	90:10	93
18	**1b**	neat	17	77:23	75
19	**1b**	neat[i]	72	84:16	78
20	**1b**	neat[j]	94	78:22	76

[a] Reactions were performed with polymer **1a** or **1b** (0.015 mmol), *p*-nitrobenzaldehyde **9a** (0.15 mmol) and cyclohexanone **10a** (0.75 mmol) in different solvents (54 μL). [b] Determined by ^{1}H NMR on the crude mixture. [c] In parentheses % of enone from dehydration of the product. [d] Determined by HPLC analysis of the crude mixture using a

chiral stationary phase. [e] Synthesis grade. [f] 16 h. [g] In parentheses combined yield of the isolated diastereomers. [h] 19 h. [i] 0.33 mmol (2.2 equiv) of cyclohexanone were used (44 h). [j] Reaction conducted in a ball-mill.

Reactions in the ball-mill were conducted using a Retsch Mixer Mill model "MM200". The milling instrument consists of a main disk, which can rotate at a frecuency of 30 s^{-1} and accommodates two grinding bowls. Both bowls (5 mL) and balls (9 mm diameter) are made of stainless steel. Typical experimental procedure for the solvent-free aldol reaction performed in the ball-mill: A ball-mill vessel was charged with cyclohexanone (67 mL, 0.65 mmol), *p*-nitrobenzaldehyde (89 mg, 0.59 mmol), **1b** (40 mg, 0.059 mmol) and 2 balls. Stirring was started in a grinding bowl using the ball-mill with a frecuency of 30 s^{-1}. After 6 h 40 min total reaction time (40 min each cycle and 10 min pause), the crude product was washed off the reaction vessel with dichloromethane (2 x 10 mL) and the combined organic fractions were filtered and concentrated under reduced pressure.

Temperature effects on the aldol reaction of cyclohexanone with *p*-nitrobenzaldehyde catalyzed by polymers **1a,b**

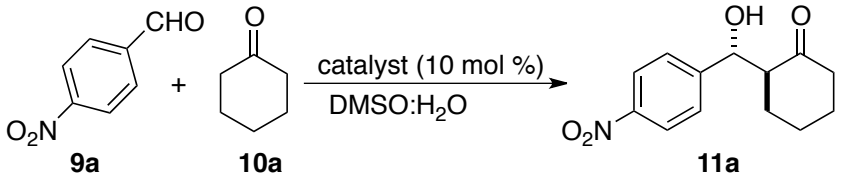

Table SI-2. Temperature effects on the aldol reaction of cyclohexanone with *p*-nitrobenzaldehyde catalyzed by polymers **1a,b**.[a]

entry	catalyst	T (ºC)	solvent	time (h)	conversion[b] (%)	yield[c] (%)	anti:syn[b]	ee anti[d] (%)
1	**1a**	35	DMSO/H_2O (83:17)	14	100	96	89:11	91
2	**1a**	35	DMSO/H_2O (91:9)	14	100	94	85:15	93
3	**1b**	35	DMSO/H_2O (83:17)	14	100	95	88:12	93
4	**1b**	35	DMSO/H_2O (91:9)	14	100	91	89:11	93
5	**1b**	60	DMSO/H_2O (83:17)	11	90	86	82:18	89

[a] Reactions were performed with polymer **1a** or **1b** (0.015 mmol), *p*-nitrobenzaldehyde (0.15 mmol) and cyclohexanone (0.75 mmol) in a mixture of DMSO:H_2O (54 μL). [b] Determined by ^1H NMR on the crude mixture. [c] Combined yield of the isolated diastereomers. [d] Determined by HPLC analysis of the crude mixture using a chiral stationary phase.

Chapter II

Screening of additives on the aldol reaction of cyclohexanone with *p*-nitrobenzaldehyde catalyzed by polymer **1b**

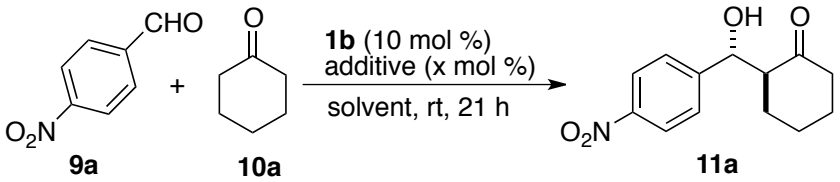

Table SI-3. Screening of additives on the aldol reaction of cyclohexanone with *p*-nitrobenzaldehyde catalyzed by **1b**.[a]

entry	solvent	additive (mol %)	conversion[b] (%)	yield[c] (%)	*anti:syn*[b]	ee *anti*[d] (%)
1	DMSO/H_2O (91:9)	none	100[e]	98	91:9	91
2	DMSO/H_2O (91:9)	4-NO_2-$C_6H_4CO_2H$ (15)	98	96	91:9	93
3	DMSO/H_2O (91:9)	CF_3CO_2H (10)	84	-	93:7	96
4	DMSO/H_2O (83:17)	none	100[e]	96	90:10	93
5	DMSO/H_2O (83:17)	DiMePEG (10)	97	90	89:11	94
6	DMSO/H_2O (83:17)	CH_3CO_2H (10)	100	97	89:11	94
7	DMSO/H_2O (83:17)	4-NO_2-$C_6H_4CO_2H$ (15)	100	97	92:8	93
8	DMSO/H_2O (83:17)	CF_3CO_2H (10)	99	90	96:4	96
9	H_2O	none	74	-	71:29	73
10	H_2O	DiMePEG (10)	71	58	90:10	89
11	H_2O	CF_3CO_2H (10)	27	-	93:7	94

[a] Reactions were performed with polymer **1b** (0.015 mmol, 10.2 mg), *p*-nitrobenzaldehyde (0.15 mmol) and cyclohexanone (0.75 mmol) in the corresponding solvent (54 μL). [b] Determined by ^{1}H NMR on the crude mixture. [c] The data in parentheses indicate the combined yield of the isolated diastereomers. [d] Determined by HPLC analysis of the crude mixture using a chiral stationary phase. [e] 19 h.

Solvent and additives effects on the aldol reaction of cyclohexanone with *p*-nitrobenzaldehyde catalyzed by polymer **2**

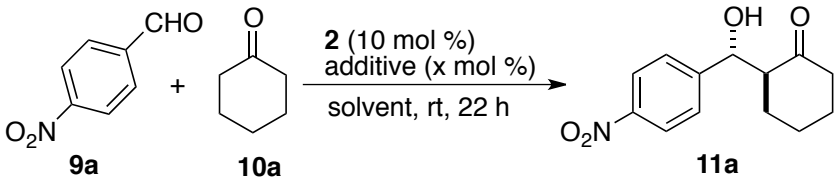

Table SI-4. Solvent and additives effects on the aldol reaction of cyclohexanone with *p*-nitrobenzaldehyde catalyzed by polymer **2**.[a]

entry	solvent	additive (mol %)	conversion[b] (%)	yield[c] (%)	*anti:syn*[b]	ee *anti*[d] (%)
1	H_2O	none	91	90	95:5	96
2	DMSO/H_2O (50:50)	none	96	95	95:5	96
3	DMF/H_2O (50:50)	none	96	94	95:5	96
4	H_2O	CF_3CO_2H (10)	90	87	92:8	95
5	H_2O	DiMePEG (10)	69	65	89:11	95

[a] Reactions were performed with polymer **2** (0.015 mmol, 10.2 mg), *p*-nitrobenzaldehyde (0.15 mmol) and cyclohexanone (0.75 mmol) in the corresponding solvent (54 µL). [b] Determined by ^{1}H NMR on the crude mixture. [c] The data in parentheses indicate the combined yield of the isolated diastereomers. [d] Determined by HPLC analysis of the crude mixture using a chiral stationary phase.

Recycling experiments with catalysts **1b** and **2**

a) Recycling experiments with catalyst **1b**. After performing the aldol reaction of *p*-nitrobenzaldehyde (**9a**, 49 mg, 0.32 mmol) with cyclohexanone (**10a**, 168 μL, 1.62 mmol) in the presence of polymer **1b** (22 mg, 0.032 mmol) swollen in 116 μL of a DMSO/H_2O (87:13) mixture containing TFA (0.015 mmol) at room temperature for 23 h, the polymer was separated by filtration and rinsed with water (2 mL) and dichloromethane (2 mL). The polymer was then dried under reduced pressure for 1 h and reused in the next run. Results have been collected in the following table:

cycle	conversion [a] (%)	yield (%)[b]	*anti:syn*[a]	ee *anti* (%)[c]
1	93	90	96:4	96
2	90	87	96:4	96
3	87	85	96:4	96
4	87	84	96:4	96
5	88	85	96:4	96
6	83	79	96:4	96
7	82	80	96:4	96

[a] Determined by ^{1}H NMR on the crude mixture. [b] Combined yield of the isolated isomers after flash chromatography. [c] Determined by HPLC analysis of the crude mixture using a chiral stationary phase.

Figure SI-1. In blue: IR spectrum of fresh catalyst **1b**; In red: IR spectrum after seven runs.

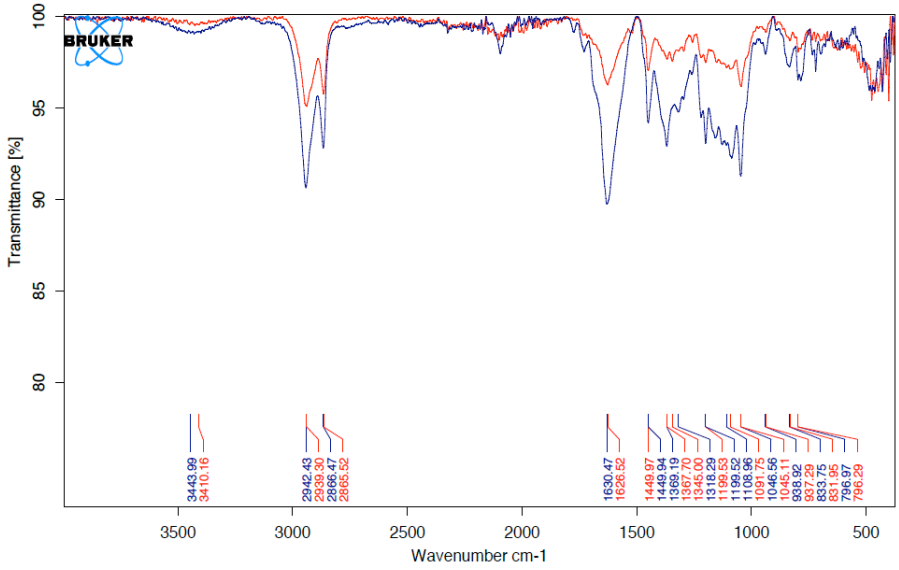

Fresh catalyst **1b**: Elemental analysis (%): N, 8.26; f = 1.47 mmol g^{-1}. Elemental analysis after seven runs (%): N, 7.53; f = 1.34 mmol g^{-1}

Figure SI-2. SEM picture of fresh catalyst **1b** (A) and after seven runs (B).

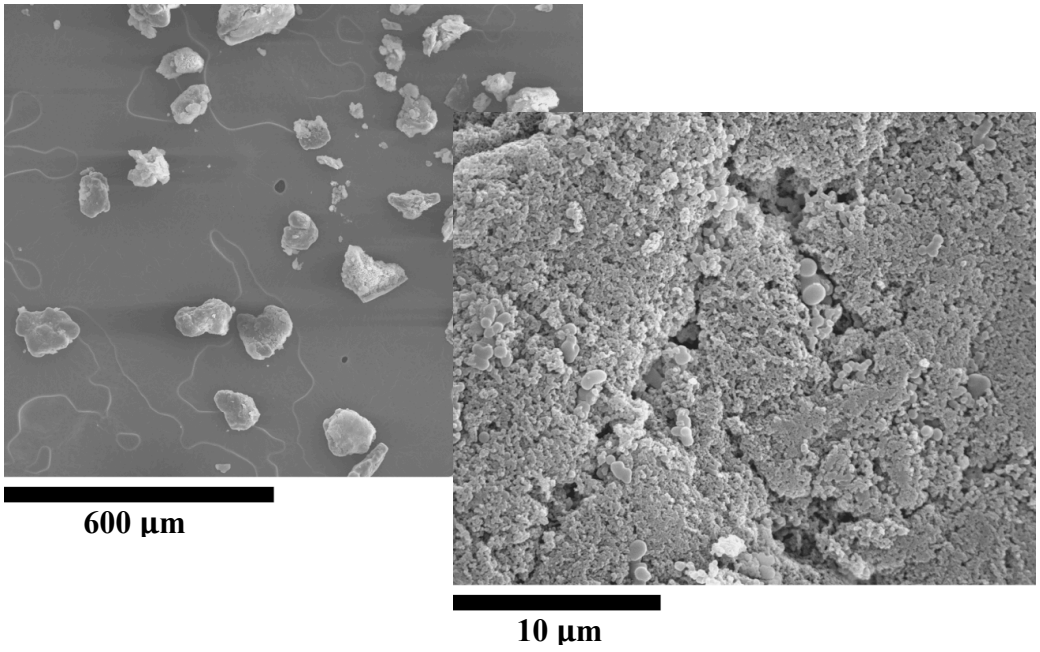

A

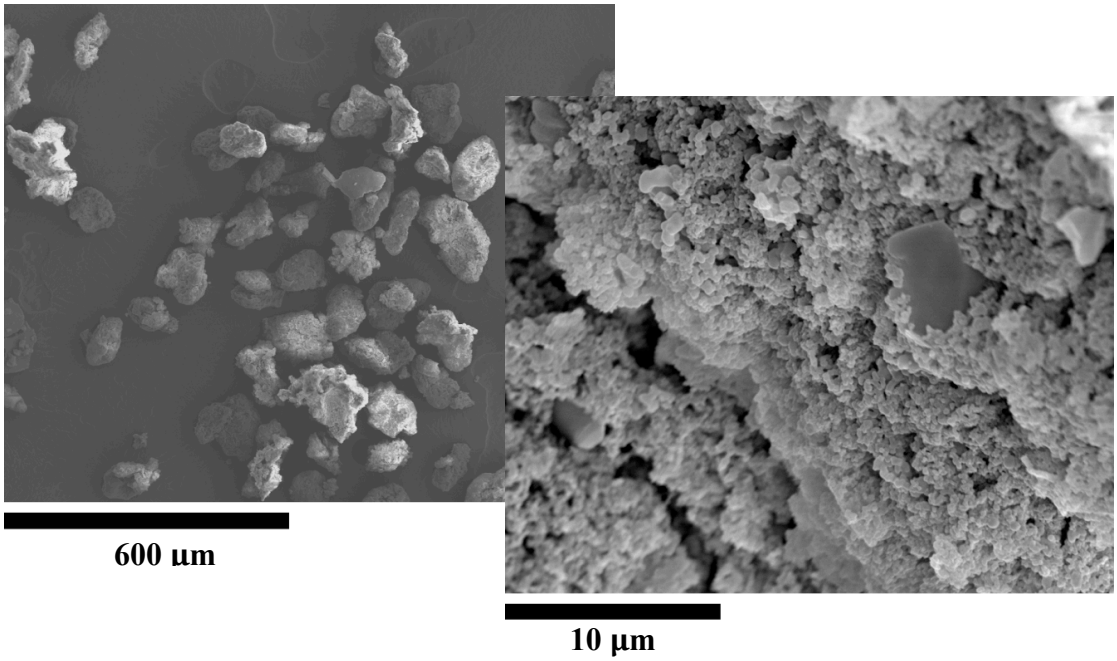

B

b) Recycling experiments with catalyst **2**. After performing the aldol reaction of *p*-nitrobenzaldehyde (**9a**, 41 mg, 0.27 mmol) with cyclohexanone (**10a**, 140 µL, 1.35 mmol) in DMF:H_2O (50:50, 98 µL) in the presence of polymer **2** (0.027 mmol, 31 mg) at room temperature for 22 h following the general procedure, the polymer was separated by filtration and rinsed with water (2 mL) and dichloromethane (2 mL). The polymer was then dried under reduced pressure for 1 h and reused in the next run. Results have been collected in the following table:

cycle	yield (%)[a]	*anti*:*syn*[b]	ee *anti* (%)[c]
1	97	96:4	97
2	98	96:4	96
3	99	96:4	96
4	98	96:4	96
5	99	95:5	95
6	99	95:5	95
7	98	96:4	94

[a] Combined yield of the isolated isomers after flash chromatography. [b] Determined by ^{1}H NMR on the crude mixture. [c] Determined by HPLC analysis of the crude mixture using a chiral stationary phase.

Figure SI-3. In blue: IR spectrum of fresh catalyst **2**; In red: IR spectrum after seven runs.

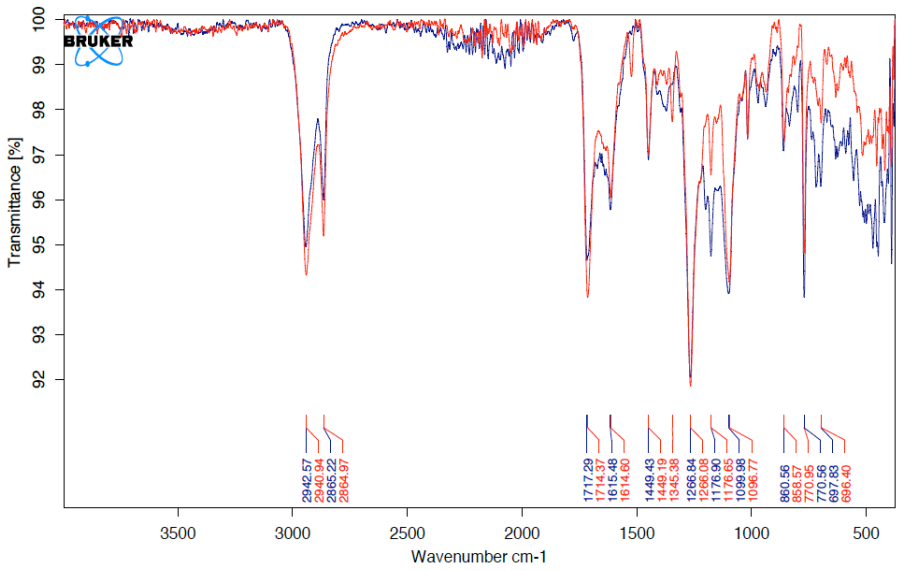

Fresh catalyst **2**: Elemental analysis (%): N, 4.89; $f = 0.87$ mmol g^{-1}. Elemental analysis after seven runs (%): N, 4.91; $f = 0.876$ mmol g^{-1}

Figure SI-4. SEM picture of fresh catalyst **2** (A) and after seven runs (B).

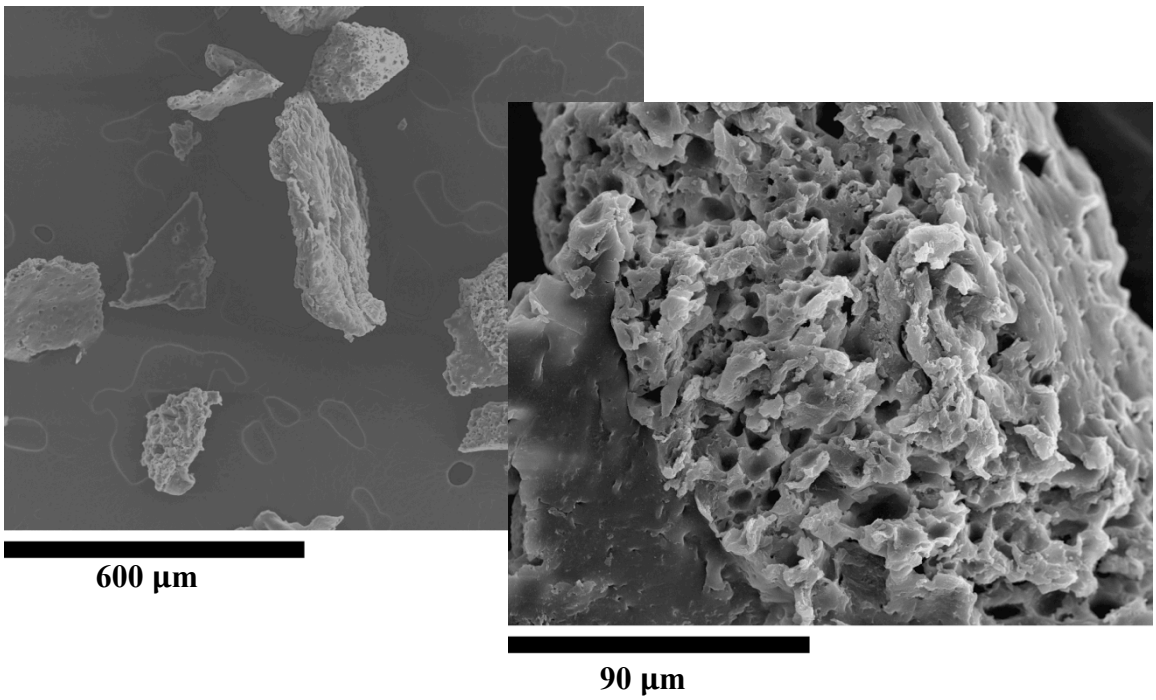

A

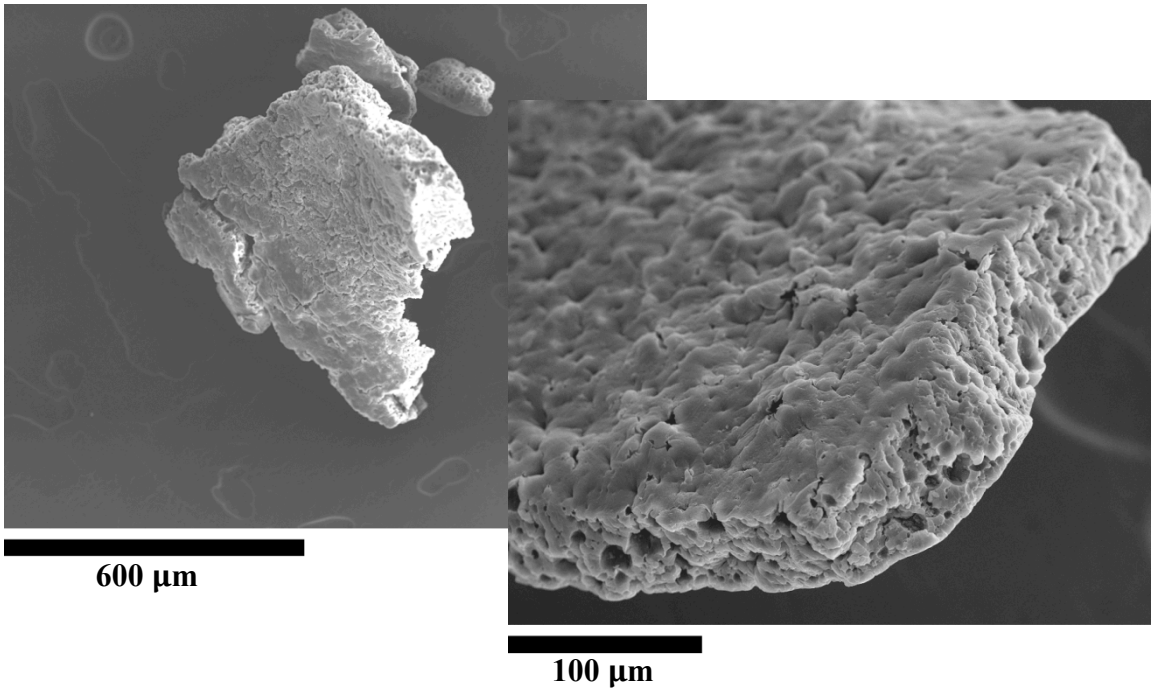

B

Chapter II

[1]HNMR and [13]CNMR spectra and chromathographic data of aldol products **11**

(2*S*,1'*R*)-2-(Hydroxy-4-nitrophenylmethyl)cyclohexan-1-one **11a**:

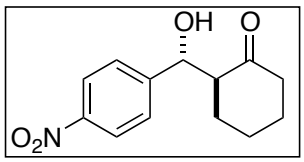

Enantiomeric excess was determined by HPLC with a Chiralpak AD-H column (90:10 Hexane:2-propanol), 1.0 mL/min, λ = 254 nm; major enantiomer t_r = 31.4 min, minor enantiomer t_r = 24.7 min. All the spectroscopic data matched with literature.[S4, S5]

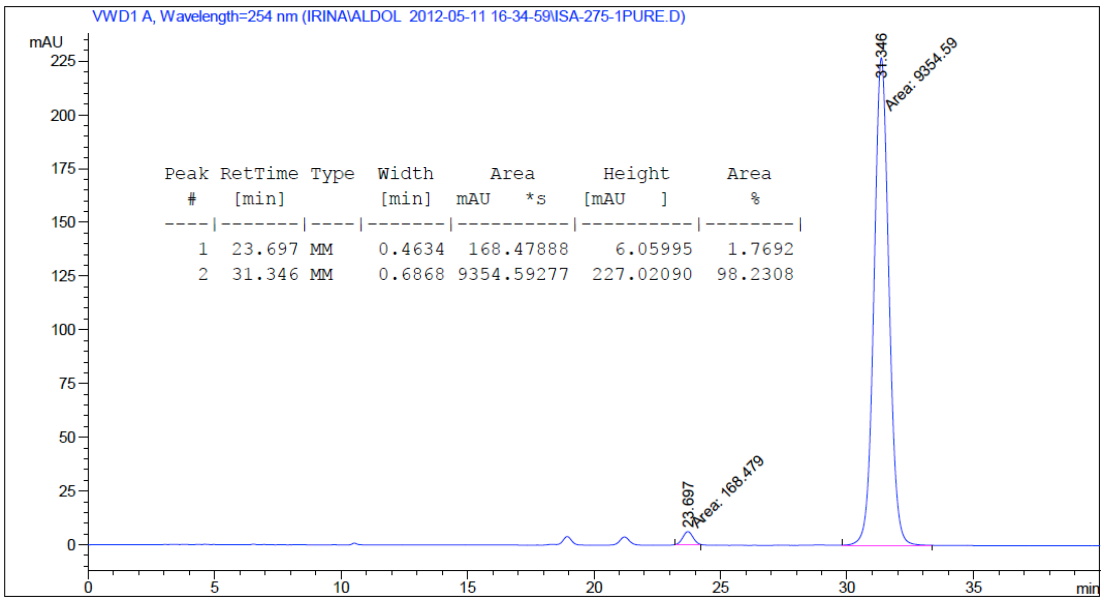

Peak #	RetTime [min]	Type	Width [min]	Area mAU *s	Height [mAU]	Area %
1	23.697	MM	0.4634	168.47888	6.05995	1.7692
2	31.346	MM	0.6868	9354.59277	227.02090	98.2308

Racemic mixture:

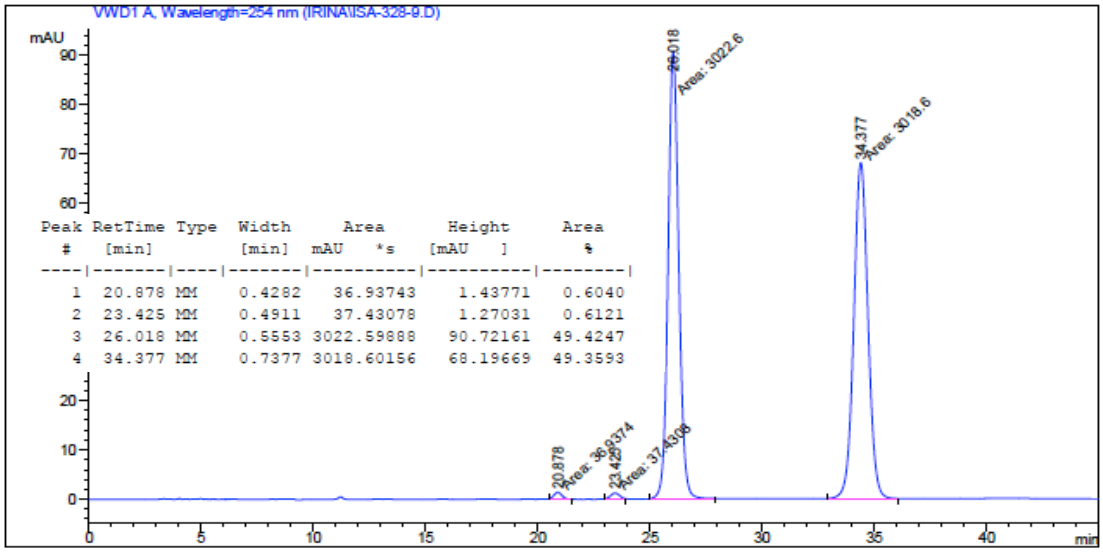

Peak #	RetTime [min]	Type	Width [min]	Area mAU *s	Height [mAU]	Area %
1	20.878	MM	0.4282	36.93743	1.43771	0.6040
2	23.425	MM	0.4911	37.43078	1.27031	0.6121
3	26.018	MM	0.5553	3022.59888	90.72161	49.4247
4	34.377	MM	0.7377	3018.60156	68.19669	49.3593

(2*S*,1'*R*)-2-(Hydroxy-2-nitrophenylmethyl)cyclohexan-1-one **11b**:

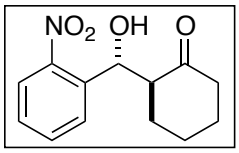

Enantiomeric excess was determined by HPLC with a Chiralpak AD-H column (90:10 hexane:2-propanol), 1.0 mL/min, λ = 254 nm; major enantiomer t_r= 14.2 min. All the spectroscopic data matched with literature.[S4, S6]

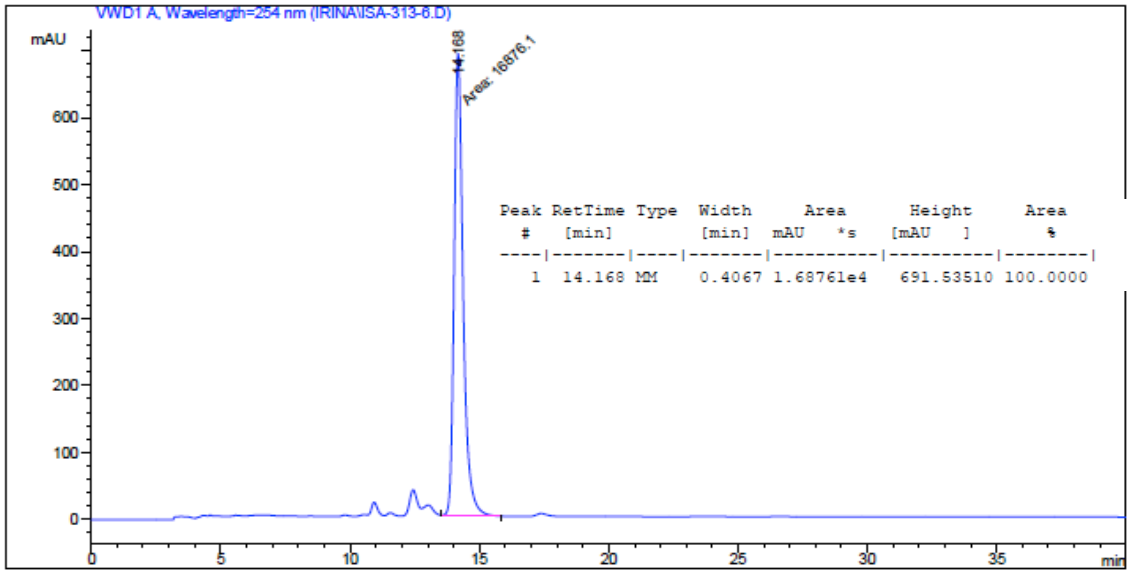

Racemic mixture:

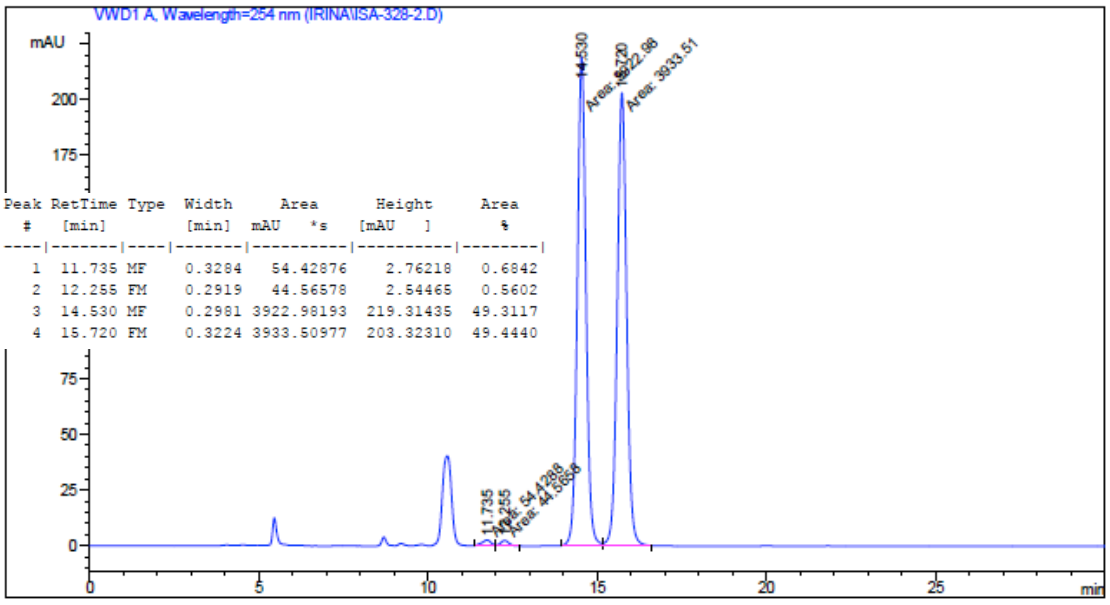

Chapter II

(2*S*,1'*R*)-2-(Hydroxy-3-nitrophenylmethyl)cyclohexan-1-one **11c**:

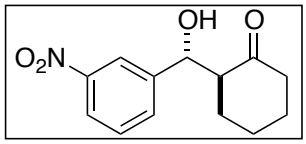

Enantiomeric excess was determined by HPLC with a Chiralpak AD-H column (95:5 hexane:2-propanol), 0.8 mL/min, λ = 254 nm; major enantiomer t_r= 39.2 min, minor enantiomer t_r= 50.1 min. All the spectroscopic data matched with literature.[S4, S6]

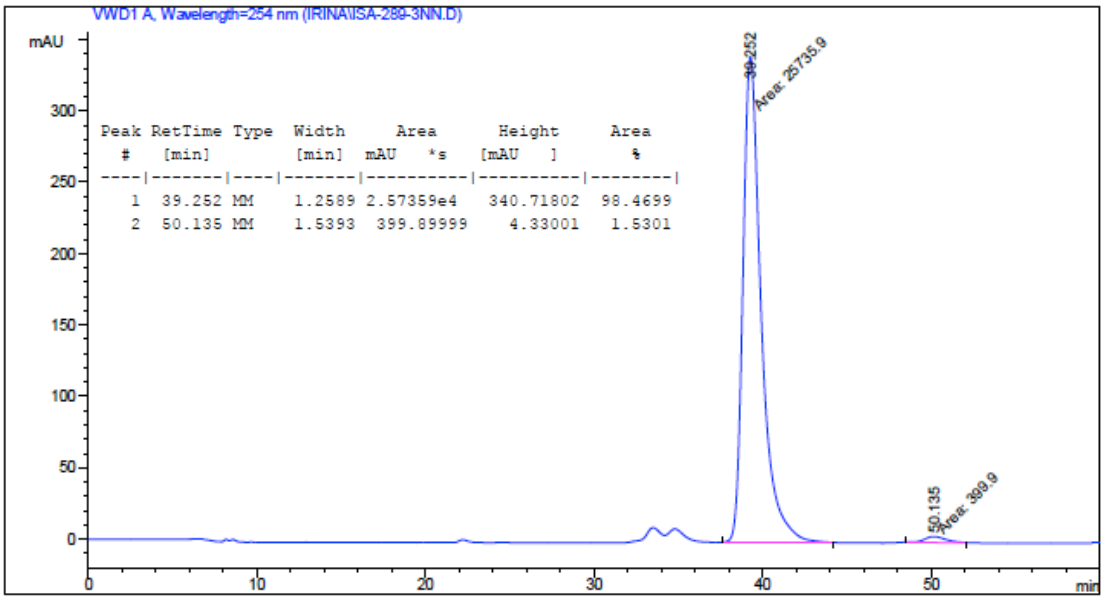

Peak #	RetTime [min]	Type	Width [min]	Area mAU *s	Height [mAU]	Area %
1	39.252	MM	1.2589	2.57359e4	340.71802	98.4699
2	50.135	MM	1.5393	399.89999	4.33001	1.5301

Racemic mixture:

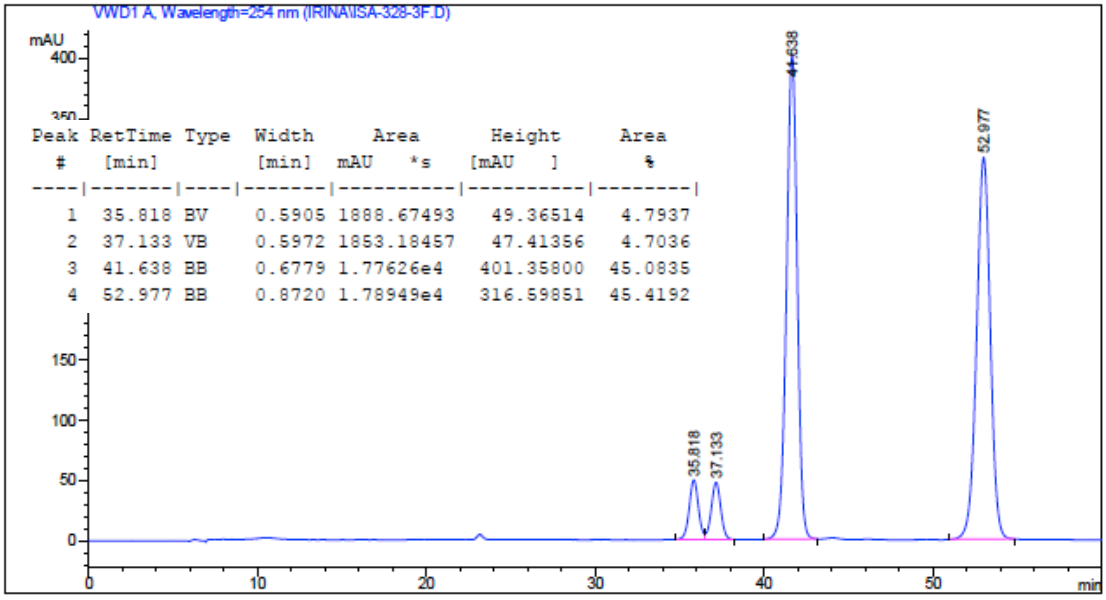

Peak #	RetTime [min]	Type	Width [min]	Area mAU *s	Height [mAU]	Area %
1	35.818	BV	0.5905	1888.67493	49.36514	4.7937
2	37.133	VB	0.5972	1853.18457	47.41356	4.7036
3	41.638	BB	0.6779	1.77626e4	401.35800	45.0835
4	52.977	BB	0.8720	1.78949e4	316.59851	45.4192

(2*S*,1'*R*)-2-(Hydroxy-4-cyanophenylmethyl)cyclohexan-1-one **11d**:

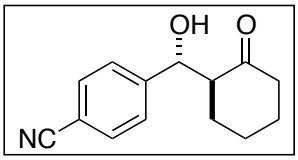

Enantiomeric excess was determined by HPLC with a Chiralpak AD-H column (80:20 Hexane:2-propanol), 1.0 mL/min, λ = 254 nm; major enantiomer t_r = 14.0 min, minor enantiomer t_r = 11.5 min. All the spectroscopic data matched with literature.[S4, S5]

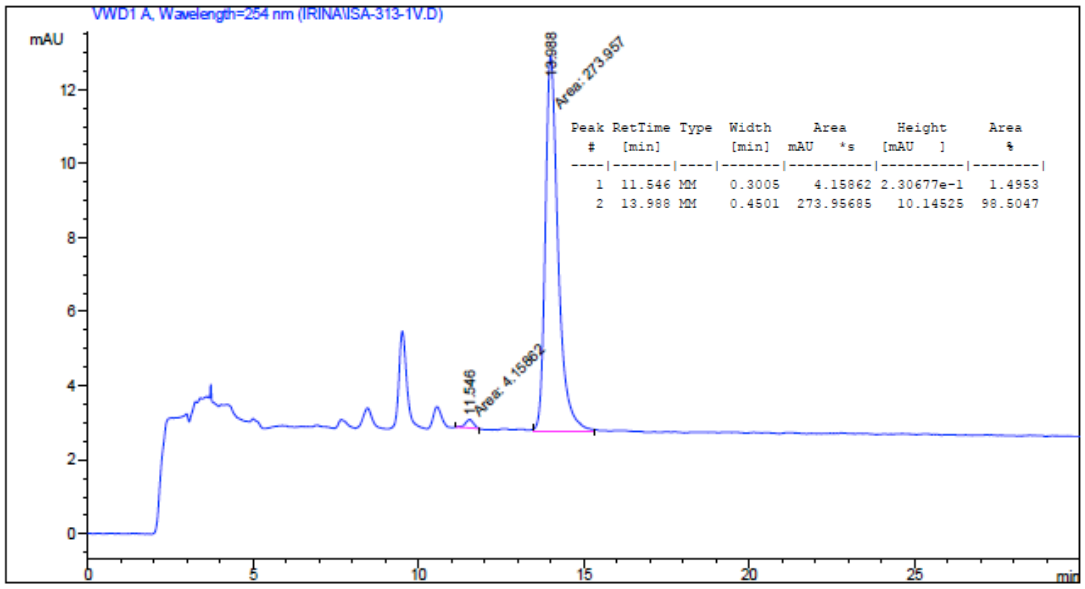

Peak #	RetTime [min]	Type	Width [min]	Area mAU *s	Height [mAU]	Area %
1	11.546	MM	0.3005	4.15862	2.30677e-1	1.4953
2	13.988	MM	0.4501	273.95685	10.14525	98.5047

Racemic mixture:

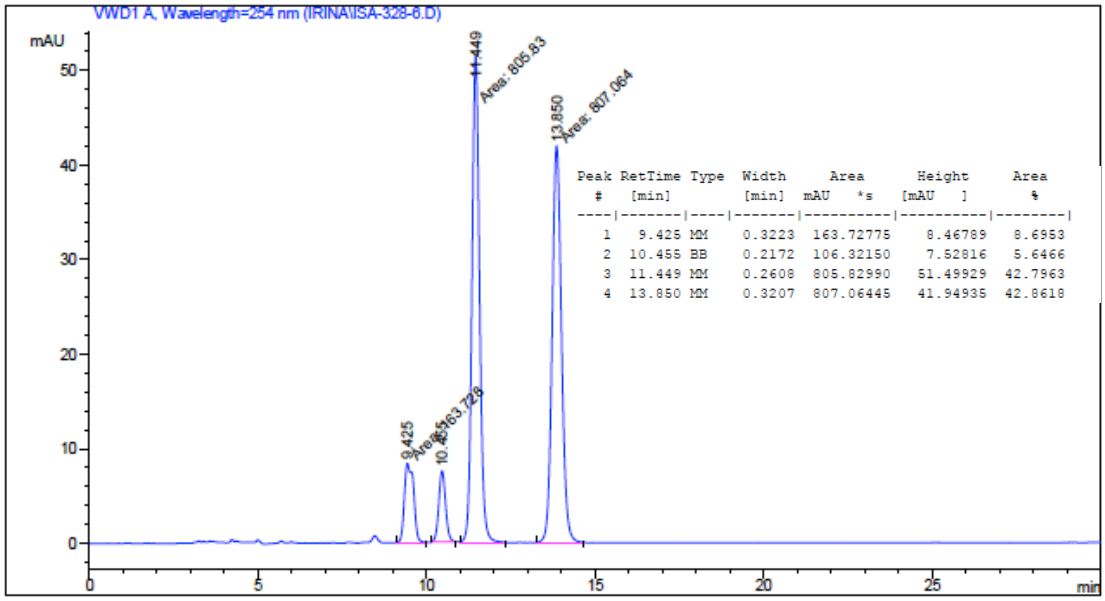

Peak #	RetTime [min]	Type	Width [min]	Area mAU *s	Height [mAU]	Area %
1	9.425	MM	0.3223	163.72775	8.46789	8.6953
2	10.455	BB	0.2172	106.32150	7.52816	5.6466
3	11.449	MM	0.2608	805.82990	51.49929	42.7963
4	13.850	MM	0.3207	807.06445	41.94935	42.8618

(2*S*,1'*R*)-2-(Hydroxy-4-trifluoromethylphenylmethyl)cyclohexan-1-one **11e**:

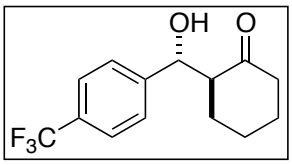

Enantiomeric excess was determined by HPLC with a Chiralpak AD-H column (90:10 Hexane:2-propanol), 1.0 mL/min, λ = 254 nm; major enantiomer t_r = 13.2 min, minor enantiomer t_r = 10.9 min. All the spectroscopic data matched with literature.[S5]

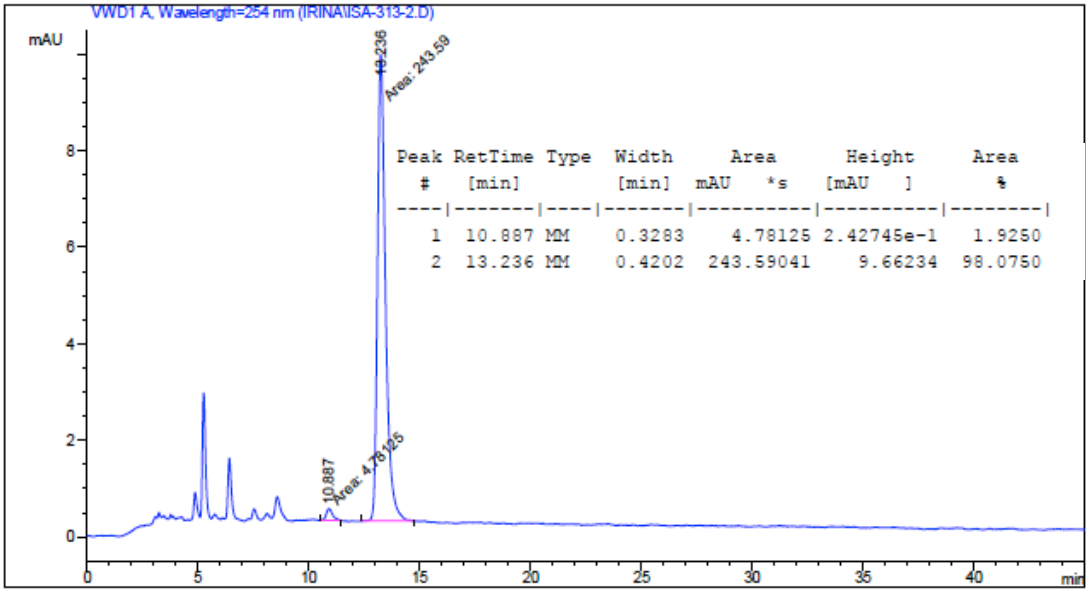

Racemic mixture:

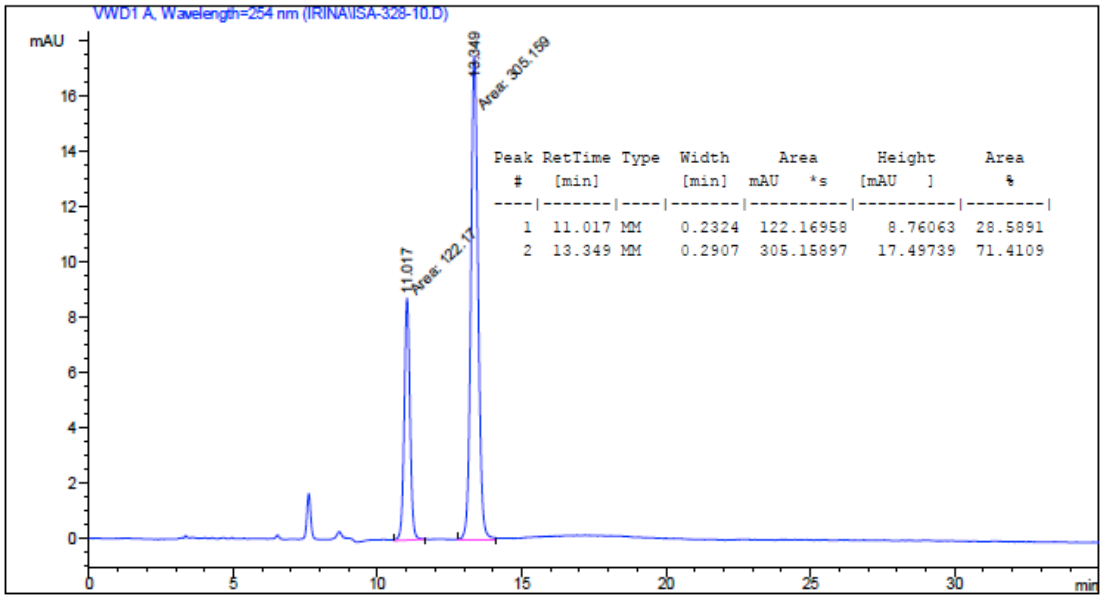

(2*S*,1'*R*)-2-(Hydroxy-2-trifluoromethylphenylmethyl)cyclohexan-1-one **11f**:

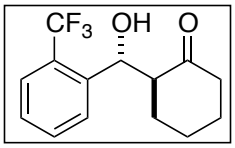

Enantiomeric excess was determined by HPLC with a Chiralpak AS-H column (90:10 Hexane:2-propanol), 0.5 mL/min, λ = 220 nm; major enantiomer t_r = 19.8 min, minor enantiomer t_r = 14.7 min. All the spectroscopic data matched with literature.[S6]

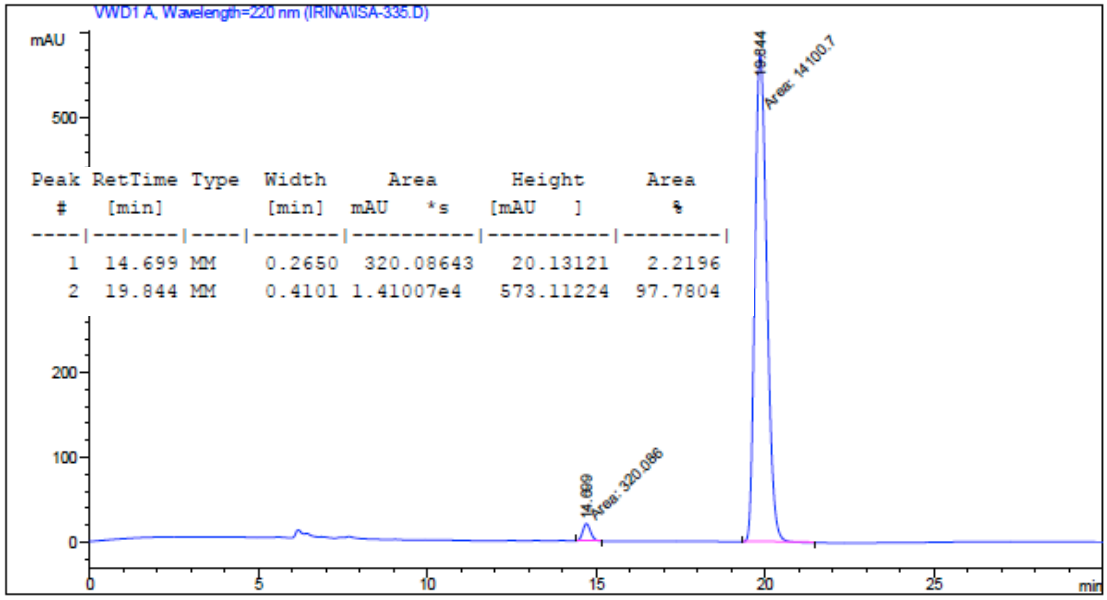

Peak #	RetTime [min]	Type	Width [min]	Area mAU *s	Height [mAU]	Area %
1	14.699	MM	0.2650	320.08643	20.13121	2.2196
2	19.844	MM	0.4101	1.41007e4	573.11224	97.7804

Racemic mixture:

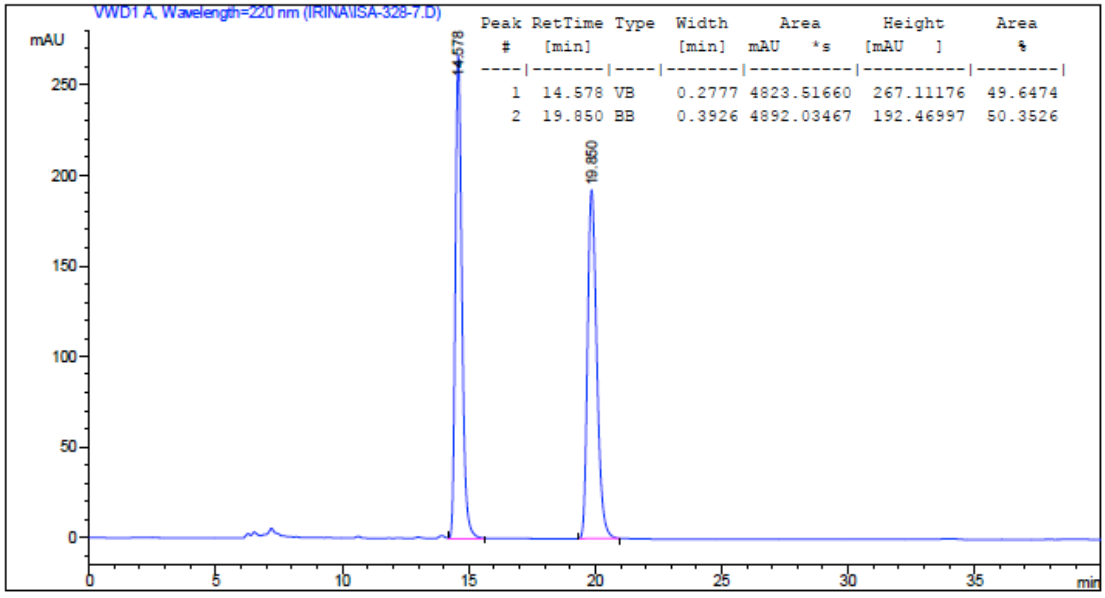

Peak #	RetTime [min]	Type	Width [min]	Area mAU *s	Height [mAU]	Area %
1	14.578	VB	0.2777	4823.51660	267.11176	49.6474
2	19.850	BB	0.3926	4892.03467	192.46997	50.3526

Chapter II

(2*S*,1'*R*)-2-(Hydroxyphenylmethyl)cyclohexan-1-one **11g**:

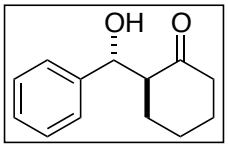

Enantiomeric excess was determined by HPLC with a Chiralcel OD-H column (99:1 Hexane:2-propanol), 1.0 mL/min, λ = 213 nm; major enantiomer t_r = 18.4 min, minor enantiomer t_r = 23.9 min. All the spectroscopic data matched with literature.[S5,S7]

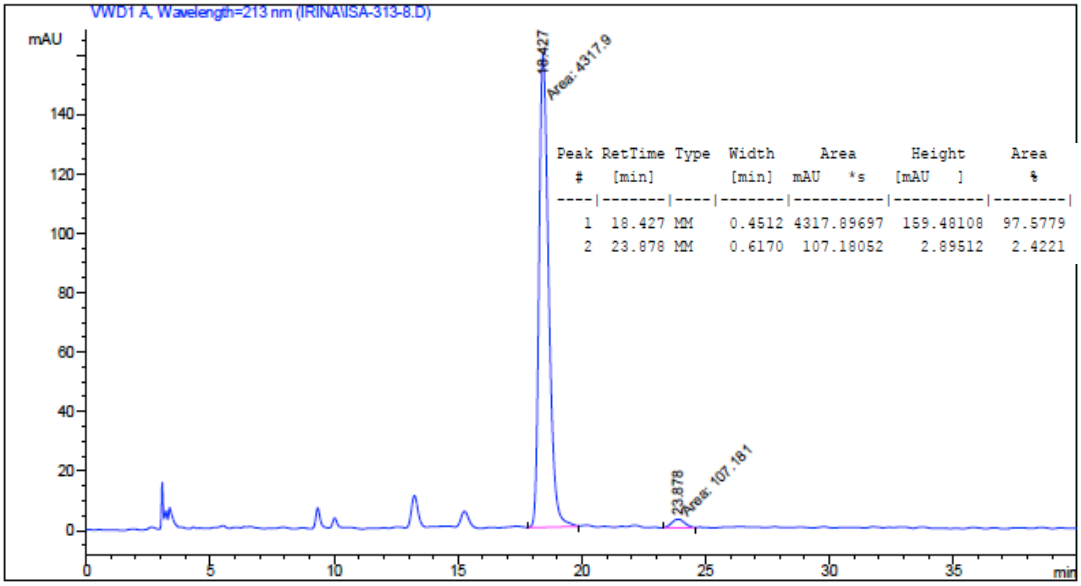

Methyl 4-((*R*)-hydroxy((*S*)-2-oxocyclohexyl)methyl)benzoate **11h**:

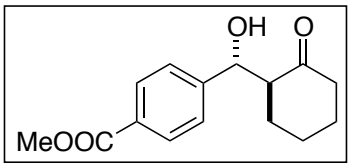

Enantiomeric excess was determined by HPLC with a Chiralpak AS-H column (90:10 Hexane:2-propanol), 1.0 mL/min; λ = 254 nm; major enantiomer t_r = 37.0 min, minor enantiomer t_r = 55.9 min. All the spectroscopic data matched with literature.[S4, S5]

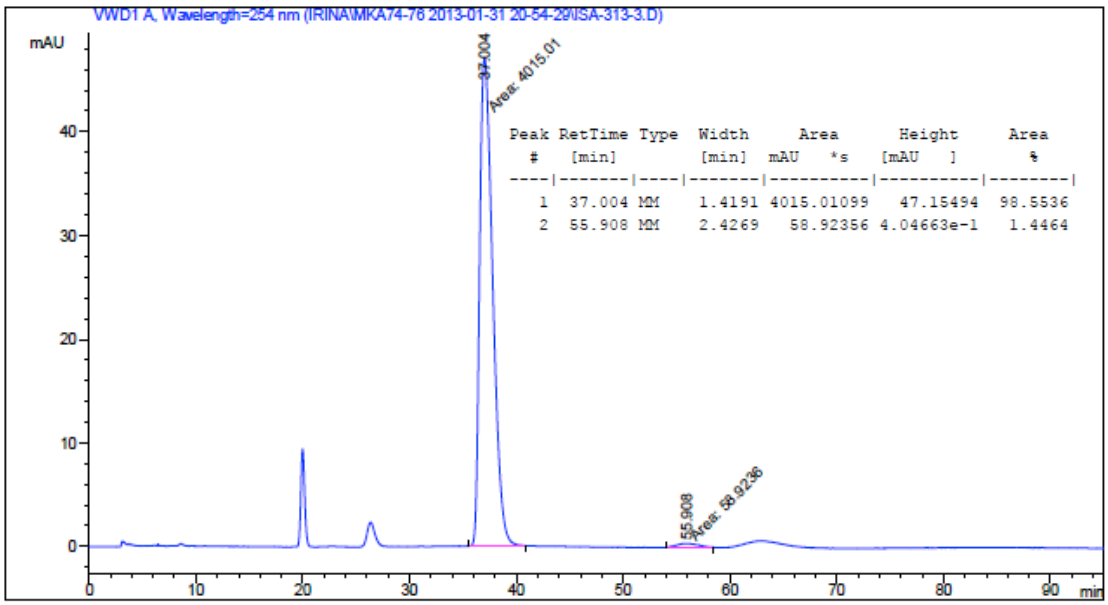

Racemic mixture:

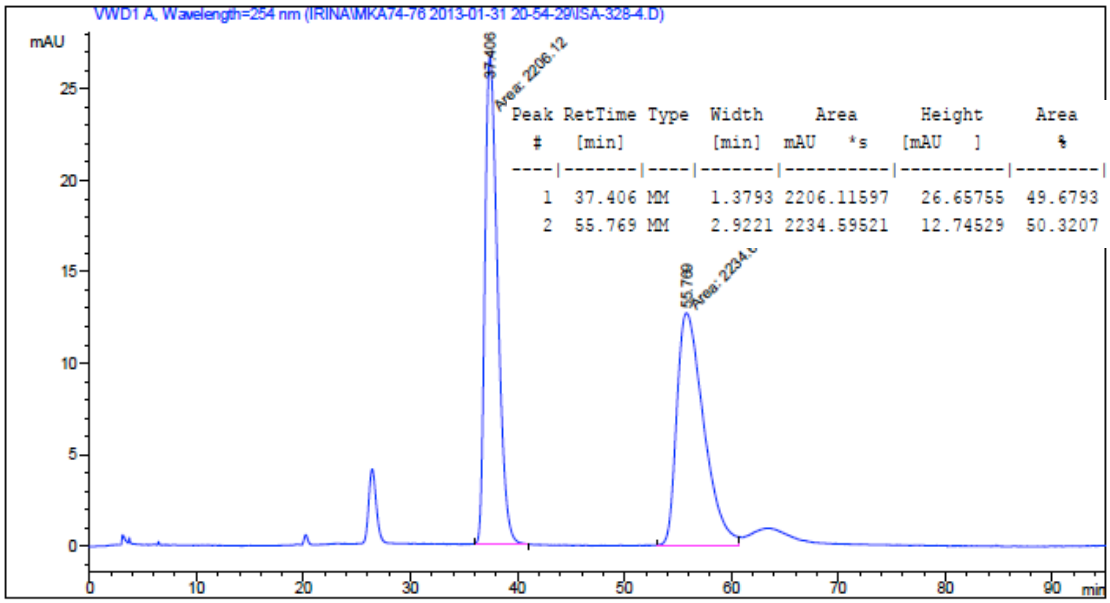

Chapter II

(2*S*,1'*R*)-2-(Hydroxynaphtalen-2-ylmethyl)cyclohexan-1-one **11i**:

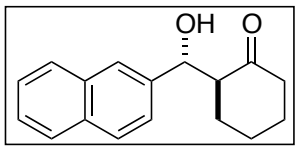

Enantiomeric excess was determined by HPLC with a Chiralpak AS-H column (90:10 Hexane:2-propanol), 0.5 mL/min, λ = 254 nm; major enantiomer t_r = 36.8 min, minor enantiomer t_r = 41.3 min. All the spectroscopic data matched with literature.[S7]

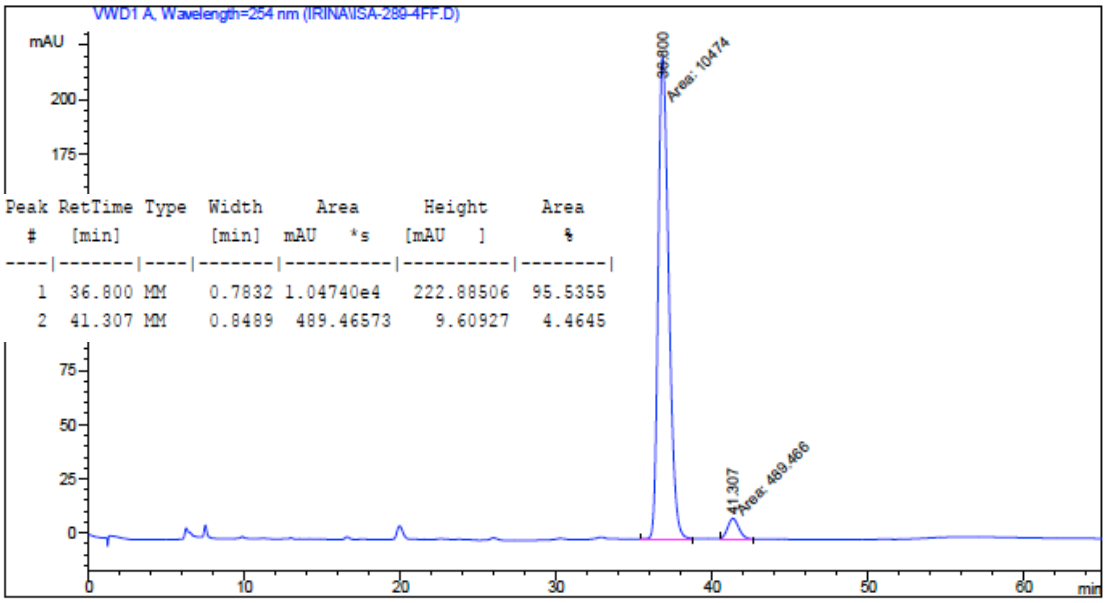

Peak #	RetTime [min]	Type	Width [min]	Area mAU *s	Height [mAU]	Area %
1	36.800	MM	0.7832	1.04740e4	222.88506	95.5355
2	41.307	MM	0.8489	489.46573	9.60927	4.4645

Racemic mixture:

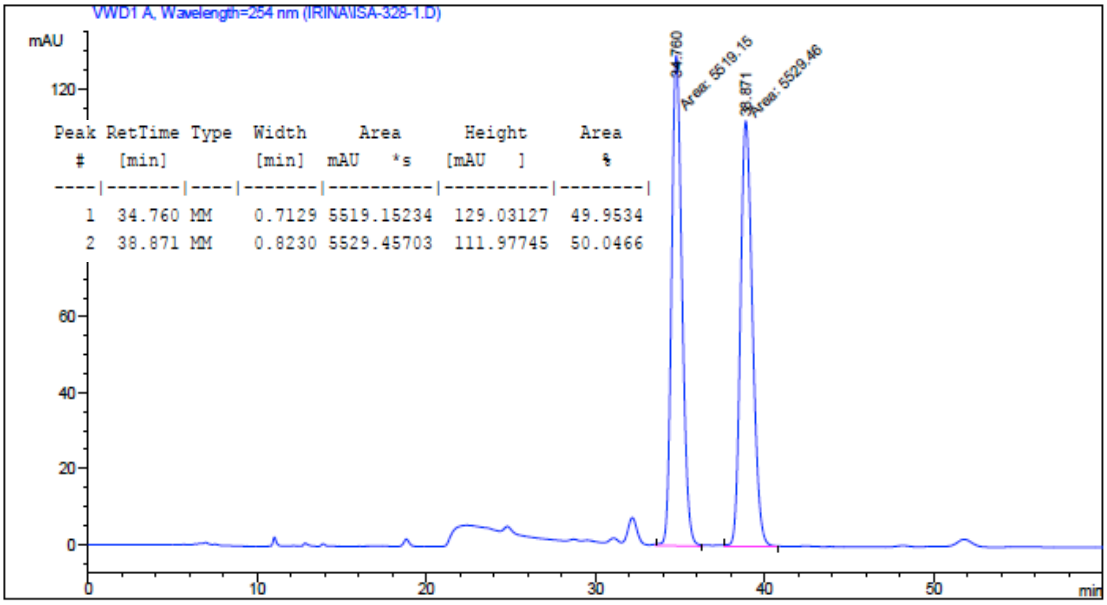

Peak #	RetTime [min]	Type	Width [min]	Area mAU *s	Height [mAU]	Area %
1	34.760	MM	0.7129	5519.15234	129.03127	49.9534
2	38.871	MM	0.8230	5529.45703	111.97745	50.0466

(2*S*,1'*R*)-2-(Hydroxy-4-bromophenylmethyl)cyclohexan-1-one **11j**:

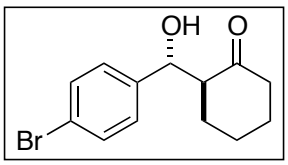

Enantiomeric excess was determined by HPLC with a Chiralpak AD-H column (90:10 Hexane:2-propanol), 1.0 mL/min; λ = 230 nm; major enantiomer t_r = 34.7 min, minor enantiomer t_r = 29.9 min. All the spectroscopic data matched with literature.[S8]

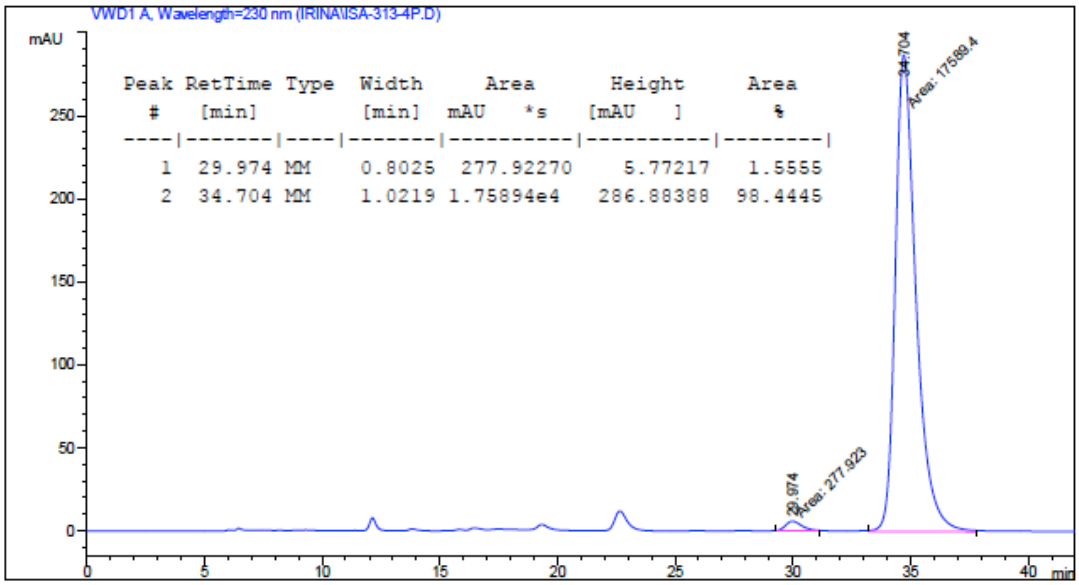

Racemic mixture:

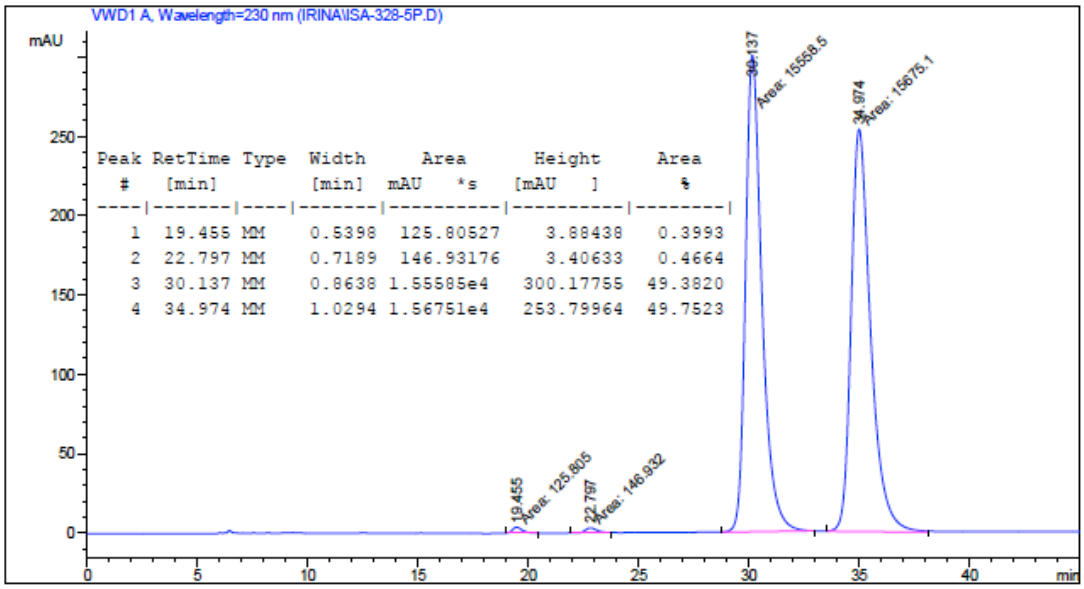

(2*S*,1'*R*)-2-(Hydroxy-4-nitrophenylmethyl)cyclopentan-1-one **11k**:

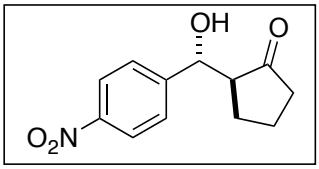

Enantiomeric excess was determined by HPLC with a Chiralpak AD-H column (97:3 Hexane:2-propanol), 1.0 mL/min; λ = 254 nm; major enantiomer t_r = 65.6 min, minor enantiomer t_r = 63.9 min. All the spectroscopic data matched with literature.[S4, S8]

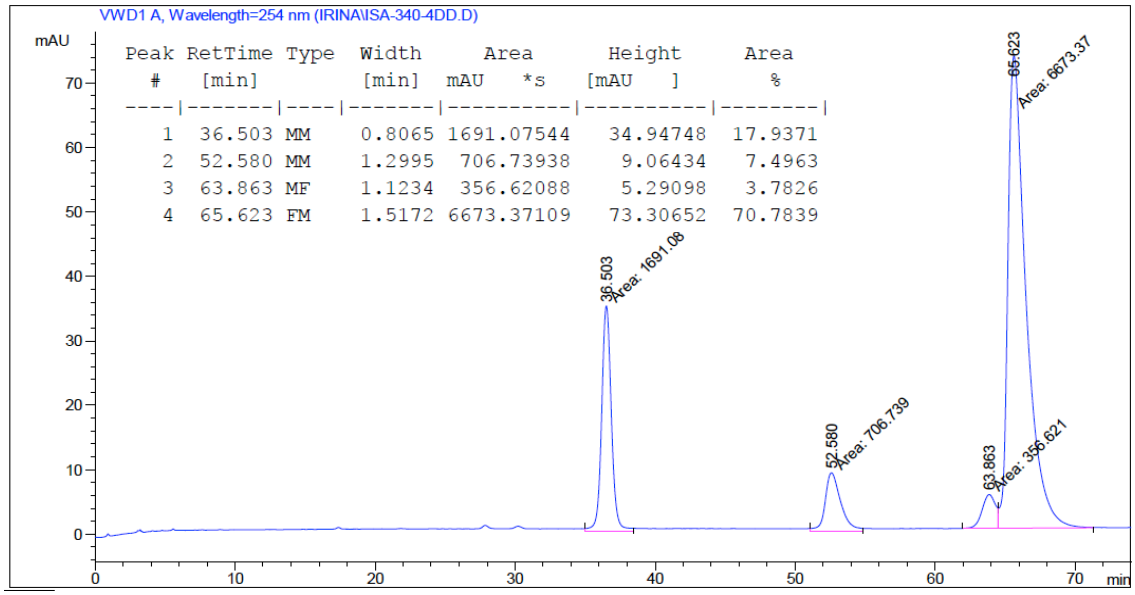

S22

(2*S*,1'*R*)-2-(Hydroxy-4-nitrophenylmethyl)tetrahydropyran-4-one **11l**:

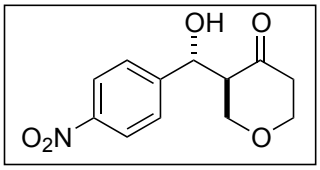

Enantiomeric excess was determined by HPLC with a Chiralpak AD-H column (80:20 Hexane:2-propanol), 1.0 mL/min; λ = 254 nm; major enantiomer t_r = 22.9 min, minor enantiomer t_r = 19.5 min. All the spectroscopic data matched with literature.[S9]

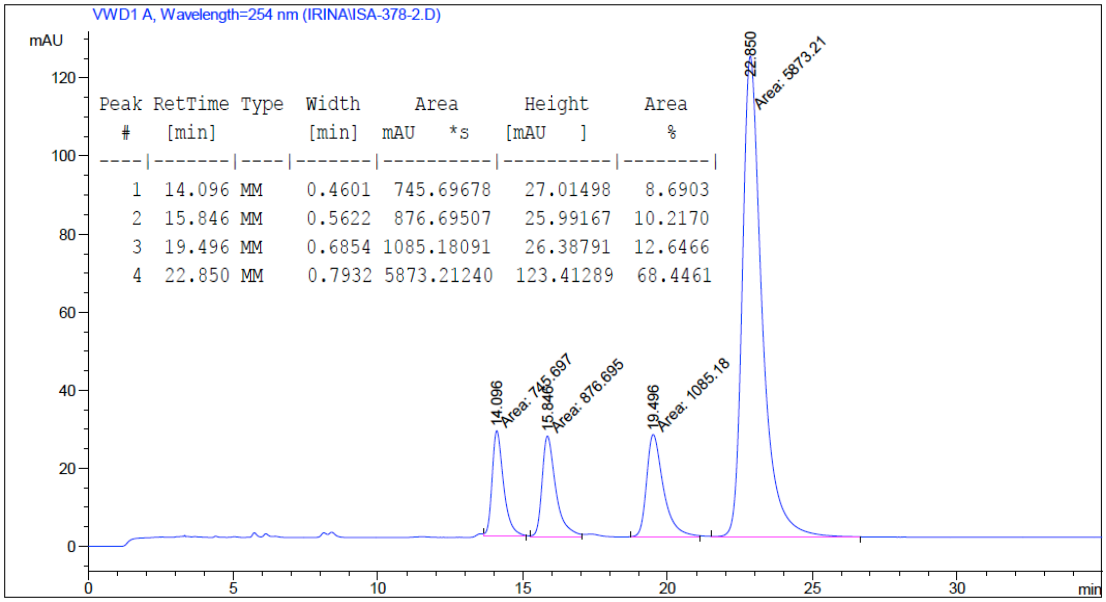

Peak #	RetTime [min]	Type	Width [min]	Area mAU *s	Height [mAU]	Area %
1	14.096	MM	0.4601	745.69678	27.01498	8.6903
2	15.846	MM	0.5622	876.69507	25.99167	10.2170
3	19.496	MM	0.6854	1085.18091	26.38791	12.6466
4	22.850	MM	0.7932	5873.21240	123.41289	68.4461

Chapter II

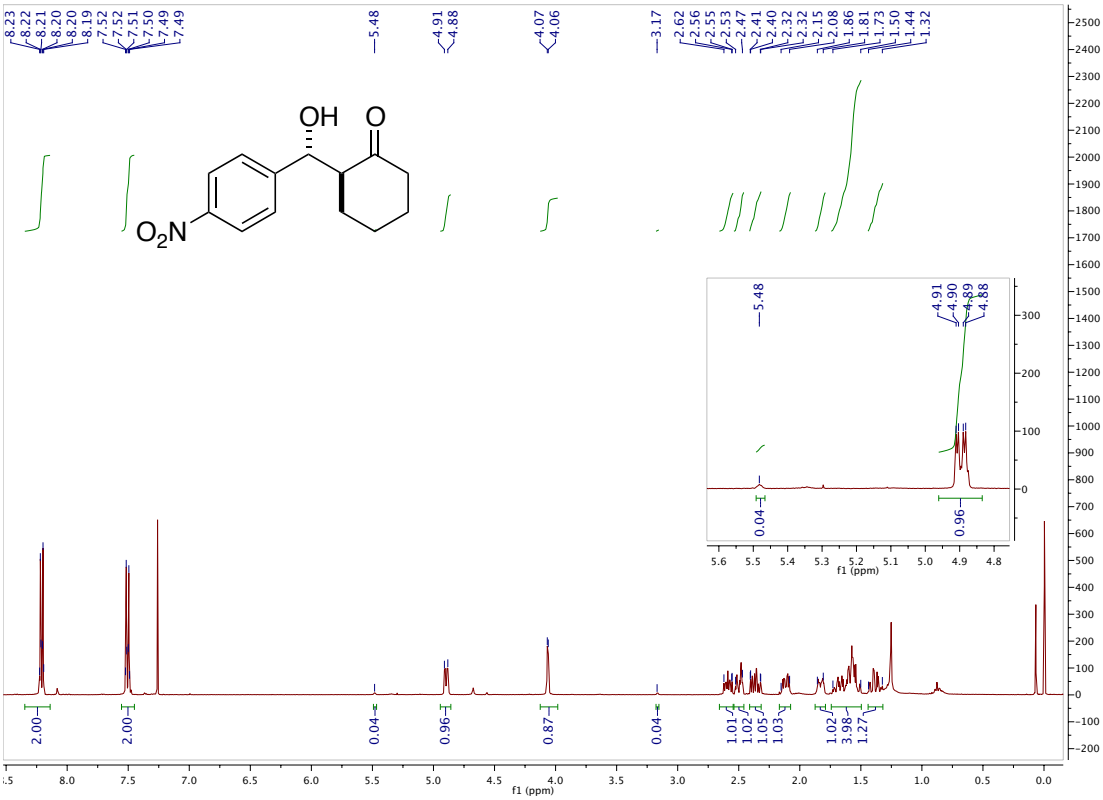
OH
O
O_2N
f1 (ppm)

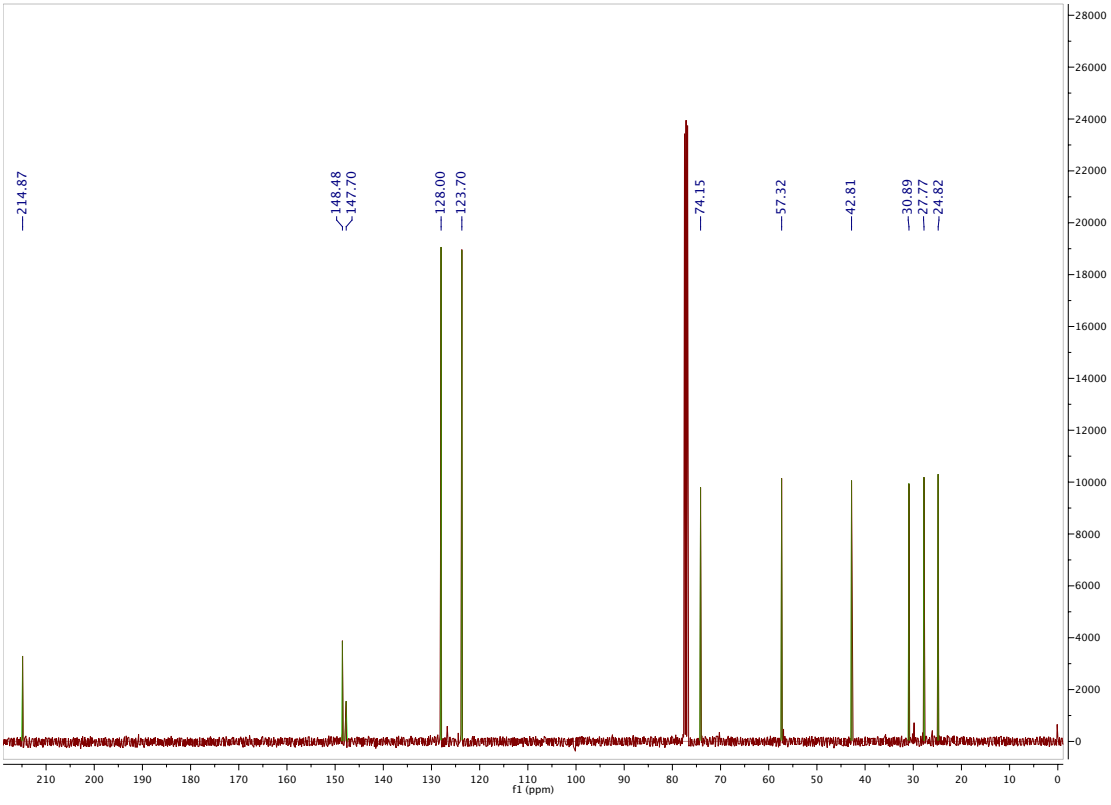
214.87
148.48
147.70
128.00
123.70
74.15
57.32
42.81
30.89
27.77
24.82
f1 (ppm)

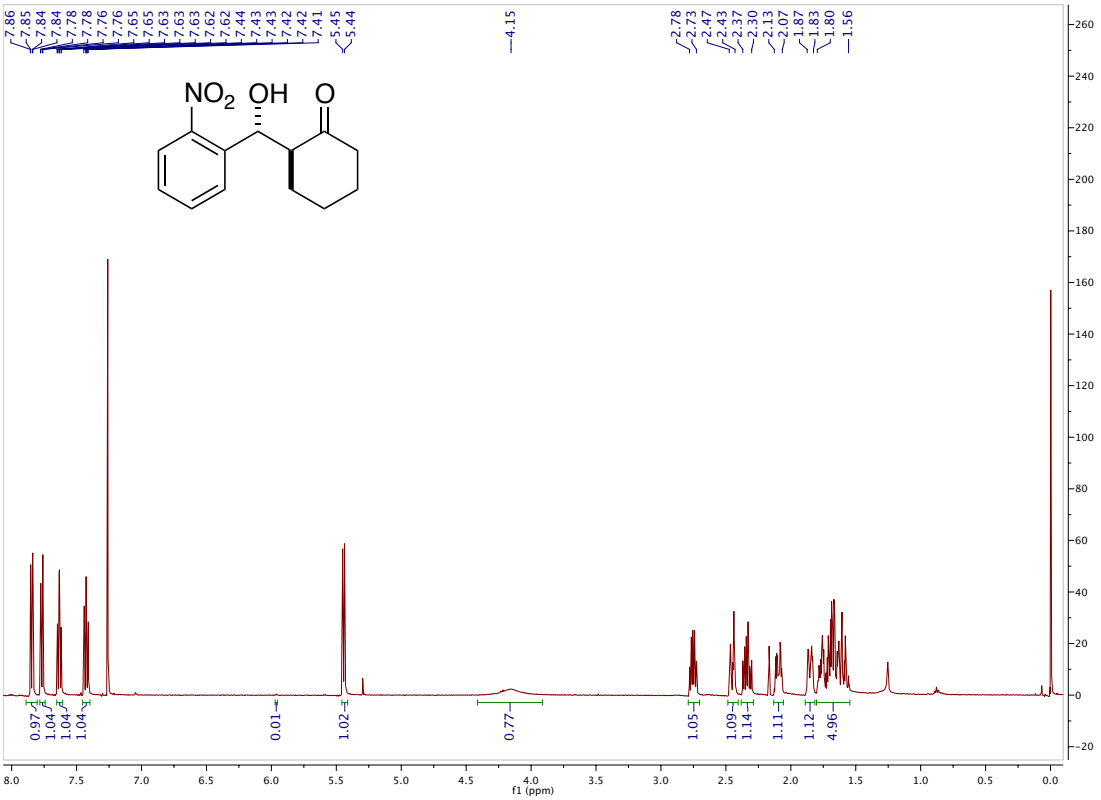
7.86
7.85
7.84
7.84
7.78
7.78
7.76
7.76
7.65
7.65
7.63
7.63
7.63
7.62
7.62
7.44
7.43
7.43
7.42
7.42
7.41
5.45
5.44
4.15
2.78
2.73
2.47
2.43
2.37
2.30
2.13
2.07
1.87
1.83
1.80
1.56
NO2 OH O
0.97
1.04
1.04
1.04
0.01
1.02
0.77
1.05
1.09
1.14
1.11
1.12
4.96
f1 (ppm)

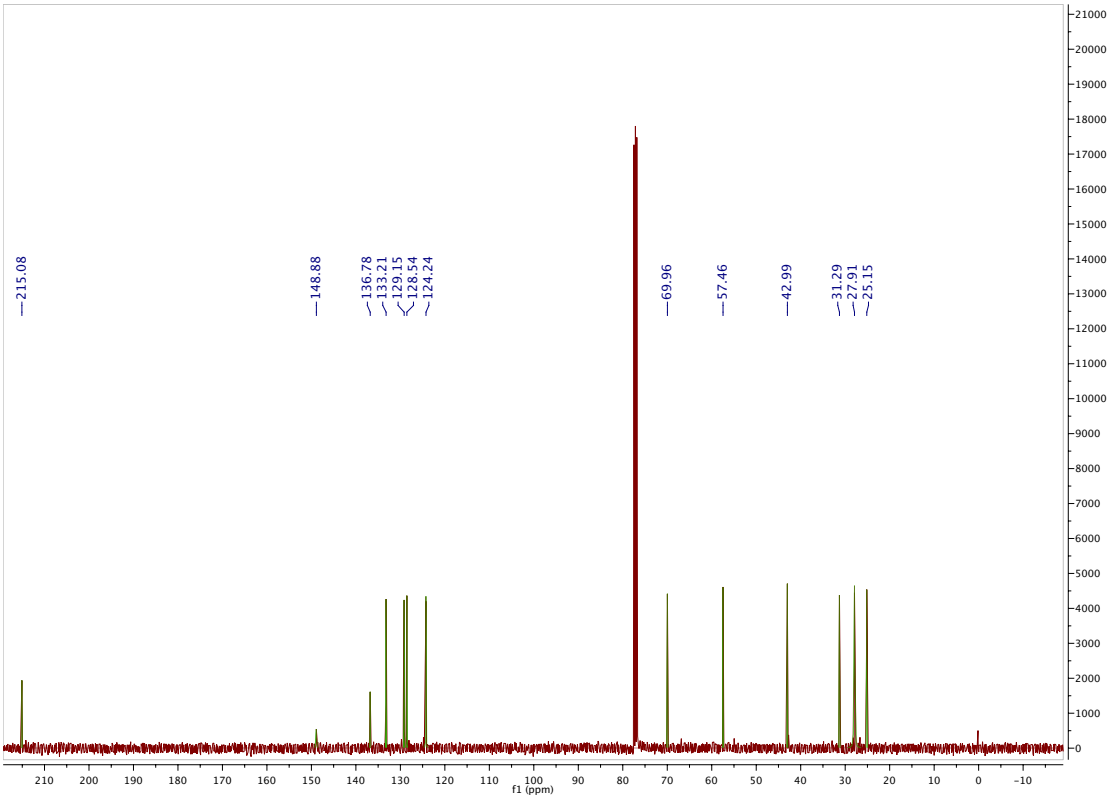
215.08
148.88
136.78
133.21
129.15
128.54
124.24
69.96
57.46
42.99
31.29
27.91
25.15
f1 (ppm)

Chapter II

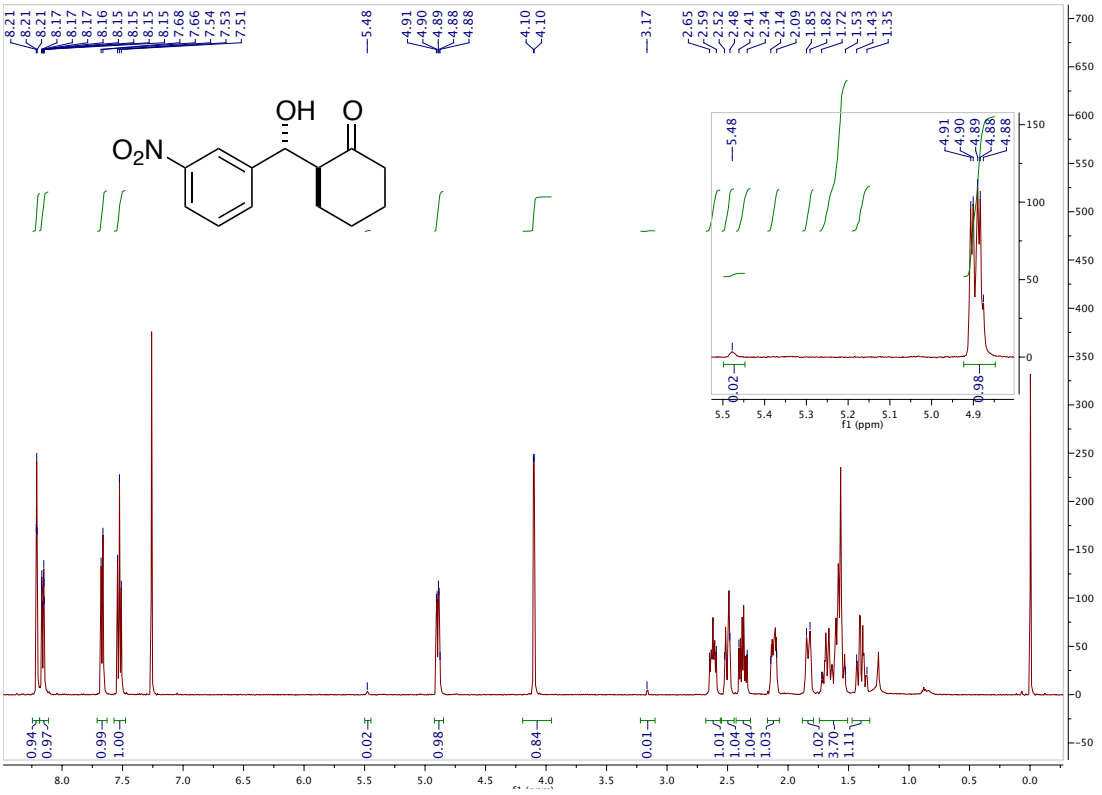

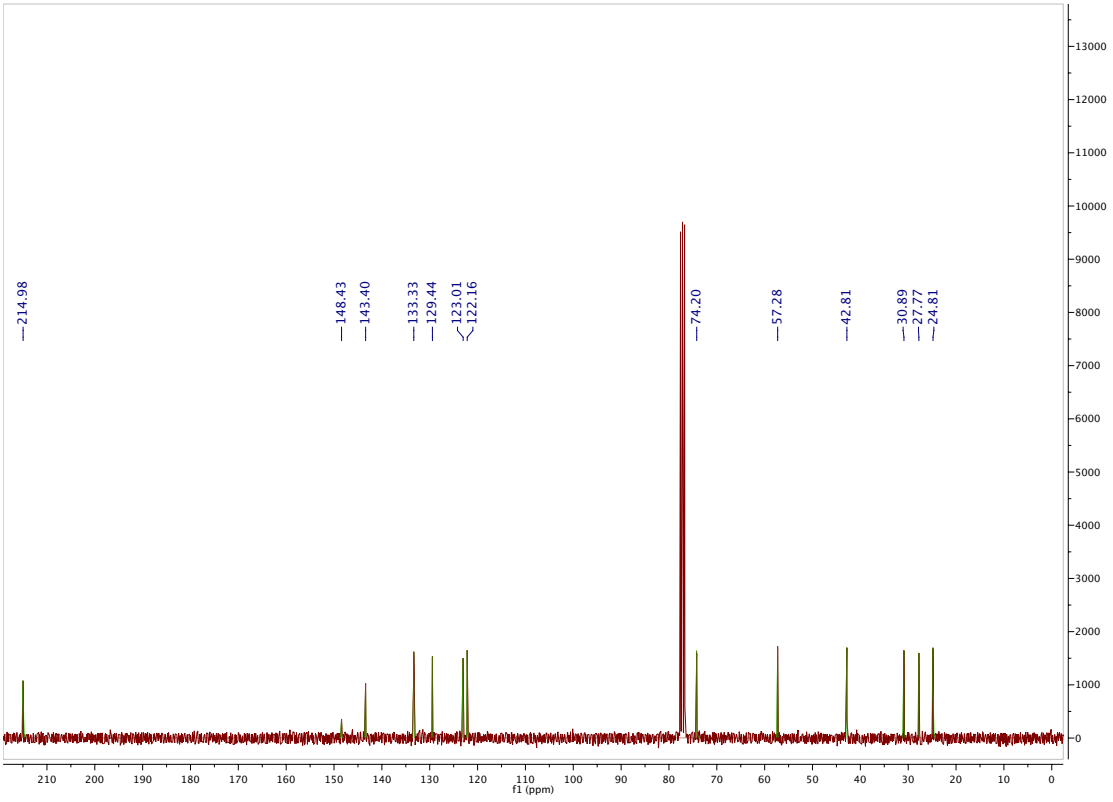

S26

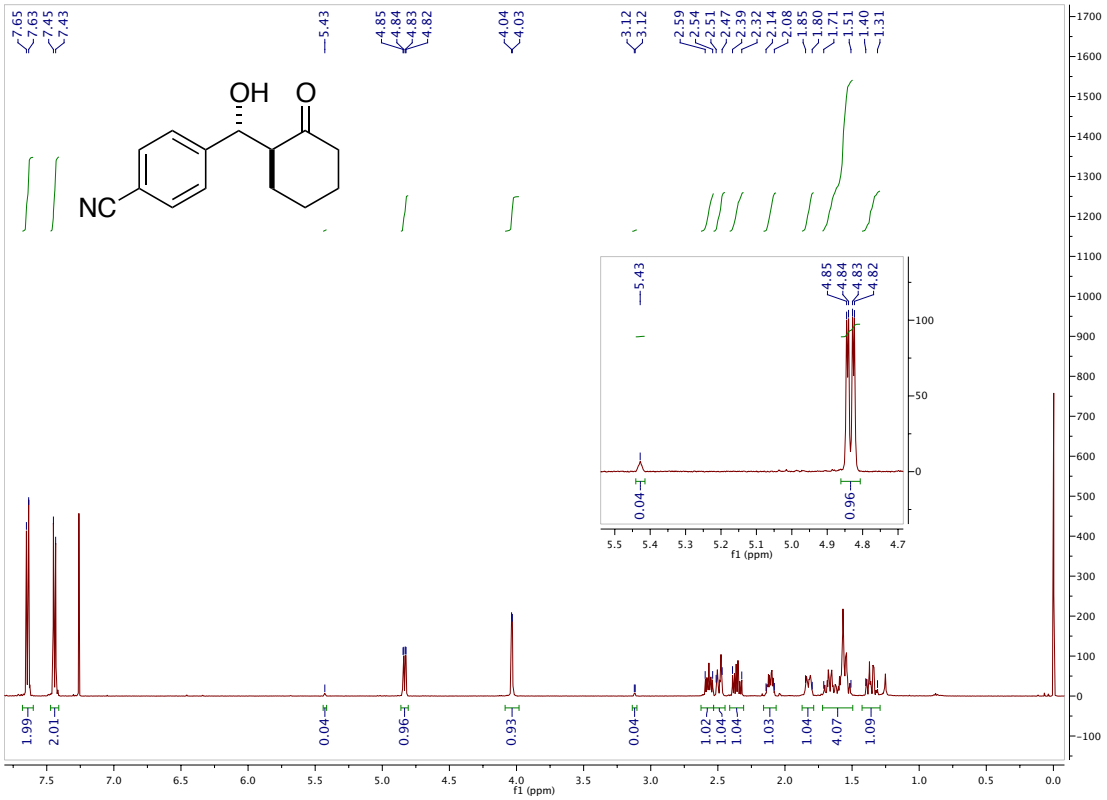
OH
O
NC
7.65
7.63
7.45
7.43
5.43
4.85
4.84
4.83
4.82
4.04
4.03
3.12
3.12
2.59
2.54
2.51
2.47
2.39
2.32
2.14
2.08
1.85
1.80
1.71
1.51
1.40
1.31
1.99
2.01
0.04
0.96
0.93
0.04
1.02
1.04
1.04
1.03
1.04
4.07
1.09
f1 (ppm)

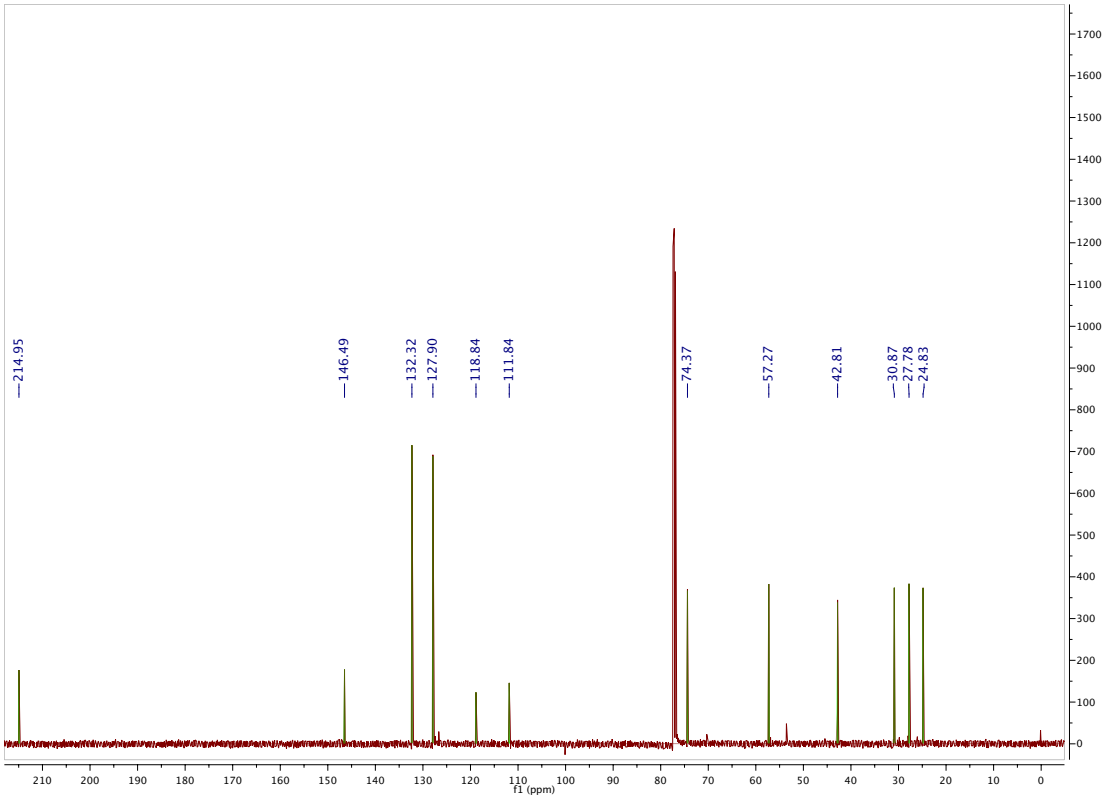
214.95
146.49
132.32
127.90
118.84
111.84
74.37
57.27
42.81
30.87
27.78
24.83
f1 (ppm)

Chapter II

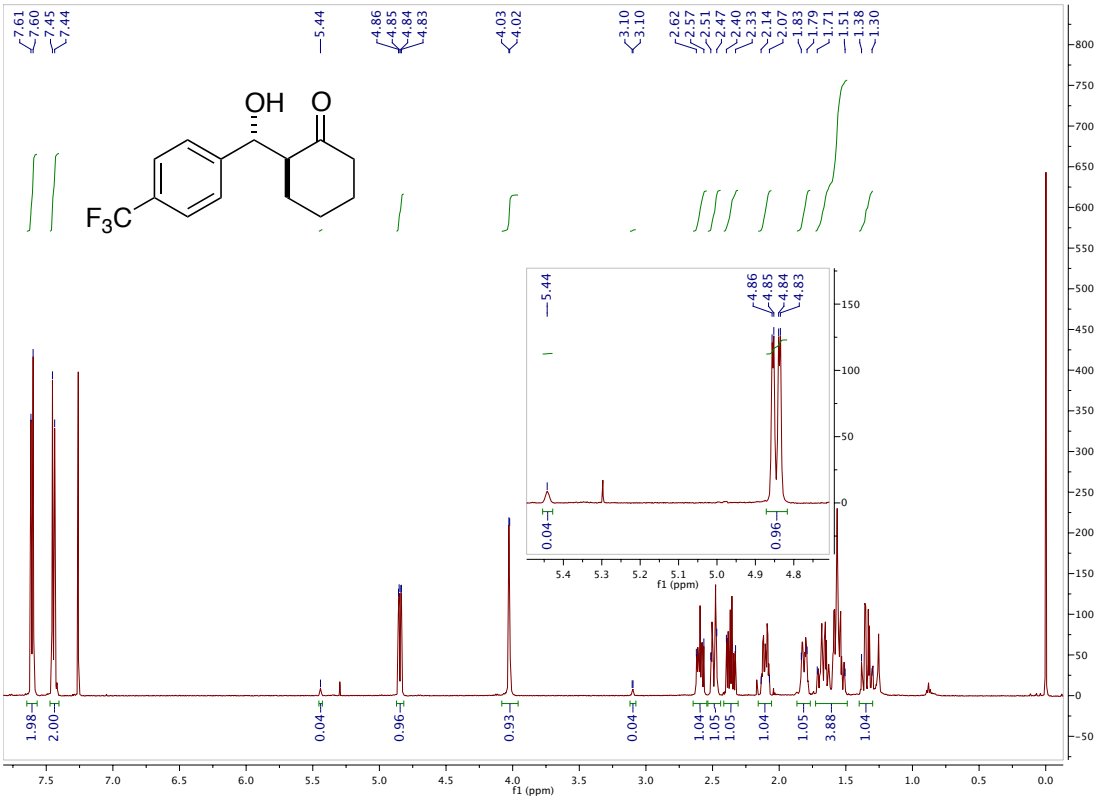
OH
O
F3C
7.61
7.60
7.45
7.44
5.44
4.86
4.85
4.84
4.83
4.03
4.02
3.10
3.10
2.62
2.57
2.51
2.47
2.40
2.33
2.14
2.07
1.83
1.79
1.71
1.51
1.38
1.30
1.98
2.00
0.04
0.96
0.93
0.04
1.04
1.05
1.05
1.04
1.05
3.88
1.04
f1 (ppm)

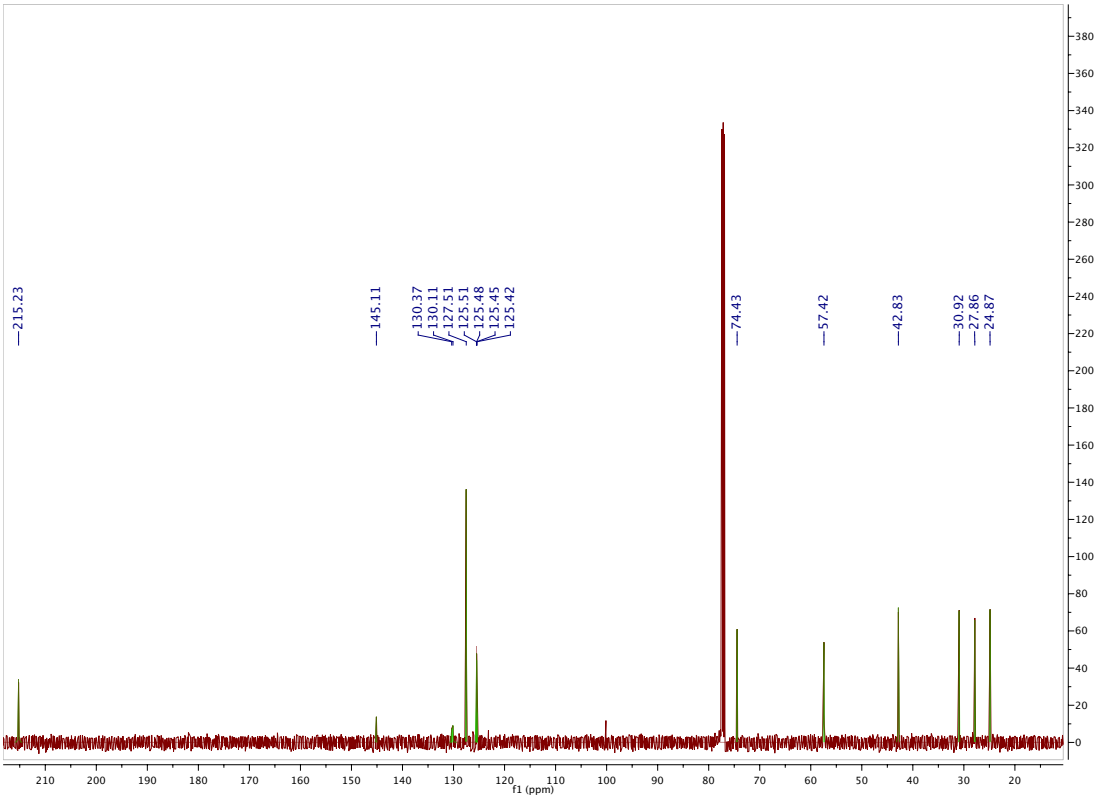
215.23
145.11
130.37
130.11
127.51
125.51
125.48
125.45
125.42
74.43
57.42
42.83
30.92
27.86
24.87
f1 (ppm)

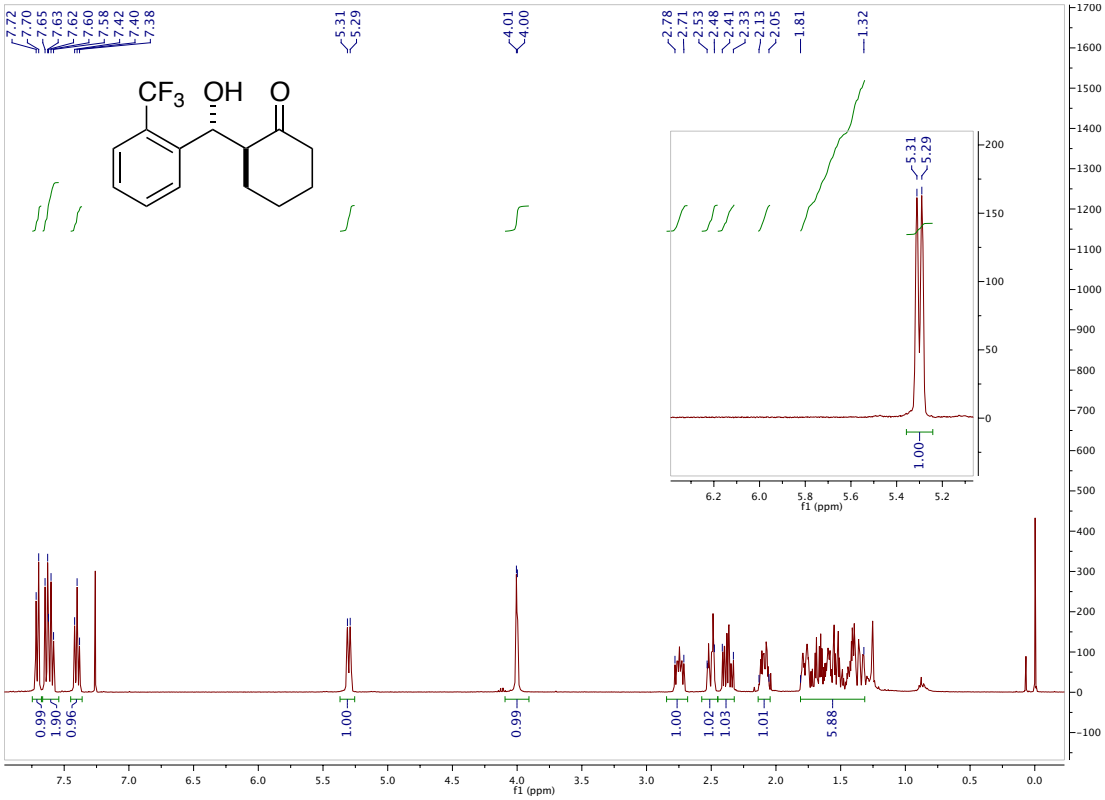
7.72
7.70
7.65
7.63
7.62
7.60
7.58
7.42
7.40
7.38
5.31
5.29
4.01
4.00
2.78
2.71
2.53
2.48
2.41
2.33
2.13
2.05
1.81
1.32
CF3 OH O
0.99
1.90
0.96
1.00
0.99
1.00
1.02
1.03
1.01
5.88
f1 (ppm)

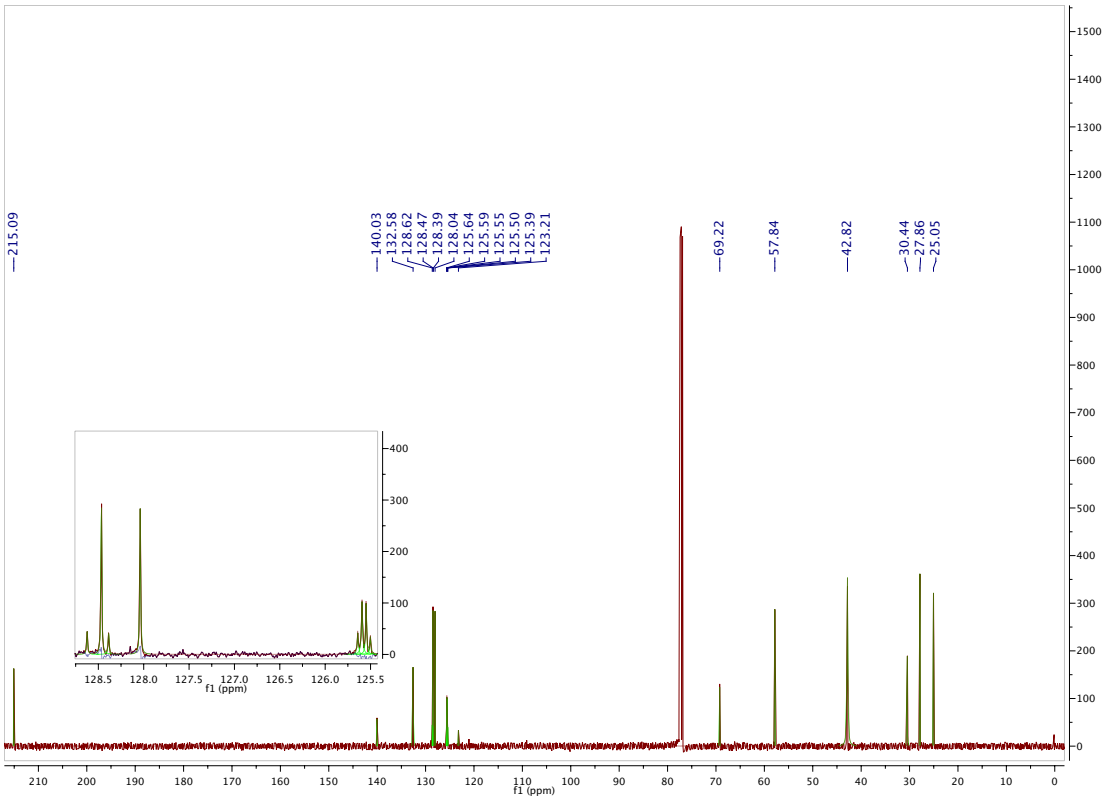
215.09
140.03
132.58
128.62
128.47
128.39
128.04
125.64
125.59
125.55
125.50
125.39
123.21
69.22
57.84
42.82
30.44
27.86
25.05
f1 (ppm)

Chapter II

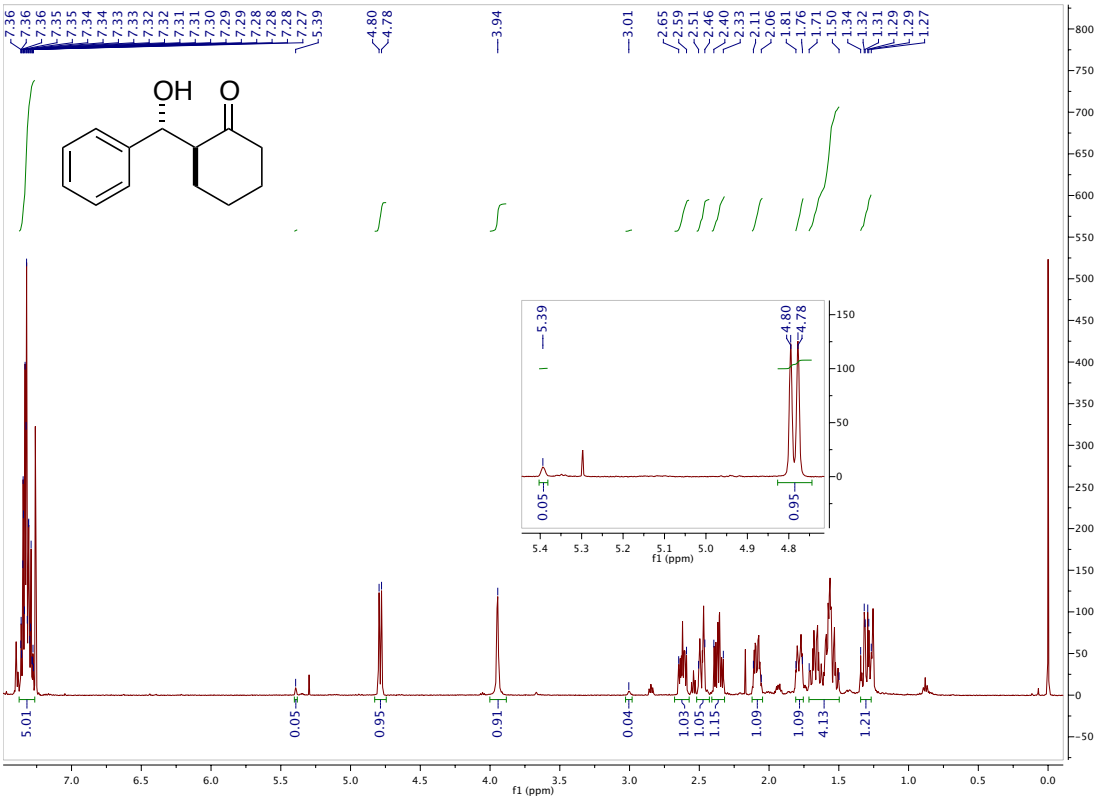

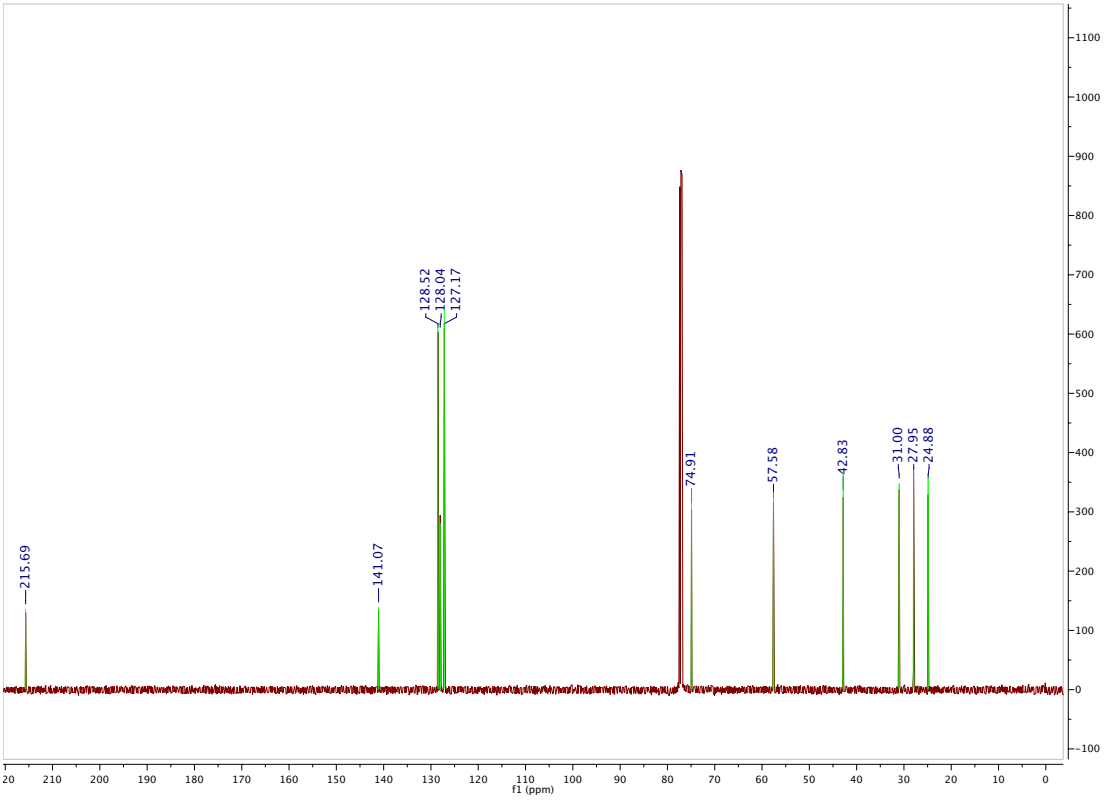

S30

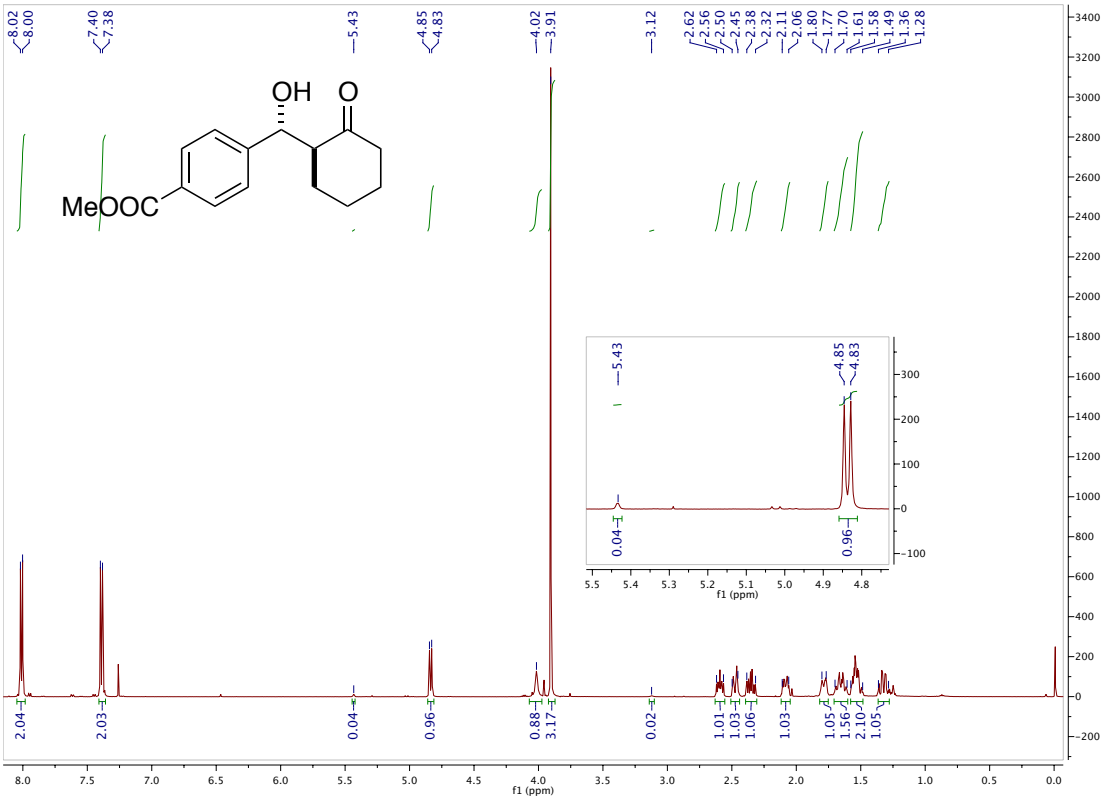
OH
O
MeOOC
f1 (ppm)

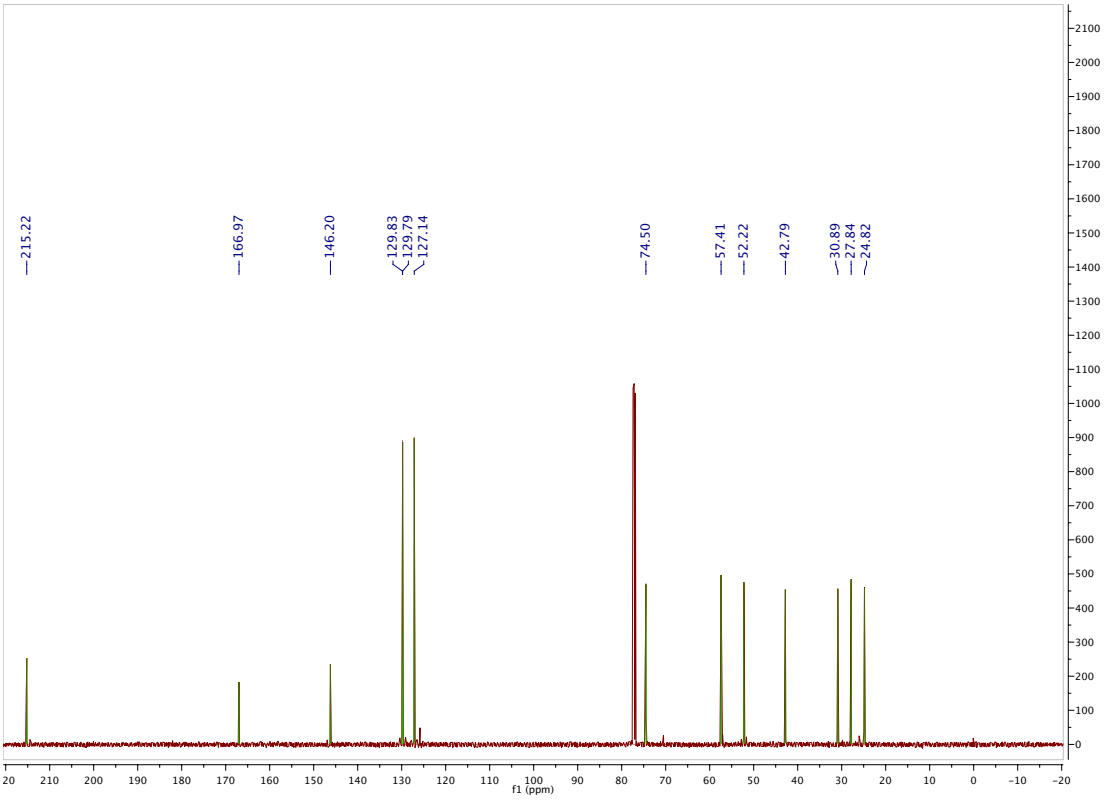
f1 (ppm)

Chapter II

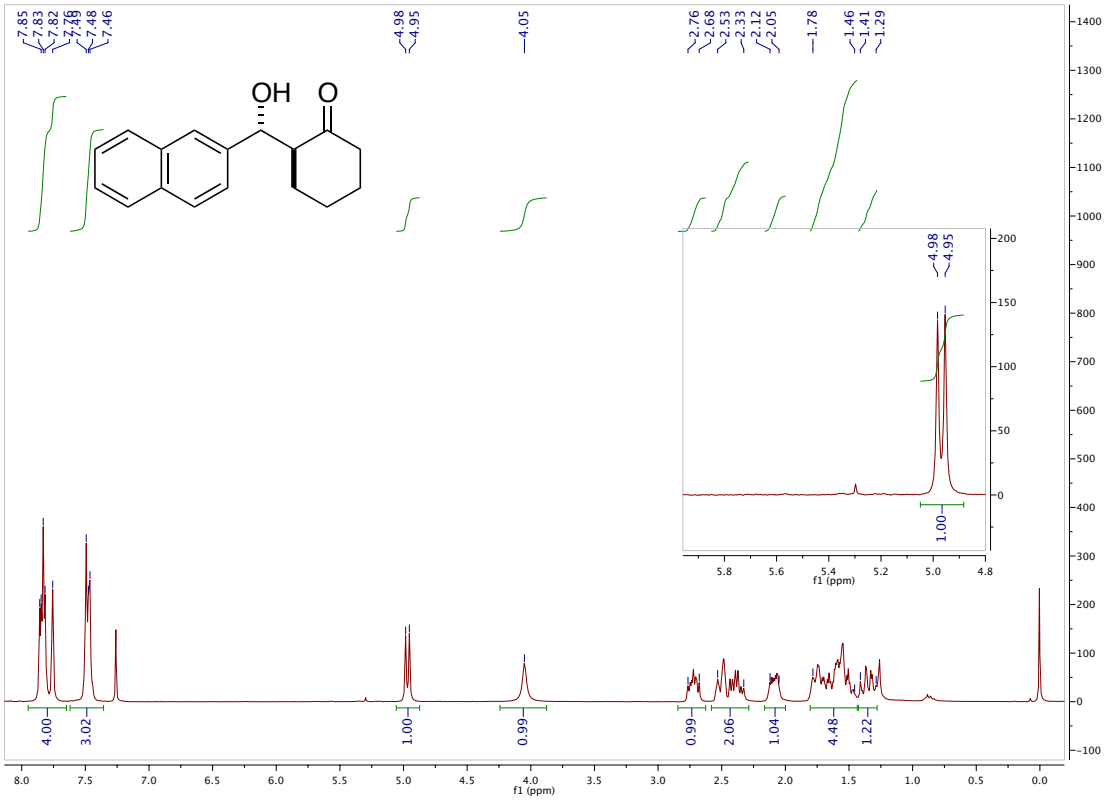
OH
O
7.85
7.83
7.82
7.48
7.46
4.98
4.95
4.05
2.76
2.68
2.33
2.12
2.05
1.78
1.46
1.41
1.29
4.00
3.02
1.00
0.99
0.99
2.06
1.04
4.48
1.22
f1 (ppm)

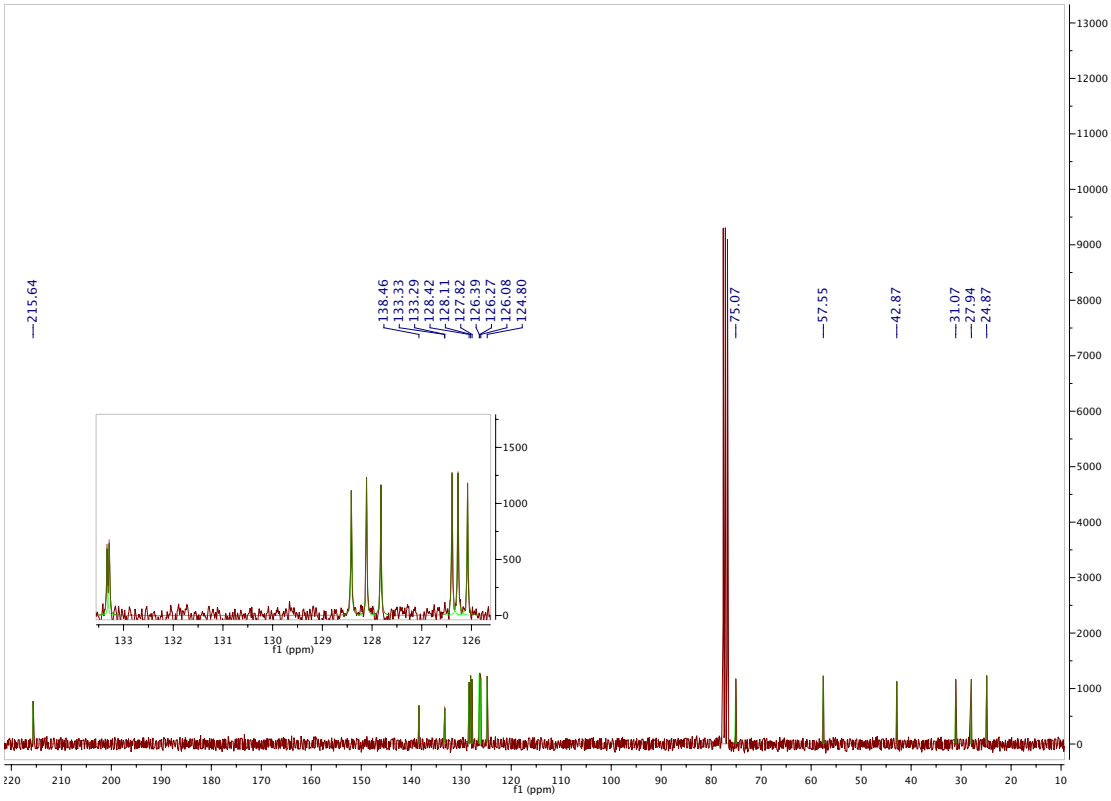
215.64
138.46
133.33
133.29
128.42
128.11
127.82
126.39
126.27
126.08
124.80
75.07
57.55
42.87
31.07
27.94
24.87
f1 (ppm)

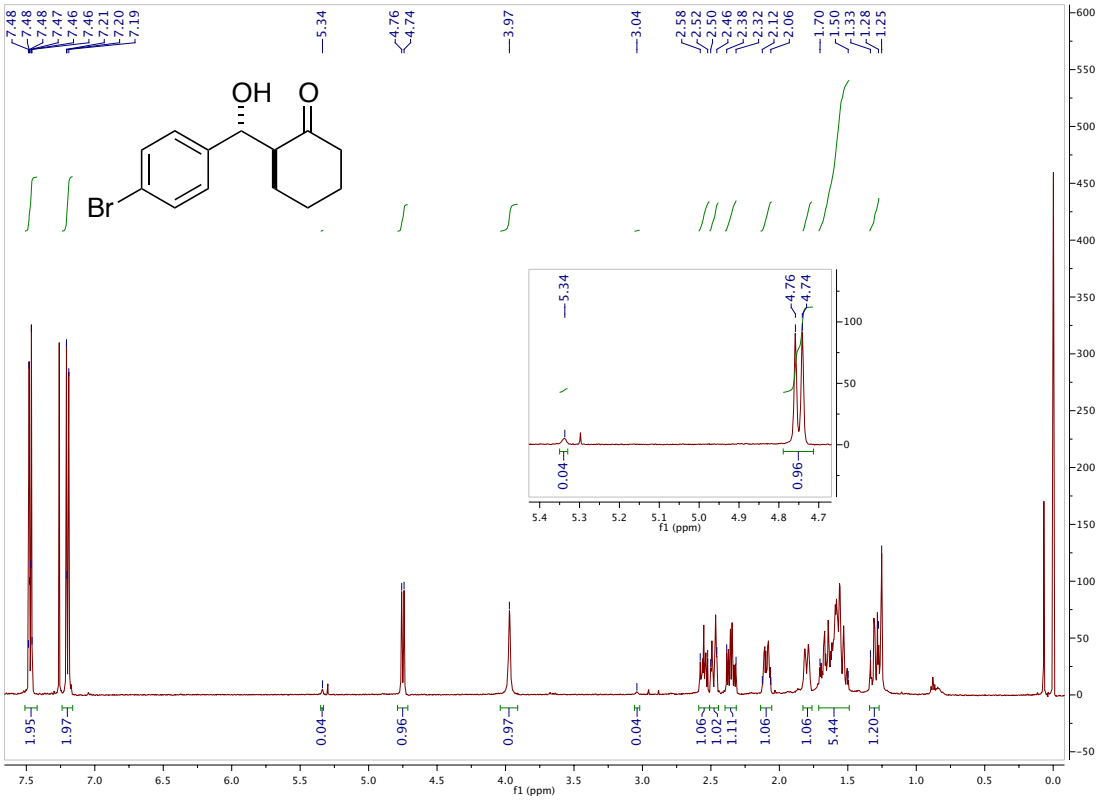
OH
O
Br
7.48
7.48
7.48
7.47
7.46
7.46
7.21
7.20
7.19
5.34
4.76
4.74
3.97
3.04
2.58
2.52
2.50
2.46
2.38
2.32
2.12
2.06
1.70
1.50
1.33
1.28
1.25
1.95
1.97
0.04
0.96
0.97
0.04
1.06
1.02
1.11
1.06
1.06
5.44
1.20
f1 (ppm)

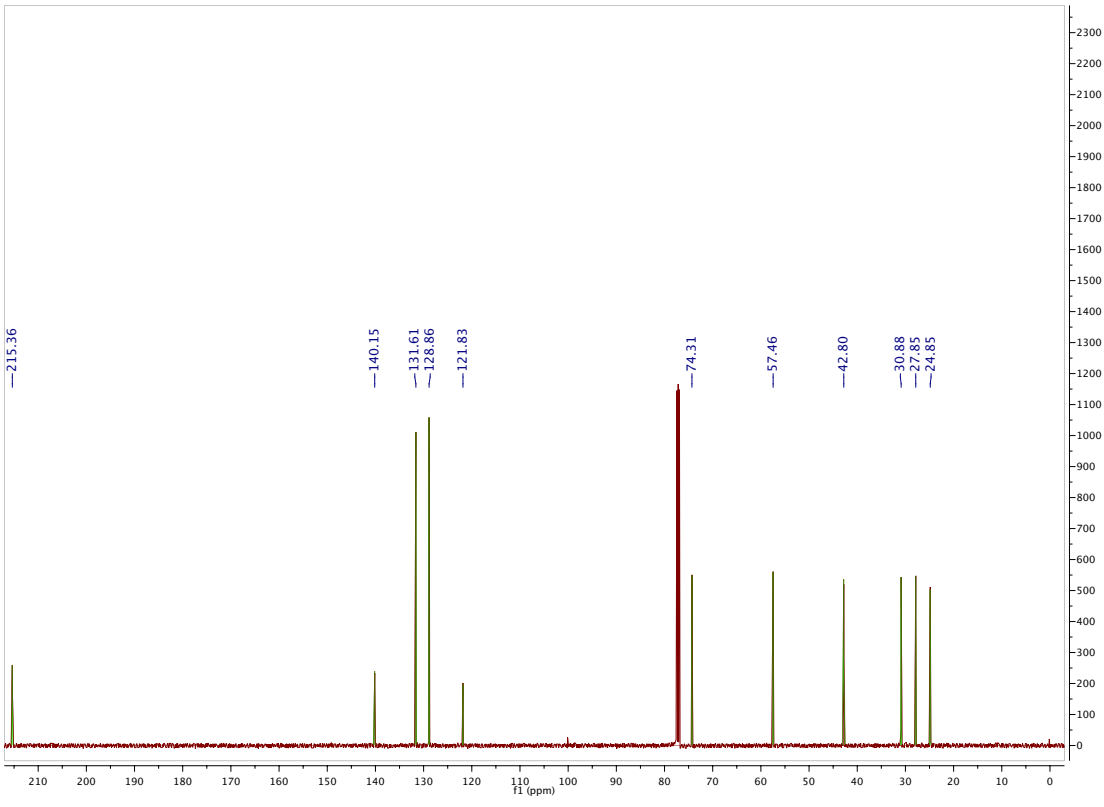
215.36
140.15
131.61
128.86
121.83
74.31
57.46
42.80
30.88
27.85
24.85
f1 (ppm)

Chapter II

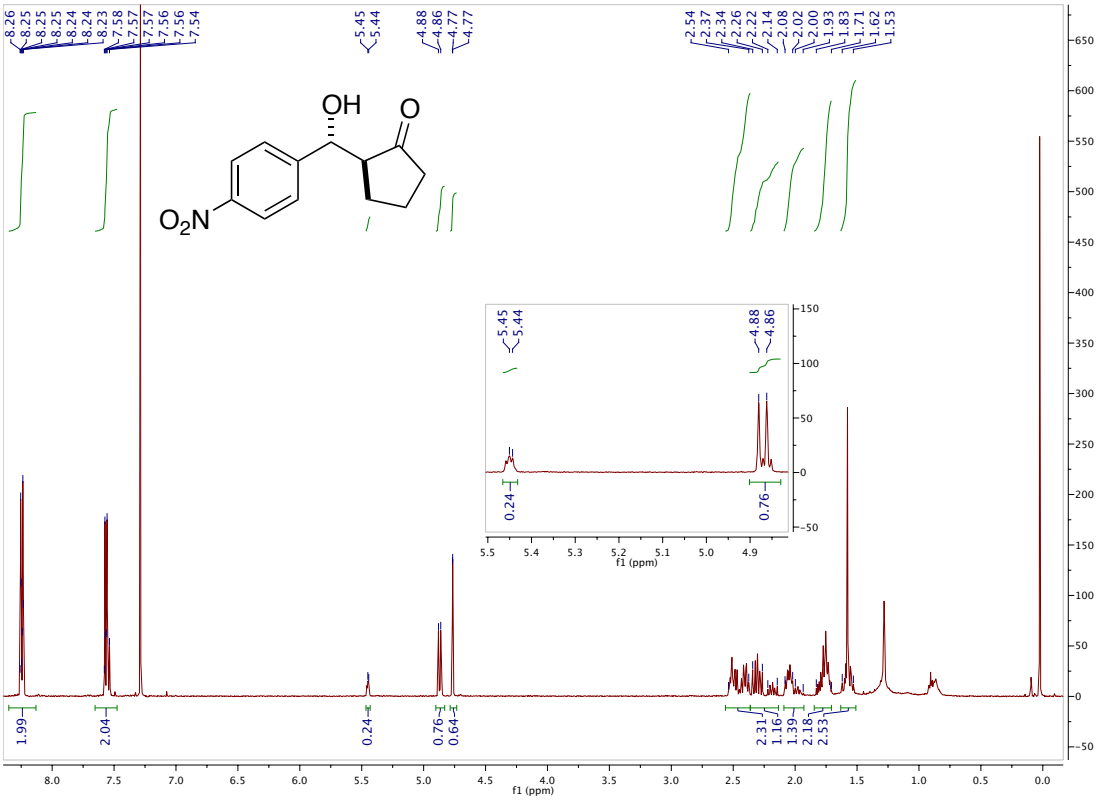
OH
O
O_2N
f1 (ppm)

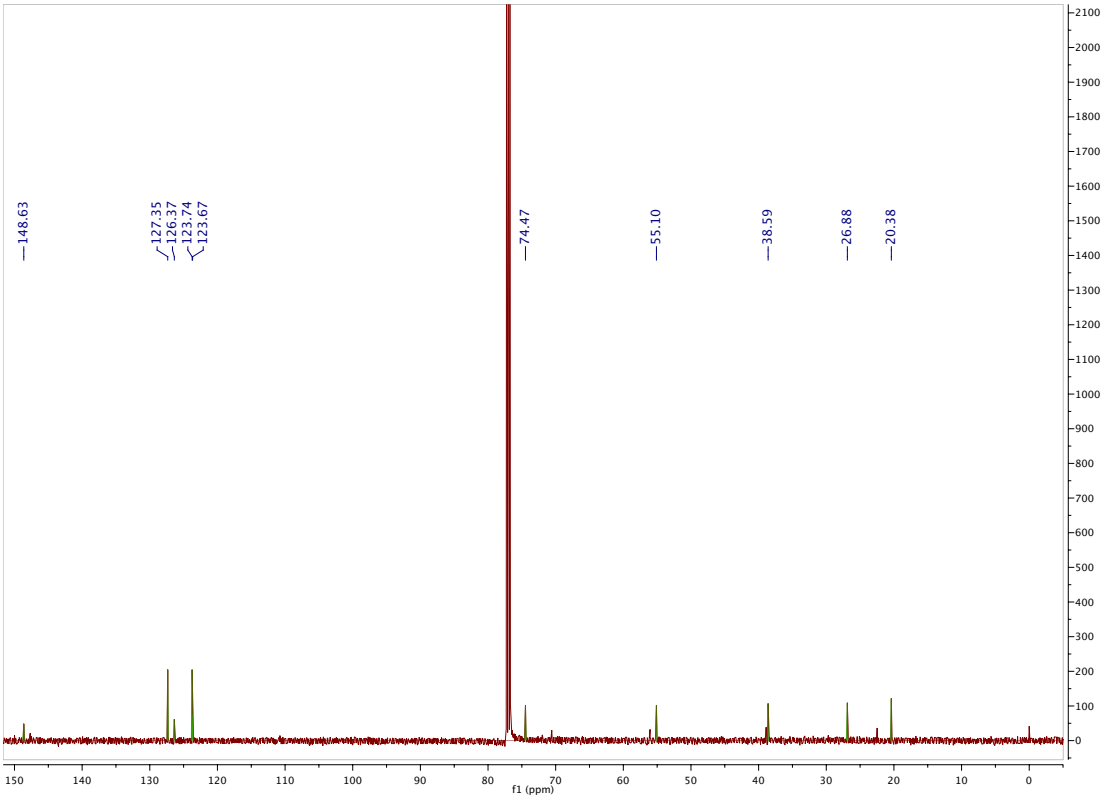
148.63
127.35
126.37
123.74
123.67
74.47
55.10
38.59
26.88
20.38
f1 (ppm)

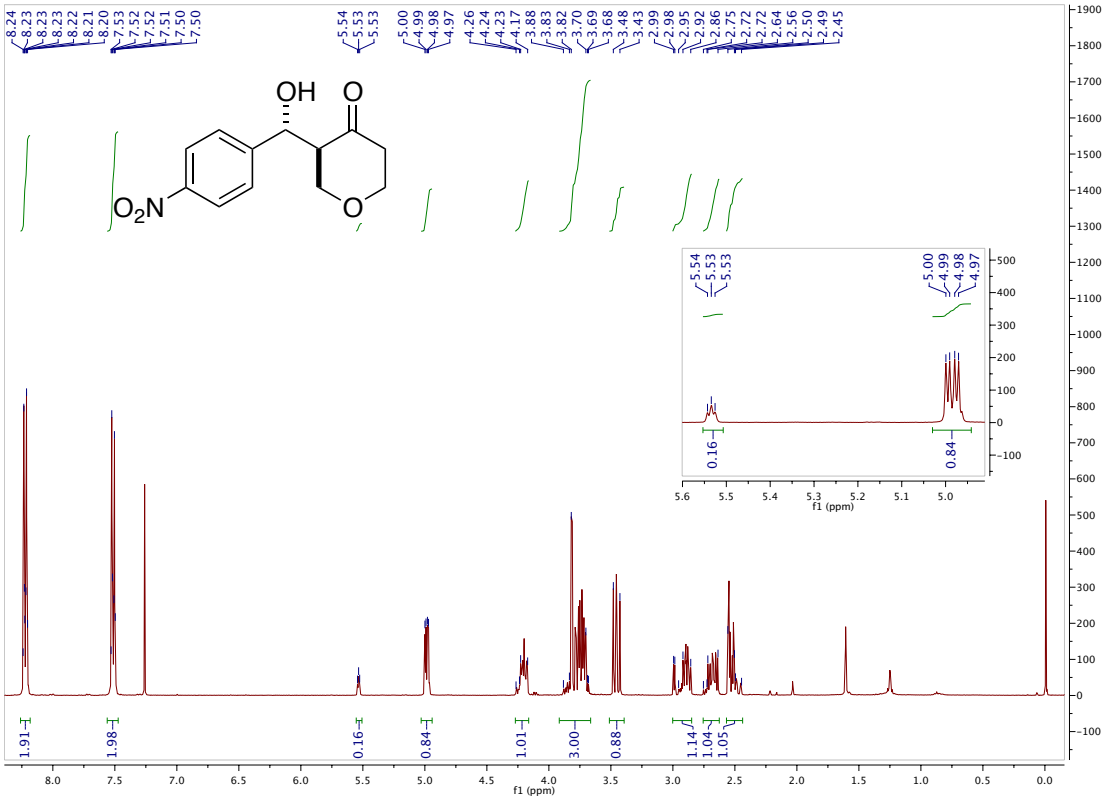
OH
O
O_2N
O
f1 (ppm)

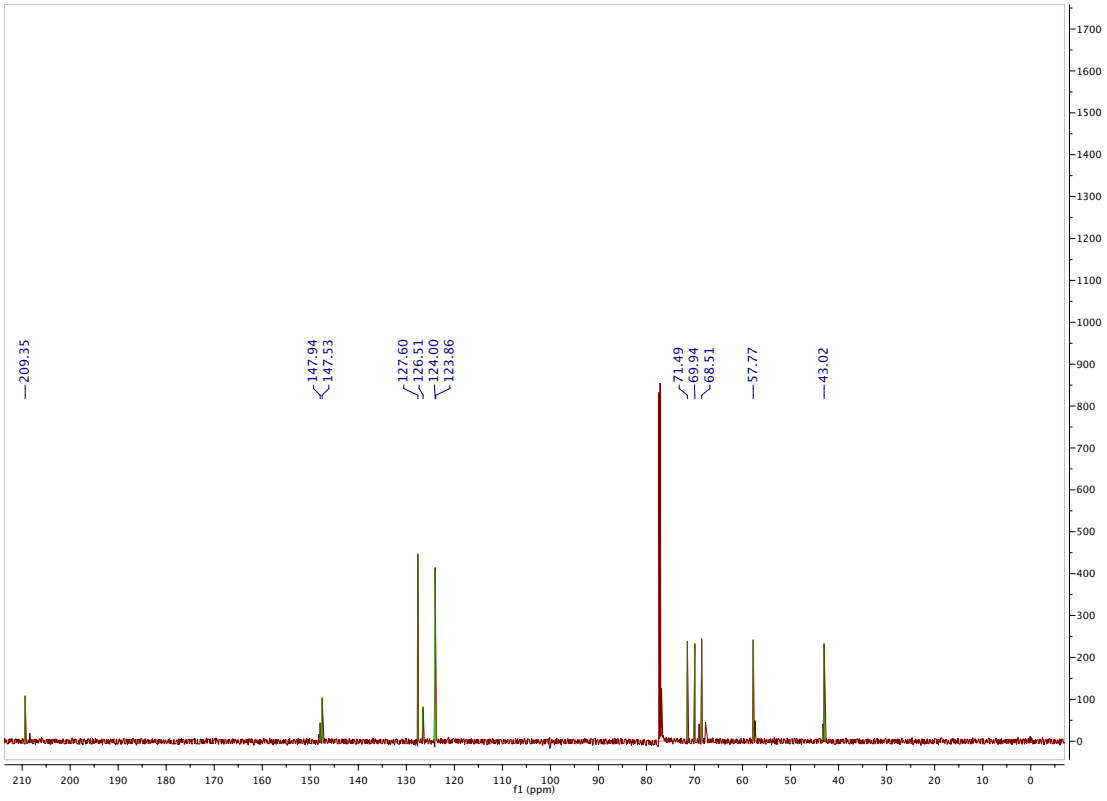
209.35
147.94
147.53
127.60
126.51
124.00
123.86
71.49
69.94
68.51
57.77
43.02
f1 (ppm)

Characterization of azido-copolymers **4a-d** and bromo-copolymer **3b**

Table SI-5. Azido-copolymers **4a-d** and bromo-copolymer **3b**

			elemental analysis			
copolymer	structure	mmolBr/gCop [a]	%N	%C	%H	*f* (mmol/g) [b]
4a	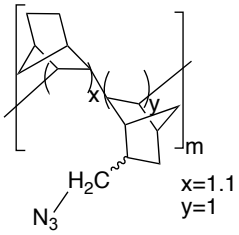	0.27	12.96	74.55	8.44	3.08
4b	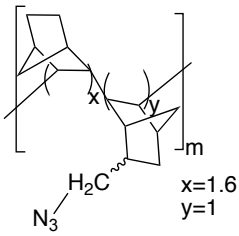	0.13	9.94	76.60	8.68	2.37
4c	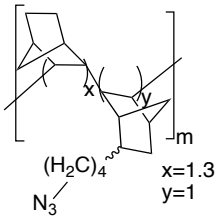	0	12.43	76.61	9.26	2.96
4d	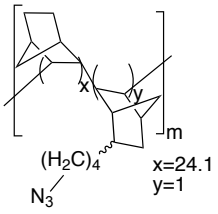	0.015	2.01	86.69	10.16	0.48
3b	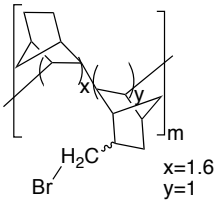	2.98		nd		2.98 [a]

[a] Determined by quantitative analysis of bromine in the copolymer. [b] Calculated from the results of elemental analysis with the formula $f = (0.714/n)\%N$, where n is the number of nitrogen atoms in the functional unit and %N is the percent of nitrogen provided by the elemental analysis.

Figure SI-5. SEM pictures of azido-copolymers **4b-c** and bromo-copolymer **3b**

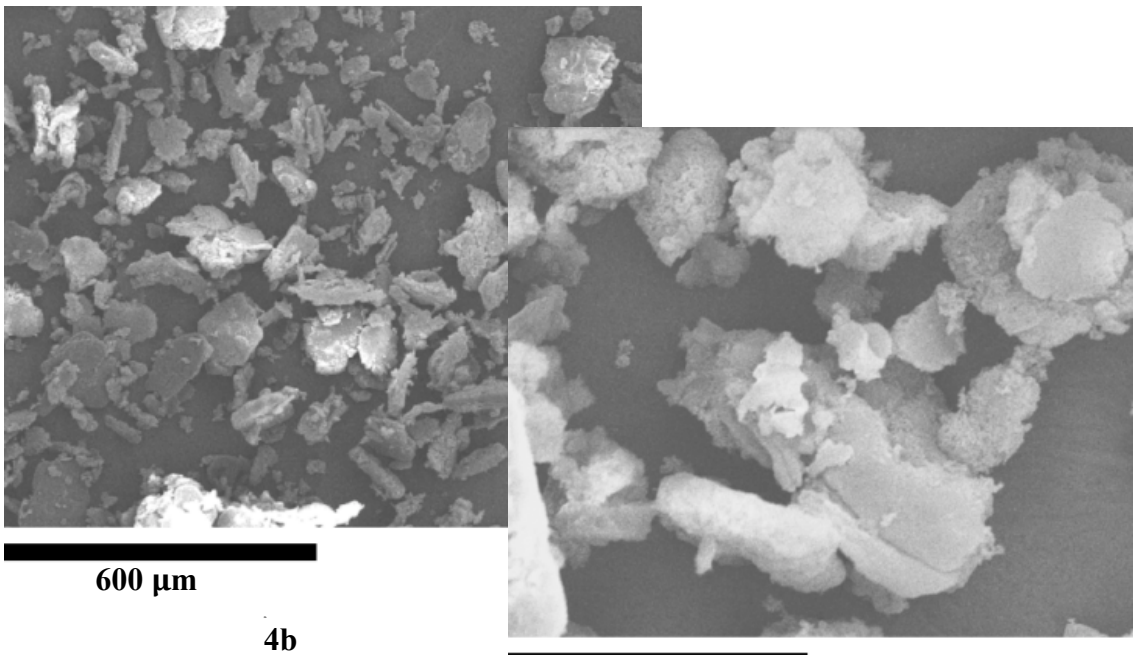

4b

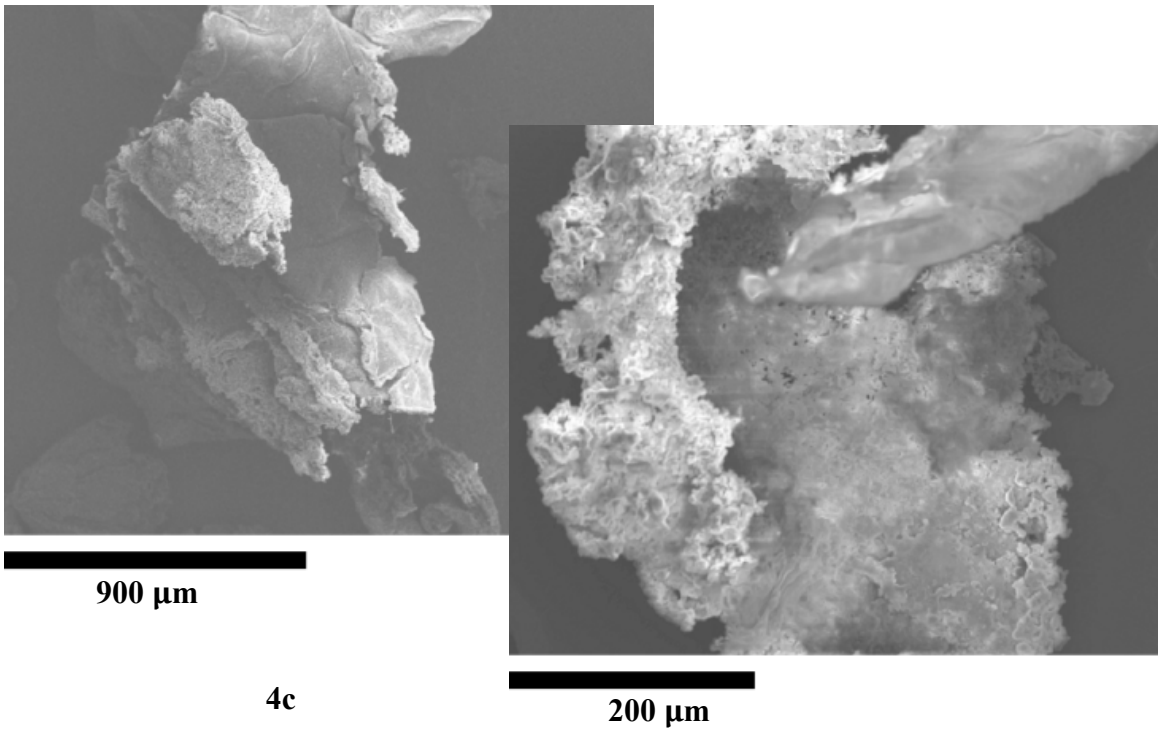

4c

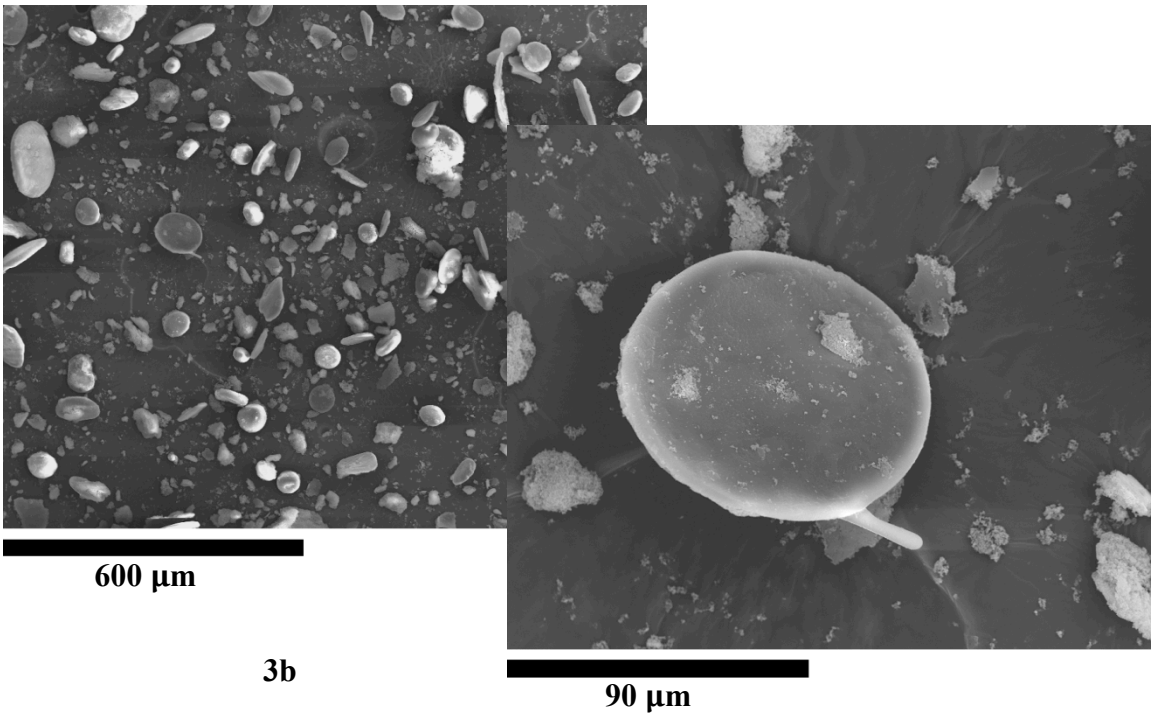

Figure SI-6. IR spectra of Azido-copolymers **4a-d** and bromo-copolymer **3b**.

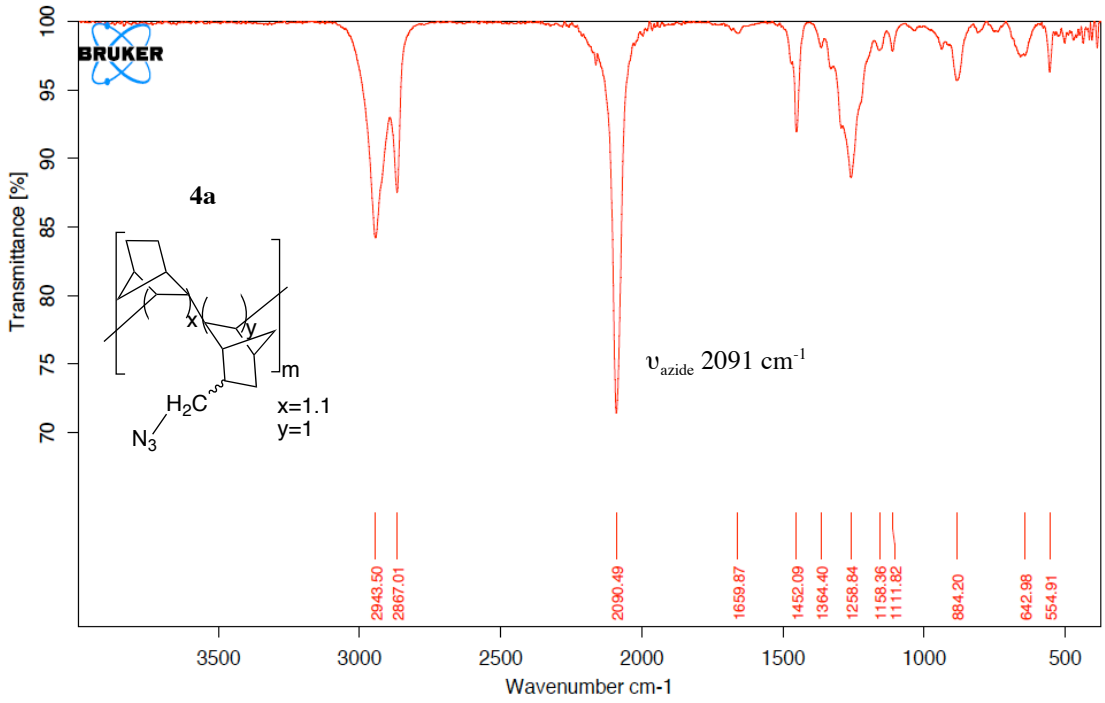

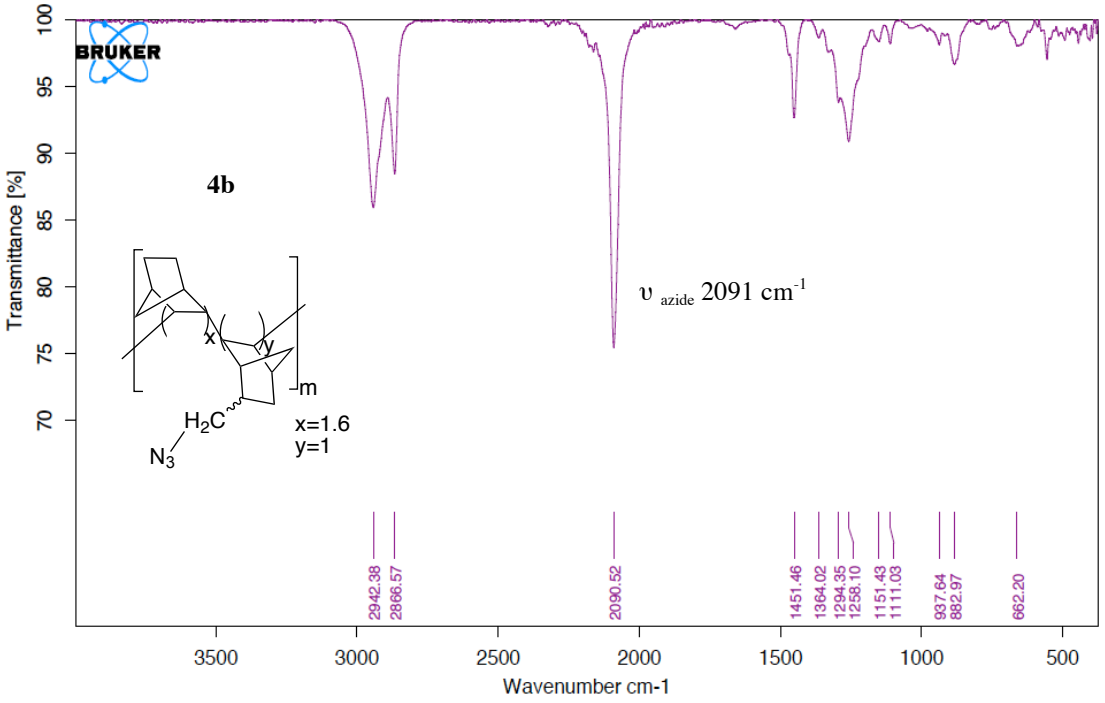
BRUKER
4b
Transmittance [%]
100
95
90
85
80
75
70
x
y
m
H2C
N3
x=1.6
y=1
υ azide 2091 cm-1
2942.38
2866.57
2090.52
1451.46
1364.02
1294.35
1258.10
1151.43
1111.03
937.64
882.97
662.20
3500
3000
2500
2000
1500
1000
500
Wavenumber cm-1

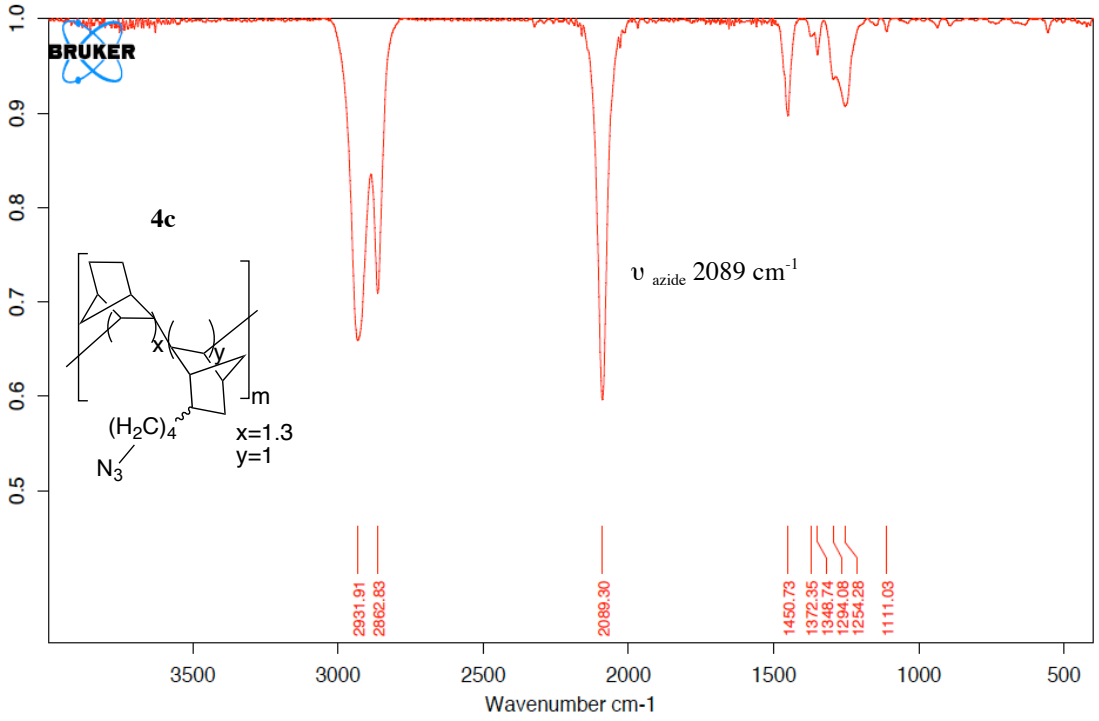
BRUKER
4c
1.0
0.9
0.8
0.7
0.6
0.5
x
y
m
(H2C)4
N3
x=1.3
y=1
υ azide 2089 cm-1
2931.91
2862.83
2089.30
1450.73
1372.35
1348.74
1294.08
1254.28
1111.03
3500
3000
2500
2000
1500
1000
500
Wavenumber cm-1

Chapter II

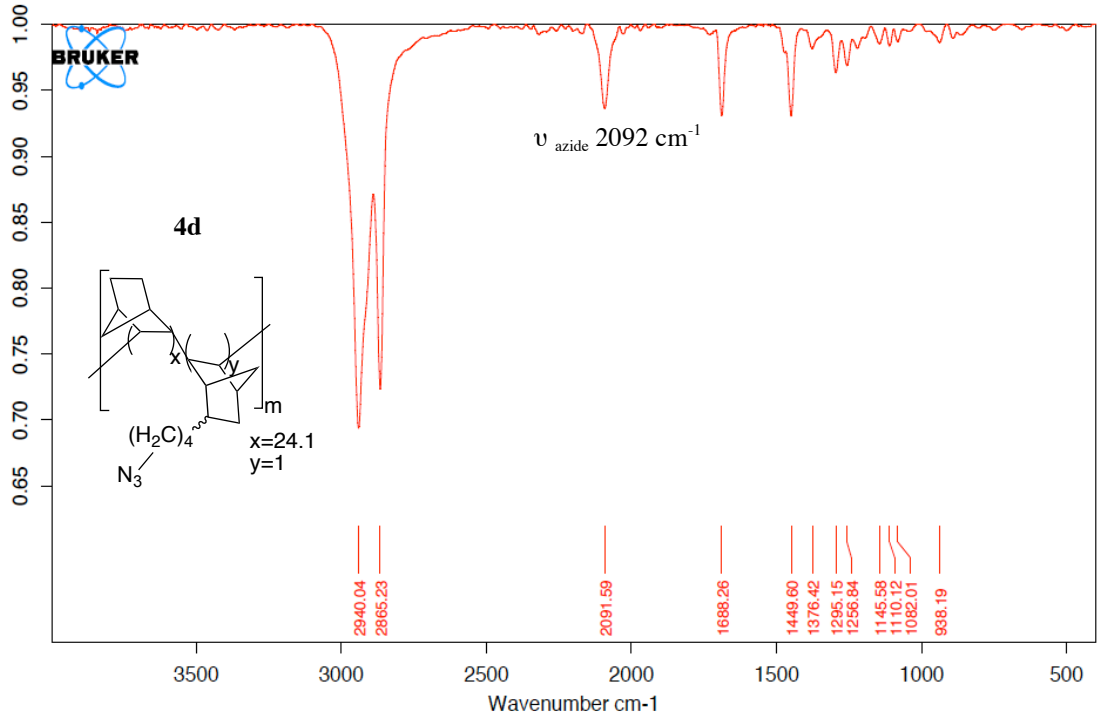

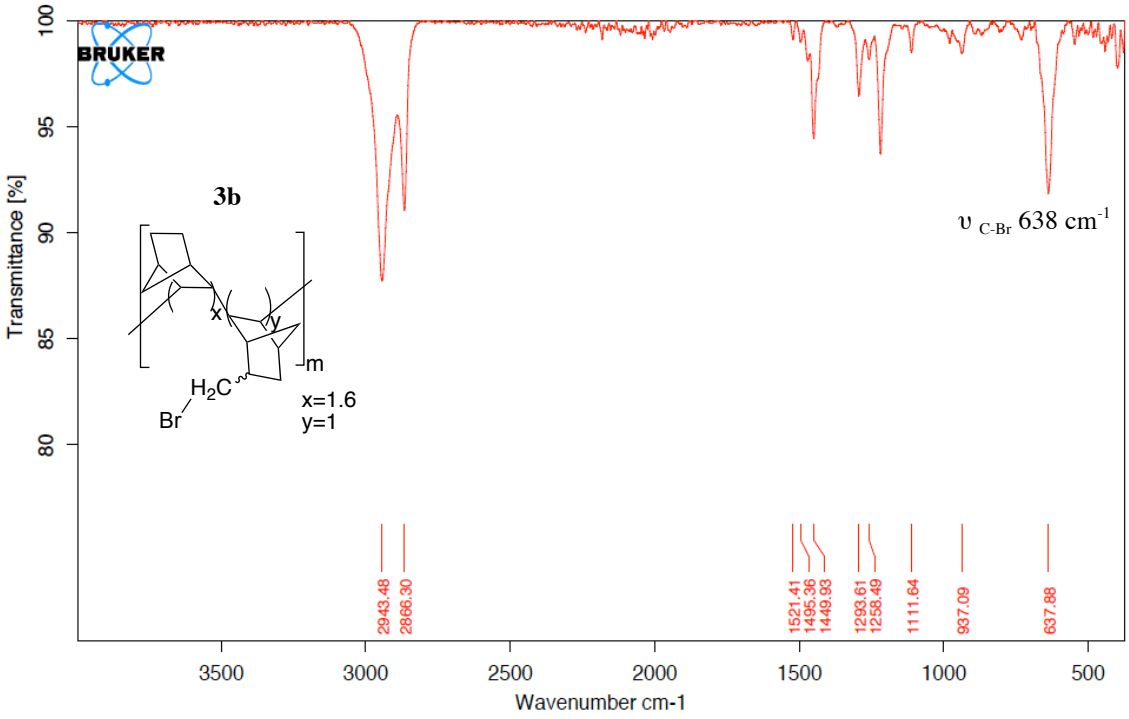

S40

Figure SI-7. Raman spectrum of bromo-copolymer **3b**.

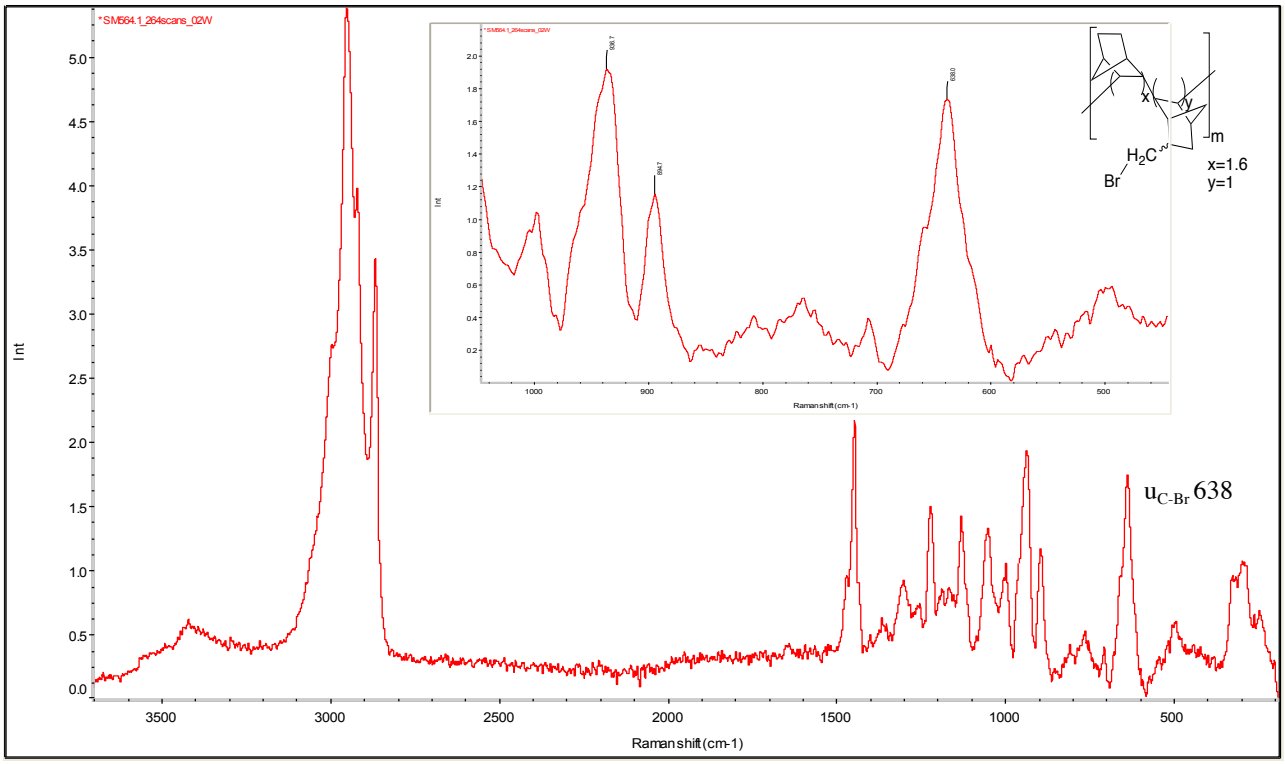

Chapter II

IR spectra of catalysts **1a-d**

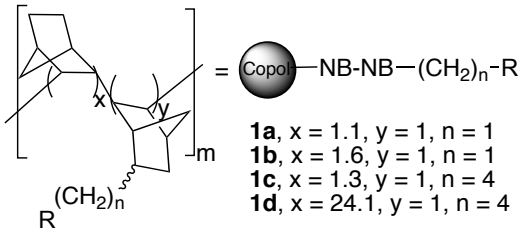

1a, x = 1.1, y = 1, n = 1
1b, x = 1.6, y = 1, n = 1
1c, x = 1.3, y = 1, n = 4
1d, x = 24.1, y = 1, n = 4

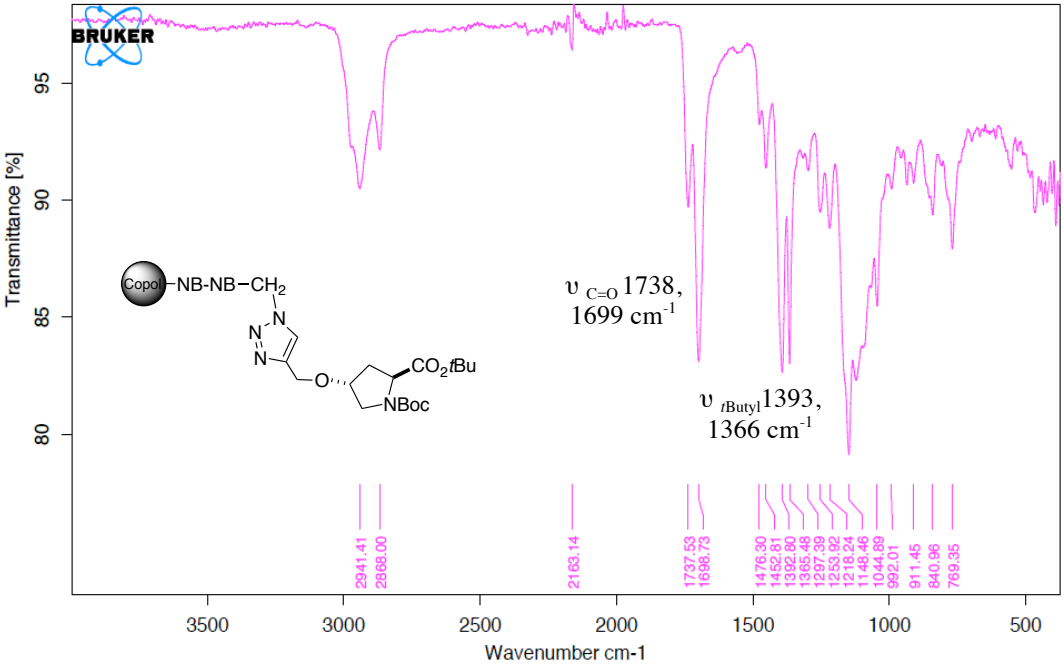

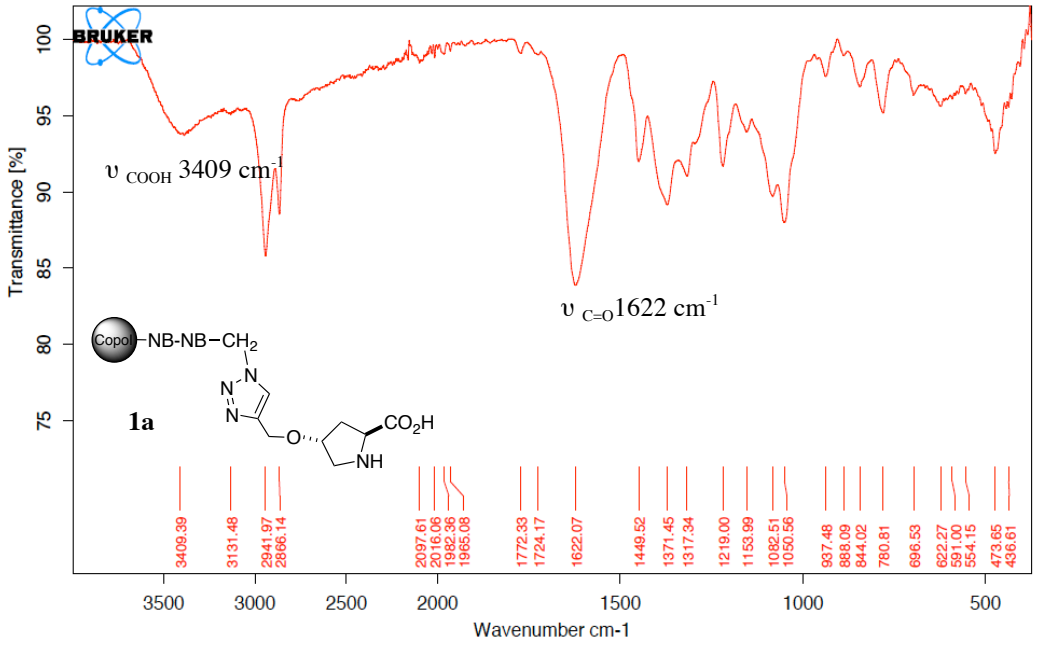

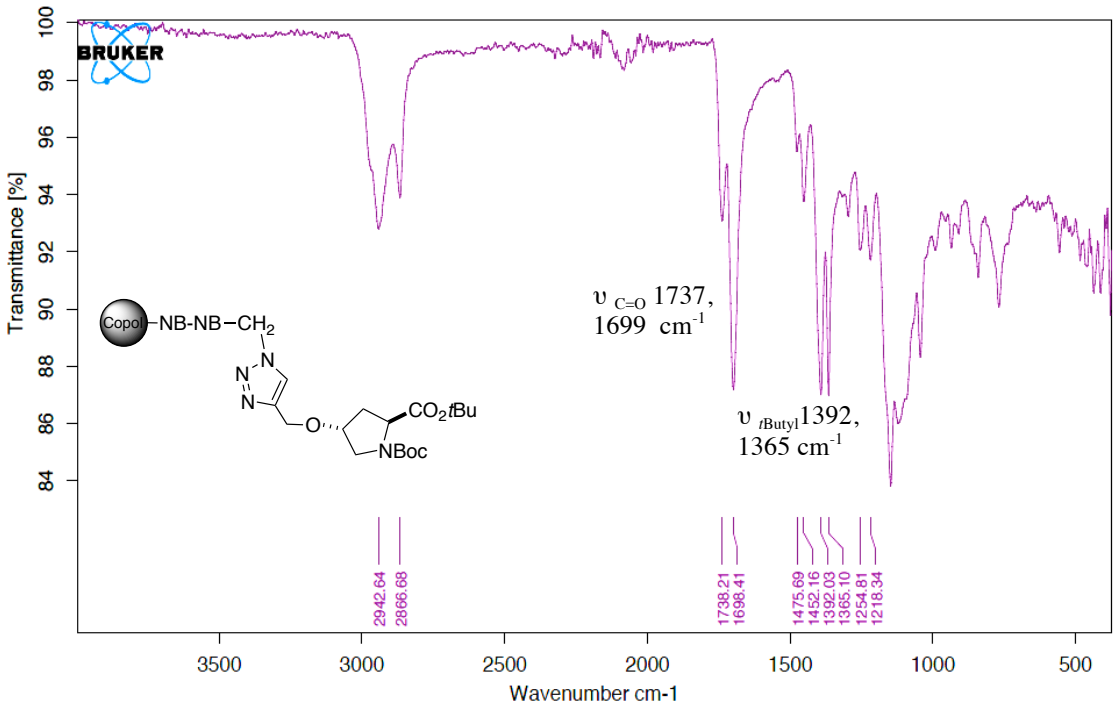
BRUKER
Transmittance [%]
100
98
96
94
92
90
88
86
84
Copol–NB-NB–CH2
CO2tBu
NBoc
υ C=O 1737, 1699 cm-1
υ tButyl 1392, 1365 cm-1
2942.64
2866.68
1738.21
1698.41
1475.69
1452.16
1392.03
1365.10
1254.81
1218.34
3500
3000
2500
2000
1500
1000
500
Wavenumber cm-1

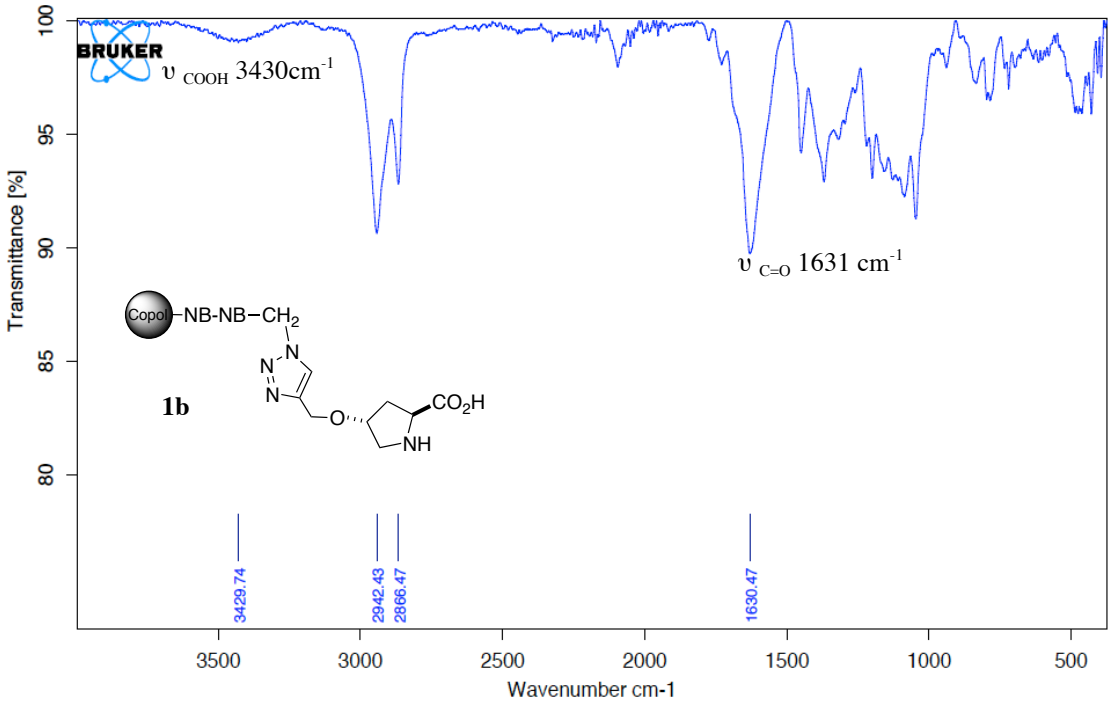
BRUKER
Transmittance [%]
100
95
90
85
80
υ COOH 3430cm-1
υ C=O 1631 cm-1
Copol–NB-NB–CH2
CO2H
NH
1b
3429.74
2942.43
2866.47
1630.47
3500
3000
2500
2000
1500
1000
500
Wavenumber cm-1

Chapter II

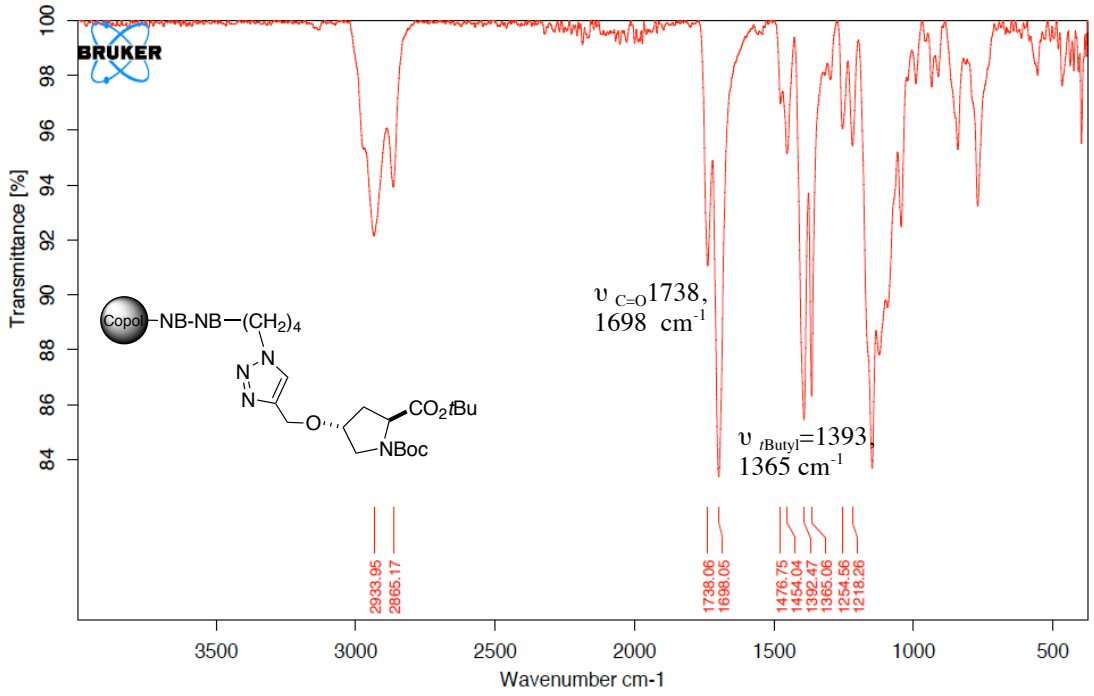

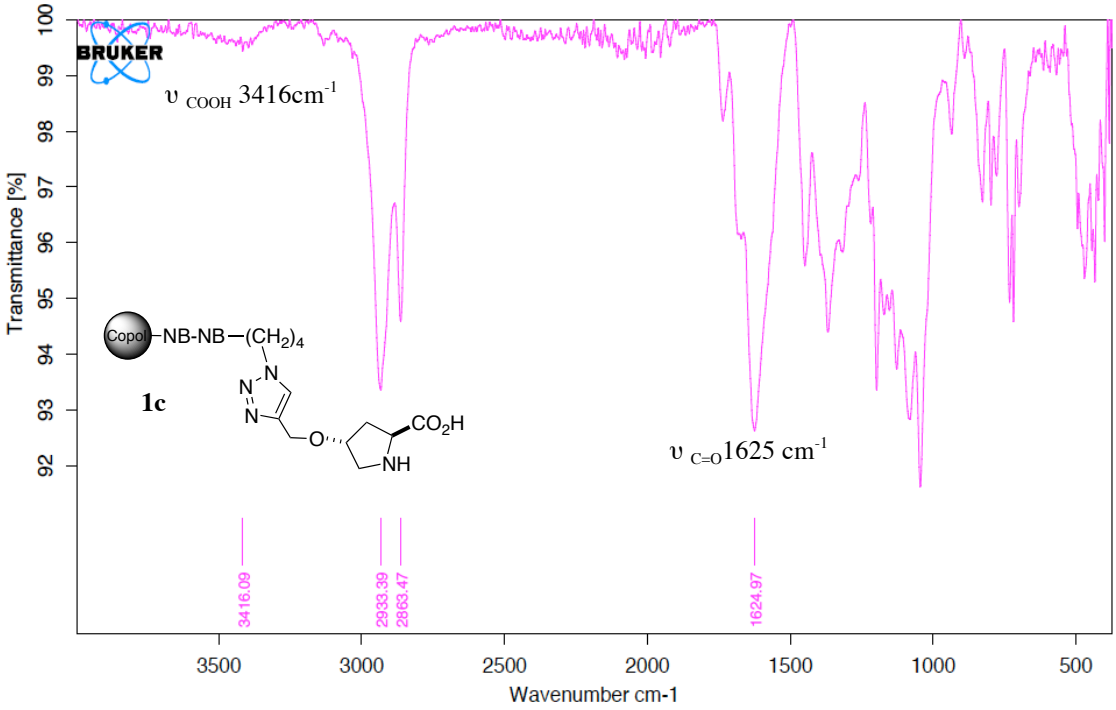

S44

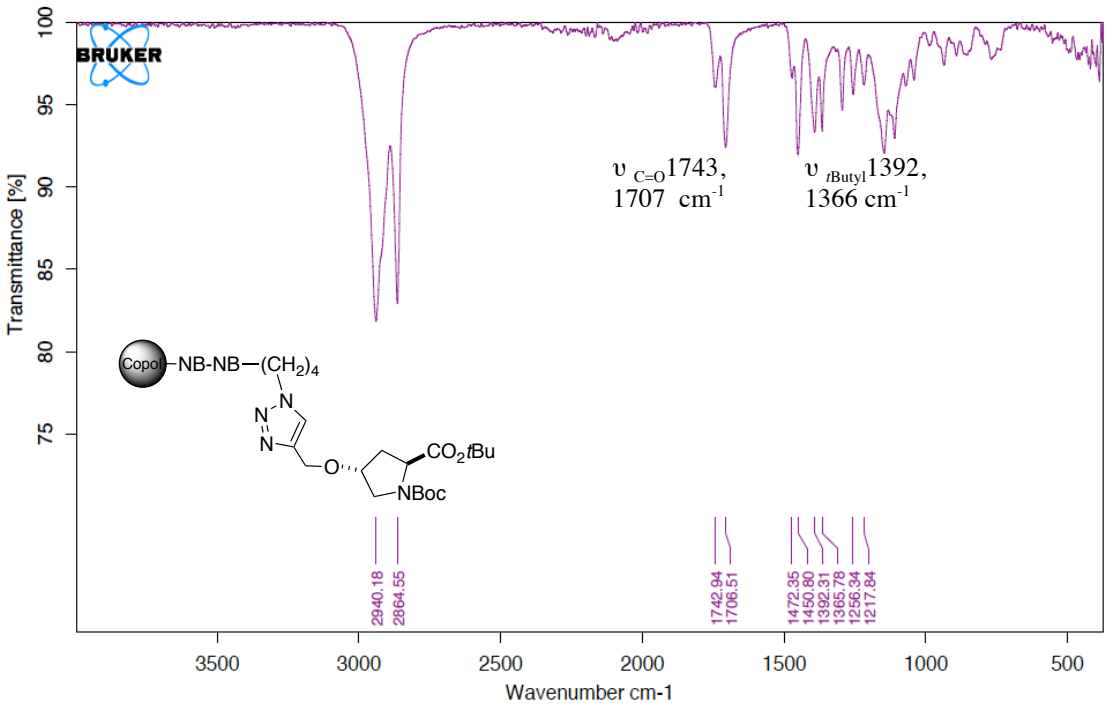
BRUKER
Transmittance [%]
100
95
90
85
80
75
υ C=O1743, 1707 cm-1
υ tButyl1392, 1366 cm-1
Copol
NB-NB—(CH2)4
CO2tBu
NBoc
2940.18
2864.55
1742.94
1706.51
1472.35
1450.80
1392.31
1365.78
1256.34
1217.84
3500
3000
2500
2000
1500
1000
500
Wavenumber cm-1

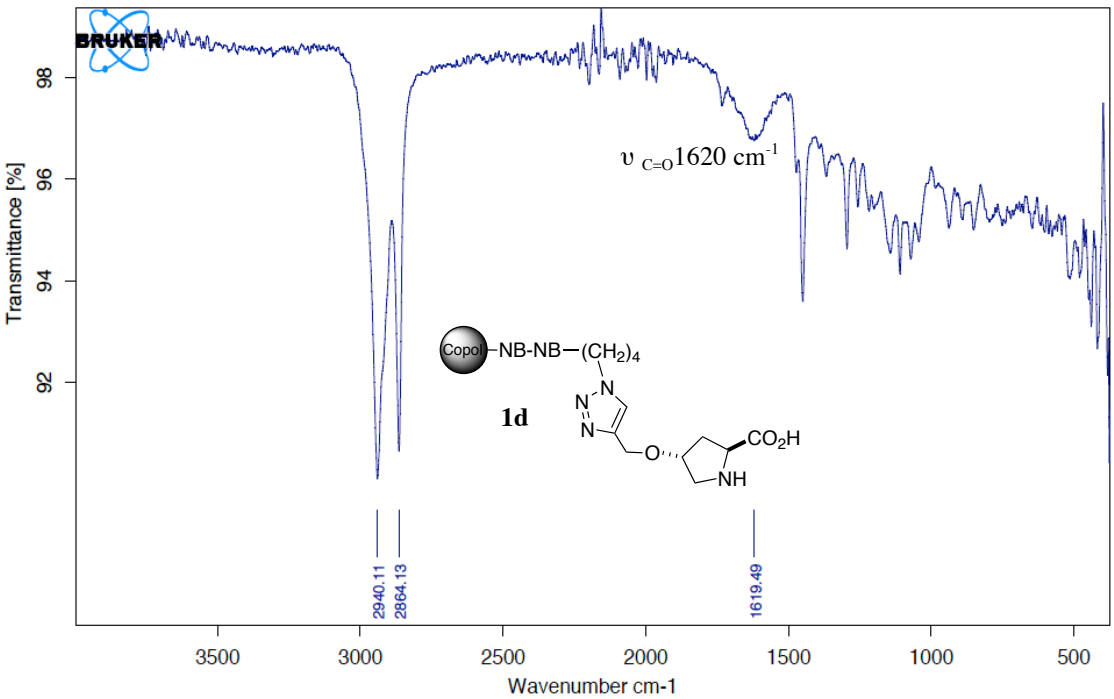
BRUKER
Transmittance [%]
98
96
94
92
υ C=O1620 cm-1
Copol
NB-NB—(CH2)4
1d
CO2H
NH
2940.11
2864.13
1619.49
3500
3000
2500
2000
1500
1000
500
Wavenumber cm-1

Chapter II

Characterization of polymers **6b** and **2**

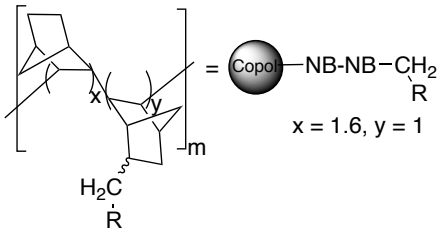

Figure SI-8. ^{13}C NMR spectrum of polymer **6b**.

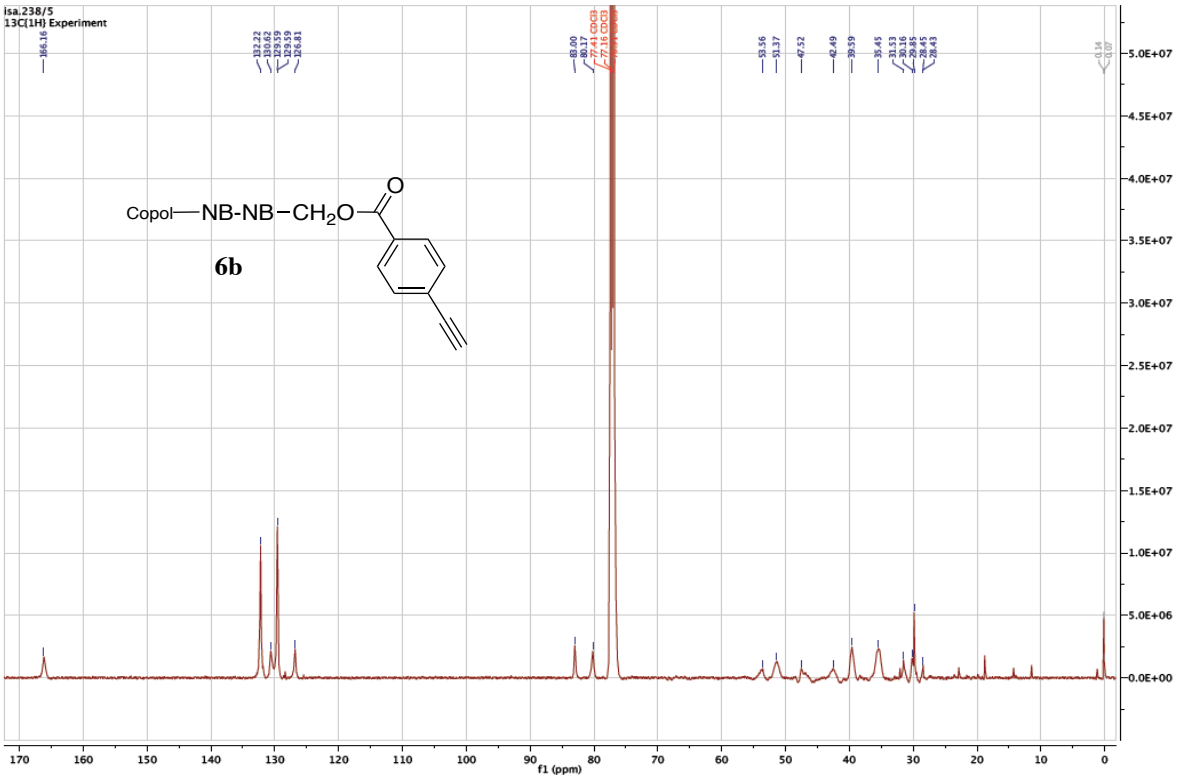

Figure SI-9. SEM pictures of polymer **6b**.

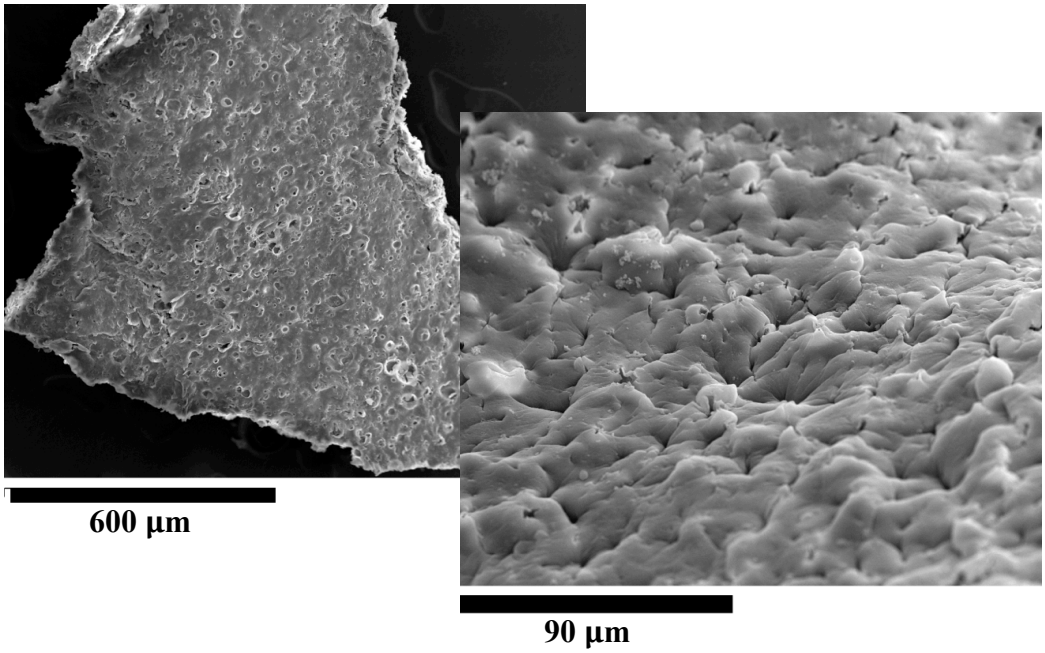

Figure SI-10. IR spectrum of polymer **6b**.

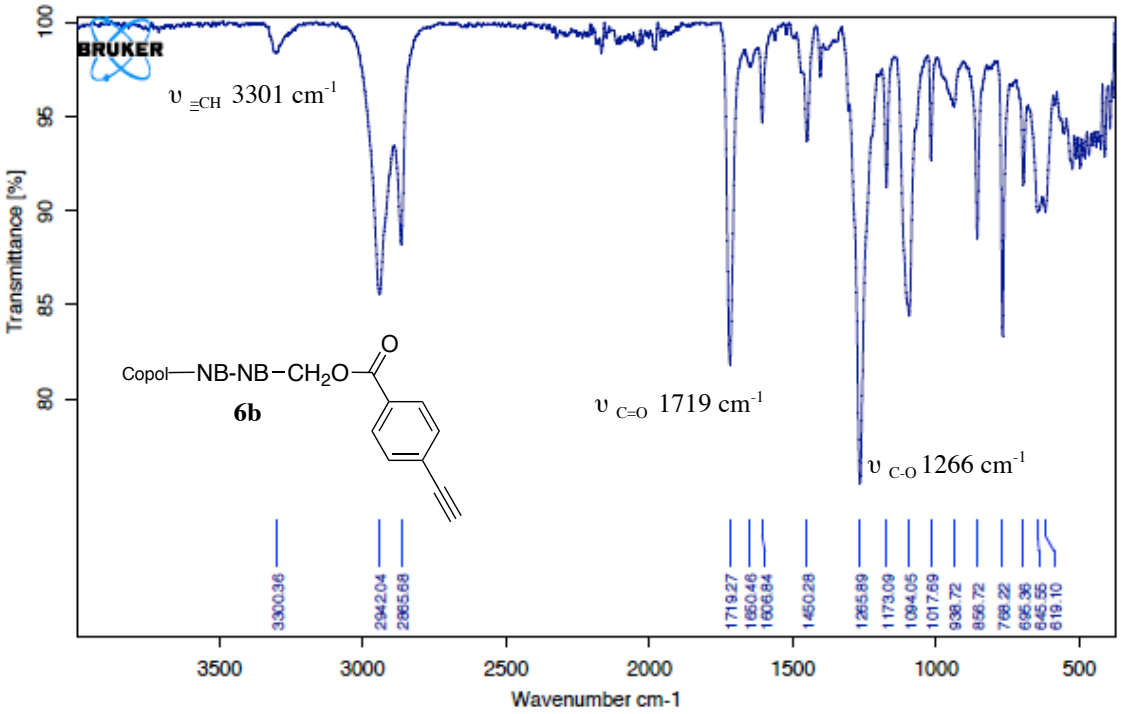

Figure SI-11. Raman spectrum of polymer **6b**.

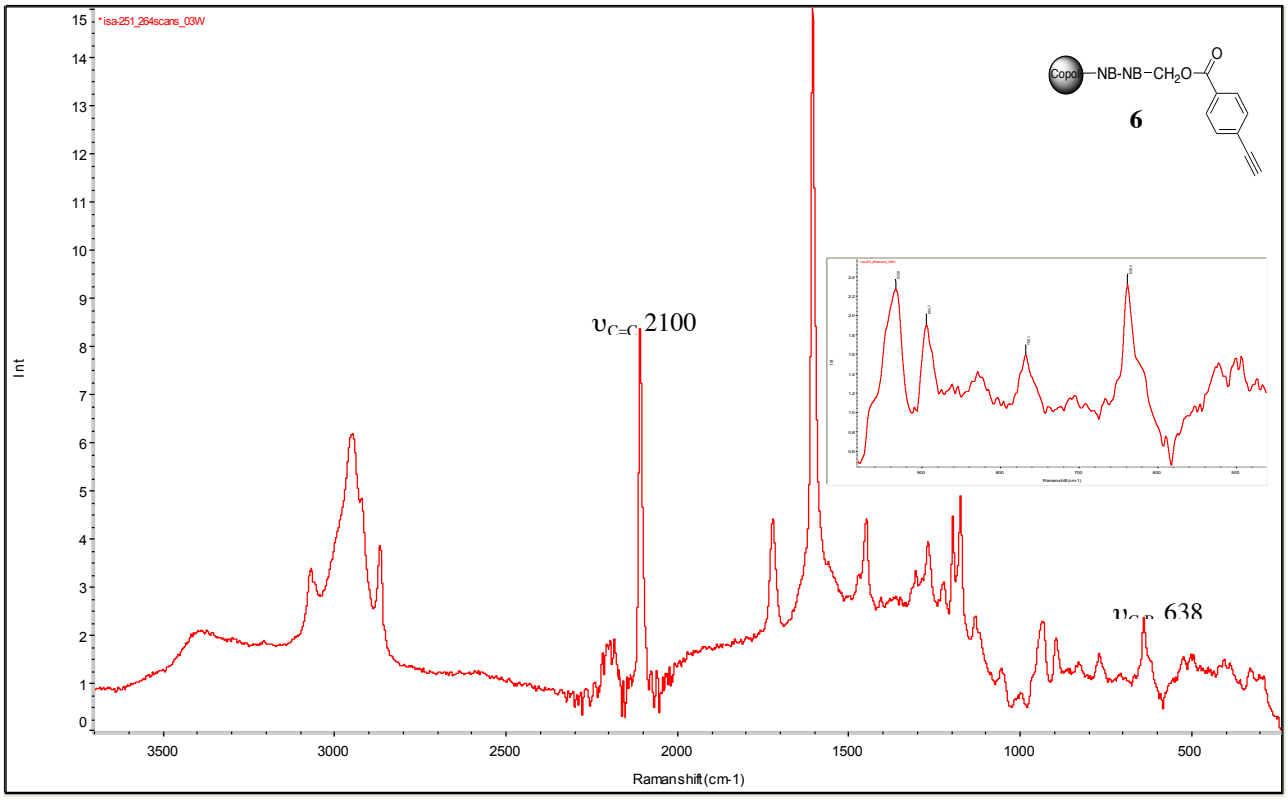

Figure SI-12. IR spectrum of catalyst **2**.

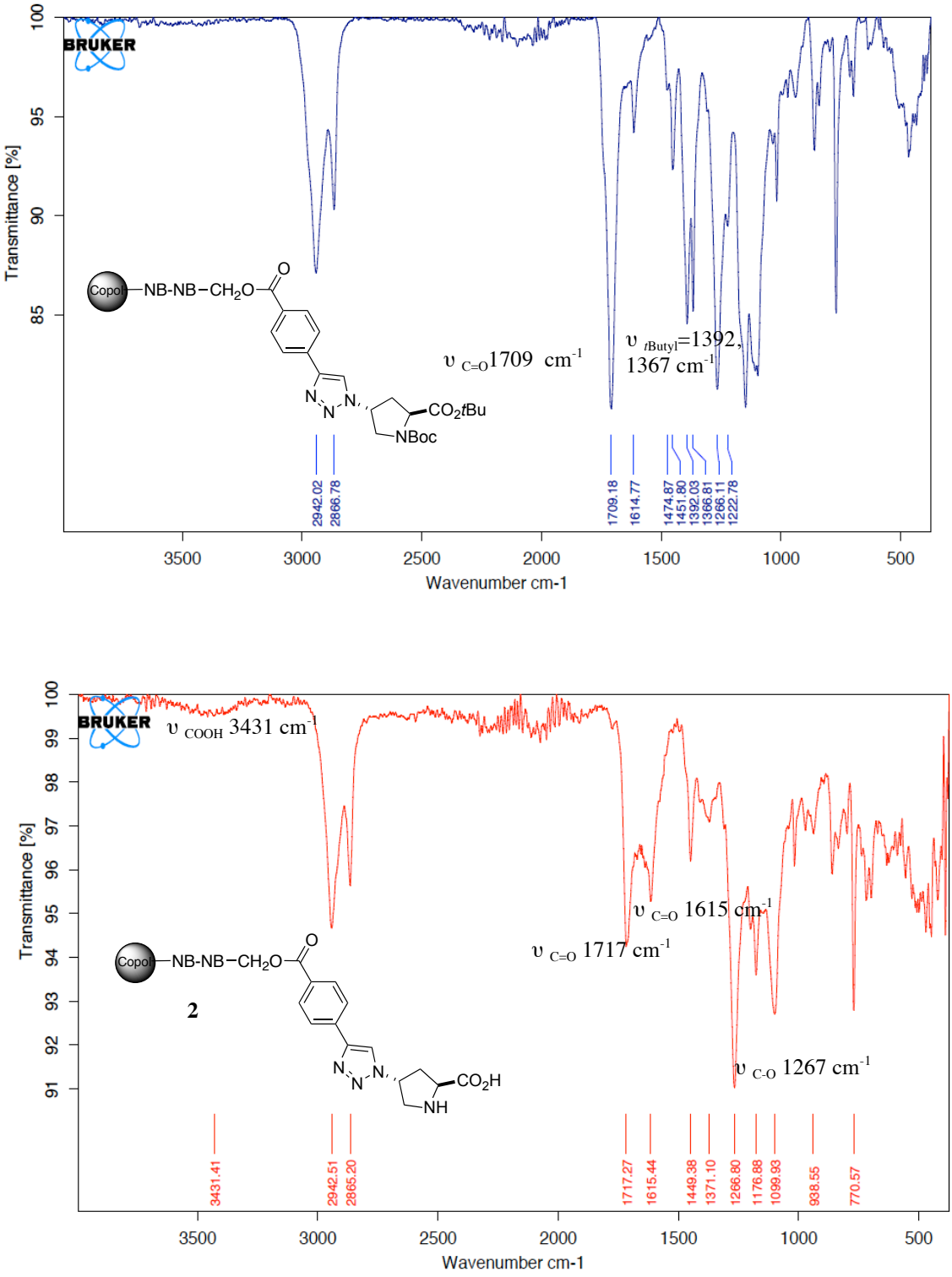

References

[S1] D. C. White, *Mikrochim. Acta* 1961, 449.

[S2] R. P. Washington and O. Steinbock, *J. Am. Chem. Soc.* 2001, **123**, 7933.

[S3] A. Melissaris, H. L. Morton, *J. Org. Chem.* 1992, **57**, 6998.

[S4] N. Mase, Y. Nakai, N. Ohara, H. Yoda, K. Takabe, F. Tanaka, C. F. Barbas III, *J. Am. Chem. Soc.* 2006, **128**, 734.

[S5] C. Ayats, A. H. Henseler, M. A. Pericàs, *ChemSusChem* 2012, **5**, 320.

[S6] J. G. Hernández, E. Juaristi, *Tetrahedron* 2011, **67**, 6953.

[S7] Y. Hayashi, T. Sumiya, J. Takahashi, H. Gotoh, T. Urushima, M. Shoji, *Angew. Chem. Int. Ed.* 2006, **45**, 958.

[S8] Z. Jiang, H. Yang., X. Han, J. Luo, M. W. Wong, Y. Lu, *Org. Biomol. Chem.* 2010, **8**, 1368.

[S9] H. Yang, S. Mahapatra, P. H. -Y. Cheong, G. R. Garter, *J. Org. Chem.* 2010, **75**, 7279.

CHAPTER III

Translation the Enantioselective Michael Reaction to a Continuous Flow Paradigm with an Immobilized, Fluorinated Organocatalyst

UNIVERSITAT ROVIRA I VIRGILI
NEW APPROACHES TO CATALYST DESIGN AND IMMOBILIZATION
Irina Sagamanova

Translating the Enantioselective Michael Reaction to a Continuous Flow Paradigm with an Immobilized, Fluorinated Organocatalyst

3.1 Introduction.

Efforts towards the development of metal-free small molecule catalysts[18] have become important since the first reports by List, Lerner, Barbas.[16] The amino acid proline has often been described as a fairly general and efficient amine-based catalyst.[18d, 138] However, in some cases proline catalysts proved to be inefficient, and new catalyst designs were needed. At the same time, MacMillan[17a] have developed the imidazolidinone catalysts and shortly after, the Jørgensen and Hayashi groups discovered α,α-diarylprolinol silyl ether derivatives, which were able to control the stereoselectivity by steric hindrance.[37,148]

Catalysts acting through enamine activation can be roughly divided in two classes according to their mode of stereochemical induction (**Figure III.1**).[18b,149] In the first one, the stereochemistry of the final adducts is controlled by a hydrogen bonding assistance (**Type A**). They incorporate an acid/hydrogen bond donor group to direct the approach of the electrophile. They are typically used for aldol, Mannich, α-amination and α-oxygenation reactions.[16,28,150] In **Type B** catalysts, the stereochemistry is controlled by steric hindrance. This concept has been applied to reactions such as α-halogenation as well as conjugate addition reactions.[17c,151]

---

[148] For the pioneering reports, see: a) Marigo, M.; Wabnitz, T. C.; Fielenbach, D.; Jørgensen, K. A. *Angew. Chem. Int. Ed*. **2005**, *44*, 794-797; b) Hayashi, Y.; Gotoh, H.; Hayashi, T.; Shoji, M. *Angew. Chem. Int. Ed*. **2005**, *44*, 4212-4215.

[149] Moyano, A. in *Stereoselective Organocatalysis: Bond Formation Methodologies and Activation Modes* (ed.: Torres, R. R.), John Wiley & Sons Inc, Hoboken, New Jersey, **2013**, *Ch. 2*, 11-80.

[150] For some examples, see: a) Enders, D.; Seki, A. *Synlett* **2002**, *1*, 26-28; b) Bøgevig, A.; Juhl, K.; Kumaragurubaran, N.; Zhuang, W.; Jørgensen, K. A. *Angew. Chem. Int. Ed*. **2002**, *41*, 1790-1793; c) Hayashi, Y.; Tsuboi, W.; Ashimine, I.; Urushima, T.; Shoji, M.; Sakai, K. *Angew. Chem. Int. Ed*. **2003**, *42*, 3677-3680.

[151] For some examples, see: a) Franzén, J.; Marigo, M.; Fielenbach, D.; Wabnitz, T. C.; Kjærsgaard, A.; Jørgensen, K. A. *J. Am. Chem. Soc*. **2005**, *127*, 18296-18304; b) Marigo, M.; Fielenbach, D.; Braunton, A.; Kjærsgaard, A.; Jørgensen, K. A. *Angew. Chem. Int. Ed*. **2005**, *44*, 3703-3706.

Chapter III

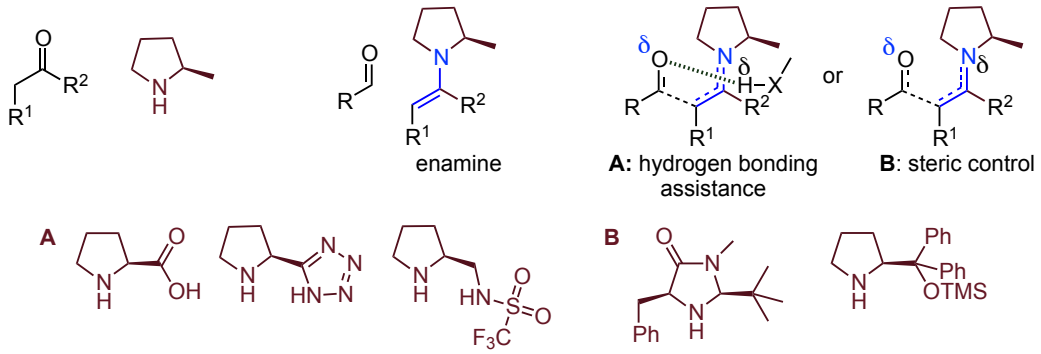

Figure III.1. The two modes of stereochemical steering with enamine catalysis.

In the first case, the attack of the electrophile takes place via a cyclic transition state (so-called List-Houk model), leading to an upper face approach.[35c] In the other case the attack of the electrophile is directed by purely steric effects, providing the opposite facial stereoselectivity (**Figure III.2 A, B**).[149]

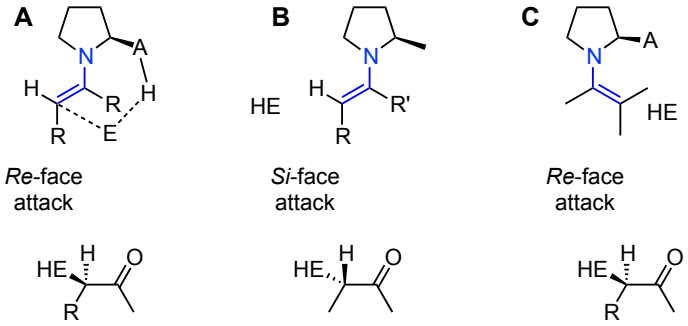

Figure III.2. Working transition state model for the electrophilic attack to the enamine intermediate.

However, it is important to note that the first class of catalysts has been the subject of some debate. In 2007, Seebach *et al.* proposed an alternative transition state,[152] in which (after protonation of the electrophile) the electrophilic attack is directed by an intramolecular reaction of the conjugated base of the amine substituent (**Figure III.2C**).

In general, the process of designing a new type of catalyst is an iterative process. The early examples of diarylmethylpyrrolidines were usually insufficient in terms of providing good levels of enantioselectivity, although good reactivities were observed for various transformations.[148a, 153] On the other hand, the diarylprolinol system was able to induce good stereocontrol, albeit with limited catalyst turnover due

[152] Seebach, D.; Beck, A. K.; Badine, D. M.; Limbach, M.; Eschenmoser, A.; Treasurywala, A. M.; Hobi, R., Prikoszovich, W.; Linder, B. *Helv. Chim. Acta.* **2007**, *90*, 425-471.
[153] a) Melchiorre, P.; Jørgensen, K. A. *J. Org. Chem.* **2003**, *68*, 4151-4157; b) Juhl. K.; Jorgensen, K. A. *Angew. Chem. Int. Ed.* **2003**, *42*, 1498-1501; c) Chi, Y. Gelllman, S. H. *J. Am. Chem. Soc.* **2006**, *128*, 6804-6805; d) Ibrahem, I.; Santoro, S.; Himo, F.; Córdova, A. *Adv. Synth. Catal.* **2011**, *353*, 245-252.

to the formation of a "parasitic" oxazolidine species. In general, the modification of proline to sterically demanding systems such as diarylprolinols has proved to be a more effective strategy for the design of new types of catalysts (**Figure III.3**). From a library of synthesized diarylprolinol silyl ethers, two of them have proven to be highly general catalysts (**Figure III.3**, *right*).[37,154]

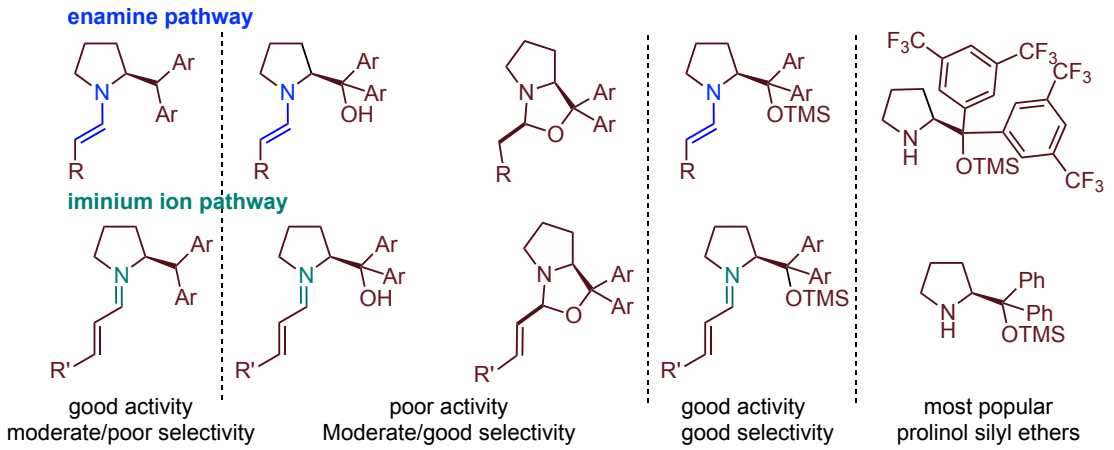

Figure III.3. Designs of aminocatalyst structures.

Diarylprolinol catalysts have also been used in heterogeneous catalytic systems thanks to their high potential in both the enamine and iminium ion activation modes. With the aim of enhancing the sustainability profile of these catalysts, several groups,[155] including our own,[71g-i,m,o] have devoted efforts to the development of immobilized analogues. A set of solid-supported derivatives has been reported, and their robustness was established through recycling and implementation of enantioselective continuous flow processes.[156]

Although they present some advantages, supported TMS-diarylprolinol catalysts suffer from deactivation problems in long time use or upon recycling. In most

---

[154] For general and comprehensive reviews in application of the diarylprolinol silyl ether catalysts, see: a) Mielgo, A.; Palomo, C. *Chem. Asian J.* **2008**, *3*, 922-948; b) Xu, L.-W.; Li, L.; Shi, Z.-H. *Adv. Synth. Catal.* **2010**, *352*, 243; c) Jiang, H.; Albrecht, Ł.; Dickmeiss, G.; Jensen, K. L.; Jørgensen, K. A. *Comprehensive Enantioselective Organocatalysis: Catalysts, Reactions, and Applications* (Ed. Dalko, P. I.), Wiley-VCH, Verlag, Weinheim **2013**, *Ch. 2*, 33-50.

[155] For selected examples, see: a) Li, Y.; Liu, X.-Y.; Zhao, G. *Tetrahedron: Asymmetry* **2006**, *17*, 2034-2039; b) Maltsev, O. V.; Kucherenko, A. S.; Zlotin, S. G. *Eur. J. Org. Chem.* **2009**, 5134-5137; c) Wang, B. G.; Ma, B. C.; Wang, Q.; Wang, W. *Adv. Synth. Catal.* **2010**, *352*, 2923-2928; d) Kristensen, T. E.; Vestli, K.; Jakobsen, M. G.; Hansen, F. K.; Hansen, T. *J. Org. Chem.* **2010**, *75*, 1620-1629; e) Mager, I.; Zeitler, K. *Org. Lett.* **2010**, *12*, 1480-1483; f) Wang, C. A.; Zhang, Z. K.; Yue, T.; Sun, Y. L.; Wang, L.; Wang, W. D.; Zhang, Y.; Liu, C.; Wang, W. *Chem. Eur. J.* **2012**, *18*, 6718-6723; g) Keller, M.; Perrier, A.; Linhardt, R.; Travers, L.; Wittmann, S.; Caminade, A.-M.; Majoral, J.-P.; Reiser, O.; Ouali, A. *Adv. Synth. Catal.* **2013**, *355*, 1748-1754; h) Zheng, W.; Lu, C.; Yang, G.; Chen, Z.; Nie, J. *Catal. Commun.* **2015**, *62,* 34-38.

[156] For recent reviews on asymmetric organocatalysis in continuous flow, see: a) Rodríguez-Escrich, C.; Pericàs, M. A. *Eur. J. Org. Chem.* **2015**, 1173-1188; b) Atodiresei, I.; Vila, C.; Rueping, M. *ACS Catal.* **2015**, *5*, 1972-1985; c) Munirathinam, R.; Huskens, J.; Verboom, W. *Adv. Synth. Catal.* **2015**, *357*, 1093-1123; d) Zhao, D.; Ding, K. *ACS Catal.* **2013**, *3*, 928-944; e) Tsubogo, T.; Ishiwata, T.; Kobayashi, S. *Angew. Chem. Int. Ed.* **2013**, *52*, 6590-6604; f) Puglisi, A.; Benaglia, M.; Chiroli, V. *Green Chem.* **2013**, *15*, 1790-1813.

cases they become much less active after the first, second or third run. Several approaches have been employed to remediate the lability of the catalytic system.

It was observed that the catalyst can be deactivated by means of desilylation. It is possible to re-activated them by re-silylation with different silylating agents as Me_3SiOTf[157] or $Me_2NCOOSiMe_3$[71g,i] (**Scheme III.1**). However, these approaches have disadvantages: they cannot be applied to work in continuous flow and reactivation is not cost effective.

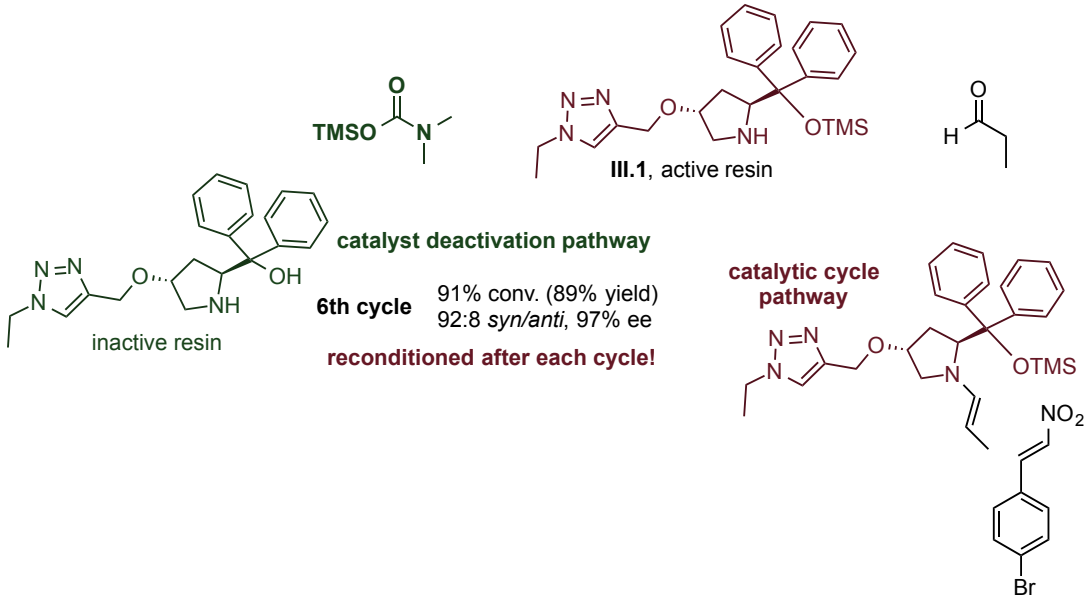

Scheme III.1. Reconditioning of the supported organocatalyst **III.1**.

Due the fact that this type of catalysts get easily deactivated, the analogous methyl ether[158] was also studied. When comparing the result of both catalysts in the Michael reaction it was observed that the methyl ether protected catalyst was less active and selective that the TMS-protected one [71g,i] (**Scheme III.2**). This evidences the crucial role of *O*-silyl protection pattern in the control of catalytic activity and selectivity of diarylprolinol ether derivatives.

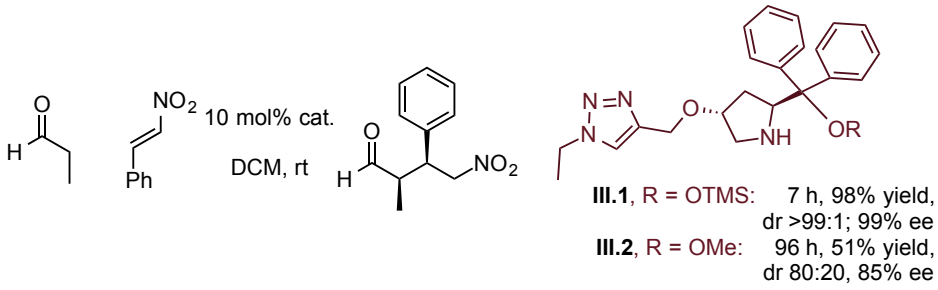

Scheme III.2. Comparison of polymer-supported organocatalysts **III.1** and **III.2.**

[157] Velera, M. C.; Dixon, S. M.; Lamb, K. S.; Shore, N. E. *Tetrahedron* **2008**, *64*, 10087-10090.
[158] For the homogeneous catalyst, see: Chi, Y.; Gellman, S. H. *Org. Lett.* **2005**, *7*, 4253-4356

Additional studies were devoted toward the preparation of catalysts with bulkier silyl ethers, which display increased stability.[71o] However, significant structural changes can compromise reactivity and they still tend to deactivate over time.

An alternative pathway to account for the deactivation of this type of catalysts was published by Zlotin *et al.* in 2011.[159] They described a study on deleterious side reactions that lower the catalytic efficiency of the TMS-diarylprolinol catalyst. For this, a diphenylprolinol organocatalyst modified with a cationic fragment was used in asymmetric Michael reactions of C- or N-nucleophiles to enals. The side-reactions were identified by electrospray ionization mass spectrometry (ESI-MS). After several recycles, inactive (or lowly active) oxidation and hydrolysis by-products were found to be the major components of the recovered mixture (**Scheme III.3 and III.4).**

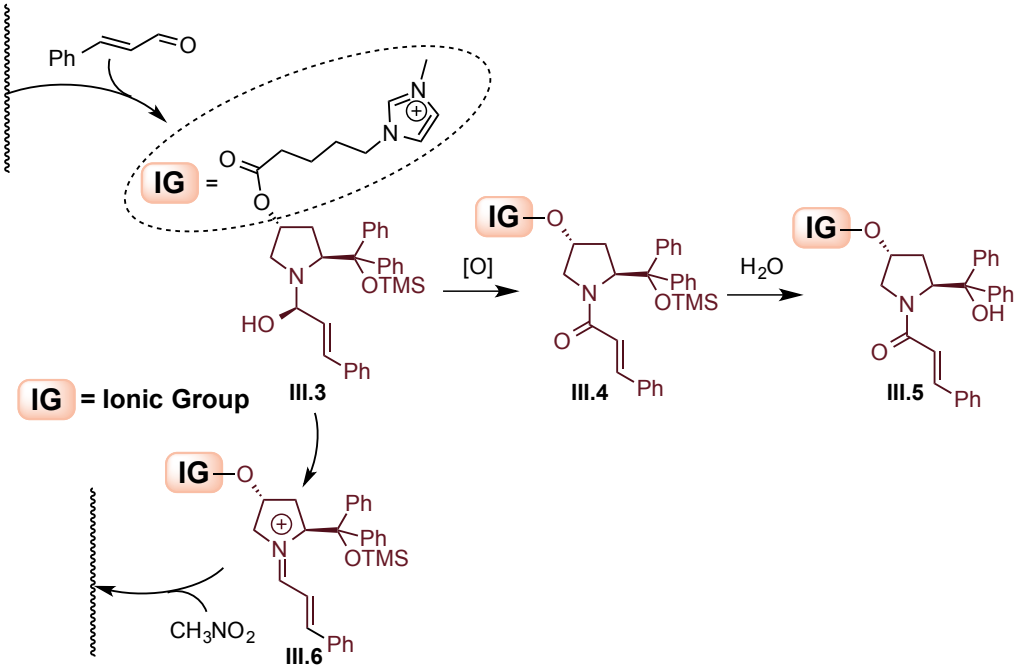

Scheme III.3. Possible deactivation pathways, according to ESI-MS(+).

Hemiaminal species **III.3,** an intermediate in the formation of iminium ion **III.6**, can undergo oxidation processes with nucleophiles or with oxidizing agents (e.g. the oxygen in the air), followed by desilylation (such as **III.4** and **III.5**). This species is formed at the beginning of the catalytic cycle before its transformation to the iminium cation **III.6**.

On the other hand, enamine intermediate **III.7** can suffer oxidation or hydrolysis, providing the catalytically inactive *N*-formyl pyrrolidine **III.8** or the

[159] Maltsev, O. V.; Chizhov, A. O; Zlotin, S. G. *Chem. Eur. J.* **2011**, *17*, 6109-6117.

Chapter III

deprotonated-prolinol **III.9**, which are still able to catalyze the Michael reaction, albeit in a less efficient way than the *O*-TMS-protected catalyst (**Scheme III.4**).

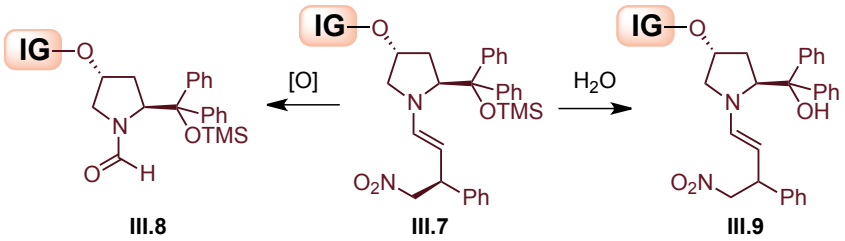

III.8 III.7 III.9

Scheme III.4. Oxidation and hydrolysis of enamine intermediates, according to ESI-MS(+).

As a conclusion, the "parasitic" products of oxidation and hydrolysis are generated under ambient atmosphere, so running reactions under oxygen-free conditions can increase the catalytic activity of the TMS-diarylprolinol for a longer time.

However, an alternative catalyst design was still needed in order to find a more robust species for work under continuous flow. From this point of view, fluorinated scaffolds seem to fulfill most of our requirements. They have been used for conformational analysis because of their structural similarities with existing secondary-amino-based organocatalysts. [160] Recently, a β-fluoroamine was employed in organocatalysis by Gilmour *et al.*[161] It can be considered as a **Type B** catalyst, that acts via the conformational effect of the fluorine group in its structure (**Figure III.4**).

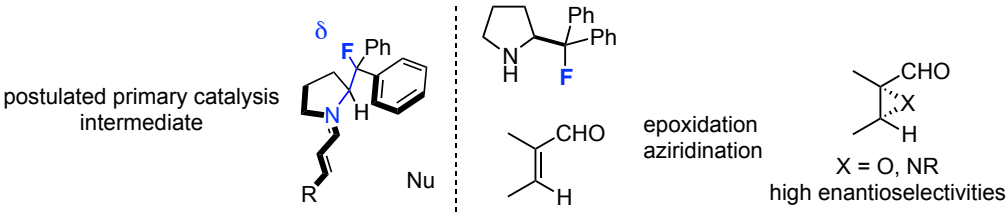

Figure III.4. β-Fluoroamines as alternative catalysts via a conformational effect.

Fluorine is increasingly used in drug design, and this has motivated advances towards understanding the physicochemical properties of this element. Attempts to use their attributes are continuously emerging in different areas of chemistry. [162] The literature provides some examples in which the conformational organization of the catalyst comes from stereoelectronic effects related to the presence of fluorine. This can lead to the stabilization of transitions states. [161]

---

[160] Hunter, L. *Beilstein J. Org. Chem.* **2010**, *6*, No. 38.
[161] a) Zimmer, L. E.; Sparr, C.; Gilmour, R. *Angew. Chem. Int. Ed.* **2011**, *50*, 11860-11871; b) Molnár, I. G.; Tanzer, E.-M.; Daniliuc, C.; Gilmour, R. *Chem. Eur. J.* **2014**, *20*, 794-800.
[162] Cahard, D.; Bizet, V. *Chem. Soc. Rev.* **2014**, *43*, 135-147.

Gilmour *et al.* introduced the use of the fluorinated system **III.10** in asymmetric organocatalysis in 2009.[163] This fluorinated pyrrolidine derivative **III.10** was designed to validate the *gauche*-effect hypothesis (see **chapter III, 3.3**) for molecular pre-organisation.[161] Indeed, in a comparative experiment, epoxidation with non-fluorinated catalyst **III.11** provided low enantioselectivity, an experiment that served as a proof of concept (**Scheme III.5**). Fluorinated aminocatalyst **III.10** has proven to be highly effective in the enantioselective epoxidations[161a,163,164] and aziridinations[161b] of enals with great success, outperforming the Jørgensen-Hayashi catalyst in some cases.[165] Nevertheless, a study concerning the use of this fluorinated organocatalyst in enamine-mediated reactions had not been disclosed at the start of this project.

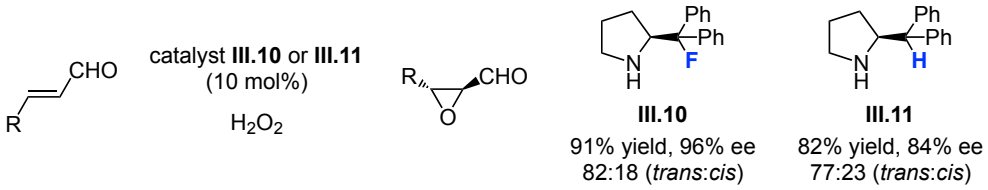

Scheme III.5. The fluorine-iminium ion gauche effect on the stereoselective epoxidation of α,β-unsaturated aldehydes.

The limited lifespan of various catalytic species reported to date remains a major concern. Therefore, we decided to immobilize the fluorinated compound **III.10**,[166] which was expected to avoid several of the issues associated to the TMS-diarylprolinol catalytic system (**Figure III.5**). Indeed, any concerns regarding the stability of this catalyst are mitigated with a robust fluorine substituent in benzylic positions,[163] much more stable than the silyl group.[161]

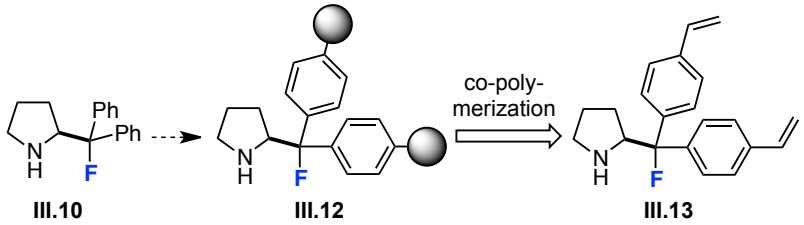

Figure III.5. Proposed design of the catalyst.

[163] a) Sparr, C.; Schweizer, W. B.; Senn, H. M.; Gilmour, R. *Angew. Chem. Int. Ed.* **2009**, *48*, 3065-3068; b) for a related precedent, see: Ho, C.-Y.; Chen, Y.-C.; Wong, M.-K.; Yang, D. *J. Org. Chem*. **2005**, *70*, 898-906.
[164] Tanzer, E.-M.; Zimmer, L. E.; Schweizer, W. B.; Gilmour. R. *Chem. Eur. J.* **2012**, *18*, 11334-11342.
[165] Alemán, J.; Fraile, A.; Marzo, L.; García Ruano, J. L.; Izquierdo, C.; Díaz-Tendero, S. *Adv. Synth. Catal*. **2012**, *354*, 1665-1671.
[166] O'Hagan, D.; Royer, F.; Tavasli, M. *Tetrahedron: Asymmetry* **2000**, *11*, 2033-2036.

Chapter III

3.2. TMS-diarylprolinol and related catalysts.

α,α-Diarylprolinol silyl ether derivatives are very successful organocatalysts. Many different articles have been published based on this catalytic system after the pioneering works by Jørgensen and Hayashi groups.[17]

Taking as a representative example the first direct enantioselective α-sulfenylation of aldehydes, developed by Jørgensen *et al.*,[17c] we can see the influence of the structure of the reported catalysts in this process (**Scheme III.6**).

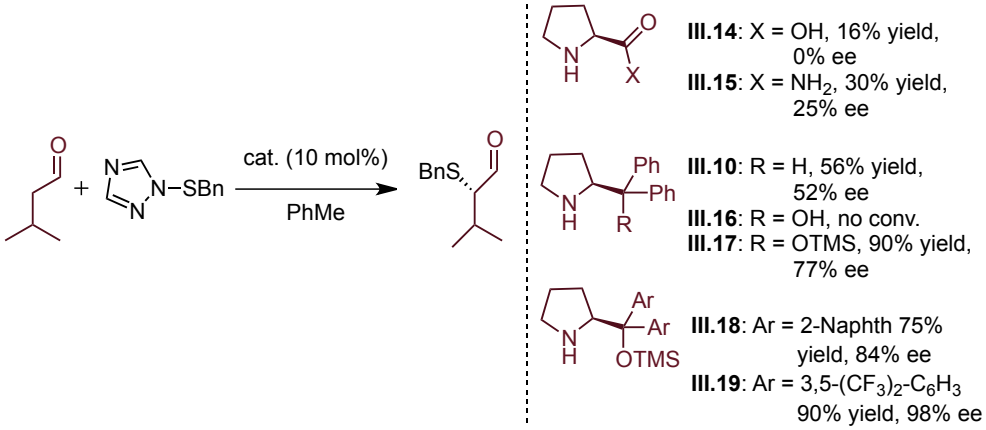

Scheme III.6. α-Sulfenylation of aldehydes.

L-Proline **III.14**, L-prolinamide **III.15**, and secondary amine catalysts **III.10** and **III.16** proved to be unreactive and/or non-selective. In the case of **III.16** no reaction occurred, probably as a result of the formation of the relatively stable and unreactive hemiaminals (**Scheme III.7**).[17c,167]

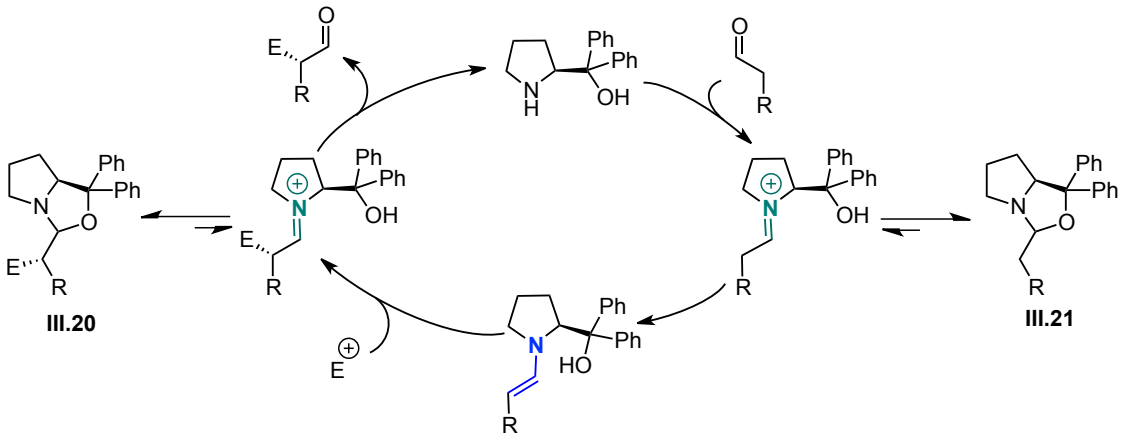

[167] Fort the formation of unreactive protonated cyclic *N,O*-acetals with OH-free prolinol, see: a) Okuyama, Y.; Nakano, H.; Hongo, H. *Tetrahedron: Asymmetry* **2000**, *11*, 1193-1198; b) Karlsson, S.; Högberg, H.-E. *Tetrahedron: Asymmetry* **2002**, *13*, 923-926; c) Schmid, M. B.; Zeitler, K.; Gschwind, R. M. *Angew. Chem. Int. Ed.* **2010**, *49*, 4997-5003.

Scheme III.7. Proposal of catalytic cycle and formation of unreactive hemiaminal species **III.20** and **III.21**.

Trimethylsilylation of the free hydroxyl moiety of **III.16**, in order to prevent hemiaminal formation, improved the rate of enamine formation with aldehydes.[168] Additional improvements were also achieved through variation of the aryl substituents in the catalyst structure (**III.18** and **III.19**).

Meanwhile, Hayashi *et al.* independently reported the asymmetric Michael reaction of aldehydes and nitroalkenes, implementing the diphenylprolinol ether system **III.17** (**Scheme III.8**).[148b] This transformation has also been the subject of intense mechanistic efforts to explain the role of the primary and secondary catalytic species (see **Chapter III**, **3.5**).[169]

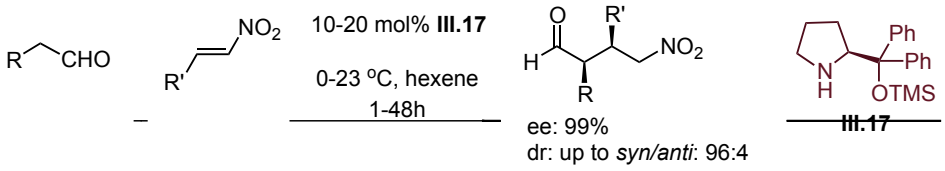

Scheme III.8. Diphenylprolinol silyl ether as an efficient organocatalyst for the Michael reaction of aldehydes and nitroalkenes.

Several transformations based on the diarylprolinol silyl ether have been developed in the recent years, including multi-component domino reactions.[170] In addition, the potential of these catalytic structures has been extended to other activation modes by using related dienamine and trienamine activation pathways (**Figure III.6**).[37]

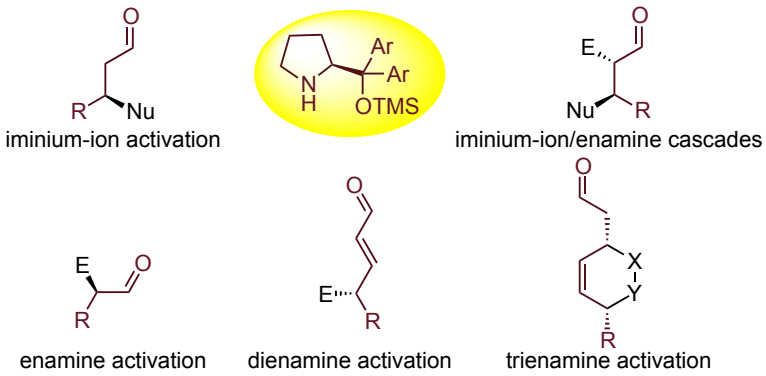

Figure III.6. Activation modes for Jørgensen-Hayashi catalyst.

[168] Dinér, P.; Kjærsgaard, A.; Lie, M. A.; Jørgensen, K. A . *Chem. Eur. J.* **2008**, *14*, 122-127.
[169] For the discussion on the mechanism, see: a) Patora-Komisarska, K.; Benohoud, M.; Ishikawa, H.; Seebach, D.; Hayashi, Y. *Helv. Chim. Acta* **2011**, *94*, 719-745; b) Burés. J.; Armstrong, A.; Blackmond, D. G. *J. Am. Chem. Soc.* **2011**, *133*, 8822-8825.
[170] For some examples, see: a) Marigo, M.; Beltelsen, S.; Landa, A.; Jørgensen, K. A. *J. Am. Chem. Soc.* **2006**, *128*, 5475-5479; b) Enders. D.; Grondal, C.; Hüttl, M. R. M. *Angew. Chem. Int. Ed.* **2007**, *46*, 1570-1581; c) Enders. D.; Wang, C.; Bats, J. W. *Angew. Chem. Int. Ed.* **2008**, *47*, 7539-7542.

Chapter III

The iminium ion and dienamine activation modes share α,β-unsaturated aldehydes as the common starting materials, providing the dienamine intermediate via a deprotonation/protonation step (**Figure III.7**).

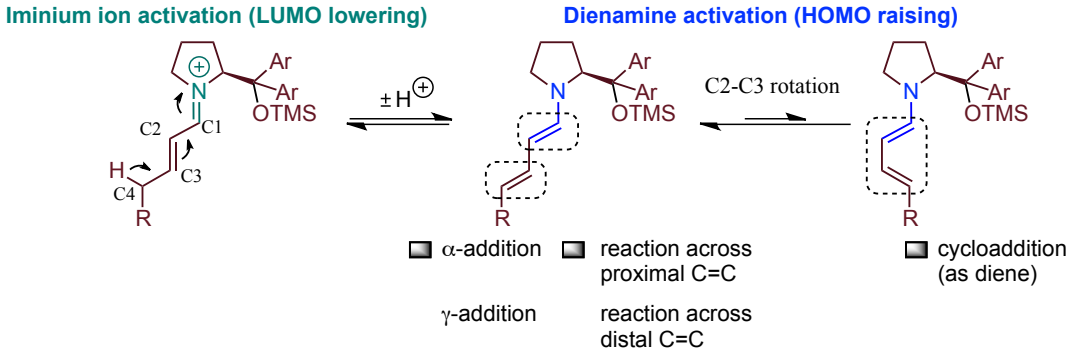

Figure III.7. Deprotonation/protonation differentiates iminium ion and dienamine activation.

In this activation mode, the diarylprolinol aminocatalysts provide activation via HOMO-raising by generating a reactive catalyst-bound dienamine species. Moreover, C2-C3 rotation of the diene opens the door to new possible reactivities.[171]

The first application of this strategy was also discovered by the Jørgensen group in 2006 in the γ-amination of α,β-unsaturated aldehydes (**Scheme III.9.A**).[172] On the other hand, there are examples of the use of dienamines in cascade reactions, described in the pioneering reports by the Barbas III, Ramachary, and Serebryakov groups (**Scheme III.9. B-C**).[173]

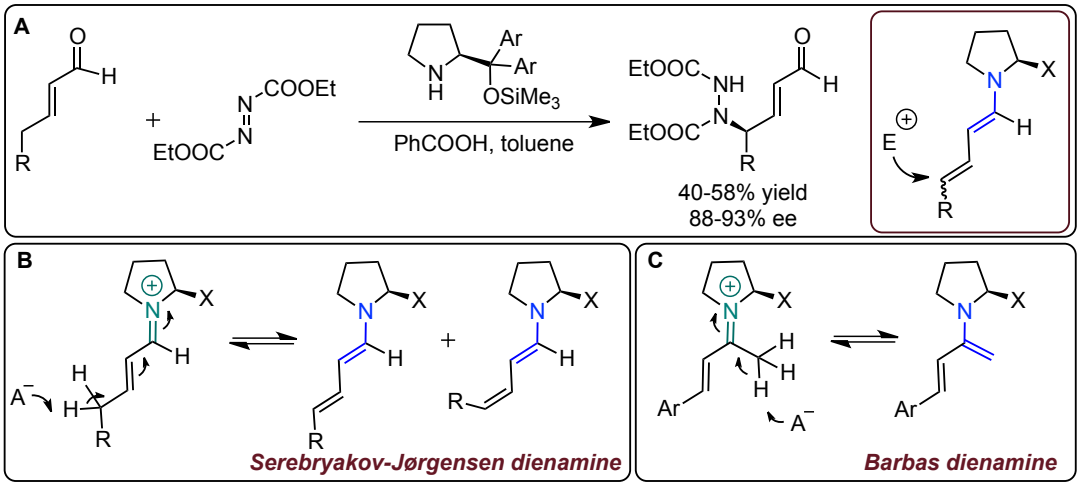

[171] Fuson, R. C. *Chem Rev.* **1935**, *16*, 1-27.
[172] Bertelsen, S.; Marigo, M.; Brandes, S.; Dinér, P.; Jørgensen, K. A. *J. Am. Chem. Soc.* **2006**, *128*, 12973-12980.
[173] a) Serebryakov, E. P.; Nigmatov, A. G.; Scherbakov, M. A.; Struchkova, M. I. *Russ. Chem. Bull.* **1998**, *47*, 82-90; b) Ramachary, D. B.; Chowdari, N. S.; Barbas III, C. F. *Tetrahedron Lett.* **2002**, *43*, 6743-6746; c) Ramachary, D. B.; Chowdari, A. S.; Barbas III, C. F. *Angew. Chem. Int. Ed.* **2003**, *42*, 4233-4237; d) Ramachary, D. B.; Ramakumar, K.; Kishor, M. *Tetrahedron Lett.* **2005**, *46*, 7037-7042.

Scheme III.9. (A) γ-Amination of α,β-unsaturated aldehydes; **(B-C)** generation of dienamine intermediates from unsaturated iminium ions.

At this point, various different reactions have been discovered that complement the enamine mode of activation.[174] These have been organized by different types of reactivity as "carbanion", "ene", or "diene" types (**Figure III.8**).[154c] In addition to the nucleophilic site at the α-position, an electrophilic site at the γ-position can be found, allowing a the sequence of reaction nucleophile-electrophile to take place. In the case of the "diene"-type reactions, electron-rich dienamines can react in inverse-electron demand Diels-Alder reactions.

The bulky stereocontrolling group of the aminocatalyst provides facial shielding and conformational restriction, in analogy to what happens with the enamine activation mode.

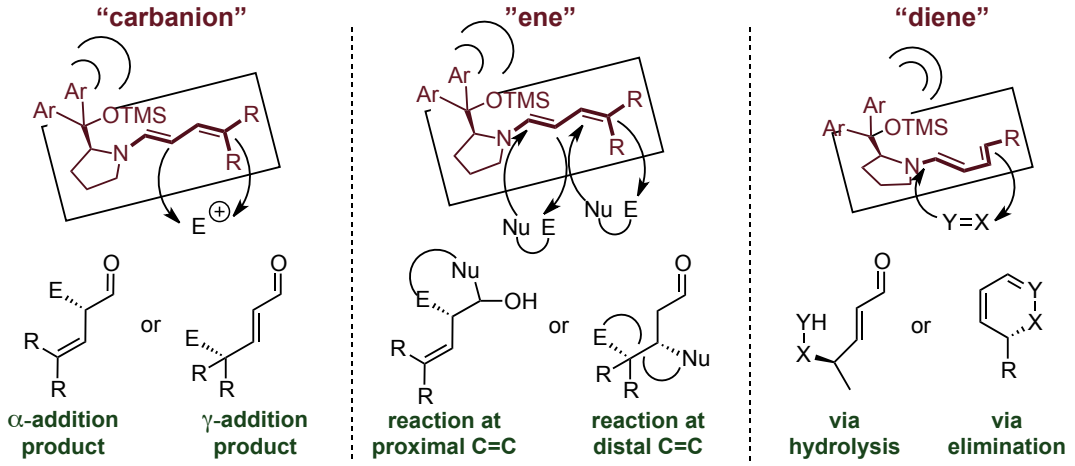

Figure III.8. "Carbanion", "ene", or "diene"-type reactivity.

In 2011, it was found that polyconjugated enals, such as 2,4-dienals, can also participate in the HOMO-raising concept by formation of a trienamine species (**Figure III.9**).[175] Two single bond rotations around C2-C3 and C4-C5 connectivities can result in the formation of two different *cis*-diene fragments. However, only reaction across the remote diene system (via C4-C5) has been observed in [4+2] cycloaddition, which could be a result of the Curtin-Hammett principle.

[174] For recent review, see: Ramachary, D. B.; Reddy, Y. V. *Eur. J. Org. Chem.* **2012**, *5*, 865-887.
[175] a) Jia, Z.-J.; Jiang, H.; Li, J.-L.; Gschwend, B.; Li, Q.-Z.; Yin, X.; Grouleff, J.; Chen, Y.-C.; Jørgensen, K. A. *J. Am. Chem. Soc.* **2011**, *133*, 5953-5061; b) Jiang, H. J.; Gschwend, B.; Albrecht, Ł.; Jørgensen, K. A. *Chem. Eur. J.* **2011**, *17*, 9032-9036.

Chapter III

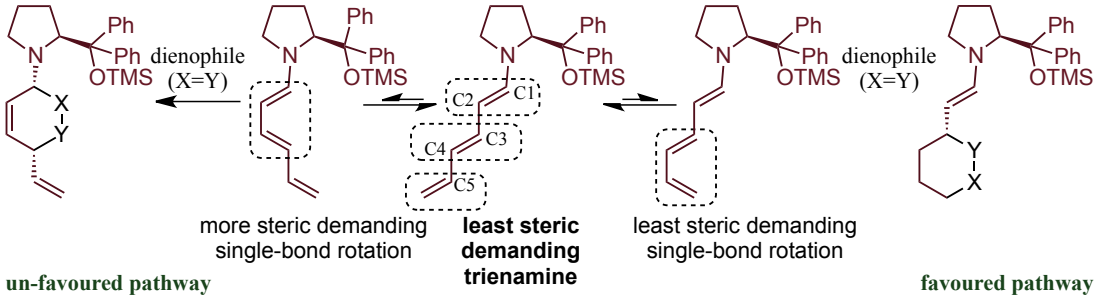

Figure III.9. Possible conformers and sites of reaction of the trienamine intermediate.

Despite of their success with different type of activation modes, TMS-diarylprolinol catalytic systems can suffer deactivation problems and catalyst designs are needed in order to provide more useful and universal catalysts for continuous flow applications.

Recently, novel catalysts **III.10** and **III.22**, related to the diarylprolinol system, have been introduced to increase the catalytic activity by incorporation of an electronegative group (fluorine or azide) at the β-position relative to the NH group: a *gauche*-effect or electrostatic interaction between these groups might be favorable for stabilizing reactive intermediates (**Scheme III.5** or **Scheme III.10**).[161,163,176]

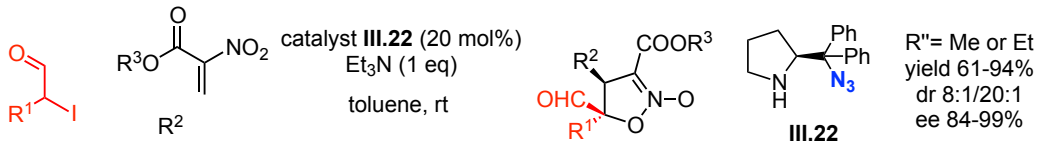

Scheme III.10. Enantioselective [4+1]-annulation catalyzed by azide-containing **III.22**.

3.3. Fluorine-iminium ion *gauche* effect.

Modern stereoelectronic theory constitutes a powerful tool for rationalizing the conformation of molecules and the outcome of organic transformations.[177] The term stereoelectronic effect involves an electronic interaction, which stabilizes a particular conformation or transition state.

Stereoelectronic interactions involving π-bonds (conjugation) are among the most important chemical phenomena, while interactions between σ-orbitals (hyperconjugation) have received less attention.[178]

---

[176] Shi, Z.; Tan, B.; Leong, Y.; Zeng, W. W.; Lu, M.; Zhong, G. *Org. Lett.* **2010**, *12*, 5402-5405.
[177] *Topics in Stereochemistry* (Ed. Denmark, S. E.), John Wiley & Sons, *Vol. 22*, **2009**.
[178] Kirsch, P. *Modern Fluoroorganic Chemistry: synthesis, reactivity, applications*, Wiley-VCH, Weinheim, Germany, **2005**.

Fluorine is the most electronegative element in the periodic table. For this reason, stereoelectronic and electrostatic effects of this element become especially important in the behavior and conformation of fluorinated organic molecules. The $C^{\delta+}$-$F^{\delta-}$ bond is highly polarized;[179] therefore, fluorine is able to stabilize some conformation via electrostatic/charge-dipole interactions. Thus, the introduction of fluorine atoms can be used as a conformational tool for the design of functional molecular systems.

The discussion of acceptor properties of C-F bonds is complicated by the presence of two conformers with either *gauche* or *anti*-orientation of the heteroatom lone pair relative to the C-C bond. **Figure III.10** illustrates the basic example 1,2-difluoroethane. It is well know that this molecule prefers *gauche* rather than an *anti* conformation.[180] *Gauche* is used to refer to conformational isomers in which two vicinal groups are separated by a 60° torsion, whereas for a 180 degrees disposition the term used is "*anti*". IUPAC defines groups as *gauche* if they have "synclinal alignment of groups attached to adjacent atoms". There are two main explanations for the *gauche* effect: hyperconjugation and bent bonds.[160,161,181]

According to the hyperconjugation model the preference for a *gauche* conformation is rationalized by taking into account stabilization through the critical donation of electrons from the neighboring σ_{C-H} orbital to the lower-lying vacant σ^*_{C-F} orbital as shown in **Figure III.10**, this is not possible in the corresponding *anti* isomer. Due to the greater electrononegativity of fluorine, the σ_{C-H} orbital is a better electron donor than the σ_{C-F} orbital, while the σ^*_{C-F} orbital is a better electron acceptor than the σ^*_{C-H} orbital.

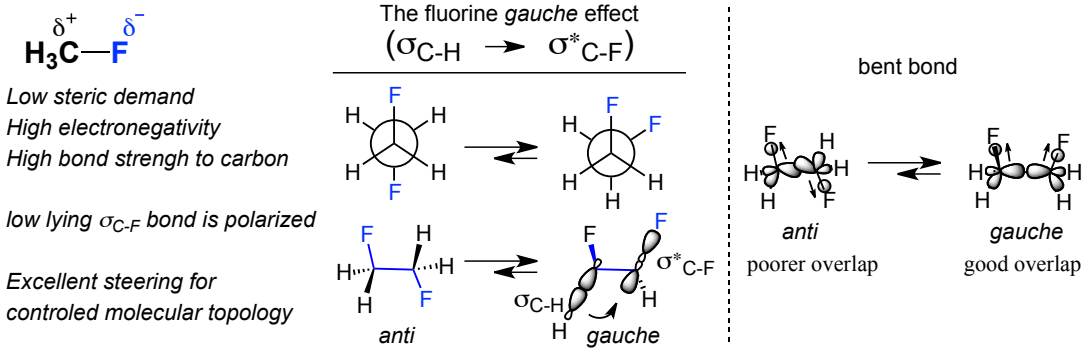

Figure III.10. Orbital interaction of 1,2-difluoroethane and bent bond theory.

[179] For review, see: O'Hagan, D. *Chem. Soc. Rev.* **2008**, *37*, 308-319.
[180] Craig, N.C.; Chen, A.; Suh, K. H.; Klee, S.; Mellau, G. C.; Winnewisser, B.P.; Winnewisser, M. *J. Am. Chem. Soc.* **1997**, *119*, 4789-4790.
[181] a) *Fluorine in medical chemistry and chemical biology* (Ed. Ojima, I.), **2009**, 13-16; b) Sparr C.; Zimmer, L. E.; Gilmour, R. *Asymmetric synthesis: more methods and applications* (Eds.: Christmann, M.; Bräse, S.), Wiley-VCH, **2012**, 117-124.

Chapter III

Wiberg *et al.* have presented an alternative hypothesis for the *gauche* effect, using bent bond analysis.[182] According to their theory, geometric changes of σ-bonds (C-C and C-H) on carbon are due to the highly polarized C-F bond. Therefore, the electron deficient C-F bond has most of its electron density on the fluorine atom, while for C-C and C-H bonds the electron density is in the middle of the bond. For the *gauche* conformer there is good overlap in the C-C bond, but for the *anti* conformer electron density is skewed in different direction towards each fluorine with resulting poorer C-C bond overlap as illustrated in **Figure III.10** (*right*). Of these two models, hyperconjugation is generally considered as the main explanation behind the *gauche* effect in difluoroethane.

The highly polarized nature of the C-F bond provides fluorinated molecules with interesting physical and electronic properties (**Figure III.11**). In the absence of overriding constraints, the *gauche* conformational preference holds for numerous fluorinated systems containing an electron-withdrawing group (X; $\sigma_{C\text{-}H} \rightarrow \sigma^*_{C\text{-}X}$). This effect can be applied in many other systems in addition to 1,2-difluoroalkanes, such as compounds, containing F-C-C-O or F-C-C-N arrays. In general, more electronegative substituents give rise to stronger *gauche* effects.

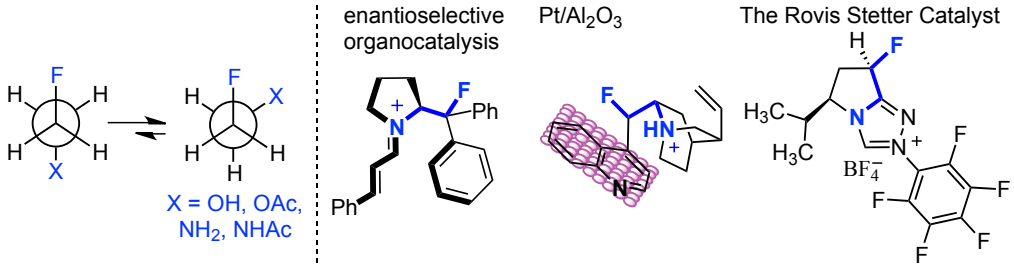

Figure III.11. Some examples of the *gauche* effect.

Pyrrolidine **III.10** was found to be highly selective for the epoxidation of α,β-unsaturated aldehydes.[163a] In the first step, aldehyde and pyrrolidine react together to form an iminium ion. In intermediate **III.23**, the fluorine atom is aligned *gauche* to the positively charged nitrogen atom, resulting in a phenyl group shielding the top (*re*) face of the alkene. Hydrogen peroxide consequently attacks from the bottom (*si*) face, leading to the depicted epoxide with high enantioselectivity.

[182] Wiberg, K. B.; Murcko, M. A.; Laidig, K. E.; MacDougall, P. J. *J. Phys. Chem.* **1990**, *94*, 6956-6959.

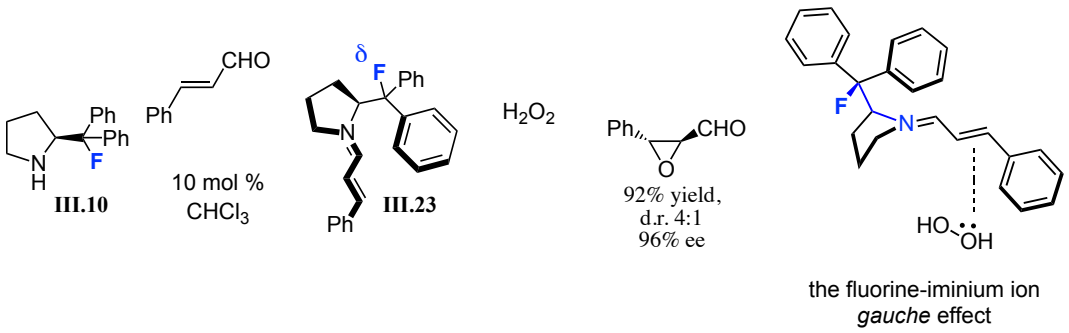

Scheme III.11. Asymmetric epoxidation reaction catalyzed by pyrrolidine **III.10**.

These results provided a proof of concept for the use of the fluorine-iminium ion *gauche* as a strategy for improving organocatalyst performance. This opens up new avenues to exploit the C-F bond as a small inert steering group for conformation control that can find further application in organocatalysis.

3.4. Covalent immobilization by polymerization.

The term polymerization refers to a chemical process where a single molecular unit (the monomer) reacts several times with itself to generate polymer chains or three-dimensional networks. The polymerization of ethylene derivatives such as styrene and vinyl chloride was discovered in 1950, leading to intensive work in industrial laboratories and practical utilization of those discoveries. In the 1984, B. Merrifield was awarded the Nobel Prize in Chemistry for discovering a method of synthesizing oligomers on a solid phase synthesis, which revolutionized the preparation of peptides and nucleotides. This strategy is now common in chemical and biochemical laboratories.[183]

Merrifield resins are made from styrene, divinylbenzene (1 or 2%) and 4-chloromethyl-1-vinylbenzene. Therefore, the polystyrene (PS) beads are functionalized with chloromethylene groups. Starting from Merrifield resin, many functional groups have been introduced into the polymer through nucleophilic substitution of the benzylic chlorine atom. This gives rise to new functional polymers as the Wang resin (**Scheme III.12**),[184] as well as alternative resins that have also been applied to organic synthesis.[185] These styrene-based polymers are commonly used for the preparation of ion exchange resins and polymeric supports.

---

[183] Merrifield, R. B. *J. Am. Chem. Soc.* **1963**, *85*, 2149-2154.
[184] Wang, S.-S. *J. Am. Chem. Soc.* **1973**, *95*, 1328-1333.
[185] Park, B. D.; Lee, H. I.; Ryoo, S.J.; Lee, Y.S. *Tetrahedron Lett.* **1997**, *38*, 591-594.

Chapter III

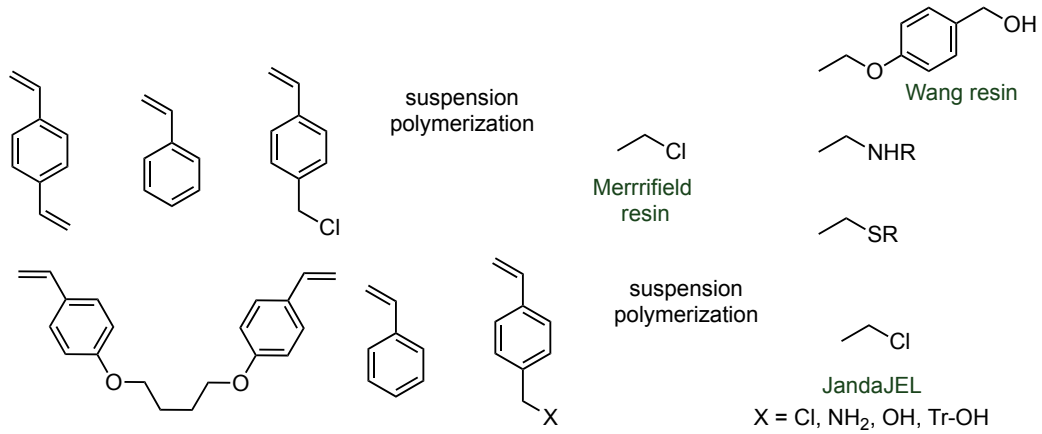

Scheme III.12. Preparation of resins by suspension co-polymerization.

It must be noted that all these resins are prepared by suspension polymerization. This is an important method for synthesizing relative unfunctionalized polymers. The radical initiator is usually an azo compound (e.g. azo-bis-2-methylpropionitrile, AIBN), or an organic peroxide (e.g. benzoyl peroxide) and the polymerization is performed at a temperature of about 50-100°C. Polyvinyl-pyrrolidine (PVP) and poly(vinyl alcohol)-co-(vinyl acetate) are the most typical stabilizers used for suspension polymerization.[186]

Another important method to obtain functional materials is the copolymerization of pre-functionalized monomers. By this way, the accessibility of the active sites depends on the degree of cross-linking agent, which can be controlled by the stoichiometry. Moreover, the structure of the cross-linkers can be varied and optimized, and the amount of functional units (e.g. a chiral moiety) incorporated in the polymer can be controlled as well.

In fact, the concept of preparing immobilized proline derivatives via copolymerization has not been extensively used in organic chemistry.[155d] There are few examples of preparation of diarylprolinols using this method by Itsuno *et al*. (**Figure III.12**).[187] The chiral polymer was obtained by copolymerization of styrene with a chiral monomer having two polymerizable vinyl groups which, as a consequence, also acts as crosslinking agent.[188] The final catalysts were generated *in situ* from monobromoborane. The resulting chiral polymers could be applied in the Diels-Alder reaction of cyclopentadiene with methacrolein to give optically active cycloadducts in high chemical yield with high *exo* selectivity.

---

[186] Arshady, R. *Colloid Polym. Sci.* **1992**, *270*, 717-732.
[187] Itsuno, S.; Kamahori, K.; Watanabe, K.; Koizumi, T.; Ito, K. *Tetrahedron: Asymmetry* **2010**, *5*, 523-526.
[188] a) Itsuno, S.; Watanabe, K.; Koizumi, T.; Ito, K. *Reactive polymers* **1995**, *24*, 219-227; b) Itsuno, S.; Ito, K. in *Trends in Organic Chemistry*, Council of Scientific Research Integration, Research Trends: **1991**, 199-211.

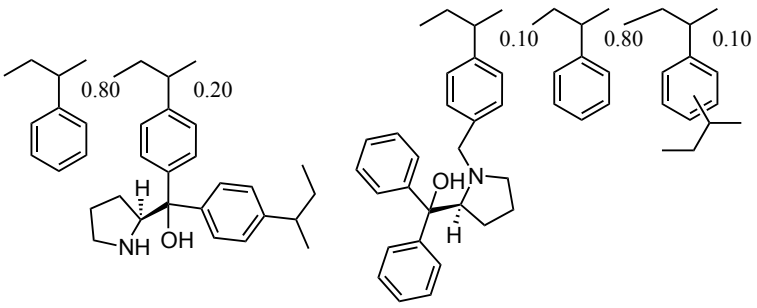

Figure III.12. Representative example by Itsuno *et al.*

3.5. Enantioselective organocatalytic Michael addition reactions.

The organocatalytic Michael addition is one of the most important and effective methods for enantioselective C-C bond formation. It is used as an important step in the synthesis of many biologically active compounds and natural products.[189]

The conjugate addition of an aldehyde to a nitroalkene, belonging to this general reaction type, is one of the most studied organocatalytic reactions in the recent years (**Scheme III.13**).[190]

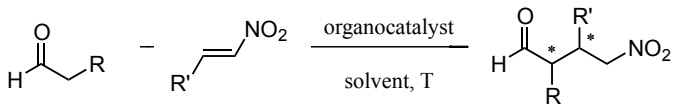

Scheme III.13. Asymmetric Michael addition of aldehydes to nitroalkenes**.**

The general mechanism of the Michael reaction between carbonyl compounds and nitroolefins via enamine catalysis is shown in **Scheme III.14**.

[189] For some examples, see: a) Andrey, O.; Vidonne, A.; Alexakis, A. *Tetrahedron Lett.* **2003**, *44*, 7901-7904; b) Nicolaou, K. C.; Sarlah, D.; Shaw, D. M. *Angew. Chem. Int. Ed.* **2007**, *46*, 4708-4711.
[190] Perlmutter, P. *Conjugate Addition Reactions in Organic Synthesis* **1992,** Pergamon Press: Oxford, UK.

Chapter III

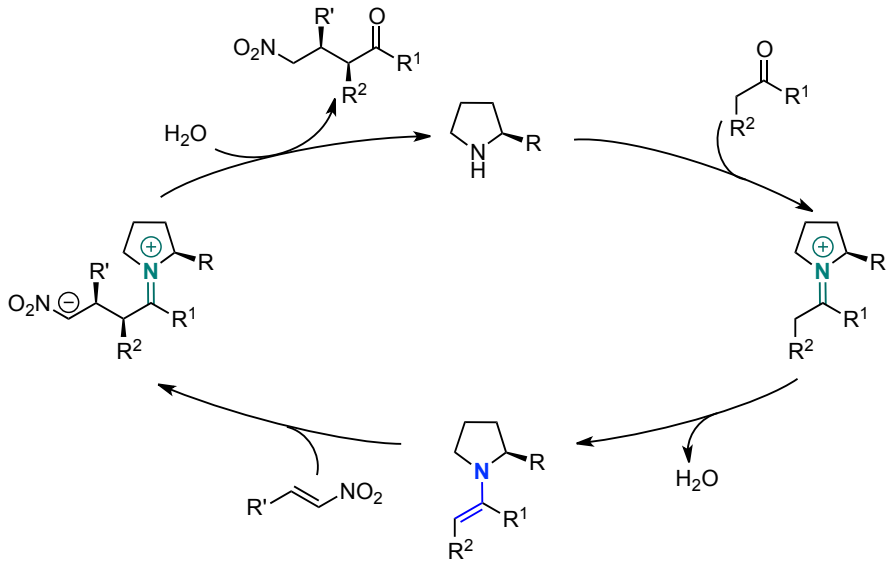

Scheme III.14. Catalytic cycle of Michael reaction of carbonyl compounds and nitroolefins.

This reaction is very appealing since the resulting γ-nitroaldehydes are valuable synthetic intermediates that can be readily converted into γ-amino acids, γ-butyrolactones, chiral pyrrolidines or tetrahydropyrans.[191] Betancort and Barbas reported the first study in this field, involving the conjugate addition of unmodified aldehydes to nitroolefins in 2001 as shown in **Scheme III.15**. All γ-formyl nitro products had *syn*-stereoselectivity and they proposed a transition state based on an acyclic synclinal model to explain the high *syn*-selectivity. In this model, there are favorable electrostatic interactions between the partially negative nitro group and the partially positive nitrogen of the enamine in the transition state as depicted in **Scheme III.15**.[192]

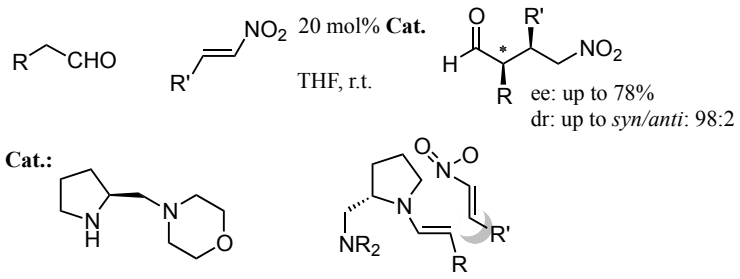

Scheme III.15. The first organocatalytic asymmetric Michael addition.

The Seebach, Hayashi and Blackmond groups have independently revised the generally accepted mechanism for organocatalyzed Michael addition of aldehydes to nitroalkenes in 2011, providing kinetic and *in situ* NMR studies (**Scheme III.16**).[169]

[191] Chen, J.-R.; Zou, Y.-Q.; Fu, L.; Ren, F.; Tan, E.; Xiao, W.-J. *Tetrahedron* **2010**, *66*, 5367-5372.
[192] Betancort, J. M.; Barbas III, C. F. *Org. Lett.* **2001**, *3*, 3737-3740.

The groups of Seebach and Hayashi have reported some mechanistic investigations in the presence of acid additives, where they found that *p*-nitrophenol (weak acid with pKa 7.15) is the most effective additive in terms of activity. This allowed lowering the catalyst loading to 1 mol%. Additional studies towards elucidation the mechanism of this reaction were investigated.[169a]

At the same time, Blackmond *et al.* also reported the kinetic and structural studies toward the mechanistical understanding of Michael addition of aldehydes to nitroalkenes. [169b]

These additional studies disclosed the formation of amino-nitro-cyclobutane intermediates **III.27**, which have been confirmed by NMR studies.[169b]

Therefore, the authors suggest a revised mechanism that is shown in **Scheme III.16**. After the zwitterionic intermediate **III.26** has been generated, two different pathways are possible: 1) cyclization to a cyclobutane derivative (**III.27**), and 2) protonation leading to an iminium ion **III.28**, which can be hydrolyzed to the desired product **III.30** or deprotonated to its corresponding enamine (**III.29**). In turn, the final product **III.30** can be epimerized in the α-carbonyl position by catalyst **III.24**.

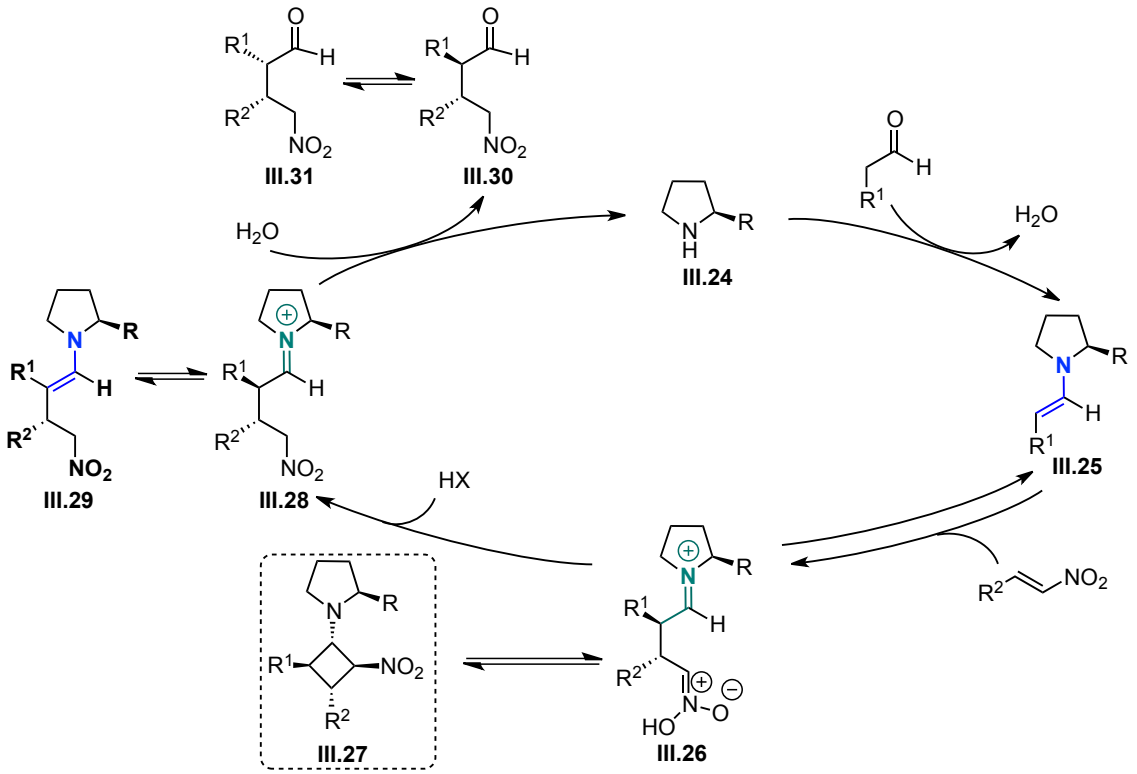

Scheme III.16. Revised mechanism of the amino catalyzed Michael addition of aldehydes to nitroolefins.

Chapter III

So far only peptidic catalysts, which can be obtained by well-established procedures, have been used under continuous flow operation in the Michael reaction between aldehydes and nitroolefins (**Scheme III.17**).[193]

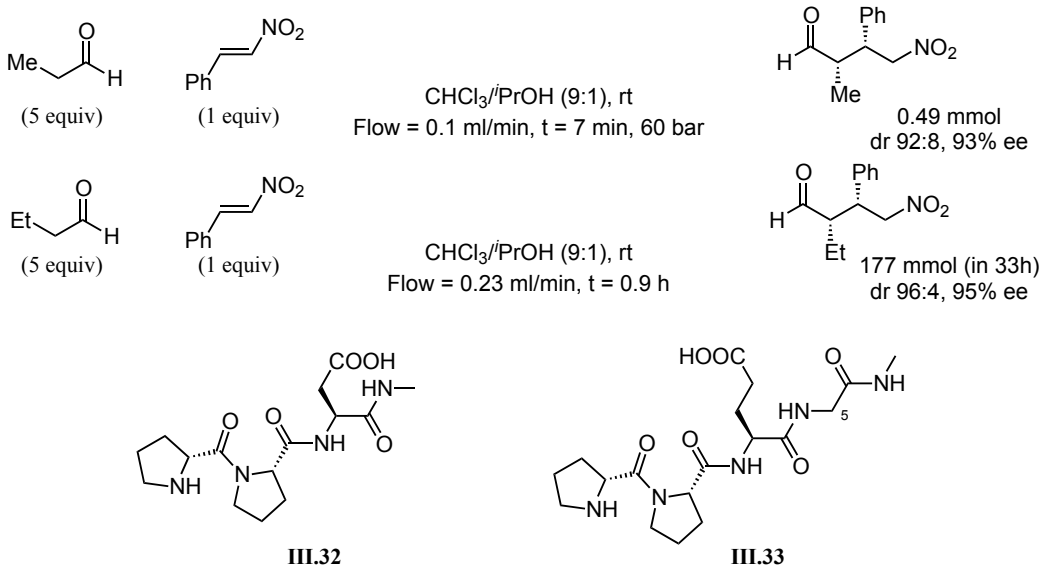

Scheme III.17. Asymmetric Michael reactions mediated by peptidic organocatalysts in flow.

Given the fact that these catalysts are anchored covalently to the polymeric support, they are much more stable towards leaching. In some cases, reuse of these catalysts is possible without any loss in activity.

However, long residence times or large amount of one of the reactants are required to obtain a good conversion. In addition, most of the experiments are limited to the lab scale demonstration, and optimization in terms of yield and selectivity is still desirable.

Flow reactors will have an increasingly important role to play in the future development of catalytic methodologies. The ability to obtain clean conversions also allows the process to be combined with other reactions in multi-step continuous flow processes, which present a number of advantages in industry, as well as academic laboratories.

[193] a) Ötvös, S. B; Mándity, I. M.; Fülöp, F. *ChemSusChem* **2012**, *5*, 266-269; b) Arakawa, Y; Wennemers, H. *ChemSusChem*, **2013**, *6*, 242–245.

3.6. Aim of the project.

Considering that recently β-fluoroamines (**III.10**) have been shown to catalyze different organocatalytic transformations via iminium ion activation,[161,163] it is surprising that no Michael addition has been reported via enamine activation mode for this type of catalyst.

The main objective of this project is to develop an efficient polymer-supported organocatalytic system for the asymmetric Michael addition of aldehydes to nitroolefins, which could display increased robustness when compared to the structurally related silyl ethers.

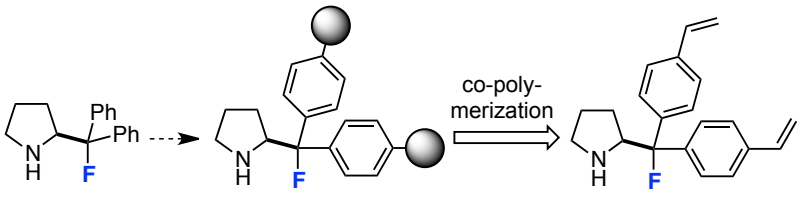

III.10 **III.12** **III.13**

Although there have been great efforts to develop organocatalysts that can exhibit high enantioselectivities and activities for this reaction, there were some problems encountered in these organocatalytic systems such as lability of silyl ethers. In addition, we would like to show new potential for β-fluoroamine catalysts in a different mode of activation.

In view of the variety of available structures, we considered to develop a supporting strategy that utilizes the vinyl double bound in **III.13** as a suitable anchoring point for co-polymerization.

We aim to demonstrate that a highly reactive and selective recyclable supported β-fluoroamine catalyst has a potential to complement immobilized prolinol derivatives in asymmetric organocatalytic transformations, with the ultimate goal of implementing novel enantioselective continuous flow processes.

UNIVERSITAT ROVIRA I VIRGILI
NEW APPROACHES TO CATALYST DESIGN AND IMMOBILIZATION
Irina Sagamanova

Article B

ACS Catalysis
Research Article
pubs.acs.org/acscatalysis

Translating the Enantioselective Michael Reaction to a Continuous Flow Paradigm with an Immobilized, Fluorinated Organocatalyst

Irina Sagamanova,[†] Carles Rodríguez-Escrich,[†] István Gábor Molnár,[§] Sonia Sayalero,[†] Ryan Gilmour,*[,§,∥] and Miquel A. Pericàs*[,†,‡]

[†]Institute of Chemical Research of Catalonia (ICIQ), The Barcelona Institute of Science and Technology, Avinguda Països Catalans 16, 43007 Tarragona, Spain

[‡]Departament de Química Orgànica, Universitat de Barcelona, 08080 Barcelona, Spain

[§]Institut für Organische Chemie, Westfälische Wilhelms-Universität Münster, Corrensstrasse 40, 48149 Münster, Germany

[∥]Excellence Cluster EXC 1003 "Cells in Motion", Westfälische Wilhelms-Universität Münster, Münster, Germany

Supporting Information

ABSTRACT: A novel polymer-supported fluorinated organocatalyst has been prepared and benchmarked in the enantioselective Michael addition of aldehydes to nitroalkenes. The system has proven to be highly efficient and displays excellent selectivities (er and dr) with a wide variety of substrates. Detailed deactivation studies have given valuable insights, thus allowing the lifespan of this immobilized aminocatalyst to be significantly extended. These data have facilitated the implementation of enantioselective, continuous flow processes allowing either the multigram synthesis of a single Michael adduct over a 13 h period or the sequential generation of a library of enantiopure Michael adducts from different combinations of substrates (13 examples, 16 runs, 18.5 h total operation). A customized in-line aqueous workup, followed by liquid−liquid separation in flow, allows for product isolation without the need of chromatography or other separation techniques.

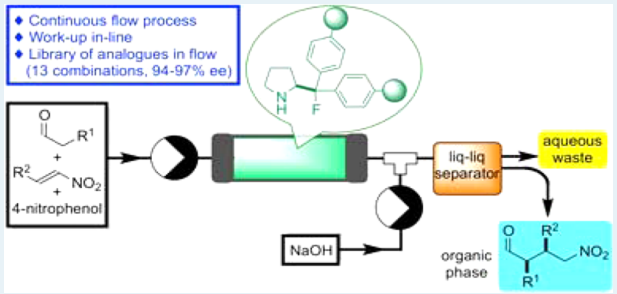

KEYWORDS: *fluorinated organocatalyst, continuous flow, polystyrene-supported catalysts, enantioselective catalysis, Michael reaction*

1. INTRODUCTION

Sustainability concerns have resulted in a change of paradigm in which not only cost reduction but also waste minimization and catalyst recovery are crucial issues in process design. In this context, continuous flow chemistry is one of the technologies expected to facilitate process intensification, reducing the footprint of chemical plants while increasing their productivity, modularity, and flexibility.[1] Despite the potential of immobilized catalysts for enantioselective flow processes, the fine chemical industry still shows some reluctance to apply these techniques because of the often limited lifespan of the reference homogeneous species. Designing more stable homogeneous catalysts and successfully translating their corresponding batch processes to an immobilized platform is therefore essential to further validate the potential of this approach. Consequently, the preparation of supported catalysts with high activity and improved stability holds great potential for both the industrial and academic chemical communities.

Since the pioneering reports by List, Lerner, Barbas,[2] and MacMillan[3] laid the foundations of modern organocatalysis, efforts to develop effective metal-free small molecule catalysts have intensified.[4] One of the most successful organocatalysts is the diarylprolinol trimethylsilyl ether, commonly known as the Jørgensen−Hayashi catalyst.[5] Given the versatility of this species, which is able to exploit both the enamine and iminium ion activation mode, several groups have tried to harness its potential by developing immobilized analogues.[6] With the aim of enhancing the sustainability profile of this catalyst, this laboratory has reported the preparation of a set of solid-supported derivatives[7] whose robustness was established through recycling and implementation of enantioselective continuous flow processes.[8] These studies revealed that the reusability of the catalyst was often compromised by the lability of the trimethylsilyl ether; this has also been investigated spectroscopically in the homogeneous paradigm.[9]

Several approaches have been employed to address this issue. First, it was demonstrated that resilylation is indeed possible,[7a] although this has obvious drawbacks from an operational point of view, and it precludes continuous flow applications. The analogous methyl ether[10] (rather than silyl) was also prepared, but the polymer-supported version proved to be less active and selective than the parent system.[7b] Although catalysts with bulkier silyl ethers display increased stability,[7d,e] significant structural changes can compromise reactivity, and they tend to deactivate

Received: August 10, 2015
Revised: September 10, 2015

 © XXXX American Chemical Society

DOI: 10.1021/acscatal.5b01746
ACS Catal. 2015, 5, 6241−6248

Chapter III

Scheme 1. Strategy for the Preparation of a Polymer-Supported Analog of 1

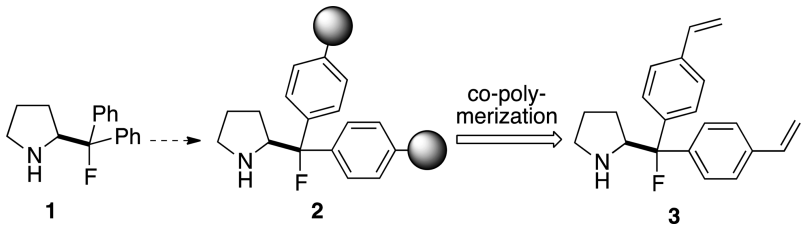

over time. With these data in hand, efforts to immobilize the fluorinated compound **1**[11] were initiated; this system was introduced in asymmetric organocatalysis by Gilmour et al. in 2009.[12] The pyrrolidine derivative, designed to validate the gauche effect hypothesis for molecular preorganization,[13] has proven to be highly effective in the enantioselective epoxidations[12a,14] and aziridinations[15] of enals with great success, outperforming the Jørgensen–Hayashi catalyst in some cases.[16] Moreover, the low steric demand of the fluorine substituent, coupled with the reactively inert C–F bond, ensures that any concerns regarding stability of this site are mitigated.

It was therefore envisaged that compound **2**, a polymer-supported analog of **1**, would display increased robustness when compared with the structurally related silyl ethers. In addition, because the active site of **1** (the pyrrolidine moiety) is not involved in the polymerization of **3** and the pyrrolidine moiety can freely rotate in polymer **2**, we anticipated that the performance of **1** would be preserved in the polymer. To test the validity of this hypothesis, compound **2** was prepared by copolymerization of the divinylated derivative **3** with styrene (Scheme 1).

Scheme 2. Preparation of the Monomer 3

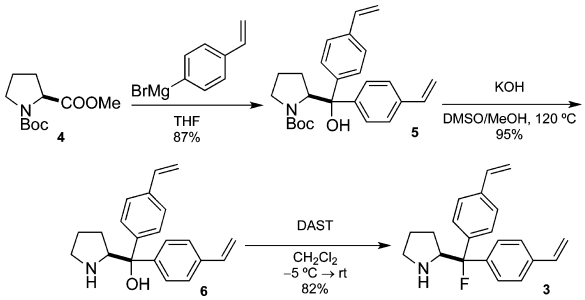

Scheme 3. Preparation of Resin 2 by Copolymerization of 3

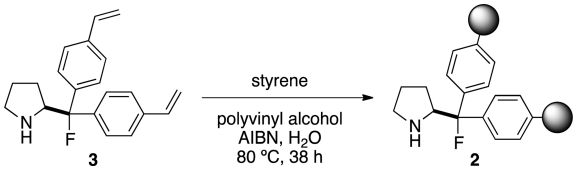

2. RESULTS AND DISCUSSION

The synthesis of the target catalyst (Scheme 2) started with the addition of 4-vinylphenyl magnesium bromide (prepared in situ) to the proline derivative **4**,[17] which furnished **5** in 87% yield.[18] The Boc group was then cleaved in basic media, presumably via the corresponding oxazolidinone, to generate amino alcohol **6**.[19] Deoxyfluorination of this amino alcohol, achieved by treatment with diethylaminosulfur trifluoride[20] (DAST), provided **3** in a concise three-step sequence and 68% overall yield. Immediate fluorination of compound **6** was essential to avoid spontaneous self-polymerization.

Polymer **2** was obtained by suspension polymerization of the chiral monomer **3** with styrene in water following a modification of the procedure reported by Itsuno for the related amino alcohol[21] (Scheme 3). Because the monomeric species has two vinyl units, a cross-linking agent (e.g., DVB) was not required. Up to 65% of the functional monomer was incorporated to the polymer, giving rise to resin batches with functionalization levels

Table 1. Effect of Additives for the Addition of Propanal to β-Nitrostyrene[a]

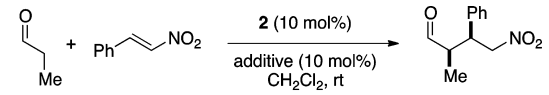

entry	additive	pK_a in H_2O[b]	t (h)	conv[c] (yield[d])	dr[c]	ee[e] (%)
1			11	100 (99)	96:4	94
2	CF_3COOH	0.52	5	14 (n.d.)	67:33	
3	2-FC_6H_4COOH	3.27	3.5	100 (97)	93:7	95
4	(*R*)-mandelic acid	3.37	5	81 (n.d.)	85:15	94
5	(*S*)-mandelic acid	3.37	5	81 (n.d.)	83:17	94
6	PhCOOH	4.20	3.5	100 (98)	95:5	94
7	CH_3CH_2COOH	4.887	4	98 (n.d.)	96:4	94
8	4-nitrophenol	7.15	1.5	100 (99)	95:5	95

[a]General conditions: (*E*)-β-nitrostyrene (22.4 mg, 0.15 mmol), propanal (33 μL, 0.45 mmol), catalyst **2** (10 mol %), additive (10 mol %) in 300 μL of CH_2Cl_2 at room temperature. [b]pK_a values taken from literature sources.[24] [c]Conversion (%) and diastereomeric ratio (dr) determined by ^1H NMR spectroscopy of the crude reaction mixture. [d]Isolated yield. [e]Determined by chiral HPLC analysis using a Chiralpak IC column.

DOI: 10.1021/acscatal.5b01746
ACS Catal. 2015, 5, 6241–6248

ranging between 0.80 and 1.15 mmol g^{-1}. This polymer was characterized by IR, elemental analysis, and SEM (see Supporting Information for details). Moreover, it was possible to confirm the presence of the fluorine substituent at the surface of the catalyst by EDX analysis

To characterize the behavior of this polymer further, the swelling ability with different solvents was determined in CH_2Cl_2, toluene, and water. As expected for a polystyrene derivative, greater swelling was observed in CH_2Cl_2 than in water, whereas toluene led to an average result (see Supporting Information for details).

Table 2. Organocatalytic Michael Addition in Batch Mode[a]

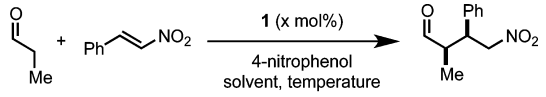

7a (3 equiv.) **8a** (1 equiv.) **9aa**

entry	catalyst/additive (mol %)	solvent	t (h)	conv[b] (yield[c]) (%)	dr[b]	ee[d] (%)
1	10	CH_2Cl_2	1	>99 (99)	96:4	95
2	10	CH_2Cl_2[e]	3	>99 (98)	97:3	95
3	10	CH_2Cl_2[f]	0.5	>99 (97)	84:16	97
4	10	CH_2Cl_2 (dry)[g]	1	>99 (98)	96:4	96
5	10	toluene	2.5	>99 (95)	95:5	95
6	10	EtOAc	16	>99 (97)	94:6	92
7	10	THF	24	93 (86)	94:6	90
8	5	CH_2Cl_2	1.5	>99 (98)	96:4	95
9	5	toluene	8	>99 (95)	96:4	95

[a]General conditions: (*E*)-*β*-nitrostyrene (22.4 mg, 0.15 mmol), propanal (33 μL, 0.45 mmol), catalyst **1**, and 4-nitrophenol in 300 μL of solvent at room temperature. [b]Conversion (%) and diastereomeric ratio (dr) determined by ^{1}H NMR spectroscopy of the crude reaction mixture. [c]Isolated yield (%). [d]Determined by chiral HPLC analysis. [e]Reaction temperature: 0 °C. [f]Reaction temperature: 40 °C. [g]Dry solvent, stored over 4 Å molecular sieves.

Table 3. Examining the Effect of Solvent on the Addition of Propanal to *β*-Nitrostyrene in the Presence of 4-Nitrophenol and Catalyst 2[a]

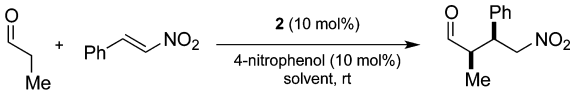

7a (3 equiv.) **8a** (1 equiv.) **9aa**

entry	solvent	t (h)	conv[b] (yield[c])	dr[b]	ee[d] (%)
1	CH_2Cl_2	1.5	100 (99)	95:5	95
2	toluene	5	100 (98)	95:5	96
3	EtOAc	16	99 (n.d.)	95:5	93
4	THF	16	65 (n.d.)	93:7	92
5	H_2O	1.5	100 (99)	95:5	95
6	CH_2Cl_2[e]	5	100 (98)	95:5	95

[a]General conditions: (*E*)-*β*-nitrostyrene (22.4 mg, 0.15 mmol), propanal (33 μL, 0.45 mmol), catalyst **2** (10 mol %), 4-nitrophenol (10 mol %) in 300 μL of solvent at room temperature. [b]Conversion (%) and diastereomeric ratio (dr) determined by ^{1}H NMR spectroscopy of the crude reaction mixture. [c]Isolated yield. [d]Determined by chiral HPLC analysis using a Chiralpak IC column. [e]5 mol % of catalyst **2** and 5 mol % of 4-nitrophenol were used.

To evaluate the catalytic activity and recyclability of this system, the well-established catalytic addition of aldehydes to nitroalkenes[22] was selected as the benchmark reaction for this study. It is worth mentioning that there are no reports of **1** acting as a catalyst for this reaction. Indeed, this study constitutes the first report of its application in the enamine activation mode.

As a model substrate set, propanal and (*E*)-*β*-nitrostyrene were selected. An initial screening of the addition reaction catalyzed by **2** is summarized in Tables 1 and 2. Gratifyingly, the reaction in CH_2Cl_2 without any additives was complete within 11 h and gave excellent stereoselectivities (entry 1). Consistent with literature reports on the homogeneous reaction, the addition of organic acids increased the reaction rate[23] while maintaining the high levels of enantioselectivity (entries 2–8). As illustrated in Table 1, relatively strong acids, such as TFA, proved detrimental (entry 2), but several carboxylic acids were tested with good results. Finally, it was observed that 4-nitrophenol (the weakest of the acids examined) as an additive[23a,d] provided the desired product with excellent levels of enantioselectivity (95% ee) within 1.5 h. Good levels of diastereocontrol (up to 96:4 syn/anti) were observed throughout this optimization process.

The organocatalytic Michael addition reaction was then optimized in batch mode using catalyst **1** to provide a data set for comparison with the immobilized system (Table 2). The initial reaction in CH_2Cl_2 reached completion in only 1 h furnishing the desired product **9aa** in quantitative yield and with excellent levels of both diastereo- and enantioselectivity (dr 97:3 syn/anti and ee 97%. Table 2, entry 1). Indeed, the selectivity of the transformation was essentially unaffected by changes in reaction medium (entries 4–7) and temperature variations (entries 2 and 3).

Next, the influence of reaction medium on the organocatalytic Michael reaction with resin **2** was examined using several

Scheme 4. Scope of the Aldehyde Reaction Partner[a]

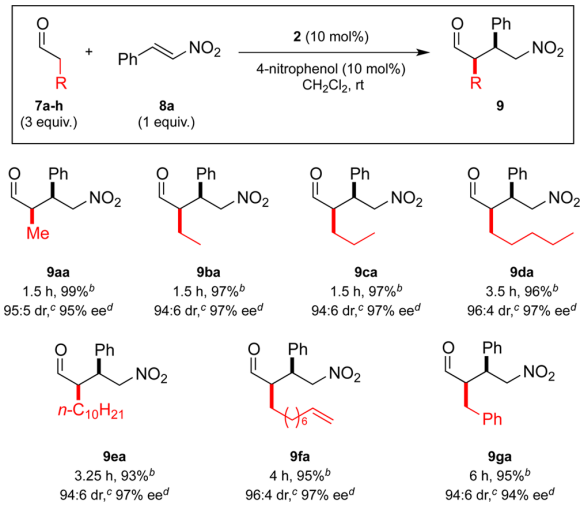

[a]General conditions: (*E*)-*β*-nitrostyrene (22.4 mg, 0.15 mmol), aldehyde (0.45 mmol), catalyst **2** (10 mol %), 4-nitrophenol (10 mol %) in 300 μL of CH_2Cl_2 at room temperature. [b]Isolated yield (%). [c]Diastereomeric ratio (dr) determined by ^{1}H NMR spectroscopy of the crude reaction mixture. [d]Determined by chiral HPLC analysis.

DOI: 10.1021/acscatal.5b01746
ACS Catal. 2015, 5, 6241–6248

Scheme 5. Scope of the Nitroalkene[a]

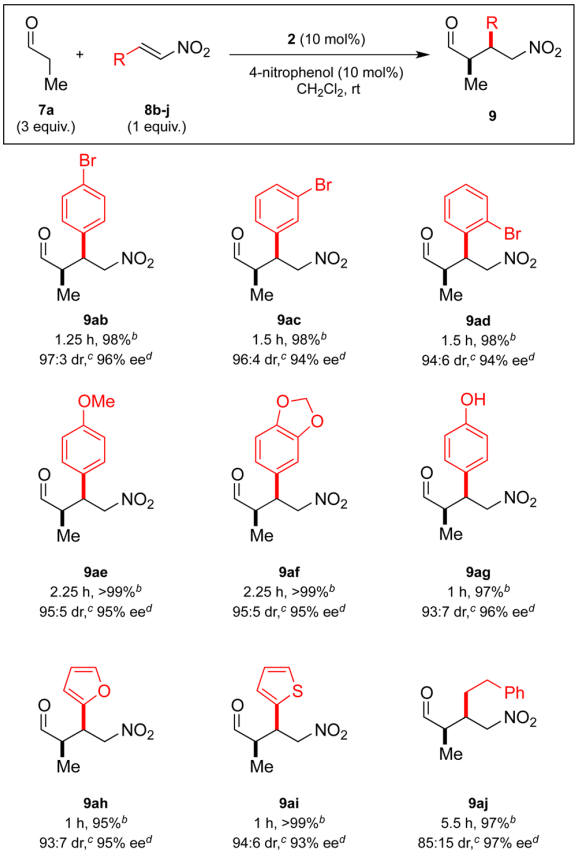

[a]General conditions: nitroalkene (0.15 mmol), propanal (33 μL, 0.45 mmol), catalyst **2** (10 mol %), 4-nitrophenol (10 mol %) in 300 μL of CH_2Cl_2 at room temperature. [b]Isolated yield (%). [c]Diastereomeric ratio (dr) determined by ^{1}H NMR spectroscopy of the crude reaction mixture. [d]Determined by chiral HPLC analysis (GC for **9ag**).

solvents while retaining 4-nitrophenol as an additive. In all cases, excellent diastereo- and enantioselectivities were recorded (up to 95:5 and 96%, respectively; see Table 3). Of the organic solvents investigated, CH_2Cl_2 proved to be beneficial in terms of reaction rate, leading to full conversions in less than 1.5 h (Table 3, entry 1). Use of toluene also led to efficient reactions (5 h, entry 2), whereas EtOAc and THF resulted in more sluggish processes (entries 3 and 4). To our delight, the reaction worked well in water (entry 5), affording the desired compound in only 1.5 h and with enantioselectivities that were comparable to those in CH_2Cl_2, irrespective of the low swelling ability of **2** in this solvent. Finally, lowering the catalyst loading to only 5 mol % was well tolerated, and the reaction reached completion in 5 h (entry 6).

An important conclusion of these studies is that immobilization of **1** (in polymer **2**) does not lead to any decrease in catalytic performance under the optimized set of reaction conditions. This being secured, the scope of the reaction was next studied. Initially, variation of the donor quickly revealed that a wide variety of aldehydes reacted smoothly with β-nitrostyrene (Scheme 4). This result sharply contrasts with a similar catalytic resin previously prepared in our group,[7a] which was extremely selective in the case of propanal.[25] Using catalyst **2**, linear aldehydes bearing longer alkyl chains gave rise to the corresponding Michael adducts in short reaction times with excellent enantioselectivities (**9aa**–**9fa**). In the case of 3-phenylpropionaldehyde, longer reaction times were required to drive the reaction to completion (**9ga**).

Variation of the nitroalkene partner was then investigated (Scheme 5). It was generally noted that using aromatic nitro olefins (**9ab**–**9ag**) led to short reaction times, regardless of the nature of the substituents (<2.5 h). Nitroalkenes with heterocyclic aromatic groups, such as the 2-furyl or 2-thienyl systems, proved to be excellent Michael acceptors for this reaction, providing the desired compounds in 1 h (**9ah**–**9ai**). Employing nitro olefins with an aliphatic side chain (adduct **9aj**) led to longer reaction times (5.5 h), and although the dr slightly decreased, high enantioselectivities were recorded (97%). The characteristically high yields obtained throughout (95–99%) are due to the simplified isolation procedure, made possible by the immobilization of the catalyst: filtration, washing with 0.1 M NaOH to remove the additive and evaporation rendered the pure products. Michael adduct **9ag** is the sole exception to this, in which the phenol-containing product had to be further purified by flash chromatography on silica gel.

To further establish the scope and limitations of the present methodology, catalytic reactions of more challenging substrates mediated by **2** were also examined (Scheme 6). To this end, we started with the β-branched donor isovaleraldehyde. Although the reaction proved to be sluggish, full conversions resulting in the formation of **9ha** were observed after 20 h using the standard conditions (10 mol % **2**, 10 mol % 4-nitrophenol). Whereas doubling the amount of additive had a remarkable effect on the reaction rate, the optimal results were obtained with 20 mol % catalyst loading in the presence of 20 mol % benzoic acid. Isovaleraldehyde was also found to react smoothly with both 2-bromo- and 4-bromonitrostyrene. After fine-tuning the reaction conditions, the desired products **9hb** and **9hc** were obtained in quantitative yield after simple extraction with 0.1 M NaOH or saturated $NaHCO_3$ without additional purification.

Scheme 6. Scope of α- and β-Branched Aldehydes[a]

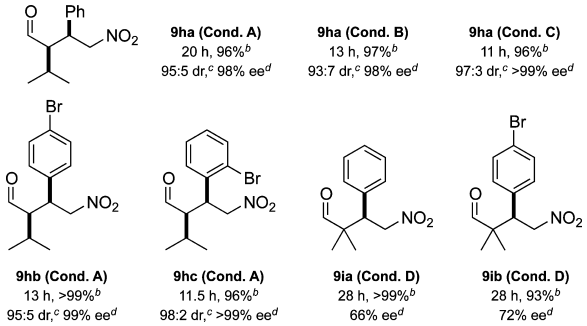

[a]Conditions A: nitroalkene (0.15 mmol), isovaleraldehyde (45 μL, 0.45 mmol), catalyst **2** (10 mol %), 4-nitrophenol (10 mol %) in 300 μL of CH_2Cl_2 at room temperature. Conditions B: 20 mol % of 4-nitrophenol. Conditions C: 20 mol % of **2** and 20 mol % PhCOOH. Conditions D (for α-branched aldehydes): nitroalkene (0.21 mmol), isobutyraldehyde (96 μL, 1.05 mmol), catalyst **2** (30 mol %), 4-nitrophenol (60 mol %) in 420 μL of CH_2Cl_2 at room temperature. [b]Isolated yield (%). [c]Diastereomeric ratio (dr) determined by ^{1}H NMR spectroscopy of the crude reaction mixture. [d]Determined by chiral HPLC analysis.

DOI: 10.1021/acscatal.5b01746
ACS Catal. 2015, 5, 6241–6248

As for α-branched aldehydes, it was found that isobutyraldehyde can be employed as the Michael donor with nitrostyrene and 4-bromonitrostyrene, giving rise to products **9ia** and **9ib**, respectively, which bear quaternary centers. Despite the severe steric hindrance of the corresponding trisubstituted enamine, full conversions were achieved after 28 h using 30 mol % catalyst and 60 mol % of 4-nitrophenol. Extraction with 0.1 M NaOH gave the Michael adducts in good yields, but with moderate enantioselectivities (66 and 72% ee, respectively). Unfortunately, trisubstituted nitroalkenes such as α-methylnitrostyrene or β-ethoxycarbonylnitrostyrene proved unreactive, even after 42 h with 20 mol % catalyst and 4-nitrophenol.

Having established the generality of the reaction, it was essential to demonstrate the stability of the catalytic resin **2** upon reuse. To that end, a standard reaction was successively run in the presence of 4-nitrophenol, and after each cycle, the mixture was simply filtered off and washed to remove all of the soluble materials. The remaining material **2** was then dried and used in the subsequent cycle. The filtrate was extracted with 0.1 M NaOH, and provided pure compound when full conversions were achieved. We were pleased to find that this polymer remained active for at least eight runs (Table 4), although some progressive loss of activity was observed in the last cycles. Despite this, even in the eighth run, the desired Michael adduct could be obtained in 68% isolated yield after 24 h. Importantly, the stereoselectivity remained constant throughout the whole process.

As outlined in the introduction, the major contributing factor to the deactivation of the Jørgensen–Hayashi catalyst (i.e., desilylation) is no longer a risk owing to the installation of the C–F unit. Consequently, the slow decay observed in reaction efficiency can be attributed to several factors, including mechanical degradation of the polymer or irreversible oxidation of reaction intermediates, as demonstrated by Zlotin et al.[26] On the basis of these precedents, a series of recycling experiments were carried out under glovebox conditions to study the effect of oxygen exclusion on catalyst stability. It was quickly noted that, after only a few reaction cycles in the glovebox, the catalytic activity decreased; however, performing another run with the same immobilized catalyst outside the glovebox immediately led to improved performance. This suggests that the absence of water results in sluggish reactions. Three additional recycling experiments were carried out to gain further insight into the factors responsible for catalyst deactivation: performing the reaction under a nitrogen atmosphere (oxygen exclusion with 0.5 and 2.0 equiv of water) and under air with 2.0 equiv of water; in these experiments, dry CH_2Cl_2 was used. The results indicate that trace amounts of water are beneficial for catalyst turnover, whereas oxygen is detrimental (Table 5).

These conditions that have allowed catalytic activity to be retained for longer periods of time were then translated into a

Table 4. Recycling Experiments[a]

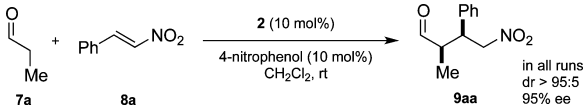

run	t (h)	conv[b] (%)	yield[c] (%)
1	1.5	100	99
2	2	100	98
3	2.5	100	97
4	4	100	98
5	6	100	97
6	12	84	83
7	24	100	97
8	24	70	68

[a]General conditions: (*E*)-β-nitrostyrene (41.0 mg, 0.275 mmol), propanal (60 μL, 0.83 mmol), catalyst **2** (10 mol %), additive (10 mol %) in 550 μL of CH_2Cl_2 at room temperature. [b]Conversion (%) and diastereomeric ratio (dr) determined by ^{1}H NMR spectroscopy of the crude reaction mixture. [c]Isolated yield (%).

Table 5. Recycling Experiments in the Presence of Water[a]

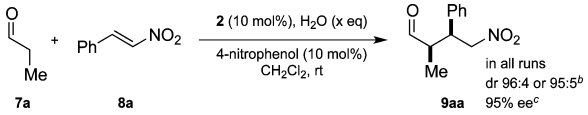

run	t (h)	conv[b] (%) (under N_2, 0.5 equiv H_2O)	conv[b] (%) (under N_2, 2.0 equiv H_2O)	conv[b] (%) (under air, 2.0 equiv H_2O)
1	1.5	100	100	93
2	2	94	96	89
3	2	79	81	80

[a]General procedure: (*E*)-β-nitrostyrene (41.0 mg, 0.275 mmol), propanal (60 μL, 0.83 mmol), catalyst **2** (10 mol %), additive (10 mol %) in 550 μL of CH_2Cl_2 at room temperature. [b]Conversion (%) and diastereomeric ratio (dr) determined by ^{1}H NMR spectroscopy of the crude reaction mixture. [c]Determined by chiral HPLC analysis.

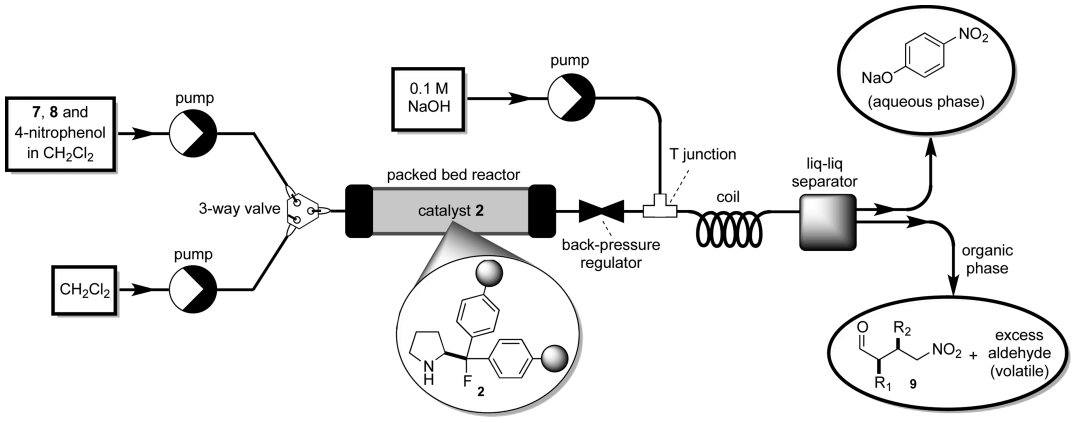

Figure 1. Continuous flow setup.

DOI: 10.1021/acscatal.5b01746
ACS Catal. 2015, 5, 6241–6248

Chapter III

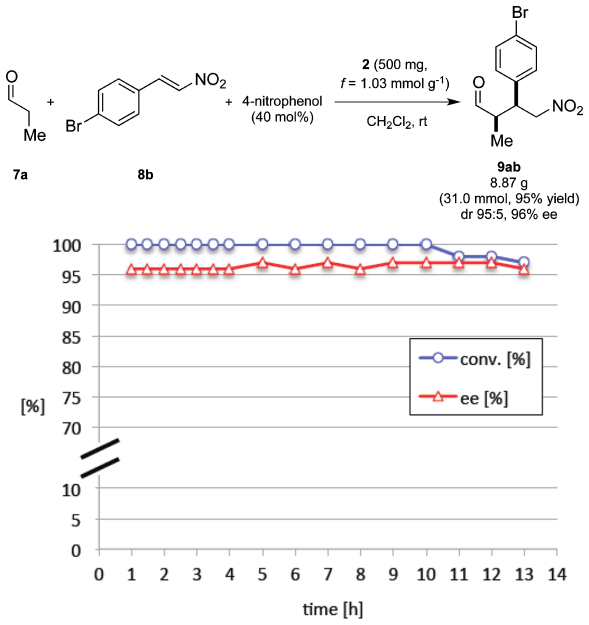

Figure 2. Continuous flow process for polymer-supported catalyst in the formation of **9ab**.

continuous flow process.[27] An overview of the setup used, in which 500 mg of resin **2** was packed in a glass column (1 cm diameter), is shown in Figure 1.

Upstream of the column, two channels were connected to a three-way valve that determined which one would feed the catalytic column. Dry, degassed CH_2Cl_2 was passed through the first channel, its purpose being to swell the resin prior to the reaction and also to rinse any remaining organic material from the column when the reagents have passed through. The second channel was fed with a solution of 4-bromonitrostyrene, propanal, and 4-nitrophenol in dry, degassed CH_2Cl_2 with 2.0 equiv of water.

Downstream, a back-pressure regulator was mounted to avoid bubble formation with volatile solvents such as CH_2Cl_2, and then further, a third pump with 0.1 M NaOH was assembled to allow for the aqueous workup and removal of 4-nitrophenol. The biphasic mixture was then separated in-line using a Zaiput liquid–liquid separator, which gave rise to a yellow aqueous phase (due to the presence of 4-nitrophenolate) and an organic phase with the desired Michael adduct and excess aldehyde (plus remaining nitrostyrene if the conversions were not complete). In most cases, simply evaporating the organic outstream furnished pure product where no further purification was necessary.

Using this setup, full conversions were obtained during the first 10 h running the flow process at 100 μL min^{-1} (Figure 2).

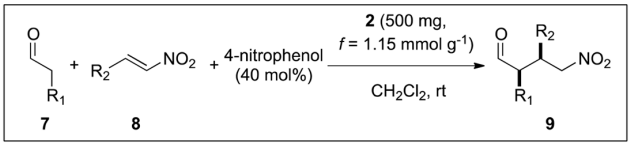

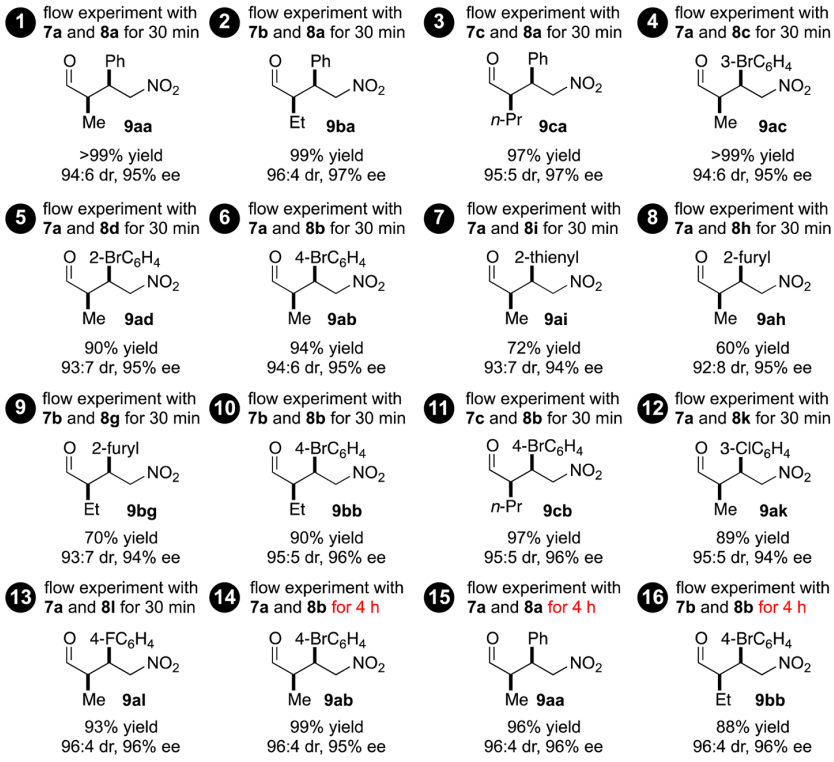

Figure 3. Continuous flow process with polymer-supported catalyst **2** applied to the preparation of a compound library.

DOI: 10.1021/acscatal.5b01746
ACS Catal. 2015, 5, 6241–6248

Over the following 3 h, a slight decrease in conversion was observed, but remained above 97%. Overall, the desired Michael adduct was obtained in 95% yield, and the effective catalyst loading for the whole operation period was determined to be 1.6%; this corresponds to an overall turnover number (TON) slightly above 60. The turnover frequency (TOF) remained essentially constant at 4.6 h^{-1} over the considered 13 h operation period.

The importance of correctly handling the packed catalyst columns is illustrated by the following fact: when a still fully active column used in a flow experiment was dried, stored in contact with the atmosphere, and then attempted to recycle after reswelling, it was found that catalytic activity was lost to a high degree. This behavior can be easily understood when the conditions of use of the catalytic column in-flow are considered. Because an excess of aldehyde reactant is employed, when flow is arrested, most of the active sites in the column will be in the active, enamine form. If the column is then dried and allowed to be in contact with air, oxidation of the labile enamine units[26] will lead to irreversible deactivation. As shown below, simply keeping the catalytic column wet with dichloromethane when not in use efficiently suppresses this problem.

The possibility of using this continuous flow setup to generate a library of compounds was then explored. With a new batch of catalyst, a similar flow process was run with different reagent combinations. Each pair of starting materials was circulated through the system for 30 min, rinsing with solvent for 1 h afterward. At the end of each day and to avoid catalyst deactivation, CH_2Cl_2 was passed at a rate of 25 μL min^{-1} before continuing the flow experiments the next day. Eight different combinations were run the first day, and five more, the second. On the third day, the first three examples were rerun for 4 h each, thus demonstrating that the catalytic activity was retained after several changes of substrates and an extended operation time. The compounds synthesized and the results obtained during the generation of this library are summarized in Figure 3. In total, 16 consecutive runs were carried out, with high yields and stereoselectivities observed in all cases. Remarkably, the last run produced the desired Michael adduct in 90% conversion, thus demonstrating the robustness of the catalyst. The overall TON for this set of experiments was 72.

To demonstrate the synthetic utility of the process, two different Michael adducts were further derivatized to the corresponding 3,4-disubstituted pyrrolidines **10** by a one-pot operation involving reduction of the nitro group and reductive amination of the corresponding amino aldehyde[28] (Scheme 7). The process was carried out on a gram scale, and the corresponding products were transformed into the *N*-tosylated derivatives **11** before determining the optical purity. Excellent yields were obtained in both reactions for the two Michael adducts tested.

Scheme 7. Derivatization of the Adducts 9aa and 9ab to Pyrrolidines 10

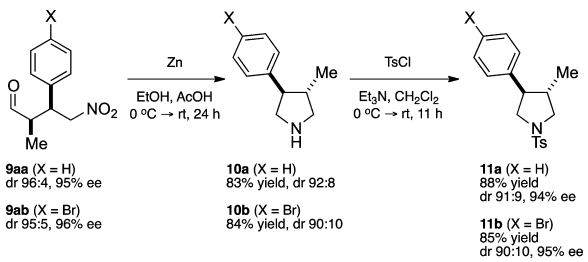

3. CONCLUSIONS

In summary, an immobilized analog of the fluorinated amino-catalyst **1** has been developed and showcased in a model transformation. Key to the success of this approach has been a polymer design that does not affect the active site in **1** and, hence, maintains its catalytic performance. The catalytic resin **2** shows great potential for the Michael addition of aldehydes to nitroalkenes in batch and flow: this is the first example of this catalytic system in enamine activation. Catalyst deactivation studies have delineated the conditions responsible for degradation, thus allowing the process to be streamlined to extend the lifespan of the catalyst. Applying this resin in a carefully designed continuous flow setup has allowed for the facile isolation of the desired Michael adducts without chromatographic purification. This catalyst system has proved to be extremely active, both in experiments that were run for extended periods of time and in the preparation of a complex library of analogs. Importantly, the immobilized system shows activity comparable with that of the batch process. This, together with the stability profile of this novel polymer-supported catalyst, is a powerful endorsement for the use of flow chemistry as an enabling synthesis technology. Application of this catalytic resin to other synthetically valuable transformations is in progress and will be reported in due course.

■ ASSOCIATED CONTENT

Supporting Information

The Supporting Information is available free of charge on the ACS Publications website at DOI: 10.1021/acscatal.5b01746.

Experimental procedures, compound and polymer characterization, NMR spectra and HPLC chromatograms (PDF)

■ AUTHOR INFORMATION

Corresponding Authors

*E-mail: ryan.gilmour@uni-muenster.de.
*E-mail: mapericas@iciq.es.

Notes

The authors declare no competing financial interest.

■ ACKNOWLEDGMENTS

Financial support from the Institute of Chemical Research of Catalonia (ICIQ) Foundation, MINECO (Grant CTQ2012-38594-C02-01), and DEC Generalitat de Catalunya (Grant 2014SGR827) is gratefully acknowledged. We also thank MINECO for support through Severo Ochoa Excellence Accreditation 2014−2018 (SEV-2013-0319). C.R.-E. thanks the AGAUR (Generalitat de Catalunya) for a Beatriu de Pinós B fellowship. R.G. and I.G.M. thank the WWU Münster, and the Deutsche Forschungsgemeinschaft (SFB 858 and DFG EXC 1003 "Cells in Motion − Cluster of Excellence", Münster) for generous financial support.

■ REFERENCES

(1) (a) Wiles, C.; Watts, P. *Green Chem.* **2014**, *16*, 55. (b) Vaccaro, L.; Lanari, D.; Marrocchi, A.; Strappaveccia, G. *Green Chem.* **2014**, *16*, 3680.
(2) List, B.; Lerner, R. A.; Barbas, C. F., III *J. Am. Chem. Soc.* **2000**, *122*, 2395.

DOI: 10.1021/acscatal.5b01746
ACS Catal. 2015, 5, 6241−6248

Chapter III

(3) Ahrendt, K. A.; Borths, C. J.; MacMillan, D. W. C. *J. Am. Chem. Soc.* **2000**, *122*, 4243.
(4) (a) Mukherjee, S.; Yang, J. W.; Hoffmann, S.; List, B. *Chem. Rev.* **2007**, *107*, 5471. (b) Melchiorre, P.; Marigo, M.; Carlone, A.; Bartoli, G. *Angew. Chem., Int. Ed.* **2008**, *47*, 6138. (c) Bertelsen, S.; Jørgensen, K. A. *Chem. Soc. Rev.* **2009**, *38*, 2178.
(5) For the pioneering reports, see: (a) Marigo, M.; Wabnitz, T. C.; Fielenbach, D.; Jørgensen, K. A. *Angew. Chem., Int. Ed.* **2005**, *44*, 794. (b) Hayashi, Y.; Gotoh, H.; Hayashi, T.; Shoji, M. *Angew. Chem., Int. Ed.* **2005**, *44*, 4212. (c) For a recent review, see: Jensen, K. L.; Dickmeiss, G.; Jiang, H.; Albrecht, Ł.; Jørgensen, K. A. *Acc. Chem. Res.* **2012**, *45*, 248.
(6) For selected examples, see: (a) Li, Y.; Liu, X.-Y.; Zhao, G. *Tetrahedron: Asymmetry* **2006**, *17*, 2034. (b) Maltsev, O. V.; Kucherenko, A. S.; Zlotin, S. G. *Eur. J. Org. Chem.* **2009**, *2009*, 5134. (c) Wang, B. G.; Ma, B. C.; Wang, Q.; Wang, W. *Adv. Synth. Catal.* **2010**, *352*, 2923. (d) Kristensen, T. E.; Vestli, K.; Jakobsen, M. G.; Hansen, F. K.; Hansen, T. *J. Org. Chem.* **2010**, *75*, 1620. (e) Mager, I.; Zeitler, K. *Org. Lett.* **2010**, *12*, 1480. (f) Wang, C. A.; Zhang, Z. K.; Yue, T.; Sun, Y. L.; Wang, L.; Wang, W. D.; Zhang, Y.; Liu, C.; Wang, W. *Chem. - Eur. J.* **2012**, *18*, 6718. (g) Keller, M.; Perrier, A.; Linhardt, R.; Travers, L.; Wittmann, S.; Caminade, A.-M.; Majoral, J.-P.; Reiser, O.; Ouali, A. *Adv. Synth. Catal.* **2013**, *355*, 1748. (h) Zheng, W.; Lu, C.; Yang, G.; Chen, Z.; Nie, J. *Catal. Commun.* **2015**, *62*, 34.
(7) (a) Alza, E.; Pericàs, M. A. *Adv. Synth. Catal.* **2009**, *351*, 3051. (b) Alza, E.; Sayalero, S.; Kasaplar, P.; Almaşi, D.; Pericàs, M. A. *Chem. - Eur. J.* **2011**, *17*, 11585. (c) Riente, P.; Mendoza, C.; Pericàs, M. A. *J. Mater. Chem.* **2011**, *21*, 7350. (d) Fan, X.; Sayalero, S.; Pericàs, M. A. *Adv. Synth. Catal.* **2012**, *354*, 2971. (e) Fan, X.; Rodríguez-Escrich, C.; Sayalero, S.; Pericàs, M. A. *Chem. - Eur. J.* **2013**, *19*, 10814.
(8) For recent reviews on asymmetric organocatalysis in continuous flow, see: (a) Rodríguez-Escrich, C.; Pericàs, M. A. *Eur. J. Org. Chem.* **2015**, *2015*, 1173. (b) Atodiresei, I.; Vila, C.; Rueping, M. *ACS Catal.* **2015**, *5*, 1972. (c) Munirathinam, R.; Huskens, J.; Verboom, W. *Adv. Synth. Catal.* **2015**, *357*, 1093. (d) Zhao, D.; Ding, K. *ACS Catal.* **2013**, *3*, 928. (e) Tsubogo, T.; Ishiwata, T.; Kobayashi, S. *Angew. Chem., Int. Ed.* **2013**, *52*, 6590. (f) Puglisi, A.; Benaglia, M.; Chiroli, V. *Green Chem.* **2013**, *15*, 1790.
(9) (a) Haindl, M. H.; Schmid, M. B.; Zeitler, K.; Gschwind, R. M. *RSC Adv.* **2012**, *2*, 5941. (b) Holland, M. C.; Gilmour, R. *Angew. Chem., Int. Ed.* **2015**, *54*, 3862.
(10) For the homogeneous catalyst, see: Chi, Y.; Gellman, S. H. *Org. Lett.* **2005**, *7*, 4253.
(11) O'Hagan, D.; Royer, F.; Tavasli, M. *Tetrahedron: Asymmetry* **2000**, *11*, 2033.
(12) (a) Sparr, C.; Schweizer, W. B.; Senn, H. M.; Gilmour, R. *Angew. Chem., Int. Ed.* **2009**, *48*, 3065. (b) For a related precedent, see: Ho, C.-Y.; Chen, Y.-C.; Wong, M.-K.; Yang, D. *J. Org. Chem.* **2005**, *70*, 898.
(13) Hunter, L. *Beilstein J. Org. Chem.* **2010**, *6*, 38. (b) Zimmer, L. E.; Sparr, C.; Gilmour, R. *Angew. Chem., Int. Ed.* **2011**, *50*, 11860.
(14) Tanzer, E.-M.; Zimmer, L. E.; Schweizer, W. B.; Gilmour, R. *Chem. - Eur. J.* **2012**, *18*, 11334.
(15) Molnár, I. G.; Tanzer, E.-M.; Daniliuc, C.; Gilmour, R. *Chem. - Eur. J.* **2014**, *20*, 794.
(16) Alemán, J.; Fraile, A.; Marzo, L.; García Ruano, J. L.; Izquierdo, C.; Díaz-Tendero, S. *Adv. Synth. Catal.* **2012**, *354*, 1665.
(17) (a) Confalone, P. N.; Huie, E. M.; Ko, S. S.; Cole, G. M. *J. Org. Chem.* **1988**, *53*, 482. (b) Matoba, K.; Yonemoto, H.; Fukui, M.; Yamazaki, T. *Chem. Pharm. Bull.* **1984**, *32*, 3918.
(18) Price, M. D.; Kurth, M. J.; Schore, N. E. *J. Org. Chem.* **2002**, *67*, 7769.
(19) Degni, S.; Wilén, C.-E.; Leino, R. *Org. Lett.* **2001**, *3*, 2551.
(20) Sparr, C.; Tanzer, E.-M.; Bachmann, J.; Gilmour, R. *Synthesis* **2010**, *42*, 1394.
(21) Itsuno, S.; Watanabe, K.; Koizumi, T.; Ito, K. *React. Polym.* **1995**, *24*, 219.
(22) For the pioneering reports of organocatalytic asymmetric addition of aldehydes to nitroalkenes, see: (a) List, B.; Pojarliev, P.; Martin, H. J. *Org. Lett.* **2001**, *3*, 2423. (b) Betancort, J. M.; Barbas, C. F., III *Org. Lett.* **2001**, *3*, 3737.
(23) For studies on the role of acidic additives and the general mechanism of diarylprolinol derivatives-catalyzed Michael addition, see: (a) Patora-Komisarska, K.; Benohoud, M.; Ishikawa, H.; Seebach, D.; Hayashi, Y. *Helv. Chim. Acta* **2011**, *94*, 719. (b) Burés, J.; Armstrong, A.; Blackmond, D. G. *J. Am. Chem. Soc.* **2011**, *133*, 8822. (c) Burés, J.; Armstrong, A.; Blackmond, D. G. *J. Am. Chem. Soc.* **2012**, *134*, 6741. (d) Sahoo, G.; Rahaman, H.; Madarász, A.; Pápai, I.; Melarto, M.; Valkonen, A.; Pihko, P. M. *Angew. Chem., Int. Ed.* **2012**, *51*, 13144. (e) Moberg, C. *Angew. Chem., Int. Ed.* **2013**, *52*, 2160.
(24) *CRC Handbook of Chemistry and Physics*, 95th ed.; Haynes, W. M., Ed.; CRC Press/Taylor and Francis Group: Boca Raton, FL, 2014−2015; section 5, pp 94−103.
(25) In that case (see ref 7a), using a silylated diarylprolinol derivative, sterics were crucial for the success of the reaction: propanal would react, but linear aldehydes with a longer chain turned out to be much slower, whereas *β*-branched substrates did not react at all.
(26) Maltsev, O. V.; Chizhov, A. O.; Zlotin, S. G. *Chem. - Eur. J.* **2011**, *17*, 6109.
(27) For some examples of the use of solid-supported catalysts in continuous-flow Michael addition of aldehydes to nitroalkenes, see: (a) Ötvös, S. B.; Mándity, I. M.; Fülöp, F. *ChemSusChem* **2012**, *5*, 266. (b) Arakawa, Y.; Wennemers, H. *ChemSusChem* **2013**, *6*, 242. (c) Porta, R.; Benaglia, M.; Coccia, F.; Cozzi, F.; Puglisi, A. *Adv. Synth. Catal.* **2015**, *357*, 377.
(28) Kano, T.; Sugimoto, H.; Tokuda, O.; Maruoka, K. *Chem. Commun.* **2013**, *49*, 7028.

DOI: 10.1021/acscatal.5b01746
ACS Catal. 2015, 5, 6241−6248

3.7. Conclusions and Outlook.

In summary, we have developed the efficient immobilized fluorinated aminocatalyst **III.12** for the asymmetric Michael addition of aldehydes to nitroolefins as a model transformation in the batch and flow application. This transformation is the first example of this catalytic system in enamine activation.

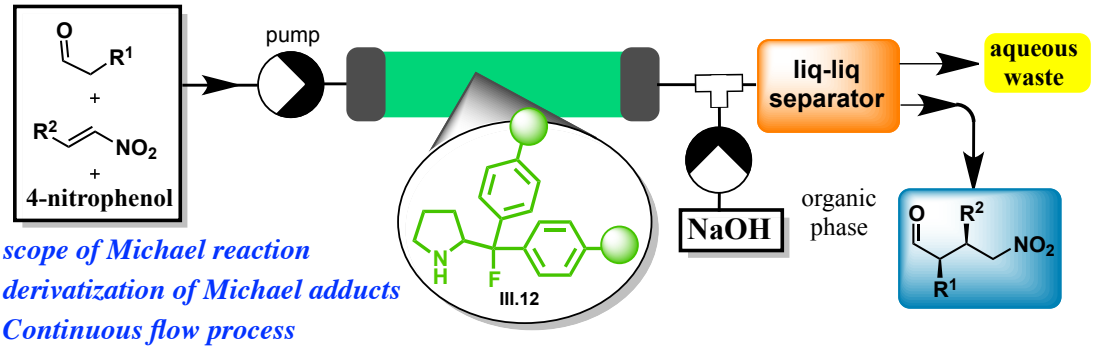

- *scope of Michael reaction*
- *derivatization of Michael adducts*
- *Continuous flow process*
- *Work-up in-line*
- *Library of analogues in flow (13 combinations, 94-97% ee)*

The key to the success of this approach has been the strategic replacement of the labile silyl ether for a fluorine substituent in the β-position of the aminocatalyst. This has provided high selectivity thanks to the conformational *gauche* effect of fluorine group.

Deactivation studies have been done for this transformation in order to increase the lifespan of the catalyst. Application of this catalyst in carefully designed continuous flow processes has allowed the easy isolation of the desired Michael adducts without chromatographic purification. In addition, these substrates were applied to the formation of 3,4-disubstituted pyrrolidines.

This β-fluorinated organocatalyst has been highly effective in the asymmetric Michael reaction of aldehydes to nitroalkenes in flow, providing the same behavior as in batch conditions. In general, this catalytic system showed high potential and stability in continuous flow.

In comparison to the literature, considerable improvement has been achieved in the stability of the catalytic system in comparison with polymer-supported silyl ester catalyst. This carefully designed catalyst can be used in continuous flow applications in order to produce desired compound in large scale. Moreover, a library of analogues can be prepared in an efficient manner with this catalytic system.

The application of this immobilized catalyst in continuous flow applications has been demonstrated and future applications will be further studied.

UNIVERSITAT ROVIRA I VIRGILI
NEW APPROACHES TO CATALYST DESIGN AND IMMOBILIZATION
Irina Sagamanova

Supporting Information for:

Translating the Enantioselective Michael Reaction to a Continuous Flow Paradigm with an Immobilized, Fluorinated Organocatalyst

Irina Sagamanova,[a] Carles Rodríguez-Escrich,[a] István Gábor Molnár,[c] Sonia Sayalero,[a] Ryan Gilmour[c,d] and Miquel A. Pericàs[a,b]**

a) Institute of Chemical Research of Catalonia (ICIQ), Av. Països Catalans 16, 43007 Tarragona (Spain).
b) Departament de Química Orgànica, Universitat de Barcelona, 08080 Barcelona (Spain).
c) Institut für Organische Chemie, Westfälische Wilhelms-Universität Münster, Corrensstrasse 40, 48149 Münster (Germany).
d) Excellence Cluster EXC 1003 "*Cells in Motion*". Westfälische Wilhelms-Universität Münster, Münster (Germany).

ryan.gilmour@uni-muenster.de; mapericas@iciq.es

Chapter III

1. General Remarks

Unless otherwise stated, all commercial reagents were used as received and all reactions were carried out directly under open air. Flash chromatography separations were carried out using 60-mesh silica gel and dry-packed columns. Thin layer chromatography was carried out using Merck TLC Silicagel 60 F254 aluminium sheets. Components were visualized by UV light (λ = 254 nm) or by staining with phosphomolybdic acid (PMA) solution. NMR spectra were registered in a Bruker Advance Ultrashield spectrometers in $CDCl_3$ at room temperature or DMSO at 373 K, operating at 400 or 500 MHz for ^{1}H, 101 or 126 MHz for $^{13}C\{1H\}$ and 136 MHz for ^{19}F. TMS was used as internal standard for ^{1}H NMR and $CDCl_3$ for ^{13}C NMR. IR spectra were recorded on a Bruker Tensor 27 FT-IR spectrometer. FAB mass spectra were obtained on a FisonsV6- Quattro instrument, ESI mass spectra were obtained on a Waters LCT Premier instrument and CI and EI spectra were obtained on a Waters GCT spectrometer. Elemental analyses CHN of the PS-resins were performed on a Thermo FlashEA 1112 elemental analyzer and F on the Metrohm761 Compact Ion Chromatograph (IC) at MedacLtd, United Kingdom. High performance liquid chromatography (HPLC) was performed on an Agilent Technologies chromatograph (1100 Series), using the specified Daicel chiral column and guard columns. Racemic standard products were prepared using DL-proline as catalyst according to reported procedures in order to establish HPLC conditions. The absolute configuration of the reaction products was confirmed by HPLC, by comparison with reported data.

Specific optical rotation measurement was carried out on a polarimeter equipped with a PMT detector using the Sodium line at 589 nm.

Environmental Scanning Electron Microscopy (ESEM) was performed on an FEI Quanta 600 scanning microscope at the Microscopy Unit of the Universitat Rovira i Virgili, Spain.

The aldehydes were distilled before use. *N*-Boc-L-proline methyl ester,[1] starting nitroalkenes[2] such as *trans*-4-bromo-β-nitrostyrene, (*E*)-2-(2-nitrovinyl)thiophene, (*E*)-2-(2-nitrovinyl) furan, (*E*)-(4-nitrobut-3-en-1-yl)benzene were synthesized according to the literature procedures.

2. Preparation of the polymer-supported pyrrolidine 2

(*S*)-bis(4-Vinylphenyl)prolinol *tert*-butyl carbamate (5)

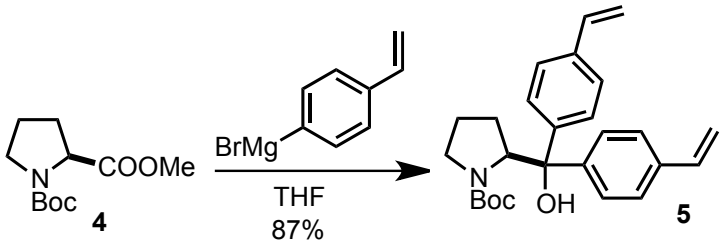

Magnesium turnings (1.23 g, 50.6 mmol) and a spatula tip of I_2 were added to a dry, 250-ml, two-necked round-bottom flask fitted with a reflux condenser and it was flame dried under nitrogen. After that, a solution of 4-bromostyrene (6.30 mL, 48.2 mmol) in 35 mL of THF was added dropwise during 10 min. Once the addition was complete, the mixture was stirred for 40 min. Then it was cooled to –5 °C and a solution of *N*-Boc-L-proline methyl ester (3.76 g, 15.09 mmol) in 25 mL of THF was added. The reaction mixture was stirred at room temperature overnight and then 20 mL of saturated aqueous NH_4Cl were added, followed by addition of 150 mL of water and extraction with Et_2O (3 × 70 mL). The combined organic layers were dried over anhydrous $MgSO_4$. After solvent removal, the crude product was purified by silica gel column chromatography with cyclohexane/EtOAc 95:5 as the eluent to afford alcohol **5**[3] as a white solid in 87% yield (5.35 g, 13.19 mmol).

^{1}H NMR (500 MHz, $CDCl_3$): δ 7.35 (bs, 4H), 7.34 (bs, 4H), 6.72 (dd, *J* = 10.9, 17.6 Hz, 1H), 6.71 (dd, *J* = 10.9, 17.6 Hz, 1H), 5.76 (dd, *J* = 1.0, 17.6 Hz, 1H), 5.74 (dd, *J* = 1.0, 17.6 Hz, 1H), 5.24 (dd, *J* = 1.0, 10.9 Hz, 1H), 5.24 (dd, *J* = 1.0, 10.9 Hz, 1H), 4.88 (dd, *J* = 3.6, 9.0 Hz, 1H), 3.35 (bs, 1H), 2.88 (bs, 1H), 2.10 (dq, *J* = 8.8, 13.4 Hz, 1H), 1.91 (ddt, *J* = 4.2, 8.1, 13.0 Hz, 1H), 1.47 (bs, 1H), 1.47 (bs, 1H), 1.44 (s, 9H), 0.85 (bs, 1H).

^{13}C NMR (126 MHz, $CDCl_3$): δ 146.10, 143.6, 136.7, 136.6, 136.5, 136.4, 128.5 (×2), 128.0 (×2), 125.9 (×2), 125.4 (×2), 114.0, 113.8, 81.7, 80.8, 65.8, 48.0, 29.8, 28.5 (×3), 23.2.

(*S*)-bis(4-Vinylphenyl)prolinol (6)

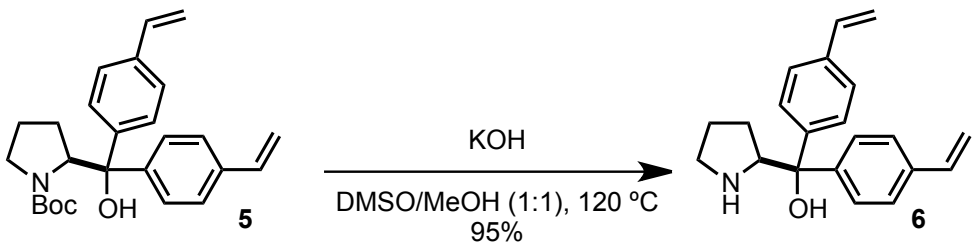

A 250-ml round-bottom flask was charged with **5** (5.30 g, 13.07 mmol), KOH (7.33 g, 0.131 mol), 87 mL MeOH and 87 mL DMSO. The solution was heated at 120 °C for 30 h. Then, crushed ice was carefully added to the solution and it was extracted with EtOAc (3 × 70 mL). The combined organic extracts were dried under $MgSO_4$ and the residue obtained after evaporation was purified by flash column chromatography (eluent DCM/MeOH from 99:1 to 95:5) to furnish amino alcohol **6**[3] as a white solid in 95% yield (3.78 g, 12.38 mmol).

^{1}H NMR (500 MHz, $CDCl_3$): δ 7.54-7.51 (m, 2H), 7.48-7.43 (m, 2H), 7.36-7.31 (m, 4H), 6.67 (dd, *J* = 10.9, 17.6, 1H), 6.66 (dd, *J* = 10.9, 17.6, 1H), 5.693 (dd, *J* = 0.9, 17.6 Hz, 1H), 5.688 (dd, *J* = 0.9, 17.6 Hz, 1H), 5.20 (dd, *J* = 0.9, 10.9 Hz, 1H), 5.19 (dd, *J* = 0.9, 10.9 Hz, 1H), 4.24 (t, *J* = 7.7 Hz, 1H), 3.04 (ddd, *J* = 4.9, 6.7, 9.3 Hz, 1H), 3.0 (dt, *J* = 7.5, 9.3 Hz, 1H), 1.80-1.52 (m, 5H).

^{13}C NMR (126 MHz, $CDCl_3$): δ 147.9, 145.1, 136.7, 136.5, 136.0, 135.8, 126.3 (×2), 126.1(×2), 126.0 (×2), 125.8 (×2), 113.7, 113.5, 77.2, 64.5, 46.9, 26.4, 25.6.

(*S*)-2-(Fluoro-bis(4-vinylphenyl)methyl)pyrrolidine (3)

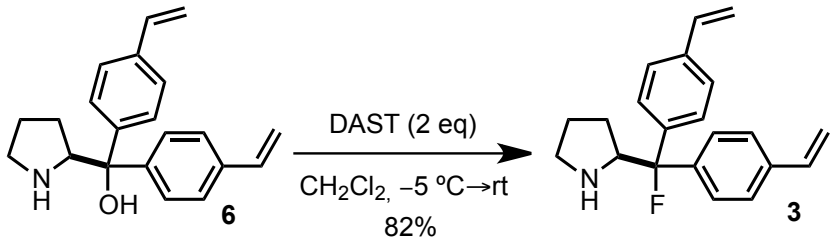

A 250 mL round-bottom flask was charged with compound **6** (1.05 g, 3.44 mmol), purged with nitrogen and dry DCM (78 mL) was added. The solution was cooled to –5 °C and DAST (0.9 mL, 6.88 mmol) was added dropwise. The reaction was gradually warmed to rt over a period of 10 h and quenched with sat. aq. $NaHCO_3$ (60 mL). The layers were separated and the aqueous phase was back-extracted with CH_2Cl_2 (3 × 20 mL). The combined organic phases were dried under $MgSO_4$ and concentrated in vacuum. The residue was purified by silica gel column chromatography (SiO_2 with 2.5% Et_3N; eluent from DCM to DCM/MeOH 95:5) to afford **3** as a yellow oil (867 mg, 2.82 mmol, 82 % yield).

IR (ATR): ν = 3276, 2943,1628, 1509, 1402, 991, 913, 828, 729, 517 cm^{-1}.

$[\alpha]_D^{25}$ (CH_2Cl_2, *c* 0.1) +106.2

^{1}H NMR (500 MHz, $CDCl_3$): δ 7.53-7.46 (m, 2H), 7.41-7-7.34 (m, 6H, C_6H_5), 6.680 (dd, *J* = 17.6, 10.9 Hz, 1H), 6.676 (dd, *J* = 10.9, 17.6 Hz, 1H), 5.723 (dd, J = 0.9, 17.6 Hz, 1H), 5.721 (d, J = 0.9, 17.6 Hz, 1H), 5.230 (dd, *J* = 0.9, 10.9 Hz, 1H), 5.234 (dd, *J* = 0.9, 10.9 Hz, 1H), 4.21-4.11 (m, 1H), 3.10-3.05 (m, 1H), 2.90-2.84 (m, 1H), 1.88 (bs, 1H), 1.82-1.66 (m, 4H).

^{13}C NMR (126 MHz, $CDCl_3$): δ 142.5 (d, *J* = 23.7 Hz), 142.1 (d, *J* = 24.3 Hz), 137.0 (d, *J* = 1.5 Hz), 136.8 (d, *J* = 1.4 Hz), 136.4, 136.3, 126.4 (×2), 126.2 (×2, d, J = 1.3 Hz), 125.9 (×2, d, *J* = 8.9 Hz), 125.2 (×2, d, *J* = 9.0 Hz), 114.3 (×2), 100.2 (d, *J* = 182.5 Hz), 64.5 (d, *J* = 22.1 Hz), 47.6, 26.6 (d, *J* = 3.4 Hz), 26.1.

^{19}F NMR (376 MHz, $CDCl_3$): δ = –169.8 (d, $^3J_{H,F}$ = 27.6 Hz).

HRMS (ESI) Calculated mass for $C_{21}H_{22}FN$ $[M+H]^+$ 308.1809, found 308.1799.

Polystyrene-supported (*S*)-2-(fluorodiphenylmethyl)pyrrolidine (2)

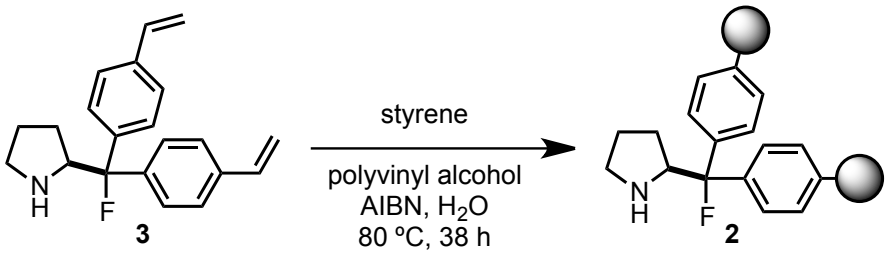

Milli-Q water (65 mL) was degassed under a stream of nitrogen during 3 h and polyvinyl alcohol (63 mg, 0.6 μmol PvOH, MW 104500) was added. The mixture was dissolved upon heating this suspension at 80 °C during 4 h. After cooling the solution to 20 °C, sequential addition of monomer **3** (923 mg, 3.0 mmol) in 0.8 mL of toluene and styrene (3.5 mL, 30.3 mmol) with AIBN (35 mg, 0.21 mmol) in 0.5 mL of toluene was carried out. After that, the mixture was stirred for 30 min at 20 °C.

The temperature was then raised to 80 °C and the reaction mixture was stirred vigorously for 38 h at 600 rpm. The resulting polymer beads were filtered and washed with hot water (50 °C) several times, then with methanol, THF and CH_2Cl_2, followed by drying under reduced pressure at 40 °C, which afforded the desired cross-linked chiral polymer (1.95 g, 67% incorporation of monomer according to elemental analysis).

Elemental analysis for the first batch: %C, 85.60; %H, 7.33; %N, 1.45; %F, 1.02.

According to the nitrogen value in the EA, the functionalization level was 1.03 mmol g^{-1}

Elemental analysis for the second batch: %C, 87.42; %H, 7.55; %N, 1.13; %F, 1.29.

According to the nitrogen value in the EA, the functionalization level was 0.807 mmol g^{-1}

Elemental analysis for the third batch: %C, 84.85; %H, 7.19; %N, 1.61; %F, 1.78.

According to the nitrogen value in the EA, the functionalization level was 1.115 mmol g^{-1}

Chapter III

The polymer was characterized by IR, EDX and ESEM-spectroscopy, all batches giving similar results.

The EDX spectrum reveals the presence of C, F and N at the polymer surface.

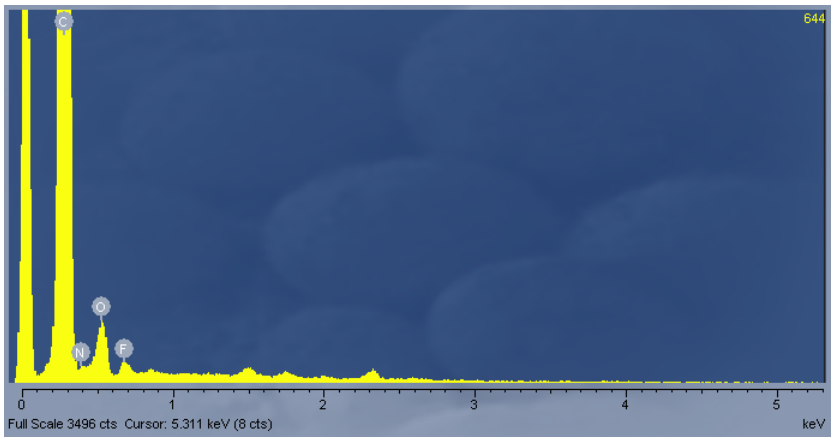

IR (ATR): ν = 3083, 3059, 3024, 2919, 2850, 1629, 1601, 1492, 1450, 1182, 987, 905, 826, 755, 697, 541 cm^{-1}.

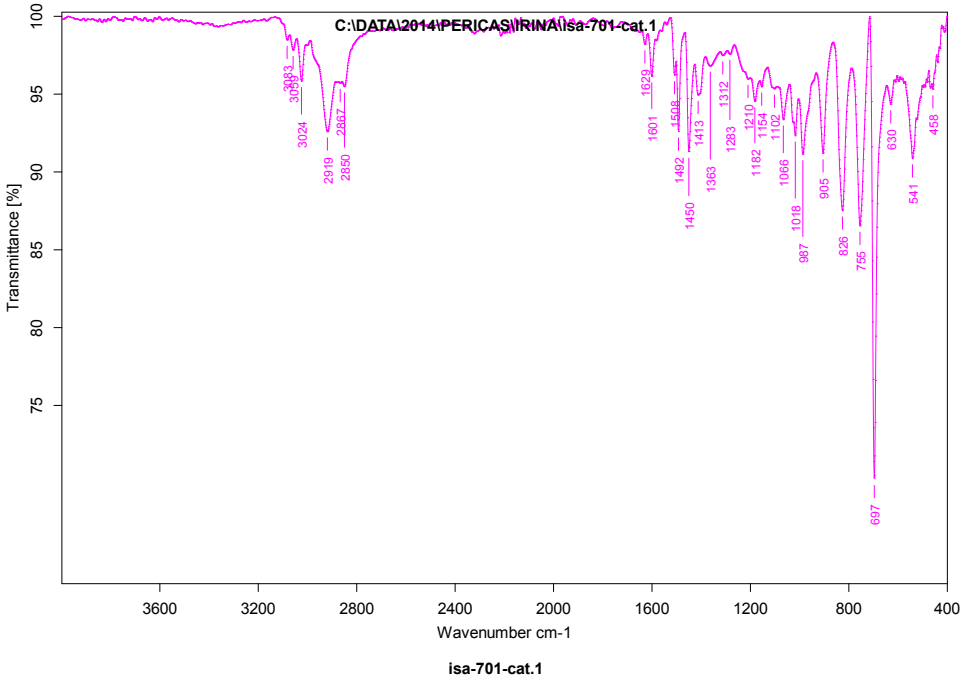

RAMAN: ν = 3057, 2908, 1629, 1602, 1582, 1149, 1322, 1182, 1030, 1001, 795, 621, 229.

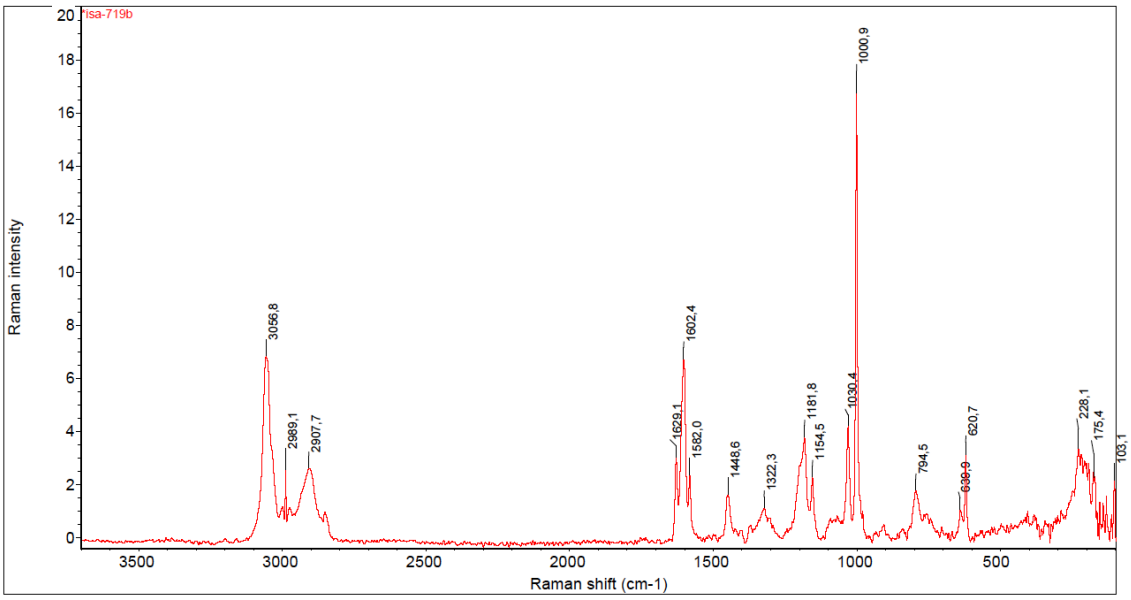

ESEM images for catalyst 2

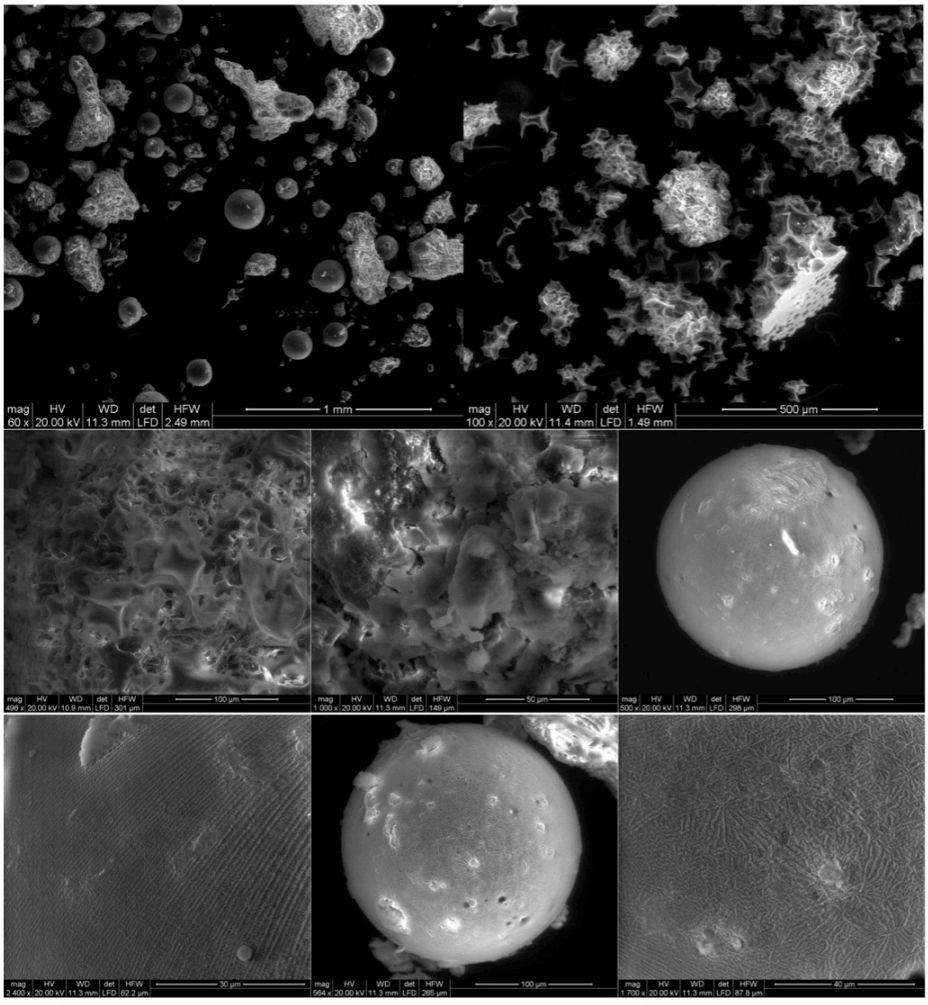

Solvent uptake tests for polymer 2

Uptake data for each solvent were determined gravimetrically and expressed as grams of solvent per grams of dry polymer.[4] Polymer (60-65 mg) was weighed into a tared 0.5 mL eppendorf tube and solvent (0.3 mL) was added. The eppendorf tubes were then closed and shaken for 3 h to ensure equilibrium was attained. After centrifugation (30 min at 4000 rpm) a syringe was used to remove excess solvent and the eppendorf tube with the swollen polymer was immediately weighed to obtain the weight of solvent absorbed.

Solvent uptake results

Entry	Solvent	Solvent uptake [$g_{solv}\ g_{pol}^{-1}$][a]	Solvent uptake [$mL_{solv}\ g_{pol}^{-1}$][b]
1	CH_2Cl_2	3.40	2.6
2	toluene	0.94	1.1
3	H_2O	0.51	0.5

[a] Solvent uptake data for polymer **2** as determined by gravimetry and expressed as grams of adsorbed solvent per grams of dry polymer; solvent uptake = (swollen mass – dry mass)/dry mass. [b] Provided in order to facilitate comparison after removing the disturbing effect of the high density of CH_2Cl_2.

3. General procedures for the Michael reaction in batch

Method A. Nitroalkene (0.15 mmol), catalyst **2** (10 mol%) and 4-nitrophenol (2.1 mg, 0.015 mmol) were weighed in a vial and CH_2Cl_2 (0.3 mL) was added, followed by the aldehyde (0.45 mmol). The suspension was stirred at RT for the specified time and filtered to separate the solid catalyst. The polymer was washed with CH_2Cl_2 and the combined organic extracts were washed with 0.1 M NaOH (10 mL) and concentrated under reduced pressure. A ^{1}H NMR spectrum was acquired to calculate the conversion and the diastereomeric ratio (dr). For volatile aldehydes, the Michael adduct was obtained as the evaporation residue without further purification. In other cases, purification by flash chromatography on silica gel (eluent cyclohexane/EtOAc 20:1 to 4:1) afforded the Michael adduct **9**.

Method B. 10 mol% of catalyst was used with 20 mol% 4-nitrophenol. The Michael adduct was obtained after extraction with 0.1 M NaOH (20 mL) without further purification in the case of volatile aldehydes.

Method C. 20 mol% of catalyst was used with 20 mol% benzoic acid. The Michael adduct was obtained after extraction with saturated $NaHCO_3$ (20 mL) without further purification in the case of volatile aldehydes.

Method D (for α-branched aldehydes). Nitroalkene (0.21 mmol), catalyst **2** (30 mol%), 4-nitrophenol (17.6 mg, 0.126 mmol) were weighed in a vial and CH_2Cl_2 (420 μL) was added, followed by isobutyraldehyde (96 μL, 1.05 mmol). The suspension was stirred at RT for 28 h and filtered to separate the solid catalyst. The polymer was washed with CH_2Cl_2 and the combined organic extracts were extracted with 0.1 M NaOH (30 mL) and concentrated under reduced pressure. A ^{1}H NMR spectrum was acquired to calculate the conversion. The Michael adduct was obtained as the evaporation residue without further purification.

Preparation of racemic samples

Racemic standard products were prepared following the same general procedures but using 20 mol% of DL-proline as catalyst according to reported procedures[5] in order to establish HPLC conditions. Chromatography was performed on silica gel (eluent cyclohexane/EtOAc 20:1 to 4:1).

4. Recycling experiments with catalyst 2

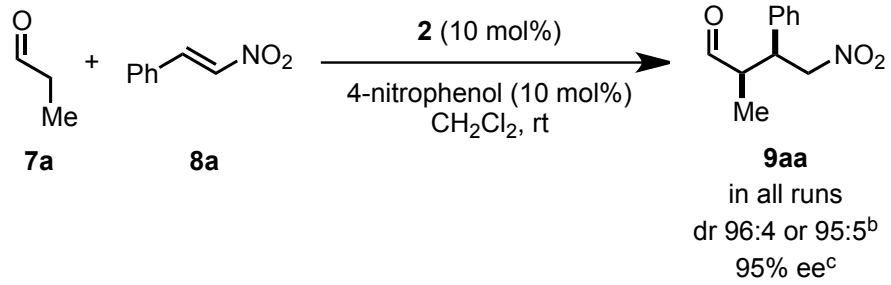

7a **8a** **9aa**

in all runs
dr 96:4 or 95:5[b]
95% ee[c]

The recycling experiment was performed by weighing (*E*)-β-nitrostyrene (41 mg, 0.275 mmol), 4-nitrophenol (3.9 mg, 0.028 mmol) and catalyst **2** (10 mol%) in a vial. Then, CH_2Cl_2 (0.55 mL, 0.5 M) and propionaldehyde (60 µl, 0.83 mmol) were added and the reaction progress was monitored by GC until consumption of starting material. After that, the reaction mixture was filtered, and rinsed with 20 mL of CH_2Cl_2. The polymer was dried and used directly in the next run.

The filtrate was extracted with 0.1 M NaOH (20 mL), concentrated at reduced pressure and purified by column chromatography on silica gel to afford the Michael adduct **9** (whenever full conversion was achieved, the adduct could be isolated without additional purification). The results are presented in the following table:

run	time (h)	conv (yield)
1	1.5	100 (99)
2	2	100 (98)
3	2.5	100 (97)
4	4	100 (98)
5	6	100 (97)
6	12	84 (83)
7	24	100 (97)
8	24	70 (68)

Recyclability of catalyst 2 in the formation of 9aa under nitrogen in the presence of H_2O

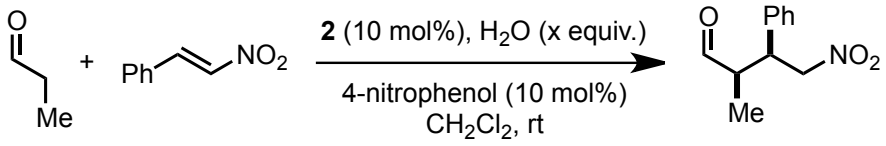

7a **8a** **9aa**
in all runs
dr 95:5, 95% ee

run*	time (h)	conv
1a	1.5	full
2a	2	94
3a	2	79
1b	1.5	full
2b	2	96
2b	2	81

* **a**: 0.5 eq of H_2O; **b**: 2.0 eq of H_2O

The recycling experiments were performed by preparation of solution of weighing (*E*)-β-nitrostyrene (41 mg, 0.275 mmol), 4-nitrophenol (3.9 mg, 0.028 mmol) and catalyst **2** (10 mol%) in degassed CH_2Cl_2 (0.55 mL, 0.5 M) inside the glovebox. Then addition of degassed H_2O (2.5 µL or 10 µL, 0.5 equiv. or 2.0 equiv.) and propionaldehyde (60 µL, 0.825 mmol) was performed under nitrogen outside the glovebox. The suspension was stirred at RT for the specified time and decanted via syringe to separate the solid catalyst, then repeatedly washed and decanted a few times more with CH_2Cl_2 (2 × 2 mL). The polymer was used directly in the next run.

Recyclability of catalyst 2 in the formation of 9aa in the presence of O_2 and H_2O

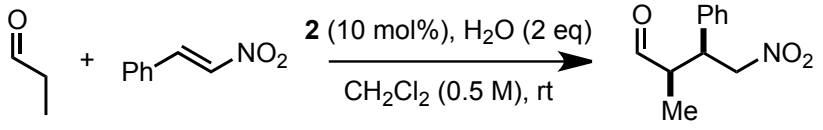

in *all runs* dr 96:4
95% ee

run	time (h)	conv
1	1.5	93
2	2	89
3	2	80
4	2	80

The recycling experiment was performed by weighing (*E*)-β-nitrostyrene (41 mg, 0.275 mmol), 4-nitrophenol (3.9 mg, 0.028 mmol) and catalyst **2** (10 mol%) in a vial. Then, dry CH_2Cl_2 (0.55 mL, 0.5M), 2 equiv. of H_2O (10 μL, 0.55 mmol) and propionaldehyde (60 μL, 0.825 mmol) were added to the reaction mixture. The suspension was stirred at RT for the specified time and decanted via syringe to separate the solid catalyst, then repeatedly washed and decanted with CH_2Cl_2 (2 × 2 mL). The polymer was used directly in the next run.

5. Continuous flow process for the preparation of 9ab

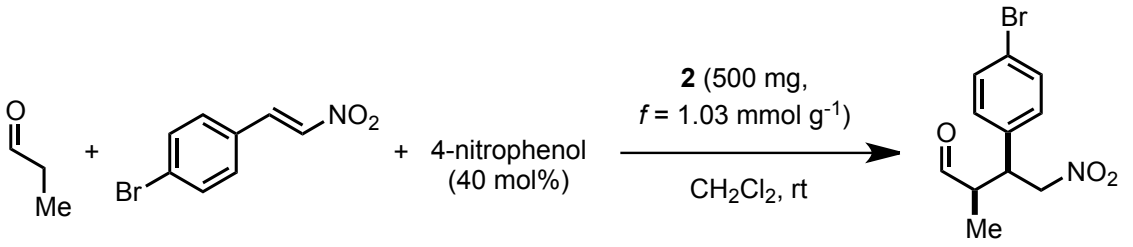

7a **8b** **9ab**
8.87 g
(31.0 mmol, 95% yield)
dr 95:5, 96% ee

For the continuous flow, dry CH_2Cl_2 was degassed; a solution of 4-nitrophenol and *trans*-β-nitrostyrene (0.5 M in this CH_2Cl_2) was prepared inside the glovebox. Addition of propionaldehyde and degassed H_2O was then performed under nitrogen. The flow process was set up under a nitrogen atmosphere (pressurized reservoir bottles).

An Omnifit glass column (1 cm internal diameter) was loaded with catalyst **2** (500 mg, 0.515 mmol, f = 1.03 mmol g^{-1}). The column was assembled to a Syrris Asia 120 Flow System. First, CH_2Cl_2 was circulated for half an hour at 100 μL min^{-1} flow rate to swell the resin. After that, the solvent channel was switched to the solution containing propionaldehyde (7.1 mL, 98 mmol), 4-nitrophenol (1.82 g, 13.1 mmol), *trans*-β-nitrostyrene (7.425 g, 32.6 mmol) and water (1.2 mL, 65.1 mmol) in 65 mL CH_2Cl_2. This feed mixture was pumped through the reactor at a flow rate of 0.1 mL min^{-1}. The reactor outlet was connected to a second pump fed with 0.1 M NaOH at 150 μL min^{-1} flow rate. Further downstream, the resulting biphasic mixture was passed through a Zaiput liquid-liquid separator and the yellow aqueous phase was discarded. The organic phase was collected in a receiving flask.

With the set-up described, running the flow process at 100 μL min^{-1}, full conversions were obtained during the first 10 h. The following three 3 h, a slight decrease in conversion was observed, but the conversions remained above 97%.

Conversion and enantioselectivity of the formed product were determined by ^{1}H NMR and HPLC analysis of periodically collected samples.

Yield 95 % (8.87 g, 31.0 mmol).

TON = 60 $mmol_{product}$ $mmol_{polymer}^{-1}$

TOF = TON/time = 4.63 h^{-1}

Chapter III

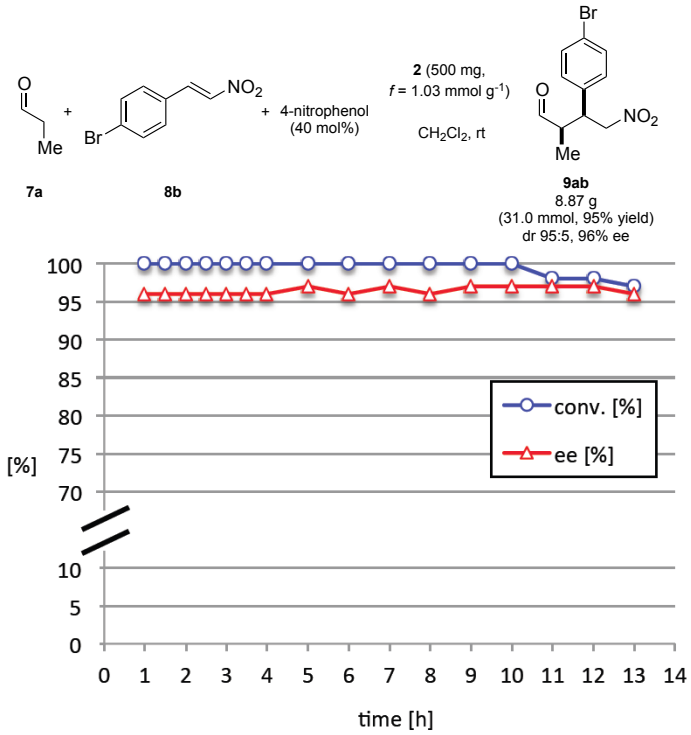
Me
Br
NO2
4-nitrophenol
(40 mol%)
2 (500 mg,
f = 1.03 mmol g-1)
CH2Cl2, rt
Br
NO2
Me
7a
8b
9ab
8.87 g
(31.0 mmol, 95% yield)
dr 95:5, 96% ee
100
95
90
85
80
75
70
10
5
0
[%]
conv. [%]
ee [%]
0 1 2 3 4 5 6 7 8 9 10 11 12 13 14
time [h]


asia
asia

6. Continuous flow process for the preparation of a library of Michael adducts

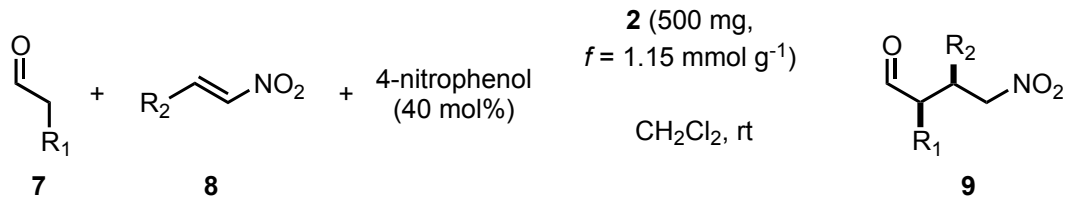

7 **8** **9**

The set-up and the way to prepare the solutions were identical to the ones previously described, except that a different batch of catalyst **2** was used (500 mg, 0.575 mmol, f = 1.15 mmol g^{-1}).

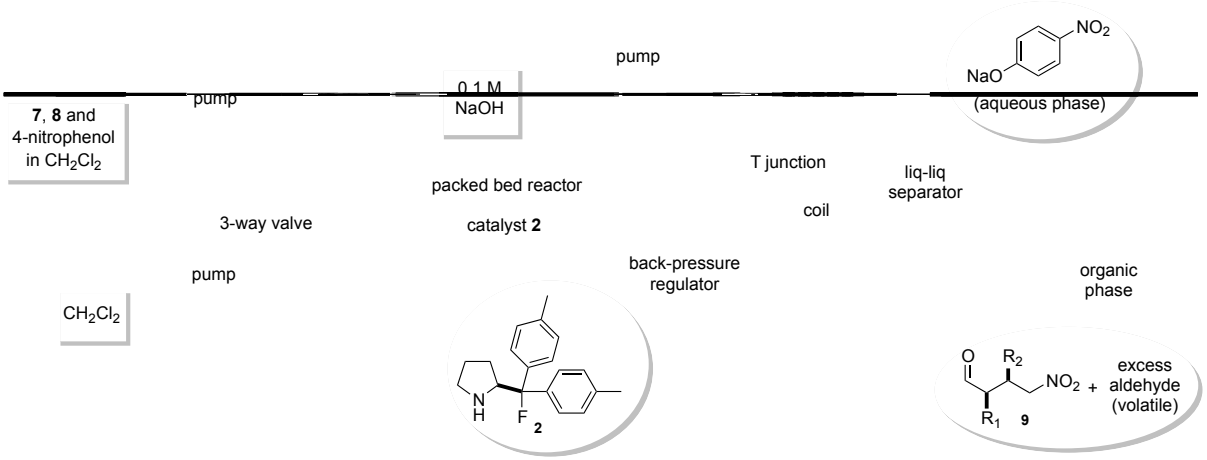

This time, the solvent channel was fed with a mixture containing aldehyde (3 equiv.), 4-nitrophenol (0.4 equiv.), nitroalkene (1 equiv.) and water (2 equiv.) in CH_2Cl_2 (0.5 M). Each of these feed mixtures was pumped through the reactor at a flow rate of 100 µL min^{-1} during 30 min. The in-line work-up and separator replicated the one described above.

After pumping each solution for 30 min, the system was rinsed by pumping CH_2Cl_2 for 1 h and the collected sample was evaporated. The same procedure was repeated for the next 8 samples.

Then, the CH_2Cl_2 flow rate was reduced to 25 µL min^{-1} and the system was maintained like this for 10 h. The following day, the same procedure was applied to the next 5 samples. The column was again kept with CH_2Cl_2 at 25 µL min^{-1} before the last experiments.

The last three members of the library were prepared following the same procedure for a longer time (4 h at 100 µL min^{-1}).

Conversion and enantioselectivity of the formed product were determined by ^{1}H NMR and HPLC analysis of periodically collected samples.

Chapter III

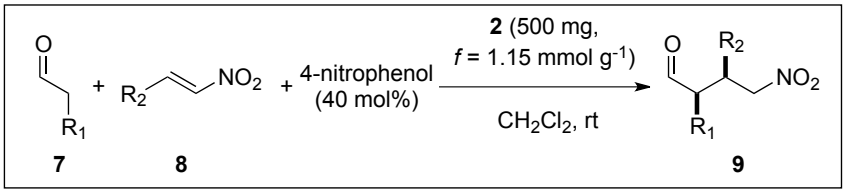

1 flow experiment with **7a** and **8a** for 30 min

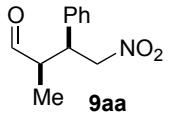

9aa

>99% yield
94:6 dr, 95% ee

2 flow experiment with **7b** and **8a** for 30 min

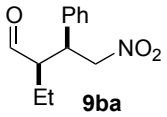

9ba

99% yield
96:4 dr, 97% ee

3 flow experiment with **7c** and **8a** for 30 min

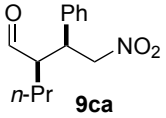

9ca

97% yield
95:5 dr, 97% ee

4 flow experiment with **7a** and **8c** for 30 min

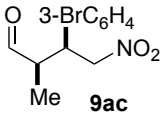

9ac

>99% yield
94:6 dr, 95% ee

5 flow experiment with **7a** and **8d** for 30 min

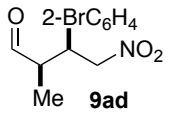

9ad

90% yield
93:7 dr, 95% ee

6 flow experiment with **7a** and **8b** for 30 min

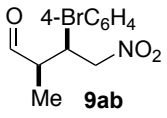

9ab

94% yield
94:6 dr, 95% ee

7 flow experiment with **7a** and **8i** for 30 min

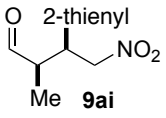

9ai

72% yield
93:7 dr, 94% ee

8 flow experiment with **7a** and **8h** for 30 min

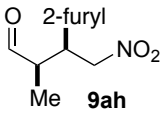

9ah

60% yield
92:8 dr, 95% ee

9 flow experiment with **7b** and **8g** for 30 min

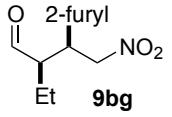

9bg

70% yield
93:7 dr, 94% ee

10 flow experiment with **7b** and **8b** for 30 min

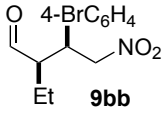

9bb

90% yield
95:5 dr, 96% ee

11 flow experiment with **7c** and **8b** for 30 min

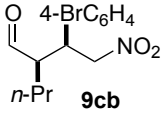

9cb

97% yield
95:5 dr, 96% ee

12 flow experiment with **7a** and **8k** for 30 min

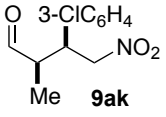

9ak

89% yield
95:5 dr, 94% ee

13 flow experiment with **7a** and **8l** for 30 min

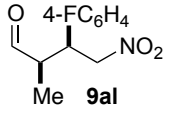

9al

93% yield
96:4 dr, 96% ee

14 flow experiment with **7a** and **8b** for 4 h

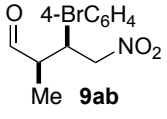

9ab

99% yield
96:4 dr, 95% ee

15 flow experiment with **7a** and **8a** for 4 h

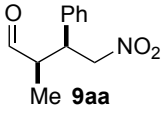

9aa

96% yield
96:4 dr, 96% ee

16 flow experiment with **7b** and **8b** for 4 h

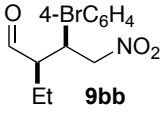

9bb

88% yield
96:4 dr, 96% ee

TON = 72 $mmol_{product}$ $mmol_{polymer}^{-1}$ (for the whole process).

1) Continuous flow reaction of propionaldehyde (300 μL, 4.05 mmol), 4-nitrophenol (75 mg, 0.54 mmol), *trans*-β-nitrostyrene (201 mg, 1.35 mmol) and water (49 μL, 2.7 mmol) in 2.7 mL CH_2Cl_2.

The solvent was removed from the collected sample to give pure **9aa** (280 mg, 1.35 mmol, 96:4 dr and 96% ee).

Productivity: 4.70 $mmol_{product}$ $mmol_{cat}^{-1}$ h^{-1}; theoretical yield during 30 min = 1.35 mmol (>99% yield).

2) Continuous flow reaction of butyraldehyde (352 μL, 3.9 mmol), 4-nitrophenol (72 mg, 0.520 mmol), *trans*-β-nitrostyrene (194 mg, 1.30 mmol) and water (47 μL, 2.60 mmol) in 2.6 mL CH_2Cl_2.

The solvent was removed from the collected sample to give pure **9ba** (284 mg, 1.28 mmol, 96:4 dr and 97% ee).

Productivity: 4.45 $mmol_{product}$ $mmol_{cat}^{-1}$ h^{-1}; theoretical yield during 30 min = 1.30 mmol (99% yield).

3) Continuous flow reaction of valeraldehyde (404 μL, 3.75 mmol), 4-nitrophenol (70 mg, 0.5 mmol), *trans*-β-nitrostyrene (186 mg, 1.25 mmol) and water (45 μL, 2.5 mmol) in 2.5 mL CH_2Cl_2.

The solvent was removed from the collected sample to give an oil, which was submitted to flash chromatography on silica gel using cyclohexane/EtOAc (20:1) as eluent to give pure **9ca** (286 mg, 1.22 mmol, 95:5 dr and 97% ee).

Productivity: 4.24 $mmol_{product}$ $mmol_{cat}^{-1}$ h^{-1}; theoretical yield during 30 min = 1.25 mmol 97% yield).

4) Continuous flow reaction of propionaldehyde (275 μL, 3.75 mmol), 4-nitrophenol (70 mg, 0.50 mmol), 1-bromo-3-(2-nitrovinyl)-benzene (285 mg, 1.25 mmol) and water (45 μL, 2.5 mmol) in 2.5 mL CH_2Cl_2.

The solvent was removed from the collected sample to give pure **9ac** (324 mg, 1.13 mmol, 94:6 dr and 94% ee).

Productivity: 3.93 $mmol_{product}$ $mmol_{cat}^{-1}$ h^{-1}; theoretical yield during 30 min = 1.25 mmol (91% yield).

5) Continuous flow reaction of propionaldehyde (275 μL, 3.75 mmol), 4-nitrophenol (70 mg, 0.50 mmol), 1-bromo-2-(2-nitrovinyl)-benzene (285 mg, 1.25 mmol) and water (45 μL, 2.5 mmol) in 2.5 mL CH_2Cl_2.

The solvent was removed from the collected sample to give pure **9ad** (322 mg, 1.13 mmol, 93:7 dr and 95% ee).

Productivity: 3.93 $mmol_{product}$ $mmol_{cat}^{-1}$ h^{-1}; theoretical yield during 30 min = 1.25 mmol (>99% yield).

6) Continuous flow reaction of propionaldehyde (275 μL, 3.75 mmol), 4-nitrophenol (70 mg,

0.50 mmol), 1-bromo-4-(2-nitrovinyl)-benzene (285 mg, 1.25 mmol) and water (45 μL, 2.5 mmol) in 2.5 mL CH_2Cl_2.

The solvent was removed from the collected sample to give pure **9ab** (335 mg, 1.17 mmol, 94:6 dr and 95% ee).

Productivity: 4.07 $mmol_{product}$ $mmol_{cat}^{-1}$ h^{-1}; theoretical yield during 30 min = 1.25 mmol 94% yield).

7) Continuous flow reaction of propionaldehyde (275 μL, 3.75 mmol), 4-nitrophenol (70 mg, 0.50 mmol), trans-2-(2-nitrovinyl)thiophene (194 mg, 1.25 mmol) and water (45 μL, 2.5 mmol) in 2.5 mL CH_2Cl_2.

An additional extraction of the aqueous phase was carried out. The solvent was removed from the collected sample to give an oil that was submitted to flash chromatography on silica gel using cyclohexane/EtOAc (from 9:1 to 4:1) as eluent to give pure **9ai** (192 mg, 0.90 mmol, 93:7 dr and 94% ee).

Productivity: 3.13 $mmol_{product}$ $mmol_{cat}^{-1}$ h^{-1}; theoretical yield during 30 min = 1.25 mmol (72% yield).

8) Continuous flow reaction of propionaldehyde (275 μL, 3.75 mmol), 4-nitrophenol (70 mg, 0.50 mmol), (*E*)-2-(2-nitroethenyl)furan (174 mg, 1.25 mmol) and water (45 μL, 2.5 mmol) in 2.5 mL CH_2Cl_2.

An additional extraction of the aqueous phase was carried out. The solvent was removed from the collected sample to give pure **9ah** (148 mg, 0.75 mmol, 92:8 dr and 95% ee).

Productivity: 2.61 $mmol_{product}$ $mmol_{cat}^{-1}$ h^{-1}; theoretical yield during 30 min = 1.25 mmol (60% yield).

9) Continuous flow reaction of butyraldehyde (324 μL, 3.6 mmol), 4-nitrophenol (69 mg, 0.48 mmol), (*E*)-2-(2-nitroethenyl)furan (167 mg, 1.20 mmol) and water (43 μL, 2.4 mmol) in 2.4 mL CH_2Cl_2.

An additional extraction of the aqueous phase was carried out. The solvent was removed from the collected sample to give an oil that was submitted to flash chromatography on silica gel using cyclohexane/EtOAc (from 20:1 to 9:1) as eluent to give pure **9bg** (177 mg, 0.84 mmol, 93:7 dr and 94% ee).

Productivity: 2.92 $mmol_{product}$ $mmol_{cat}^{-1}$ h^{-1}; theoretical yield during 30 min = 1.20 mmol (70% yield).

10) Continuous flow reaction of butyraldehyde (324 μL, 3.6 mmol), 4-nitrophenol (69 mg, 0.48 mmol), 1-bromo-4-(2-nitrovinyl)-benzene (274 mg, 1.20 mmol) and water (43 μL, 2.4 mmol) in 2.4 mL CH_2Cl_2.

The solvent was removed from the collected sample to give an oil that was submitted to flash chromatography on silica gel using cyclohexane/EtOAc (from 20:1 to 9:1) as eluent to give pure **9bb** (324 mg, 1.08 mmol, 95:5 dr and 96% ee).

Productivity: 3.76 $mmol_{product}$ $mmol_{cat}^{-1}$ h^{-1}; theoretical yield during 30 min = 1.20 mmol (90% yield).

11) Continuous flow reaction of valeraldehyde (371 μL, 3.45 mmol), 4-nitrophenol (64 mg, 0.46 mmol), 1-bromo-4-(2-nitrovinyl)-benzene (262 mg, 1.15 mmol) and water (42 μL, 2.3 mmol) in 2.3 mL CH_2Cl_2.

The solvent was removed from the collected sample to give an oil that was submitted to flash chromatography on silica gel using cyclohexane/EtOAc (from 20:1) as eluent to give pure **9cb** (352 mg, 1.12 mmol, 95:5 dr and 96% ee).

Productivity: 3.90 $mmol_{product}$ $mmol_{cat}^{-1}$ h^{-1}; theoretical yield during 30 min = 1.15 mmol (97% yield).

12) Continuous flow reaction of propionaldehyde (275 μL, 3.75 mmol), 4-nitrophenol (70 mg, 0.50 mmol), 1-chloro-3-(2-nitrovinyl)-benzene (229 mg, 1.25 mmol) and water (45 μL, 2.5 mmol) in 2.5 mL CH_2Cl_2.

The solvent was removed from the collected sample to give pure **9ak** (269 mg, 1.11 mmol, 95:5 dr and 94% ee).

Productivity: 4.70 $mmol_{product}$ $mmol_{cat}^{-1}$ h^{-1}; theoretical yield during 30 min = 1.25 mmol 89% yield).

13) Continuous flow reaction of propionaldehyde (275 μL, 3.75 mmol), 4-nitrophenol (70 mg, 0.50 mmol), 1-fluoro-4-(2-nitrovinyl)-benzene (209 mg, 1.25 mmol) and water (45 μL, 2.5 mmol) in 2.5 mL CH_2Cl_2.

The solvent was removed from the collected sample to give pure **9al** (261 mg, 1.16 mmol, 96:4 dr and 95% ee).

Productivity: 4.03 $mmol_{product}$ $mmol_{cat}^{-1}$ h^{-1}; theoretical yield during 30 min = 1.25 mmol (93% yield).

14) Continuous flow reaction of propionaldehyde (2.2 mL, 30 mmol), 4-nitrophenol (556 mg, 4.0 mmol), 1-bromo-4-(2-nitrovinyl)-benzene (2.28 g, 10.0 mmol) and water (360 μL, 0.36 mmol) in 20 mL CH_2Cl_2.

The solvent was removed from the collected sample to give pure **9ab** (2.840 g, 9.93 mmol, 96:4 dr and 95% ee).

Productivity: 4.32 $mmol_{product}$ $mmol_{cat}^{-1}$ h^{-1}; theoretical yield during 4 h = 10.0 mmol (99% yield).

15) Continuous flow reaction of propionaldehyde (2.1 mL, 28.8 mmol), 4-nitrophenol (534 mg, 3.84 mmol), *trans*-β-nitrostyrene (1.43 g, 9.6 mmol) and water (350 μL, 0.346 mmol) in 19.5 mL CH_2Cl_2.

The solvent was removed from the collected sample to give an oil that was submitted to flash chromatography on silica gel using cyclohexane/EtOAc (from 20:1 to 9:1) as eluent to give pure **9aa** (1.970 g, 9.20 mmol, 96:4 dr and 96% ee).

Productivity: 4.00 $mmol_{product}$ $mmol_{cat}^{-1}$ h^{-1}; theoretical yield during 4 h = 9.5 mmol (96% yield).

16) Continuous flow reaction of propionaldehyde (2.45 mL, 27 mmol), 4-nitrophenol (556 mg, 4.0 mmol), 1-bromo-4-(2-nitrovinyl)-benzene (2.05 g, 9.0 mmol) and water (324 μL, 0.24 mmol) in 18 mL CH_2Cl_2.

The solvent was removed from the collected sample to give an oil that was submitted to flash chromatography on silica gel using cyclohexane/EtOAc (from 20:1 to 9:1) as eluent to give pure **9bb** (2.367 g, 7.89 mmol, 96:4 dr and 96% ee).

Productivity: 3.43 $mmol_{product}$ $mmol_{cat}^{-1}$ h^{-1}; theoretical yield during 4 h = 9.0 mmol (88% yield).

7. Derivatization of Michael adducts 9: preparation of 10 and 11

Preparation of pyrrolidine derivatives

General procedure for the synthesis of pyrrolidines 10a,b

The corresponding Michael adduct **9** (2.29 mmol) was dissolved in EtOH (23 mL) in a round-bottom flask equipped with a magnetic stirrer and AcOH (5.3 mL, 92 mmol) was added. The solution was cooled to –5 ºC and Zn powder (2.25 g, 34.4 mmol) was added portionwise within 1 h. The reaction mixture was cooled to room temperature and stirred for 24 h. Then the insoluble residue was filtered off on celite with ethanol (3 × 12 mL). The organic layer was concentrated in vacuo and the residue was cooled to –5 ºC, then 1 N NaOH (around 60 mL) was added slowly until pH 10-11, and extracted with CH_2Cl_2 (2 × 50 mL) The combined organic phase was dried with anhydrous $MgSO_4$ and concentrated in vacuo. The enantiomeric excess was determined after *N*-tosylation.

General procedure for the synthesis of *N*-tosylated pyrrolidines 11

The corresponding pyrrolidine **11** (1.36 mmol) and Et_3N (0.45 mL, 3.1 mmol) in 12 mL of CH_2Cl_2 under nitrogen was cooled to 0 ºC, then TsCl was added (310 mg, 1.63 mmol). The reaction mixture was brought to room temperature and stirred for 11 h. Then, water (10 mL) was added to the solution and it was extracted with CH_2Cl_2 (3 × 20 mL). The combined organic extracts were dried under $MgSO_4$ and the residue obtained after evaporation was purified by flash chromatography on silica gel (eluent cyclohexane/EtOAc 98:2 to 95:5) to furnish tosyl derivatives **11**.

8. Physical and spectroscopic data for Michael adducts 9

(2*R*,3*S*)-2-Methyl-4-nitro-3-phenylbutanal (9aa)

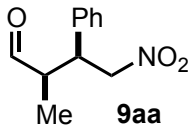

9aa

The title compound was prepared from (*E*)-β-nitrostyrene and propionaldehyde according to **General Procedure A** in 99% yield (30.9 mg, 0.149 mmol) after 1.5 h (dr 96:4, 95% ee). All spectroscopic data matched those reported in the literature.[6]

Major diastereomer:

^{1}H NMR (500 MHz, $CDCl_3$): δ 9.72 (d, *J* = 1.7 Hz, 1H), 7.37-7.27 (m, 3H), 7.19-7.14 (m, 2H), 4.80 (dd, *J* = 5.5, 12.7 Hz, 1H), 4.68 (dd, *J* = 9.3, 12.7 Hz, 1H), 3.81 (dt, *J* = 5.5, 9.2 Hz, 1H), 2.77 (dqd, *J* = 1.7, 7.2, 9.0 Hz, 1H), 1.00 (d, *J* = 7.2 Hz, 3H).

^{13}C NMR (126 MHz, $CDCl_3$): δ 202.4, 136.7, 129.2 (×2), 128.3, 128.2 (×2), 78.2, 48.6, 44.2, 12.3.

HPLC: Daicel Chiralpak IC column, hexane/*i*-PrOH (90:10), flow rate 0.8 mL min^{-1}, 214 nm. t_R major = 50.7 min, t_R minor = 43.0 min.

(2*R*,3*S*)-2-Ethyl-4-nitro-3-phenylbutanal (9ba)

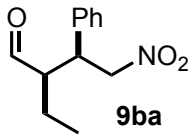

9ba

The title compound was prepared from (*E*)-β-nitrostyrene and butyraldehyde according to **General Procedure A** in 97% yield (32.1 mg, 0.145 mmol) after 1.5 h (dr 94:6, 98% ee). Purification was carried out by flash chromatography on silica gel using cyclohexane/EtOAc (from 20:1 to 9:1) as eluent. All spectroscopic data matched those reported in the literature.[6]

Major diastereomer:

^{1}H NMR (500 MHz, $CDCl_3$): δ 9.72 (d, *J* = 2.6 Hz, 1H), 7.37-7.32 (m, 2H), 7.32-7.27 (m, 1H), 7.19-7.16 (m, 2H), 4.72 (dd, *J* = 4.9, 12.7 Hz, 1H), 4.63 (dd, *J* = 9.7, 12.7 Hz, 1H), 3.79 (dt, *J* = 4.9, 9.8 Hz, 1H), 2.68 (dddd, *J* = 2.6, 4.9, 7.5, 10.1 Hz, 1H), 1.55-1.48 (m, 2H), 0.84 (t, *J* = 7.5 Hz, 3H).

^{13}C NMR (101 MHz, $CDCl_3$): δ 203.3, 136.9, 129.3 (×2), 128.3, 128.1 (×2), 78.7, 55.2, 42.9, 20.5, 10.8.

HPLC: Daicel Chiralpak IC column, hexane/*i*-PrOH (90:10), flow rate 1.0 mL min^{-1}, 214 nm. t_R major = 30.3 min, t_R minor = 27.0 min.

(2*R*,3*S*)-2-Propyl-4-nitro-3-phenylbutanal (9ca)

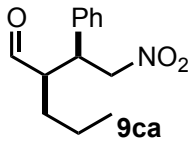

Title compound was prepared from (E)-β-nitrostyrene and *n*-pentanal according to **General Procedure A** in 97% yield (34.4 mg, 0.146 mmol) after 1.5 h (dr 94:6, 97% ee). Purification was carried out by flash chromatography on silica gel using cyclohexane/EtOAc (20:1) as eluent. All spectroscopic data matched those reported in the literature.[7]

Major diastereomer:

^{1}H NMR (500 MHz, $CDCl_3$): δ 9.73 (d, *J* = 2.8 Hz, 1H), 7.40-7.30 (m, 3H), 7.22-7.17 (m, 2H), 4.73 (dd, *J* = 5.3, 12.8 Hz, 1H), 4.67 (dd, *J* = 9.5, 12.8 Hz, 1H), 3.80 (dt, *J* = 5.3, 9.6 Hz, 1H), 2.73 (tt, *J* = 3.3, 9.5, Hz, 1H), 1.57-1.44 (m, 1H), 1.44-1.30 (m, 3H), 0.83 (t, *J* = 7.2 Hz, 3H).

^{13}C NMR (101 MHz, $CDCl_3$): δ 203.3, 136.9, 129.3 (×2), 128.3, 128.1 (×2), 78.6, 54.0, 43.3, 29.6, 19.9, 14.1.

HPLC: Daicel Chiralpak IC column, hexane/*i*-PrOH (90:10), flow rate 1.0 mL min^{-1}, 214 nm. t_R major = 26.0 min, t_R minor = 22.9 min.

(2*R*,3*S*)-2-Pentyl-4-nitro-3-phenylbutanal (9da)

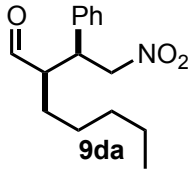

Title compound was prepared from (E)-β-nitrostyrene and *n*-heptanal according to **General Procedure A** in 96% yield (38.0 mg, 0.144 mmol) after 3.5 h (dr 96:4, 97% ee). Purification was carried out by flash chromatography on silica gel using cyclohexane/EtOAc (20:1) as eluent. All spectroscopic data matched those reported in the literature.[8]

Major diastereomer:

^{1}H NMR (500 MHz, $CDCl_3$): δ 9.71 (d, J = 2.7 Hz, 1H), 7.37-7.32 (m, 2H), 7.32-7.27 (m, 1H), 7.19-7.15 (m, 2H), 4.71 (dd, *J* = 5.1, 12.8 Hz, 1H), 4.64 (dd, *J* = 9.7, 12.8 Hz, 1H), 3.77 (dt, *J* = 5.1, 9.7 Hz, 1H), 2.73-2.66 (m, 1H), 1.54-1.43 (m, 1H), 1.45-1.33 (m, 1H), 1.32-1.26 (m, 1H), 1.22-1.06 (m, 5H), 0.81 (t, *J* = 7.0 Hz, 3H).

^{13}C NMR (126 MHz, $CDCl_3$): δ 203.4, 137.0, 129.3 (×2), 128.3, 128.1 (×2), 78.6, 54.1, 43.3, 31.7, 27.5, 26.2, 22.4, 14.0.

HPLC: Daicel Chiralpak IC column, hexane/*i*-PrOH (90:10), flow rate 1.0 mL min^{-1}, 214 nm. t_R major = 22.2 min, t_R minor = 19.6 min.

(2*R*,3*S*)-2-Decyl-4-nitro-3-phenylbutanal (9ea)

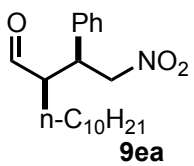

Title compound was prepared from (*E*)-β-nitrostyrene and *n*-dodecyl

aldehyde according to **General Procedure A** in 93% yield (46.7 mg, 0.140 mmol) after 3.25 h (dr 94:6, 97% ee). Purification was carried out by flash chromatography on silica gel using cyclohexane/EtOAc (20:1) as eluent. All spectroscopic data matched those reported in the literature.[9]

Major diastereomer:

^{1}H NMR (400 MHz, $CDCl_3$): δ 9.70 (d, *J* = 2.7 Hz, 1H), 7.37-7.27 (m, 3H), 7.20-7.15 (m, 2H), 4.71 (dd, *J* = 5.2, 12.8 Hz, 1H), 4.64 (dd, *J* = 9.5, 12.8 Hz, 1H), 3.77 (dt, *J* = 5.2, 9.6 Hz, 1H), 2.74-2.65 (m, 1H), 1.51-1.11 (m, 18H), 0.87 (t, *J* = 6.9 Hz, 3H).

^{13}C NMR (101 MHz, $CDCl_3$): δ 203.4, 137.0, 129.3 (×2), 128.3, 128.1 (×2), 78.6, 54.1, 43.3, 32.0, 29.6, 29.5 (×2), 29.4, 29.3, 27.5, 26.5, 22.8, 14.0.

HPLC: Daicel Chiralpak IC column, hexane/*i*-PrOH (95:5), flow rate 0.8 mL min^{-1}, 214 nm. t_R major = 30.8 min, t_R minor = 26.4 min.

(2*R*,3*S*)-2-(Undec-10-enal)-4-nitro-3-phenylbutanal (9fa)

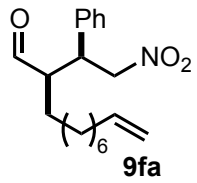

9fa

Title compound was prepared from (*E*)-β-nitrostyrene and undecylenic aldehyde according to **General Procedure A** in 95% yield (45.5 mg, 0.143 mmol) after 4 h (dr 96:4, 97% ee). Purification was carried out by flash chromatography on silica gel using cyclohexane/EtOAc (20:1) as eluent. All spectroscopic data matched those reported in the literature.[10]

Major diastereomer:

^{1}H NMR (500 MHz, $CDCl_3$): δ 9.70 (d, *J* = 2.7 Hz, 1H), 7.38-7.31 (m, 2H), 7.31-7.28 (m, 1H), 7.19-7.15 (m, 2H), 5.78 (ddt, *J* = 6.7, 10.2, 17.0 Hz, 1H), 5.00-4.94 (m, 1H), 4.92 (ddt, *J* = 1.2, 2.3, 10.2 Hz, 1H), 4.70 (dd, *J* = 5.1, 12.8 Hz, 1H), 4.64 (dd, *J* = 9.6, 12.8, Hz, 1H), 3.77 (dt, *J* = 5.1, 9.7, Hz, 1H), 2.73-2.66 (m, 1H), 2.02-1.96 (m, 2H), 1.52-1.44 (m, 1H), 1.42-1.34 (m, 1H), 1.33-1.24 (m, 4H), 1.22-1.11 (m, 6H).

^{13}C NMR (126 MHz, $CDCl_3$): δ 203.3, 139.2, 136.9, 129.3 (×2), 128.3, 128.1 (×2), 114.4, 78.6, 54.1, 43.3, 33.8, 29.5, 29.1, 29.0, 28.9, 27.5, 26.5.

HPLC: Daicel Chiralpak IC column, hexane/*i*-PrOH (95:5), flow rate 0.8 mL min^{-1}, 214 nm. t_R major = 36.8 min, t_R minor = 31.7 min.

(2*R*,3*S*)-2-(Benzyl)-4-nitro-3-phenylbutanal (9ga)

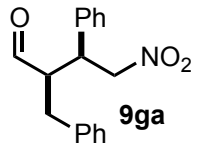

9ga

The title compound was prepared from (*E*)-β-nitrostyrene and aldehyde according to **General Procedure A** in 95% yield (33.9 mg, 0.144 mmol)

after 6 h (dr 94:6, 94% ee). Purification was carried out by flash chromatography on silica gel using cyclohexane/EtOAc (20:1 to 9:1) as eluent. All spectroscopic data matched those reported in the literature.[11]

Major diastereomer:

^{1}H NMR (500 MHz, $CDCl_3$): δ 9.72 (d, *J* = 2.3 Hz, 1H), 7.41-7.35 (m, 2H), 7.35-7.24 (m, 3H), 7.24-7.19 (m, 3H), 7.05-7.00 (m, 2H), 4.73 (dd, *J* = 5.9, 12.8 Hz, 1H), 4.70 (dd, *J* = 8.6, 12.8 Hz, 1H), 3.83 (dt, *J* = 5.9, 8.8 Hz, 1H), 3.12 (tdd, *J* = 2.3, 5.7, 9.0 Hz, 1H), 2.82-2.72 (m, 2H).

^{13}C NMR (126 MHz, $CDCl_3$): δ 203.1, 137.3, 136.9, 129.4 (×2), 129.0 (×2), 128.9 (×2), 128.5, 128.2 (×2), 127.1, 78.2, 55.5, 43.6, 34.4.

HPLC: Daicel Chiralpak IC column, hexane/*i*-PrOH (90:10), flow rate 1.0 mL min^{-1}, 214 nm. t_R major = 31.5 min, t_R minor = 24.2 min.

(2*R*,3*S*)-3-(4-Bromophenyl)-2-methyl-4-nitrobutanal (9ab)

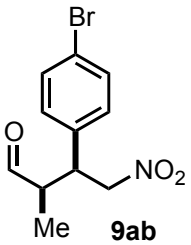

9ab

Title compound was prepared from 1-bromo-4-(2-nitrovinyl)-benzene and propionaldehyde according to **General Procedure A** in 98% yield (42.2 mg, 0.147 mmol) after 1.25 h (dr 97:3, 96% ee). All spectroscopic data matched those reported in the literature.[12]

Major diastereomer:

^{1}H NMR (500 MHz, $CDCl_3$): δ 9.69 (d, *J* = 1.6 Hz, 1H), 7.51-7.44 (m, 2H), 7.08-7.03 (m, 2H), 4.79 (dd, *J* = 5.3, 12.8 Hz, 1H), 4.64 (dd, *J* = 9.6, 12.8 Hz, 1H), 3.78 (dt, *J* = 5.3, 9.3 Hz, 1H), 2.75 (dqd, *J* = 1.6, 7.3, 9.0 Hz, 1H), 1.00 (d, *J* = 7.3 Hz, 3H).

^{13}C NMR (101 MHz, $CDCl_3$): δ 201.9, 135.8, 132.4 (×2), 129.9 (×2), 122.3, 78.0, 48.3, 43.7, 12.4.

HPLC: Daicel Chiralpak IC column, hexane/*i*-PrOH (90:10), flow rate 1.0 mL min^{-1}, 214 nm. t_R major = 38.3 min, t_R minor = 35.7 min.

(2*R*,3*S*)-3-(3-Bromophenyl)-2-methyl-4-nitrobutanal (9ac)

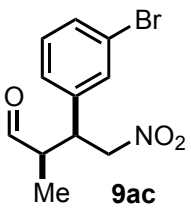

9ac

Title compound was prepared from 1-bromo-3-(2-nitrovinyl)-benzene and propionaldehyde according to **General Procedure A** in 98% yield (42.0 mg, 0.147 mmol) after 1.5 h (dr 96:4, 94% ee). All spectroscopic data matched those reported in the literature.[12b]

Major diastereomer:

^{1}H NMR (400 MHz, $CDCl_3$): δ 9.69 (d, *J* = 1.5 Hz, 1H), 7.43 (ddd, *J* = 1.0, 1.9, 8.0 Hz, 1H), 7.33 (t, *J* = 1.9 Hz, 1H), 7.23 (t, *J* = 7.8, 1H), 7.11 (dt, *J* = 1.3, 7.8 Hz, 1H), 4.79 (dd, *J* = 5.2, 12.9 Hz, 1H), 4.65 (dd, *J* = 9.5, 12.9 Hz, 1H), 3.77 (dt, *J* = 5.2, 9.3 Hz, 1H), 2.76 (dqd, *J* = 1.5, 7.3, 8.9 Hz, 1H), 1.01 (d, *J* = 7.3 Hz, 3H).

^{13}C NMR (101 MHz, $CDCl_3$): δ 201.8, 139.2, 131.5, 131.3, 130.8, 126.9, 123.3, 77.9, 48.4, 43.8, 12.4.

HPLC: Daicel Chiralpak IC column, hexane/*i*-PrOH (90:10), flow rate 1.0 mL min^{-1}, 204 nm. t_R major = 32.4 min, t_R minor = 28.0 min.

(2*R*,3*S*)-3-(2-Bromophenyl)-2-methyl-4-nitrobutanal (9ad)

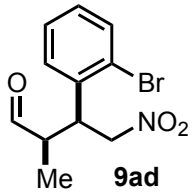

9ad

Title compound was prepared from 1-bromo-2-(2-nitrovinyl)-benzene and propionaldehyde according to **General Procedure A** in 98% yield (42.3 mg, 0.148 mmol) after 1.5 h (dr 96:4, 94% ee). All spectroscopic data matched those reported in the literature.[10,12b]

Major diastereomer:

^{1}H NMR (400 MHz, $CDCl_3$): δ 9.74 (d, *J* = 1.6 Hz, 1H), 7.61 (dd, *J* = 1.2, 7.9 Hz, 1H), 7.32 (td, *J* = 1.4, 7.6 Hz, 1H), 7.21-7.14 (m, 2H), 4.87 (dd, *J* = 8.9, 13.0 Hz, 1H), 4.77 (dd, *J* = 4.9, 13.0 Hz, 1H), 4.4-4.3 (m, 1H), 3.1-2.9 (m, 1H), 1.06 (d, *J* = 7.4 Hz, 3H).

^{13}C NMR (126 MHz, $CDCl_3$): δ 202.0, 136.4, 134.0, 129.6 (×2), 128.2 (×2), 76.9, 48.2, 42.9, 12.5.

HPLC: Daicel Chiralpak IC column, hexane/*i*-PrOH (80:20), flow rate 0.6 mL min^{-1}, 214 nm. t_R major = 33.7 min, t_R minor = 36.4 min.

(2*R*,3*S*)-3-(4-Methoxyphenyl)-2-methyl-4-nitrobutanal (9ae)

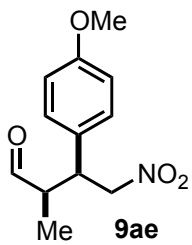

9ae

Title compound was prepared from 1-methoxy-4-(2-nitrovinyl)-benzene and propionaldehyde according to **General Procedure A** in >99% yield (35.4 mg, 0.150 mmol) after 2.25 h (dr 95:5, 95% ee). All spectroscopic data matched those reported in the literature.[7]

^{1}H NMR (400 MHz, $CDCl_3$): δ 9.71 (d, *J* = 1.8 Hz, 1H), 7.11-7.05 (m, 2H), 6.90-6.83 (m, 2H), 4.76 (dd, *J* = 5.5, 12.5 Hz, 1H), 4.63 (dd, *J* = 9.5, 12.5 Hz, 1H), 3.79-3.73 (m, 1H), 3.79 (s, 3H), 2.76 (dqd, *J* = 1.8, 7.3, 9.0 Hz, 1H), 1.00 (d, *J* = 7.3 Hz, 3H).

^{13}C NMR (126 MHz, $CDCl_3$): δ 202.5, 159.4, 129.3 (×2), 128.4, 114.6 (×2), 78.5, 55.4, 48.7, 43.5, 12.2.

HPLC: Daicel Chiralpak IC column, hexane/*i*-PrOH (80:20), flow rate 1.0 mL min^{-1}, 214 nm. t_R major = 26.9 min, t_R minor = 23.9 min.

(2*R*,3*S*)-3-(Benzo[d][1.3]dioxol-5-yl)-2-methyl-4-nitrobutanal (9af)

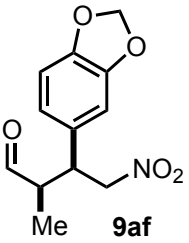

9af

The title compound was prepared from 5-[(*E*)-2-nitrovinyl)-1,3-benzodioxole and propionaldehyde according to **General Procedure A** in >99% yield (37.5 mg, 0.149 mmol) after 2.25 h (dr 95:5, 95% ee). All spectroscopic data matched those reported in the literature.[13]

^{1}H NMR (500 MHz, $CDCl_3$): δ 9.69 (d, *J* = 1.7 Hz, 1H), 6.77-6.74 (m, 1H), 6.65-6.60 (m, 2H), 5.95 (s, 2H), 4.74 (dd, *J* = 5.3, 12.6 Hz, 1H), 4.60 (dd, *J* = 9.6, 12.6 Hz, 1H), 3.71 (dt, *J* = 5.3, 9.3 Hz, 1H), 2.70 (dqd, *J* = 1.7, 7.3, 9.1 Hz, 1H), 1.01 (t, *J* = 7.3 Hz, 3H).

^{13}C NMR (126 MHz, $CDCl_3$): δ 202.3, 148.4, 147.5, 130.2, 121.8, 108.8, 108.1, 101.4, 78.5, 48.7, 44.0, 12.3.

HPLC: Daicel Chiralpak IC column, hexane/*i*-PrOH (80:20), flow rate 0.8 mL min^{-1}, 214 nm. t_R major = 39.7 min, t_R minor = 35.7 min.

(2*R*,3*S*)-3-(4-Hydroxyphenyl)-2-methyl-4-nitrobutanal (9ag)

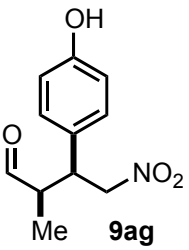

9ag

The title compound was prepared from 1-hydroxy-4-(2-nitrovinyl)-benzene and propionaldehyde according to **General Procedure A** in 97% yield (32.6 mg, 0.146 mmol) after 1 h (dr 93:7, 96% ee). In this case **extraction with 0.1 M NaOH was not performed.** Purification was carried out by flash chromatography on silica gel using cyclohexane/EtOAc (from 9:1 to 4:1) as eluent. Yellow solid.

$[\alpha]_D^{25}$ ($CHCl_3$, *c* 0.1) = +31.5.

IR (ATR): ν = 3369; 1713; 1548; 1515; 1377; 1218; 770; 535 cm^{-1}.

mp = 90-92 ºC.

^{1}H NMR (500 MHz, $CDCl_3$): δ 9.69 (d, *J* = 1.7 Hz, 1H), 7.03-6.99 (m, 2H), 6.79-6.75 (m, 2H), 5.60 (bs, 1H), 4.75 (dd, *J* = 5.5, 12.6 Hz, 1H), 4.63 (dd, *J* = 9.5, 12.6 Hz, 1H), 3.75 (dt, *J* = 5.5, 9.1 Hz, 1H), 2.72 (dqd, *J* = 1.7, 7.2, 9.0 Hz, 1H), 0.99 (d, *J* = 7.2 Hz, 3H).

^{13}C NMR (126 MHz, $CDCl_3$): δ 202.9, 155.6, 129.4 (×2), 128.4, 116.1 (×2), 78.5, 48.5, 43.5, 12.1.

HRMS (ESI) Calculated mass for $C_{11}H_{12}NO_4$: $[M–H]^-$ = 222.0772, found = 222.0768.

HPLC: Daicel Chiralpak IC column, hexane/*i*-PrOH (80:20), flow rate 0.8 mL min^{-1}, 214 nm.

t_R major = 20.5 min, t_R minor = 19.3 min.

(2*R*,3*S*)-3-(2-Furyl)-2-methyl-4-nitrobutanal (9ah)

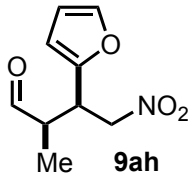

9ah

Title compound was prepared from (E)-2-(2-nitrovinyl)furan and propionaldehyde according to **General Procedure A** in 95% yield (28.1 mg, 0.143 mmol) after 1 h (dr 93:7, 95% ee). All spectroscopic data matched those reported in the literature.[12a]

^{1}H NMR (500 MHz, $CDCl_3$): δ 9.71 (d, *J* = 1.0 Hz, 1H), 7.35 (dd, *J* = 0.8, 1.9 Hz, 1H), 6.30 (dd, *J* = 1.9, 3.3 Hz, 1H), 6.18(d, *J* = 3.3 Hz, 1H), 4.75 (dd, *J* = 8.6, 12.8 Hz, 1H), 4.70 (dd, *J* = 6.0, 12.8 Hz, 1H), 4.09 (dt, *J* = 6.6, 8.6 Hz, 1H), 2.80 (quintd, *J* = 1.0, 7.3 Hz, 1H), 1.07 (d, *J* = 7.3 Hz, 3H).

^{13}C NMR (126 MHz, $CDCl_3$): δ 201.7, 150.0, 142.8, 110.6, 108.9, 75.9, 47.2, 37.8, 11.1.

GC: Betadex120, injector T = 230 °C, isotherm at 100 °C, flow rate 1.5 mL min^{-1}.

t_R major = 307.8 min, t_R minor = 316.9 min.

(2*R*,3*S*)-3-(2-Thienyl)-2-methyl-4-nitrobutanal (9ai)

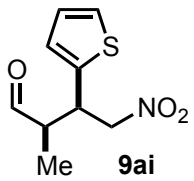

9ai

The title compound was prepared from (E)-2-(2-nitrovinyl)thiophene and propionaldehyde according to **General Procedure A** in >99% yield (31.9 mg, 0.150 mmol) after 1 h (dr 93:7, 93% ee). All spectroscopic data matched those reported in the literature.[7]

^{1}H NMR (500 MHz, $CDCl_3$): δ 9.70 (d, *J* = 1.2 Hz, 1H), 7.24 (dd, *J* = 1.2, 5.1 Hz, 1H), 6.96 (dd, *J* = 3.5, 5.1 Hz, 1H), 6.91-6.88 (m, 1H), 4.78 (dd, *J* = 5.9, 12.8 Hz, 1H), 4.68 (dd, *J* = 8.7, 12.8, Hz, 1H), 4.24 (dt, *J* = 5.9, 8.2 Hz, 1H), 2.79 (quintd, *J* = 1.2, 7.3, Hz, 1H), 1.13 (t, *J* = 7.3 Hz, 3H).

^{13}C NMR (126 MHz, $CDCl_3$): δ 201.8, 139.0, 127.3, 126.9, 125.5, 78.5, 49.0, 39.6, 11.7.

HPLC: Daicel Chiralpak IC column, hexane/*i*-PrOH (90:10), flow rate 0.8 mL min^{-1}, 214 nm.

t_R major = 49.3 min, t_R minor = 35.2 min.

(2*R*,3*S*)-2-Methyl-3-nitromethyl-5-phenylpentanal (9aj)

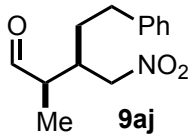

9aj

The title compound was prepared from (E)-(4-nitrobut-3-en-1-yl)benzene and propionaldehyde according to **General Procedure A** in 97% yield (34.3 mg, 0.146 mmol) after 5.5 h (dr 85:15, 97% ee). All spectroscopic data matched those reported in the literature.[14]

^{1}H NMR (500 MHz, $CDCl_3$): δ 9.62 (d, *J* = 0.6 Hz, 1H), 7.33-7.27 (m, 2H), 7.24-7.19 (m, 1H), 7.24-7.19 (m, 2H), 4.54 (dd, *J* = 5.8, 12.4 Hz, 1H), 4.45 (dd, *J* = 7.6, 12.4, Hz, 1H), 2.83-2.76 (m, 1H), 2.73-2.55 (m, 3H), 1.75-1.58 (m, 2H), 1.16 (d, *J* = 7.3 Hz, 3H).

^{13}C NMR (126 MHz, $CDCl_3$): δ 202.6, 140.6, 128.8 (×2), 128.4 (×2), 126.6, 76.9, 47.2, 37.0, 33.4, 30.4, 9.3.

HPLC: Daicel Chiralpak IC column, hexane/*i*-PrOH (90:10), flow rate 0.8 mL min^{-1}, 214 nm. t_R major = 28.0 min, t_R minor = 23.3 min.

(2*R*,3*S*)-2-(Isopropyl)-4-nitro-3-phenylbutanal (9ha)

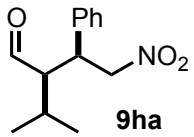

9ha

The title compound was prepared from (*E*)-β-nitrostyrene and isovaleraldehyde according to **General Procedure C (as well as A and B)** in 96% yield (34.5 mg, 0.147 mmol). Full conversion was observed in 11 h (dr 97:3, >99% ee). All spectroscopic data matched those reported in the literature.[6]

Major diastereomer:

^{1}H NMR (400 MHz, $CDCl_3$): δ 9.93 (d, *J* = 2.4 Hz, 1H), 7.38-7.27 (m, 3H), 7.22-7.17 (m, 2H), 4.67 (dd, *J* = 4.4, 12.5 Hz, 1H), 4.57 (dd, *J* = 9.9, 12.5 Hz, 1H), 3.90 (dt, *J* = 4.4, 10.3 Hz, 1H), 2.77 (ddd, *J* = 2.5, 4.2, 10.7 Hz, 1H), 1.72 (heptd, *J* = 4.2, 7.1 Hz, 1H), 1.10 (d, *J* = 7.2 Hz, 3H), 0.89 (d, *J* = 7.0 Hz, 3H).

^{13}C NMR (101 MHz, $CDCl_3$): δ 204.5, 137.2, 129.3 (×2), 128.2, 128.1 (×2), 79.1, 58.9, 42.1, 28.1, 21.8, 17.1.

HPLC: Daicel Chiralpak IC column, hexane/*i*-PrOH (90:10), flow rate 0.8 mL min^{-1}, 214 nm. t_R major = 28.9 min, t_R minor = 25.9 min.

(2*R*,3*S*)-3-(4-Bromophenyl)-2-isopropyl-4-nitrobutanal (9hb)

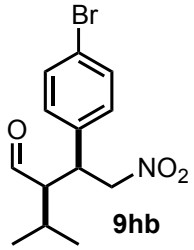

9hb

The title compound was prepared from 1-bromo-4-(2-nitrovinyl)-benzene and isovaleraldehyde according to **General Procedure B (as well as C)** in 96% yield (45.3 mg, 0.144 mmol) after 13 h (dr 95:5, 99% ee). All spectroscopic data matched those reported in the literature.[15]

Major diastereomer:

^{1}H NMR (500 MHz, $CDCl_3$): δ 9.91 (d, *J* = 2.2 Hz, 1H), 7.50-7.46 (m, 2H), 7.10-7.05 (m, 2H), 4.67 (dd, *J* = 4.2, 12.7 Hz, 1H), 4.54 (dd, *J* = 10.1, 12.7 Hz, 1H), 3.87 (dt, *J* = 4.2, 10.4 Hz, 1H), 2.74 (ddd, *J* = 2.2, 4.2, 10.7 Hz 1H), 1.70 (heptd, *J* = 4.1, 7.1 Hz 1H), 1.11 (d, *J* = 7.2 Hz, 3H), 0.87 (d, *J* = 7.0 Hz, 3H).

^{13}C NMR (126 MHz, $CDCl_3$): δ 204.0, 136.3, 132.5 (×2), 129.8 (×2), 122.2, 78.8, 58.7, 41.6, 28.1, 21.8, 17.1.

HPLC: Daicel Chiralpak IC column, hexane/*i*-PrOH (90:10), flow rate 0.8 mL min^{-1}, 214 nm. t_R major = 27.6 min, t_R minor = 26.0 min.

(2*R*,3*S*)-3-(2-Bromophenyl)-2-isopropyl-4-nitrobutanal (9hc)

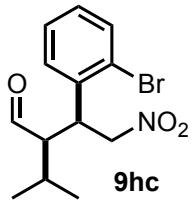

9hc

The title compound was prepared from 1-bromo-2-(2-nitrovinyl)-benzene and isovaleraldehyde according to **General Procedure C** in 96% yield (45.1 mg, 0.144 mmol after 11.5 h (dr 98:2, >99% ee).

$[\alpha]_D^{25}$ ($CHCl_3$, *c* 0.1) +68.5.

IR (ATR): ν = 3062, 2962, 2740, 1716, 1549, 1471, 1432, 1376, 1023, 756, 452 cm^{-1}.

Major diastereomer:

^{1}H NMR (500 MHz, $CDCl_3$): δ 9.92 (d, *J* = 2.0 Hz, 1H), 7.63-7.59 (m, 1H), 7.30 (td, *J* = 1.3, 7.5 Hz, 1H), 7.19-7.13 (m, 2H), 4.92-4.79 (m, 1H), 4.65 (dd, *J* = 4.2, 12.7 Hz, 1H), 4.43 (bs, 1H), 3.10 (bs, 1H), 1.79 (quintd, *J* = 4.8, 7.1 Hz 1H), 1.18 (d, *J* = 7.1 Hz, 3H), 0.92 (d, *J* = 6.9 Hz, 3H).

^{13}C NMR (126 MHz, $CDCl_3$): δ 204.3, 136.4, 134.2, 129.6 (×2), 128.2 (×2), 77.4, 57.9, 40.9, 28.5, 21.8, 18.2.

Note: the broad peaks observed in ^{13}C NMR could only be resolved in DMSO at 373 K.

^{1}H NMR (500 MHz, DMSO-d_6, 373 K): δ 9.84 (d, *J* = 2.7 Hz, 1H), 7.63 (dd, *J* = 1.3, 8.0 Hz, 1H), 7.48 (dd, J = 1.7, 7.8 Hz, 1H), 7.39 (td, J = 1.3, 7.4 Hz, 1H), 7.22 (ddd, *J* = 1.7, 7.3, 8.0 Hz, 1H), 4.90 (dd, *J* = 9.0, 13.3 Hz, 1H), 4.89 (dd, *J* = 5.5, 13.3 Hz, 1H), 4.43 (dt, *J* = 5.5, 9.2 Hz, 1H), 2.90 (ddd, *J* = 2.7, 4.8, 9.4 Hz, 1H), 1.72 (heptd, *J* = 4.8, 7.0 Hz, 1H), 1.07 (d, *J* = 7.1 Hz, 3H), 0.87 (d, *J* = 6.9 Hz, 3H).

^{13}C NMR (126 MHz, DMSO-d_6, 373 K): δ 203.7, 137.0, 132.8, 128.9, 128.8, 127.6, 124.1, 77.2, 57.9, 40.2, 26.8, 20.6, 17.5.

HRMS (ESI) Calculated mass for $C_{13}H_{16}BrNNaO_3$: $[M+Na]^+$ 336.0206, found 336.0195.

HPLC: Daicel Chiralpak IC column, hexane/*i*-PrOH (95:5), flow rate 0.6 mL min^{-1}, 214 nm. t_R major = 27.6 min, t_R minor = 25.6 min.

(3*R*)-2,2-Dimethyl-4-nitro-3-phenylbutanal (9ia)

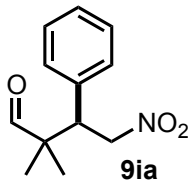

9ia

The title compound was prepared from (*E*)-β-nitrostyrene and isobutyraldehyde according to **General Procedure D** in 98% yield (45.6 mg, 0.205 mmol) after 28 h (66% ee). All spectroscopic data matched those reported in the literature.[16]

^{1}H NMR (500 MHz, $CDCl_3$): δ 9.53 (s, 1H), 7.37-7.25 (m, 3H), 7.22-7.17 (m, 2H), 4.85 (dd, *J* = 11.2, 13.1 Hz, 1H), 4.69 (dd, *J* = 4.2, 13.1 Hz, 1H), 3.78 (dd, *J* = 4.2, 11.2 Hz, 1H), 1.14 (s, 3H), 1.01 (s, 3H).

^{13}C NMR (126 MHz, $CDCl_3$): δ 204.4, 135.5, 129.2 (×2), 128.9 (×2), 128.3, 76.5, 48.7, 48.4, 21.9, 19.1.

HPLC: Daicel Chiralpak IC column, hexane/*i*-PrOH (90:10), flow rate 1.0 mL min^{-1}, 214 nm. t_R major = 25.2 min, t_R minor = 41.4 min.

(3*R*)-3-(4-Bromophenyl)-2,2-dimethyl-4-nitrobutanal (9ib)

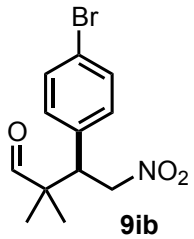

9ib

The title compound was prepared from trans-1-bromo-4-(2-nitrovinyl) benzene and isobutyraldehyde according to **General Procedure D** in 93% yield (59.1 mg, 0.2 mmol) after 28 h (72% ee). All spectroscopic data matched those reported in the literature.[15]

^{1}H NMR (500 MHz, $CDCl_3$): δ 9.50 (s, 1H), 7.49-7.44 (m, 2H), 7.11-7.07 (m, 2H), 4.82 (dd, *J* = 11.4, 13.1 Hz, 1H), 4.69 (dd, *J* = 4.1, 13.2 Hz, 1H), 3.75 (dd, *J* = 4.1, 11.4 Hz, 1H), 1.12 (s, 3H), 1.02 (s, 3H).

^{13}C NMR (126 MHz, $CDCl_3$): δ 203.9, 134.7, 132.1 (×2), 130.9 (×2), 122.4, 76.2, 48.3, 48.1, 21.9, 19.1.

HPLC: Daicel Chiralpak IC column, hexane/*i*-PrOH (90:10), flow rate 1.0 mL min^{-1}, 214 nm. t_R major = 24.5 min, t_R minor = 41.5 min.

9. Physical and spectroscopic data of the Michael adducts prepared during the generation of the library of compounds

(2*R*,3*S*)-3-(2-Furyl)-2-ethyl-4-nitrobutanal (9bg)

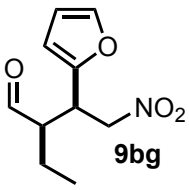

9bg

Title compound was prepared from (*E*)-2-(2-nitrovinyl)furan and butyraldehyde as specified in section 6 of this Supporting Information. All spectroscopic data matched those reported in the literature.[17]

^{1}H NMR (500 MHz, $CDCl_3$): δ 9.72 (d, *J* = 1.8 Hz, 1H), 7.36 (dd, *J* = 0.8, 1.9 Hz, 1H), 6.31 (dd, *J* = 1.8, 3.3 Hz, 1H), 6.20 (d, *J* = 3.3 Hz, 1H), 4.70 (dd, *J* = 9.0, 12.8 Hz, 1H), 4.66 (dd, *J* = 5.3, 12.8 Hz, 1H), 4.01 (dt, *J* = 5.3, 8.8 Hz, 1H), 2.76 (dddd, *J* = 1.8, 5.3, 7.2, 8.8 Hz, 1H), 1.63-1.52 (m, 2H), 0.90 (t, *J* = 7.5 Hz, 3H).

^{13}C NMR (126 MHz, $CDCl_3$): δ 202.5, 150.2, 142.8, 110.6, 109.0, 76.3, 53.6, 36.7, 20.2, 11.1.

HPLC: Daicel Chiralpak IC column, hexane/*i*-PrOH (90:10), flow rate 1.0 mL min^{-1}, 210 nm. t_R major = 35.7 min, t_R minor = 27.0 min.

(2*R*,3*S*)-3-(4-Bromophenyl)-2-ethyl-4-nitrobutanal (9bb)

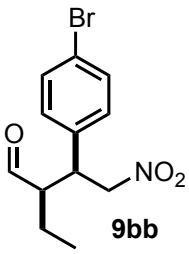

9bb

Title compound was prepared from 1-bromo-4-(2-nitrovinyl)-benzene and butyraldehyde as specified in section 6 of this Supporting Information. All spectroscopic data matched those reported in the literature.[18]

^{1}H NMR (500 MHz, $CDCl_3$): δ 9.71 (d, *J* = 2.3 Hz, 1H), 7.50-7.46 (m, 2H), 7.09-7.05 (m, 2H), 4.72 (dd, *J* = 4.8, 12.8 Hz, 1H), 4.59 (dd, *J* = 10.0, 12.8 Hz, 1H), 3.77 (dt, *J* = 4.8, 10.0 Hz, 1H), 2.66 (dddd, *J* = 2.3, 4.2, 8.3, 10.0 Hz, 1H), 1.57-1.44 (m, 2H), 0.84 (t, *J* = 7.5 Hz, 3H).

^{13}C NMR (126 MHz, $CDCl_3$): δ 202.8, 136.0, 132.5 (×2), 129.8 (×2), 122.3, 78.4, 54.8, 42.2, 20.5, 10.7.

HPLC: Daicel Chiralpak IC column, hexane/*i*-PrOH (95:5), flow rate 0.6 mL min^{-1}, 214 nm. t_R major = 85.6 min, t_R minor = 81.1 min.

(2*R*,3*S*)-3-(4-Bromophenyl)-2-propyl-4-nitrobutanal (9cb)

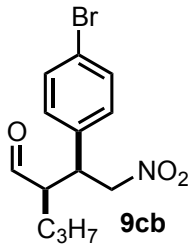

9cb

Title compound was prepared from 1-bromo-4-(2-nitrovinyl)-benzene and *n*-pentanal as specified in section 6 of this Supporting Information. All spectroscopic data matched those reported in the literature.[19]

^{1}H NMR (500 MHz, $CDCl_3$): δ 9.70 (d, *J* = 2.5 Hz, 1H), 7.50-7.46 (m, 2H), 7.08-7.05 (m, 2H), 4.69 (dd, *J* = 4.9, 12.9 Hz, 1H), 4.61 (dd, *J* = 9.8, 12.9 Hz, 1H), 3.75 (dt, *J* = 4.9, 9.8 Hz, 1H), 2.71-2.66 (m, 1H), 1.51-1.43 (m, 1H), 1.40-1.27 (m, 2H), 1.23-1.12 (m, 1H), 0.84 (t, *J* = 7.1 Hz, 3H).

^{13}C NMR (126 MHz, $CDCl_3$): δ 202.9, 136.0, 132.5 (×2), 129.8 (×2), 122.3, 78.3, 53.7, 42.7, 29.6, 19.8, 14.1.

HPLC: Daicel Chiralpak IC column, hexane/*i*-PrOH (95:5), flow rate 0.6 mL min^{-1}, 214 nm. t_R major = 49.4 min, t_R minor = 46.6 min.

(2*R*,3*S*)-3-(3-Chlorophenyl)-2-methyl-4-nitrobutanal (9ak)[20]

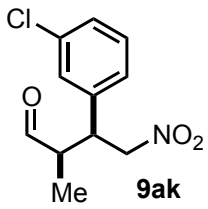

9ak

Title compound was prepared from 1-chloro-3-(2-nitrovinyl)-benzene and propionaldehyde as specified in section 6 of this Supporting Information.

$[\alpha]_D^{25}$ ($CHCl_3$, *c* 0.1) –22.9.

^{1}H NMR (500 MHz, $CDCl_3$): δ 9.70 (d, *J* = 1.5 Hz, 1H), 7.31-7.26 (m, 2H), 7.20-7.15 (m, 1H), 7.09-7.04 (m, 1H), 4.80 (dd, *J* = 5.2, 12.9 Hz, 1H), 4.66 (dd, *J* = 9.5, 12.9 Hz, 1H), 3.79 (dt, *J* = 5.2, 9.3 Hz, 1H), 2.77 (dqd, *J* = 1.5, 7.3, 8.9 Hz 1H), 0.87 (d, *J* = 7.3 Hz, 3H).

^{13}C NMR (126 MHz, $CDCl_3$): δ 201.8, 139.3, 135.1, 130.5, 128.6, 128.4, 126.5, 77.9, 48.4, 43.9, 12.4.

HPLC: Daicel Chiralpak IC column, hexane/*i*-PrOH (90:10), flow rate 1.0 mL min^{-1}, 210 nm. t_R major = 35.9 min, t_R minor = 31.4 min.

HRMS (ESI) Calculated mass for $C_{11}H_{11}ClNO_3$: $[M–H]^-$ 240.0433, found 240.0432.

(2*R*,3*S*)-3-(4-Fluorophenyl)-2-methyl-4-nitrobutanal (9al)

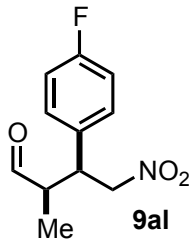

9al

Title compound was prepared from 1-fluoro-4-(2-nitrovinyl)-benzene and propionaldehyde as specified in section 6 of this Supporting Information. All spectroscopic data matched those reported in the literature.[21]

^{1}H NMR (500 MHz, $CDCl_3$): δ 9.71 (d, *J* = 1.6 Hz, 1H), 7.17-7.12 (m, 2H), 7.07-7.01 (m, 2H), 4.79 (dd, *J* = 5.3, 12.7 Hz, 1H), 4.64 (dd, *J* = 9.6, 12.9 Hz, 1H), 3.81 (dt, *J* = 5.3, 9.3 Hz, 1H), 2.75 (dqd, *J* = 1.6, 7.3, 8.9 Hz 1H), 1.01 (d, *J* = 7.3 Hz, 3H).

^{13}C NMR (126 MHz, $CDCl_3$): δ 202.1, 162.5 (d, *J* = 247.4 Hz), 132.5 (d, *J* = 3.4 Hz), 129.8 (×2, d, *J* = 8.1 Hz), 116.2 (×2, d, *J* = 21.5 Hz), 78.3, 48.6, 43.5, 12.3.

^{19}F NMR (376 MHz, $CDCl_3$): –113.8 (tt, *J* = 5.1, 8.3 Hz).

HPLC: Daicel Chiralpak IC column, hexane/*i*-PrOH (80:20), flow rate 0.6 mL min^{-1}, 210 nm. t_R major = 38.1 min, t_R minor = 34.0 min.

10. Physical and spectroscopic data for pyrrolidine derivatives 10 and 11

(3*S*,4*R*)-3-Methyl-4-phenylpyrrolidine (10a)

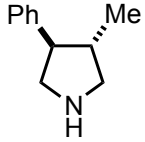

10a

Reaction performed with **9aa** (475 mg, 2.29 mmol, dr 94:6, 95% ee).

The final compound was isolated as a yellow oil in 83% yield (306.2 mg, 1.9 mmol, dr 92:8).

$[\alpha]_D^{25}$ ($CHCl_3$, *c* 0.1) +59.5.

Major diastereomer:

^{1}H NMR (500 MHz, $CDCl_3$): δ 7.33-7.27 (m, 2H), 7.24-7.17 (m, 3H), 3.41 (dd, *J* = 7.9, 10.5 Hz, 1H), 3.34 (dd, *J* = 7.9, 10.5 Hz, 1H), 3.01 (t, *J* = 10.1 Hz, 1H), 2.83-2.73 (m, 1H), 2.71-2.64 (m, 2H), 2.27-2.17 (m, 1H), 1.01 (d, *J* = 6.6 Hz, 3H).

^{13}C NMR (126 MHz, $CDCl_3$): δ 142.8, 128.6 (×2), 127.7 (×2), 126.5, 55.5, 55.3, 54.4, 43.1, 17.1.

HRMS (ESI) Calculated mass for $C_{11}H_{16}N$: $[M+H]^+$ 162.1277, found 162.1275.

(3*S*,4*R*)-*N*-Tosyl-3-methyl-4-phenylpyrrolidine (11a)

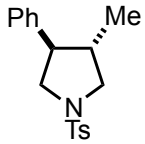

11a

Reaction performed with **10a** (250 mg, 1.55 mmol, dr 92:8).

Final compound was isolated as a yellow oil in 88% yield (429 mg, 1.36 mmol, dr 91:9, 94% ee). All spectroscopic data matched those reported in the literature.[22]

Major diastereomer:

^{1}H NMR (500 MHz, $CDCl_3$): δ 7.77-7.73 (m, 2H), 7.37-7.34 (m, 2H), 7.30-7.26 (m, 2H), 7.25-7.20 (m, 1H), 7.10-7.06 (m, 2H), 3.75-3.66 (m, 2H), 3.28 (t, *J* = 10.1, 1H), 2.92 (t, *J* = 9.8 Hz, 1H), 2.65 (td, *J* = 8.0, 10.2 Hz, 1H), 2.46 (s, 3H), 2.23-2.10 (m, 1H), 0.87 (d, *J* = 6.5 Hz, 3H).

^{13}C NMR (126 MHz, $CDCl_3$): δ 143.6, 139.3, 134.2, 129.8 (×2), 128.8 (×2), 127.7 (×2), 127.6 (×2), 127.3, 55.1, 55.0, 52.3, 40.9, 21.7, 15.6.

HPLC: Daicel Chiralpak AD-H column, hexane/*i*-PrOH (95:5), flow rate 1.0 mL min^{-1}, 214 nm.

t_R major = 16.9 min, t_R minor = 18.9 min.

(3*S*,4*R*)-3-Methyl-4-(4-bromophenyl)pyrrolidine (10b)

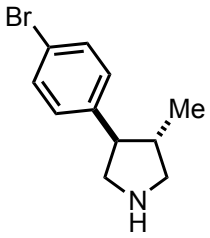

10b

Reaction performed with **9ab** (2.318 g, 8.10 mmol, 95:5 dr, 96% ee).

The final compound was isolated as a yellow oil in 84% yield (1.625 g, 6.77 mmol, dr 90:10).

IR (ATR): ν = 3334, 2957, 2926, 2871, 1638, 1529, 1488, 1404, 1073, 1009, 818, 515 cm^{-1}.

$[\alpha]_D^{25}$ ($CHCl_3$, *c* 0.1) +9.7.

Major diastereomer:

^1H NMR (500 MHz, $CDCl_3$): δ 7.44-7.39 (m, 2H), 7.12-7.09 (m, 2H), 3.38 (dd, *J* = 8.0, 11.0 Hz, 1H), 3.32 (dd, *J* = 7.5, 10.6 Hz, 1H), 2.94 (dd, *J* = 9.0, 11.0 Hz, 1H), 2.66 (dd, *J* = 8.7, 10.6 Hz, 1H), 2.64 (q, *J* = 8.9 Hz, 1H), 2.23-2.09 (m, 2H), 0.99 (d, *J* = 6.6 Hz, 3H).

^{13}C NMR (126 MHz, $CDCl_3$): δ 142.1, 131.7 (×2), 129.4 (×2), 120.1, 55.6, 55.4, 53.9, 43.3, 17.1.

HRMS (ESI+) Calculated mass for $C_{11}H_{15}BrN$ $[M+H]^+$ 240.0382, found 240.0384.

(3*S*,4*R*)-*N*-Tosyl-3-methyl-4-phenylpyrrolidine (11b)

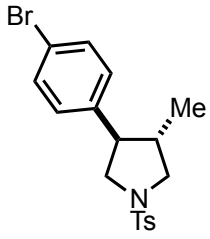

11b

Reaction performed with **10b** (598 mg, 2.5 mmol, dr 90:10).

The final compound was isolated as a yellow oil in 85 % yield (836 mg, 2.12 mmol, dr 90:10, 95% ee).

IR (ATR): ν = 2960, 2927, 2874, 1596, 1488, 1340, 1160, 1090, 1009, 814, 661, 588, 547 cm^{-1}.

$[\alpha]_D^{25}$ ($CHCl_3$, *c* 0.1) +7.6.

Major diastereomer:

^1H NMR (500 MHz, $CDCl_3$): δ 7.76-7.72 (m, 2H), 7.42-7.38 (m, 2H), 7.38-7.34 (m, 2H), 6.98-6.94 (m, 2H), 3.71-3.66 (m, 2H), 3.24 (t, *J* = 10.0, 1H), 2.90 (t, *J* = 9.8 Hz, 1H), 2.62 (td, *J* = 8.1, 10.0 Hz, 1H), 2.46 (s, 3H), 2.13 (tquint, *J* = 6.6, 10.0 Hz, 1H), 1.86 (d, *J* = 6.6 Hz, 3H).

^{13}C NMR (126 MHz, $CDCl_3$): δ 143.7, 134.5, 134.1, 132.0 (×2), 129.9 (×2), 129.3 (×2), 127.7 (×2), 121.1, 55.0, 54.8, 51.7, 41.0, 21.7, 15.6.

HRMS (ESI+) Calculated mass for $C_{18}H_{21}BrNO_2S$ $[M+H]^+$ 394.0471, found 394.0468.

HPLC: Daicel Chiralpak AD-H column, hexane/*i*-PrOH (98:2), flow rate 1.0 mL min^{-1}, 210 nm.

t_R major = 36.7 min, t_R minor = 42.0 min.

11. NMR spectra for intermediates of the preparation of catalyst 2

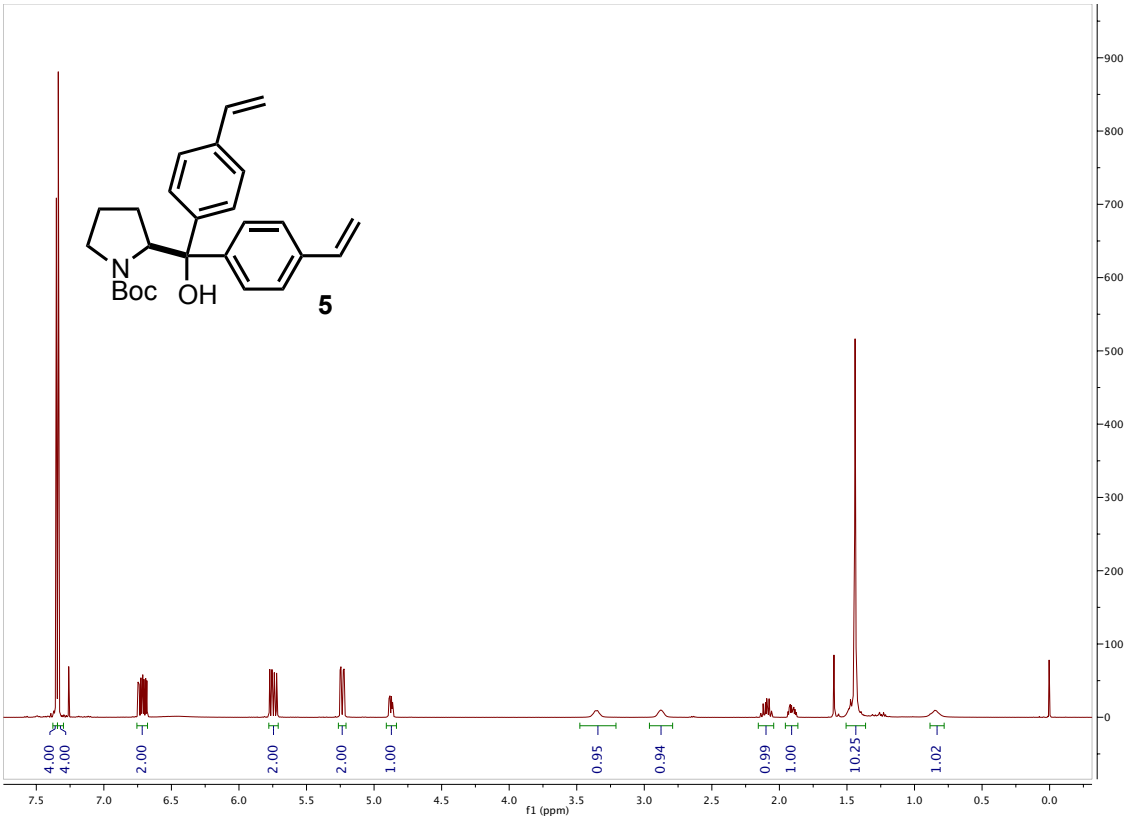

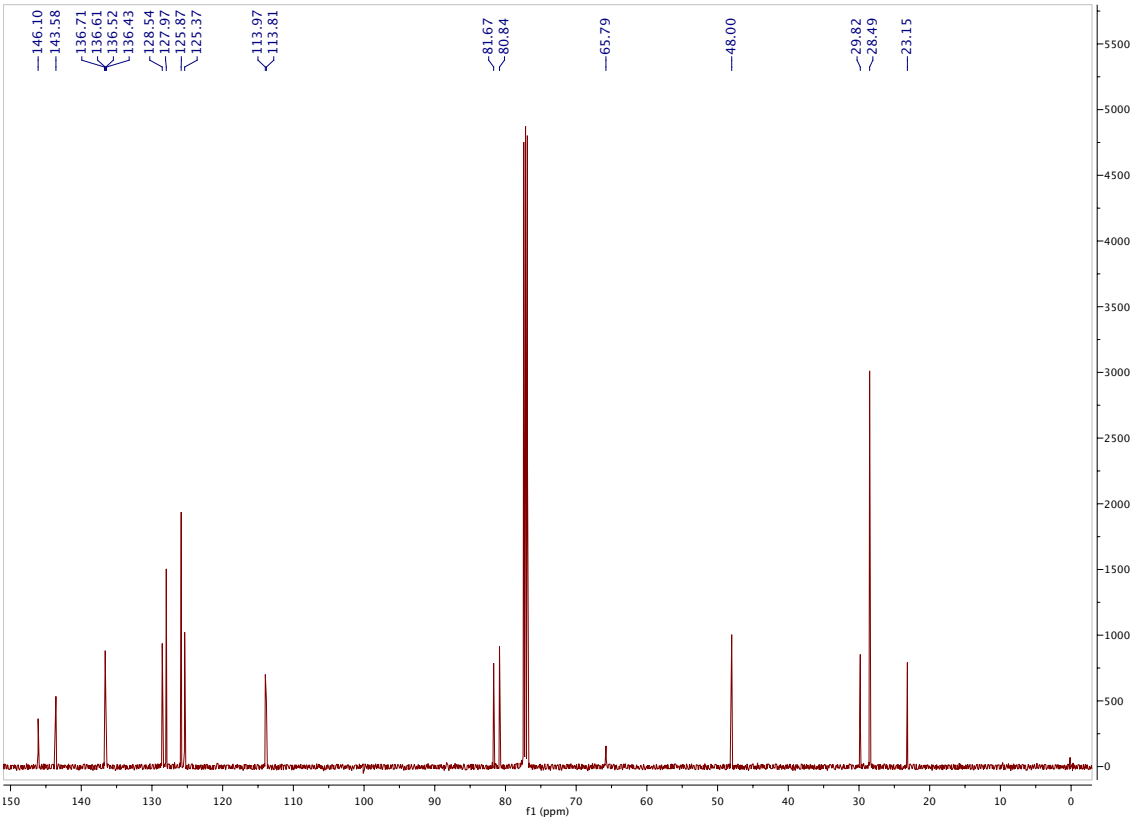

Chapter III

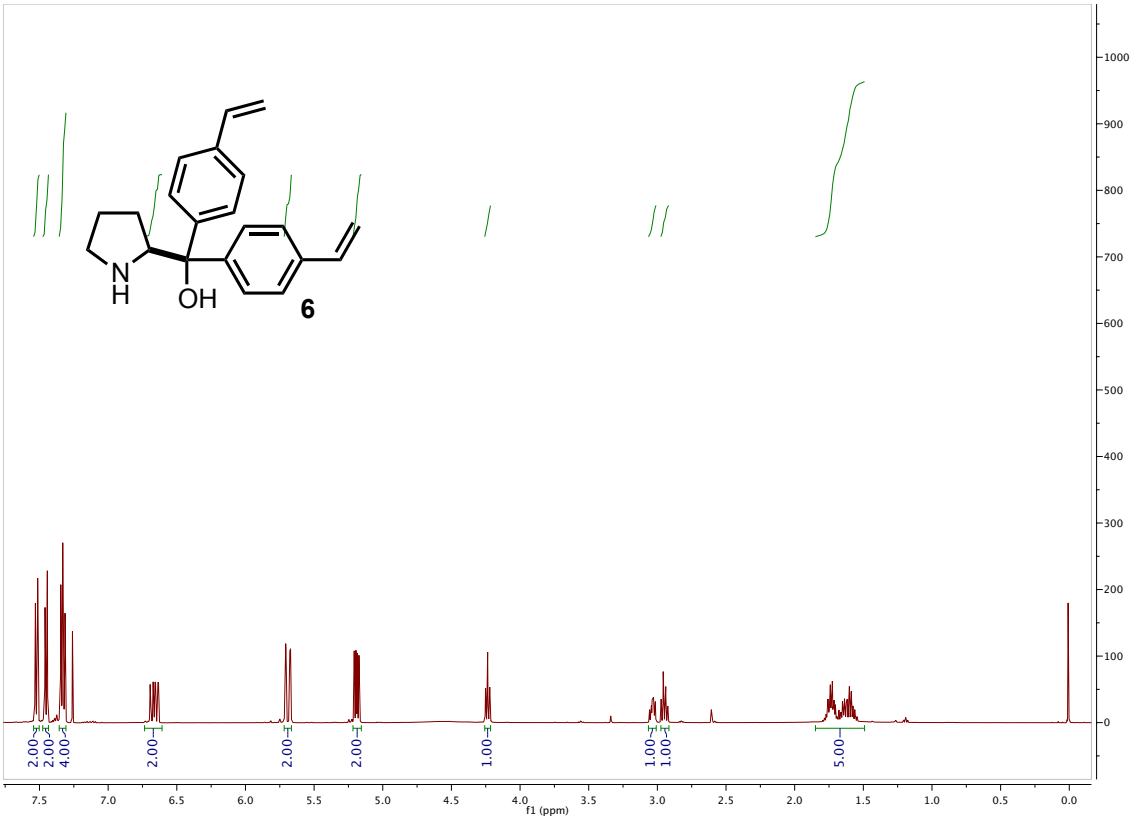
N
H
OH
6
2.00
2.00
4.00
2.00
2.00
2.00
1.00
1.00
1.00
5.00
f1 (ppm)

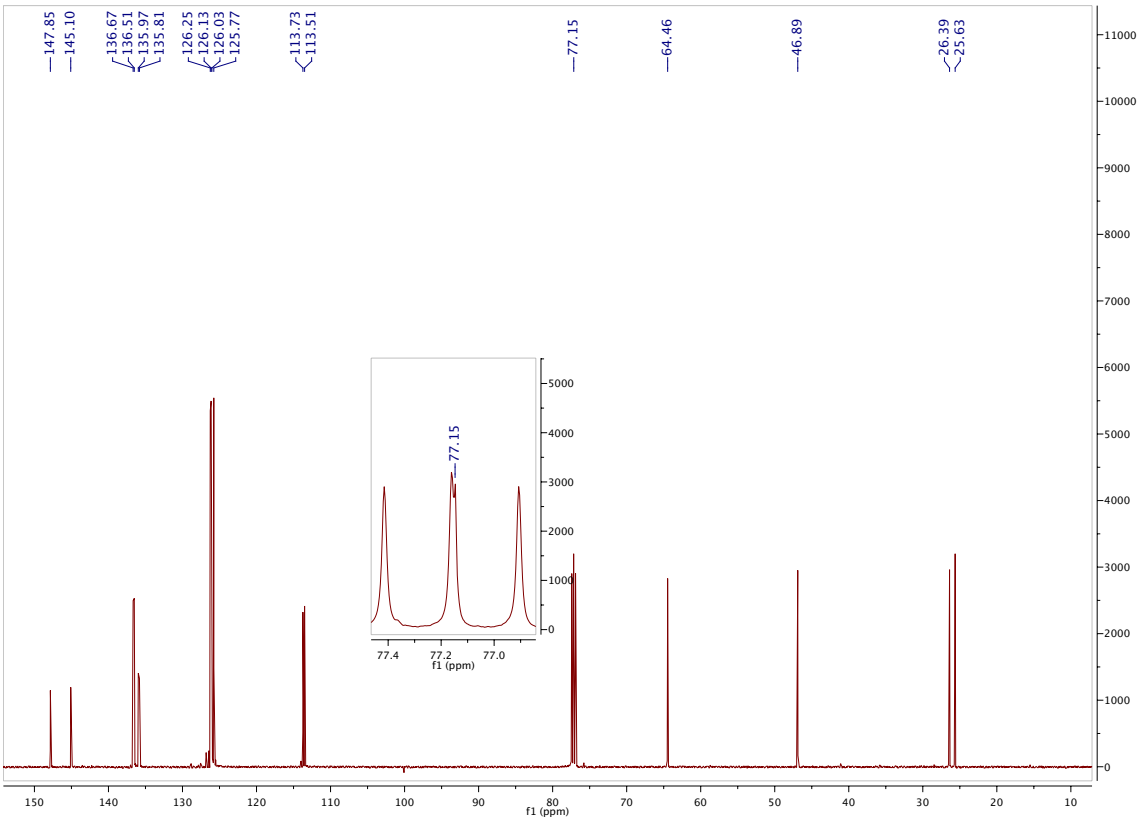
147.85
145.10
136.67
136.51
135.97
135.81
126.25
126.13
126.03
125.77
113.73
113.51
77.15
64.46
46.89
26.39
25.63
77.15
f1 (ppm)

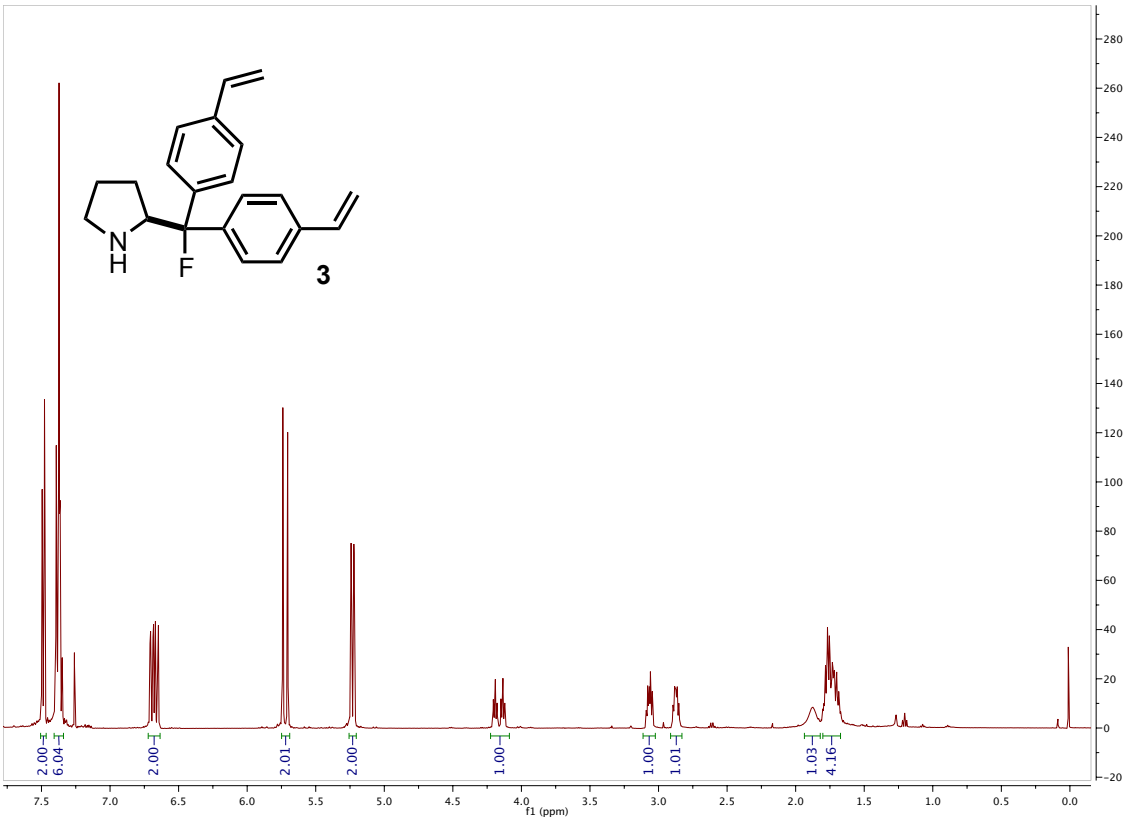
N
H
F
3
2.00
6.04
2.00
2.01
2.00
1.00
1.00
1.01
1.03
4.16
f1 (ppm)

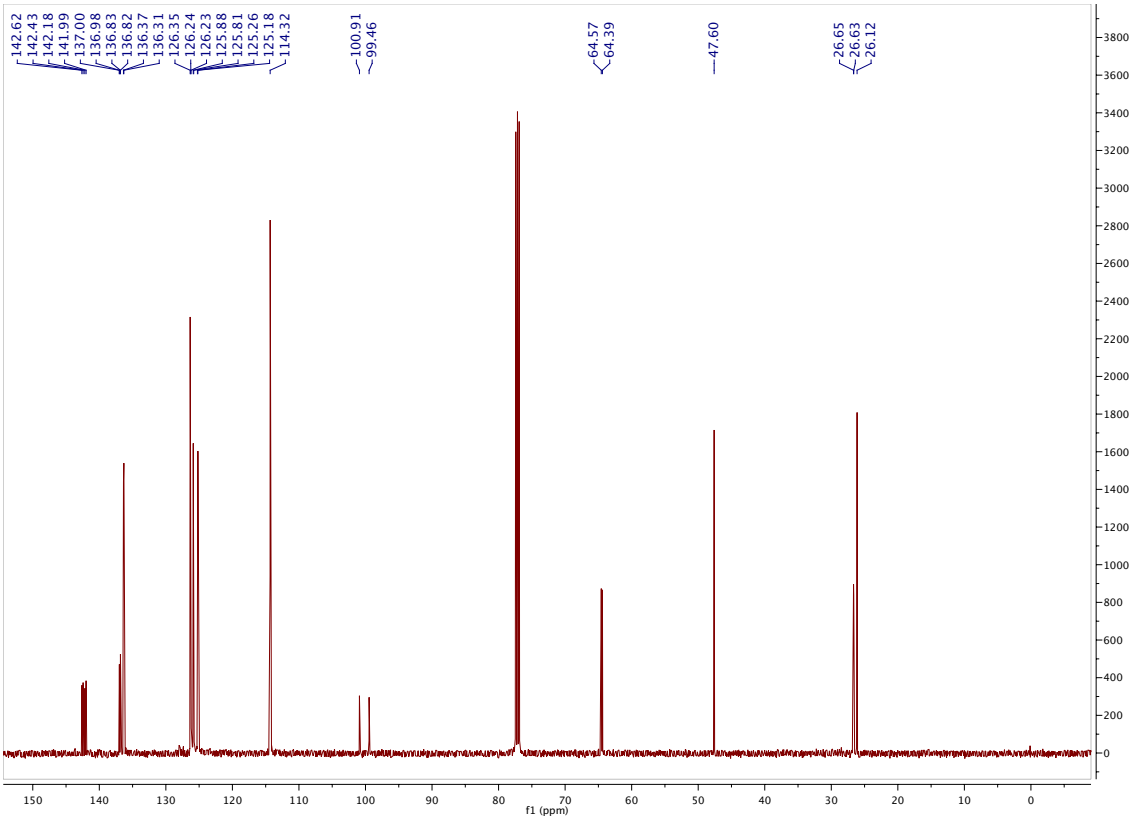
142.62
142.43
142.18
141.99
137.00
136.98
136.83
136.82
136.37
136.31
126.35
126.24
126.23
125.88
125.81
125.26
125.18
114.32
100.91
99.46
64.57
64.39
47.60
26.65
26.63
26.12
f1 (ppm)

Chapter III

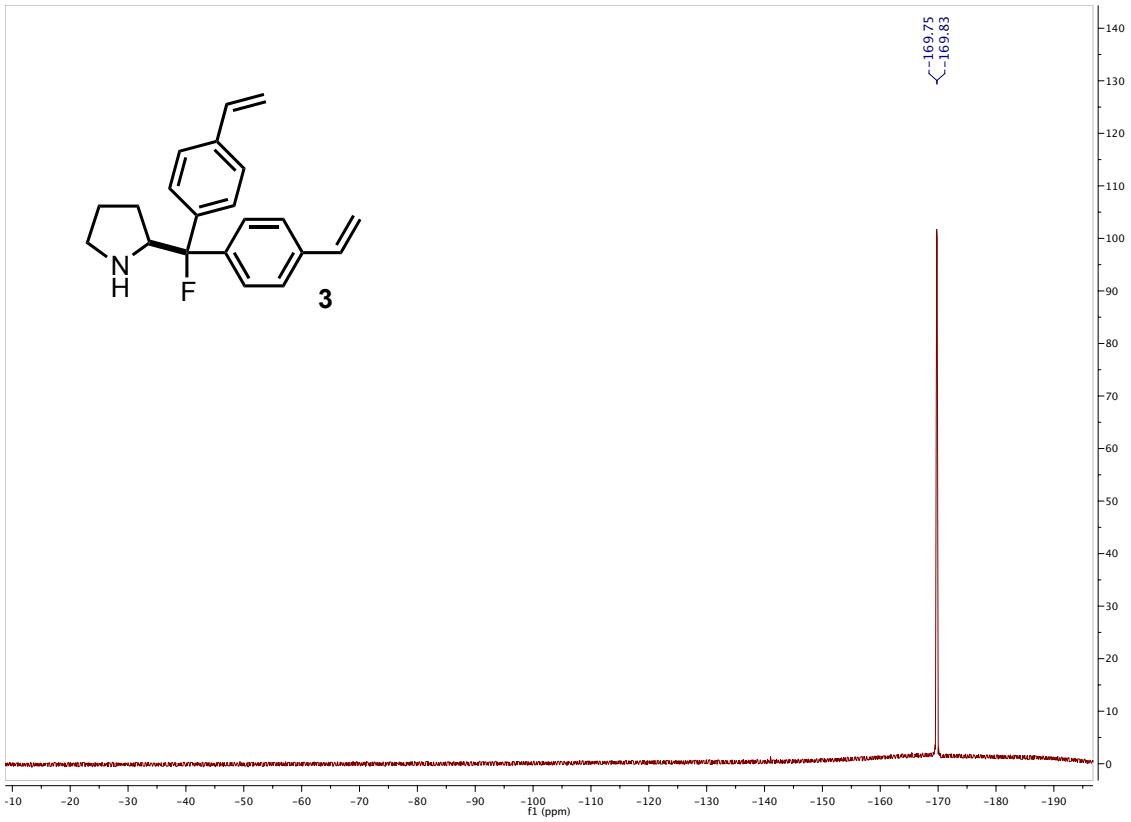

12. NMR spectra for Michael adducts 9

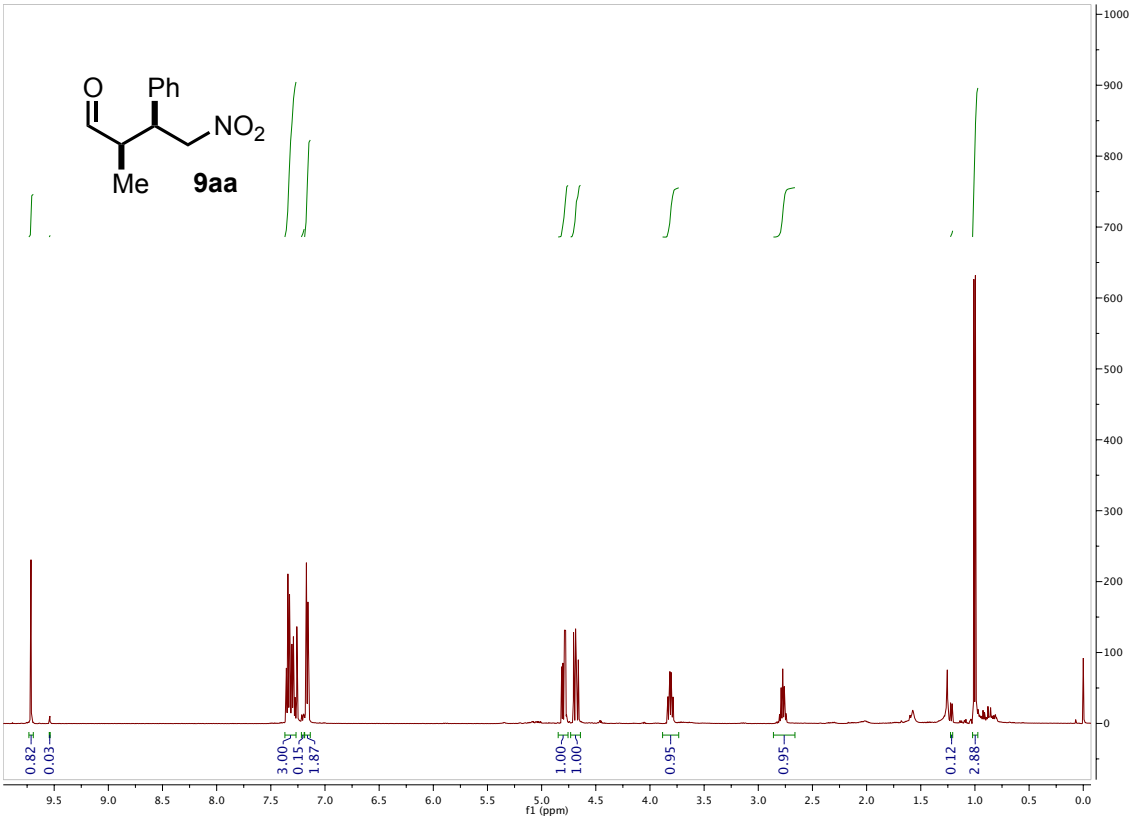

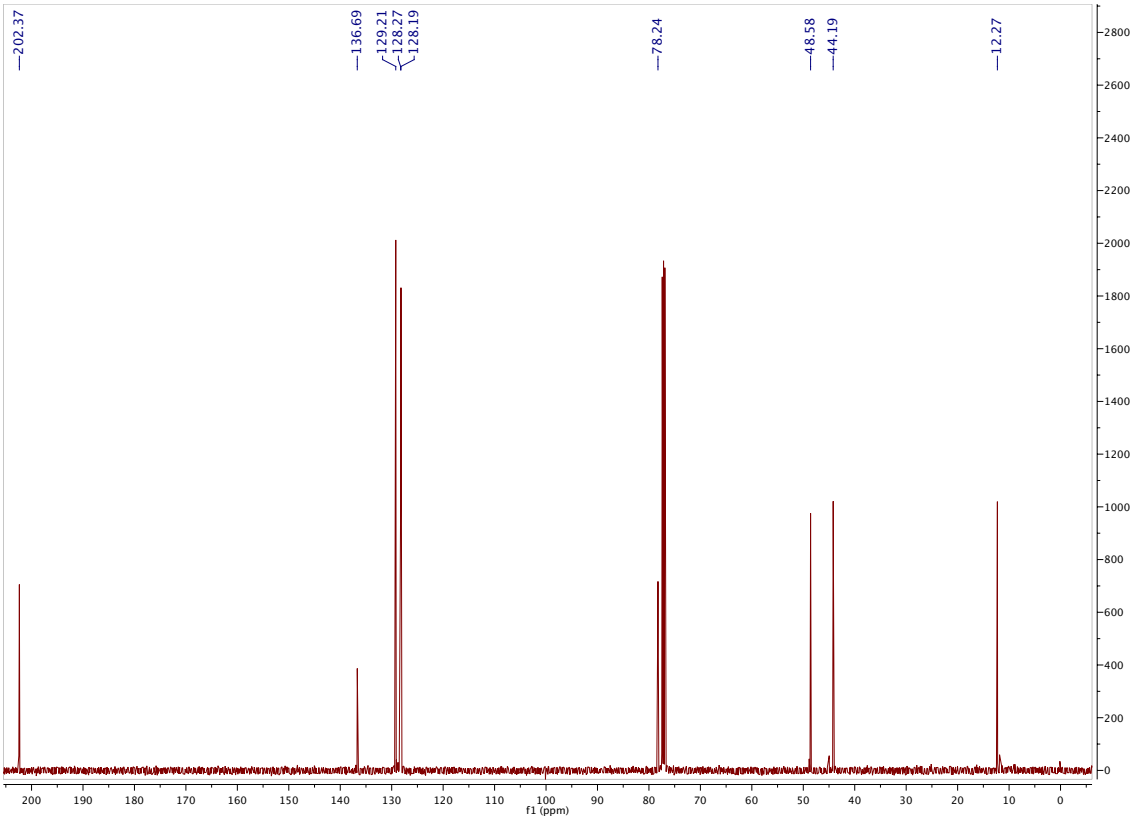

Chapter III

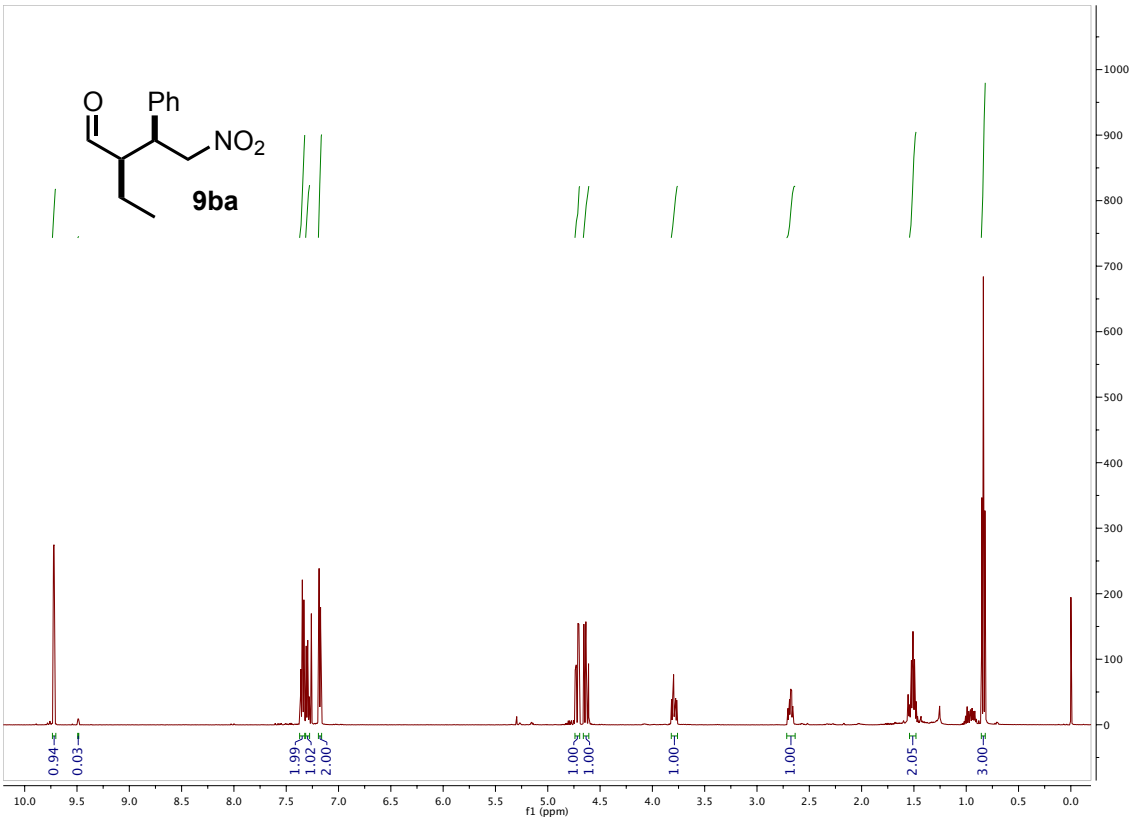
O
Ph
NO2
9ba
0.94
0.03
1.99
1.02
2.00
1.00
1.00
1.00
1.00
2.05
3.00
f1 (ppm)

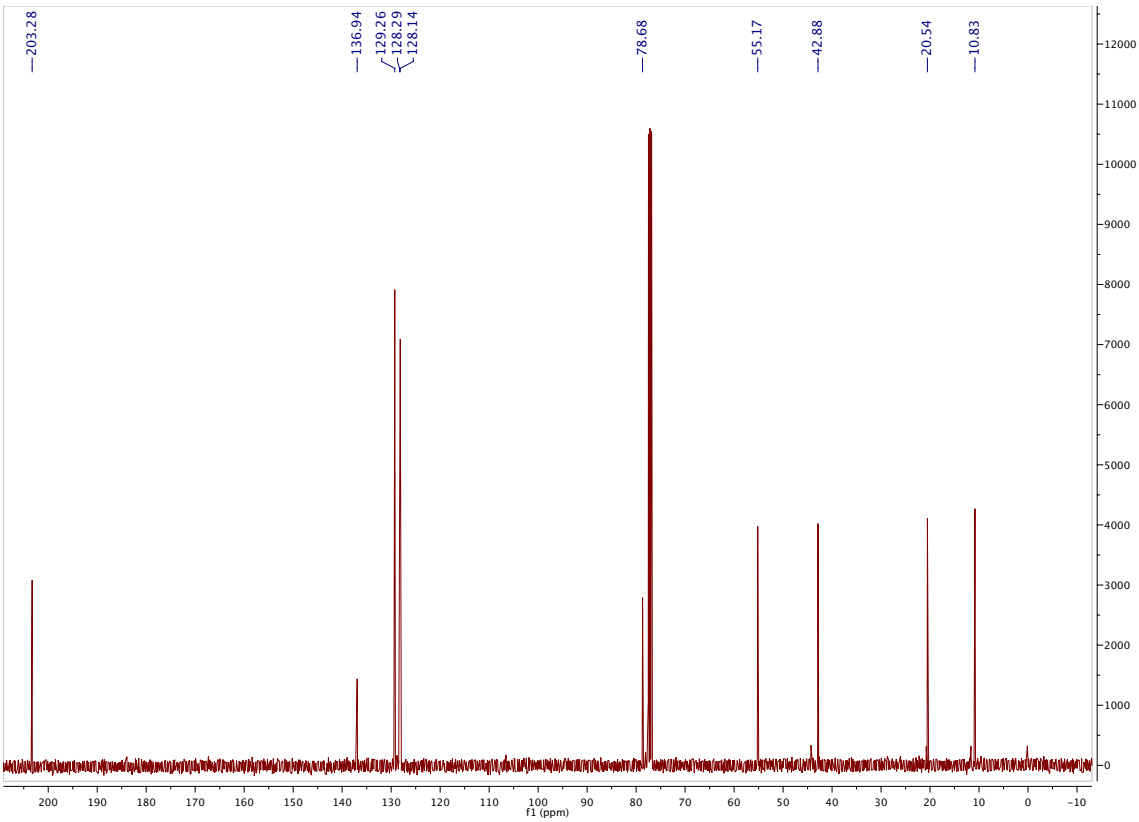
203.28
136.94
129.26
128.29
128.14
78.68
55.17
42.88
20.54
10.83
f1 (ppm)

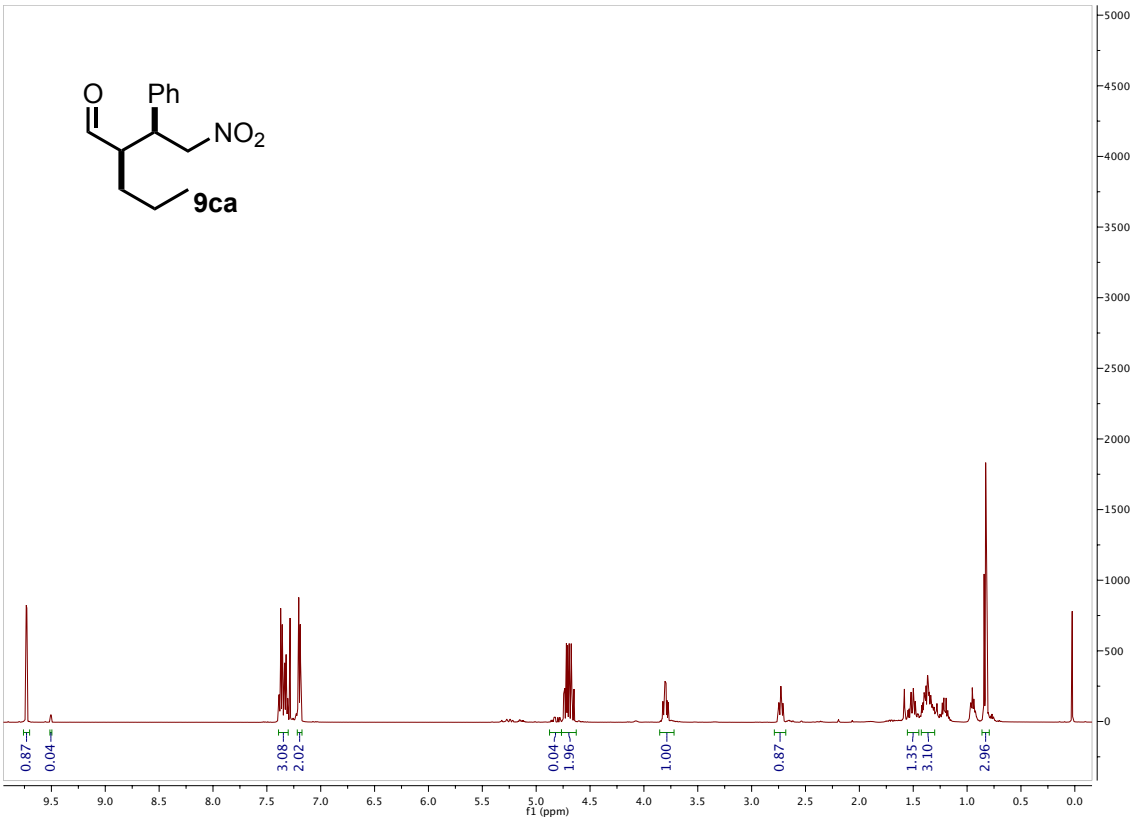
O
Ph
NO2
9ca
0.87
0.04
3.08
2.02
0.04
1.96
1.00
0.87
1.35
3.10
2.96
f1 (ppm)

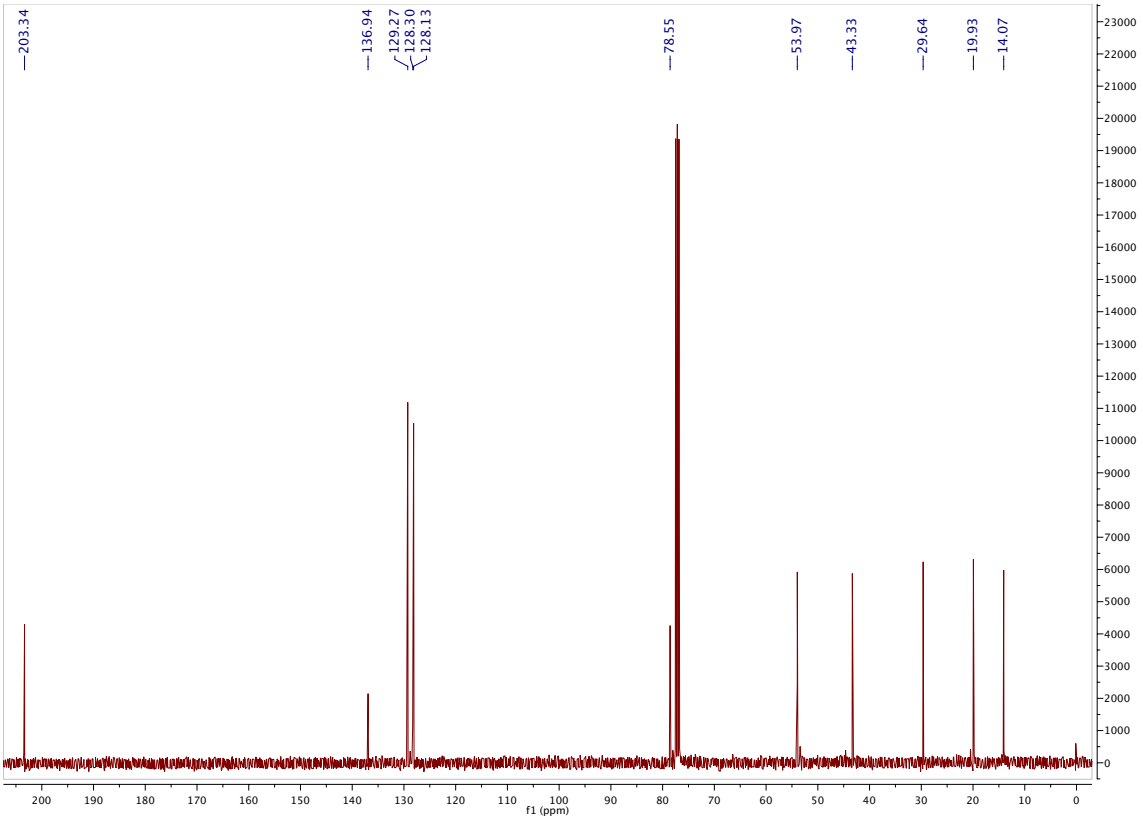
203.34
136.94
129.27
128.30
128.13
78.55
53.97
43.33
29.64
19.93
14.07
f1 (ppm)

Chapter III

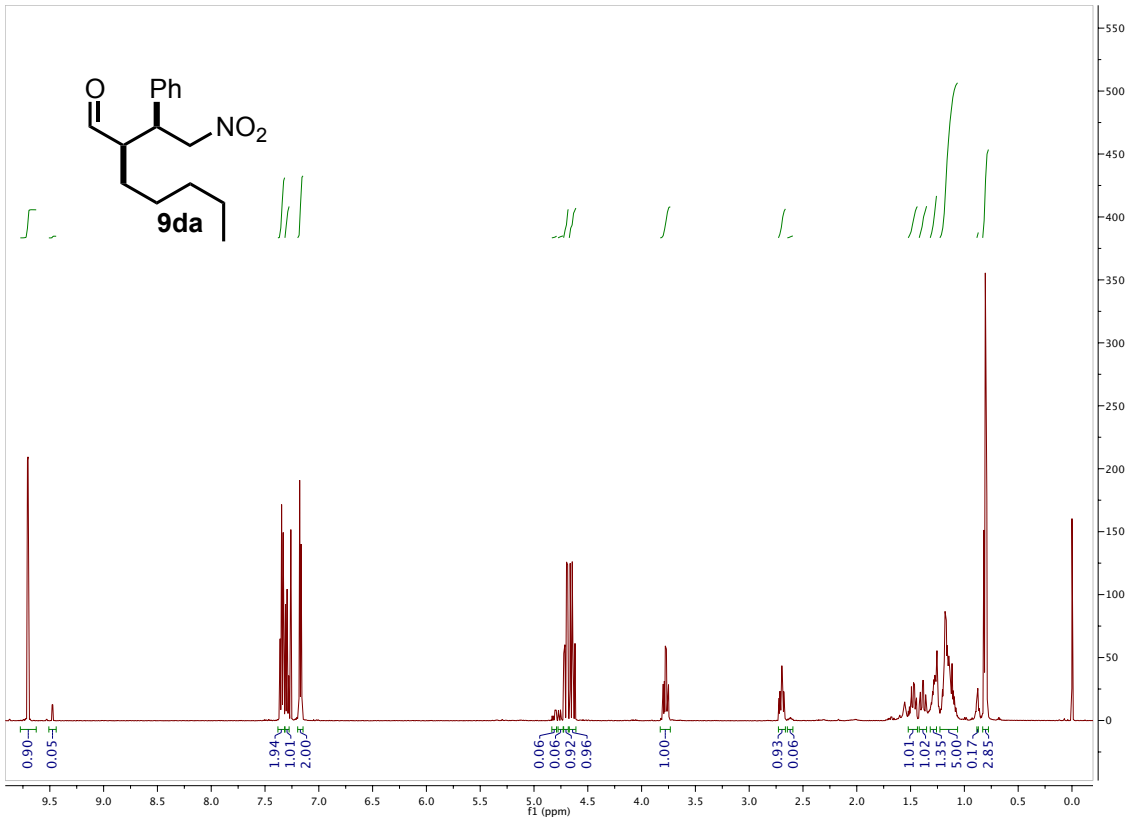
O
Ph
NO2
9da
0.90
0.05
1.94
1.01
2.00
0.06
0.06
0.92
0.96
1.00
0.93
0.06
1.01
1.02
1.35
5.00
0.17
2.85
f1 (ppm)

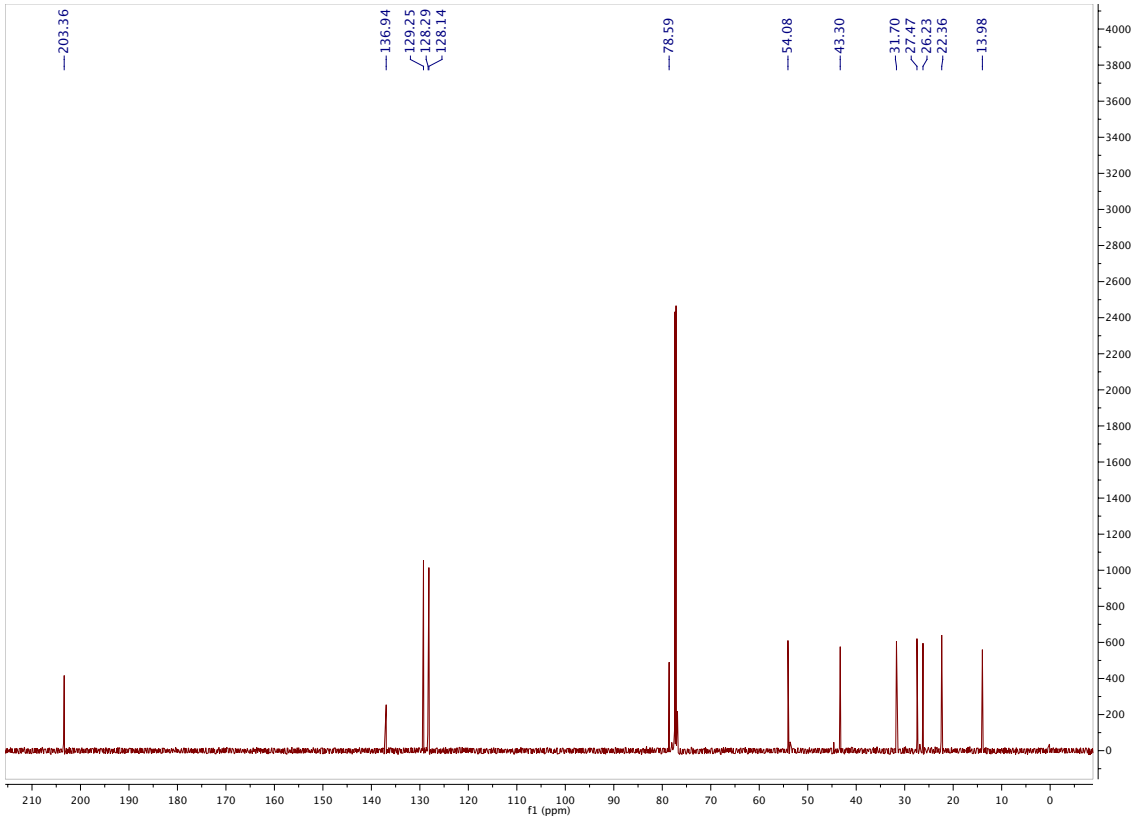
203.36
136.94
129.25
128.29
128.14
78.59
54.08
43.30
31.70
27.47
26.23
22.36
13.98
f1 (ppm)

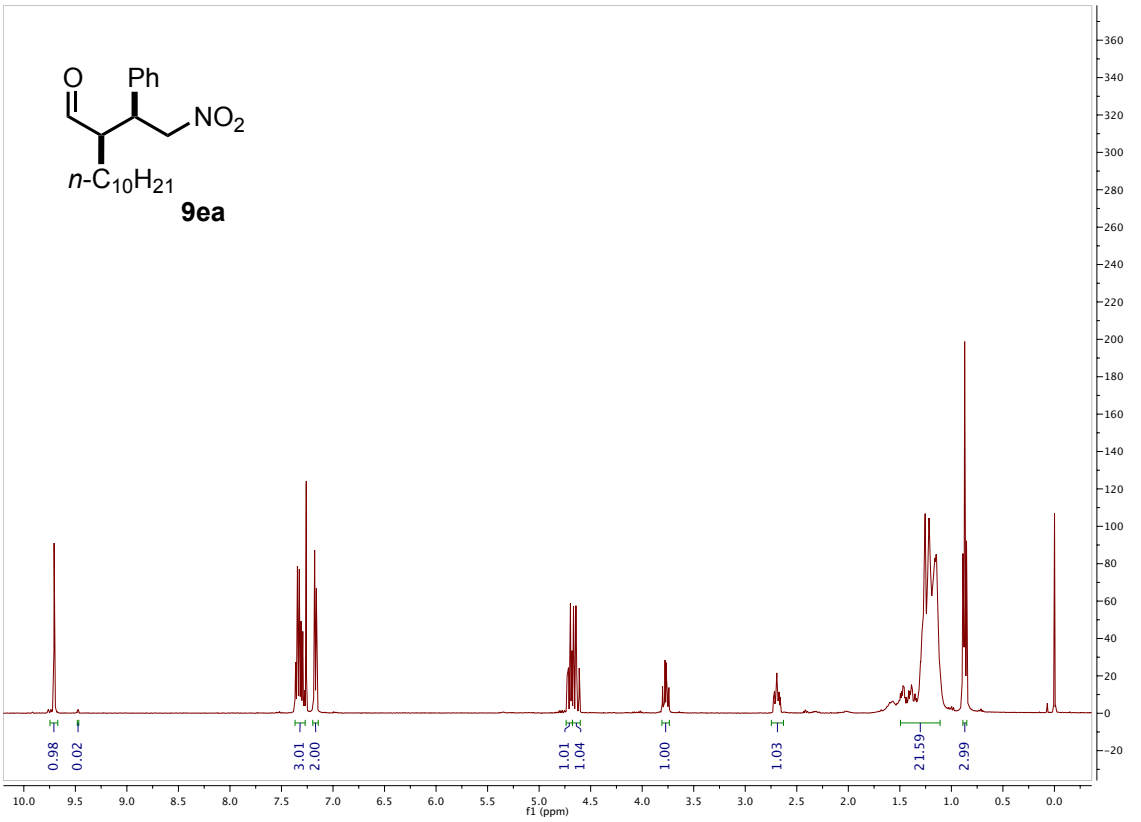
O
Ph
NO2
n-C10H21
9ea
0.98
0.02
3.01
2.00
1.01
1.04
1.00
1.03
21.59
2.99
f1 (ppm)

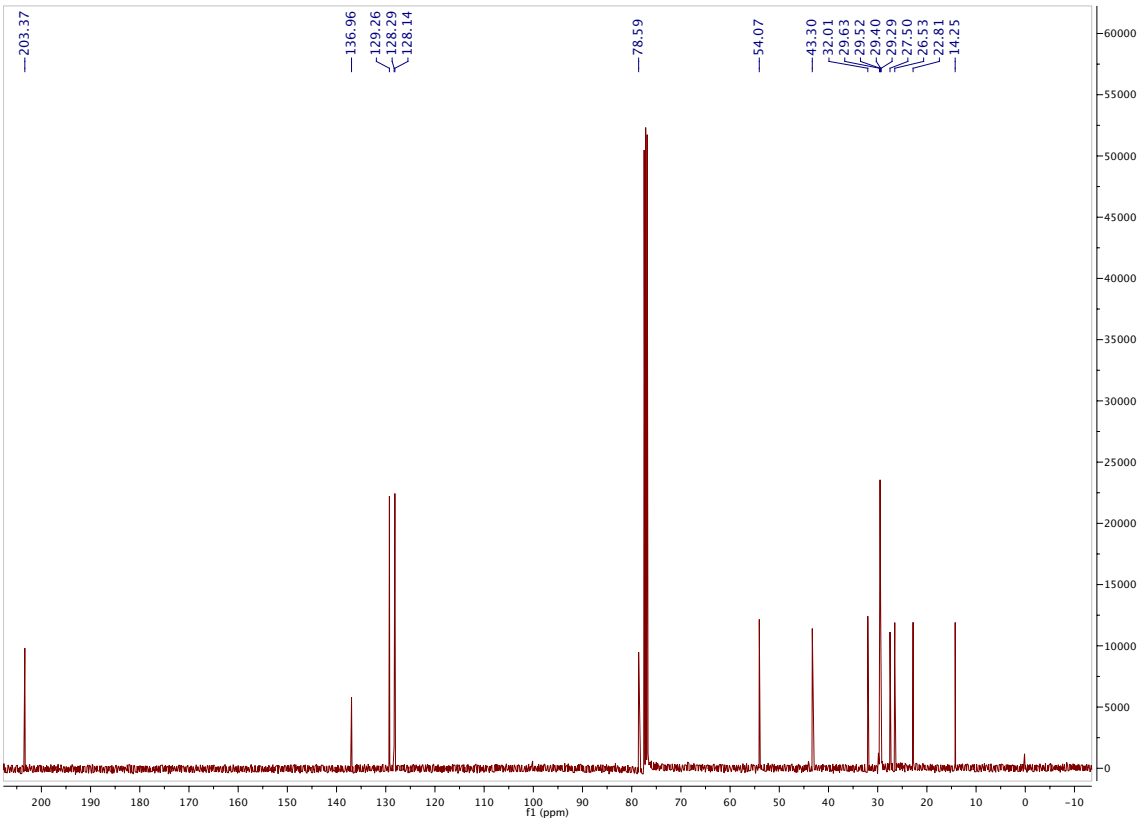
203.37
136.96
129.26
128.29
128.14
78.59
54.07
43.30
32.01
29.63
29.52
29.40
29.29
27.50
26.53
22.81
14.25
f1 (ppm)

Chapter III

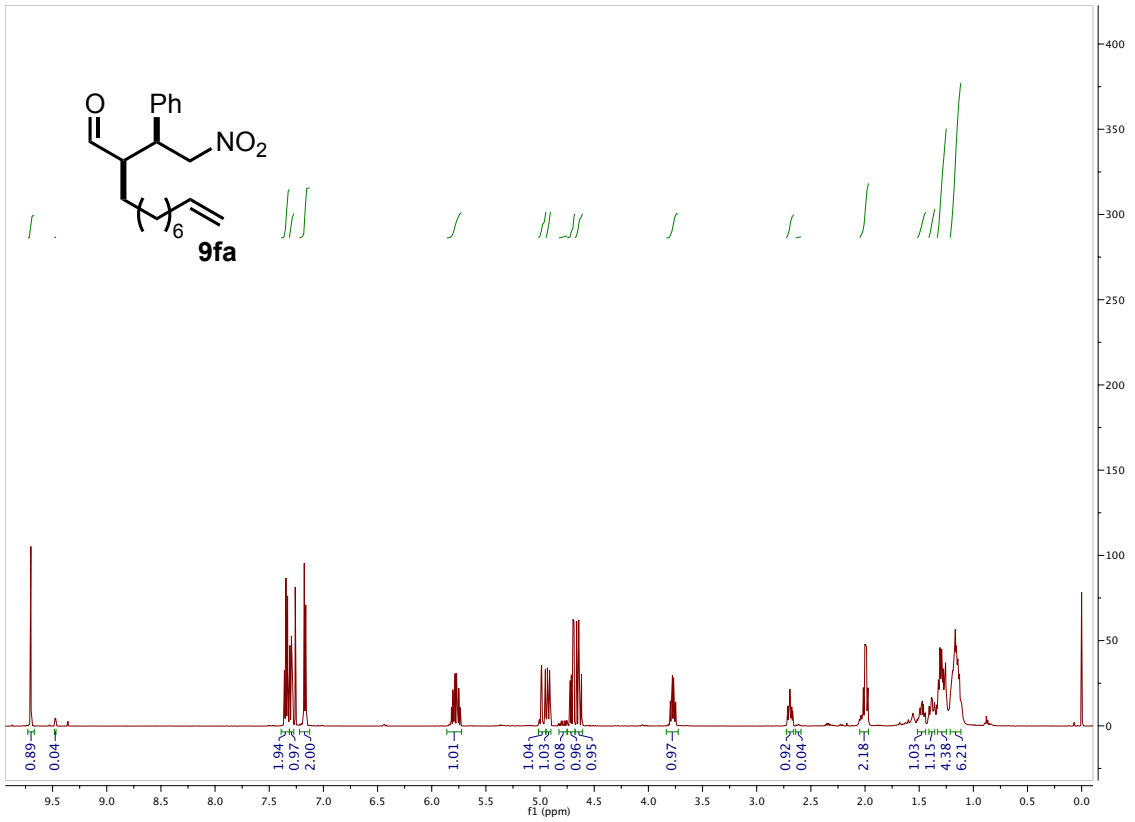
O
Ph
NO2
6
9fa
0.89
0.04
1.94
0.97
2.00
1.01
1.04
1.03
0.08
0.96
0.95
0.97
0.92
0.04
2.18
1.03
1.15
4.38
6.21
f1 (ppm)

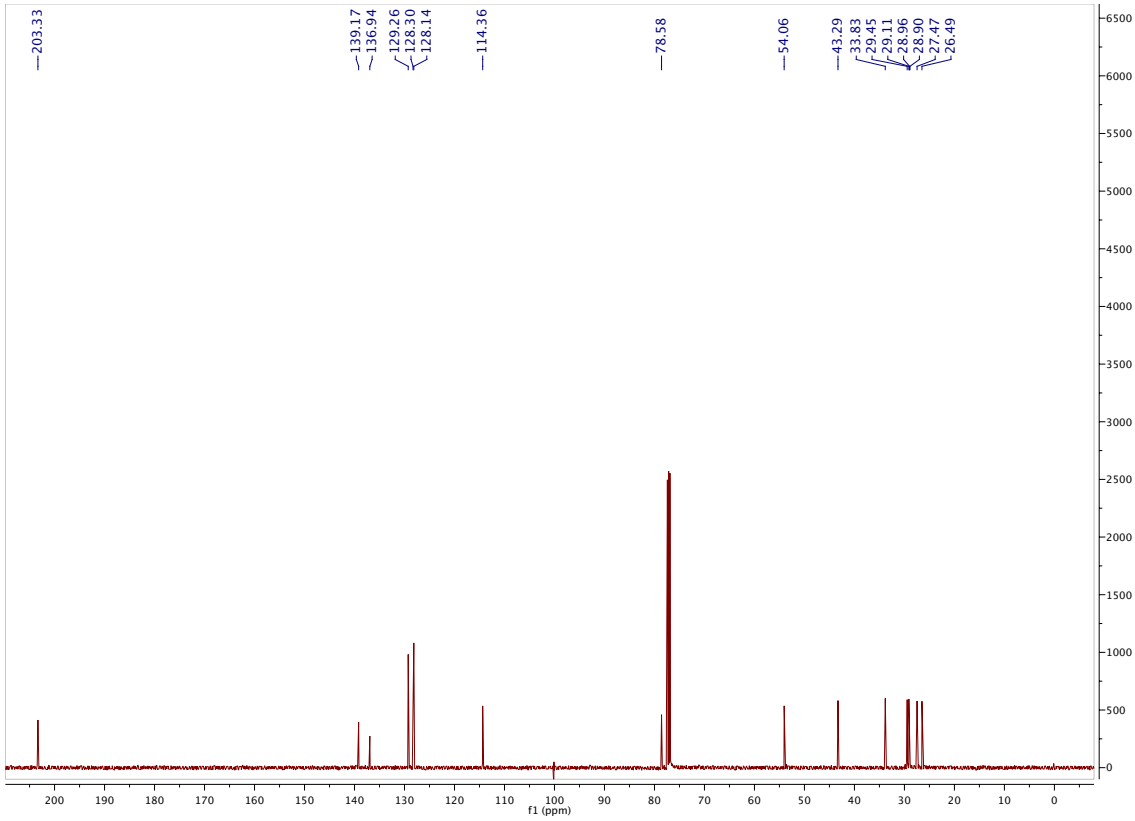
203.33
139.17
136.94
129.26
128.30
128.14
114.36
78.58
54.06
43.29
33.83
29.45
29.11
28.96
28.90
27.47
26.49
f1 (ppm)

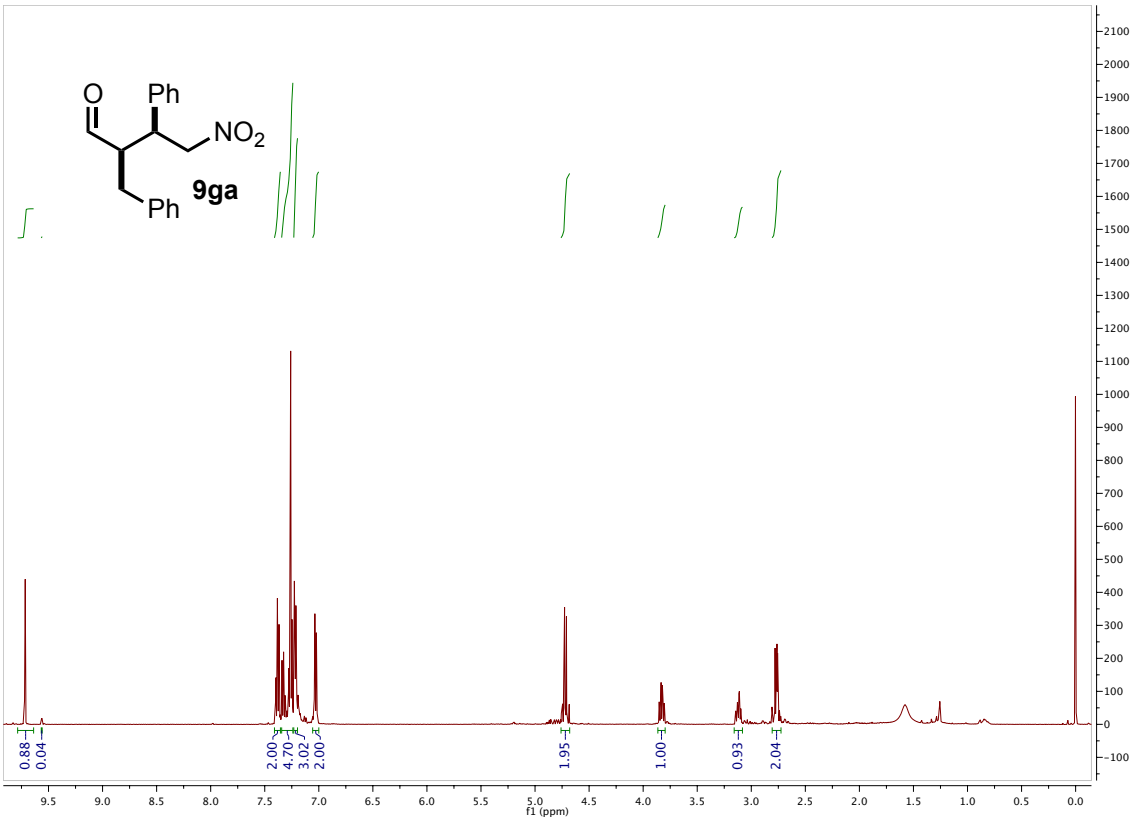
O
Ph
NO2
Ph
9ga
0.88
0.04
2.00
4.70
3.02
2.00
1.95
1.00
0.93
2.04
f1 (ppm)

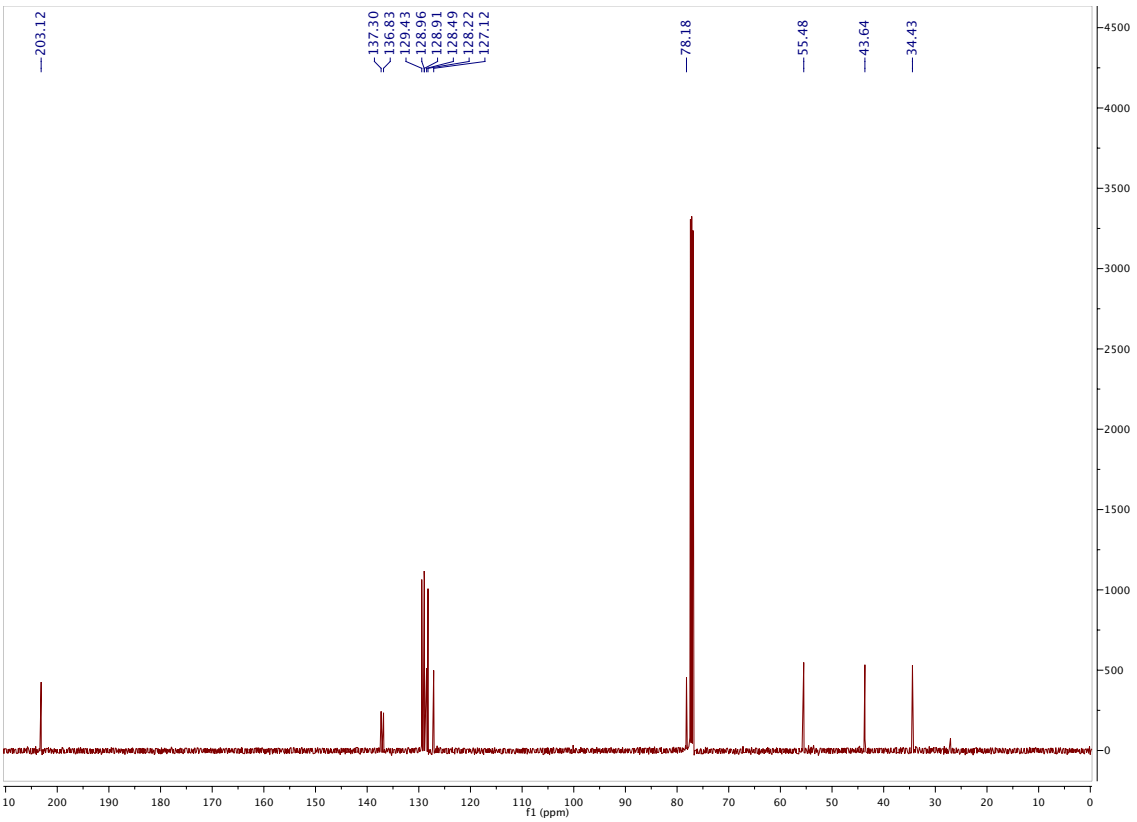
203.12
137.30
136.83
129.43
128.96
128.91
128.49
128.22
127.12
78.18
55.48
43.64
34.43
f1 (ppm)

Chapter III

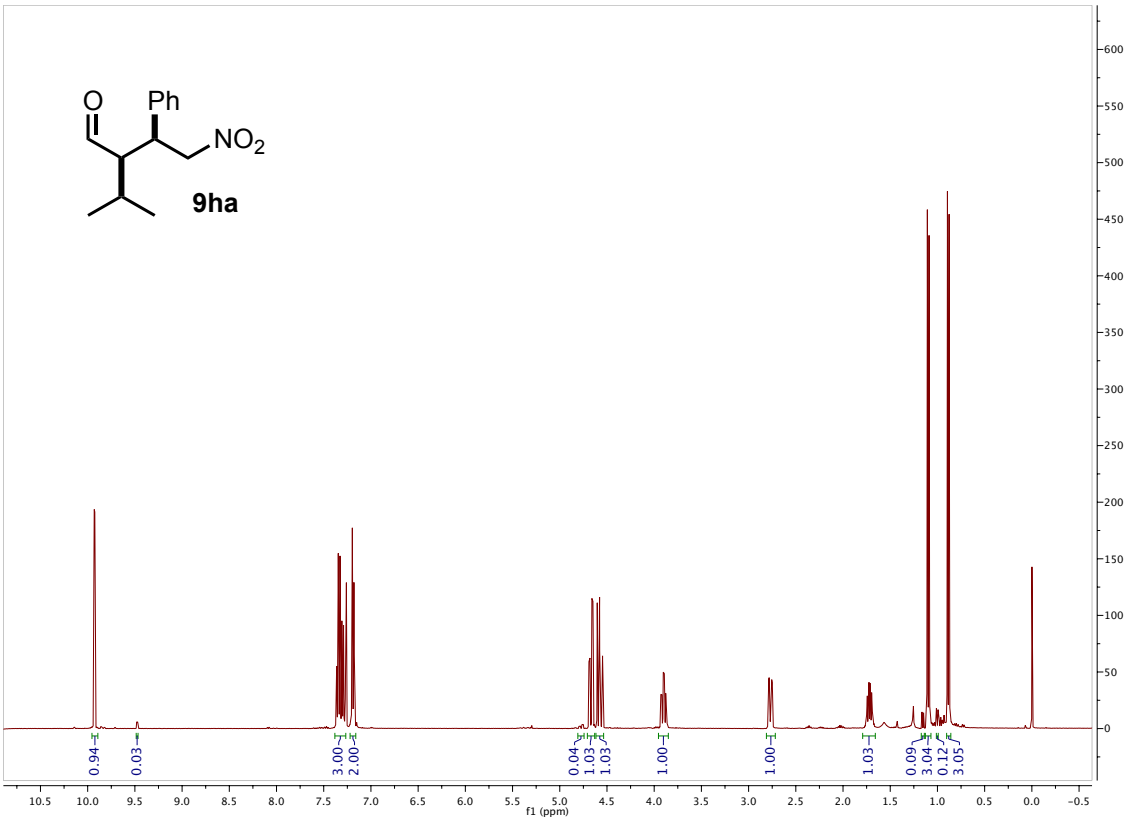
O
Ph
NO2
9ha
0.94
0.03
3.00
2.00
0.04
1.03
1.03
1.00
1.00
1.03
0.09
3.04
0.12
3.05
f1 (ppm)

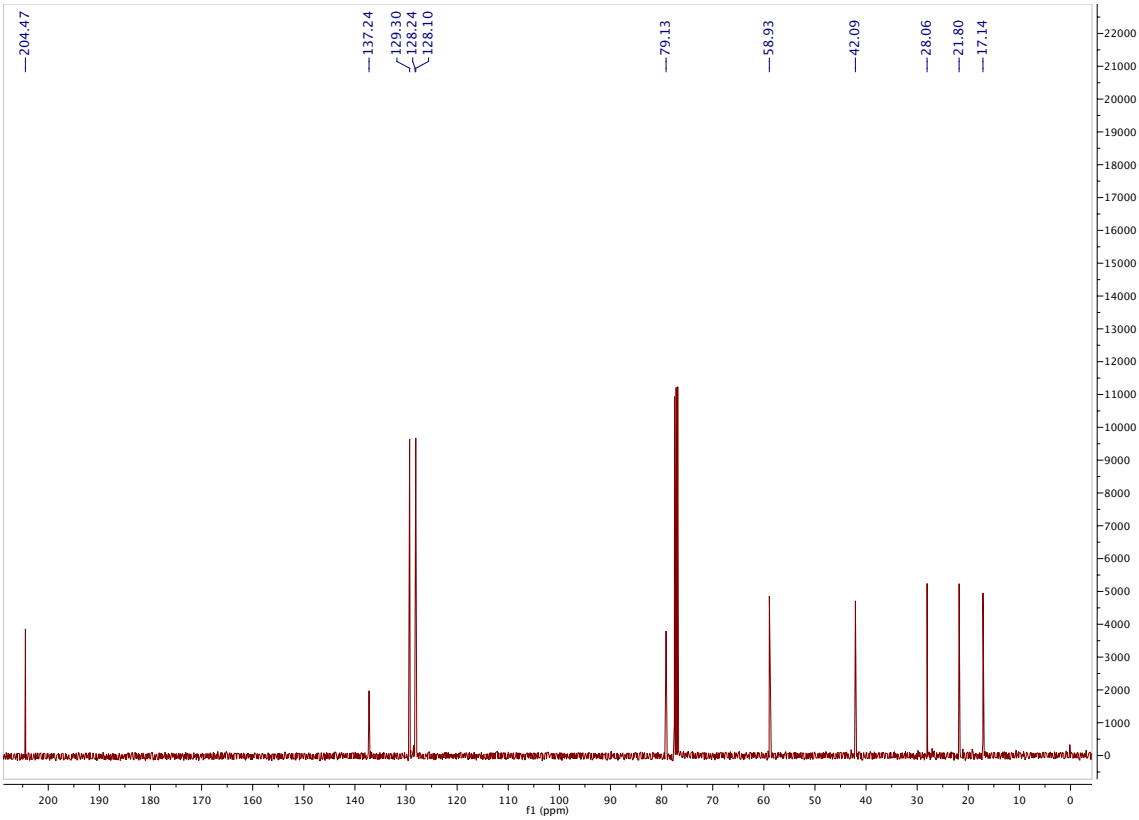
204.47
137.24
129.30
128.24
128.10
79.13
58.93
42.09
28.06
21.80
17.14
f1 (ppm)

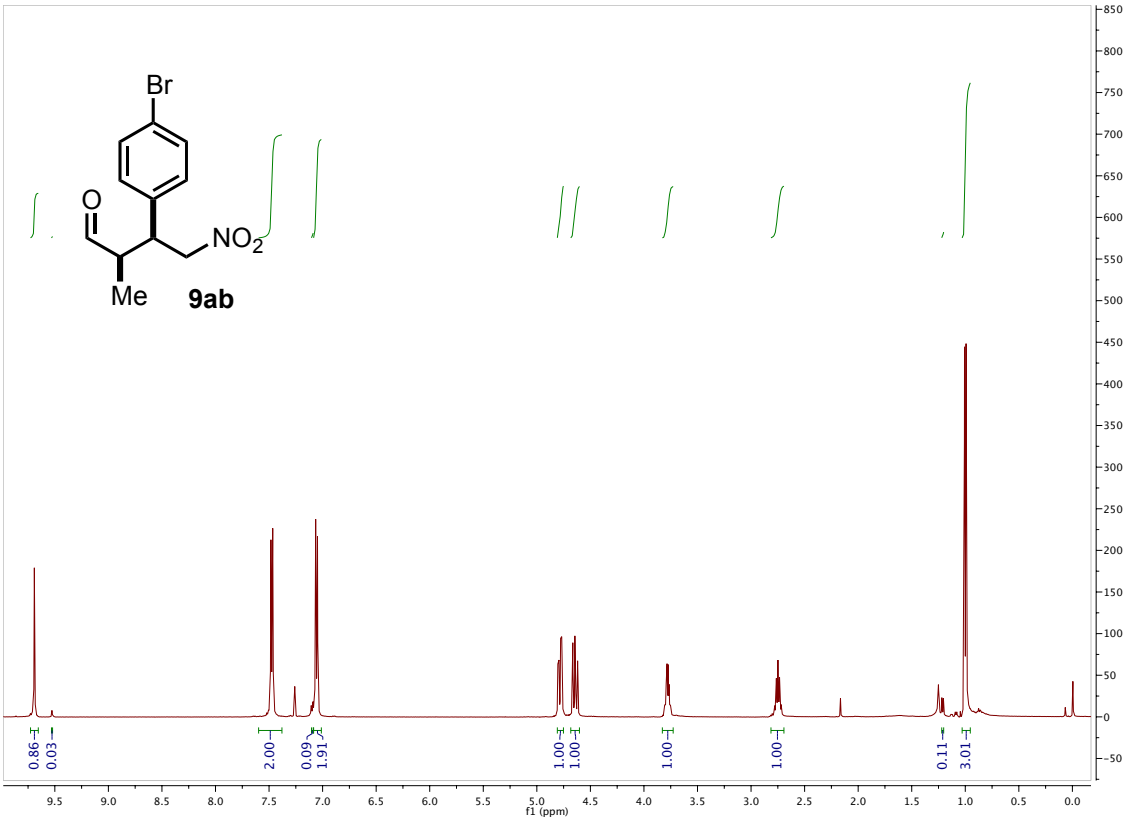
Br
O
NO2
Me
9ab
0.86
0.03
2.00
0.09
1.91
1.00
1.00
1.00
1.00
0.11
3.01
f1 (ppm)

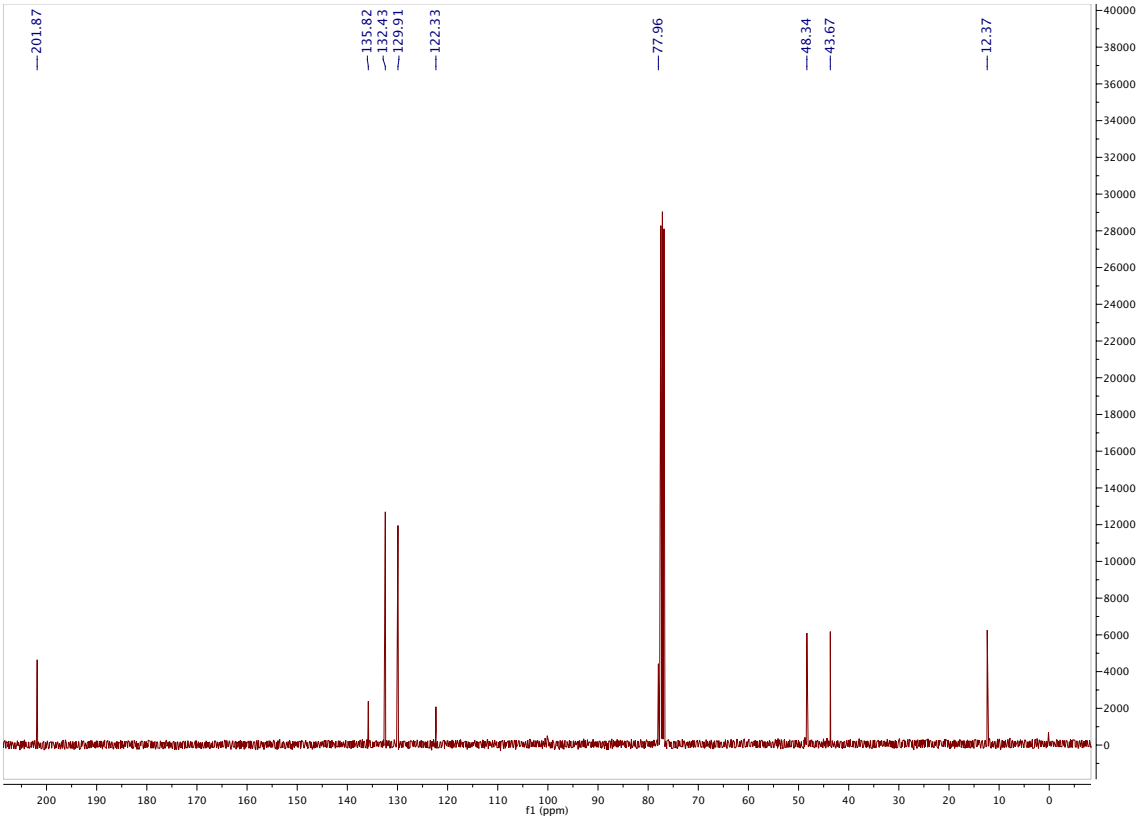
201.87
135.82
132.43
129.91
122.33
77.96
48.34
43.67
12.37
f1 (ppm)

Chapter III

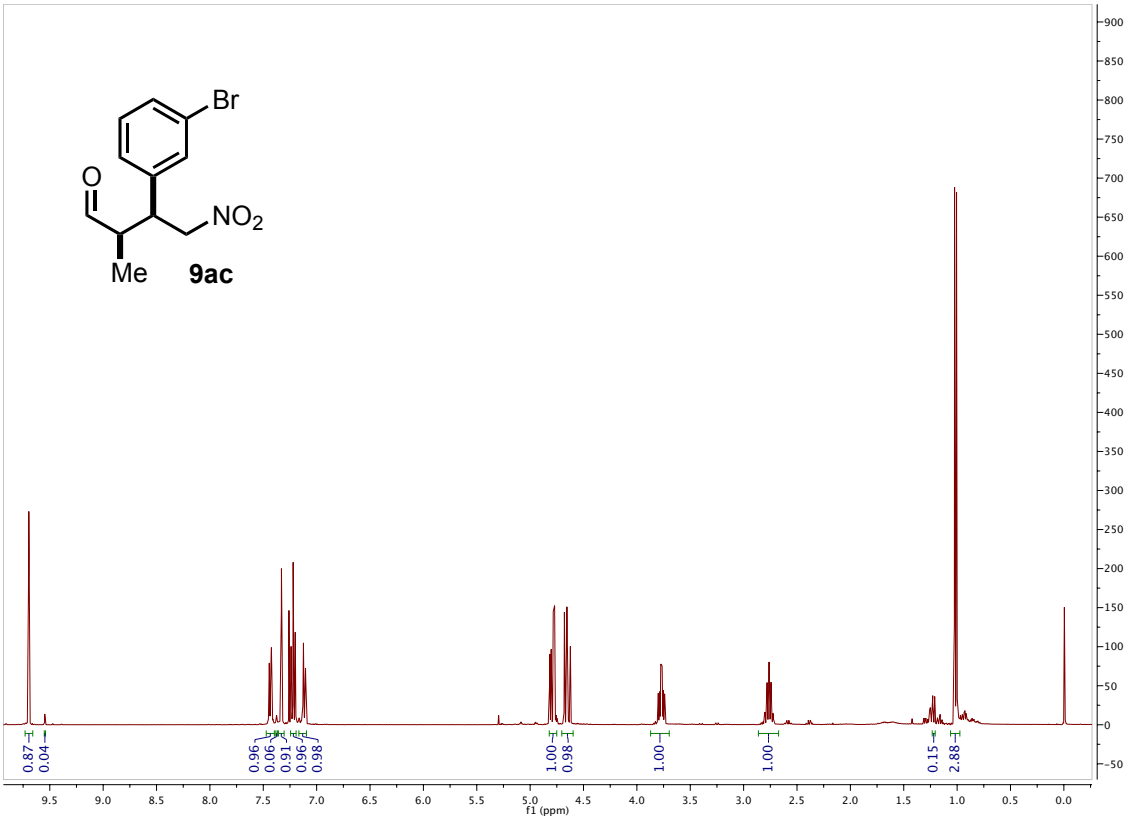
Br
O
NO2
Me
9ac
0.87
0.04
0.96
0.06
0.91
0.96
0.98
1.00
0.98
1.00
1.00
0.15
2.88
f1 (ppm)

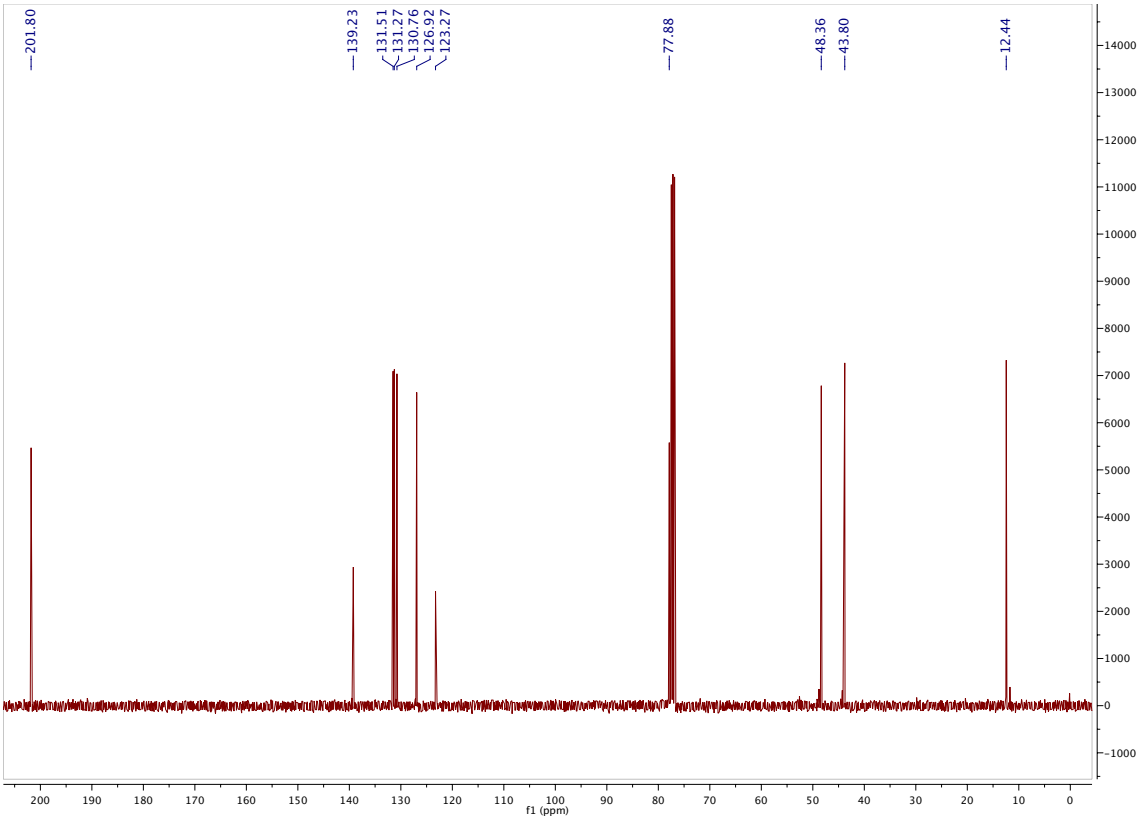
201.80
139.23
131.51
131.27
130.76
126.92
123.27
77.88
48.36
43.80
12.44
f1 (ppm)

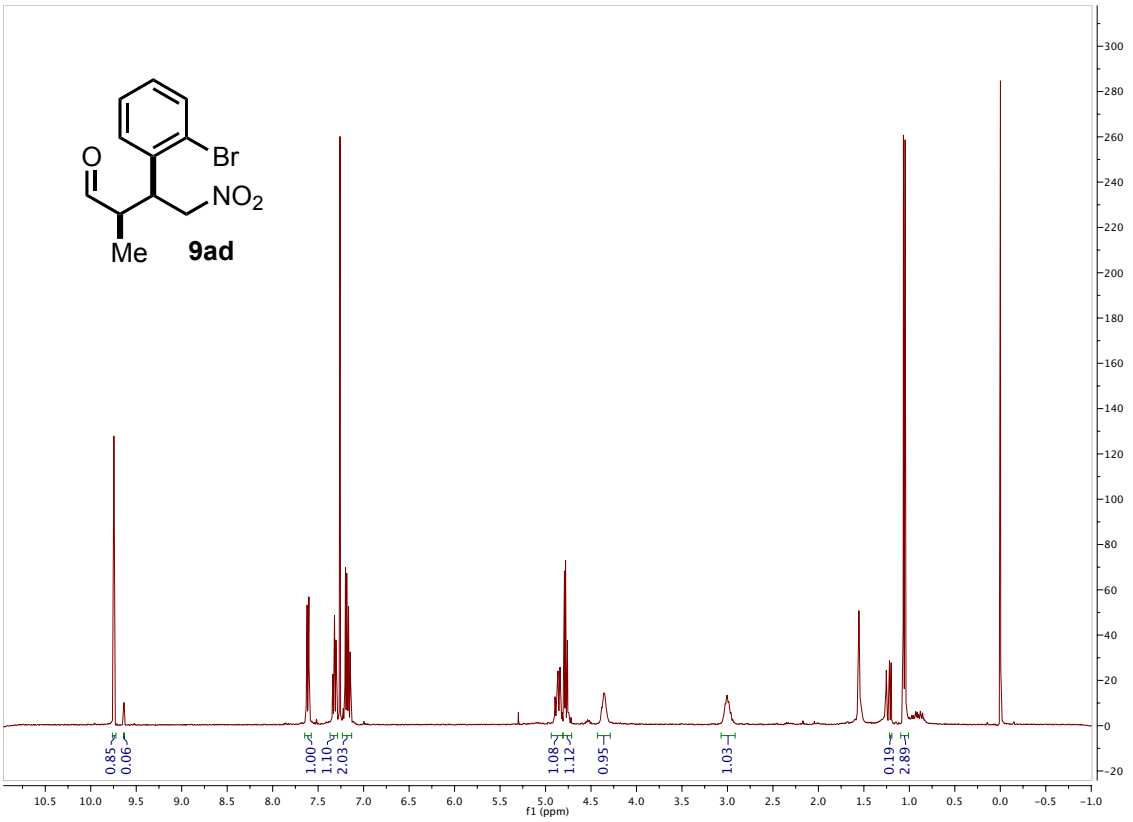
O
Br
NO2
Me
9ad
0.85
0.06
1.00
1.10
2.03
1.08
1.12
0.95
1.03
0.19
2.89
f1 (ppm)

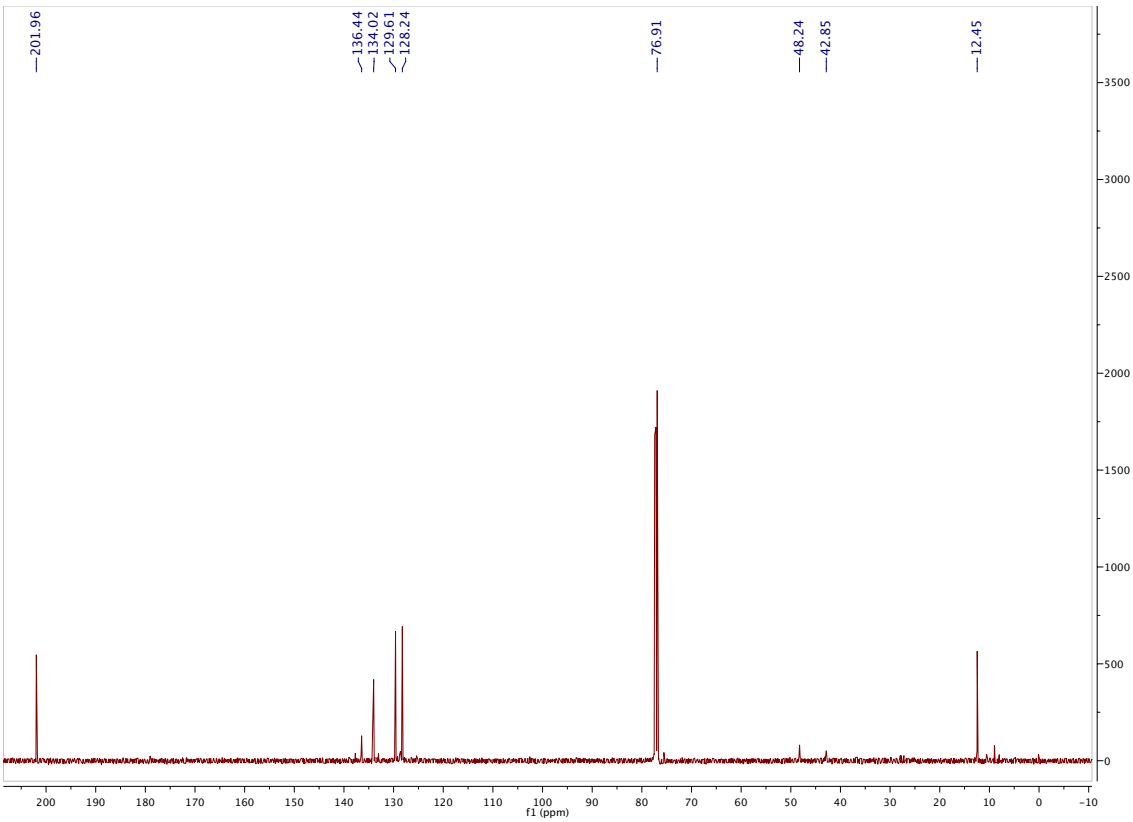
201.96
136.44
134.02
129.61
128.24
76.91
48.24
42.85
12.45
f1 (ppm)

Chapter III

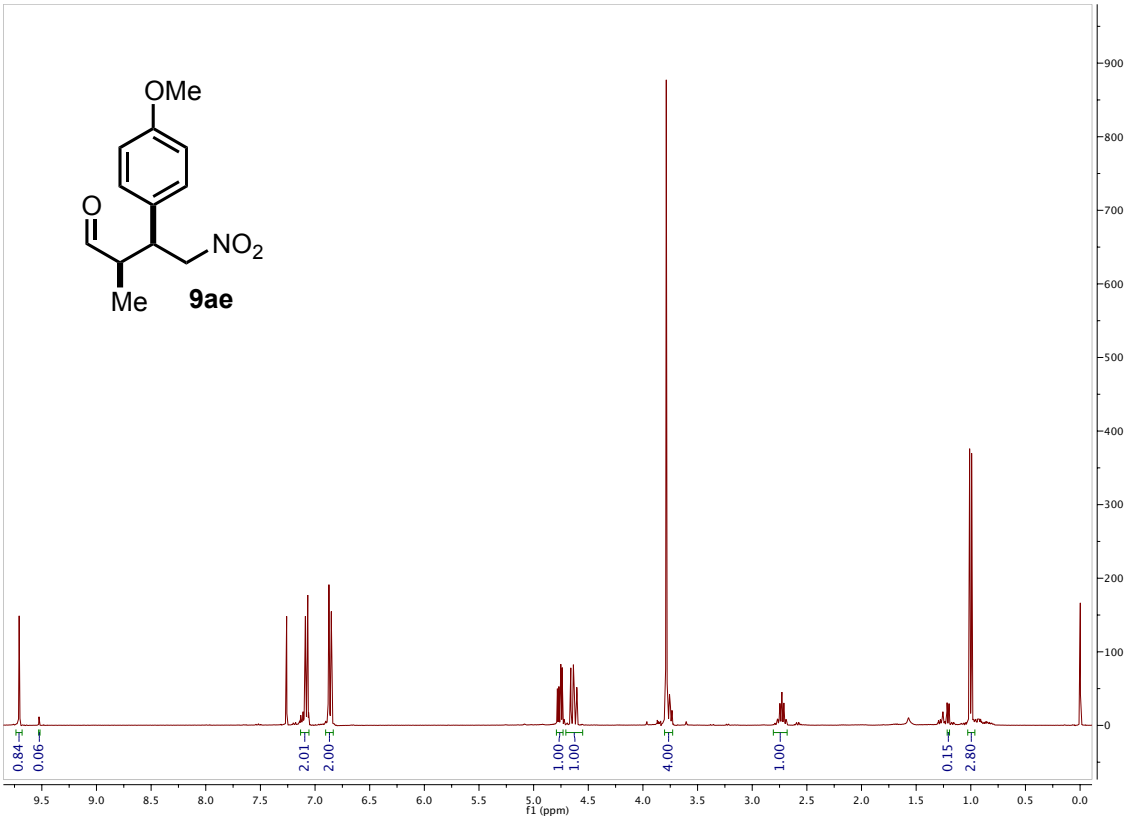
OMe
O
NO2
Me
9ae
0.84
0.06
2.01
2.00
1.00
1.00
4.00
1.00
0.15
2.80
f1 (ppm)

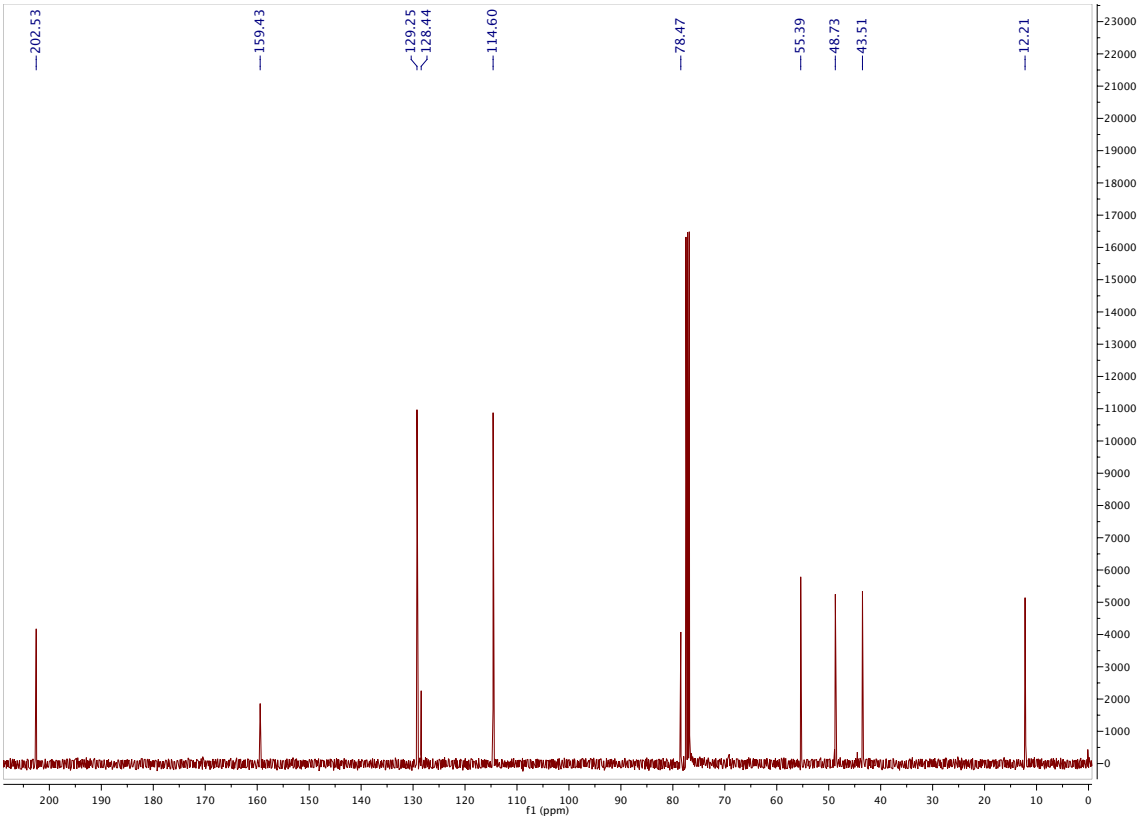
202.53
159.43
129.25
128.44
114.60
78.47
55.39
48.73
43.51
12.21
f1 (ppm)

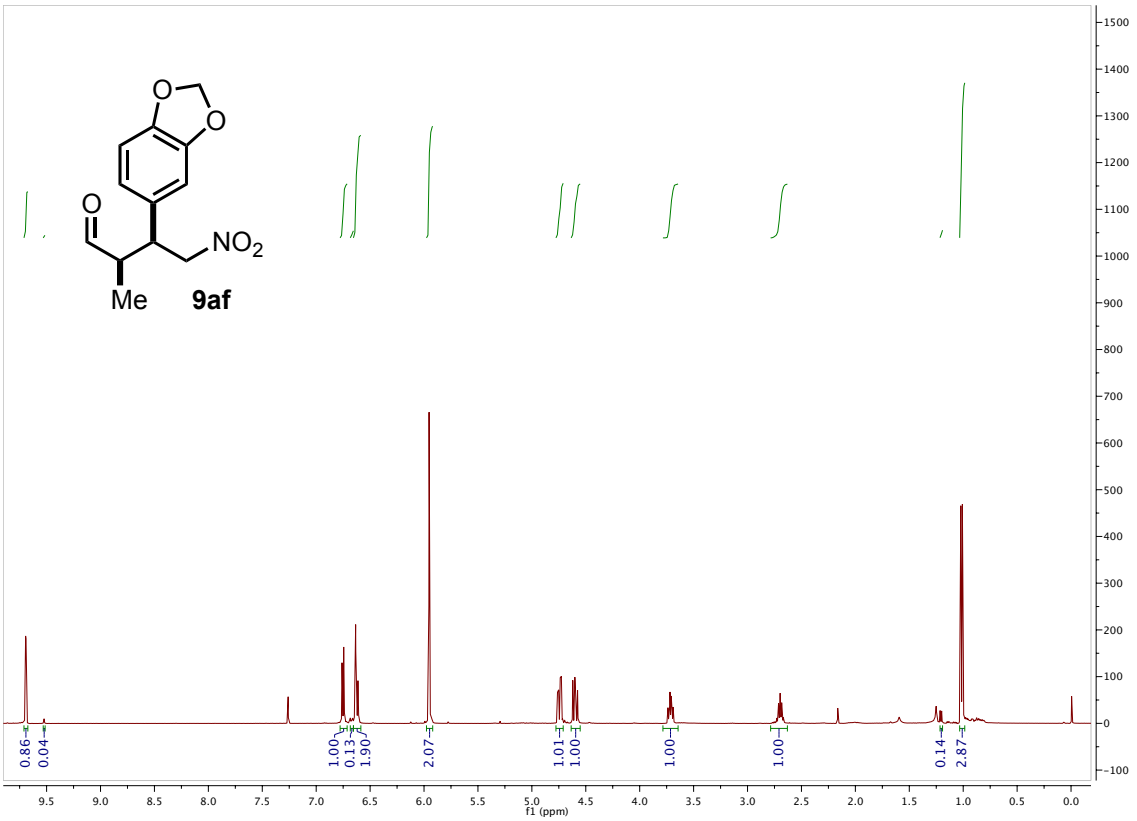
O
O
O
NO2
Me
9af
0.86
0.04
1.00
0.13
1.90
2.07
1.01
1.00
1.00
1.00
0.14
2.87
f1 (ppm)

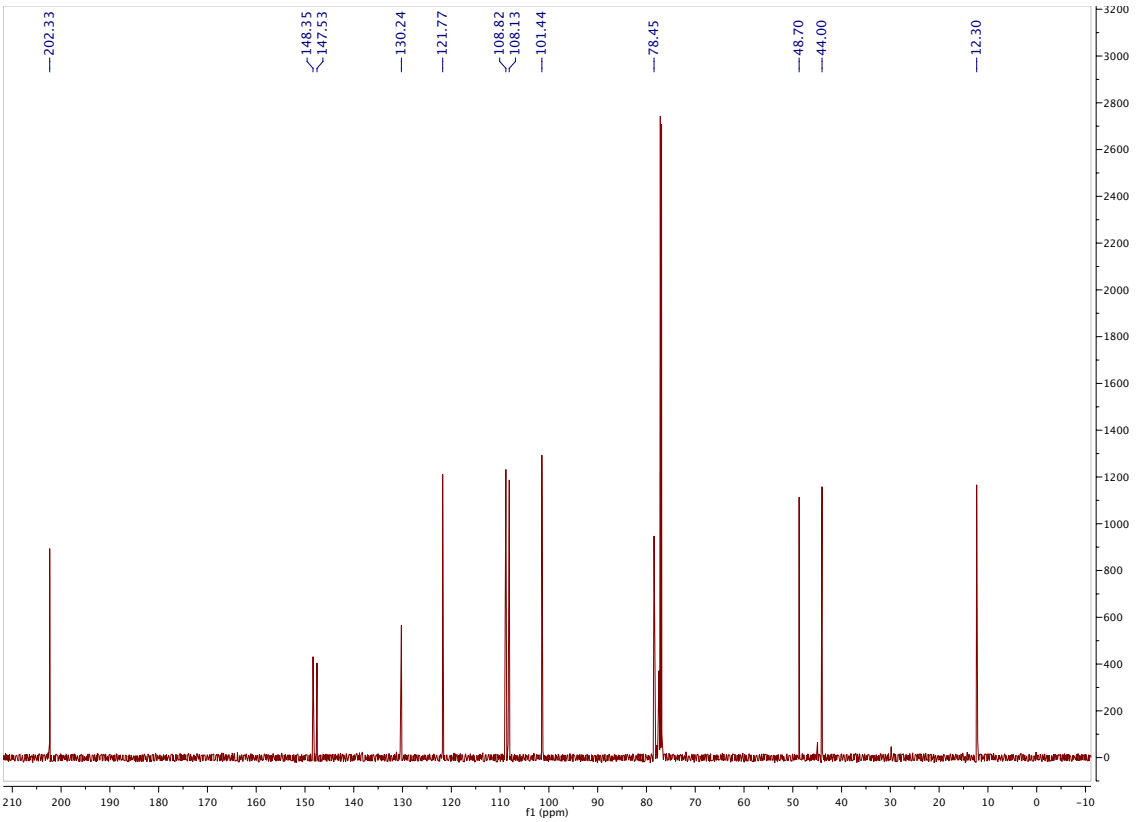
202.33
148.35
147.53
130.24
121.77
108.82
108.13
101.44
78.45
48.70
44.00
12.30
f1 (ppm)

Chapter III

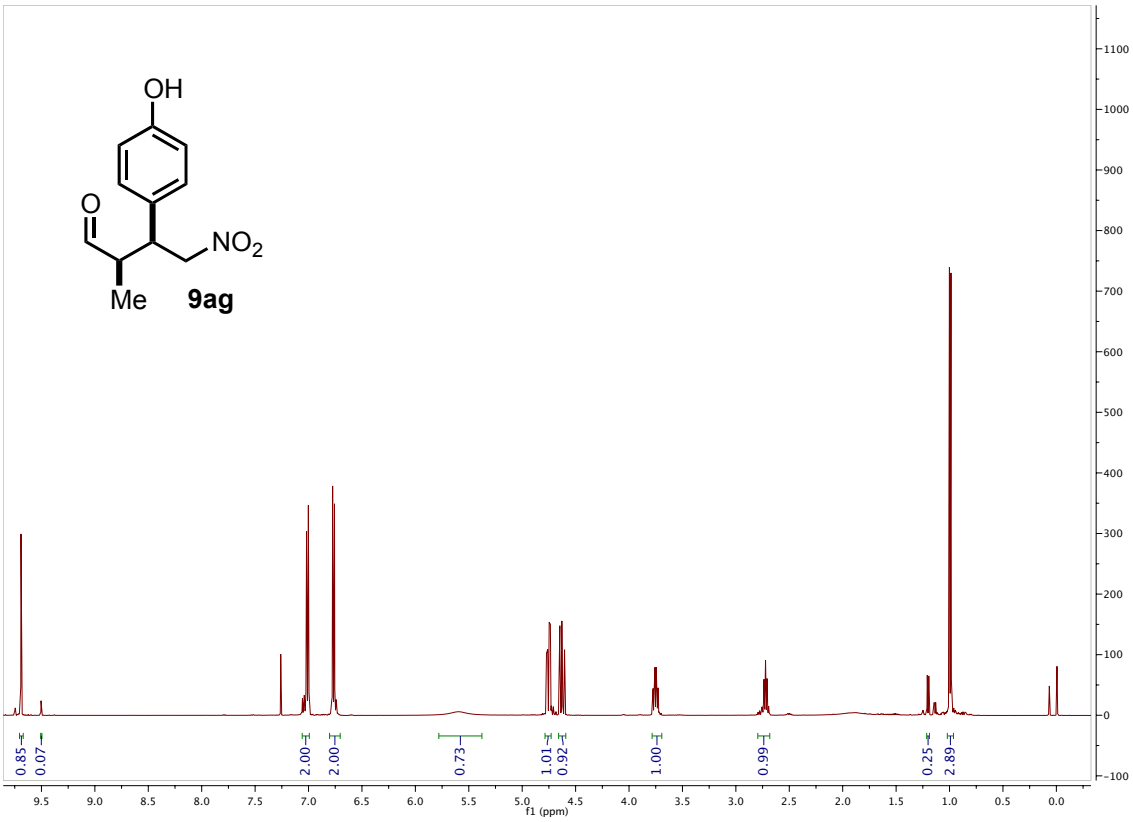
OH
O
NO2
Me
9ag
0.85
0.07
2.00
2.00
0.73
1.01
0.92
1.00
0.99
0.25
2.89
f1 (ppm)

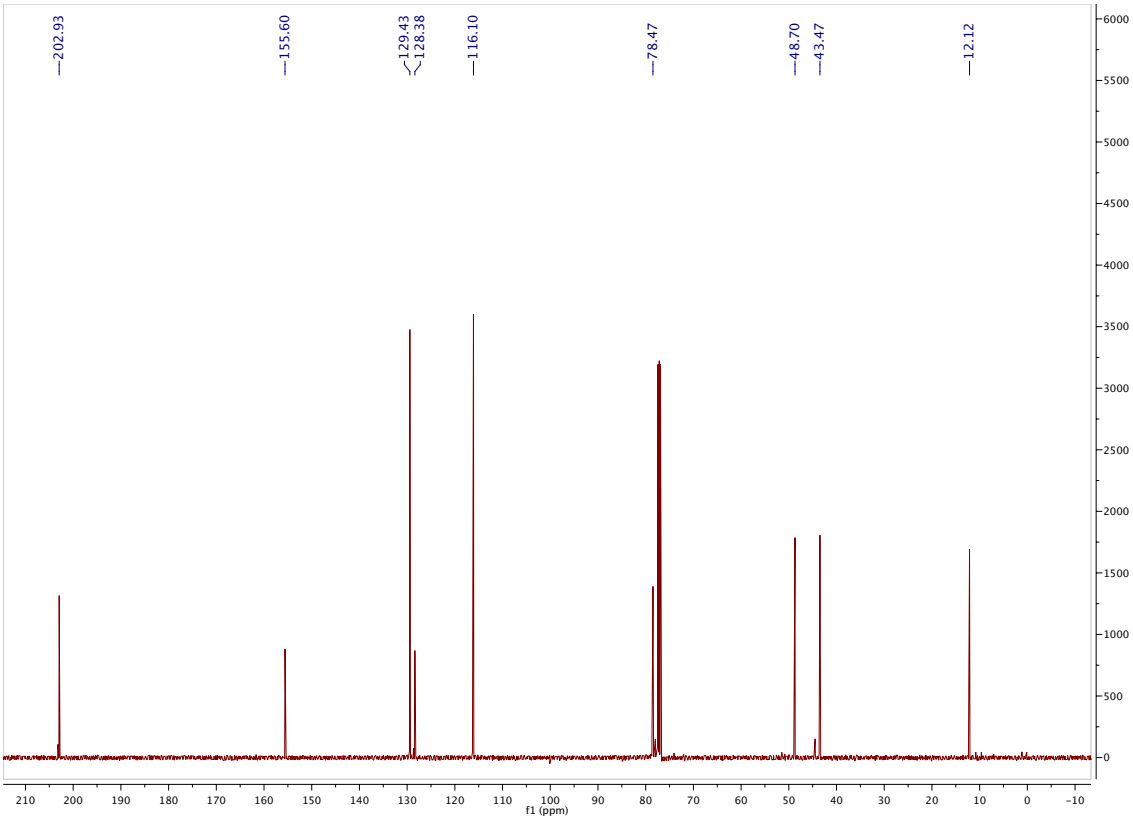
202.93
155.60
129.43
128.38
116.10
78.47
48.70
43.47
12.12
f1 (ppm)

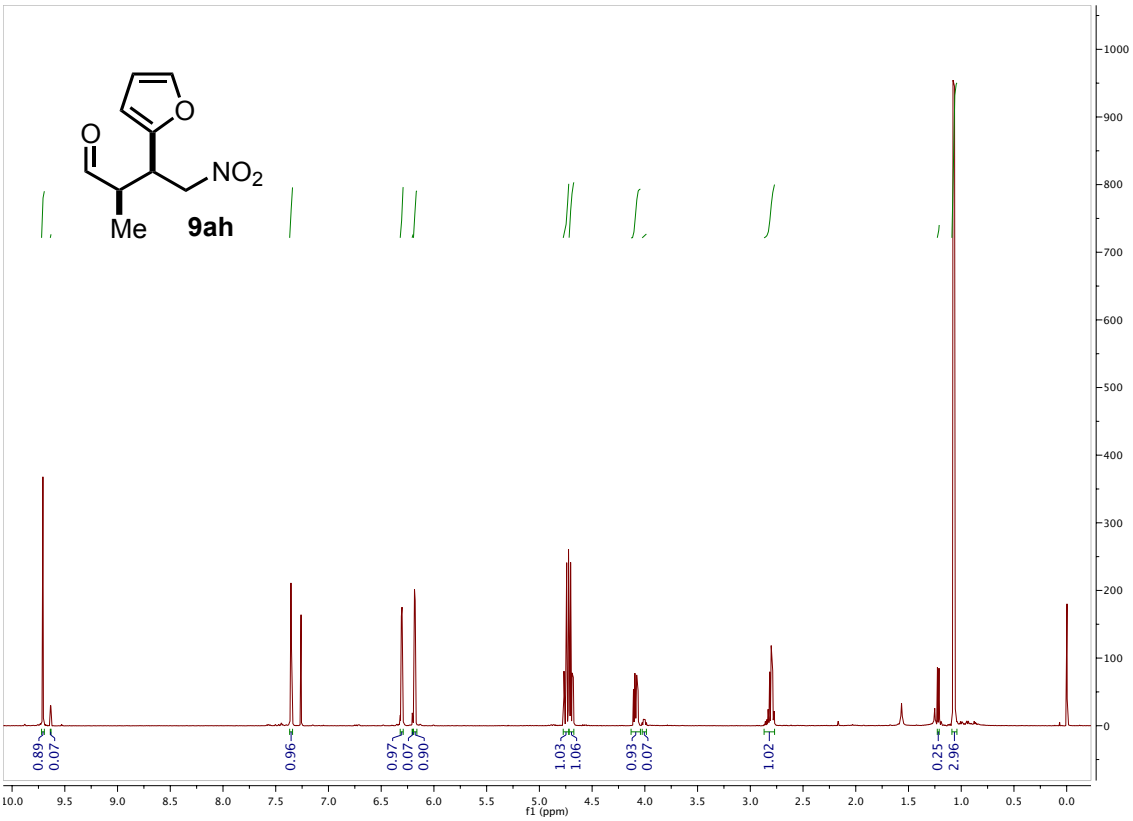
O
O
NO2
Me
9ah
0.89
0.07
0.96
0.97
0.07
0.90
1.03
1.06
0.93
0.07
1.02
0.25
2.96
f1 (ppm)

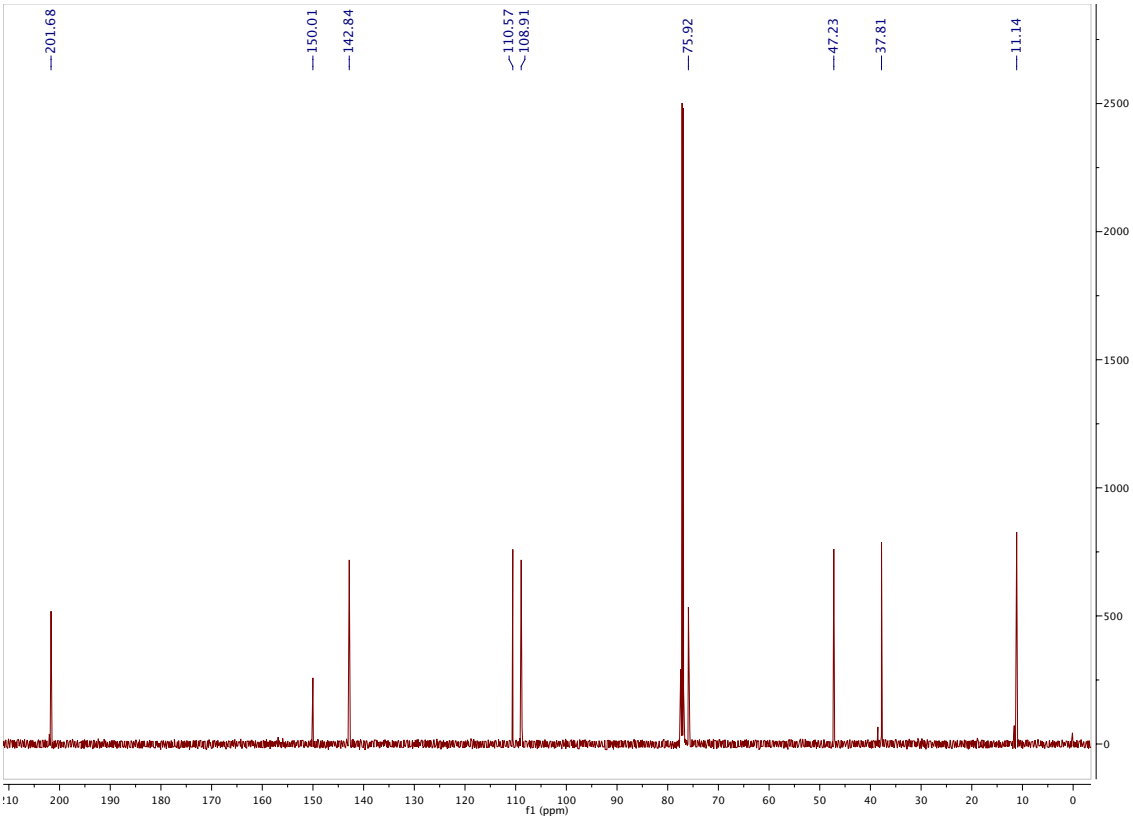
201.68
150.01
142.84
110.57
108.91
75.92
47.23
37.81
11.14
f1 (ppm)

Chapter III

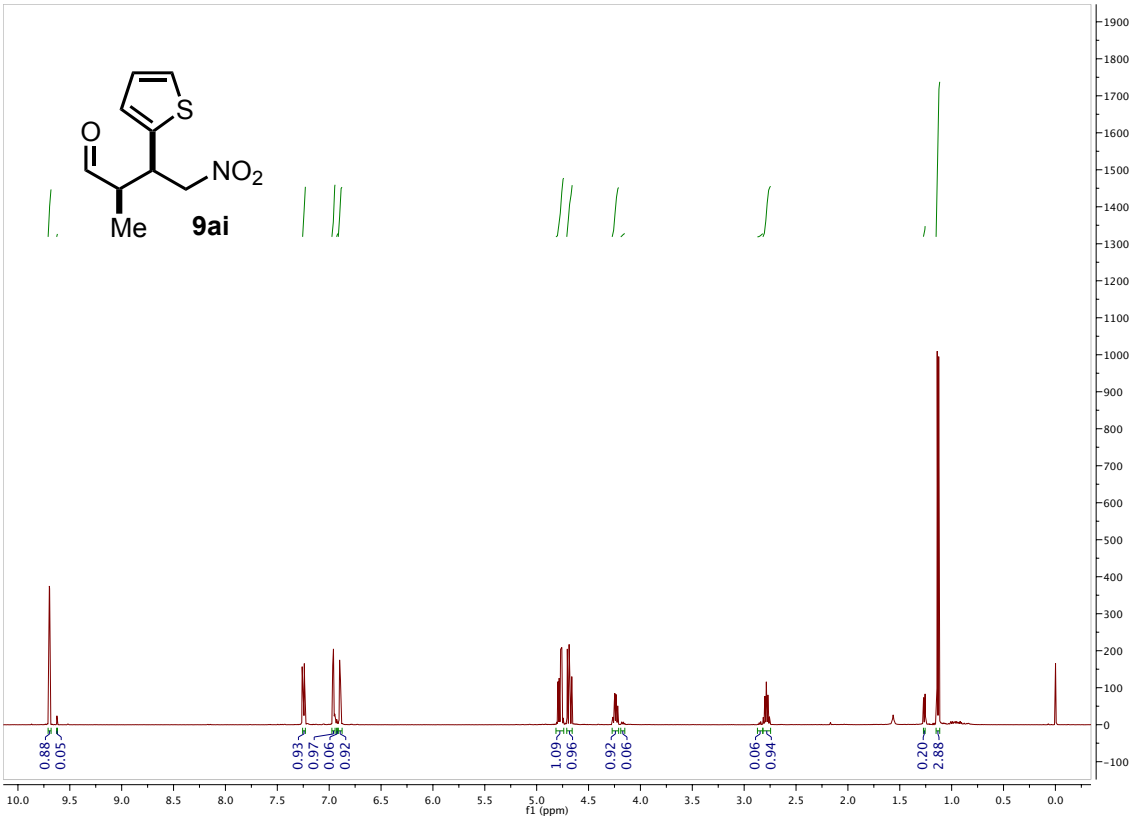
O
S
NO2
Me
9ai
0.88
0.05
0.93
0.97
0.06
0.92
1.09
0.96
0.92
0.06
0.06
0.94
0.20
2.88
f1 (ppm)

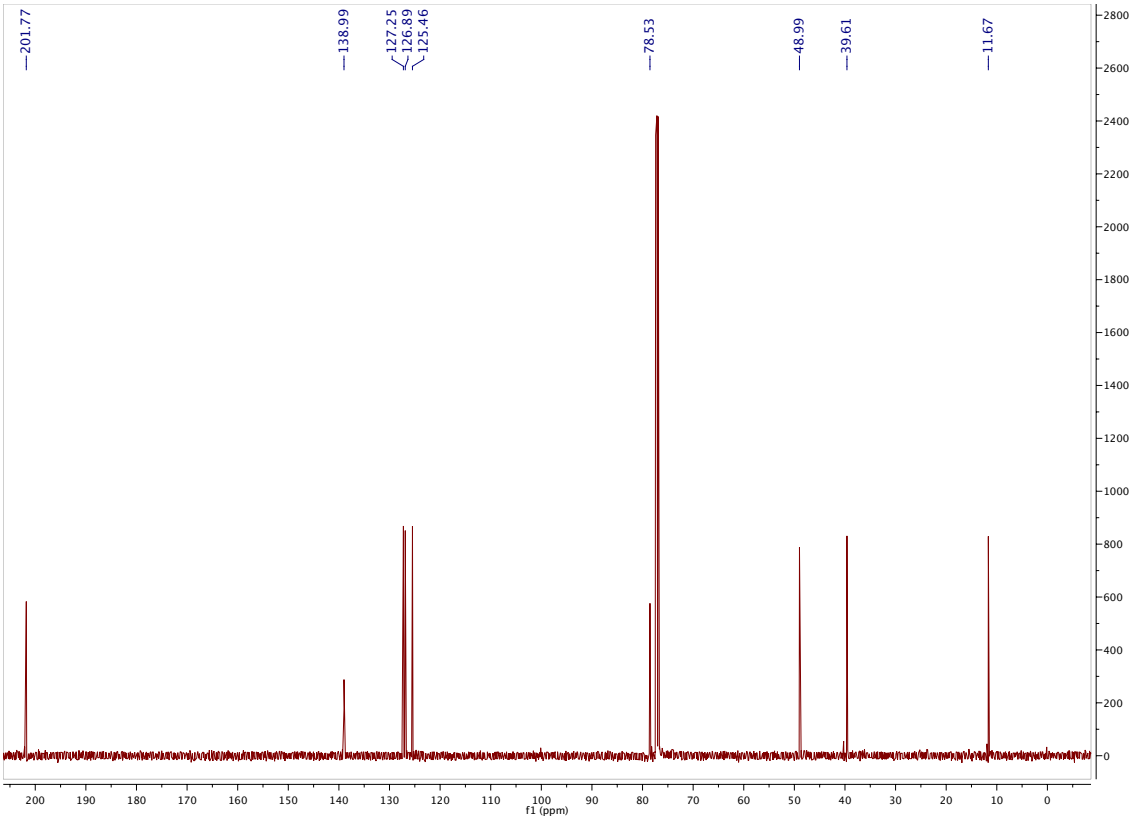
201.77
138.99
127.25
126.89
125.46
78.53
48.99
39.61
11.67
f1 (ppm)

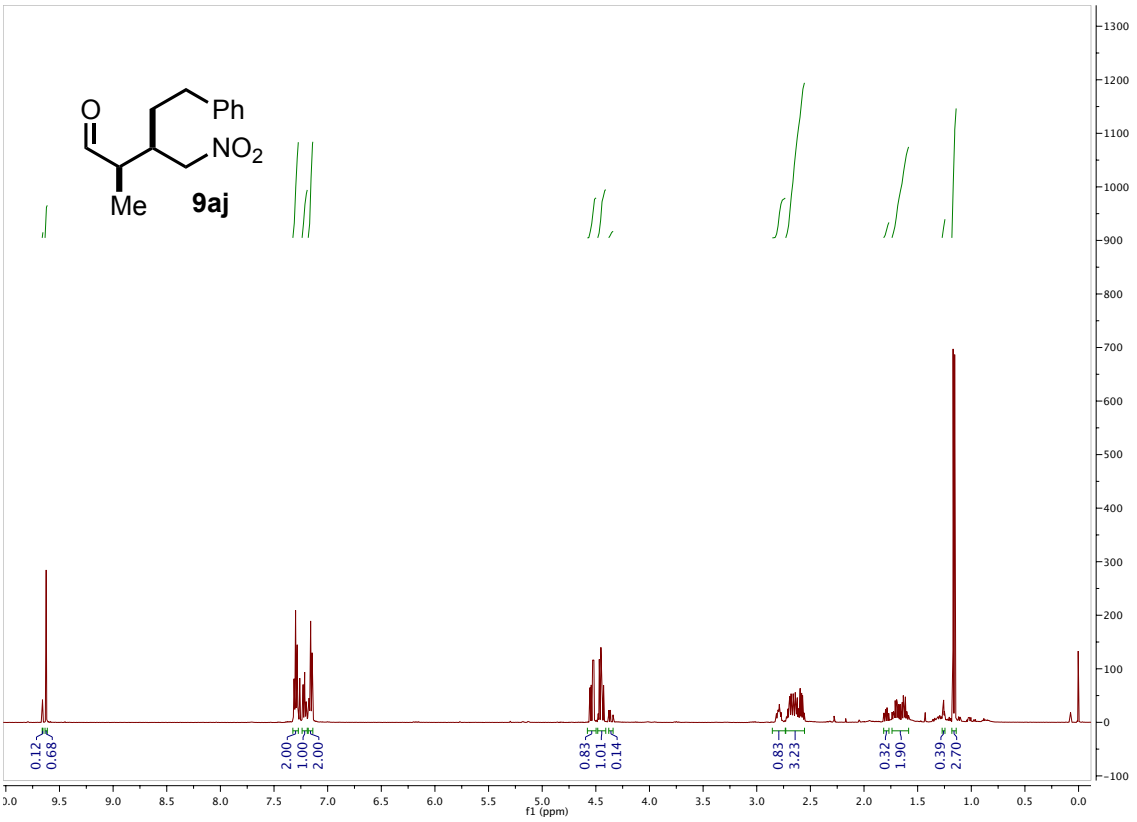
O
Ph
NO2
Me
9aj
0.12
0.68
2.00
1.00
2.00
0.83
1.01
0.14
0.83
3.23
0.32
1.90
0.39
2.70
f1 (ppm)

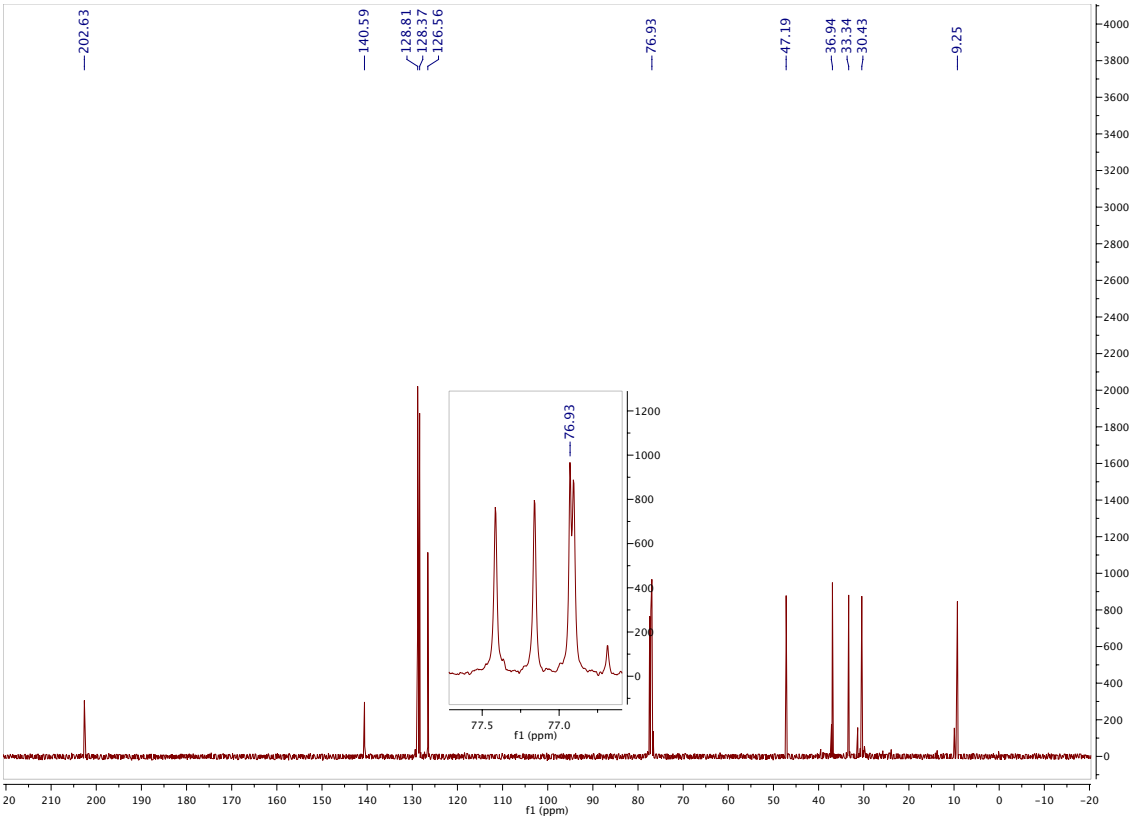
202.63
140.59
128.81
128.37
126.56
76.93
47.19
36.94
33.34
30.43
9.25
77.5
77.0
f1 (ppm)

Chapter III

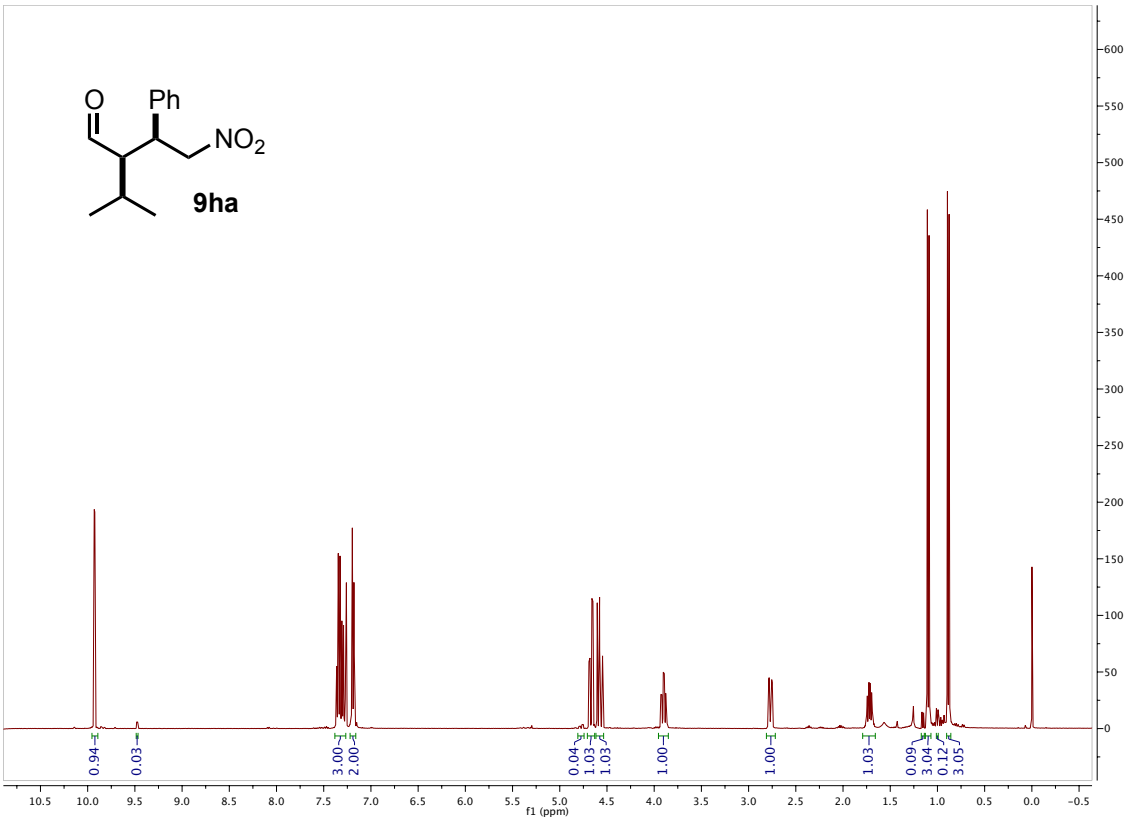
O
Ph
NO2
9ha
0.94
0.03
3.00
2.00
0.04
1.03
1.03
1.00
1.00
1.03
0.09
3.04
0.12
3.05
f1 (ppm)

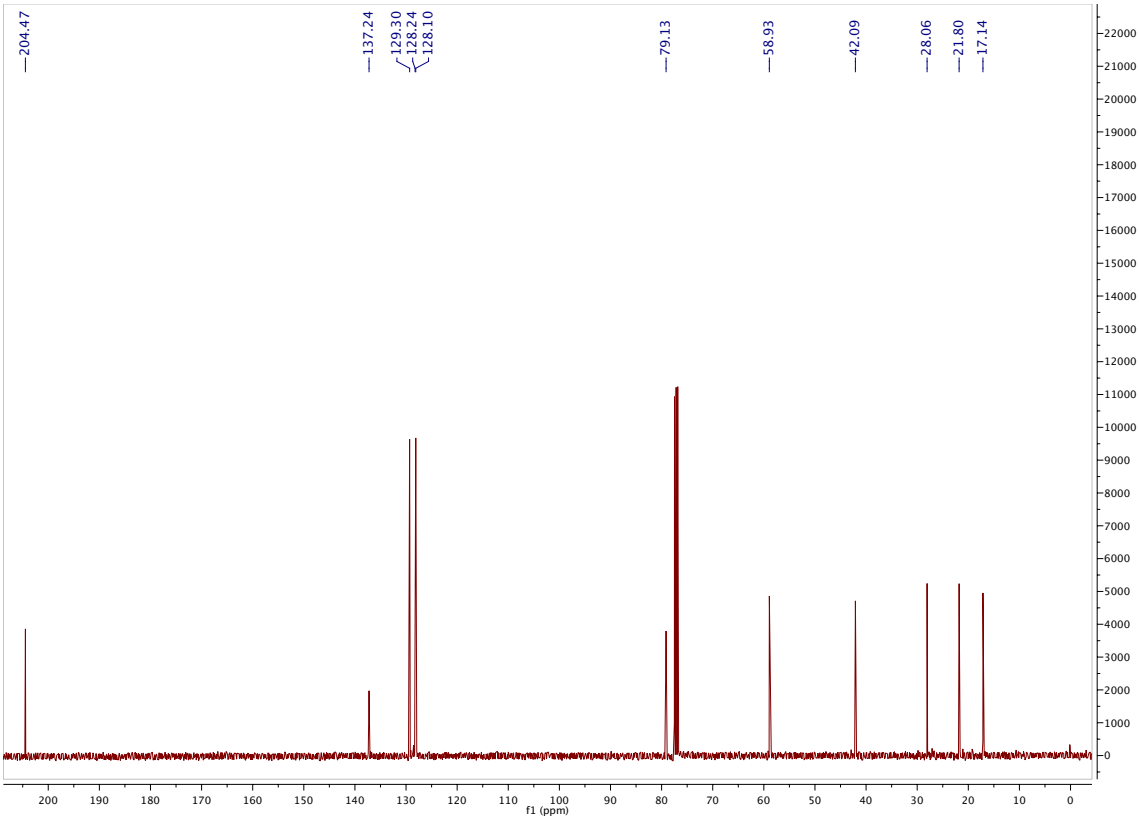
204.47
137.24
129.30
128.24
128.10
79.13
58.93
42.09
28.06
21.80
17.14
f1 (ppm)

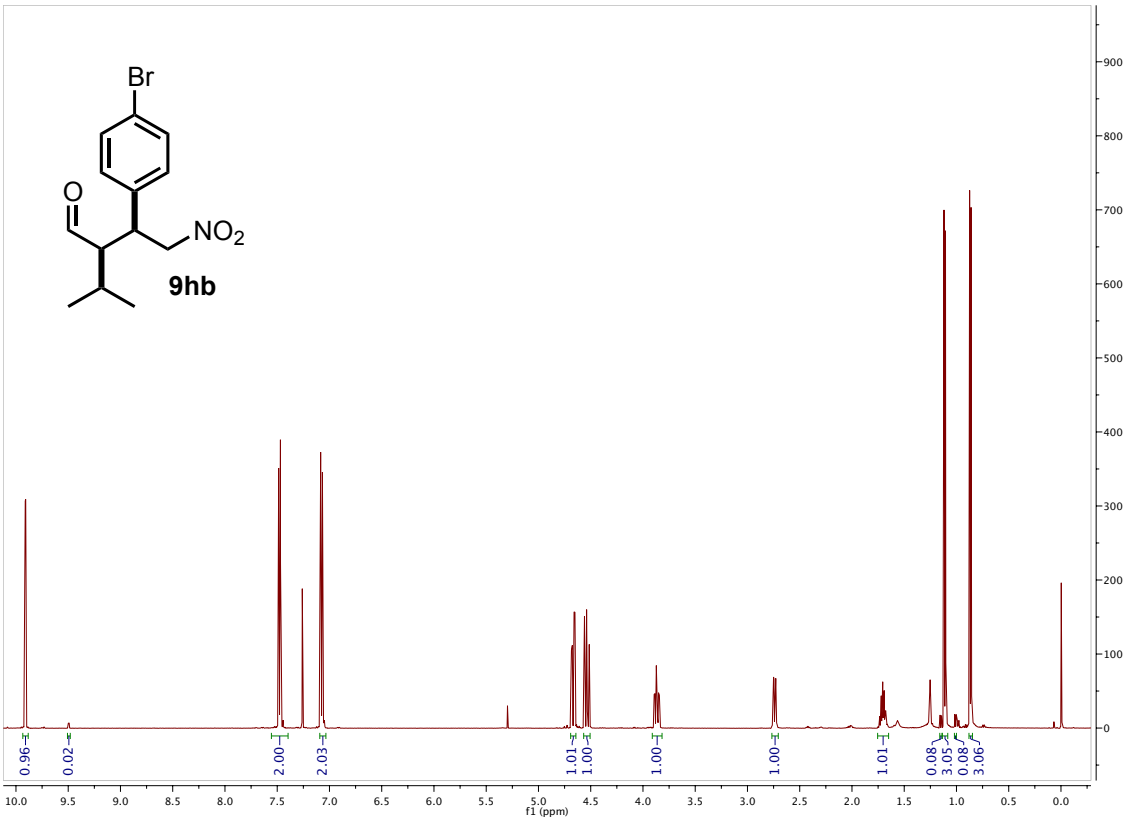
Br
O
NO2
9hb
0.96
0.02
2.00
2.03
1.01
1.00
1.00
1.00
1.01
0.08
3.05
0.08
3.06
f1 (ppm)

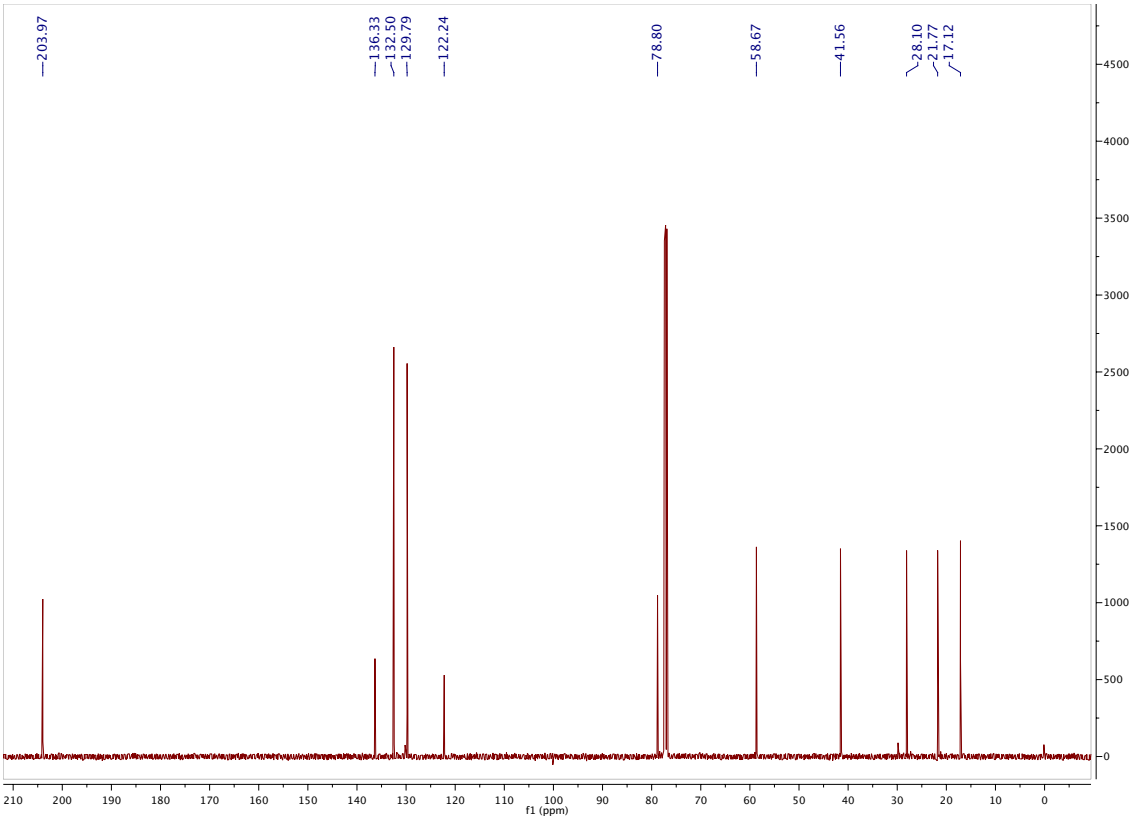
203.97
136.33
132.50
129.79
122.24
78.80
58.67
41.56
28.10
21.77
17.12
f1 (ppm)

Chapter III

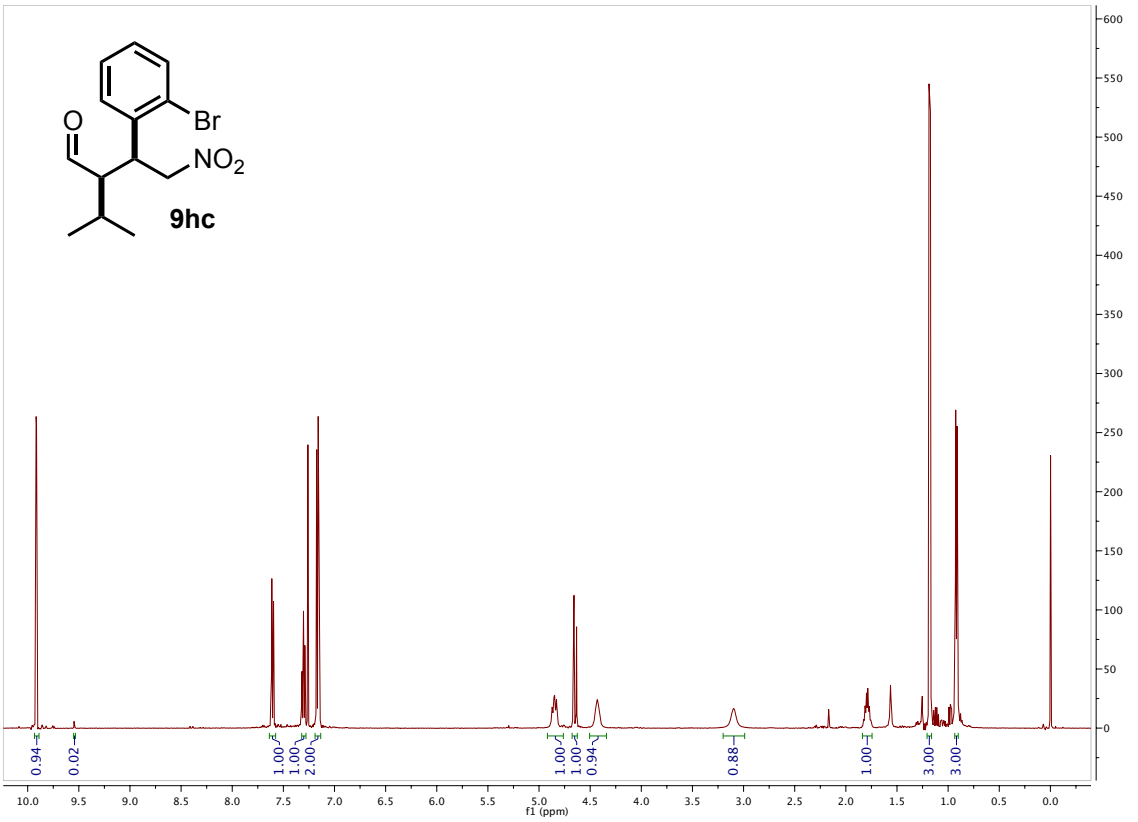
O
Br
NO2
9hc
0.94
0.02
1.00
1.00
2.00
1.00
1.00
0.94
0.88
1.00
3.00
3.00
f1 (ppm)

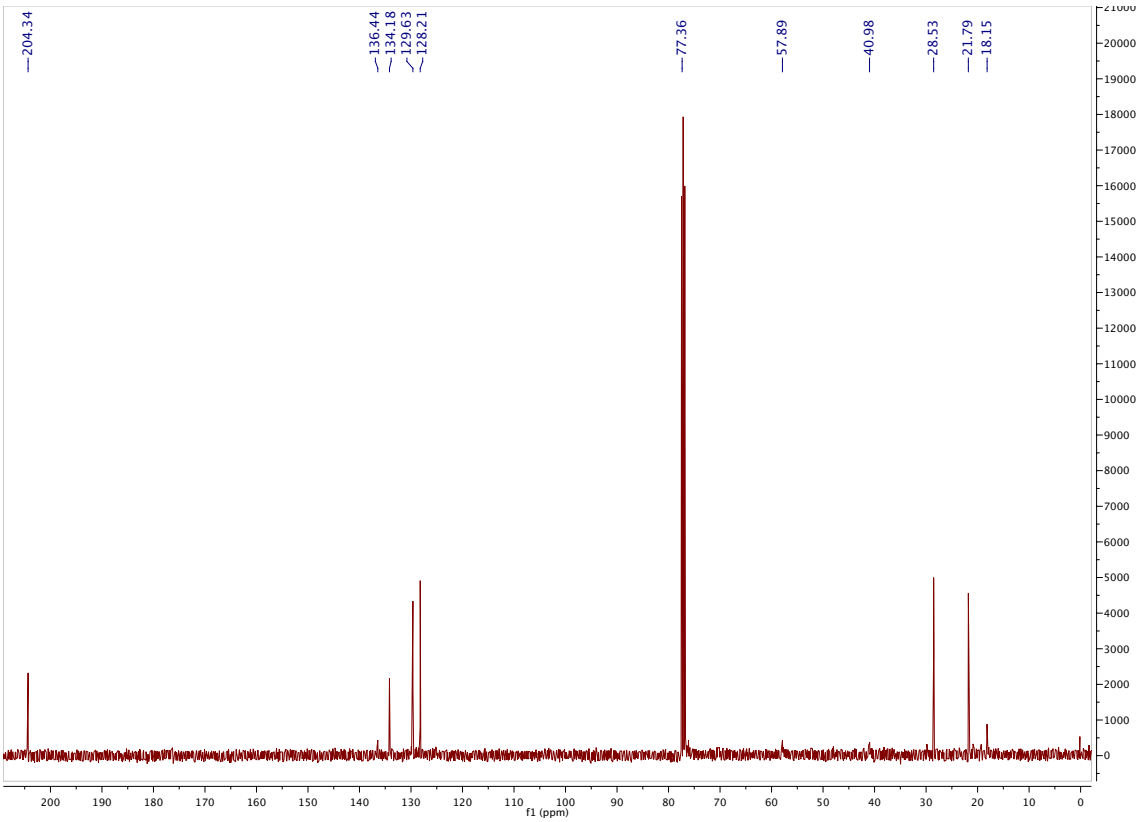
204.34
136.44
134.18
129.63
128.21
77.36
57.89
40.98
28.53
21.79
18.15
f1 (ppm)

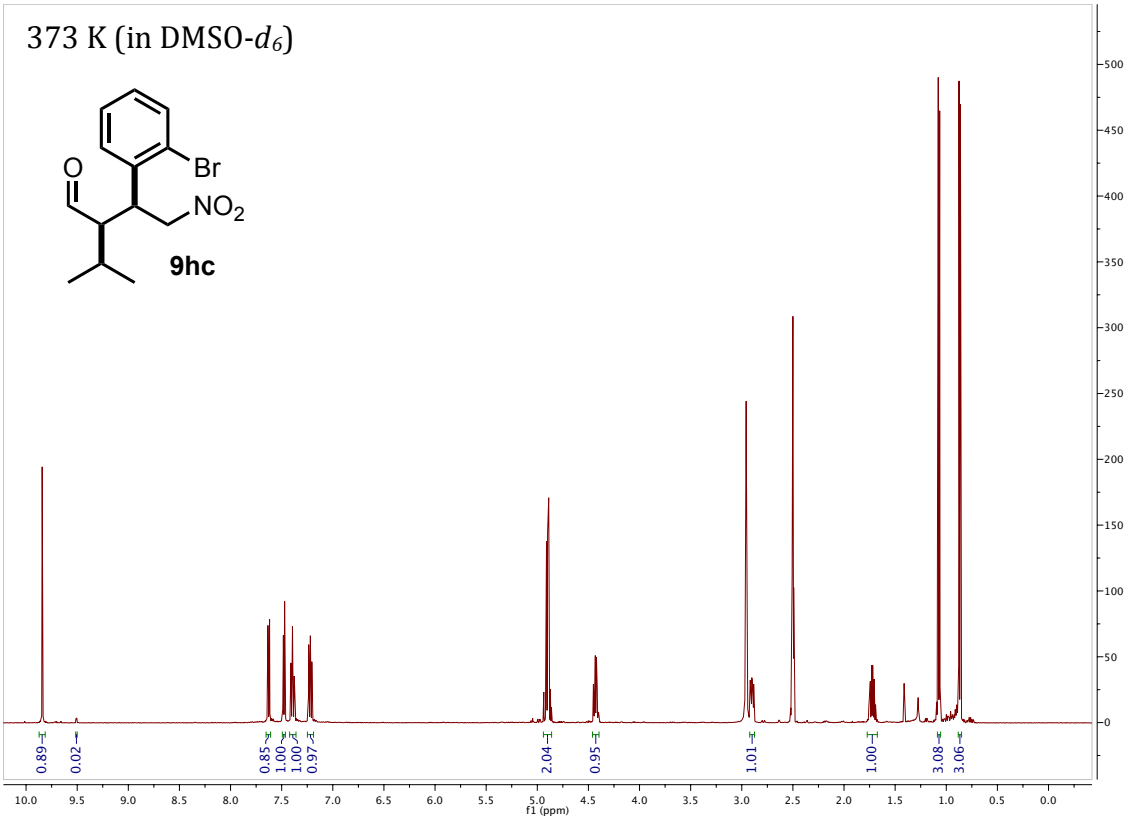
373 K (in DMSO-d_6)
O
Br
NO_2
9hc
0.89
0.02
0.85
1.00
1.00
0.97
2.04
0.95
1.01
1.00
3.08
3.06
f1 (ppm)

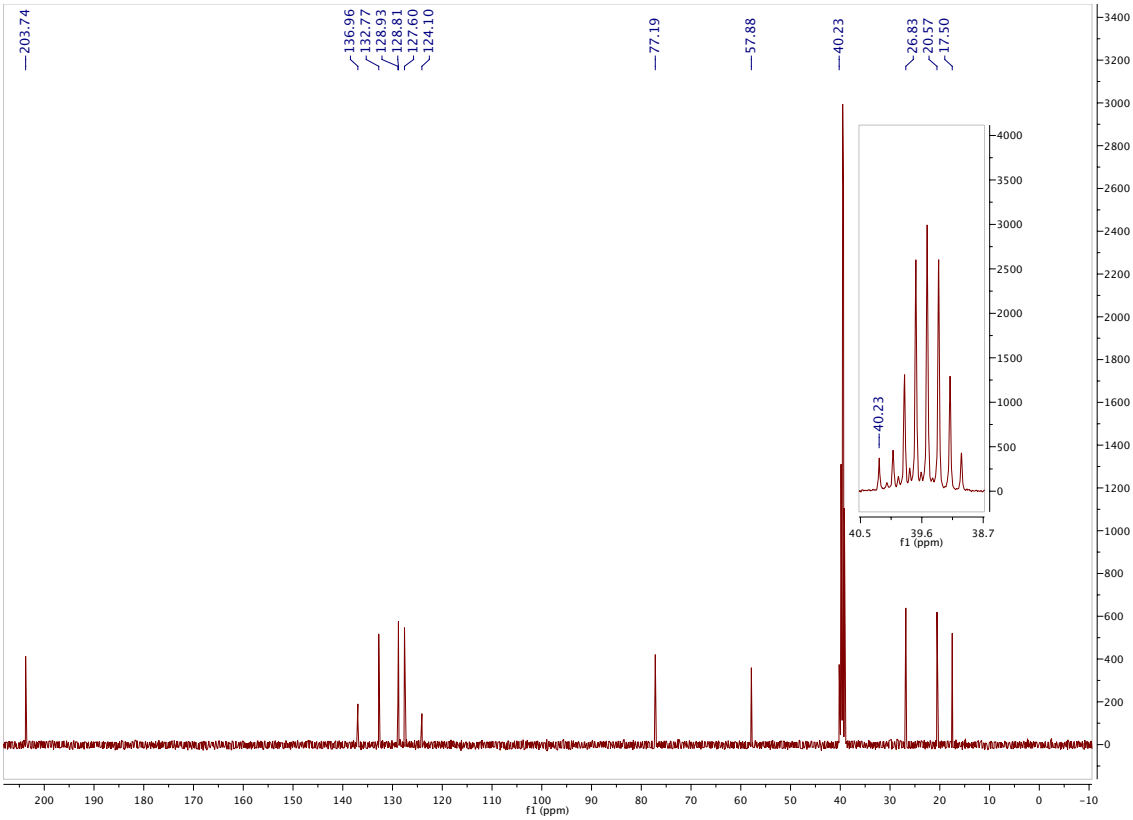
203.74
136.96
132.77
128.93
128.81
127.60
124.10
77.19
57.88
40.23
26.83
20.57
17.50
40.23
f1 (ppm)

Chapter III

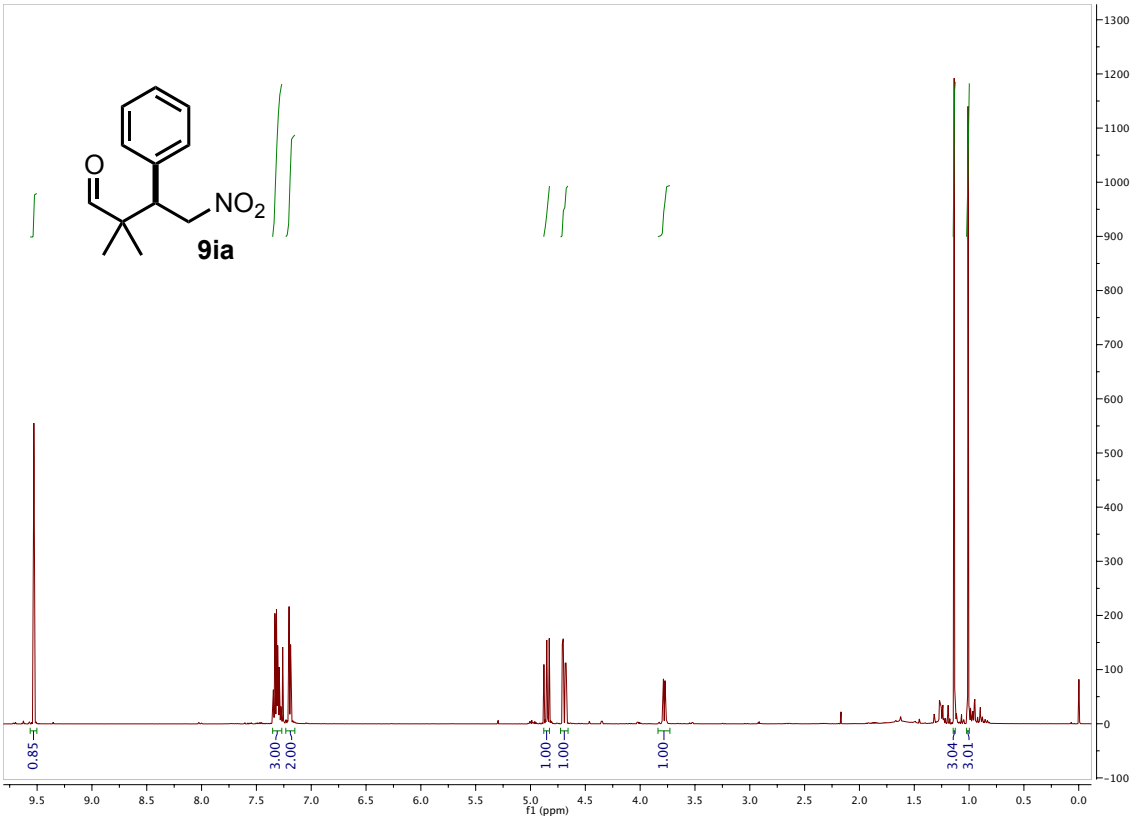
O
NO2
9ia
0.85
3.00
2.00
1.00
1.00
1.00
3.04
3.01
f1 (ppm)

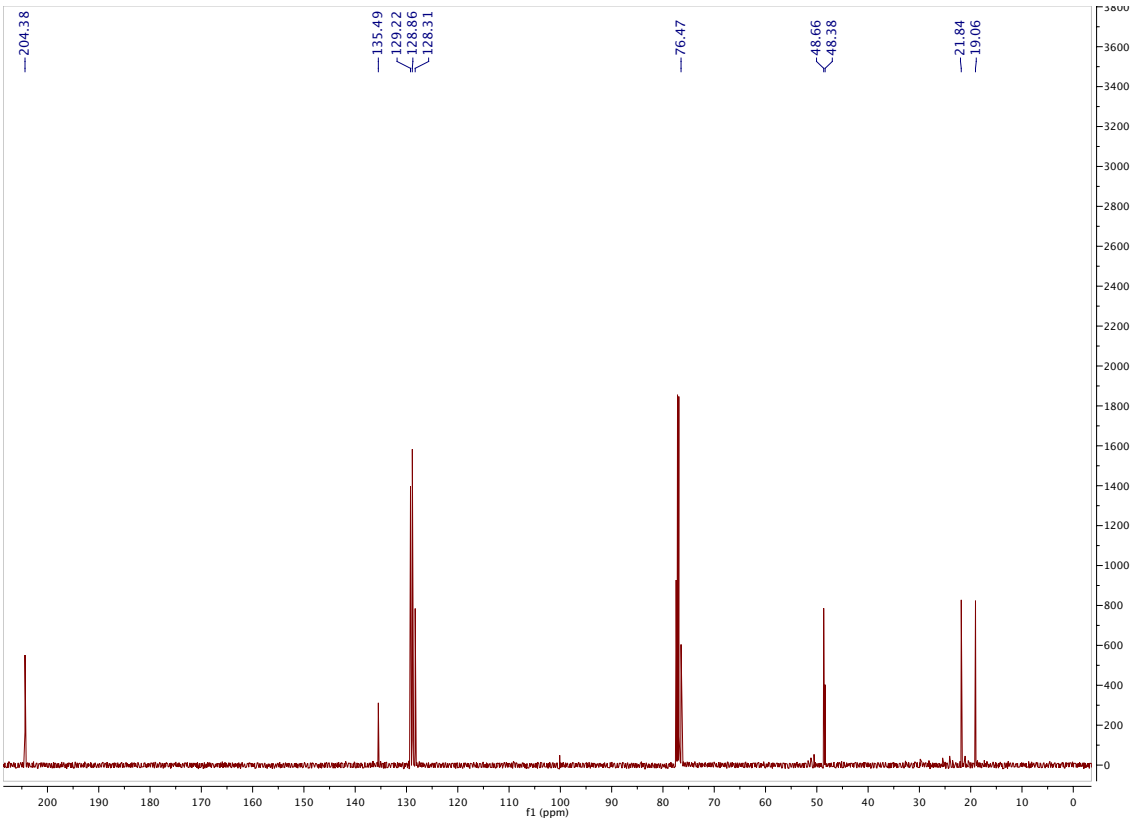
204.38
135.49
129.22
128.86
128.31
76.47
48.66
48.38
21.84
19.06
f1 (ppm)

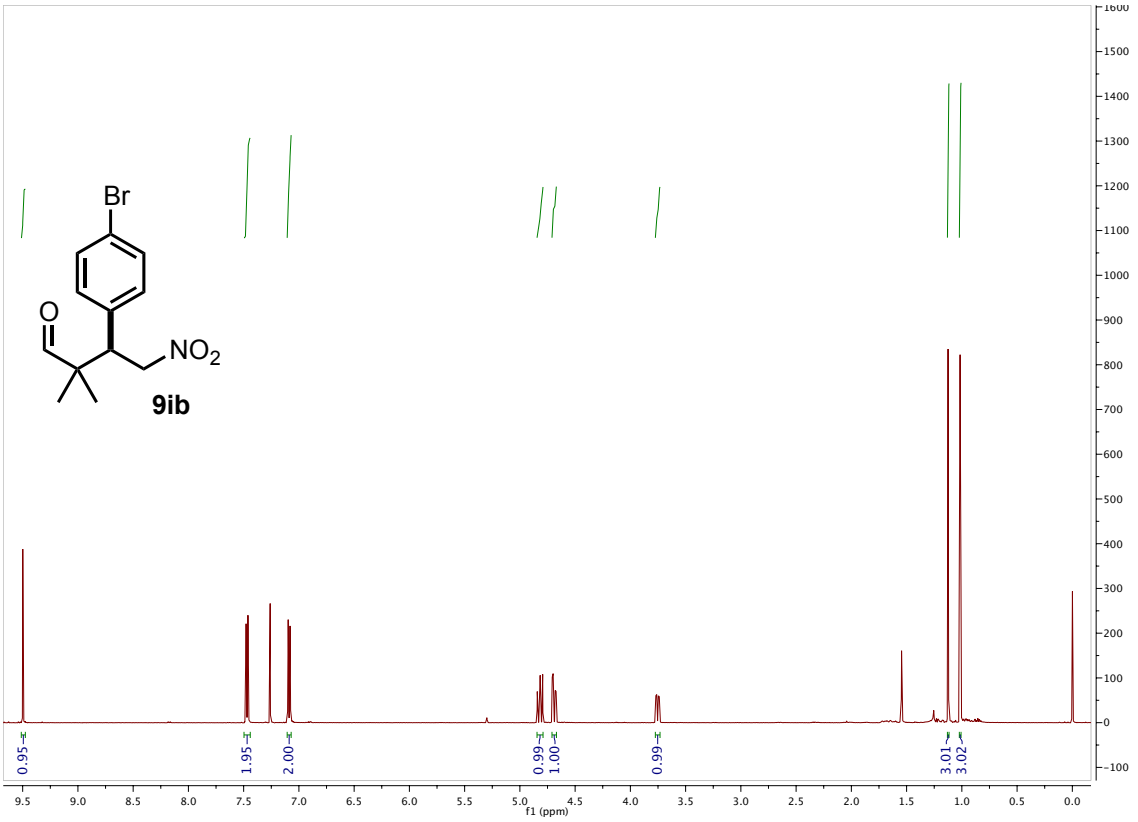
Br
O
NO2
9ib
0.95
1.95
2.00
0.99
1.00
0.99
3.01
3.02
f1 (ppm)

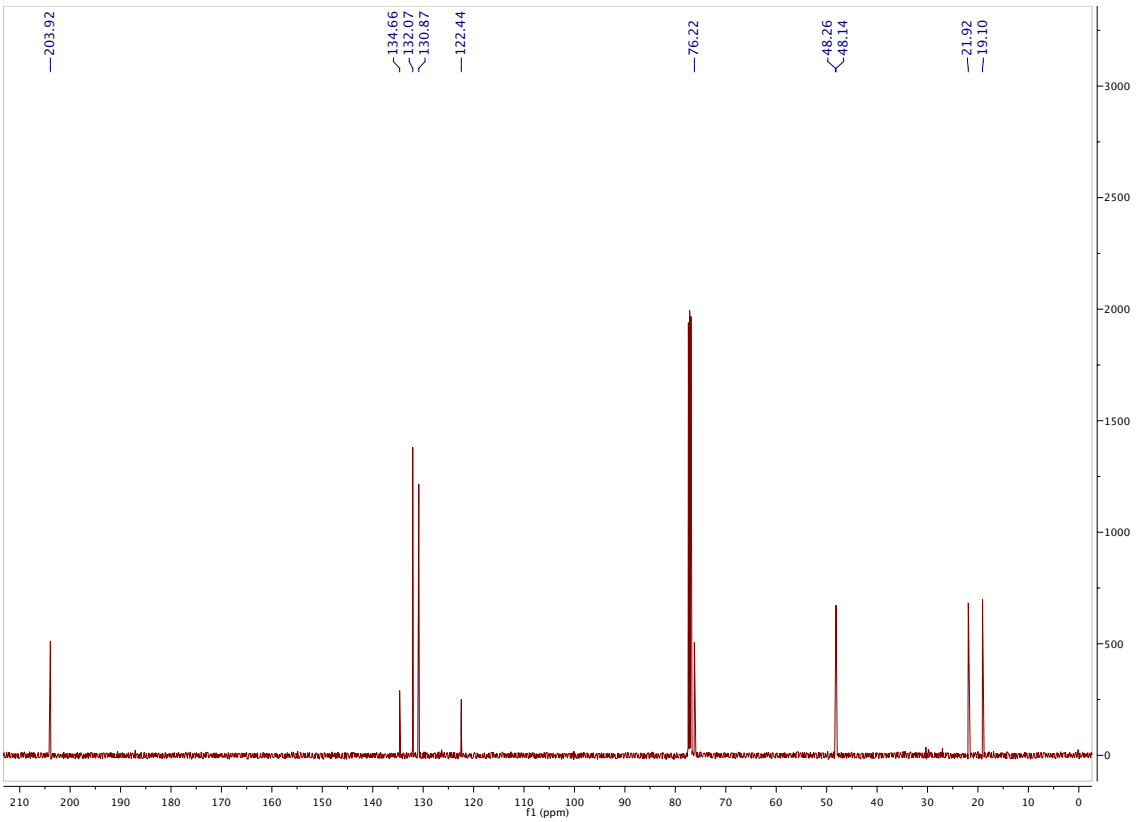
203.92
134.66
132.07
130.87
122.44
76.22
48.26
48.14
21.92
19.10
f1 (ppm)

Chapter III

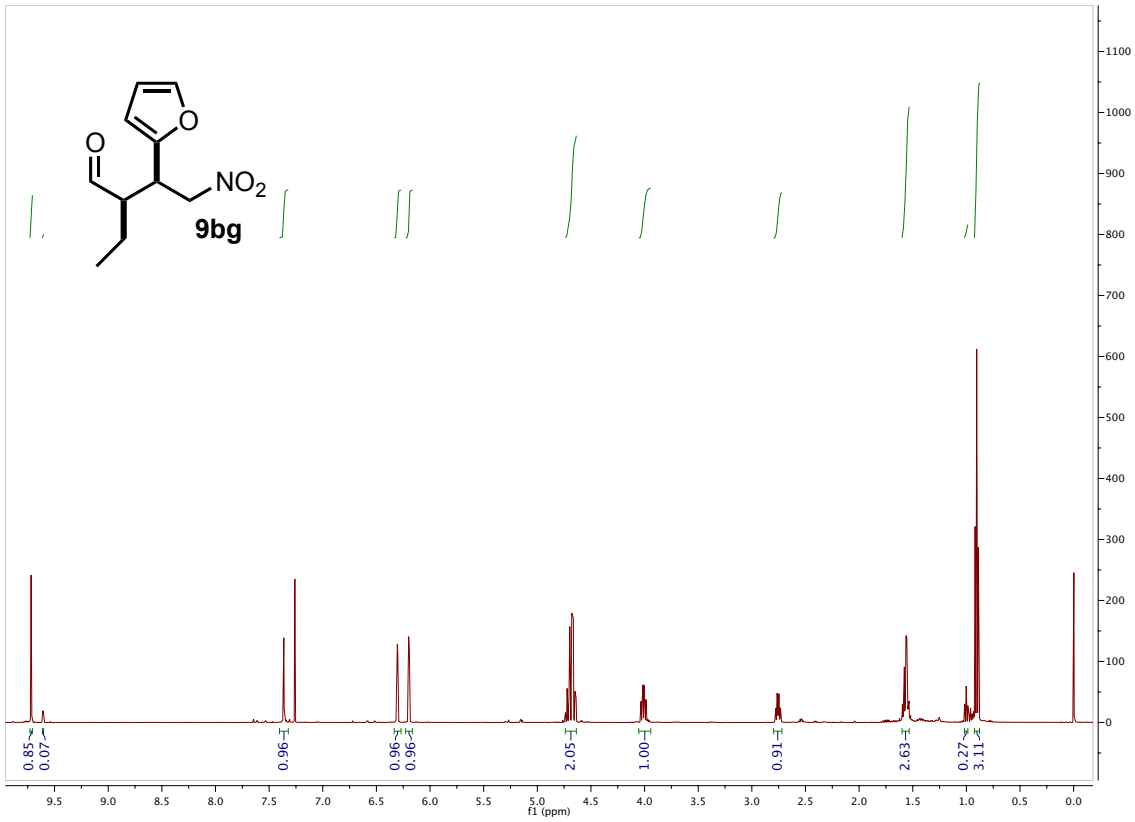
O
O
NO2
9bg
0.85
0.07
0.96
0.96
0.96
2.05
1.00
0.91
2.63
0.27
3.11
f1 (ppm)

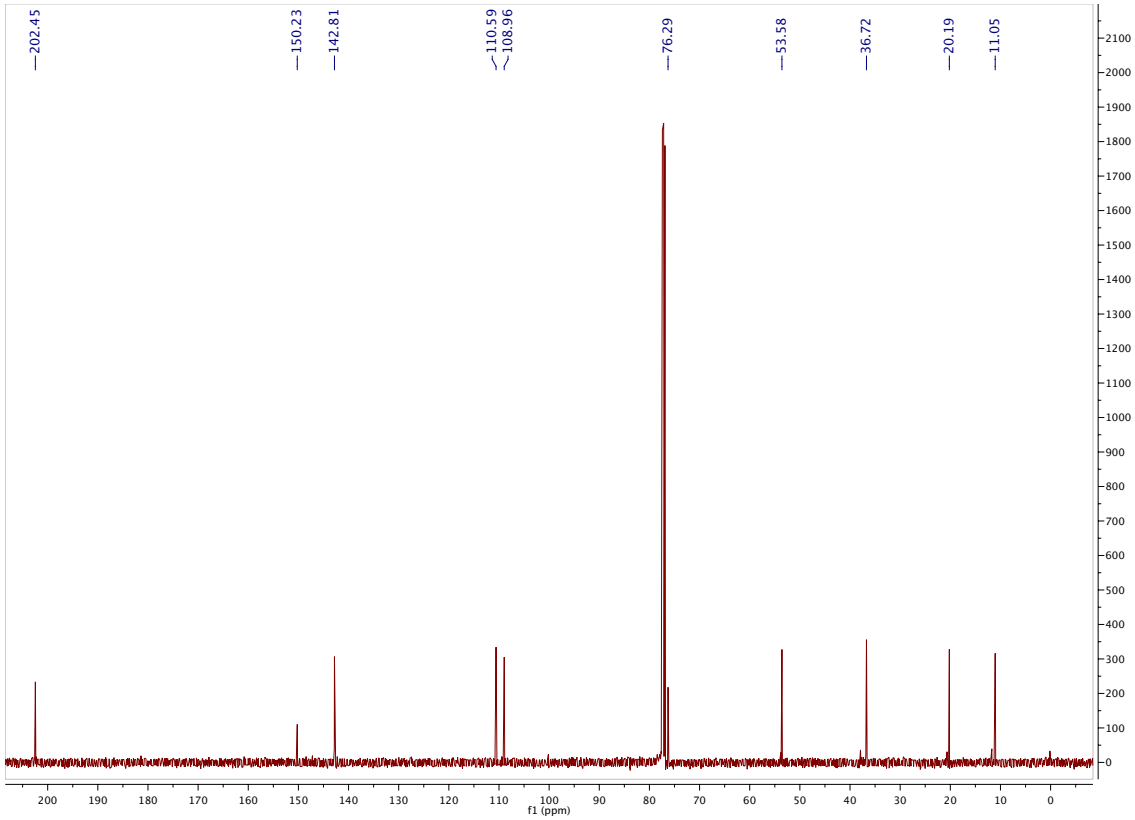
202.45
150.23
142.81
110.59
108.96
76.29
53.58
36.72
20.19
11.05
f1 (ppm)

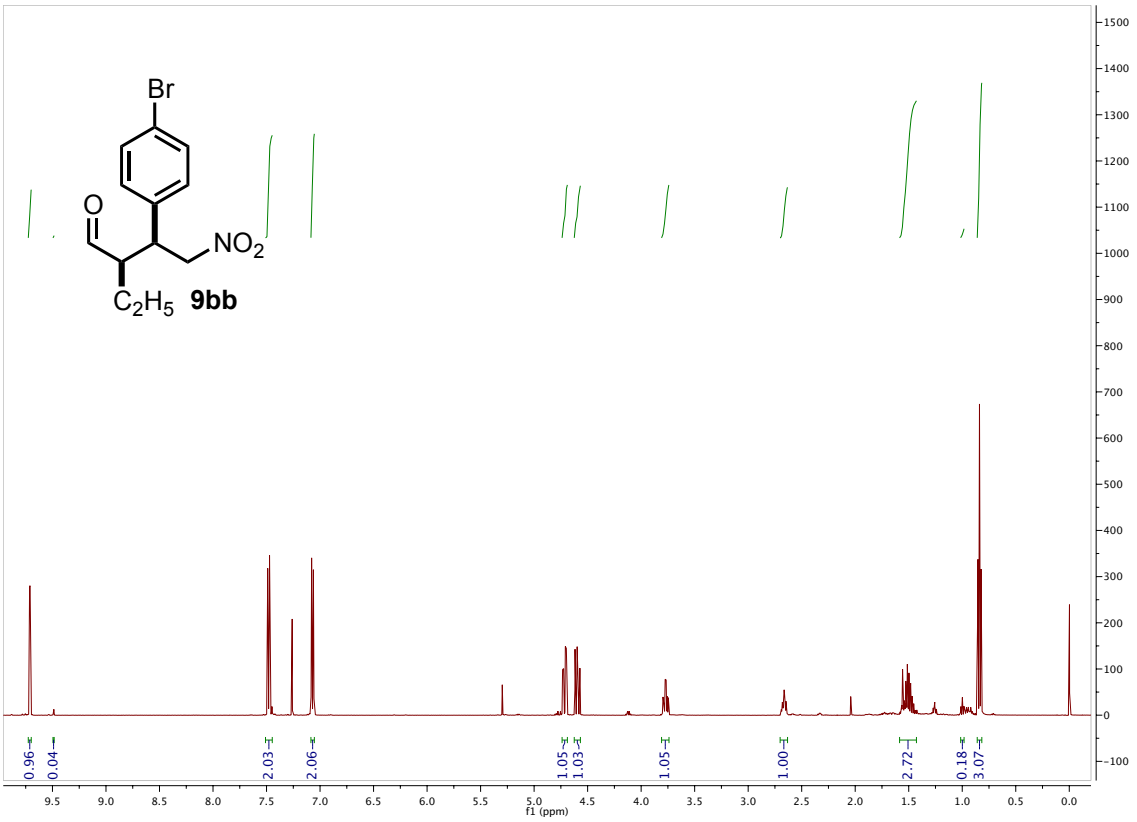
Br
O
NO2
C2H5
9bb
0.96
0.04
2.03
2.06
1.05
1.03
1.05
1.00
2.72
0.18
3.07
f1 (ppm)

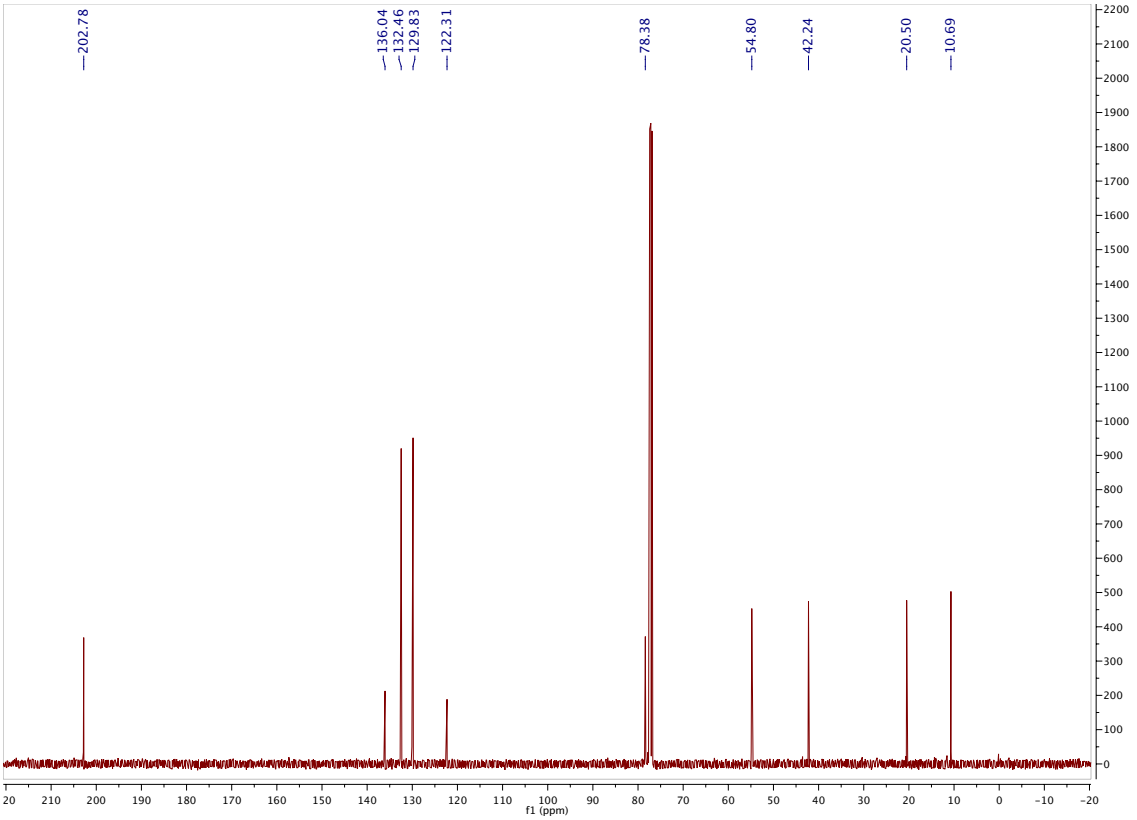
202.78
136.04
132.46
129.83
122.31
78.38
54.80
42.24
20.50
10.69
f1 (ppm)

Chapter III

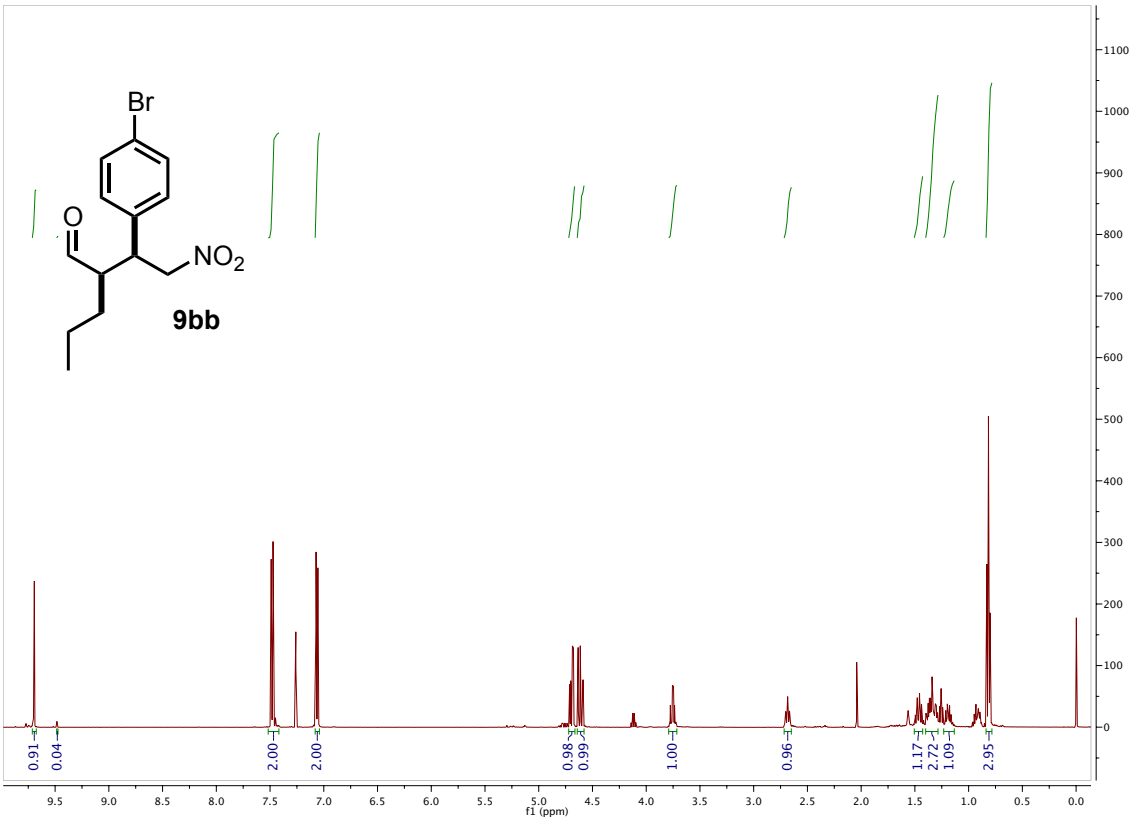
Br
O
NO2
9bb
0.91
0.04
2.00
2.00
0.98
0.99
1.00
0.96
1.17
2.72
1.09
2.95
f1 (ppm)

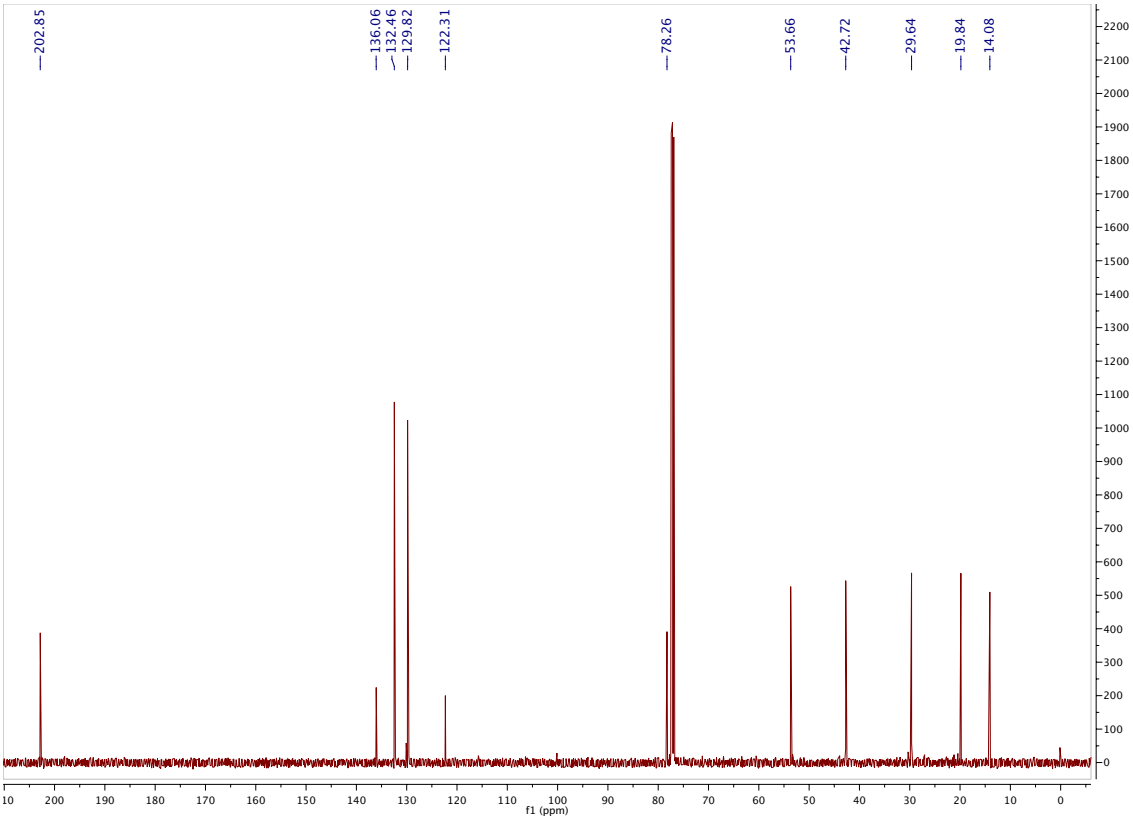
202.85
136.06
132.46
129.82
122.31
78.26
53.66
42.72
29.64
19.84
14.08
f1 (ppm)

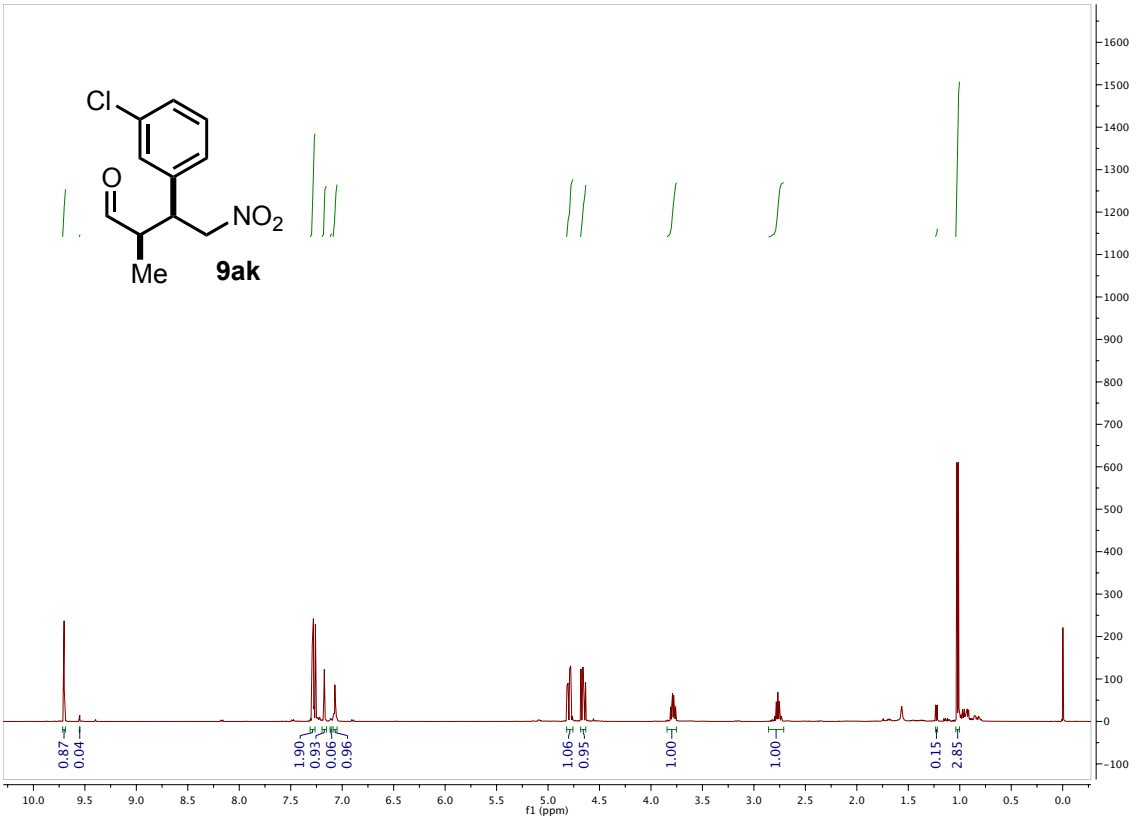
Cl
O
NO2
Me
9ak
0.87
0.04
1.90
0.93
0.06
0.96
1.06
0.95
1.00
1.00
0.15
2.85
f1 (ppm)

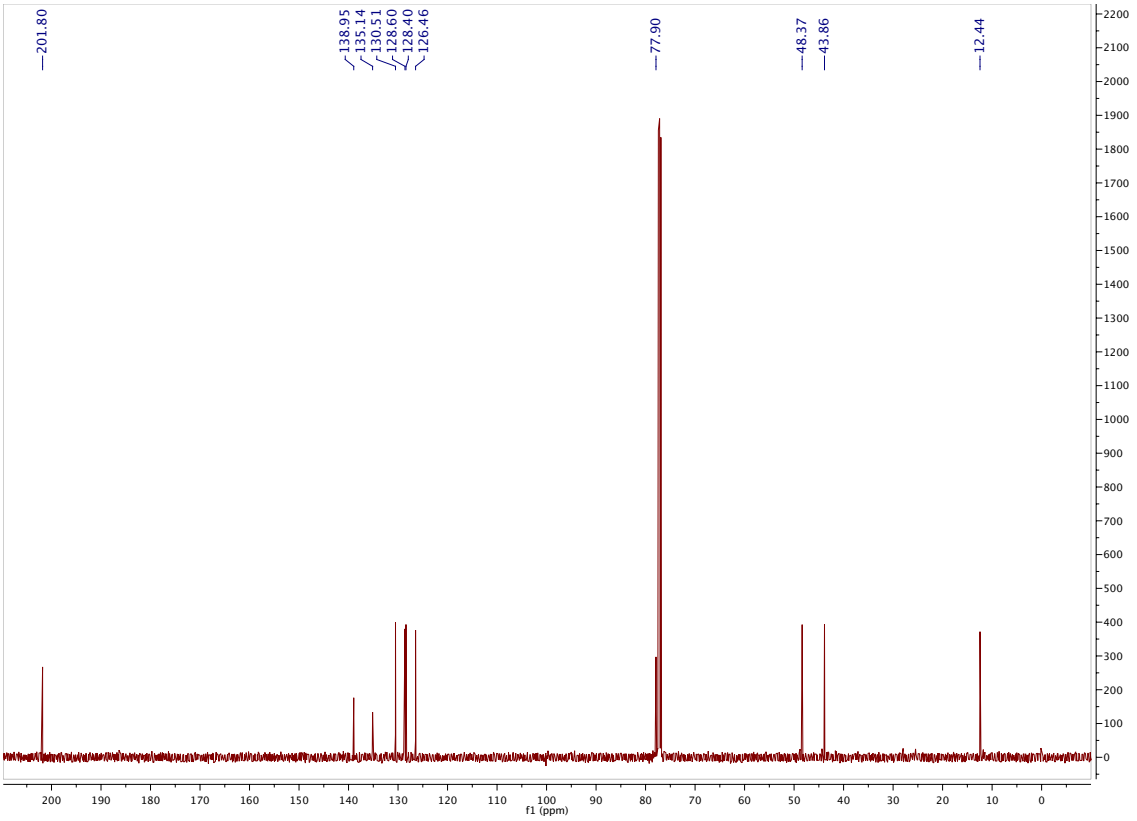
201.80
138.95
135.14
130.51
128.60
128.40
126.46
77.90
48.37
43.86
12.44
f1 (ppm)

Chapter III

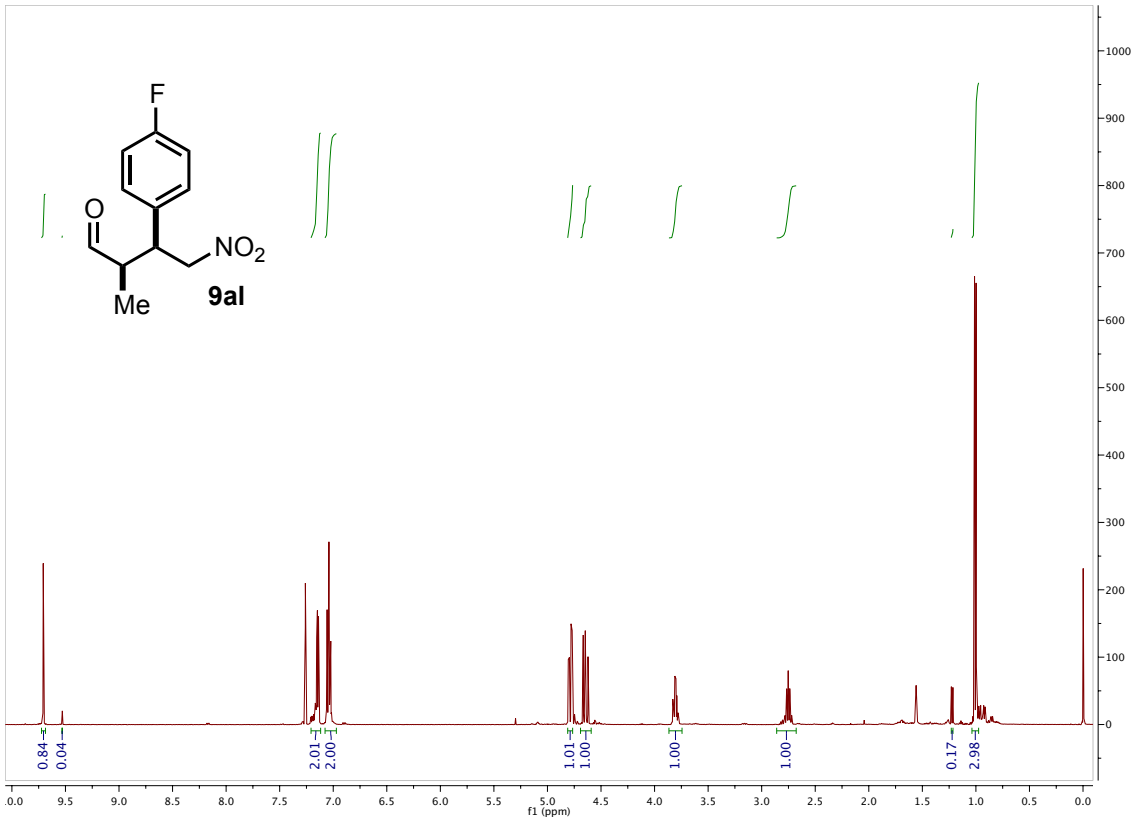
F
O
NO2
Me
9al
0.84
0.04
2.01
2.00
1.01
1.00
1.00
1.00
0.17
2.98
f1 (ppm)

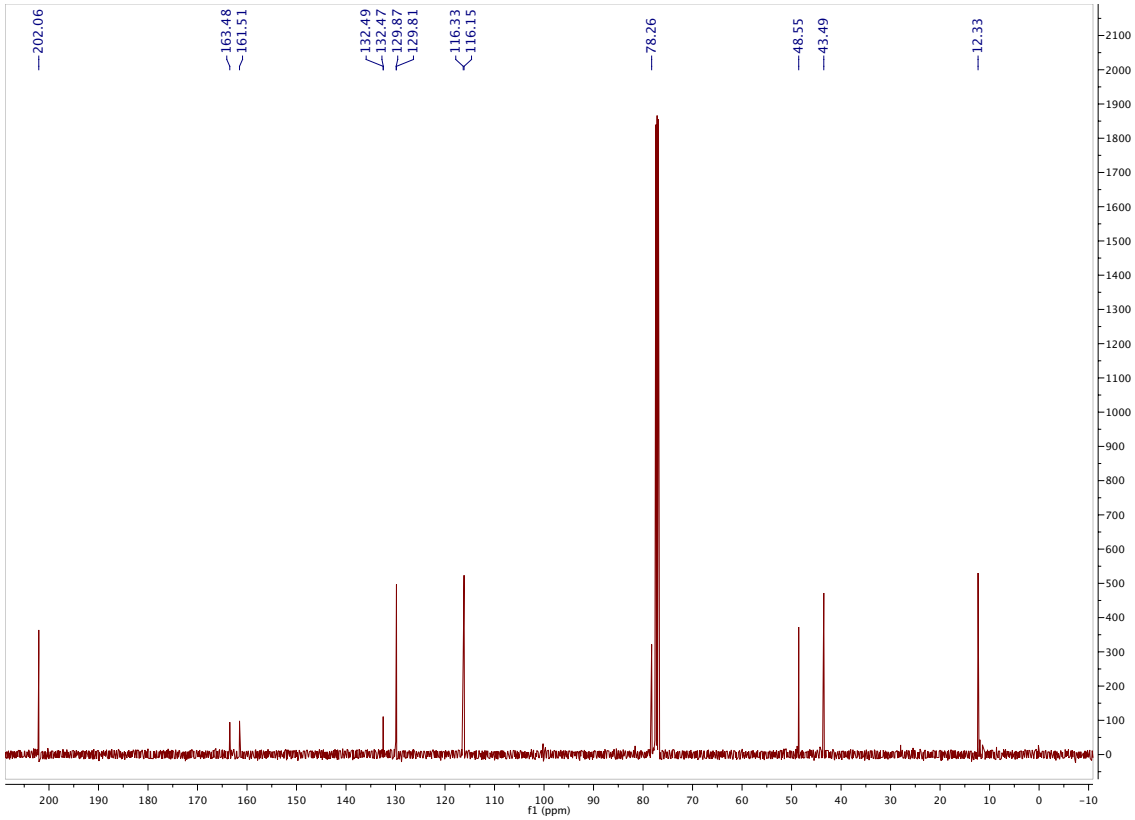
202.06
163.48
161.51
132.49
132.47
129.87
129.81
116.33
116.15
78.26
48.55
43.49
12.33
f1 (ppm)

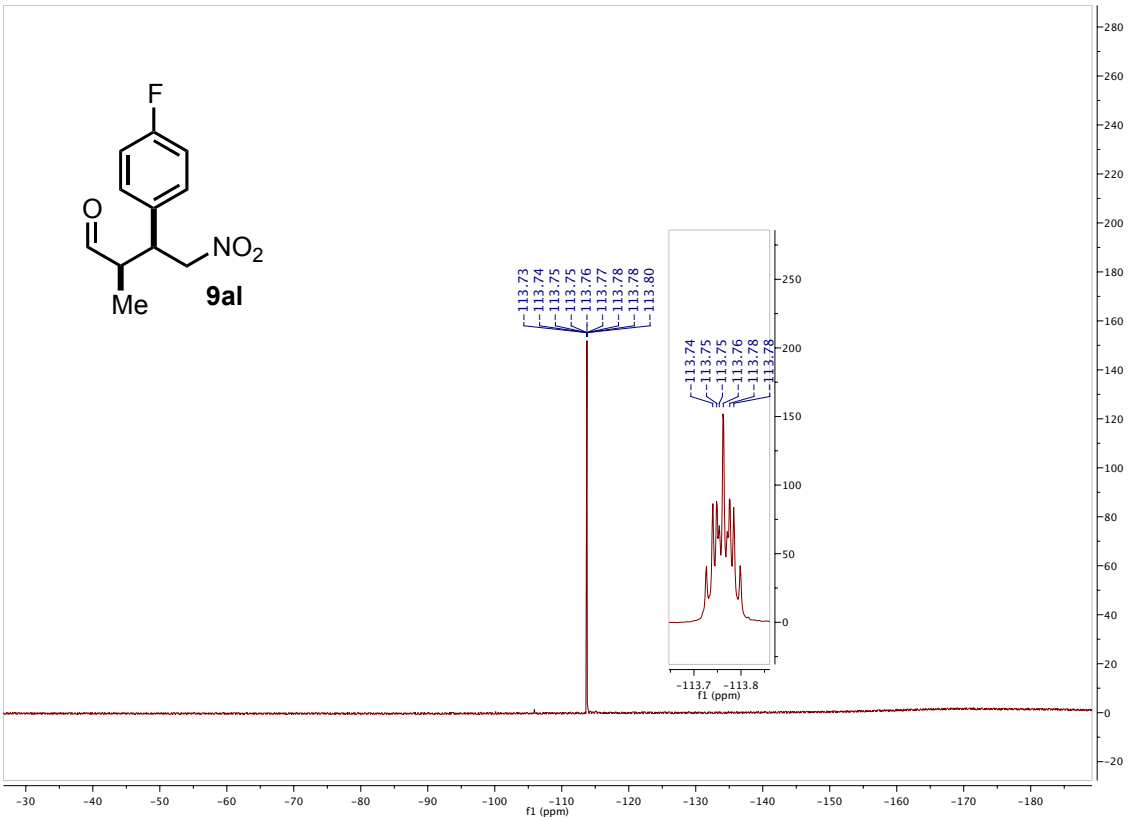
F
O
NO2
Me
9al
113.73
113.74
113.75
113.75
113.76
113.77
113.78
113.78
113.80
113.74
113.75
113.75
113.76
113.78
113.78
f1 (ppm)
f1 (ppm)

13. NMR spectra for pyrrolidine derivatives 10 and 11

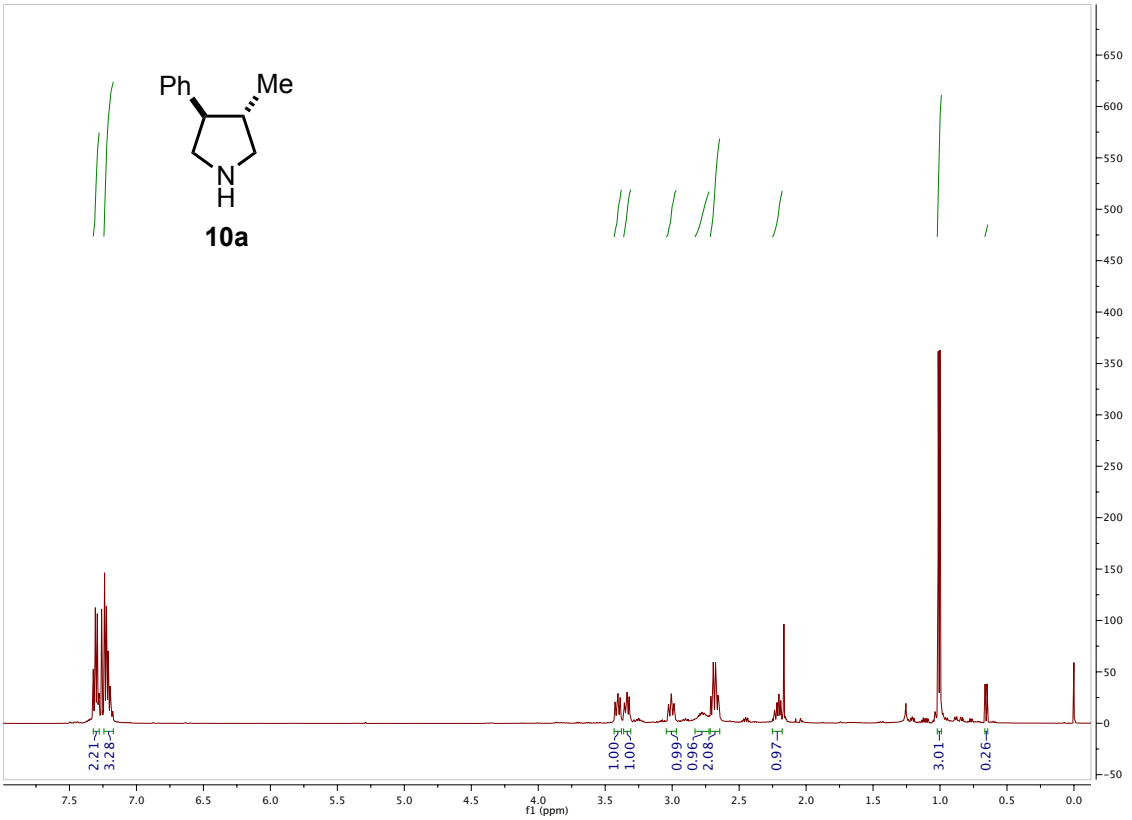

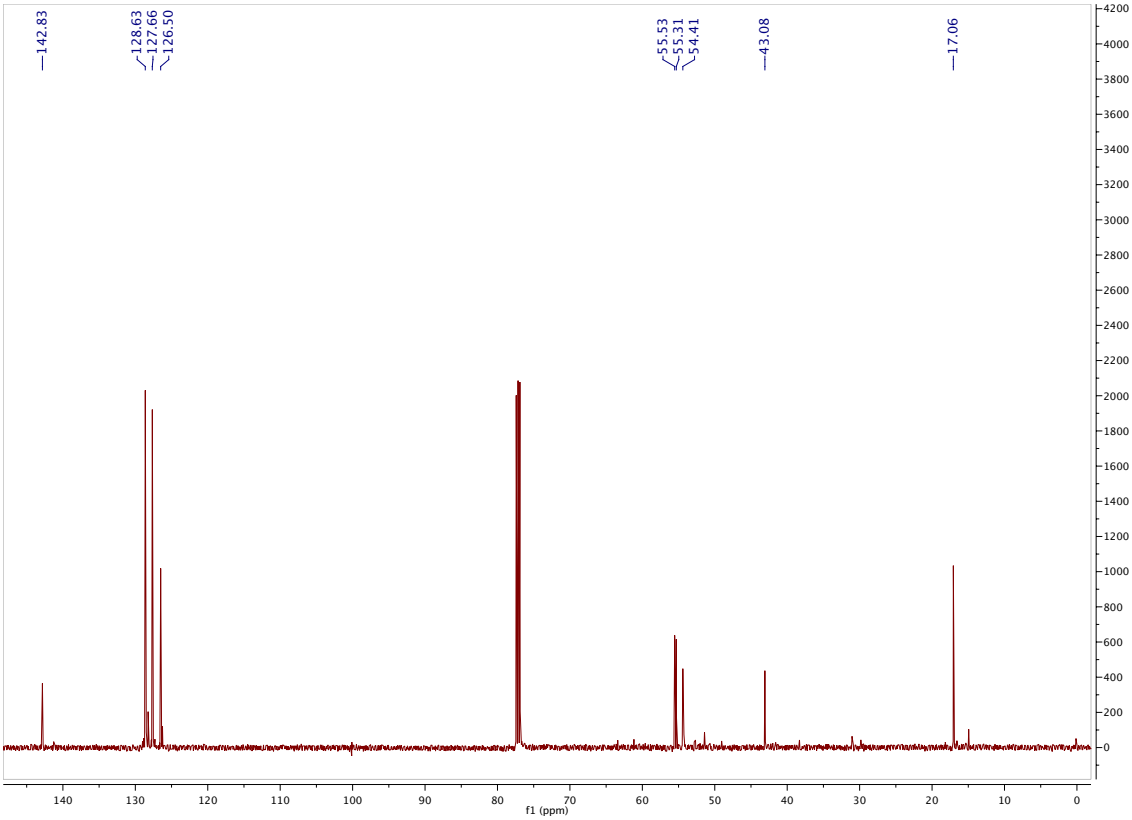

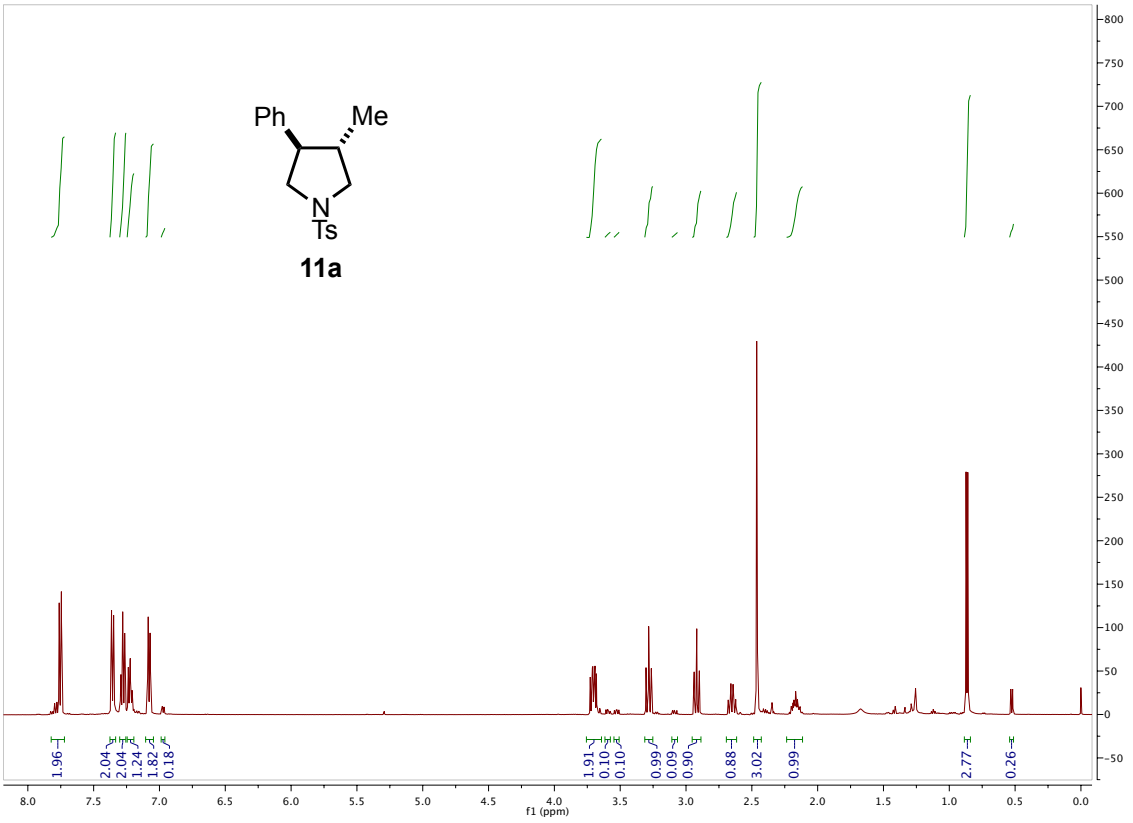
Ph
Me
N
Ts
11a
1.96
2.04
2.04
1.24
1.82
0.18
1.91
0.10
0.10
0.99
0.09
0.90
0.88
3.02
0.99
2.77
0.26
f1 (ppm)

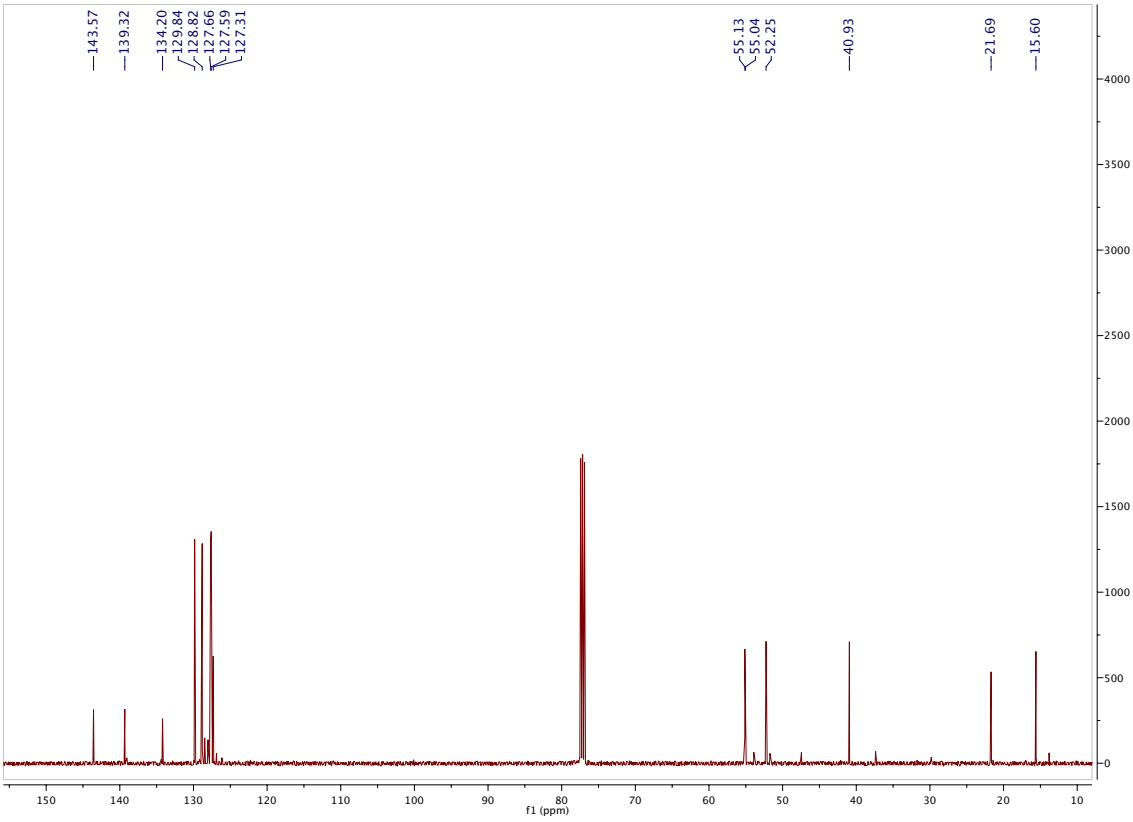
143.57
139.32
134.20
129.84
128.82
127.66
127.59
127.31
55.13
55.04
52.25
40.93
21.69
15.60
f1 (ppm)

Chapter III

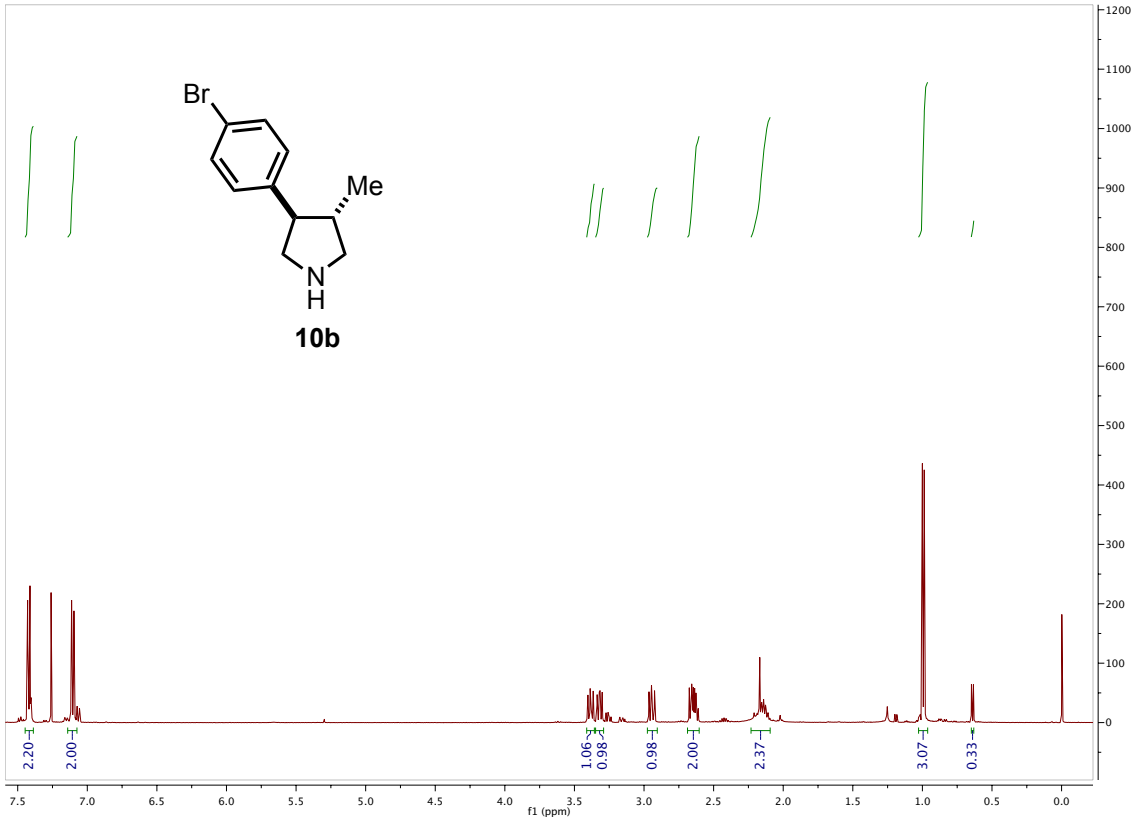
Br
Me
N
H
10b
2.20
2.00
1.06
0.98
0.98
2.00
2.37
3.07
0.33
f1 (ppm)

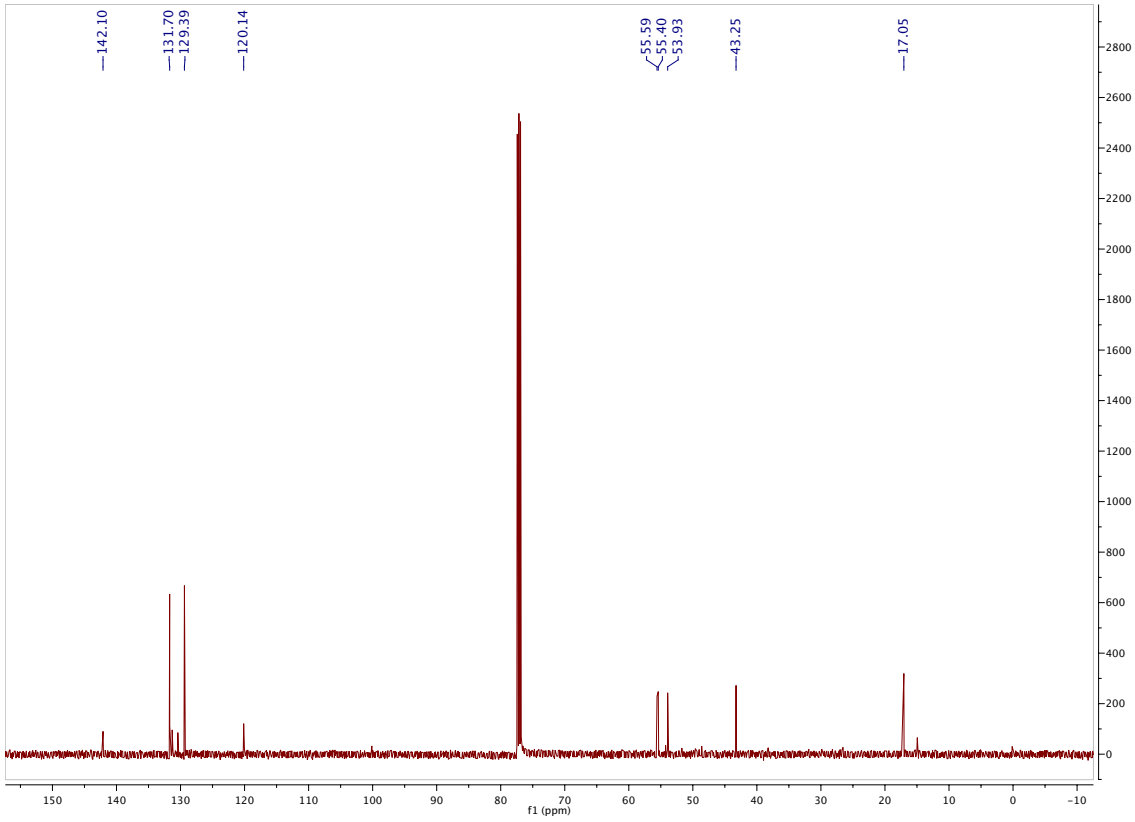
142.10
131.70
129.39
120.14
55.59
55.40
53.93
43.25
17.05
f1 (ppm)

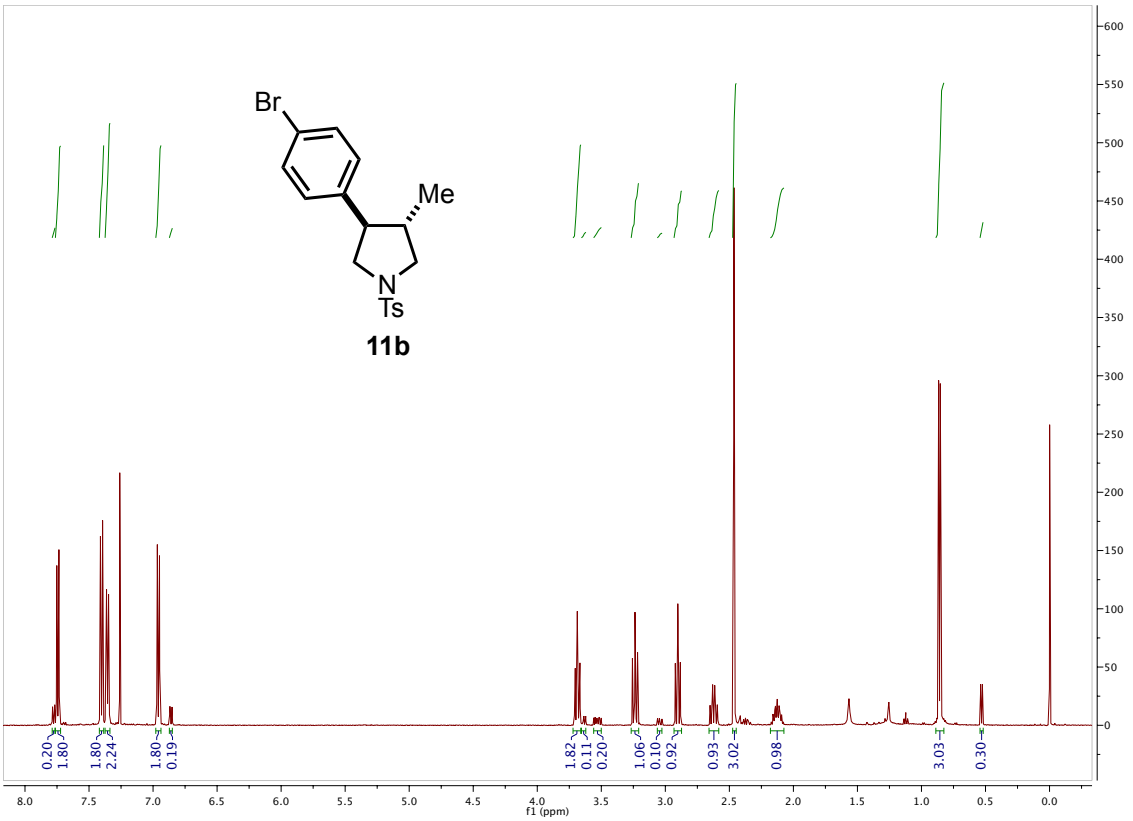
Br
Me
N
Ts
11b
0.20
1.80
1.80
2.24
1.80
0.19
1.82
0.11
0.20
1.06
0.10
0.92
0.93
3.02
0.98
3.03
0.30
f1 (ppm)

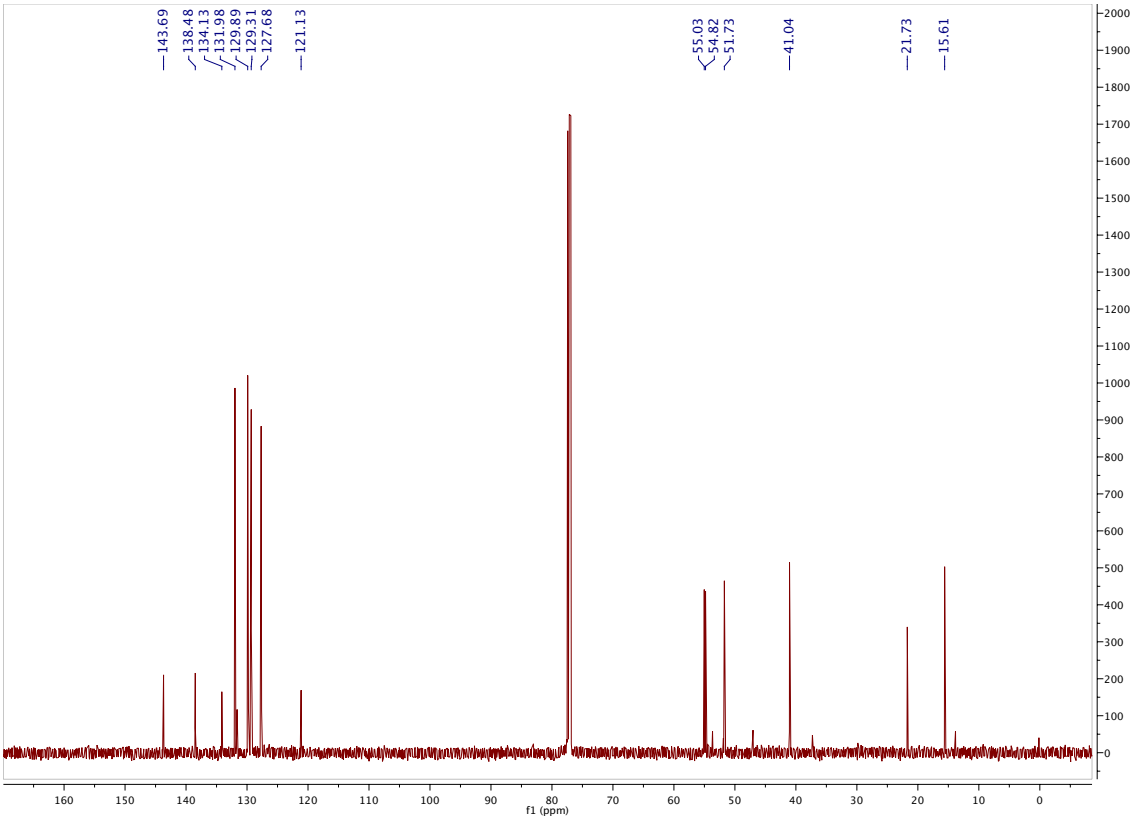
143.69
138.48
134.13
131.98
129.89
129.31
127.68
121.13
55.03
54.82
51.73
41.04
21.73
15.61
f1 (ppm)

14. Chiral HPLC chromatograms for Michael adducts 9

(2*R*,3*S*)-2-Methyl-4-nitro-3-phenylbutanal (9aa).

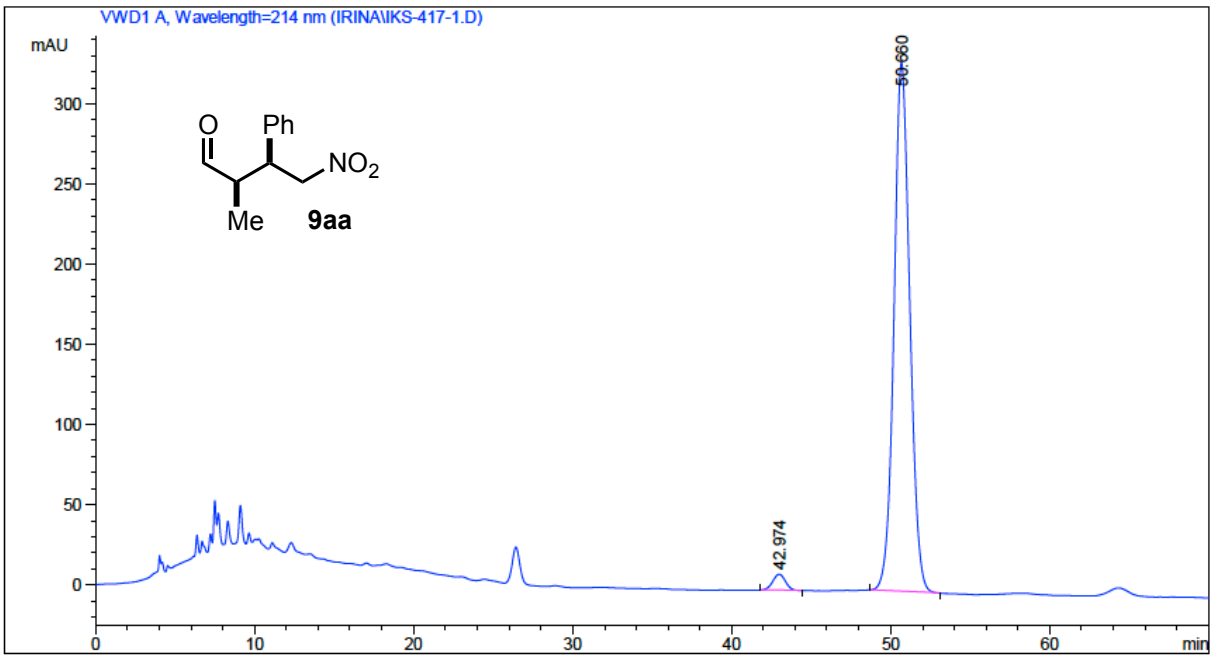

Peak #	RetTime [min]	Type	Width [min]	Area mAU *s	Height [mAU]	Area %
1	42.974	BB	0.8376	558.50861	10.02870	2.3981
2	50.660	BB	1.0587	2.27312e4	329.90790	97.6019

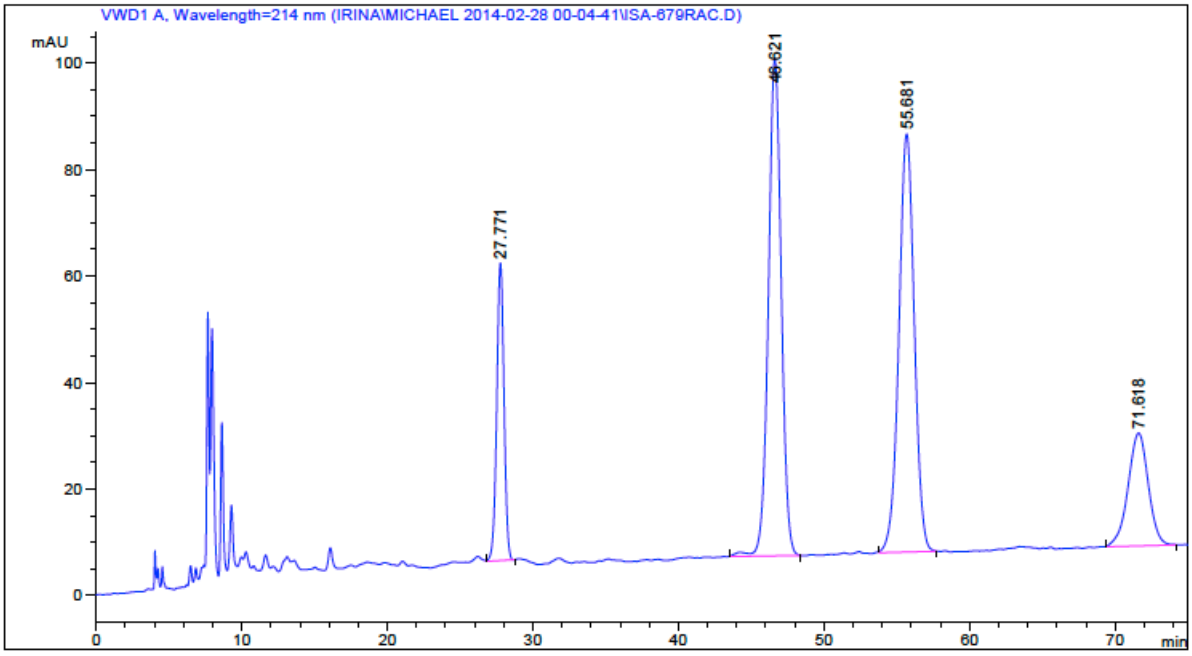

Peak #	RetTime [min]	Type	Width [min]	Area mAU *s	Height [mAU]	Area %
1	27.771	VB	0.5339	1929.99622	55.89649	12.4587
2	46.621	BB	0.9458	5745.55371	93.26810	37.0892
3	55.681	BB	1.1341	5769.60205	78.49923	37.2444
4	71.618	BB	1.4908	2046.02295	21.18382	13.2077

(2*R*,3*S*)-2-Ethyl-4-nitro-3-phenylbutanal (9ba).

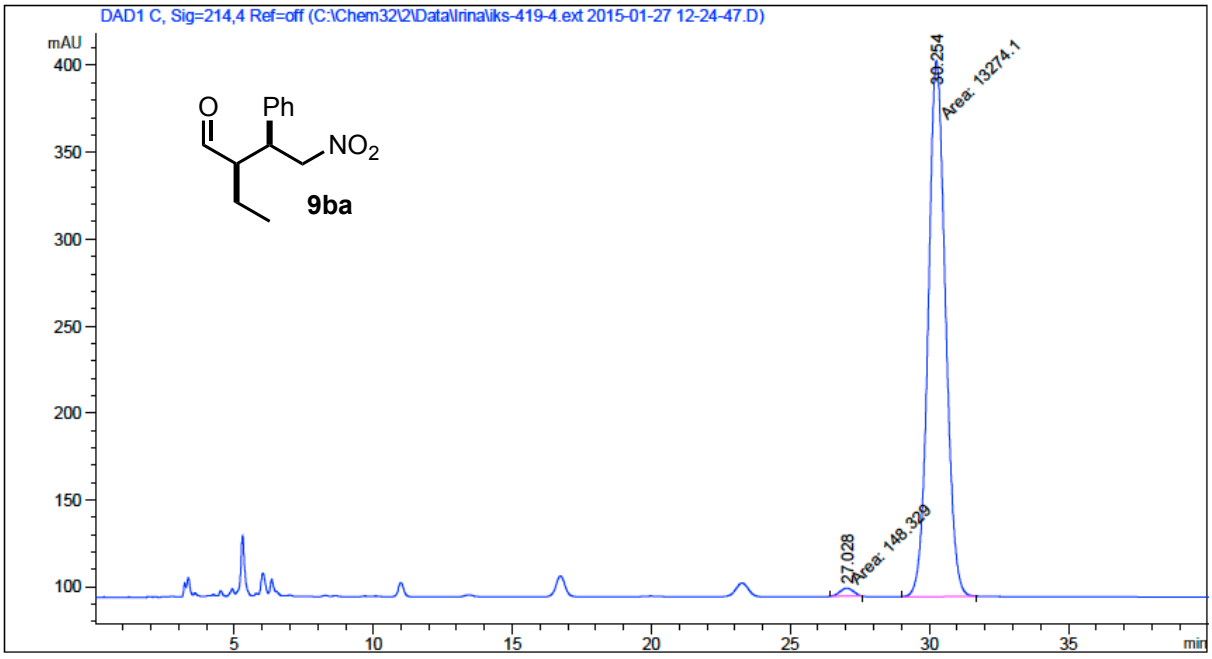

Peak #	RetTime [min]	Type	Width [min]	Area [mAU*s]	Height [mAU]	Area %
1	27.028	MM	0.5442	148.32927	4.54302	1.1051
2	30.254	MM	0.7179	1.32741e4	308.18759	98.8949

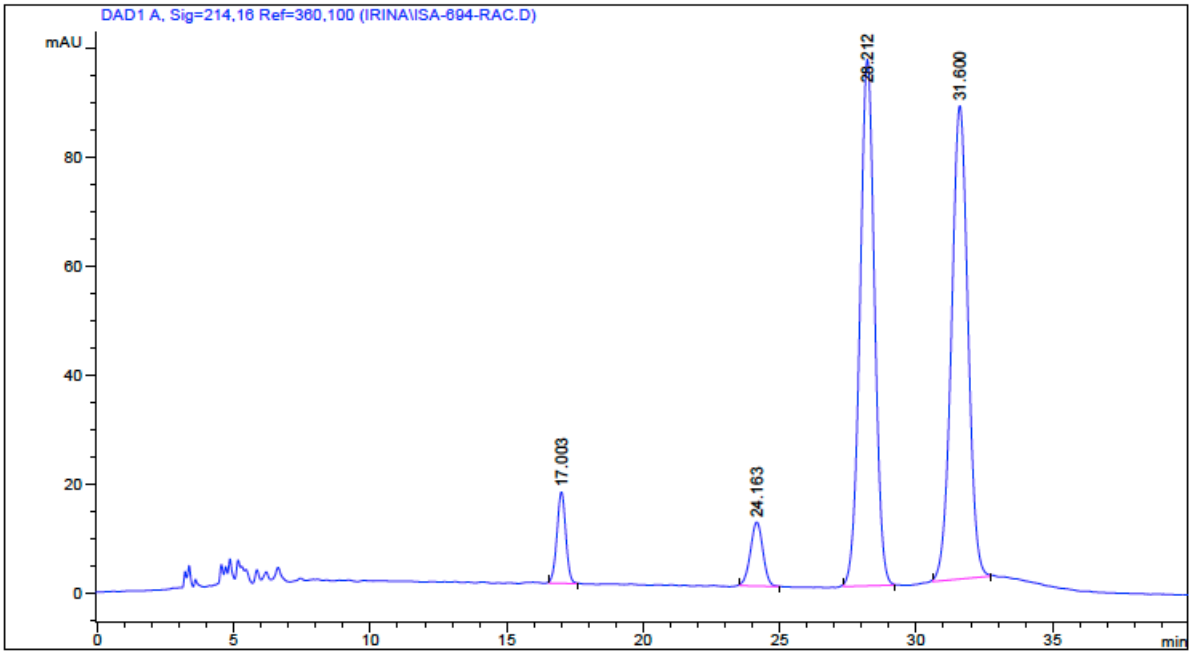

Peak #	RetTime [min]	Type	Width [min]	Area [mAU*s]	Height [mAU]	Area %
1	17.003	BB	0.3452	378.30066	16.76839	4.7336
2	24.163	BB	0.4913	373.75708	11.74257	4.6768
3	28.212	BB	0.5706	3602.64600	96.70171	45.0794
4	31.600	BB	0.6401	3637.08179	86.92855	45.5103

Chapter III

(2*R*,3*S*)-2-Propyl-4-nitro-3-phenylbutanal (9ca).

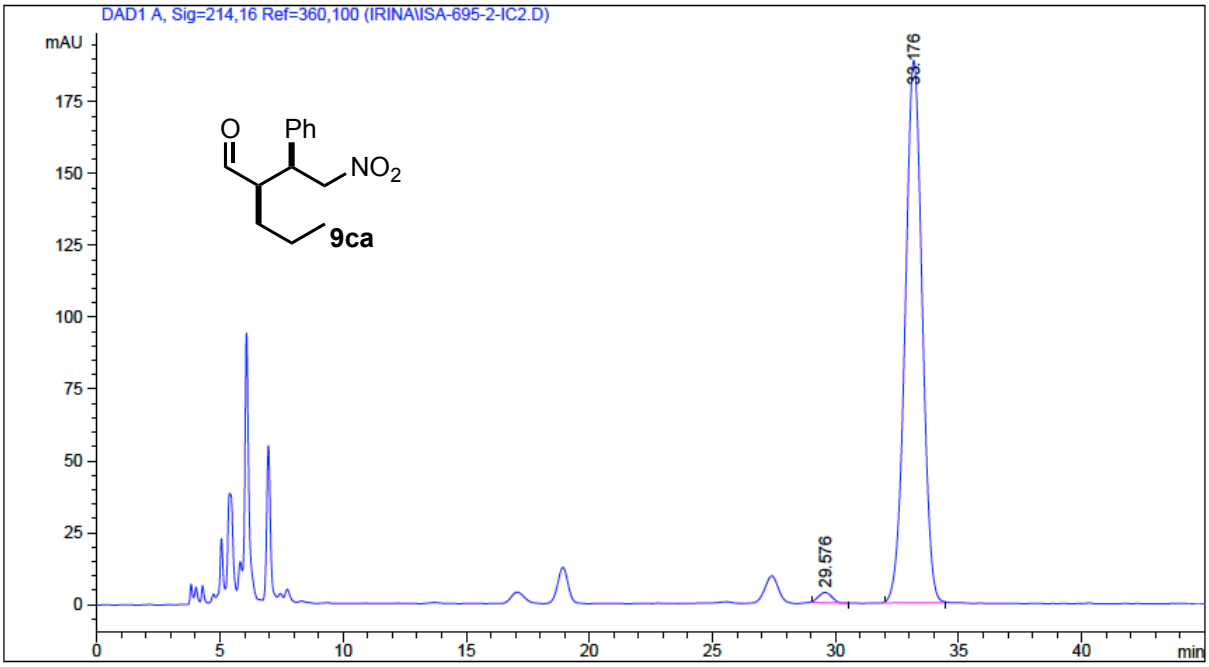

Peak #	RetTime [min]	Type	Width [min]	Area [mAU*s]	Height [mAU]	Area %
1	29.576	BB	0.5158	132.10237	3.55276	1.4382
2	33.176	BB	0.7417	9052.96484	188.71964	98.5618

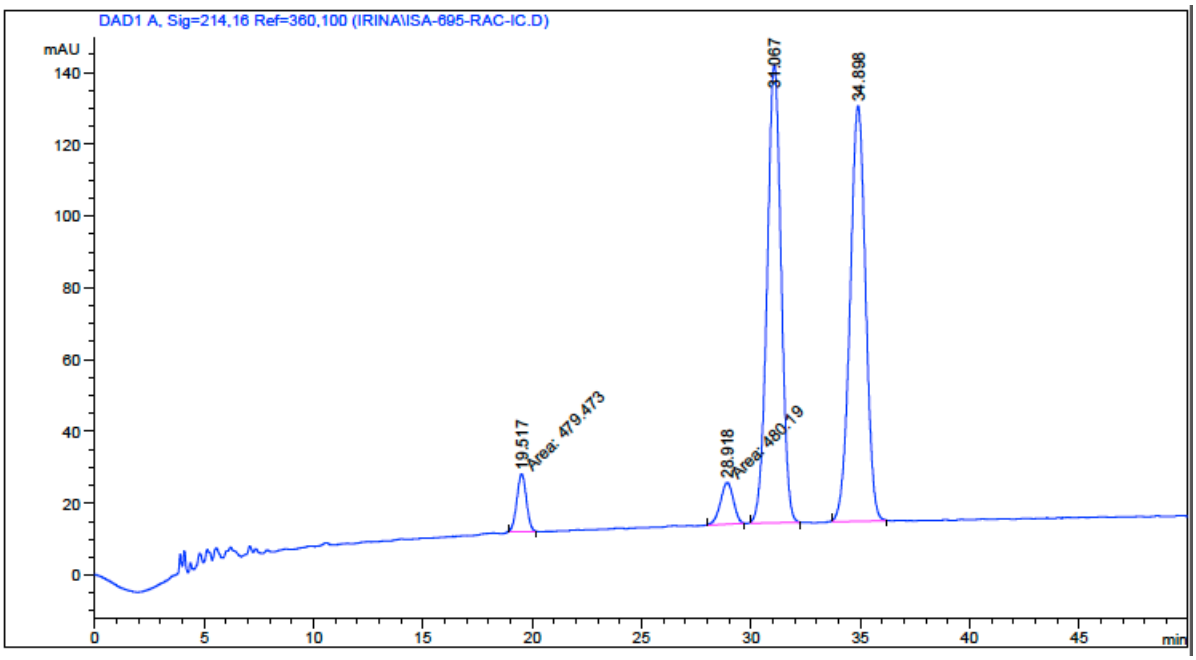

Peak #	RetTime [min]	Type	Width [min]	Area [mAU*s]	Height [mAU]	Area %
1	19.517	MM	0.5009	479.47299	15.95300	3.8776
2	28.918	MM	0.6891	480.18970	11.61382	3.8834
3	31.067	BB	0.6926	5699.99951	127.73183	46.0968
4	34.898	BB	0.7652	5705.62793	115.72260	46.1423

(2*R*,3*S*)-2-Pentyl-4-nitro-3-phenylbutanal (9da).

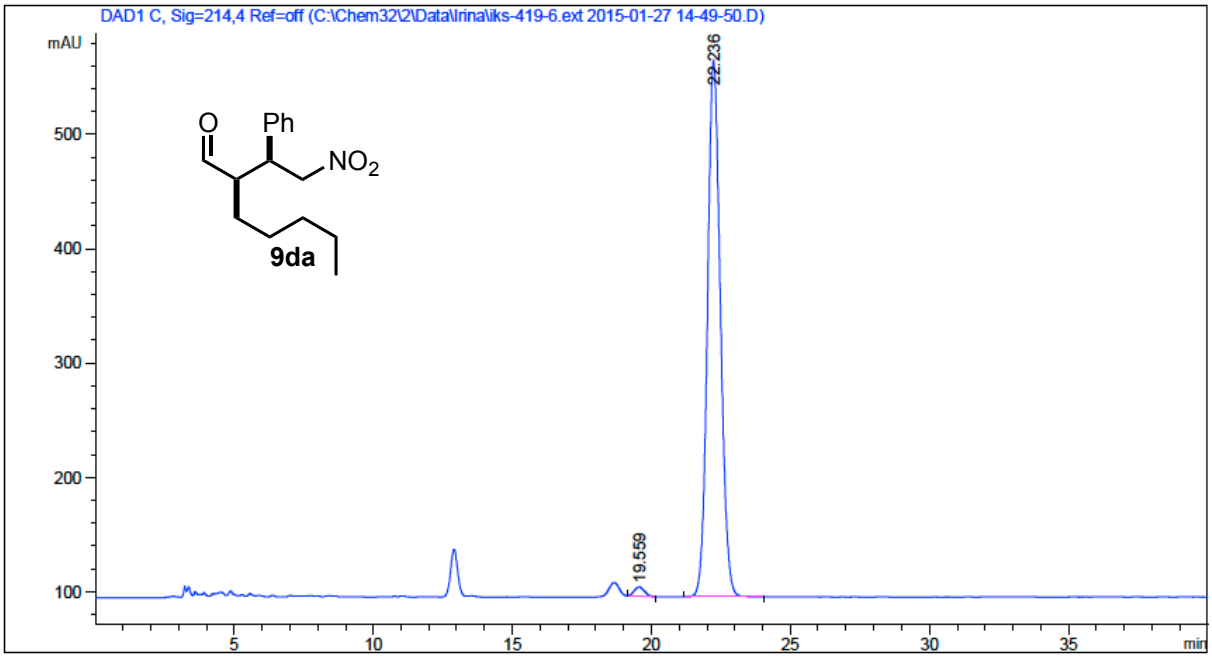

Peak #	RetTime [min]	Type	Width [min]	Area [mAU*s]	Height [mAU]	Area %
1	19.559	BB	0.3909	203.23190	8.03891	1.3300
2	22.236	BB	0.4951	1.50771e4	468.93716	98.6700

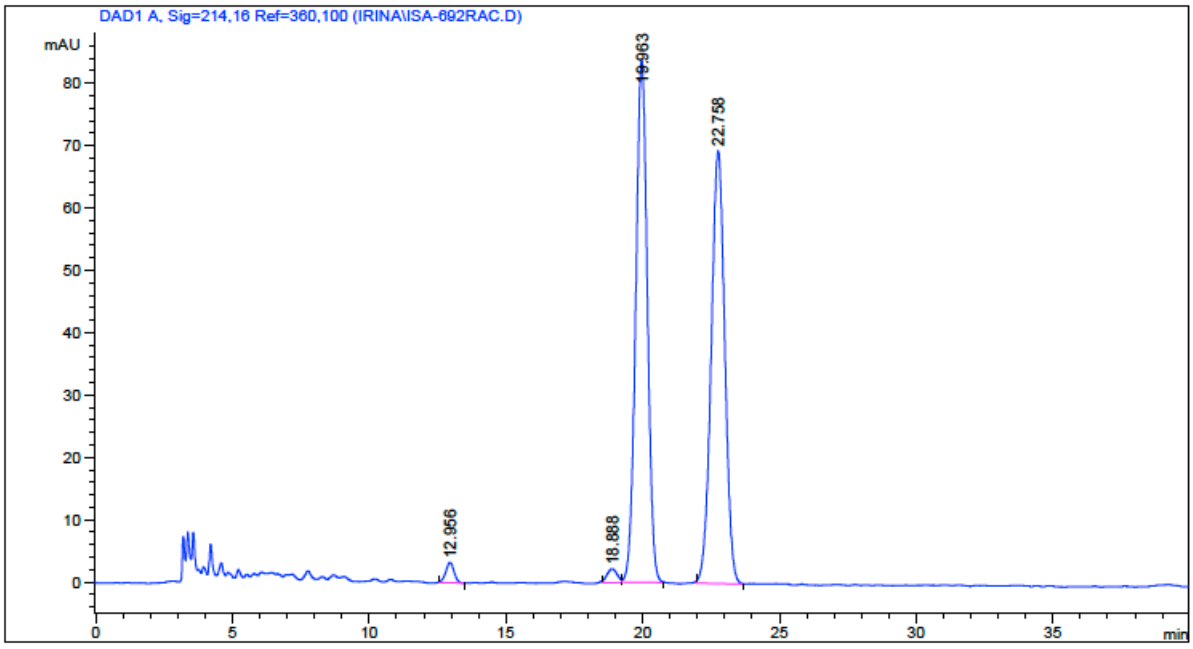

Peak #	RetTime [min]	Type	Width [min]	Area [mAU*s]	Height [mAU]	Area %
1	12.956	BB	0.3243	67.33094	3.24246	1.3520
2	18.888	BV	0.3687	53.77660	2.11467	1.0798
3	19.963	VB	0.4579	2468.34399	83.74474	49.5635
4	22.758	BB	0.5342	2390.71118	69.34342	48.0047

Chapter III

(2*R*,3*S*)-2-Decyl-4-nitro-3-phenylbutanal (9ea).

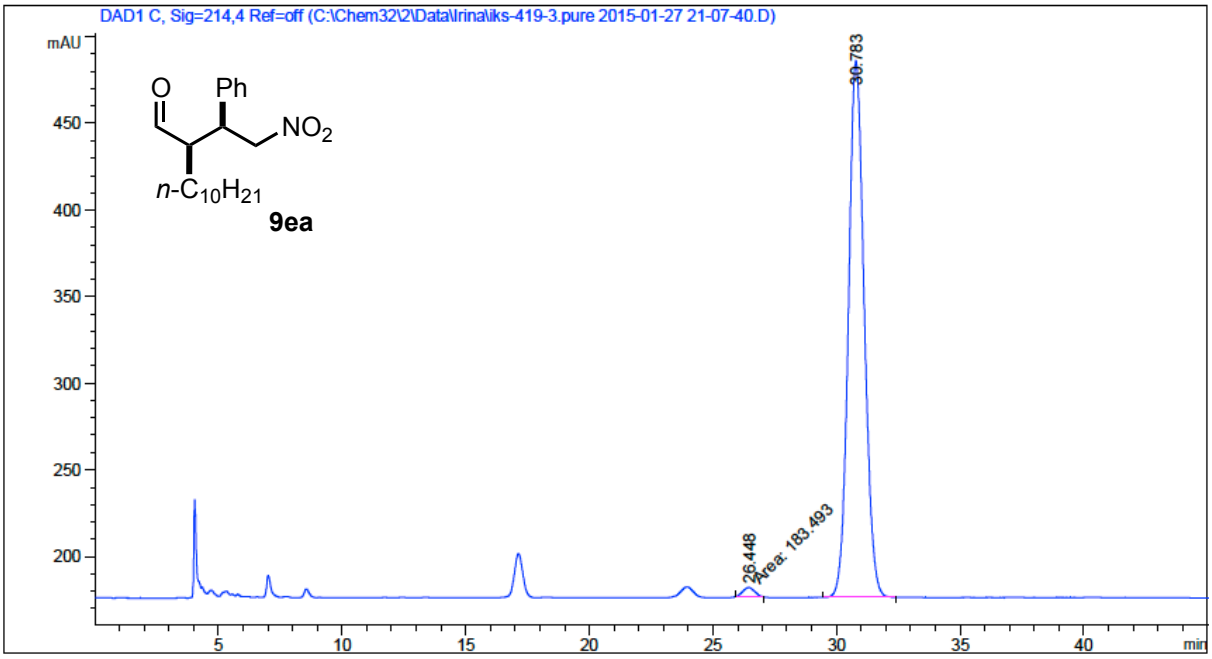

Peak #	RetTime [min]	Type	Width [min]	Area [mAU*s]	Height [mAU]	Area %
1	26.448	MM	0.5672	183.49313	5.39196	1.3219
2	30.783	BB	0.6819	1.36978e4	309.74420	98.6781

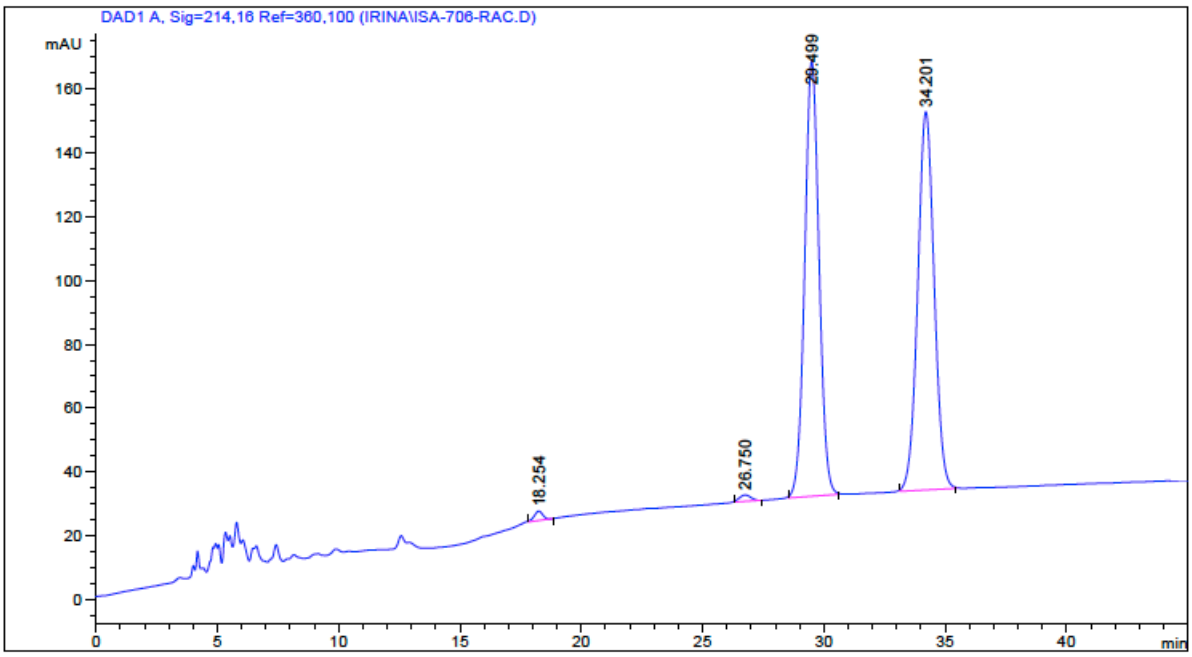

Peak #	RetTime [min]	Type	Width [min]	Area [mAU*s]	Height [mAU]	Area %
1	18.254	BB	0.3718	70.95798	2.91731	0.6283
2	26.750	BB	0.4893	65.31441	1.98809	0.5784
3	29.499	BB	0.6321	5583.16797	136.23596	49.4384
4	34.201	BB	0.7271	5573.74365	118.42125	49.3549

(2*R*,3*S*)-2-(Undec-10-enal)-4-nitro-3-phenylbutanal (9fa).

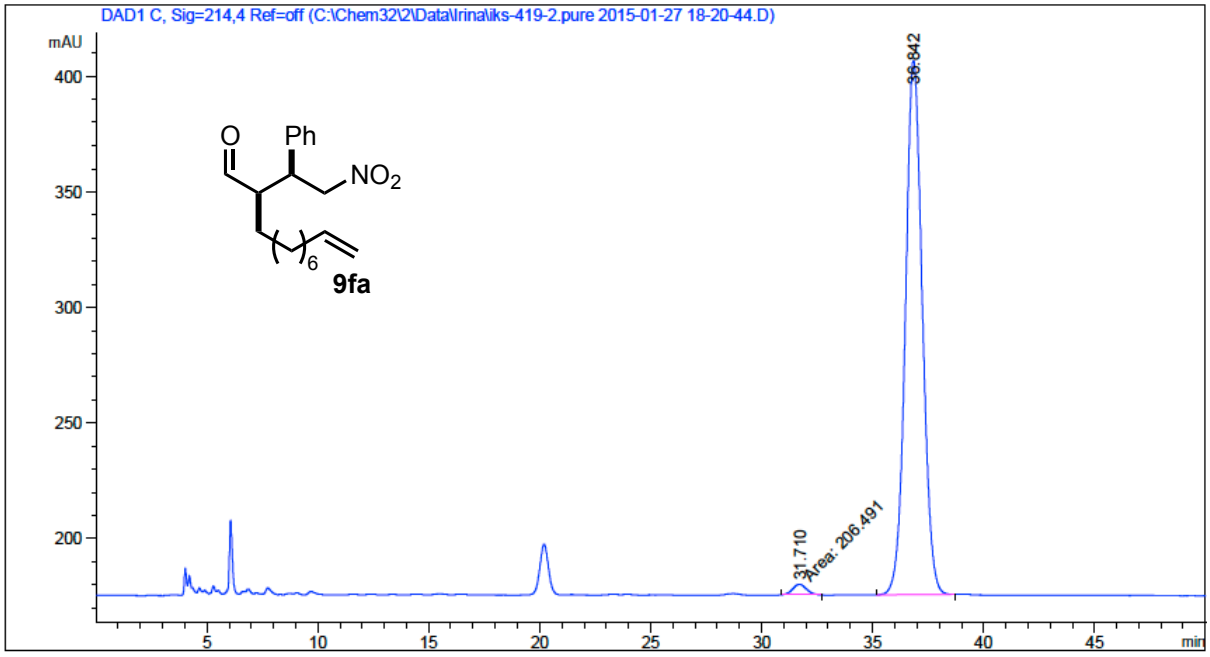

Peak #	RetTime [min]	Type	Width [min]	Area [mAU*s]	Height [mAU]	Area %
1	31.710	MM	0.7418	206.49109	4.63935	1.6634
2	36.842	BB	0.8118	1.22071e4	231.25949	98.3366

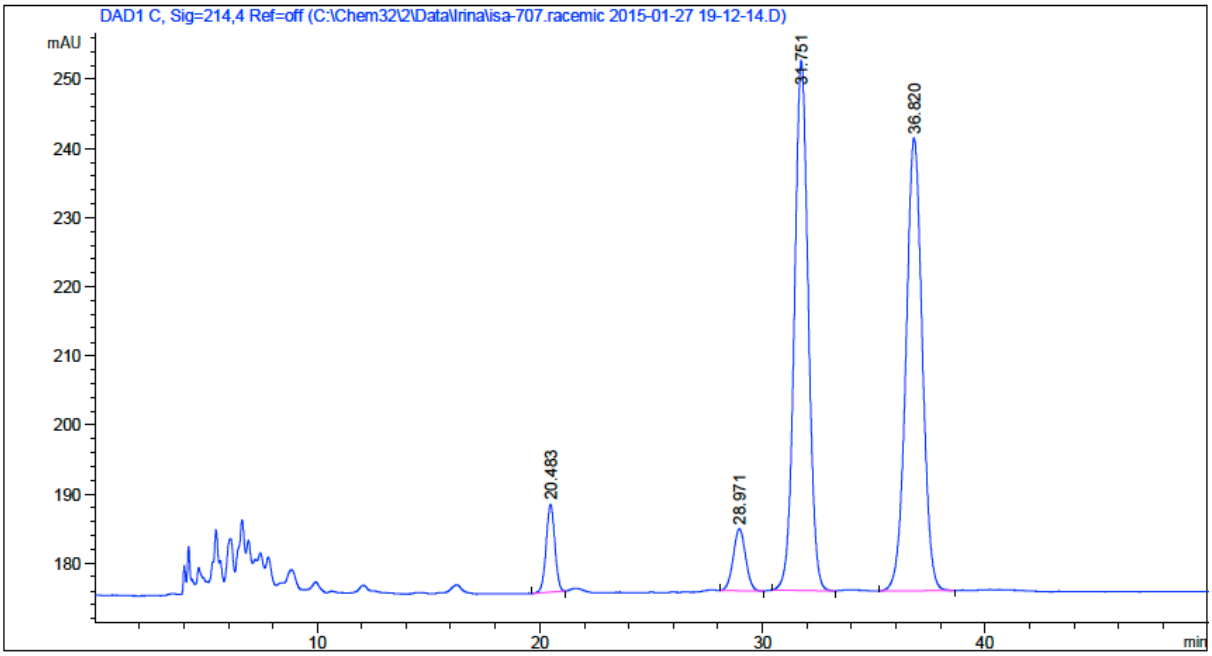

Peak #	RetTime [min]	Type	Width [min]	Area [mAU*s]	Height [mAU]	Area %
1	20.483	BB	0.4223	346.11459	12.68730	4.7078
2	28.971	BB	0.5464	347.00287	8.98837	4.7199
3	31.751	BB	0.6664	3327.62012	76.66579	45.2622
4	36.820	BB	0.7732	3331.13672	65.51259	45.3100

Chapter III

(2*R*,3*S*)-2-(Benzyl)-4-nitro-3-phenylbutanal (9ga).

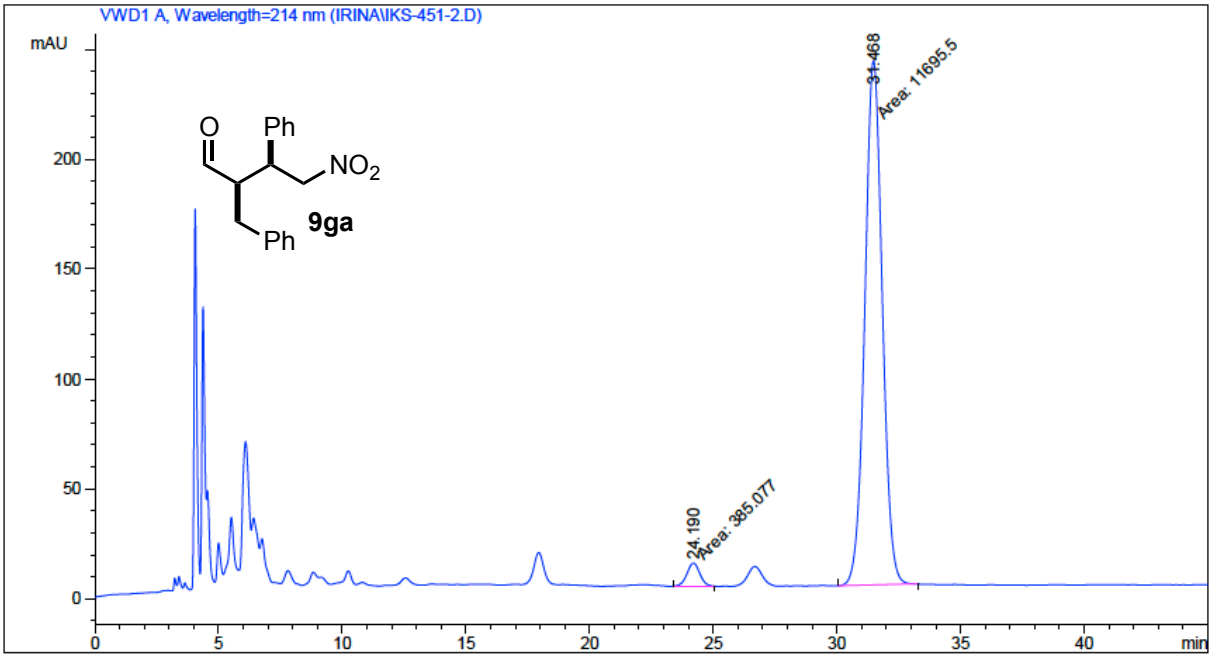

Peak #	RetTime [min]	Type	Width [min]	Area mAU *s	Height [mAU]	Area %
1	24.190	MM	0.6069	385.07721	10.57503	3.1876
2	31.468	MM	0.8163	1.16955e4	238.78075	96.8124

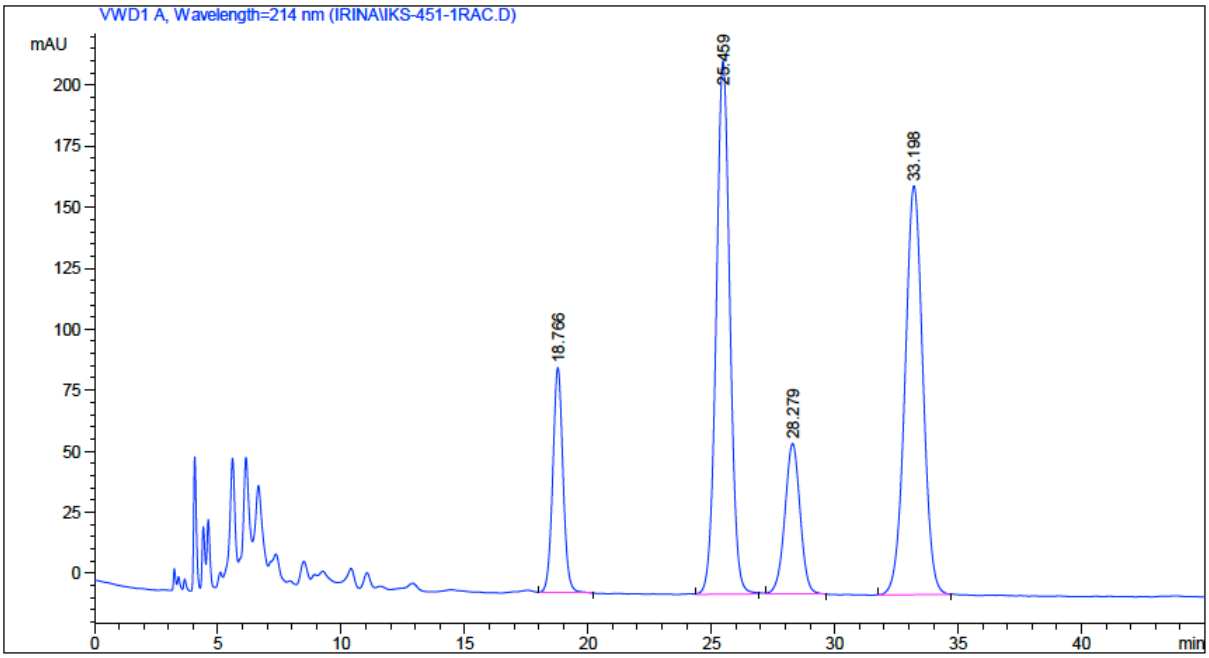

Peak #	RetTime [min]	Type	Width [min]	Area mAU *s	Height [mAU]	Area %
1	18.766	VB	0.4452	2685.25610	92.43137	12.0794
2	25.459	BB	0.5928	8430.15918	218.51674	37.9224
3	28.279	BB	0.6679	2673.69556	61.79315	12.0274
4	33.198	BB	0.7754	8440.89355	167.60902	37.9707

(2*R*,3*S*)-3-(4-Bromophenyl)-2-methyl-4-nitrobutanal (9ab).

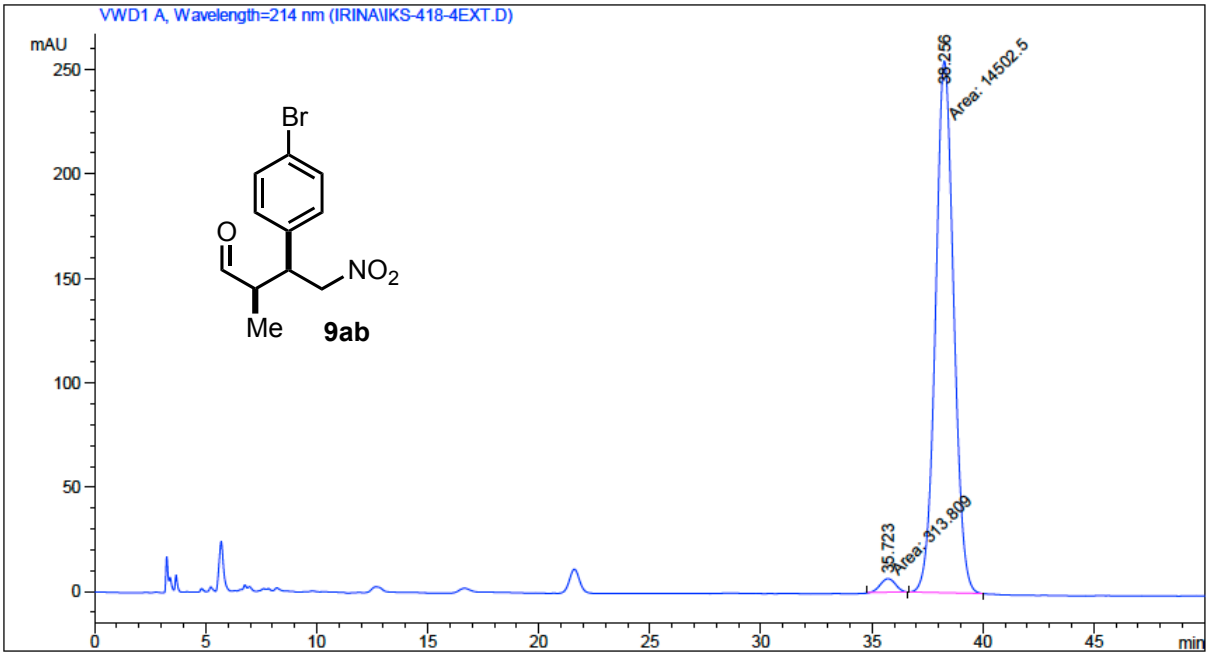

Peak #	RetTime [min]	Type	Width [min]	Area mAU *s	Height [mAU]	Area %
1	35.723	MM	0.7982	313.80875	6.55251	2.1180
2	38.256	MM	0.9489	1.45025e4	254.72652	97.8820

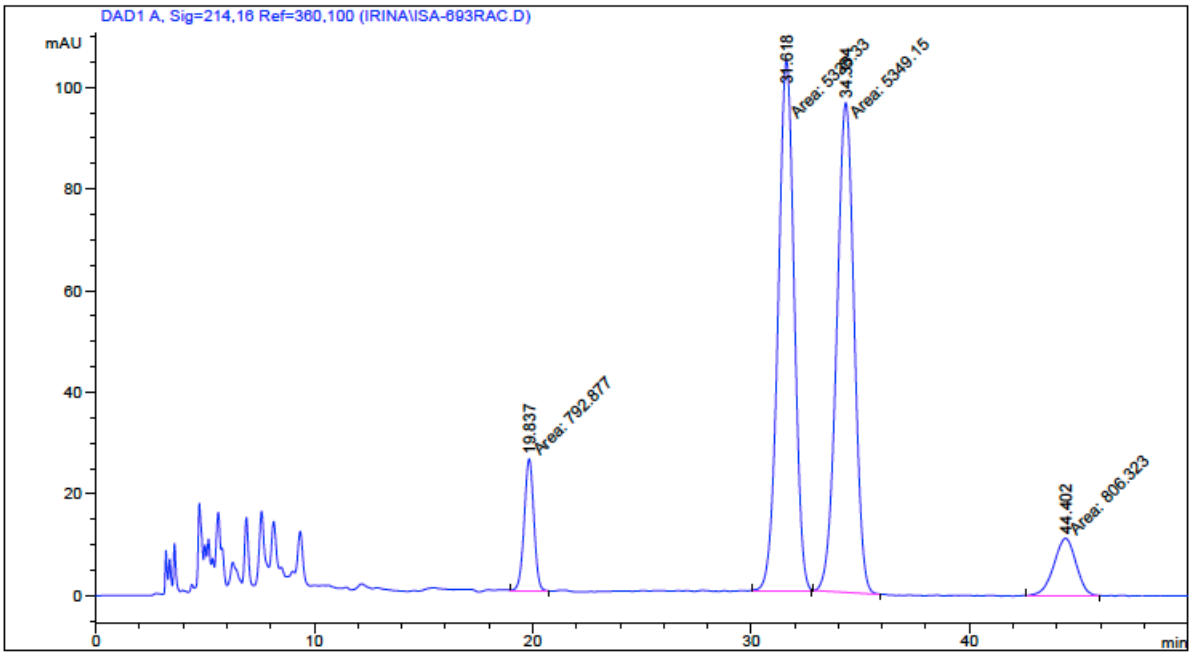

Peak #	RetTime [min]	Type	Width [min]	Area [mAU*s]	Height [mAU]	Area %
1	19.837	MM	0.5105	792.87695	25.88616	6.4542
2	31.618	MM	0.8526	5336.33057	104.31425	43.4389
3	34.334	MM	0.9251	5349.15381	96.36600	43.5433
4	44.402	MM	1.1865	806.32269	11.32605	6.5636

Chapter III

(2*R*,3*S*)-3-(3-Bromophenyl)-2-methyl-4-nitrobutanal (9ac).

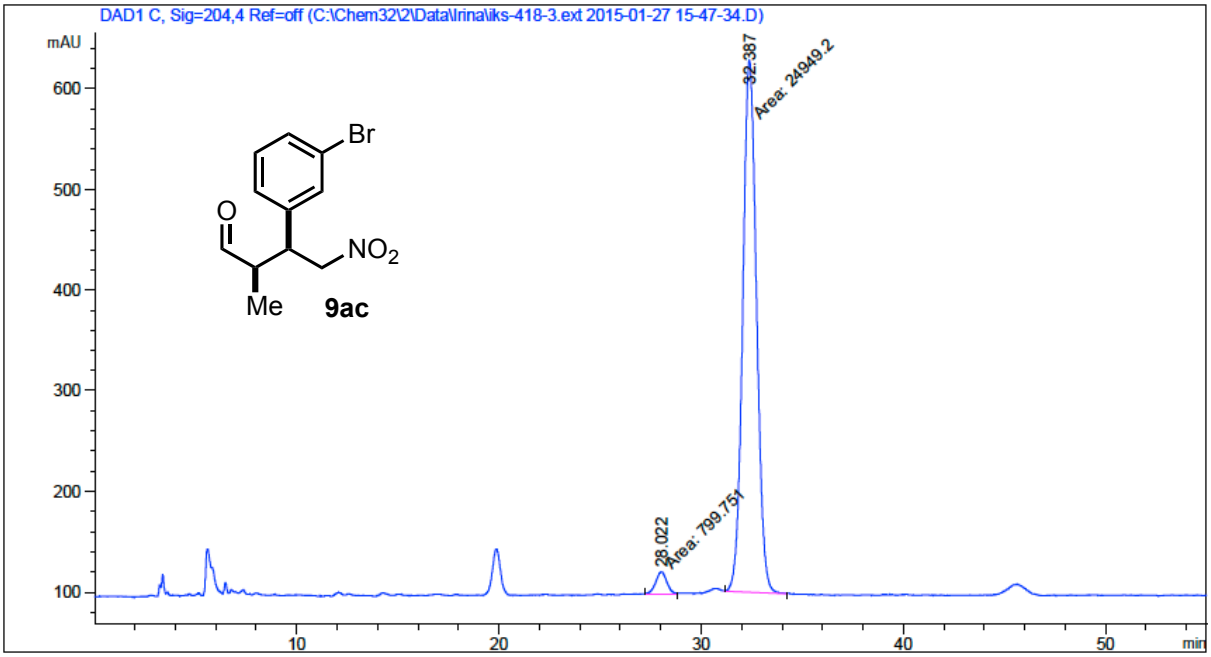

Peak #	RetTime [min]	Type	Width [min]	Area [mAU*s]	Height [mAU]	Area %
1	28.022	MM	0.6160	799.75092	21.63675	3.1060
2	32.387	MM	0.7871	2.49492e4	528.26935	96.8940

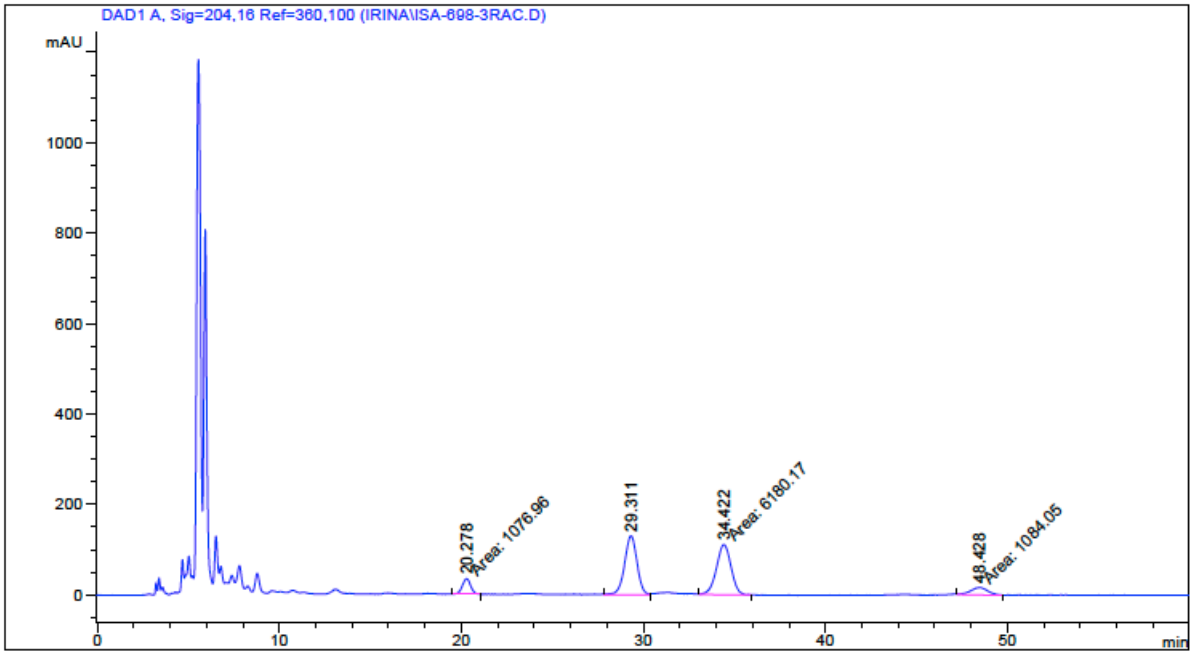

Peak #	RetTime [min]	Type	Width [min]	Area [mAU*s]	Height [mAU]	Area %
1	20.278	MM	0.5249	1076.95789	34.19263	7.4147
2	29.311	VV	0.7109	6183.54395	130.00151	42.5726
3	34.422	MM	0.9308	6180.16650	110.66006	42.5493
4	48.428	MM	1.1103	1084.05188	16.27334	7.4635

(2*R*,3*S*)-3-(2-Bromophenyl)-2-methyl-4-nitrobutanal (9ad).

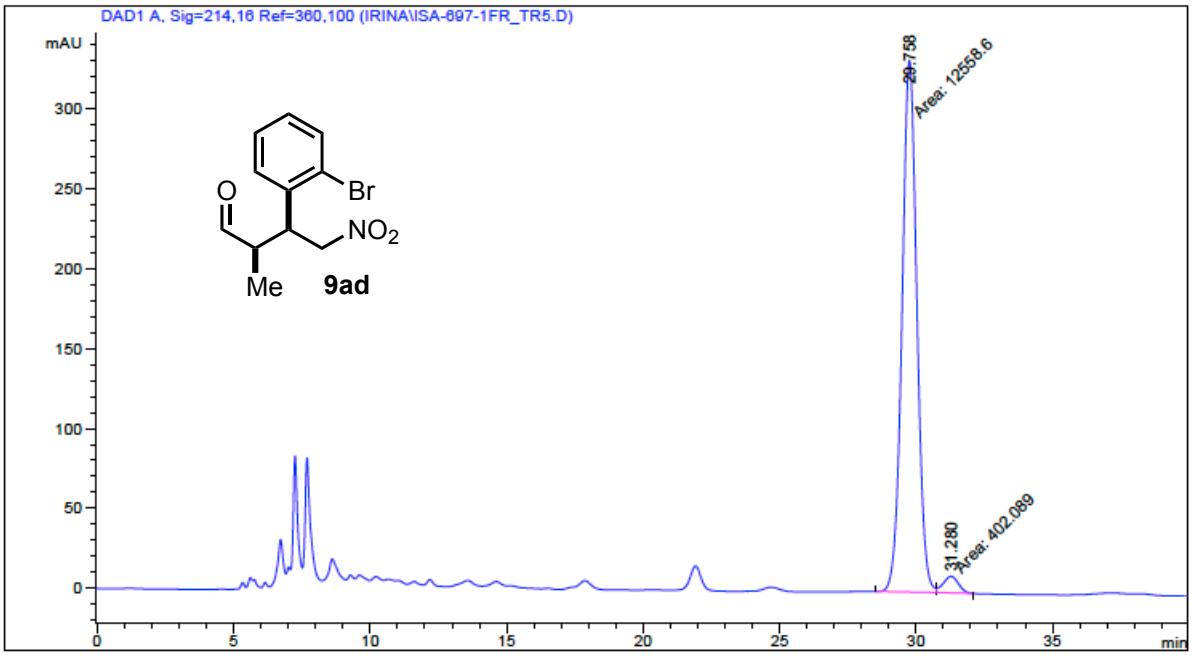

Peak #	RetTime [min]	Type	Width [min]	Area [mAU*s]	Height [mAU]	Area %
1	29.758	MM	0.6289	1.25586e4	332.79510	96.8976
2	31.280	MM	0.6450	402.08917	10.39060	3.1024

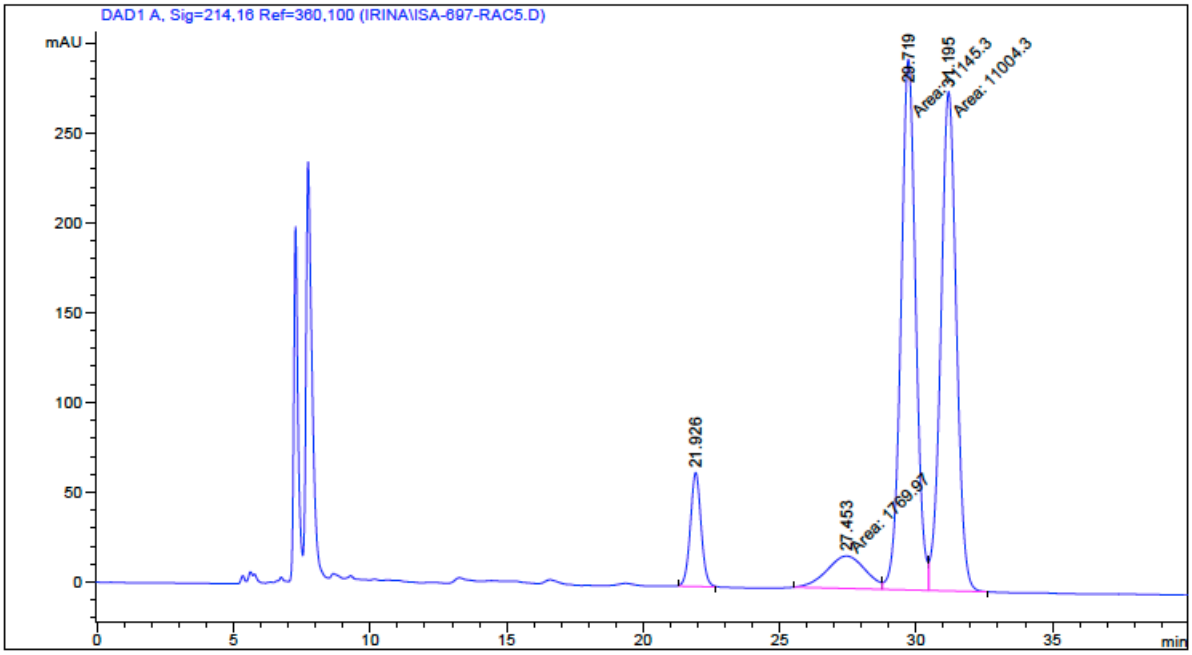

Peak #	RetTime [min]	Type	Width [min]	Area [mAU*s]	Height [mAU]	Area %
1	21.926	BB	0.4201	1740.72607	63.43788	6.7837
2	27.453	MF	1.6321	1769.96729	18.07419	6.8977
3	29.719	MF	0.6288	1.11453e4	295.42670	43.4339
4	31.195	FM	0.6596	1.10043e4	278.04858	42.8846

Chapter III

(2*R*,3*S*)-3-(4-Methoxyphenyl)-2-methyl-4-nitrobutanal (9ae).

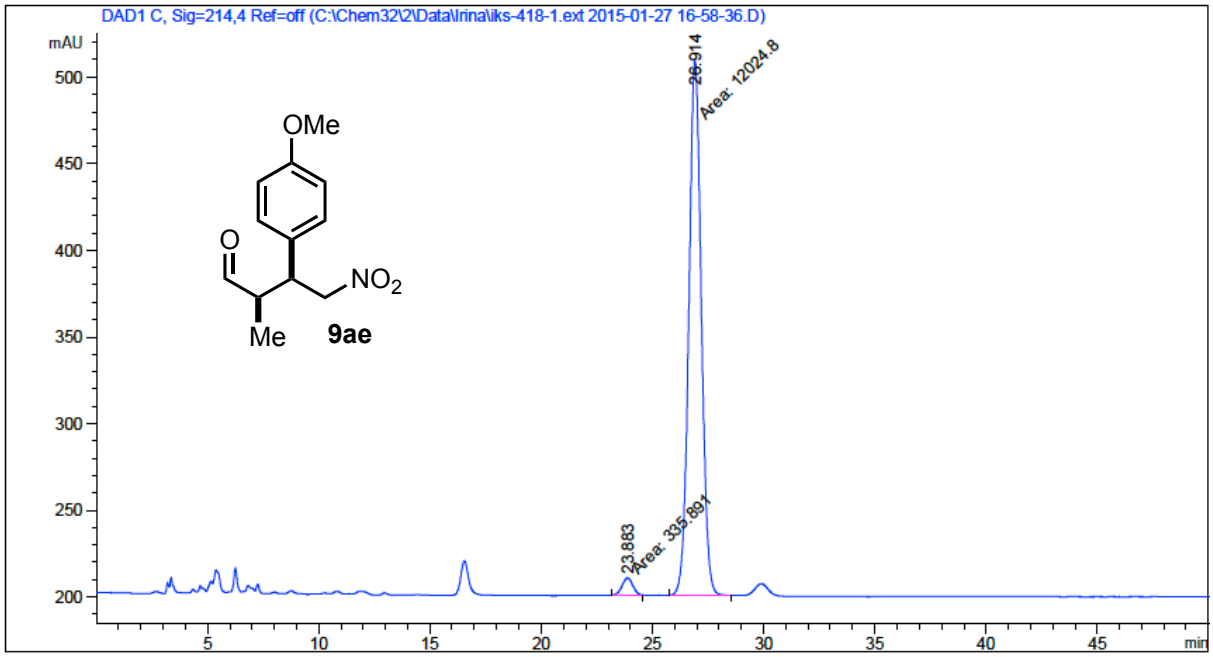

Peak #	RetTime [min]	Type	Width [min]	Area [mAU*s]	Height [mAU]	Area %
1	23.883	MM	0.5601	335.89127	9.99550	2.7174
2	26.914	MM	0.6493	1.20248e4	308.68286	97.2826

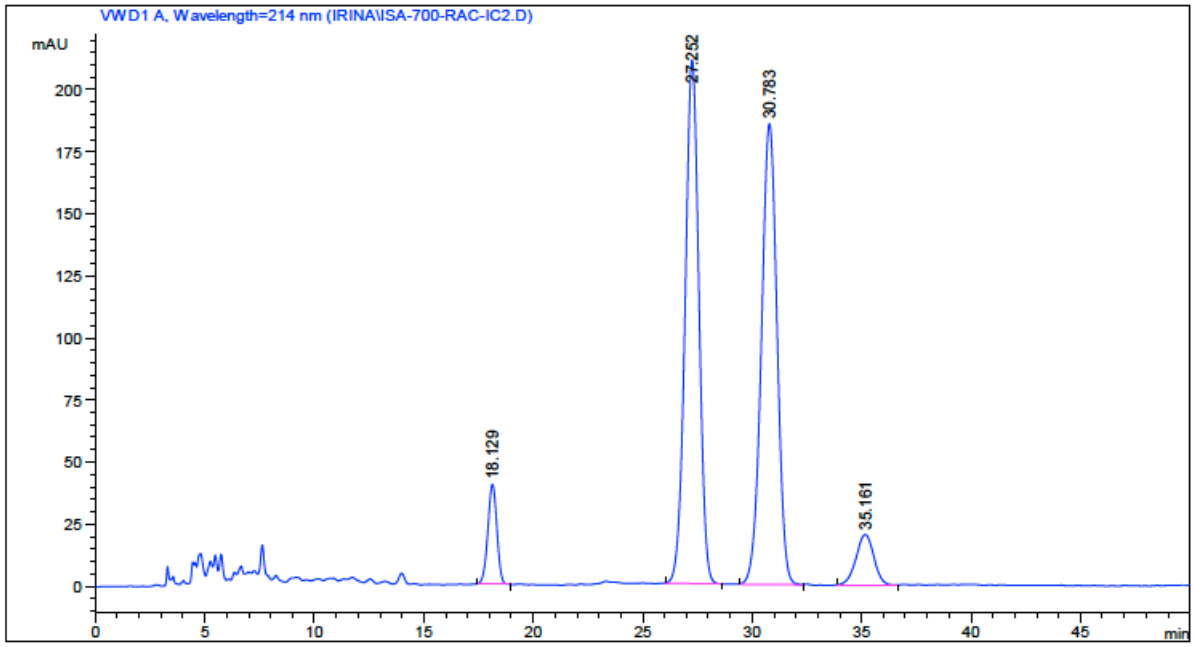

Peak #	RetTime [min]	Type	Width [min]	Area mAU *s	Height [mAU]	Area %
1	18.129	BB	0.4481	1164.62073	40.26600	5.6134
2	27.252	BB	0.6751	9202.43750	210.88942	44.3549
3	30.783	BV	0.7717	9222.98145	185.66164	44.4540
4	35.161	BB	0.8780	1157.22534	20.37963	5.5777

(2*R*,3*S*)-3-(Benzo[d][1.3]doixol-4-yl)-2-methyl-4-nitrobutanal (9af).

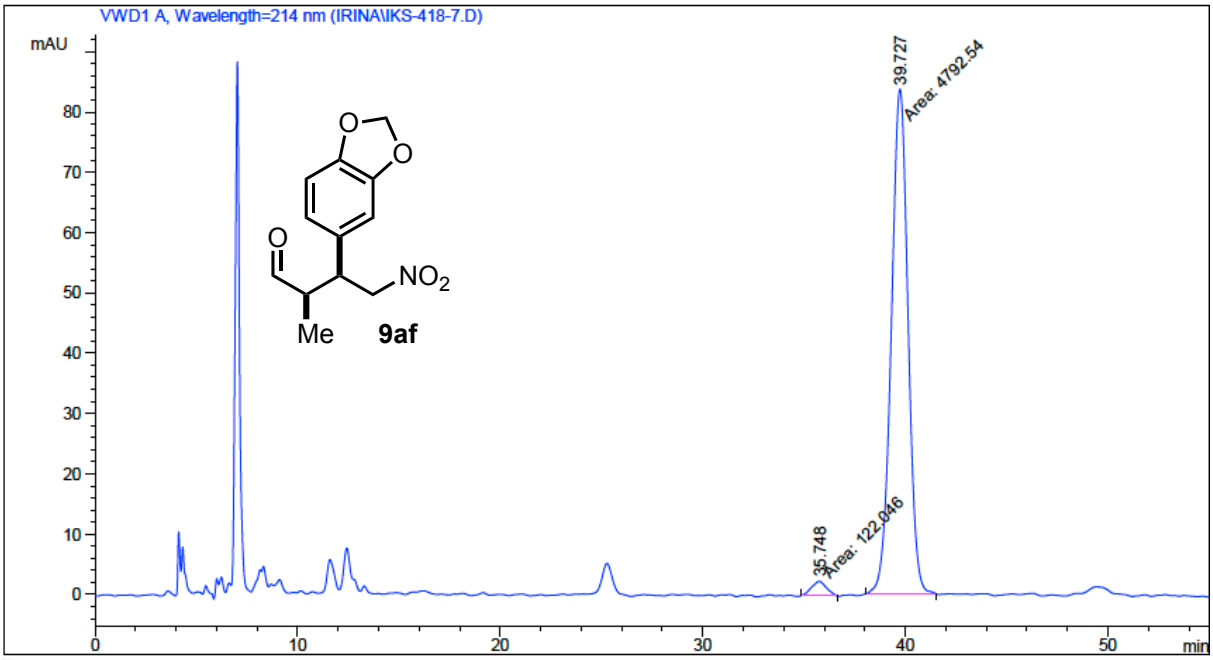

Peak #	RetTime [min]	Type	Width [min]	Area mAU *s	Height [mAU]	Area %
1	35.748	MM	0.8563	122.04570	2.37533	2.4833
2	39.727	MM	0.9543	4792.53906	83.69820	97.5167

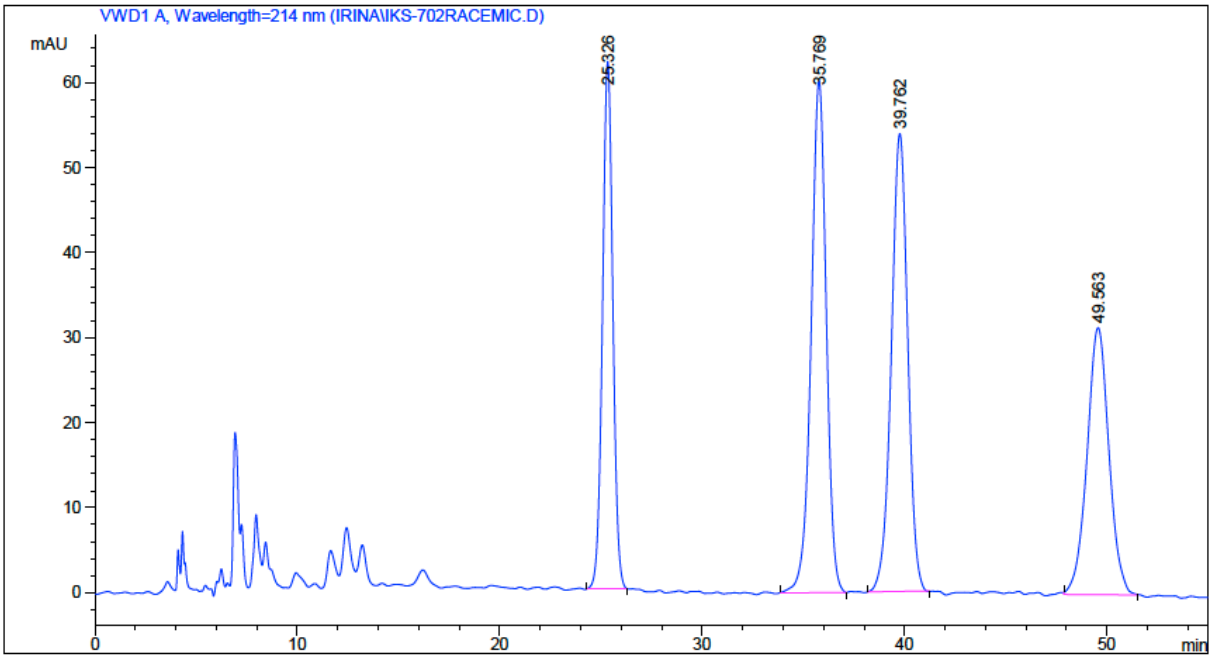

Peak #	RetTime [min]	Type	Width [min]	Area mAU *s	Height [mAU]	Area %
1	25.326	BB	0.5447	2200.60327	62.05896	20.4974
2	35.769	BB	0.7964	3134.02832	60.22061	29.1917
3	39.762	BB	0.8702	3038.69360	53.90651	28.3037
4	49.563	BB	1.1235	2362.68628	31.41464	22.0071

Chapter III

(2*R*,3*S*)-3-(4-Hydroxyphenyl)-2-methyl-4-nitrobutanal (9ag).

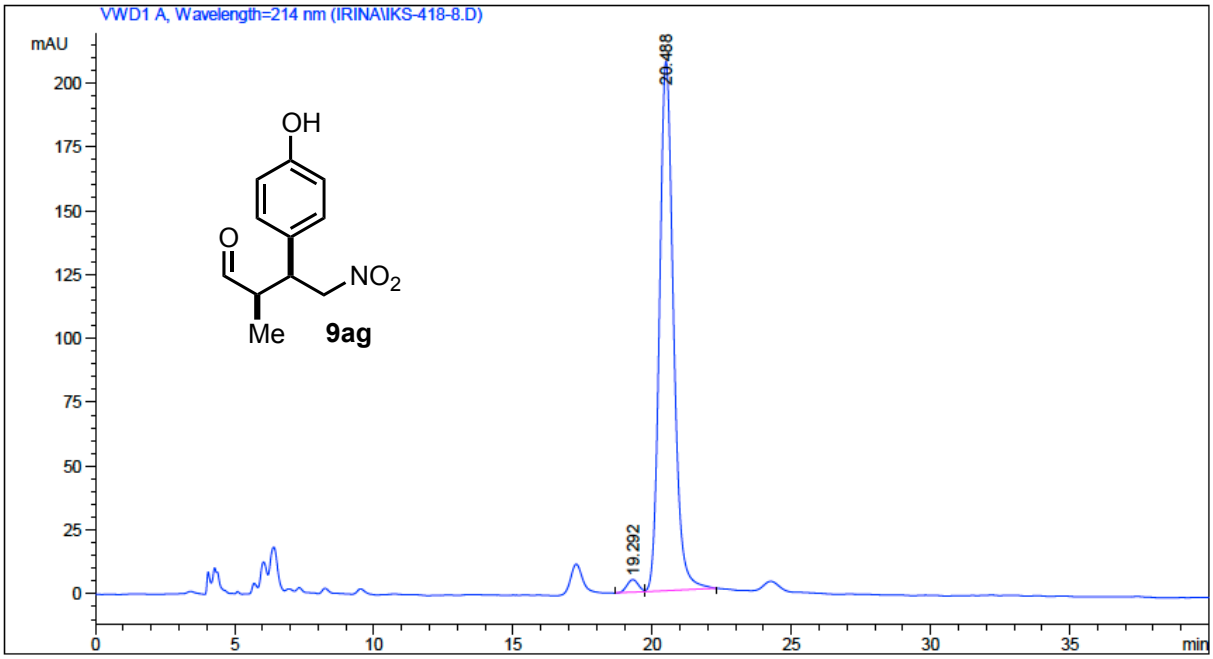

Peak #	RetTime [min]	Type	Width [min]	Area mAU *s	Height [mAU]	Area %
1	19.292	BV	0.4468	144.16074	5.00380	1.9501
2	20.488	VB	0.5343	7248.39941	207.47240	98.0499

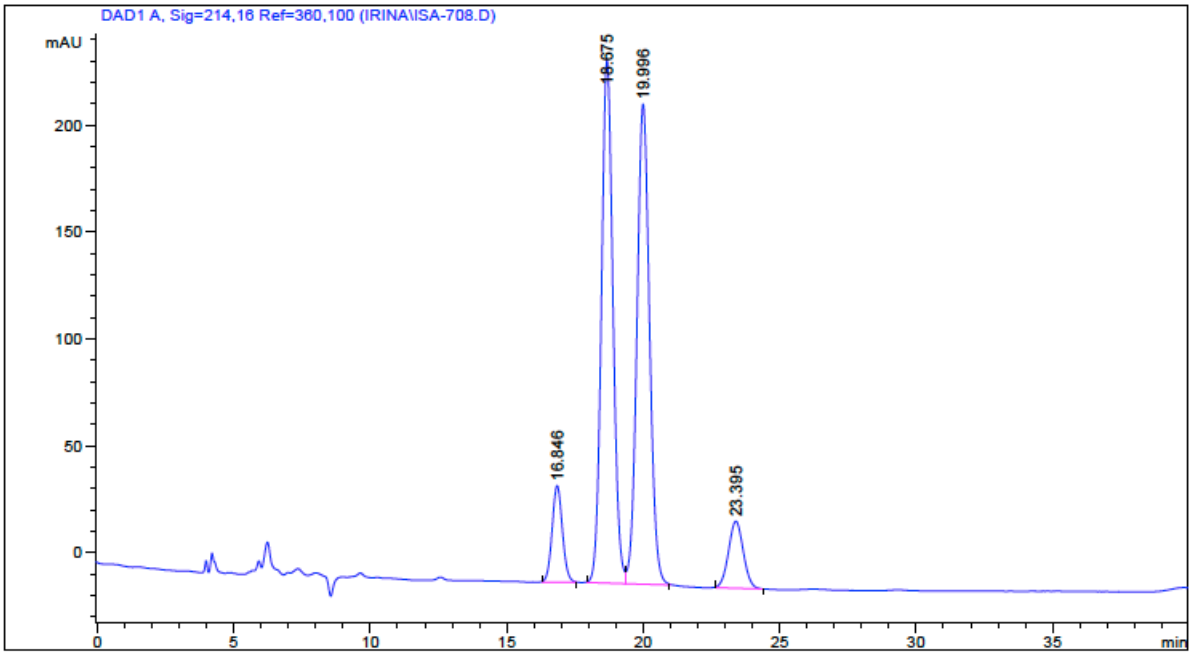

Peak #	RetTime [min]	Type	Width [min]	Area [mAU*s]	Height [mAU]	Area %
1	16.846	BB	0.4046	1186.57617	45.15331	7.0840
2	18.675	BV	0.4531	7191.37939	244.53070	42.9334
3	19.996	VB	0.4934	7184.86621	224.48988	42.8945
4	23.395	BB	0.5819	1187.26501	31.34532	7.0881

(2*R*,3*S*)-3-(2-Furyl)-2-methyl-4-nitrobutanal (9ah).

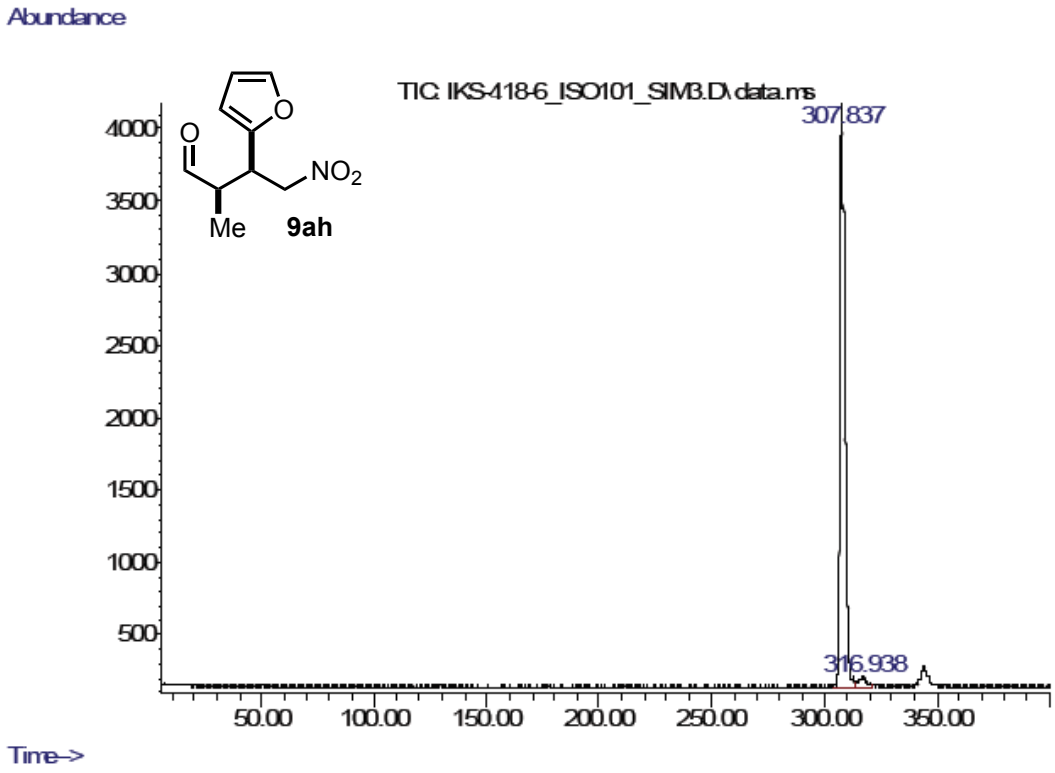

peak #	R.T. min	first scan	max scan	last scan	PK TY	peak height	corr. area	corr. % max.	% of total
1	307.837	55661	56378	57429	M3	4054	6037541	100.00%	97.511%
2	316.938	57521	58073	58899	M3	74	154102	2.55%	2.489%

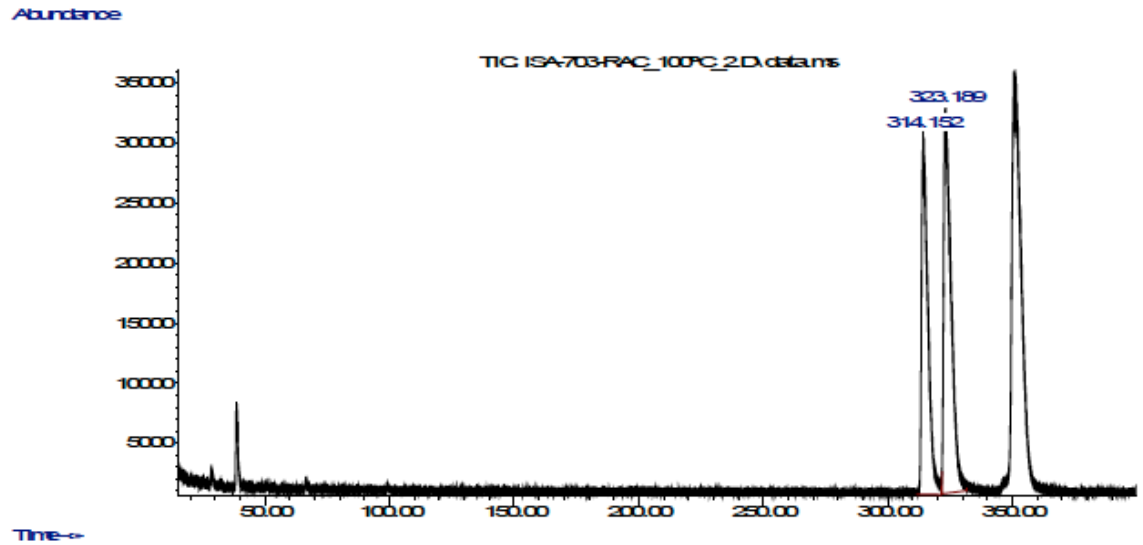

peak #	R.T. min	first scan	max scan	last scan	PK TY	peak height	corr. area	corr. % max.	% of total
1	314.152	149093	150388	154056	M	30549	53378389	93.44%	49.304%
2	323.189	154191	154932	157592	M	31007	57126710	100.00%	50.696%

Chapter III

(2*R*,3*S*)-3-(2-Thienyl)-2-methyl-4-nitrobutanal (9ai).

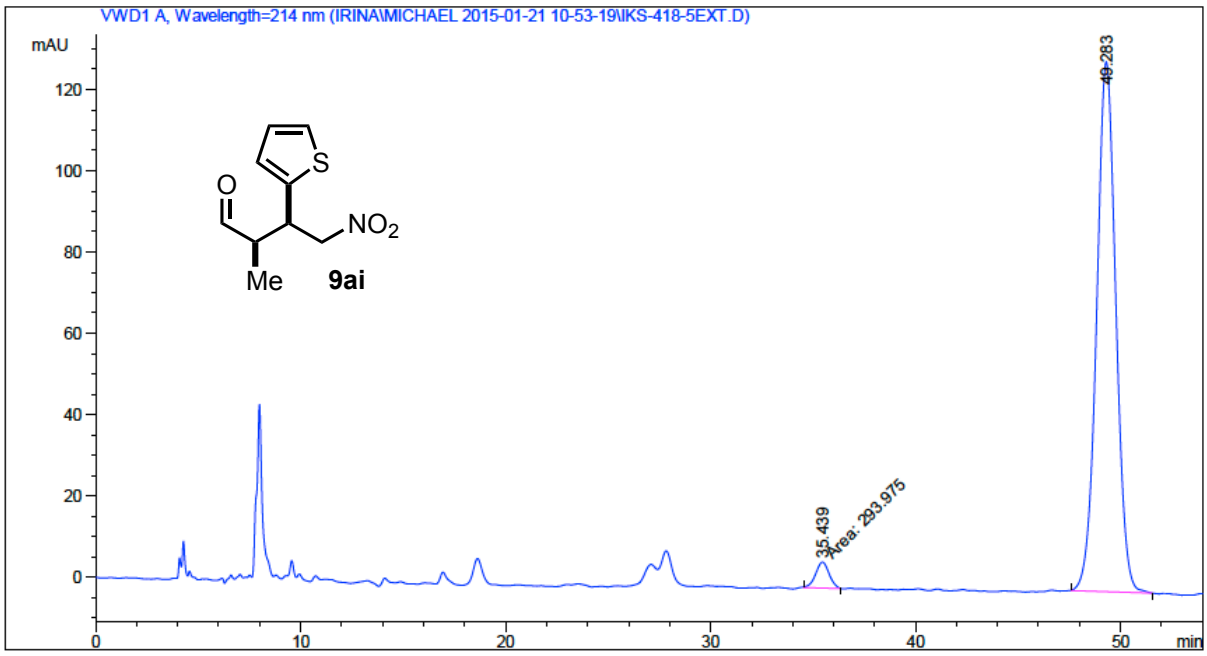

Peak #	RetTime [min]	Type	Width [min]	Area mAU *s	Height [mAU]	Area %
1	35.439	MM	0.7652	293.97467	6.40286	3.3500
2	49.283	BB	0.9992	8481.50586	130.37624	96.6500

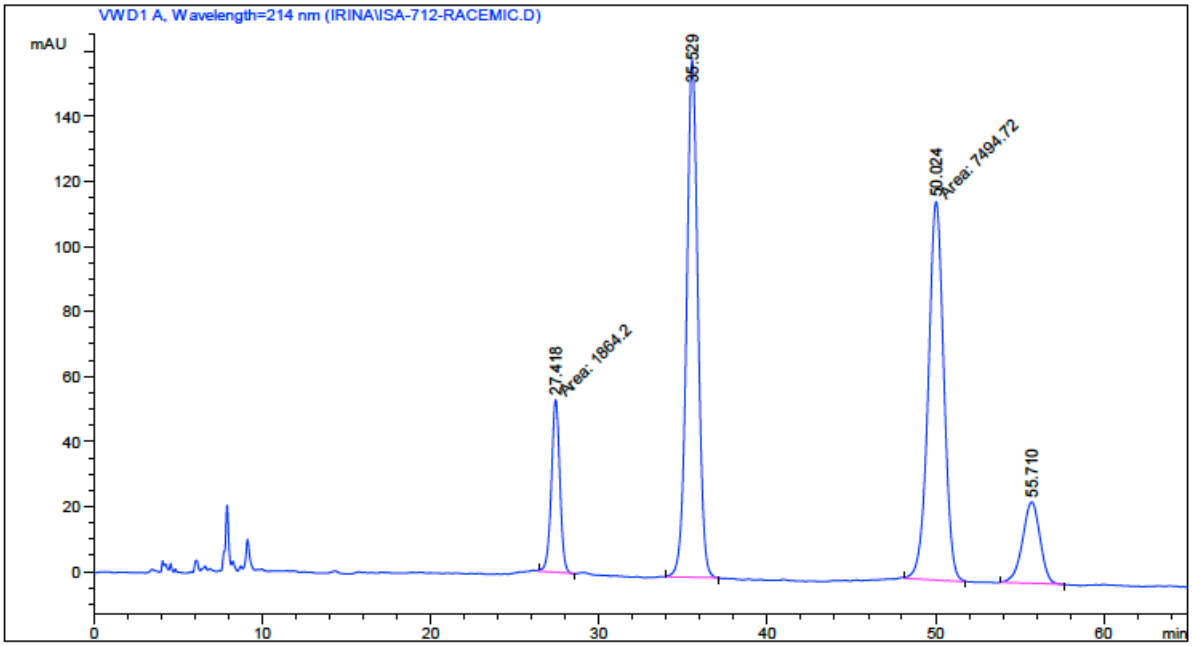

Peak #	RetTime [min]	Type	Width [min]	Area mAU *s	Height [mAU]	Area %
1	27.418	MM	0.5855	1864.19543	53.06997	9.9989
2	35.529	BB	0.7163	7453.97803	158.87428	39.9807
3	50.024	MM	1.0733	7494.72119	116.37984	40.1992
4	55.710	BB	1.0988	1831.06384	25.05183	9.8212

(2*R*,3*S*)-2-Methyl-3-nitromethyl-5-phenyl-pentanal (9aj).

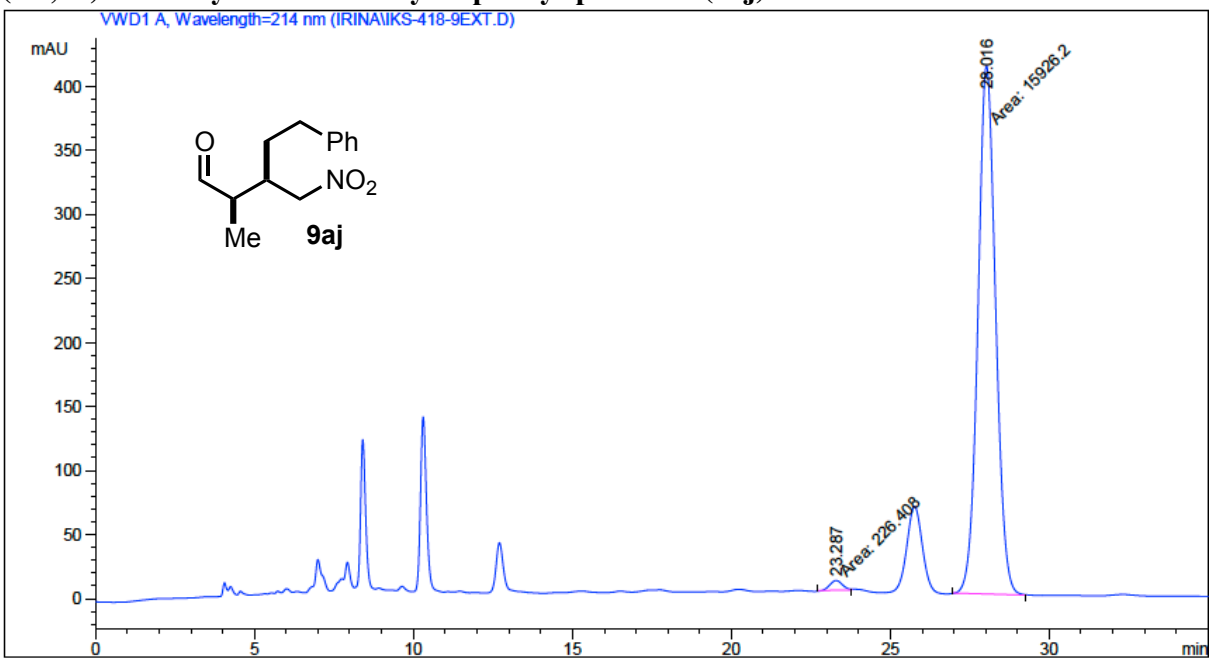

Peak #	RetTime [min]	Type	Width [min]	Area mAU *s	Height [mAU]	Area %
1	23.287	MM	0.4751	226.40776	7.94318	1.4017
2	28.016	MM	0.6430	1.59262e4	412.79849	98.5983

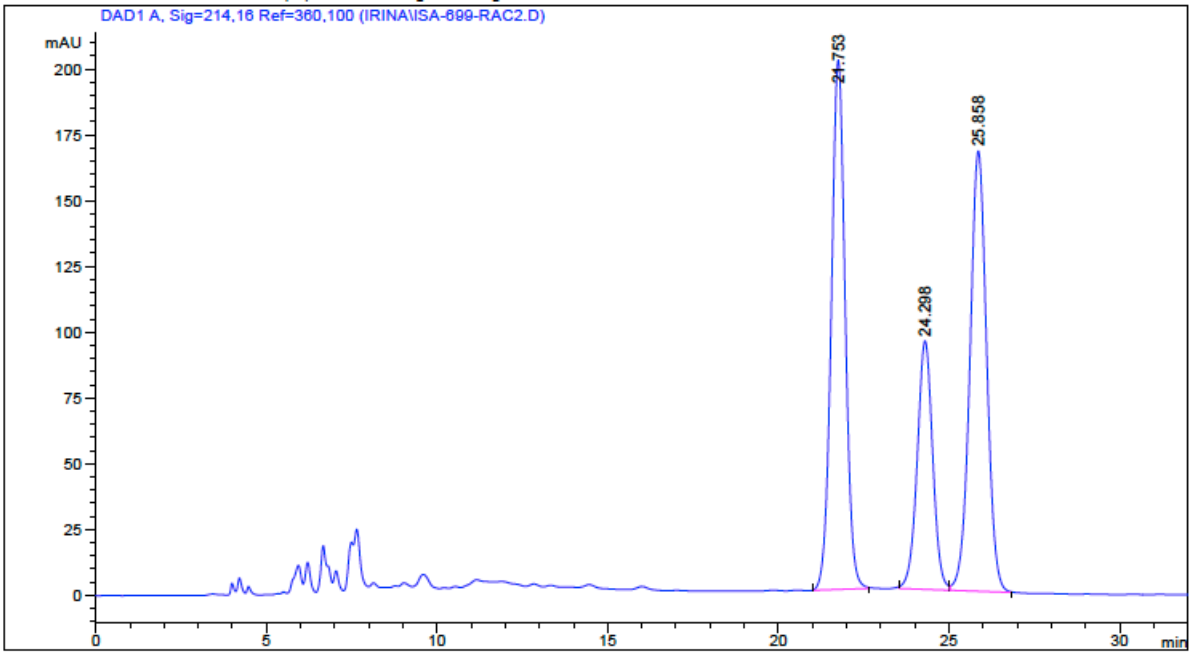

Peak #	RetTime [min]	Type	Width [min]	Area [mAU*s]	Height [mAU]	Area %
1	21.753	BB	0.4334	5681.10205	201.21049	39.5894
2	24.298	BV	0.4848	2969.48389	94.44492	20.6932
3	25.858	VB	0.5214	5699.46582	167.33006	39.7174

(the *anti* pair of enantiomers co-elute at 24.3 min)

Chapter III

(2*R*,3*S*)-2-(Isopropyl)-4-nitro-3-phenylbutanal (9ha).

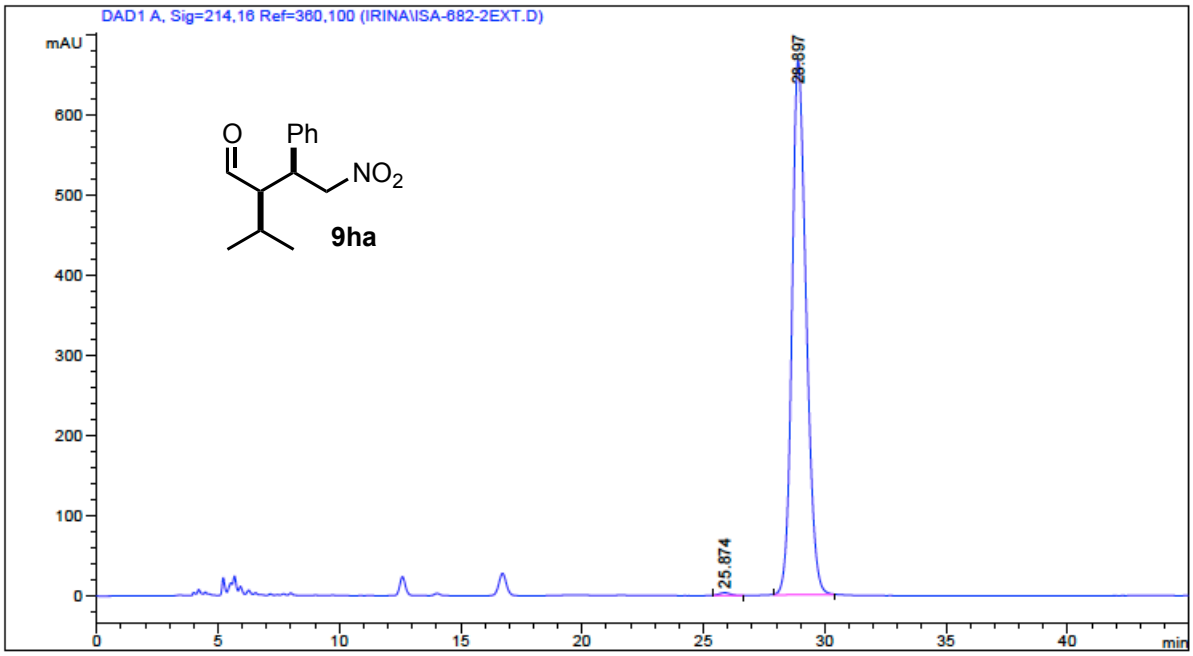

Peak #	RetTime [min]	Type	Width [min]	Area [mAU*s]	Height [mAU]	Area %
1	25.874	BB	0.4837	108.74268	3.43168	0.3992
2	28.897	BB	0.6211	2.71346e4	666.32635	99.6008

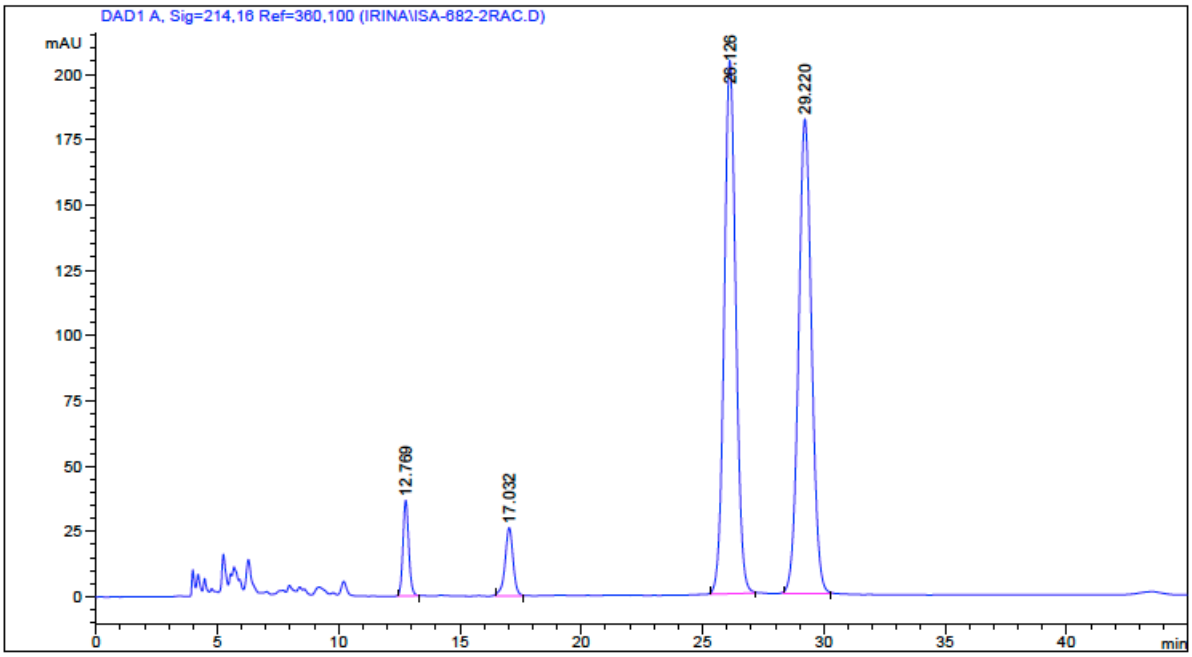

Peak #	RetTime [min]	Type	Width [min]	Area [mAU*s]	Height [mAU]	Area %
1	12.769	BB	0.2556	606.68066	36.56857	4.1079
2	17.032	BB	0.3487	600.59625	26.08041	4.0667
3	26.126	BB	0.5113	6775.45361	204.11130	45.8772
4	29.220	BB	0.5759	6785.93848	181.61182	45.9482

(2*R*,3*S*)-3-(4-Bromophenyl)-2-isopropyl-4-nitrobutanal (9hb).

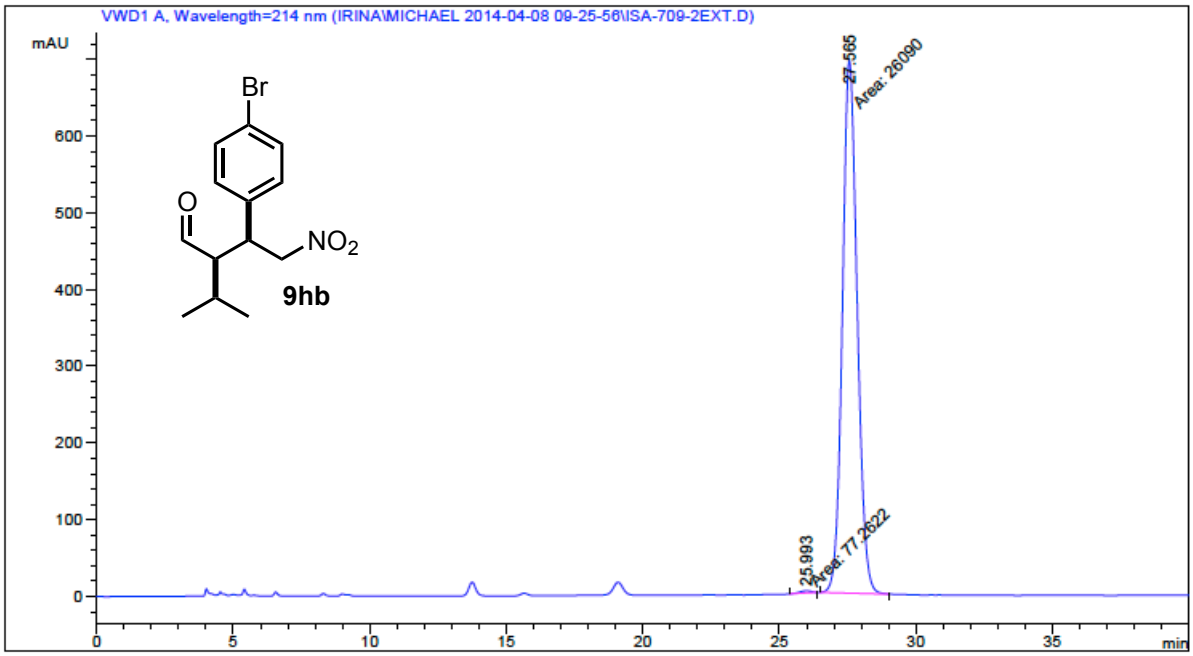

Peak #	RetTime [min]	Type	Width [min]	Area mAU *s	Height [mAU]	Area %
1	25.993	MM	0.4876	77.26217	2.64107	0.2953
2	27.565	MM	0.6267	2.60900e4	693.89972	99.7047

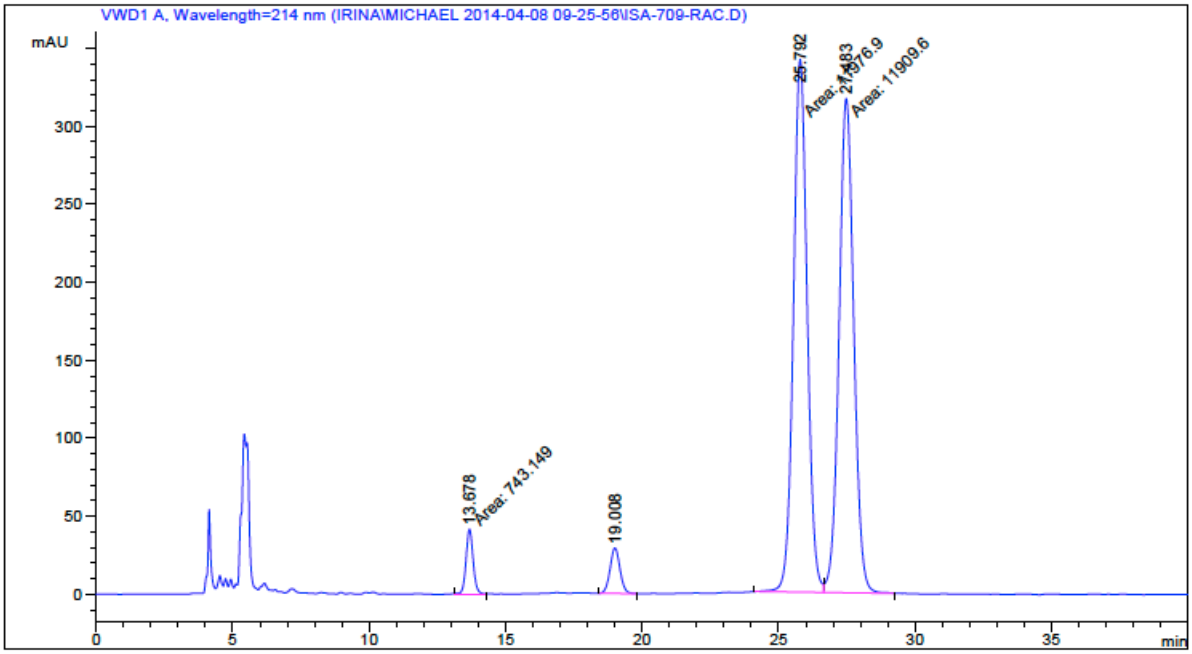

Peak #	RetTime [min]	Type	Width [min]	Area mAU *s	Height [mAU]	Area %
1	13.678	MM	0.2990	743.14886	41.42190	2.9295
2	19.008	BB	0.3900	738.19281	29.16183	2.9099
3	25.792	MF	0.5846	1.19769e4	341.43930	47.2130
4	27.483	FM	0.6266	1.19096e4	316.77783	46.9476

Chapter III

(2*R*,3*S*)-3-(2-Bromophenyl)-2-isopropyl-4-nitrobutanal (9hc).

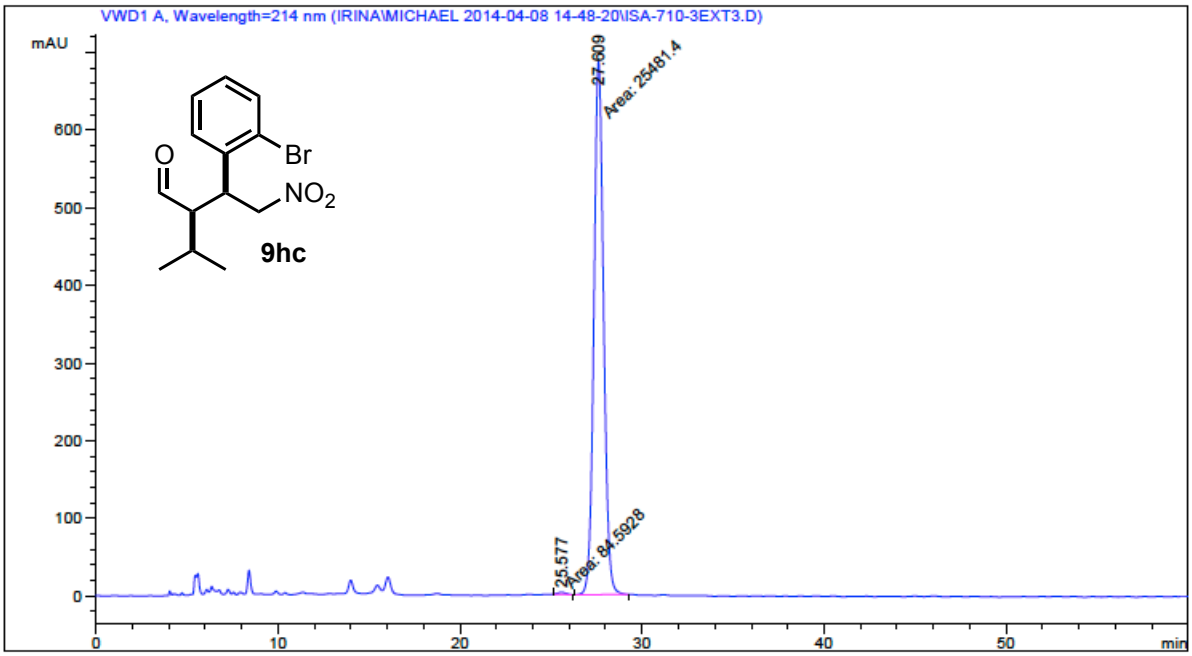

Peak #	RetTime [min]	Type	Width [min]	Area mAU *s	Height [mAU]	Area %
1	25.577	MM	0.5227	84.59280	2.69721	0.3309
2	27.609	MM	0.6173	2.54814e4	687.97156	99.6691

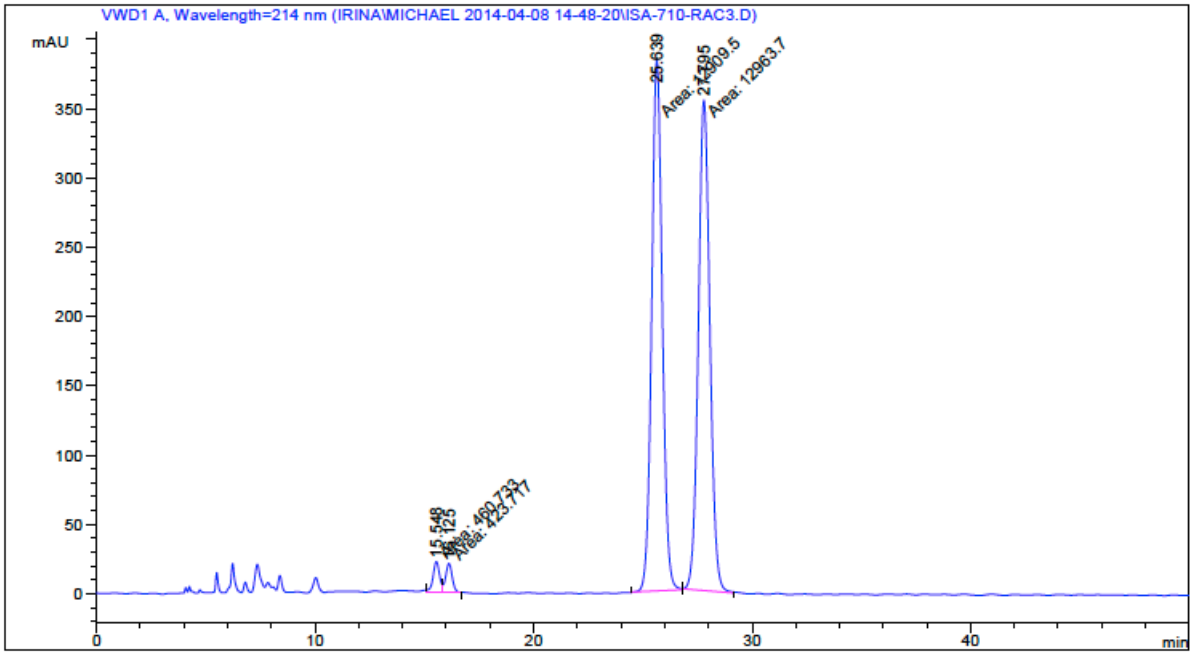

Peak #	RetTime [min]	Type	Width [min]	Area mAU *s	Height [mAU]	Area %
1	15.548	MF	0.3500	460.73251	21.94126	1.7219
2	16.125	FM	0.3415	423.71658	20.67804	1.5835
3	25.639	MM	0.5610	1.29095e4	383.50455	48.2460
4	27.795	MM	0.6106	1.29637e4	353.87683	48.4486

(3*R*)-2,2-Dimethyl-4-nitro-3-phenylbutanal (9ia).

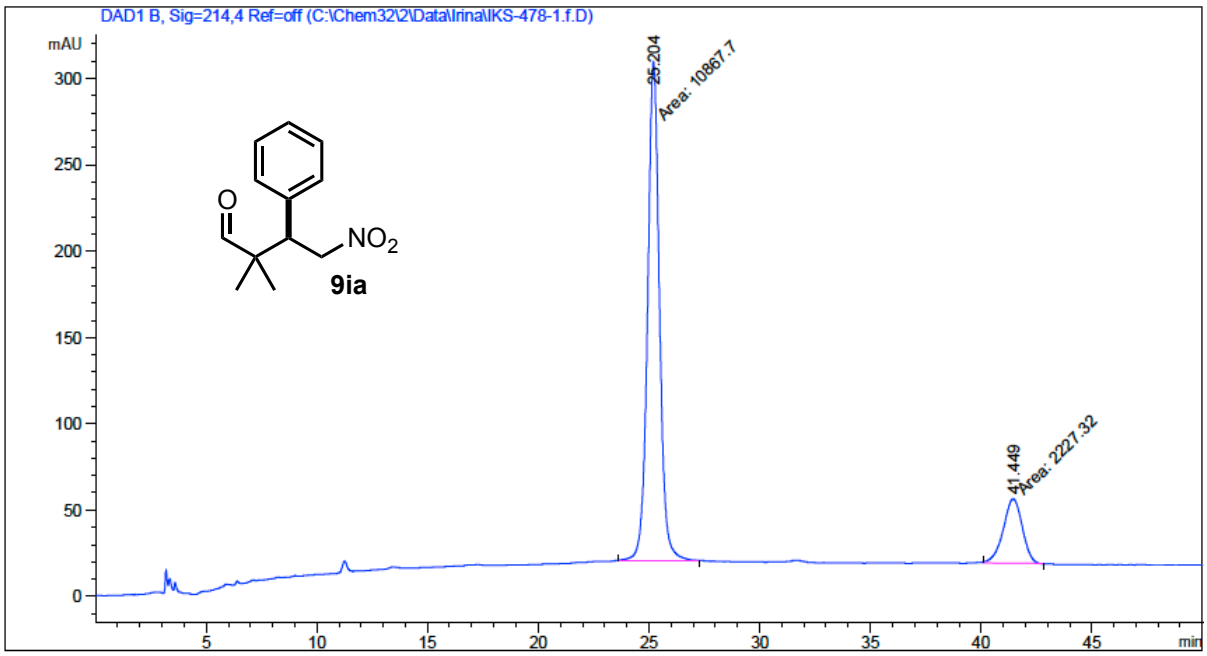

Peak #	RetTime [min]	Type	Width [min]	Area [mAU*s]	Height [mAU]	Area %
1	25.204	MM	0.6261	1.08677e4	289.31650	82.9911
2	41.449	MM	0.9978	2227.31934	37.20277	17.0089

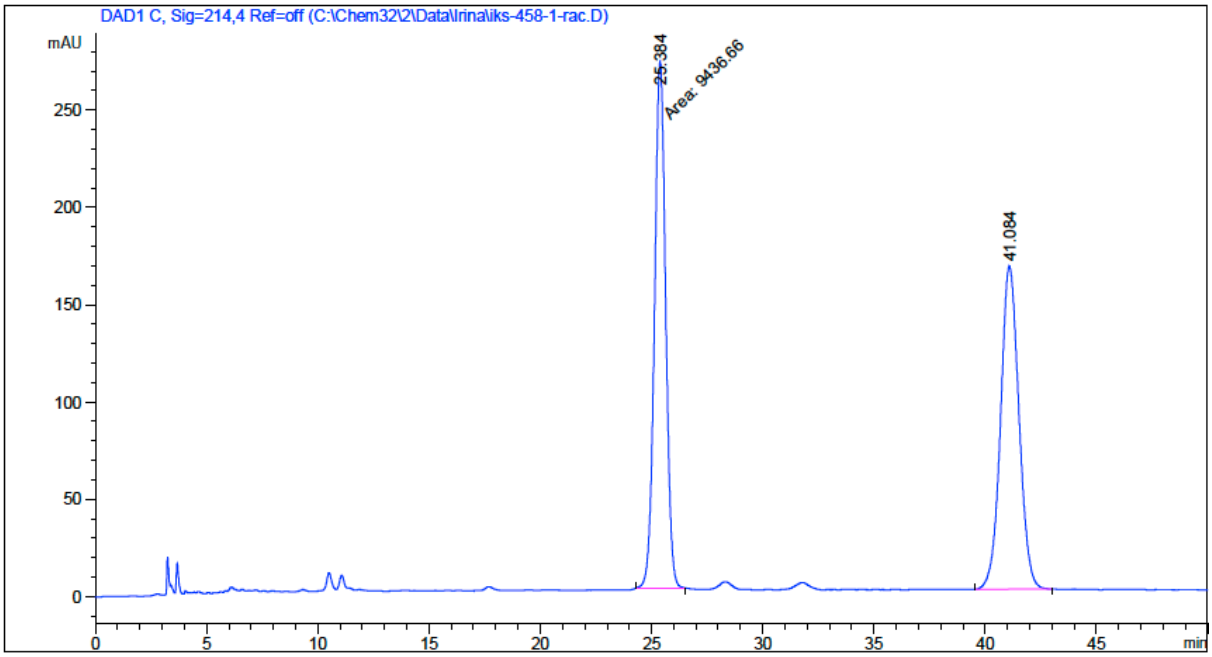

Peak #	RetTime [min]	Type	Width [min]	Area [mAU*s]	Height [mAU]	Area %
1	25.384	MM	0.5800	9436.65918	271.15076	49.8303
2	41.084	BB	0.8650	9500.93359	166.17598	50.1697

Chapter III

(3*R*)-3-(4-Bromophenyl)-2,2-dimethyl-4-nitrobutanal (9ib).

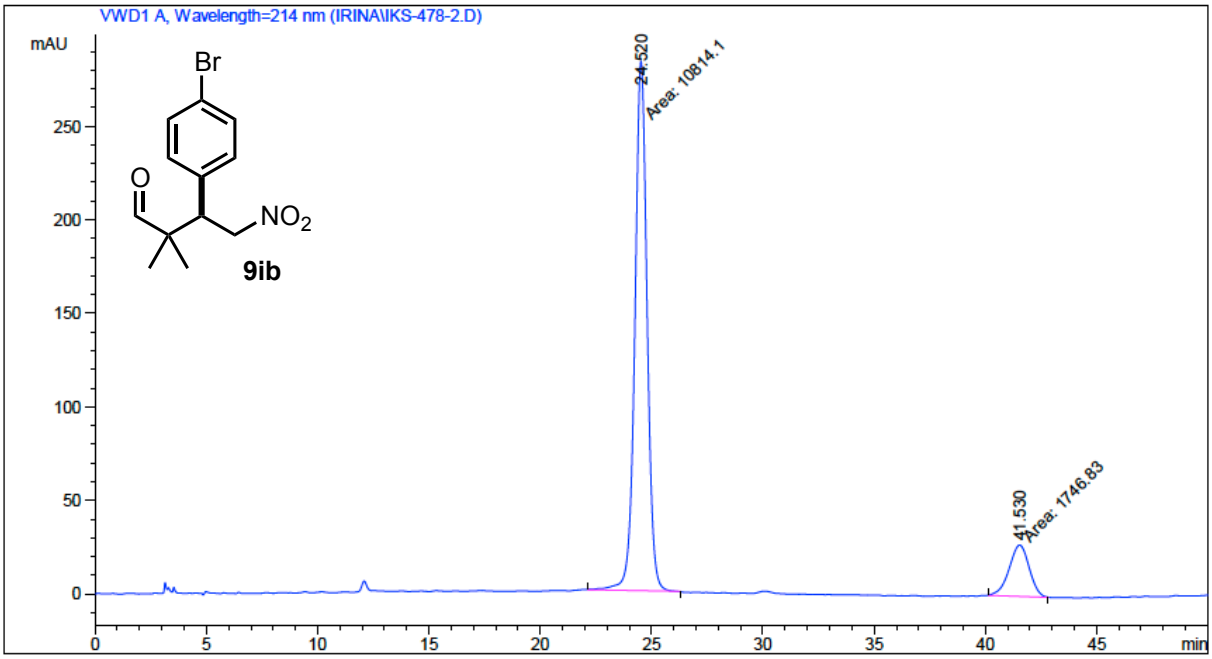

Peak #	RetTime [min]	Type	Width [min]	Area mAU *s	Height [mAU]	Area %
1	24.520	MM	0.6360	1.08141e4	283.40088	86.0932
2	41.530	MM	1.0543	1746.83325	27.61395	13.9068

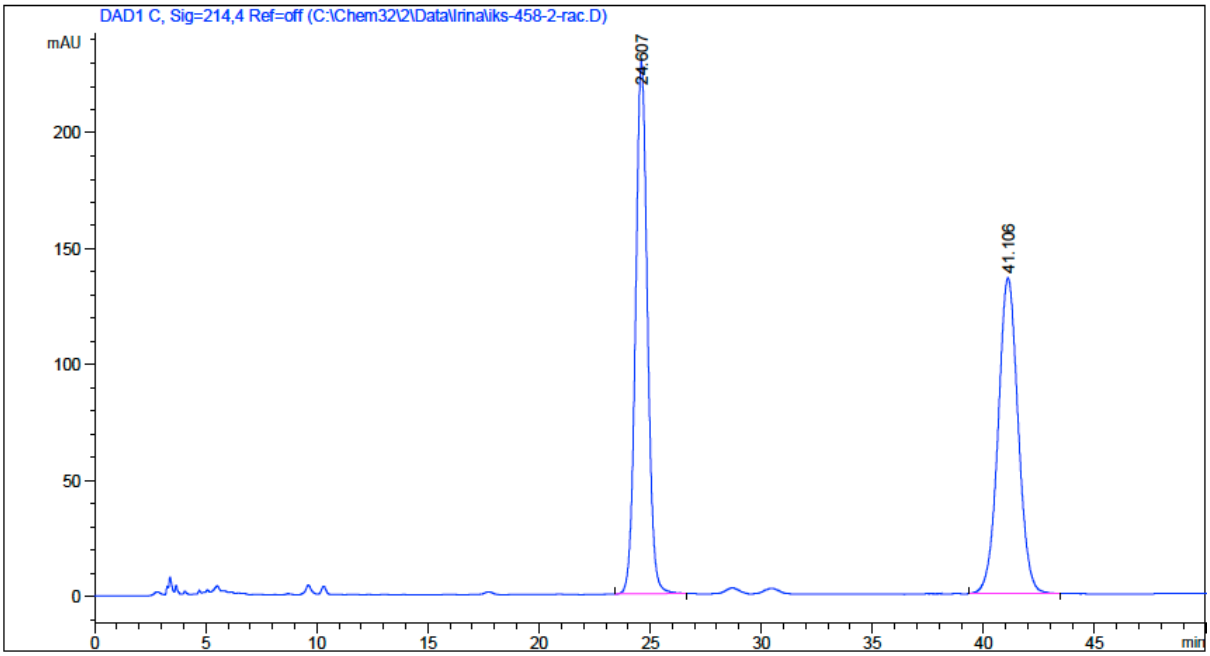

Peak #	RetTime [min]	Type	Width [min]	Area [mAU*s]	Height [mAU]	Area %
1	24.607	BB	0.5711	8532.66309	229.82976	50.0935
2	41.106	BB	0.9543	8500.79883	136.16943	49.9065

(2*R*,3*S*)-3-(2-Furyl)-2-ethyl-4-nitrobutanal (9bg).

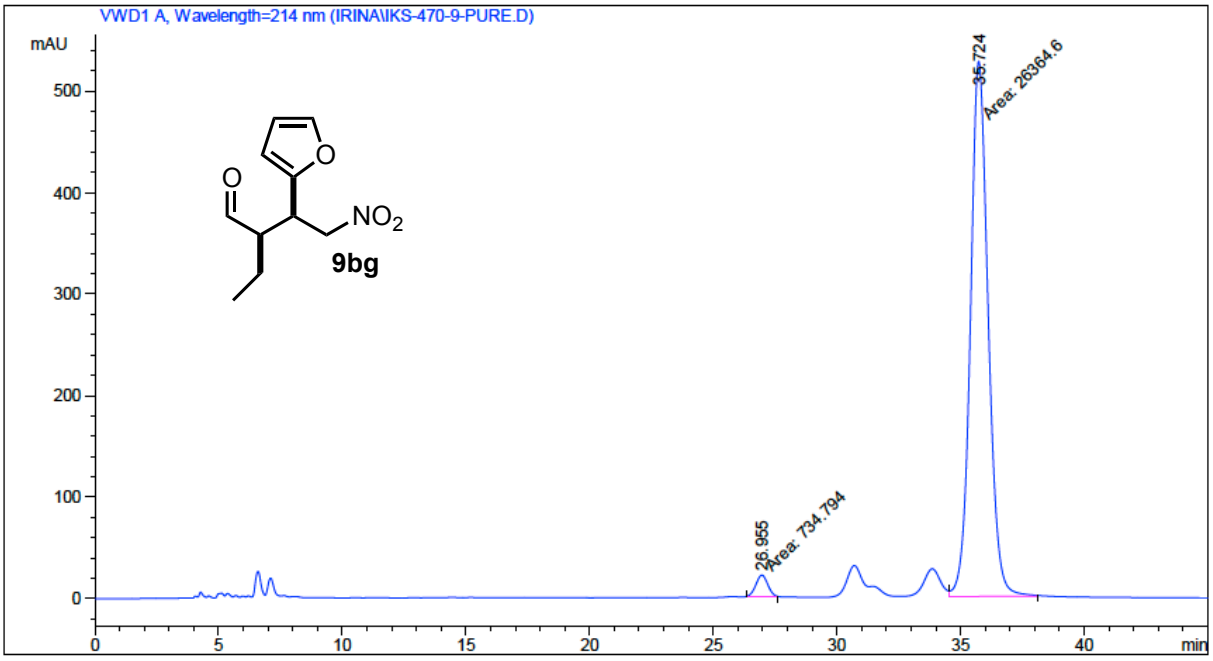

Peak #	RetTime [min]	Type	Width [min]	Area mAU *s	Height [mAU]	Area %
1	26.955	FM	0.5694	734.79431	21.50702	2.7115
2	35.724	MM	0.8330	2.63646e4	527.49030	97.2885

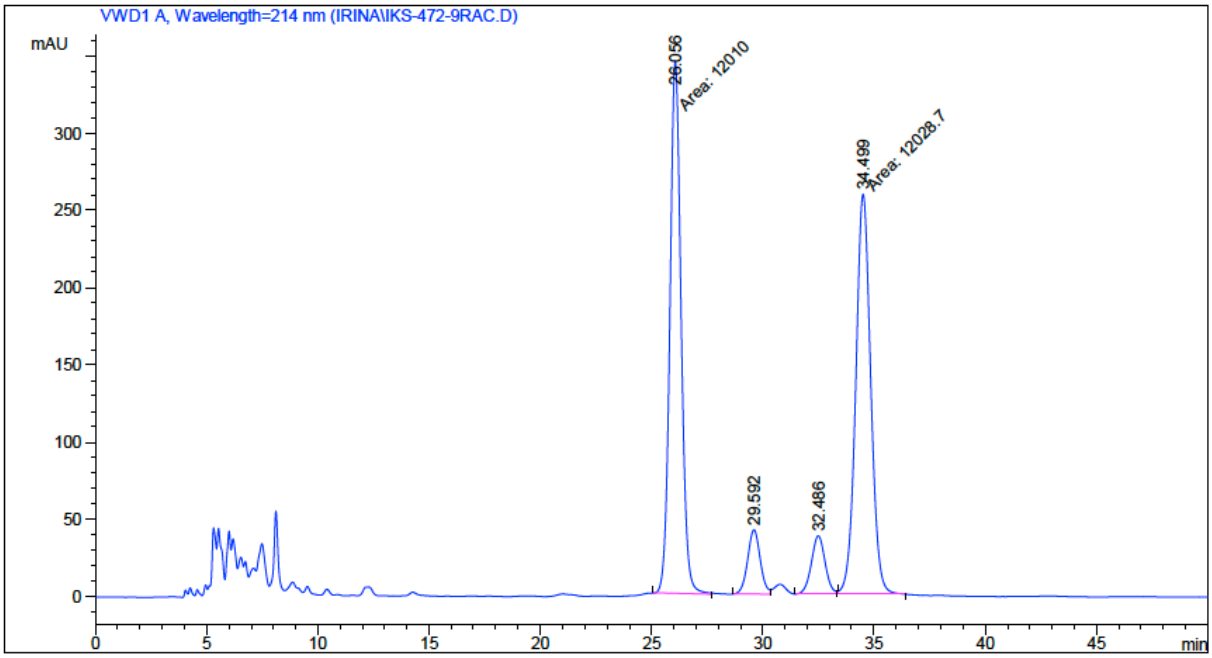

Peak #	RetTime [min]	Type	Width [min]	Area mAU *s	Height [mAU]	Area %
1	26.056	MM	0.5815	1.20100e4	344.20395	43.9582
2	29.592	BV	0.6073	1637.53479	41.63997	5.9936
3	32.486	VV	0.6632	1645.20557	37.93390	6.0217
4	34.499	MM	0.7759	1.20287e4	258.39108	44.0265

Chapter III

(2*R*,3*S*)-3-(4-Bromophenyl)-2-ethyl-4-nitrobutanal (9bb).

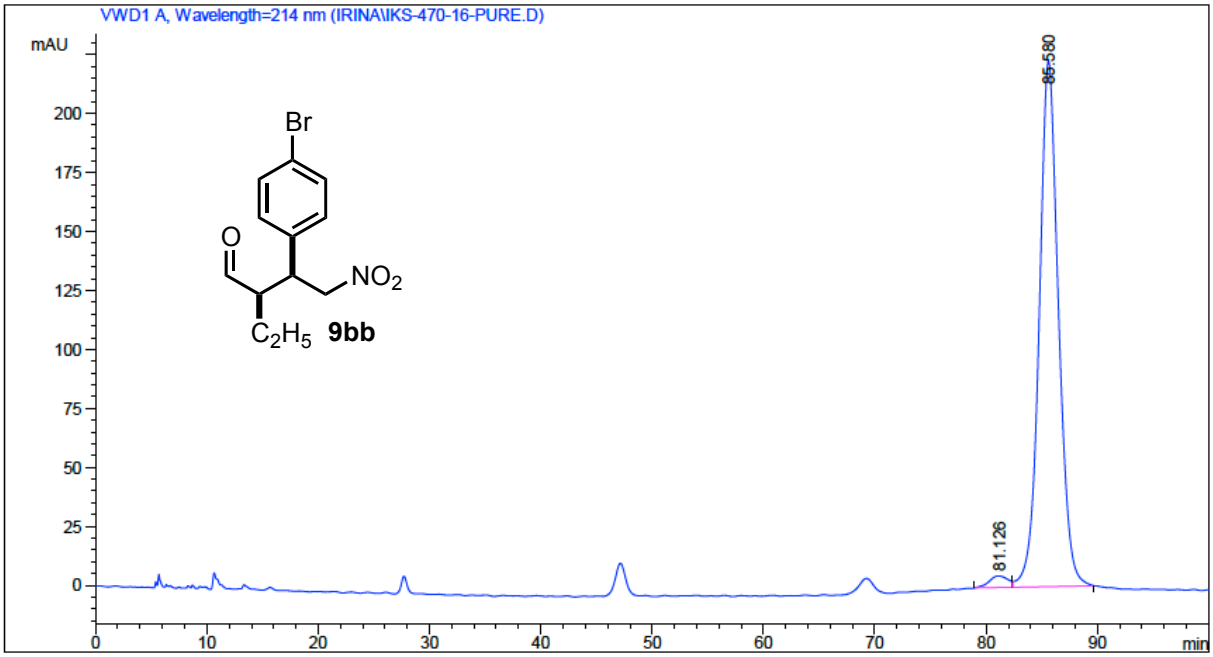

Peak #	RetTime [min]	Type	Width [min]	Area mAU *s	Height [mAU]	Area %
1	81.126	BV	1.4121	598.55127	4.98100	2.1850
2	85.580	VB	1.7493	2.67948e4	222.85602	97.8150

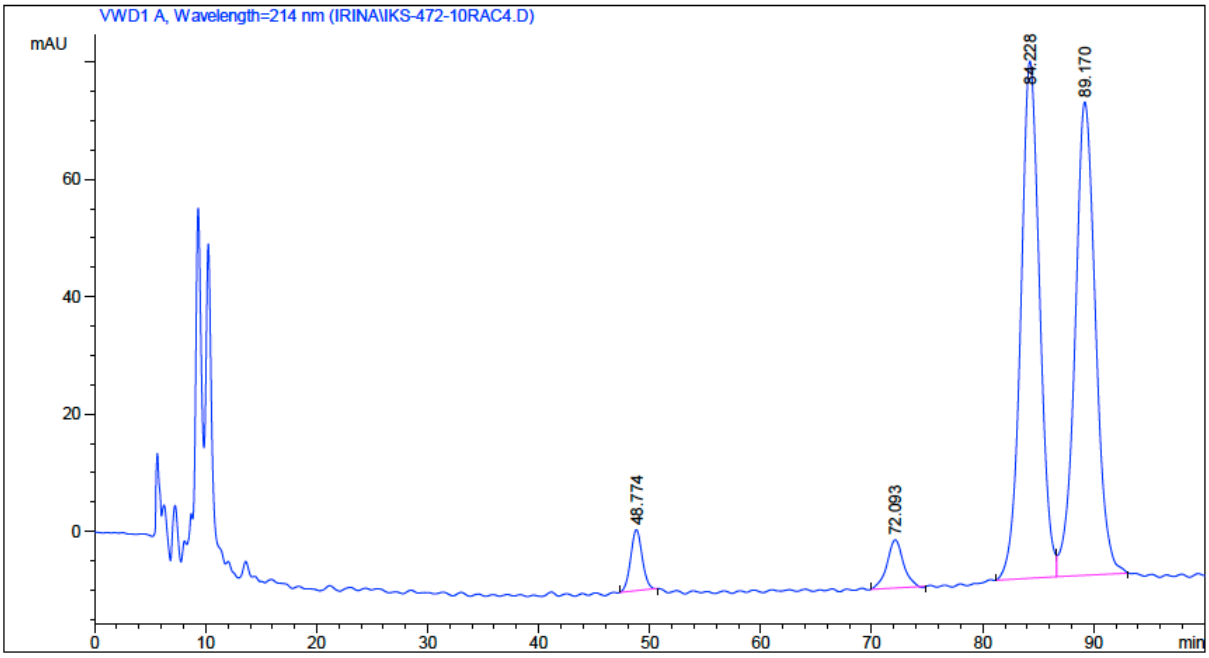

Peak #	RetTime [min]	Type	Width [min]	Area mAU *s	Height [mAU]	Area %
1	48.774	BB	1.0776	758.31635	10.43774	3.3900
2	72.093	BB	1.3097	848.48456	8.23556	3.7931
3	84.228	BV	1.7310	1.04227e4	88.11145	46.5942
4	89.170	VB	1.8539	1.03397e4	80.65015	46.2227

(2*R*,3*S*)-3-(4-Bromophenyl)-2-propyl-4-nitrobutanal (9cb).

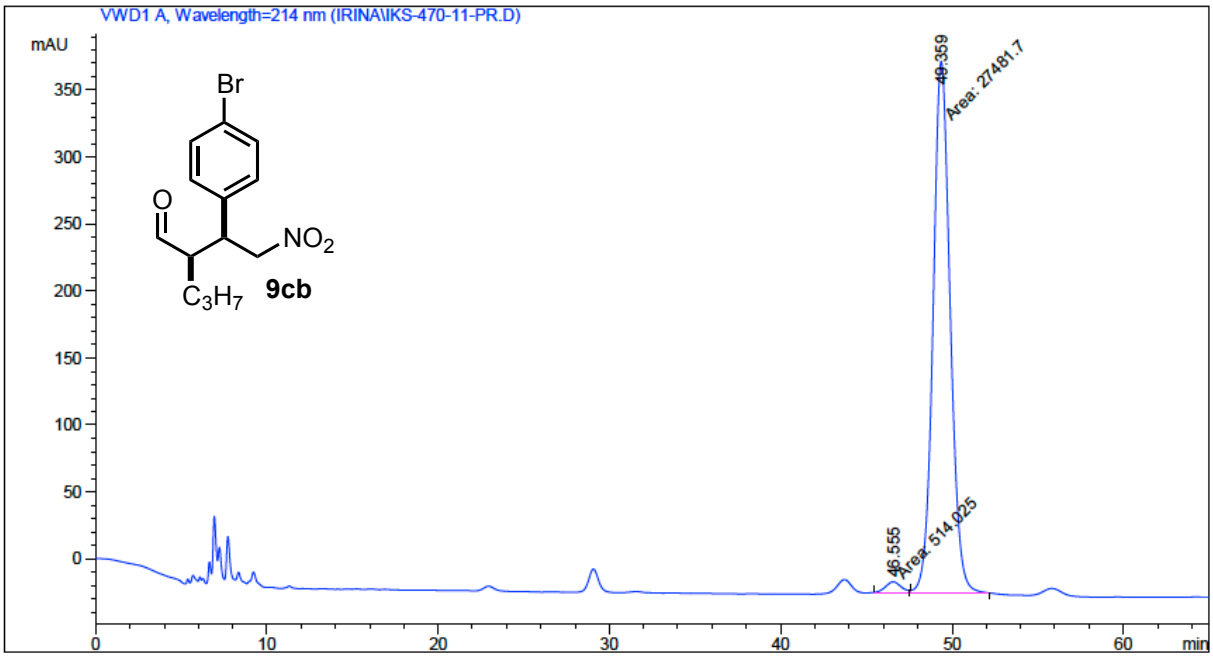

Peak #	RetTime [min]	Type	Width [min]	Area mAU *s	Height [mAU]	Area %
1	46.555	MM	1.0562	514.02533	8.11120	1.8361
2	49.359	MM	1.1547	2.74817e4	396.65521	98.1639

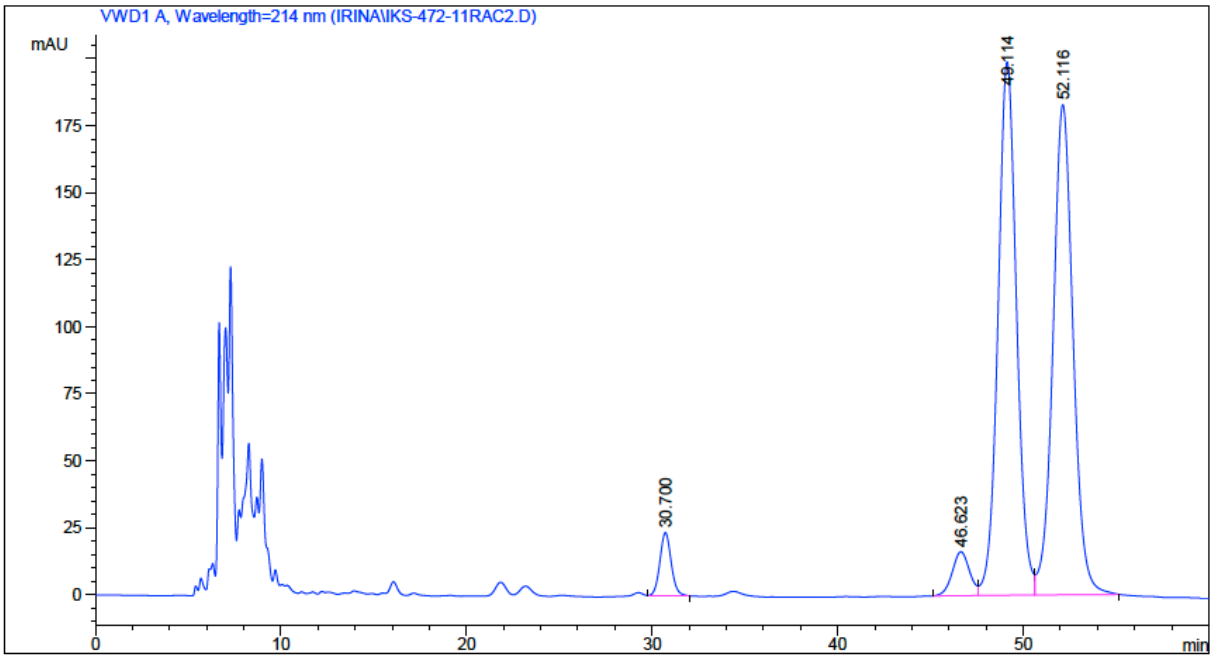

Peak #	RetTime [min]	Type	Width [min]	Area mAU *s	Height [mAU]	Area %
1	30.700	VB	0.6518	1014.20746	23.71842	3.4118
2	46.623	BV	0.9664	1069.32349	16.45359	3.5972
3	49.114	VV	1.0608	1.38529e4	199.06885	46.6011
4	52.116	VB	1.1443	1.37901e4	182.96663	46.3899

Chapter III

(2*R*,3*S*)-3-(3-Chlorophenyl)-2-methyl-4-nitrobutanal (9ak).

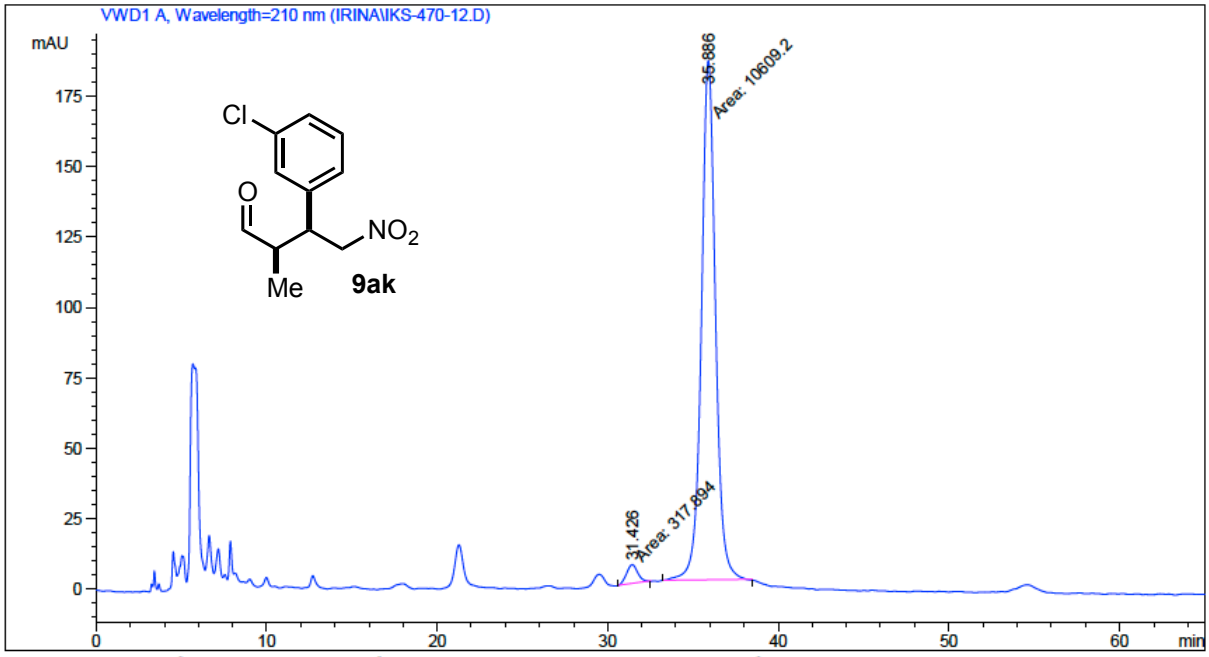

Peak #	RetTime [min]	Type	Width [min]	Area mAU *s	Height [mAU]	Area %
1	31.426	MM	0.7770	317.89423	6.81910	2.9092
2	35.886	MM	0.9587	1.06092e4	184.43420	97.0908

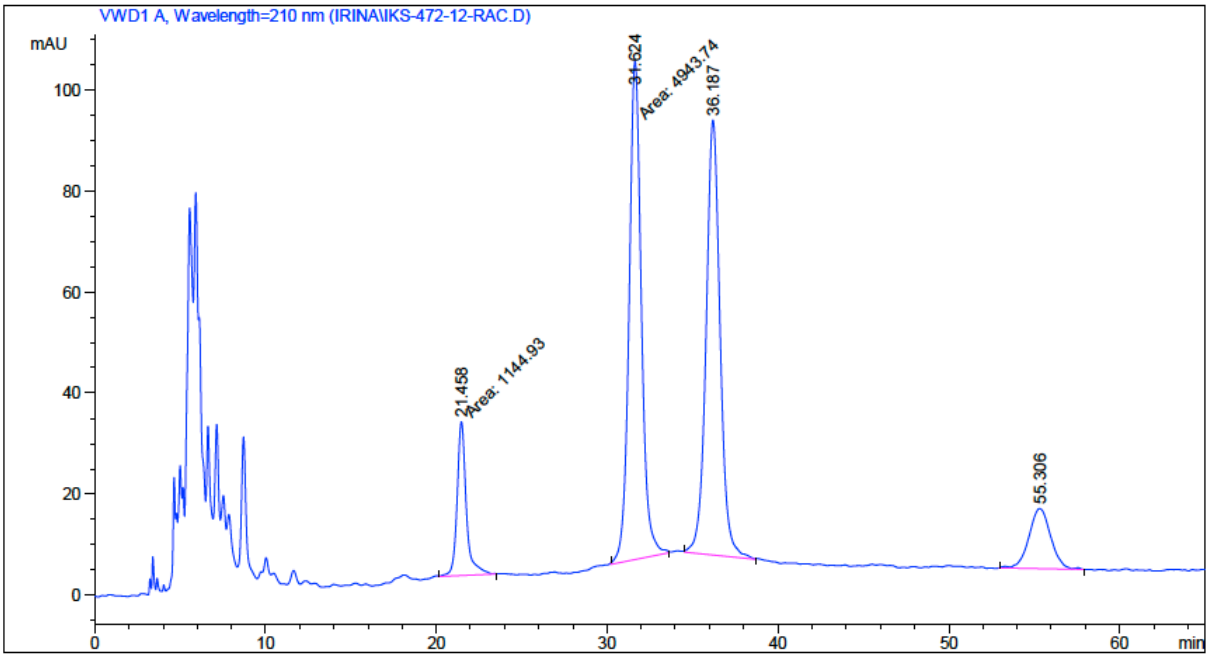

Peak #	RetTime [min]	Type	Width [min]	Area mAU *s	Height [mAU]	Area %
1	21.458	MM	0.6261	1144.92798	30.47638	9.4936
2	31.624	MM	0.8340	4943.73633	98.79398	40.9928
3	36.187	BB	0.8628	4907.52832	86.11941	40.6926
4	55.306	BB	1.3364	1063.81958	11.94098	8.8210

(2*R*,3*S*)-3-(4-Fluorophenyl)-2-methyl-4-nitrobutanal (9al).

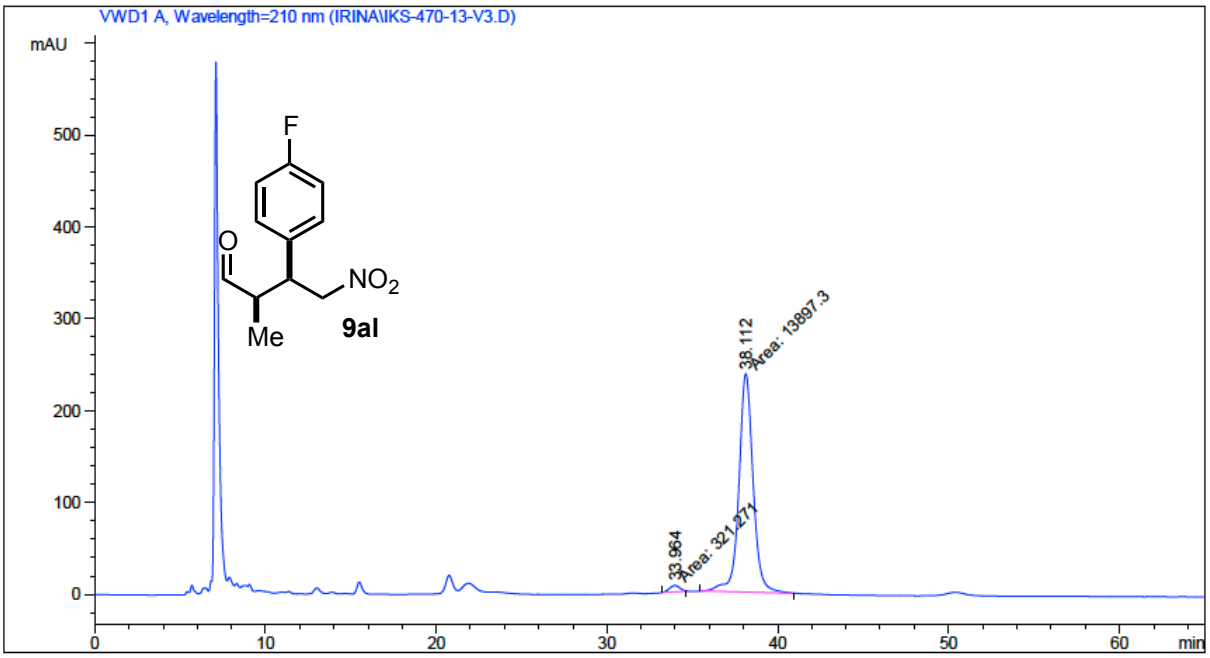

Peak #	RetTime [min]	Type	Width [min]	Area mAU *s	Height [mAU]	Area %
1	33.964	MF	0.7391	321.27115	7.24421	2.2595
2	38.112	MF	0.9734	1.38973e4	237.94481	97.7405

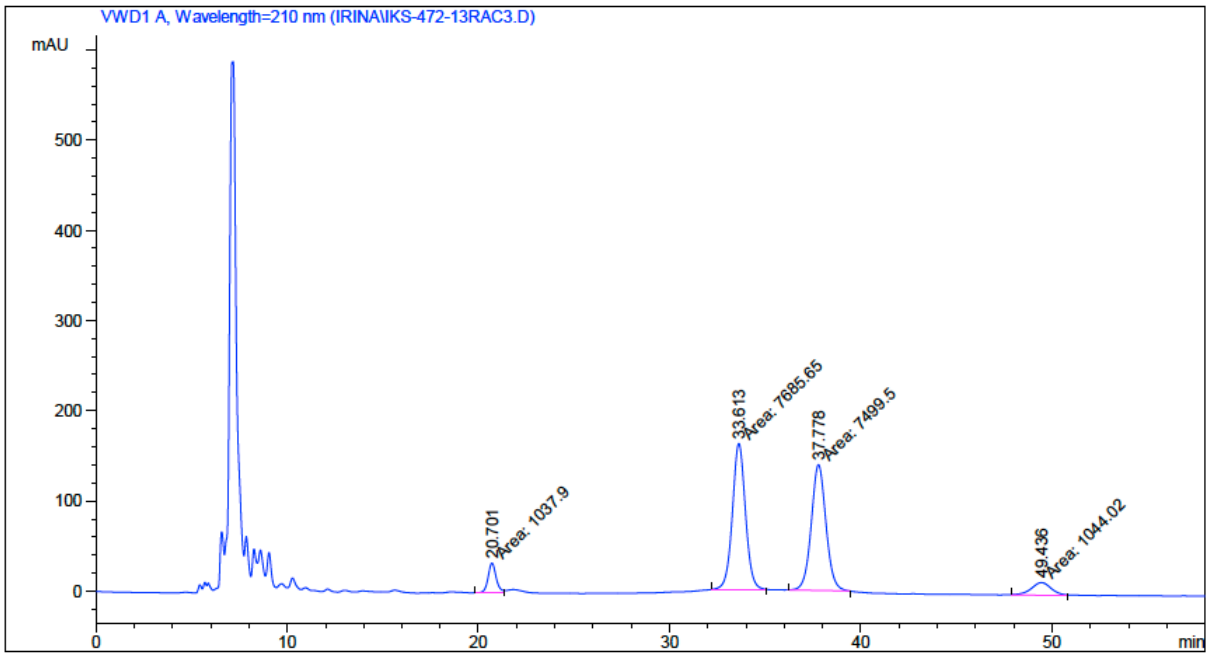

Peak #	RetTime [min]	Type	Width [min]	Area mAU *s	Height [mAU]	Area %
1	20.701	MM	0.5157	1037.90369	33.54559	6.0109
2	33.613	MM	0.7915	7685.64697	161.83443	44.5104
3	37.778	MM	0.8961	7499.50293	139.49060	43.4324
4	49.436	MM	1.2333	1044.02271	14.10875	6.0463

15. Chiral HPLC chromatograms for 11a,b

N-Tosyl-(3*R*,4*R*)-3-methyl-4-phenylpyrrolidine (11a).

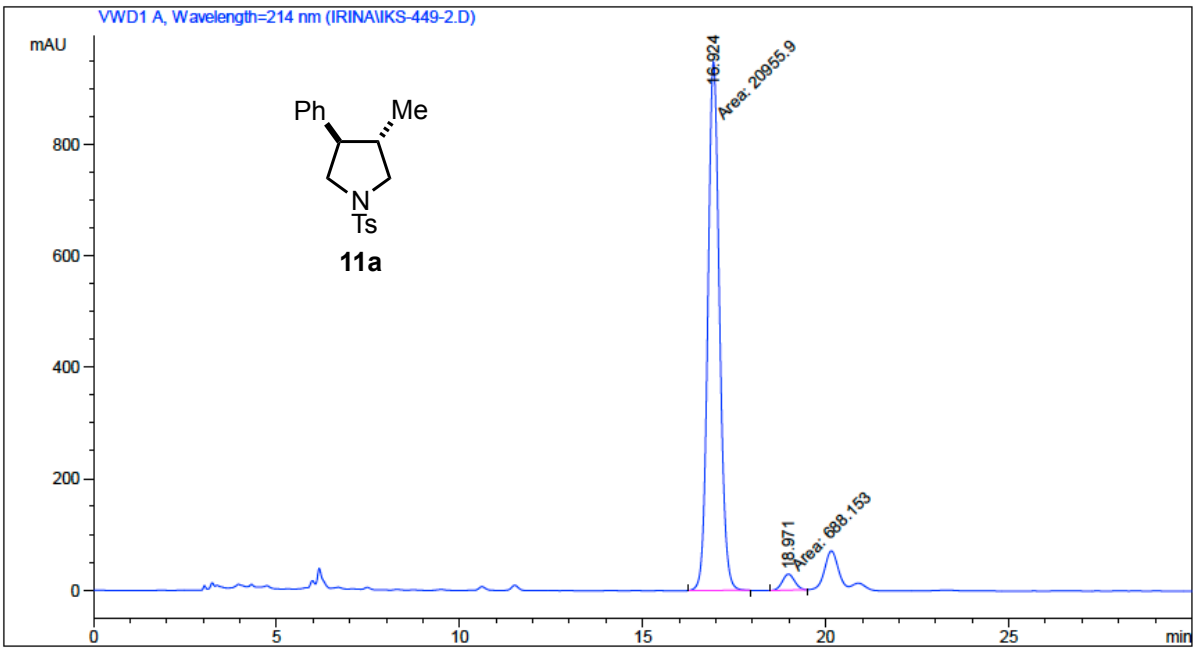

Peak #	RetTime [min]	Type	Width [min]	Area mAU *s	Height [mAU]	Area %
1	16.924	MM	0.3682	2.09559e4	948.55493	96.8206
2	18.971	MM	0.3957	688.15265	28.98798	3.1794

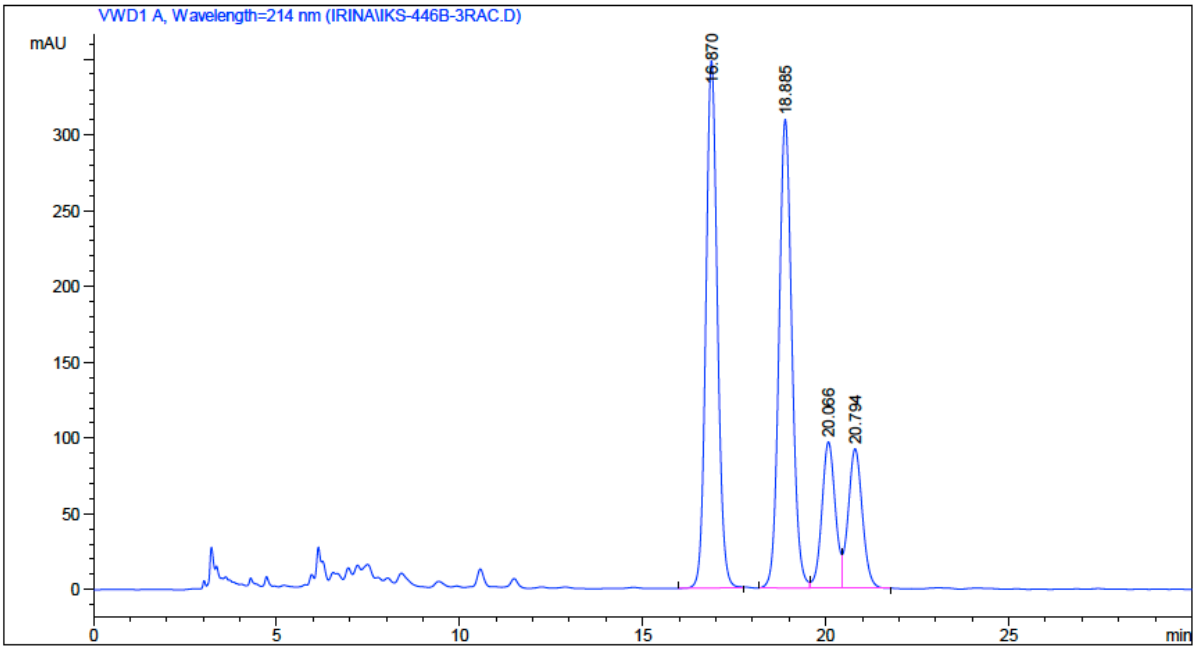

Peak #	RetTime [min]	Type	Width [min]	Area mAU *s	Height [mAU]	Area %
1	16.870	BB	0.3361	7595.73096	348.13577	37.6662
2	18.885	BV	0.3772	7604.74902	309.24307	37.7109
3	20.066	VV	0.3914	2469.98364	96.64324	12.2483
4	20.794	VB	0.4118	2495.43188	92.23053	12.3745

_N_-Tosyl-(3_R_,4_R_)-3-methyl-4-(4-bromophenyl)pyrrolidine (11b).

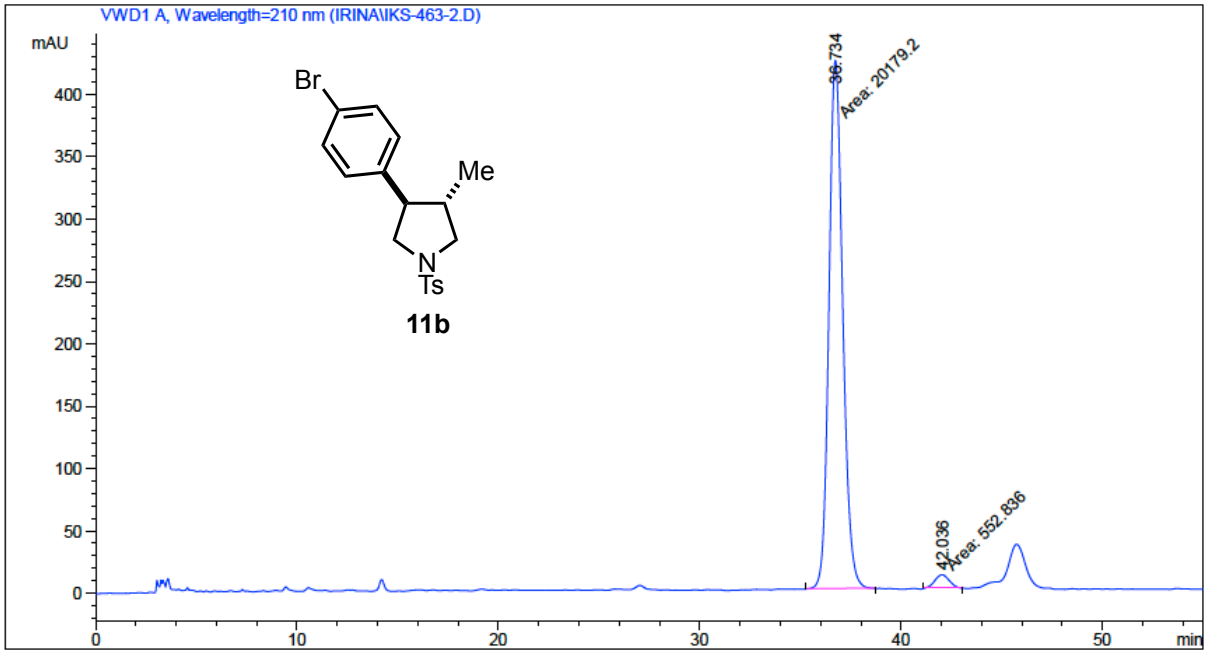

Peak #	RetTime [min]	Type	Width [min]	Area mAU *s	Height [mAU]	Area %
1	36.734	MM	0.7940	2.01792e4	423.60297	97.3334
2	42.036	MM	0.8435	552.83569	10.92371	2.6666

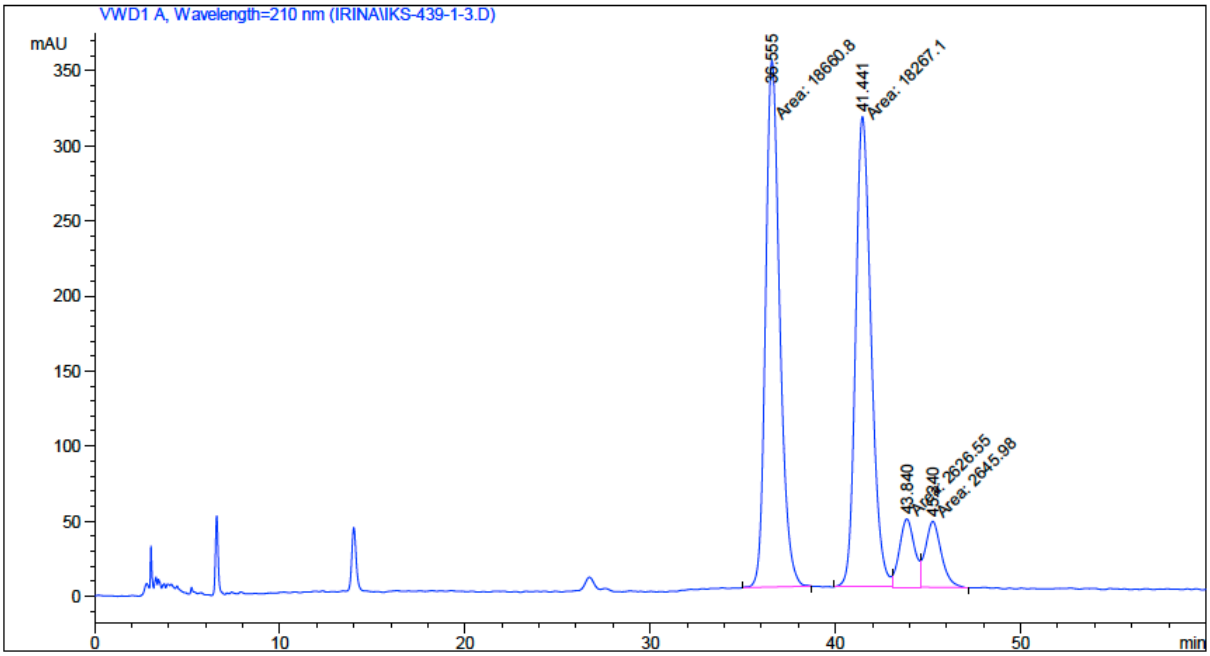

Peak #	RetTime [min]	Type	Width [min]	Area mAU *s	Height [mAU]	Area %
1	36.555	MM	0.8861	1.86608e4	350.98160	44.2195
2	41.441	MM	0.9723	1.82671e4	313.13354	43.2865
3	43.840	MF	0.9580	2626.54980	45.69462	6.2240
4	45.240	FM	0.9992	2645.98022	44.13443	6.2700

16. References

[1] Confalone, P. N.; Huie, E. M.; Ko, S. S.; Cole, G. M. *J. Org. Chem.* **1988**, *53*, 482-487.
[2] Quan, X.-J.; Ren, Z.-H.; Wang, Y.-Y.; Guan, Z.-H. *Org. Lett.* **2014**, *16*, 5728-5731.
[3] Price, M. D.; Kurth, M. J.; Schore, N. E. *J. Org. Chem.* **2002**, *67*, 7769-7773.
[4] Washington, R. P.; Steinbock, O. *J. Am. Chem. Soc.* **2001**, *123*, 7933-7934.
[5] a) List, B.; Pojarliev, P.; Martin, H. J. *Org. Lett.* **2001**, *3*, 2423-2425; b) Enders, D.; Seki, A. *Synlett* **2002**, 26-28.
[6] Betancort, J. M.; Barbas III, C. F. *Org. Lett.* **2001**, *3*, 3737-3740.
[7] Andrey, O.; Alexakis, A.; Tomassini, A.; Bernardinelli, G. *Adv. Synth. Catal.* **2004**, *346*, 1147-1168.
[8] Wang, W.; Wang, J.; Li, H. *Angew. Chem. Int. Ed.* **2005**, *44*, 1369-1371.
[9] Xu, K.; Zhang, S.; Hu, Y.; Zha, Z.; Wang, Z. *Chem. Eur. J.* **2013**, *19*, 3573-3578.
[10] Wang, B. G.; Ma, B. C.; Wang, Q.; Wang, W. *Adv. Synth. Catal.* **2010**, *352*, 2923-2928.
[11] Wiesner, M.; Neuburger, M.; Wennemers, H. *Chem. Eur. J.* **2009**, *15*, 10103-10109.
[12] a) Hayashi, Y.; Gotoh, H.; Hayashi, T.; Shoji, M. *Angew. Chem. Int. Ed.* **2005**, *44*, 4212-4215; b) Reddy, R. J.; Kuan, H.-H.; Chou, T.-Y.; Chen, K. *Chem. Eur. J.* **2009**, *15*, 9294-9298.
[13] Patora-Komisarska, K.; Benohoud, M.; Ishikawa, H.; Seebach, D.; Hayashi, Y. *Helv. Chim. Acta* **2011**, *94*, 719-745
[14] Zu, L.; Li, H.; Wang, J.; Yu, X.; Wang, W. *Tetrahedron Lett.* **2006**, *47*, 5131-5134.
[15] Li, Y.; Liu, X.-Y.; Zhao, G. *Tetrahedron: Asymmetry* **2006**, *17*, 2034-2039.
[16] Mase, N.; Thayumanavan, R.; Tanaka, F.; Barbas III, C. F. *Org. Lett.* **2004**, *6*, 2527-2530.
[17] Cheng, Y.-Q.; Bian, Z.; He, Y.-B.; Han, F.-S.; Kang, C.-Q.; Ning, Z.-L.; Gao, L.-X. *Tetrahedron: Asymmetry* **2009**, *20*, 1753-1758.
[18] Wiesner, M.; Revell, J. D.; Wennemers, H. *Angew. Chem. Int. Ed.* **2008**, *47*, 1871-1874.
[19] Zhu, S.; Yu, S.; Ma, D. *Angew. Chem. Int. Ed.* **2008**, *47*, 545-548.
[20] Yang, R.-Y.; Da, C.-S.; Yi, L.; Wu, F.-C.; Li, H. *Lett. Org. Chem.* **2009**, *6*, 44-49.
[21] Husmann, R.; Jörres, M.; Raabe, G.; Bolm, C. *Chem. Eur. J.* **2010**, *16*, 12549-12552.
[22] Denmark, S. E.; Marcin, L. R. *J. Org. Chem.* **1995**, *49*, 3221-3235.

CHAPTER IV

Polymer-Supported Organocatalysts for Asymmetric Epoxidation and Aziridination of α,β-Unsaturated Aldehydes

UNIVERSITAT ROVIRA I VIRGILI
NEW APPROACHES TO CATALYST DESIGN AND IMMOBILIZATION
Irina Sagamanova

Polymer-Supported Organocatalysts for Asymmetric Epoxidation and Aziridination of α,β-Unsaturated Aldehydes

Introduction.

Our group has previously demonstrated the usefulness of triazole rings in catalysis either by exploring the properties of the triazole as a donor group for transition metal complexes or by using it as a linker to heterogenize organocatalysts (**Figure IV.1**). [71b,i;194]

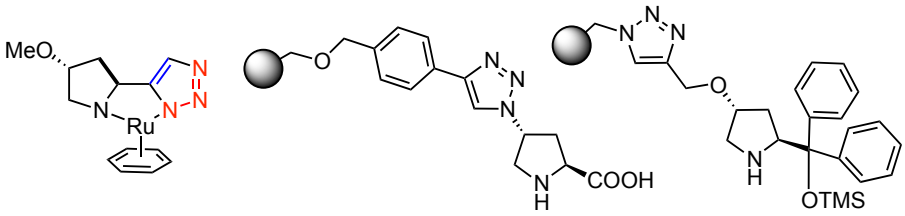

Figure IV.1. Examples of triazoles used in catalysis.

Click chemistry methods have become a successful strategy for the easy access to immobilized catalysts. However, systems bearing nitrogen-rich substituents such as 1,2,3-triazoles can show different behaviour in asymmetric reactions compared to the ones that do not present this linker.

The polymer field has largely exploited the CuAAC reaction (see **Chapter I**) for click polymerization and polymer modification.[195] In 2006, Reiser *et al.* reported the CuAAC-immobilization of TEMPO on azide-derived Merrifield resin.[196]

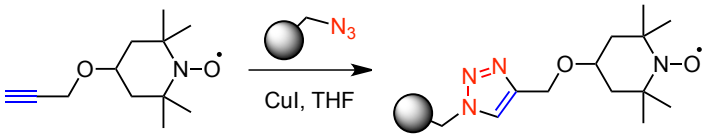

Scheme IV.1. CuAAC immobilization of TEMPO.

[194] Cambeiro, X. C.; Pericàs, M. A. *Adv. Synth. Catal.* **2011**, *353*, 113-124.
[195] a) Lutz, J.-F. *Angew. Chem., Int. Ed.* **2007**, *46*, 1018-1025; b) *Macromol. Rapid Commun.* (Ed.: Binder, W. H.) **2008**, *29*, 943-949; c) Meldal, M. *Macromol. Rapid Commun.* **2008**, *29*, 1016-1051.
[196] Gheorghe, A.; Matsuno, A.; Reiser, O. *Adv. Synth. Catal.* **2006**, *348*, 1016-1020.

In the same year, our research group immobilized for the first time 4-hydroxyproline on polystyrene supports, using the CuAAC strategy (**Scheme IV.2 a**).[71a] This type of catalyst (**IV.2**) can perform highly enantioselective asymmetric aldol reactions in water in the presence of a catalytic amount of DiMePEG. Noteworthy, the selectivity observed was superior than the one observed with the monomeric counterpart, thus suggesting that the polystyrene backbone in supported catalyst (**IV.2**) can act as a hydrophobic pocket; this would mimic the case of type-I aldolase enzymes. Later, this resin (**IV.2**) was successfully applied in the α-aminoxylation of aldehydes and ketones[71b,d] and in the asymmetric Mannich reaction under continuous flow.[71d] The same strategy was used in a different work in order to rationalize the catalytic activity of polystyrene-"clicked" proline and to prove the beneficial role of the triazole spacer in the asymmetric transformation (see **Chapter II, 2.2**).[71]

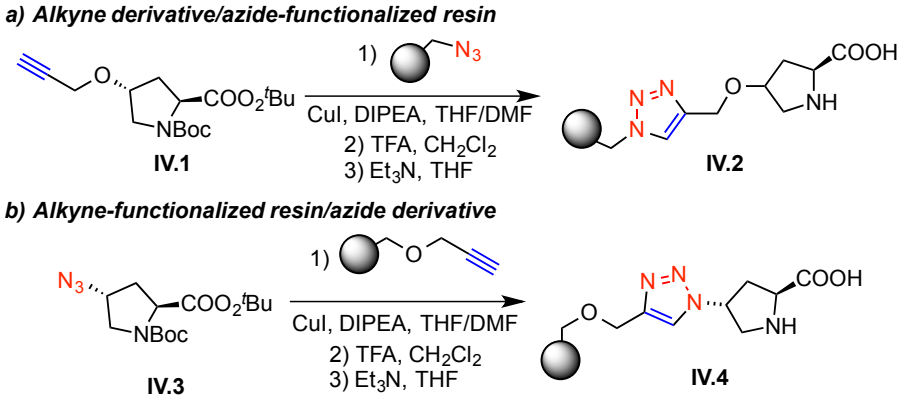

Scheme IV.2. The two main strategies to immobilize organocatalysts via CuAAC used in our group.

Two different ways of immobilizing organocatalysts onto polystyrene beads with a 1,2,3-triazole linker (illustrated in **Scheme IV.2**) can be used in the synthesis of immobilized organocatalysts. For azide-functionalized resins, a 4-hydroxyproline (or the corresponding modified catalyst) is reacted with propargyl bromide under basic conditions in order to install the alkyne moiety (**IV.1**) essential for the click reaction. The other strategy uses the "click" chemistry between the azide derivative of the desired organocatalyst (**IV.3**) and a conveniently propargylated resin.

When considering the use of triazole as a linker in the immobilization of catalytic species, one must bear in mind that a detrimental effect of the triazole linker has been observed in metal-based supported catalysts (**Scheme IV.3**). Triazoles have a tendency to form coordination complexes with metals, which can interfere with the

desired reaction pathway, providing low enantioselectivity in cases like catalyst **IV.5**.[197] In the phenylation reaction of aldehydes, triazole-containing catalyst **IV.5** provided a non chiral catalytic pathway that yielded racemic products.

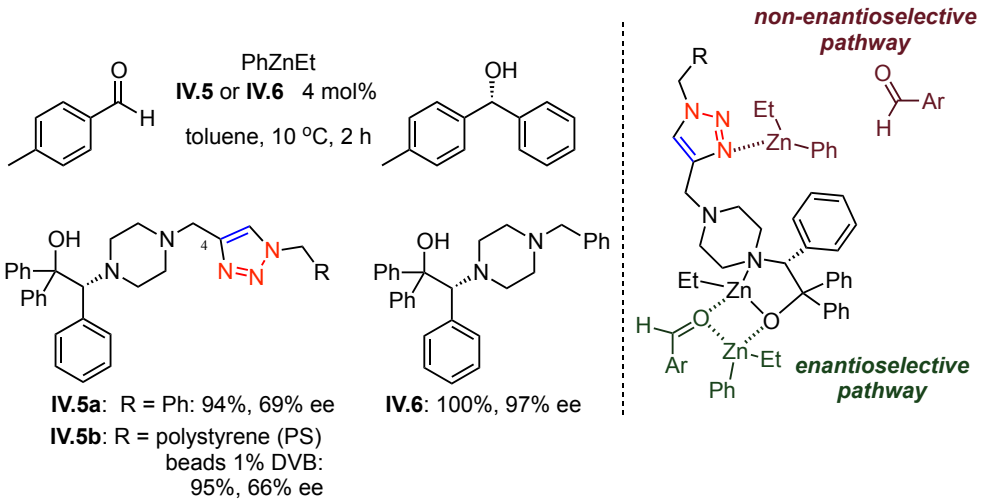

Scheme IV.3. Influence of the triazole linker on the enantioselectivity in the phenylation reaction of aldehydes.

Negative effects of the triazole moiety on the performance of the catalyst can sometimes be also observed in organocatalytic reactions; in particular, our group has reported this situation in the asymmetric α-amination of aldehydes catalyzed by a polymer-supported triazole, containing diphenyprolinol silyl ethers.[71o] Additional studies on the homogeneous analogue (**Scheme IV.4**) have shown that catalyst deactivation is due to an alternative reaction pathway: the nucleophilic attack of the aminocatalyst to dibenzylazodicarboxylate (DBAD, **IV.7**), leading to triazane formation (**IV.8**). This intermediate eliminates to generate an imine (**IV.9**) and dibenzyl hydrazine-1,2-dicarboxylate (**IV.10**) in a process triggered by the presence of the 1,2,3-triazole unit in the substituent at C-4.

[197] Bastero, A.; Font, D.; Pericàs, M. A. *J. Org. Chem.* **2007**, *72*, 2460-2468.

Chapter IV

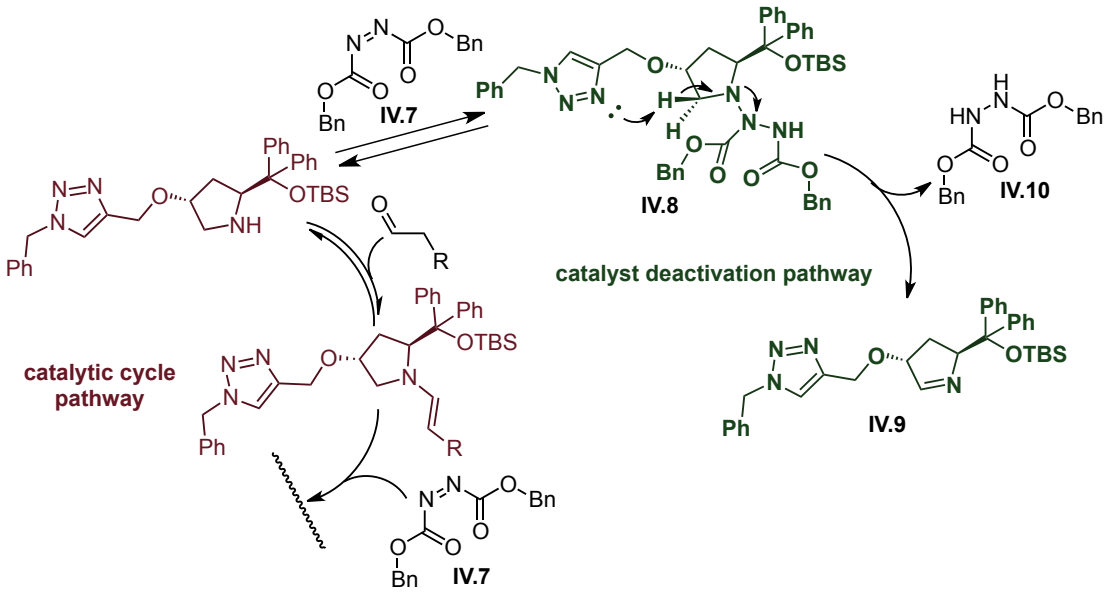

Scheme IV.4. Influence of the triazole linker on the α-amination of aldehydes.

These interactions, however, can also be used to one's advantage. For instance in the palladium-catalyzed asymmetric allylic amination reaction (**Scheme IV.5**) [198] a positive effect of the pair triazole/metal binding was observed. The coordination of triazole was investigated by DFT calculations and NOE experiments on the corresponding homogeneous ligands.

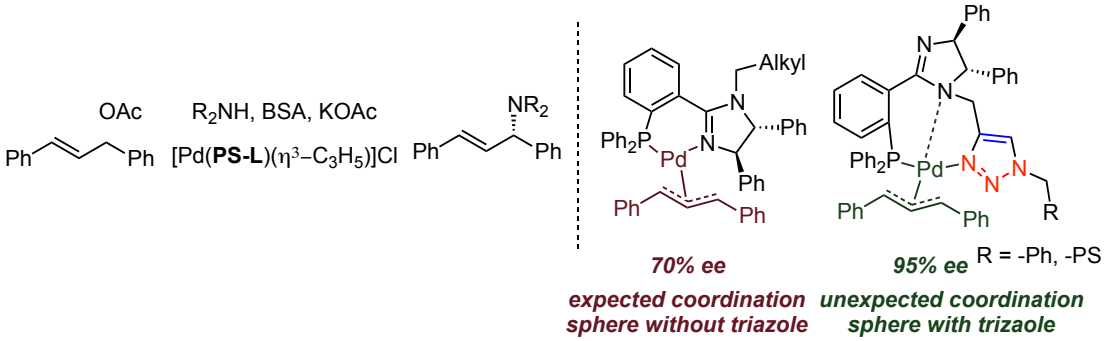

Scheme IV.5. Positive effect via triazole/metal binding.

Overall, click chemistry has proven to be an efficient strategy for the covalent immobilization of catalysts for several reasons. There are very limited detection means for fast monitoring of the reactions taking place in solid phase. However, the strong signal of the azide functional group in IR spectra facilitates the monitoring of reaction completion. Moreover, the high efficiency of the reaction provides high yields with few side reactions, reducing the risk of anchoring unwanted compounds onto the solid support.

---

[198] de la Fuente, V.; Marcos, R.; Cambeiro, X. C.; Castillón, S.; Claver, C.; Pericàs, M. A. *Adv. Synth. Catal.* **2011**, *353*, 3255-3261.

Nowadays, developments in supported enantioselective catalysts are mainly focused on their separation and recycling. Some of the immobilized catalysts have been used in continuous flow operation, which is an extremely useful tool for synthetic chemists.

The synthesis of the optimal model of polymer-supported catalytic system is an ongoing research, often characterized by the search for a balance between stability and activity in different potential applications. Therefore, complementary to the successful design of the co-polymerized supported catalyst introduced in **Chapter III**, we also developed new polymer-supported β-fluoroamines via click chemistry (**Figure IV.2**).

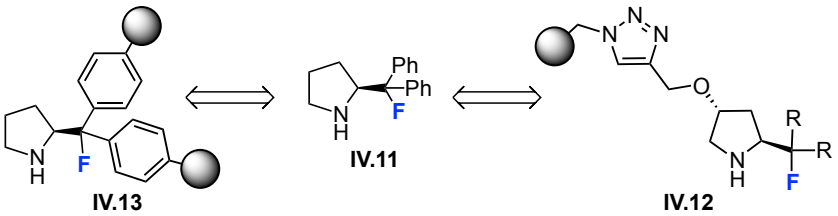

Figure IV.2. General proposed design for substituted β-fluoroamine catalytic systems.

Herein, we will present the preliminary results for these catalysts working via iminium ion activation, in particular for the epoxidation or aziridination of α,β-unsaturated aldehydes.

4.2. Epoxidation of α,β-unsaturated aldehydes.

Asymmetric epoxidation is a fundamental reaction in organic synthesis. Epoxides are highly useful intermediates in the synthesis of natural products and pharmaceuticals.[199] The three-membered ring, thanks to its inherent polarity and strain, undergoes stereospecific ring-opening reactions with nucleophiles for the generation of 1,2-difunctional compounds.[200]

Therefore, many methods have been developed to date. Katsuki and Sharpless were the first ones to develop a practical method for catalytic asymmetric epoxidation, using titanium-tartrate complexes as epoxidation catalysts for allylic alcohols (**Scheme**

[199] a) Johnson, R. A.; Sharpless, K. B. *Catalytic Asymmetric Synthesis, 2nd ed.* (Ed.: Ojima, I.), Wiley, New York, **2000**, *Ch. 6A*, 229-280; b) *Aziridines and Epoxides in Organic Synthesis* (Ed.: Yudin, A. K.), Wiley-VCH, Weinheim, Germany, **2006**.
[200] For some examples, see: a) Rickborn, B. in *Comprehensive Organic Synthesis* (Eds.: Trost, B. M.; Fleming, I.; Pattenden, G.), Pergamon Press, Oxford, **1991**, *Vol. 3*, 733-775; b) Jacobsen, E. N. *Acc. Chem. Res.* **2000**, *33*, 421-431; c) Pineschi, M. *Eur. J. Org. Chem.* **2006**, *22*, 4979-4988.

IV.6A).[201] Significant efforts in organometallic strategies were also made in the independent contributions of Jacobsen and Katsuki (**Scheme IV.6B**)[202] in the asymmetric epoxidation of unfunctionalized and particularly conjugated *(Z)*-disubstituted olefins.

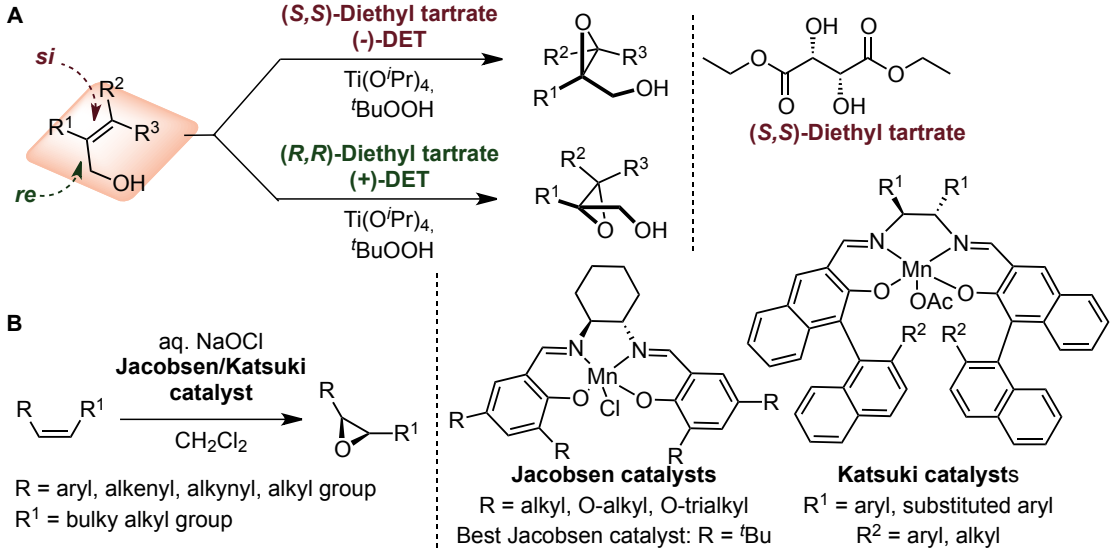

Scheme IV.6. Asymmetric epoxidation of allylic alcohols (A) and alkenes (B).

In recent years, the work of several groups, in particular Shi, Denmark, Yang, and Armstrong, focused in dioxirane-based systems for asymmetric epoxidation of a wide range of trisubstituted and 1,2-*trans*-disubstituted alkenes.[203] Dioxiranes feature a relatively weak O-O bond (**IV.8**) and they are readily attacked even by poor nucleophiles such as olefins. The general method to produce a dioxirane is through the use of a ketone and a stoichiometric oxidant (usually Oxone) (**Scheme IV.7**).

[201] a) Katsuki, T.; Sharpless, K. B. *J. Am. Chem. Soc.* **1980**, *102*, 5974-5976; for mechanism of asymmetric epoxidation, see: b) Finn, M. G.; Sharpless, K. B. *J. Am. Chem. Soc.* **1991**, *113*, 113-126.
[202] a) Zhang, W.; Loebach, J. L.; Wilson, S. R.; Jacobsen, E. N. *J. Am. Chem. Soc.* **1990**, *112*, 2801-2803; b) Irie, R.; Noda, K.; Ito, Y.; Matsumoto, N.; Katsuki, T. *Tetrahedron Lett.* **1990**, *31*, 7345-7348.
[203] a) Yang, D.; Wong, M. K.; Yip, Y. C. *J. Org. Chem.* **1995**, *60*, 3887-3889; b) Armstrong, A.; Hayter, B. R. *Chem. Commun.* **1998**, 621-622; c) Tu, Y.; Wang, Z.-X.; Shi, Y. *J. Am. Chem. Soc.* **1996**, *118*, 9806-9807; d) Denmark, S. E.; Forbes, D. C.; Hays, D. S.; DePue, J. S.; Wilde, R.G. *J. Org. Chem.* **1995**, *60*, 1391-1407.

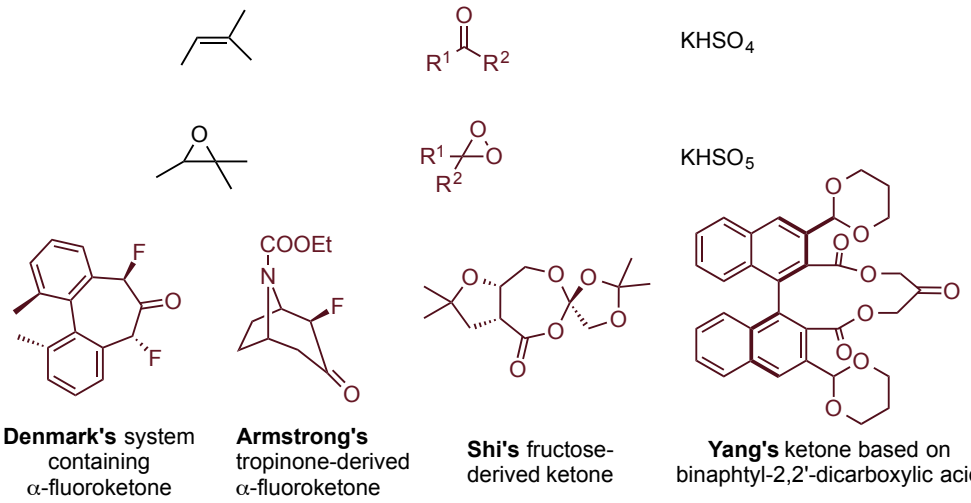

Denmark's system containing α-fluoroketone

Armstrong's tropinone-derived α-fluoroketone

Shi's fructose-derived ketone

Yang's ketone based on binaphtyl-2,2'-dicarboxylic acid

Scheme IV.7. Organocatalytic approaches for trisubstituted and 1,2-trans-disubstituted alkenes.

However, there are only a few different methods for the asymmetric epoxidation of electron-deficient olefins. Due to the value of the corresponding optically active epoxides, much effort has been devoted to the development of a general, highly enantioselective method applicable to this transformation.

The first general approach for the epoxidation of electron-deficient olefins was reported by Weitz and Scheffer,[204] using alkaline hydroperoxides. The epoxide formation occurs via a two-step mechanism, which was reported by Bunton and Minkoff in 1990 (**Scheme IV.8**).[205] Under basic conditions, epoxidation involves the conjugate addition of peroxide anion to the β-position of the α,β-unsaturated ketone, and the attack of the transient enolate to the peroxide O-O bond to cleave the hydroxide anion.

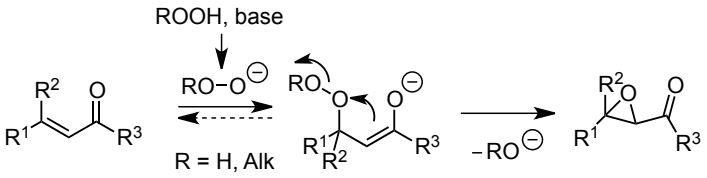

Scheme IV.8. Mechanism of the Weitz-Scheffer epoxidation.

Particular attention has been paid to the development of an asymmetric version of the Weitz-Scheffer epoxidation, due to the importance of enantiomerically enriched

[204] Weitz, E.; Scheffer, A. *Chem. Ber.* **1921**, *54*, 2344-2353.
[205] Bunton, C. A.; Minkoff, G. J. *J. Chem. Soc.* **1949**, 665-667.

Chapter IV

α,β-epoxyketones as chiral building blocks and products of pharmaceutical and biological interest (**Figure IV.3**).[206]

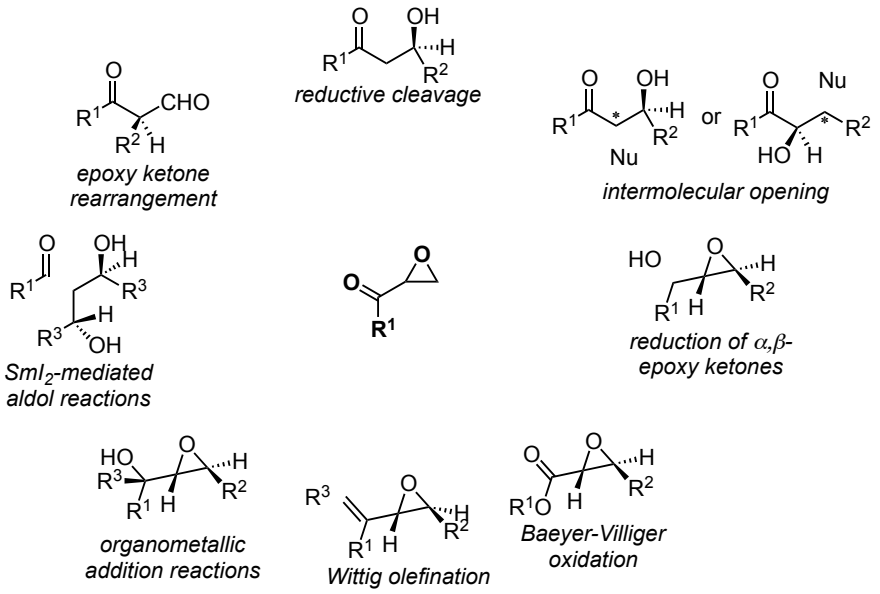

Figure IV.3. Selected transformations of α,β-epoxy ketones.

Since the pioneering work by Wynberg *et al.* in 1976,[207] which represented one of the first methods for the synthesis of optically active epoxides via phase transfer catalysis (PTC) (**Scheme IV.9**), numerous investigations have been developed.[208]

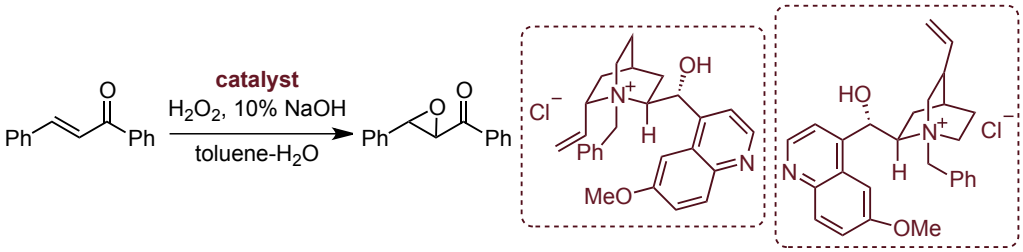

Scheme IV.9. First asymmetric Weitz-Scheffer epoxidation by Wynberg.

The Juliá-Colonna epoxidation is another classic asymmetric epoxidation system,[209] based on a triphasic system: aqueous solution of hydrogen peroxide and sodium hydroxide, insoluble polyamino acid catalyst (poly-L-alanine (PLA) or poly-L-

[206] For a review, see: Lauret, C. *Tetrahedron* **2001**, *12*, 2359-2383.
[207] a) Helder, R.; Hummelen, J. C.; Laane, R. W. P. M.; Wiering, J. S.; Wynberg. H. *Tetrahedron Lett.* **1976**, *21*, 1831–1834; b) Wynberg, H.; Greijdanus, B. *J. Chem. Soc., Chem. Commun.* **1978**, *62*, 427–428.
[208] a) Lygo, B.; Wainwright, P. G. *Tetrahedron Lett.* **1998**, *39*, 1599-1602; b) Lygo, B.; Wainwright, P. G. *Tetrahedron* **1999**, *55*, 6289-6300; c) Corey, E. J.; Zhang, F.-Y. *Org. Lett.* **1999**, *1*, 1287-1290; d) Lopez-Pedrosa, J.-M.; Pitts, M. R.; Roberts, S. M.; Saminathan, S.; Whittall, J. *Tetrahedron Lett.* **2004**, *45*, 5073-5075.
[209] a) Juliá, S.; Masan, J.; Vega, J. C. *Angew. Chem., Int. Ed.* **1980**, *19*, 929-931; b) Juliá, S.; Guixer, J.; Masana, J.; Rocas, J.; Colonna, S.; Annuziata, R.; Molinari, H. *J. Chem. Soc., Perkin Trans. 1*, **1982**, 1317-1324.

leucine (PLL)) and a solution of sodium chalcone in an organic solvent (**Scheme IV.10**). Despite the excellent enantioselectivity, this methodology has been limited to α,β-enones, in particular chalcone and simple analogues; in addition, long reaction times are required.

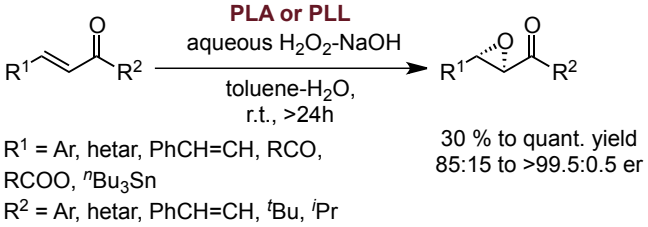

Scheme IV.10. Julia-Colonna epoxidation under triphasic reaction conditions.

Organocatalytic asymmetric epoxidation methods have been recently extended by the use of proline-derived chiral amines, increasing the range of synthetically accessible epoxides. Particular attention was paid to hydrogen peroxide as oxidant due to its advantages over many other alternatives: high oxygen content, low price, availability, and environmental acceptability.

Jørgensen *et al.*[210] demonstrated the first direct approach for obtaining α,β-epoxy aldehydes by the combination of an iminium and enamine activation with nucleophilic oxidants such as simple as hydrogen peroxide. The generally accepted mechanism of the organocatalytic epoxidation of α,β-unsaturated aldehydes is shown in **Scheme IV.11**. The first step involves condensation of the trimethylsilyl prolinol catalyst **IV.14** with the α,β-unsaturated aldehyde to form the iminium ion intermediate (**IV.15**). This is followed by nucleophilic addition of the peroxide to the β-carbon atom of the conjugated iminium ion species. In the next step, the epoxide is formed via attack of the α-carbon atom on the electrophilic oxygen atom of **IV.16**. Hydrolysis of the iminium ion intermediate **IV.17** produces the α,β-epoxy aldehyde and regenerates the catalyst (**IV.14**).

[210] a) Marigo, M.; Franzén, J.; Poulsen, T. B.; Zhang, W.; Jørgensen, K. A. *J. Am. Chem. Soc.* **2005**, *127*, 6964-6965; b) W. Z. Zhang, M. Marigo, K. A. Jørgensen, *Org. Biomed. Chem.* **2005**, 3883-3885.

Chapter IV

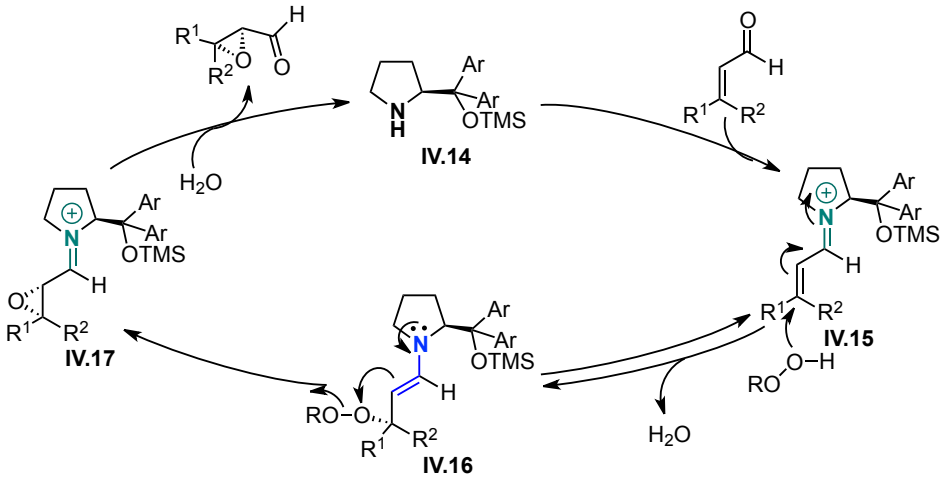

Scheme IV.11. Accepted mechanism for the organocatalytic epoxidation of α,β-unsaturated aldehydes.

Several studies have been carried out on the organocatalytic epoxidation using different chiral pyrrolidine derivatives and imidazolidinone salts with varying nucleophilic oxidants.[211] MacMillan and co-workers have established iminium catalysis with a chiral imidazolidinone as a strategy for the formation of oxiranes from a wide array of α,β-unsaturated aldehydes, using hypervalent iodine reagents as oxidants.[210b] However, simpler *tert*-butyl hydroperoxide, *m*-CPBA and hydrogen peroxide failed as oxidants for this transformation.

In 2009, Gilmour *et al.* reported a novel, fluorinated organocatalyst for the enantioselective epoxidation of α,β-unsaturated aldehydes (**Scheme IV.12**).[163a] They illustrated the importance of the fluorine-iminium ion interaction through a control experiment with a nonfluorinated counterpart of the catalyst (only 85% ee in the case of $CHPh_2$).

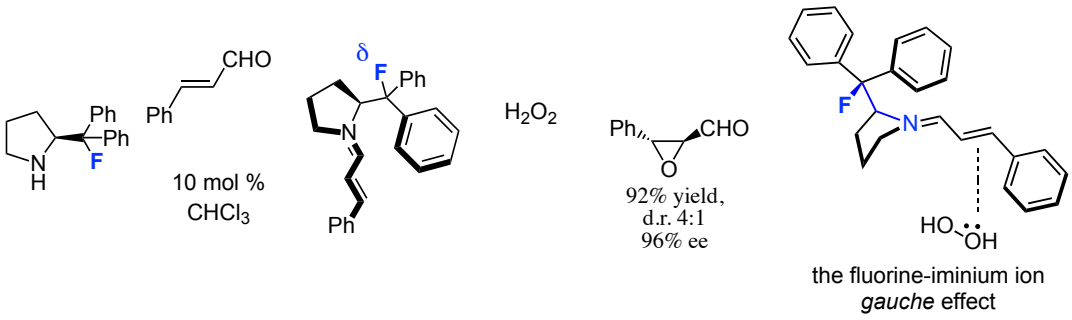

Scheme IV.12. A fluorinated organocatalyst for the stereoselective epoxidation of α,β-unsaturated aldehydes.

[211] a) Sundén, H.; Ibrahem, I.; Córdova, A. *Tetrahedron Lett.* **2006**, *47*, 99-103; b) Lee, S.; MacMillan, D. W. C. *Tetrahedron* **2006**, *62*, 11413-11424; c) Zhao, G.-L.; Ibrahem, I.; Sundén, H.; Córdova, A. *Adv. Synth. Catal.* **2007**, *349*, 1210-1224.

4.3. Aziridination of α,β-unsaturated aldehydes.

The aziridine moiety is one of the most important three-membered rings, and it is present in the structure of many natural products (**Figure IV.4**).[199b,212] Mitomycin A, C together with porfiromycin, represent an important class of naturally occurring mitosanes, which antitumour properties resulting from their ability to cross-link DNA via nucleophilic ring opening of the aziridine moiety.[213] FR compounds are structurally related to mitosanes, where the acetal-like core of these molecules reveals a relationship with them. They have also shown similar anticancer activity. Other examples, such as azinomycins are naturally occurring metabolites, which demonstrate activity against a wide range of tumours.

A number of synthetic aziridines have also been shown to exhibit useful biological properties. See for instance, the structures **IV.18** and **IV.19**[214] presented in **Figure IV.4**. There are irreversible inhibitors of enzymes, such as diaminopimelic acid epimerase or glutamate racemase.

Several research groups have developed methodologies to access important biological compounds from aziridines; for example, key intermediates for the synthesis of some bioactive compounds by Fujisawa Research (FR-66979 and FR-00482).[215] Preparation of aziridines, especially in an optically active manner, has become an important aim in organic chemistry.[216] However, they have received limited application in the synthesis of natural compounds due to difficulties in their preparation and handling.

---

[212] a) Osborn, H. M. O.; Sweeney, J. *Tetrahedron: Asymmetry* **1997**, *8*, 1693-1715; b) Sweeney, J. B. *Chem. Soc. Rev.* **2002**, *31*, 247-258; c) Watson, I. D. G.; Yu, L.; Yudin, A. K. *Acc. Chem. Res.* **2006**, *39*, 194-206.
[213] Kasai, M.; Kono, M. *Synlett* **1992**, *10*, 778-790.
[214] **IV.18**: a) Gerhart, F.; Higgins, W.; Tardif, C.; Ducep, J. *J. Med. Chem.* **1990**, *33*, 2157-2162; **IV.19**: b) Tanner, M. E.; Miao, S. *Tetrahedron Lett.* **1994**, *35*, 4073-4076.
[215] Judd, T. C.; Williams, R. M. *Angew. Chem. Int. Ed.* **2002**, *41*, 4683-4685.
[216] Recent review on catalytic methods: a) Pellissier, H. *Tetrahedron* **2010**, *66*, 1509-1555; For a review on the use of chiral catalysts, see: b) Müller, P.; Fruit, C. *Chem. Rev.* **2003**, *103*, 2905-2919; c) Möβner, C.; Bolm, C. *In Transition Metals for Organic Synthesis, 2nd ed.* (Eds.: Beller, M.; Bolm, C.), Wiley-WCH, Verlag: Weinheim, **2004**; 389–402; For a review on the use of chiral auxiliaries: d) Tanner, D. *Angew. Chem. Int. Ed.* **1994**, *33*, 599-619; c) Furmeier, S.; Metzger, J. O. *Eur. J. Org.Chem.* **2003**, 649-659.

Chapter IV

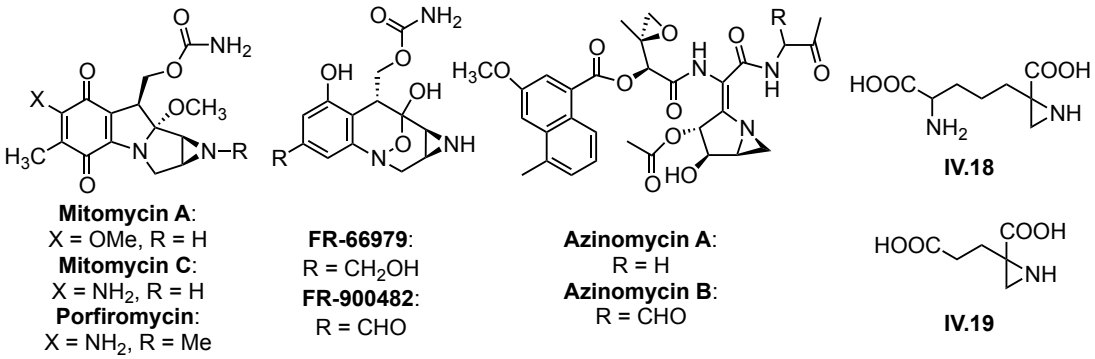

Figure IV.4. Aziridine-containing products.

Aziridines are nitrogen analogues of epoxides and display similar reactivity patterns as electrophilic reagents. Therefore, the ring strain of aziridines renders these compounds susceptible to regio- and stereoselective ring opening with various nucleophiles (**Figure IV.5**).[199b,217] Ring opening of aziridines can be provided by a variety of biologically active molecules such as α and β-amino acids, amino alcohols, amines, diamines, β-lactams and oxazolidinones.

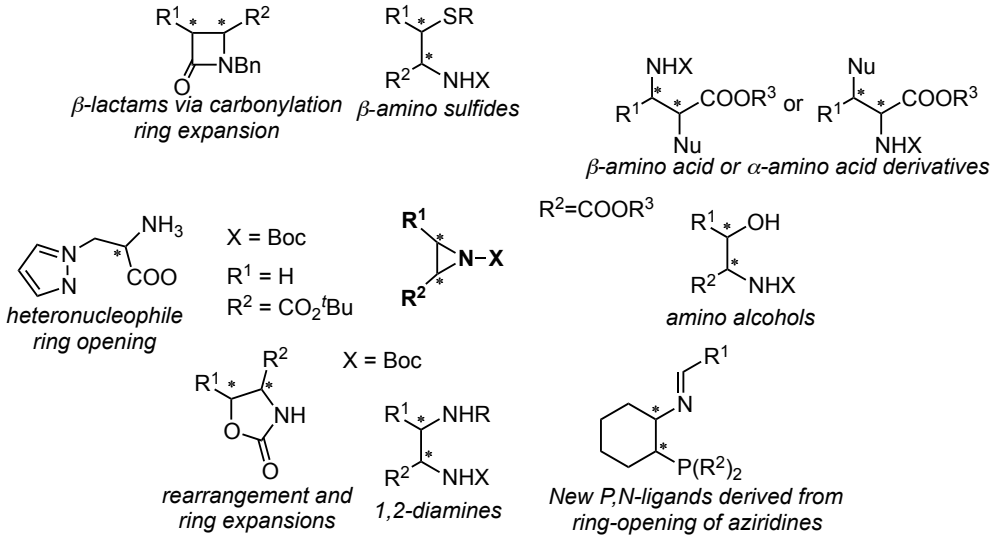

Figure IV.5. Selected examples of ring-opening of aziridines.

Several strategies have been established for the synthesis of aziridines (**Figure IV.6**), cyclization and addition processes being, perhaps, the most succesful.[199b] Cyclization processes, involving ring-closure of 1,2 amino alcohols or their equivalents, often provide the aziridines, which opens the possibility of preparing them in an enantiopure manner. In 1888, the first reaction to afford aziridines was reported. This

[217] M^{c}Coull, W. M.; Davis, F. A. *Synthesis* **2000**, *10*, 1347-1365.

involved the chlorination of ethanolamines with thionyl chloride, followed by alkali-induced cyclization.[218]

On the other hand, addition processes can be classified as nitrene addition to olefins or carbene and ylide addition to imines.

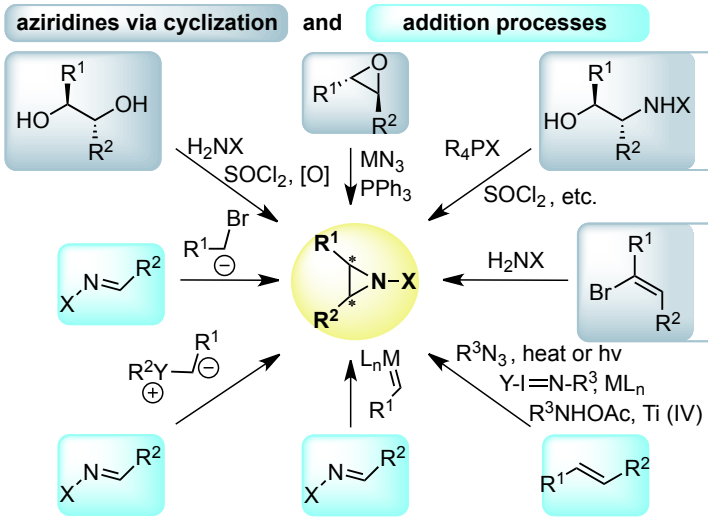

Figure IV.6. Overview of general aziridination methods.

High selectivity has been achieved through the use of chiral substrates or chiral auxiliaries.[215] The first asymmetric practical approach was introduced in the early 1990s by the group of Evans and co-workers,[219] who developed a useful method for the formal nitrene transfer using copper-catalysis. Several new achiral ligands have been introduced for Cu-catalyzed aziridination, using for the first time [*N*-(*p*-toluenesulfonyl)imino]phenyliodinane (PhI=NTs) as the nitrene source (**Scheme IV.13A**).[220]

As an extension of this methodology, an alternative approach has been tackled, involving the activation of an imine by a Lewis acid.[221] The corresponding activated imine is then prone to react with a diazo compound. In 1999 Wulff *et al.* reported the aziridination of benzhydryl imines in the presence of a chiral Lewis acid (**Scheme IV.13B**),[222a] further optimization resulting in new ligands.[222] However, the benzhydryl substituent was present in the final molecules, which is not convenient for synthetic purposes.

---

[218] Gabriel, S. *Chem. Ber.* **1888**, *21*, 1049-1057; b) Gabriel, S. *Chem. Ber.* **1888**, *21*, 2664-2669.
[219] Evans, D. A.; Faul, M. M.; Bilodeau, M. T. *J. Org. Chem.* **1991**, *56*, 6744-6746.
[220] a) Li, Z.; Conser, K. R.; Jacobsen, E. N. *J. Am. Chem. Soc.* **1993**, *115*, 5326-5327; b) Evans, D. A.; Faul, M. M.; Bilodeau, M. T.; Anderson, B. A.; Barnes, D. M. *J. Am. Chem. Soc.* **1993**, *115*, 5328-5329.
[221] Casarrubios, L.; Pérez, J. A.; Brookhart, M.; Templeton, J. L. *J. Org. Chem.* **1996**, *61*, 8358-8359.
[222] a) Antilla, J. C.; Wulff, W. D. *J. Am. Chem. Soc.* **1999**, *121*, 5099-5100; b) Antilla, J. C.; Wulff, W. D. *Angew. Chem., Int. Ed.* **2000**, *39*, 4518-4521; c) Loncaric, C.; Wulff, W. D. *Org. Lett.* **2001**, *3*, 3675-3678.

Chapter IV

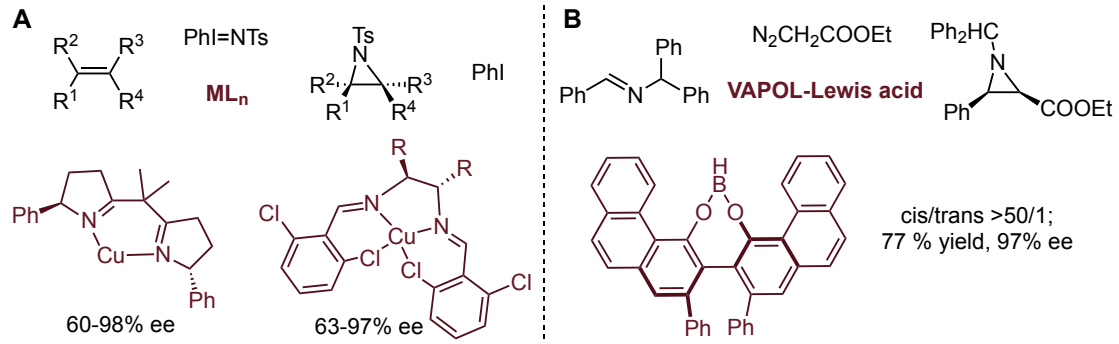

Scheme IV.13. Nitrene transfer (A) or acid catalysis (B).

Later, highly successful catalytic aziridination employing sulphonium ylides was developed by the group of Aggarwal via diazo decomposition with metal catalysts, its association to chiral sulphide, and subsequent transfer to an appropriate imine (**Scheme IV.12**).[223] However, the preparation of a broad substrate scope can be difficult due to the *in situ* generation of carbene from the diazomethane precursor.

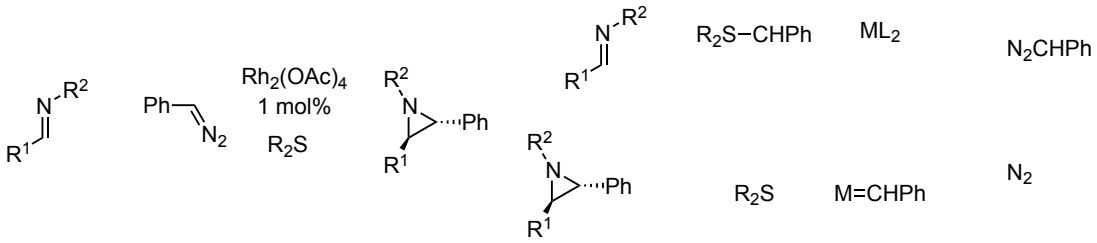

Scheme IV.12. Preparation of aziridines from imines and phenyldiazomethane.

Among these methods, with regard to the development of catalytic methods, the most successful approaches can be divided in the transfer of nitrogen to olefins and transfer of carbon to imines (**Figure IV.7**).[216a,224]

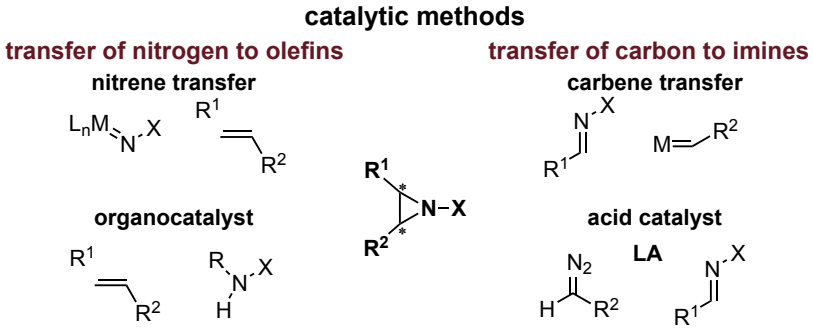

Figure IV.7. Catalytic methods to prepare aziridine derivatives.

[223] a) Aggarwal, V. K.; Thompson, A.; Jones, R. V. H.; Standen, M. C. H. *J. Org. Chem.* **1996**, *61*, 8368-8369; b) Aggarwal, V. K. *Synlett* **1998**, *4*, 329-336; c) Aggarwal, V. K.; Alonso, E.; Fang, F.; Ferrara, M.; Hynd, G.; Porcelloni, M. *Angew. Chem. Int. Ed.* **2001**, *40*, 1433-1436.
[224] Zhang, Y.; Lu, Z.; Wulff, W. D. *Synlett* **2009**, *17*, 2715-2739.

Some of these have been already mentioned above; however, more practical asymmetric methods are still required for the enantioselective synthesis of aziridines due to limitation of functionalized groups with the previous methods.

In the field of organocatalysis MacMillan and co-workers pioneered the organocatalytic amino conjugate addition to α,β-unsaturated aldehydes to generate enantioenriched β-amino aldehydes (**Scheme IV.14**).[225]

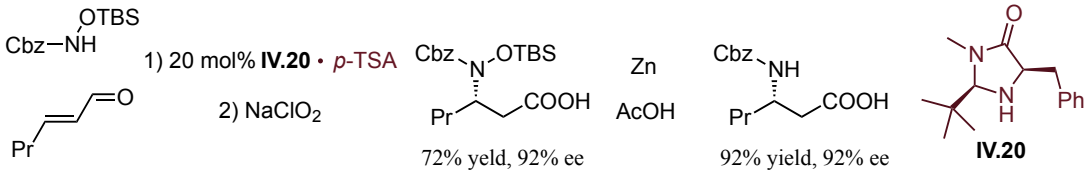

Scheme IV.14. Enantioselective two-step synthesis of β-amino acids.

The idea to develop a reaction where the nitrogen-atom source would first act as a nucleophile and, at a later stage, become electrophilic (**Figure IV.8**) was introduced by the group of Córdova in 2007.[226]

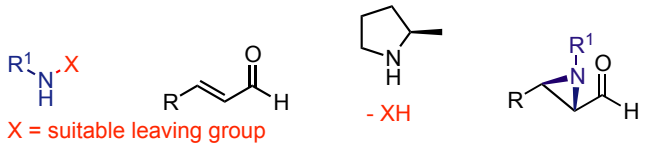

Figure IV.8. Proposed design of aziridination of α,β-unsaturated aldehydes.

They demonstrated for the first time that the Jørgensen-Hayashi catalyst[226] is able to catalyze the aziridination of α,β-unsaturated aliphatic aldehydes (**Scheme IV.15**), a work followed by others.[227]

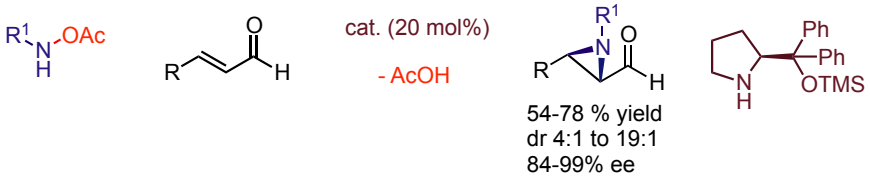

Scheme IV.15. Aziridination of α,β-unsaturated aliphatic aldehydes.

---

[225] Chen, Y. K.; Yoshida, M.; MacMillan, D. W. C. *J. Am. Chem. Soc.* **2006**, *128*, 9328-9329.
[226] Vesely, J.; Ibrahem, I.; Zhao, G.-L.; Rios, R.; Córdova, A. *Angew. Chem. Int. Ed.* **2007**, *46*, 778-781.
[227] a) Arai, H.; Sugaya, N.; Sasaki, N.; Makino, K.; Lectard, S.; Hamada, Y. *Tetrahedron Lett.* **2009**, *50*, 3329-333; b) Deiana, L.; Dziedzic, P.; Zhao, G.-L.; Vesely, J.; Ibrahem, I.; Rios, R.; Sun, J.; Córdova A. *Chem. Eur. J.* **2011**, *17*, 7904-7917; c) Jiang, H.; Halskov, K. S.; Johansen, T. K.; Jørgensen, K. A. *Chem. Eur. J.* **2011**, *17*, 3842-3846; d) Desmarchelier, A.; Pereira de Sant'Ana, D.; Terrasson, V.; Campagne, J.; Moreau, X.; M.; Greck, C.; Marcia de Figueiredo, R. *Eur. J. Org. Chem.* **2011**, 4046-4052; e) Halskov, K. S.; Naicker, T.; Jensen, M. E.; Jørgensen, K. A. *Chem. Commun.* **2013**, *49*, 6382-6384; for examples of the chiral primary amines, derived from cinchona alkaloids in catalytic aziridination, see: f) Armstrong, A.; Baxter, C. A.; Lamont, S. G.; Pape, A. R.; Wincewicz, R. *Org. Lett.* **2007**, *9*, 351-353; i) Pesciaioli, F.; De Vincentiis, F.; Galzerano, P.; Bencivenni, G.; Bartoli, G.; Mazzanti, A.; Melchiorre, P. *Angew. Chem.* **2008**, *120*, 8831-8834; j) De Vincentiis, F.; Bencivenni, G.; Pesciaioli, F.; Mazzanti, A.; Bartoli, G.; Galzerano, P.; Melchiorre, P. *Chem. Asian J.* **2010**, *5*, 1652-1656; k) Jiang, H.; Holub, N.; Jørgensen, K. A. *Proc. Nat. Acad. Sci. USA* **2010**, *107*, 20630-20635; l) Armstrong, A.; Pullin, R. D. C.; Jenner, C. R.; Foo, K.; White, A. P. *Tetrahedron: Asymmetry* **2014**, *25*, 74-86.

The mechanism of this reaction (**Scheme IV.16**) proceeds via reversible formation of an iminium ion intermediate (**IV.22**), initially formed between α,β-unsaturated aldehyde and the chiral catalyst (**IV.21**). Efficient shielding of the *Si* face of the iminium intermediate due to the bulky aryl substituent leads to nucleophilic azo-conjugate addition to the β-carbon atom of the electrophile at the *Re* face of iminium intermediate (**IV.22**). Next, a 3-*exo*-*tet* nucleophilic attack of the chiral enamine intermediate (**IV.23**) to the electrophilic nitrogen atom takes place from its *Re* face and the leaving group (R^2OH) is released. This intramolecular ring closure provides an iminium ion intermediate (**IV.24**), and subsequent hydrolysis gives the corresponding aziridine product and releases the amine catalyst (**IV.21**).[226]

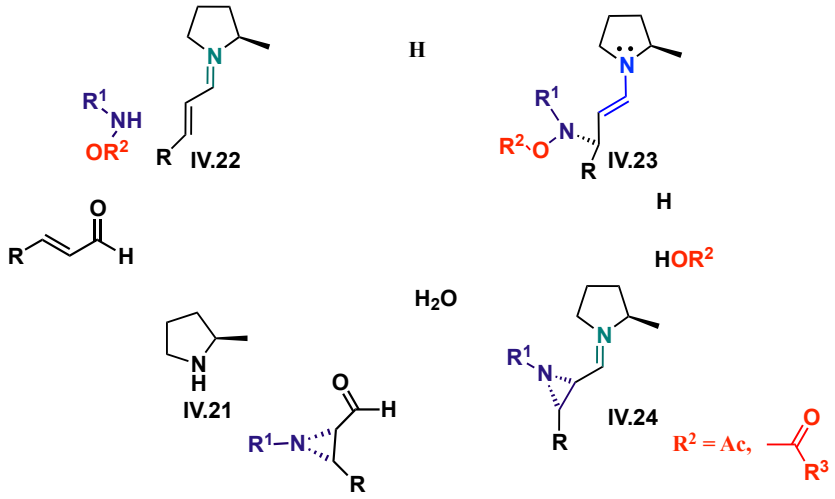

Scheme IV.16. A plausible reaction pathway for enantioselective aziridination catalyzed by a chiral amine.

Recently, Gilmour *et al.* explored the use of β-fluoroiminium ion (**IV.25**) in the enantioselective aziridination of small, medium and macro-cyclic enals (**Scheme IV.17**),[161b] because of their importance in life sciences.[228]

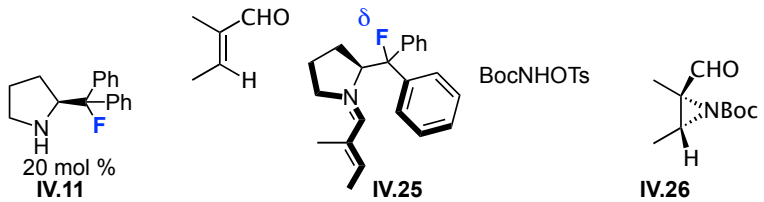

Scheme IV.17. Aziridination of enals.

However, high catalyst loadings (20 mol%) were required for this type of reactions, and preparation of new polymer supported organocatalysts seemed interesting as it may open up the possibility of re-using the catalytic species.

---

[228] Park, K.-H.; Kurth, M. J. *Tetrahedron* **2002**, *58*, 8629-8659.

4.4. Aim of the project.

As already mentioned in the introduction (see also **Chapter III**), the development of new types of catalysts is still important due to deactivation of the Jørgensen-Hayashi and related catalyst. Given the fact that the most common strategy for preparation of the supported organocatalyst in our group involved click chemistry, we considered to develop a new type of catalyst, involving the triazole ring.

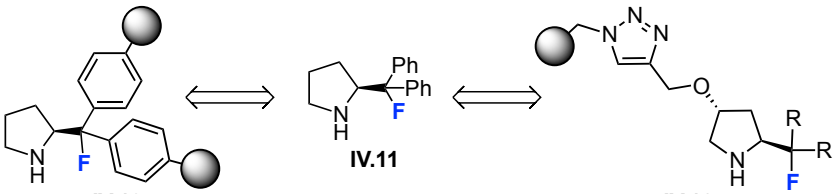

IV.13 **IV.11** **IV.12**

Recently, iminium ion catalysis has been successfully applied to the enantioselective epoxidation of α,β-unsaturated aldehydes by the groups of Jørgensen and MacMillan, using catalytic amounts of chiral secondary amines or amine salts. Córdova *et al.* also provided the first asymmetric aziridination of α,β-unsaturated aldehydes with the Jørgensen-Hayashi catalyst.

However, polymer-supported versions of the Jørgensen-Hayashi catalyst often deactivate upon recycling in different types of transformations. Therefore, an alternative catalyst design is needed in order to increase their recyclability and allow their implementation in continuous flow applications.

In 2009, a new design of the catalyst (**IV.11**) was provided by Gilmour *et al.*, which showed high performance in iminium ion catalysis both for the epoxidation and the aziridination of enals.

Inspired by these findings, we reasoned that it should be possible to develop a conceptually similar asymmetric epoxidation with hydroperoxides using a polymer-supported version of catalyst (**IV.12**). The goal was to study the robustness of this new type of catalyst and the possibility of continuous flow applications. Moreover, we aimed to extend this methodology to multistep synthesis by ring-opening of the highly electrophilic products.

Another reaction working via iminium ion activation mode, such as the aziridination of α,β-unsaturated aldehydes, was also selected. This transformation required 20 mol% of catalyst loading and still needed optimization for continuous flow applications. Aziridines are analogues of epoxides but, in contrast with them, the development of catalytic asymmetric methods for their synthesis is much more limited and has proven to be a considerable challenge.

Therefore we decided to explore both transformations with a supported version of the Gilmour fluorinated catalyst.

The goal of this project will be to develop an efficient and general method for the catalytic asymmetric epoxidation and aziridination of α,β-unsaturated aldehydes with the novel catalyst **IV.12**. In addition to these processes, the role of triazole function will be evaluated during the course of this study.

4.5. Synthesis of polymer-supported β-fluoroamines.

The synthesis of the pyrrolidine derivatives containing the linker needed for immobilization is summarized in **Scheme IV.18** and **Scheme IV.19**. This approach required the preparation of the key propargyloxy-proline intermediates **IV.30A** and **IV.30B** in three steps from commercially available (2*S*,4*R*)-*N*-Boc-4-hydroxy-proline (**IV.27**).[71a,b] Methylation of **IV.27**, followed by propargylation resulted in the propargyloxy-proline **IV.29**. During the propargylation step, the final compound can suffer partial racemization and a slightly updated procedure has been described in this Thesis. [229] Then, Grignard addition of phenylmagnesium bromide, or 2-naphthylmagnesiumbromide the afforded desired compounds **IV.30A** or **IV.30B**.

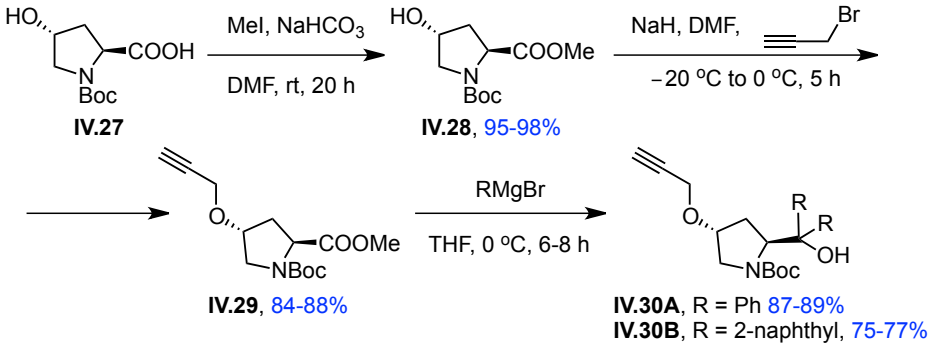

IV.27

IV.28, 95-98%

IV.29, 84-88%

IV.30A, R = Ph 87-89%
IV.30B, R = 2-naphthyl, 75-77%

Scheme IV.18. Synthesis of the key propargyloxy-proline intermediate **IV.30A** and **IV.30B**.

Deprotection of the Boc-group provided amino alcohols **IV.31A** and **IV.31B**.[71o] Afterwards, a deoxyfluorination protocol using diethylaminosulfur trifluoride (DAST) gave access to the β-fluoroamine derivatives **IV.32A** and **IV.32B**.

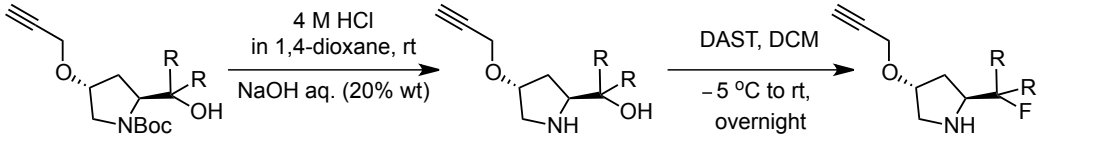

IV.30A, R = Ph 87-89%
IV.30B, R = 2-naphthyl, 75-77%

IV.31A, R = Ph, 95-97%
IV.31B, R = 2-naphthyl, 98%

IV.32A, R = Ph, 68-71%
IV.32B, R = 2-naphthyl**,** 80%

"DAST"-Et_2NSF_3

Scheme IV.19. Synthesis of the β-fluoroamine derivatives

[229] Compound **IV.29** cannot be separated from its C2 diastereomer. The dr can be determined by non chiral GC. We found that both diastereomers can be separated after Boc deprotection and silylation of the hydroxy group in diaryl derivatives like **IV.31**. The experimental procedure and the isolation of the minor *cis*-diastereomer will be described in the experimental part of this Chapter.

In the last step, a CuAAC reaction with azidomethylpolysterene gave the desired PS-organocatalysts with good functionalization levels, as determined by elemental analysis (**Scheme IV.20**).

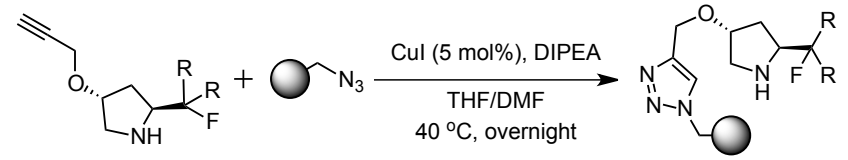

IV.32A, R = Ph
IV.32B, R = 2-naphthyl

IV.12A, R = Ph, *f* = 0.45 mmol/g
IV.12B, R = 2-naphthyl, *f* = 0.42 mmol/g

Scheme IV.20. Synthesis of polymer-supported catalysts.

Monomeric catalyst **IV.12.C** was synthesized using the same conditions with CuI and DIPEA with 89% yield (**Scheme IV.21**).

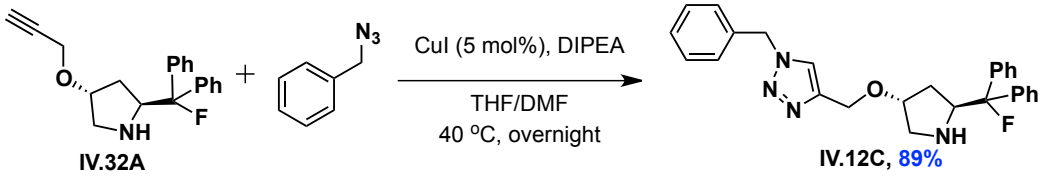

IV.32A

IV.12C, 89%

Scheme IV.21. Preparation of the homogeneous version of the catalyst.

4.6. Preliminary results and discussion of epoxidation of α,β-unsaturated aldehydes.

We began by testing the epoxidation of cinnamaldehyde with H_2O_2, using catalyst **IV.12A** (**Table IV.1**). After 17 h (**entry 1**) only formation of 31% of *cis* isomer was observed, accompanied by a 69% of benzaldehyde, which was confirmed by chromatographic purification. Since the excess of hydrogen peroxide was quenched by addition of a saturated aqueous solution of $Na_2S_2O_3$, benzaldehyde appears to arise during the course of the reaction.

Table IV.1. Screening of solvents.[a]

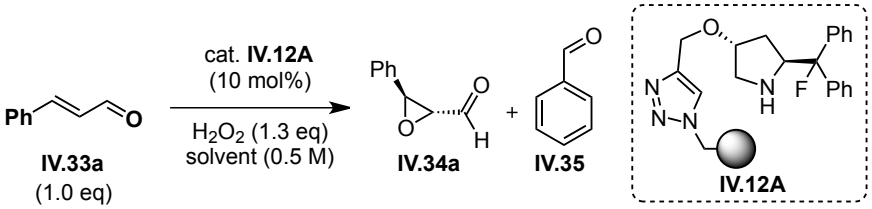

entry	solvent	time (h)	IV.34a, % ($dr_{trans/cis}$)[b]	IV.35, %[b]	IV.33a, %[b]
1	$CHCl_3$	3	31 (52:48)	51	18
1a	$CHCl_3$	17	31 (0:100)	69	0
2	DCM	1	57 (56:44)	17	26
2a	DCM	12	27 (0:100)	73	0
3	$CHCl_3$:H_2O (1:1)	1	57 (72:28)	12	31
3a	$CHCl_3$:H_2O (1:1)	2	54 (41:59)	46	0
4	DCM:H_2O (1:1)	1	65 (66:34)	16	19
4a	DCM:H_2O (1:1)	2	52 (45:55)	48	0
5	toluene	1	46 (40:60)	19	35
6	THF	1	-	4	96

[a] Conditions: 0.11 mmol of aldehyde, 0.13 mmol of H_2O_2, 10 mol% of the catalyst, 0.5 M in CH_2Cl_2. [b] Determined by ^1H NMR of the crude mixture (ratio between **IV.33a**, **IV34a** and **IV.35**).

After additional experiments, we found that the diastereoselectivities of generated epoxides were not constant during the reaction (for example, **entry 1 and 1a**). Indeed, benzaldehyde formation appeared to happen much faster on the *trans*-isomer (the major component of the mixture).

This unwanted side reaction took place by nucleophilic attack of the hydroperoxide anion and cleavage of the C-C bond as shown in **Figure IV.9**[230]. Using

[230] Wright, P.; Abbot, J. *Int. J. Chem. Kinet.* **1993**, *25*, 901-911.

different solvents in the presence of water, the reaction was completed in less than 2 h (**entry 3-4**), but still high amounts of benzaldehyde were observed.

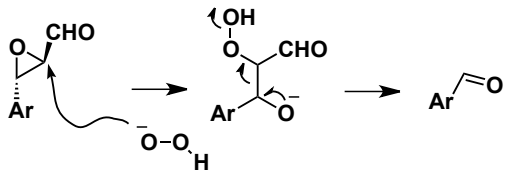

Figure IV.9. Formation of benzaldehyde in the epoxidation of cinnamaldehyde.

Then we examined different additives in the epoxidation reaction in an attempt to decrease the reaction time and suppress by-product formation. We found that the reaction proceeds faster in the presence of acids, however still high amounts of benzaldehyde were observed (***Table IV.2***). The reductive work-up also appeared to have an effect in the reaction outcome. As indicated in ***Table IV.2***, it was found that, under the same conditions (**entries 1-2**), changing the work-up time (3 or 1 h) provided different enantioselectivity (73 or 81% ee). Increasing the amount of acid from 10 to 30 mol% does not improve the reaction rate (**entry 2-3**). Unfortunately, after screening several additives moderate enantioselectivities were obtained in most cases (72-81% ee). This can be attributed to the design of the polymer-supported catalyst if we compare the results obtained with **IV.11** (93-96% ee). Further screening in the presence of molecular sieves or $MgSO_4$ as additive to remove the water present in the reaction mixture did not improve significantly the previous results.

Table IV.2. Epoxidation of cinnamaldehyde with different additives.[a]

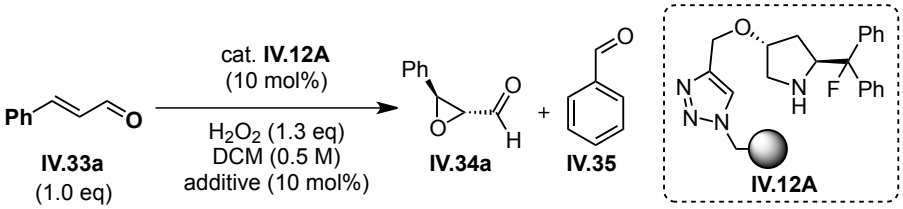

entry	additive	time (h)	IV.34a, % ($dr_{trans/cis}$)[b]	IV.35, %[b]	IV.33a, %[b]	IV.34a, ee, %[c]
1	PhCOOH	3	55 (66:34)	37	8	73
2	PhCOOH	1	61 (73:27)	19	20	81
3	PhCOOH (30 mol%)	1	61 (66:34)	19	20	81
4	2-fluorobenzoic acid	3	59 (55:45)	41	0	74
5	S-(+)-mandelic acid	3	48 (51:49)	43	9	76
6	R-(-)-mandelic acid	3	72 (42:58)	28	0	72
7	Mol. Sieves (4Å)	12	62 (76:24)	19	19	81
8	$MgSO_4$ (1.3 eq)	2	68 (63:27)	26	6	79

[a] Conditions: 0.11 mmol of aldehyde, 0.13 mmol of H_2O_2, 10 mol% of the catalyst and 10 mol% of additive, 0.5 M in CH_2Cl_2; [b] Determined by ^1H NMR of the crude mixture (ratio between **IV.33a**, **IV34a** and **IV.35**); [c]

Determined by chiral GC.

Additionally, we also attempted the catalytic epoxidation of α,β-unsaturated aldehydes with different oxidants. However, no promising results were achieved although the desired compound was the major one in this transformation (***Table IV.3***).

Table IV.3. Screening of oxidants.[a]

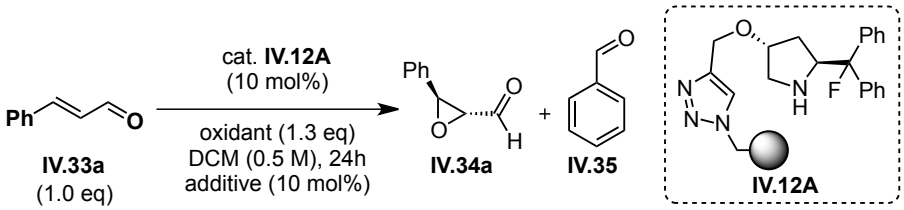

entry	oxidant	additive	IV.34a, % ($dr_{trans/cis}$)[b]	% IV.35[b]	IV.33a,%[b]	IV.34a, ee, %[c]
1	^{t}BuOOH	-	89 (75:25)	6	5	68
2	^{t}BuOOH	PhCOOH	90 (75:25)	5	5	69
3	Cumyl hydroperoxide	-	76 (79:21)	17	7	71

[a] Conditions: 0.11 mmol of aldehyde, 0.13 mmol of oxidant, 10 mol% of the catalyst and in some cases 10 mol % of additive in DCM (0.5 M); [b] Determined by ^{1}H NMR of the crude mixture (ratio between **IV.33a**, **IV34a** and **IV.35**);[c] Determined by chiral GC

A similar behaviour was observed with catalyst **IV.12B** (R = naphthyl), which provided the same enantioselectivity, as well as amount of by-product in this transformation, when compared to catalyst **IV.12A**.

In order to understand the effect of the triazole linker, we decided to study the behaviour of catalyst **IV.12C**, the homogeneous version of our triazole-linked, supported catalysts. Thus, we screened a series of different pyrrolidine derivatives (**Table IV.4**).

Table IV.4. Screening of other pyrrolidine derivatives.[a]

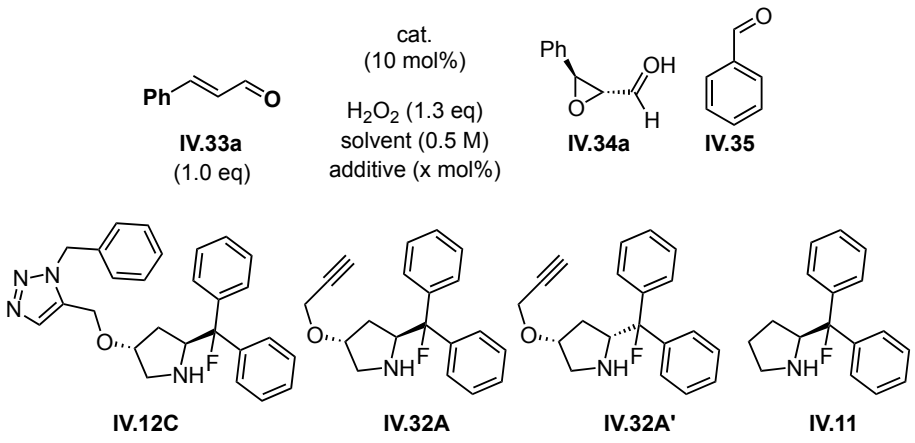

entry	catalyst	PhCOOH (mol%)	solvent	time (h)	IV.34a, % ($dr_{trans/cis}$)[b]	IV.35, %[b]	IV.33a,%[b]	IV.34a, ee, %[c]
1	**IV.12C**	-	$CHCl_3$	5	56 (66:34)	19	15	83
2	**IV.12C**	5	CH_2Cl_2	1	90 (76:24)	10	0	83
3	**IV.12C**	10	CH_2Cl_2	2	94 (78:22)	6	0	83
4	**IV.32A**	-	CH_2Cl_2	2	87 (73:27)	13	0	80
5	**IV.32A**	-	$CHCl_3$	3	73 (64:36)	27	0	80
6	**IV.32A'**	-	CH_2Cl_2	1.5	69 (73:27)	27	4	84[d]
7	**IV.32A'**	10	CH_2Cl_2	1.5	77 (76:24)	23	0	84[d]
8	**IV.11**	-	$CHCl_3$	3	90 (83:17)	10	0	91
9[e]	**IV.11**	-	$CHCl_3$	1	80 (80:20)	20	0	91

[a] Conditions: 0.11 mmol of aldehyde, 0.13 mmol of H_2O_2, 10 mol% of the catalyst in 0.5 M solvent; [b] Determined by ^1H NMR of the crude mixture (ratio between **IV.33a**, **IV34a** and **IV.35**); [c] Determined by chiral GC. *An other enantiomer of the *trans*-epoxide was obtained as the major compound. [e] New bottle of H_2O_2 (30%).

The pyrrolidine derivative **IV.32A'** had been obtained as a by-product arising from the epimerization of an intermediate en route to the desired catalyst (see, **experimental part**). This organocatalyst promoted the enantioselective epoxidation of α,β-unsaturated aldehydes, providing the other enantiomer of the *trans*-epoxide with similar enantioselectivity. This seems to point out that the configuration of the substituent at C4 has little influence on the reaction outcome. In addition, high enantioselectivities were observed for the asymmetric epoxidation with catalyst **IV.11**. When we used the Gilmour catalyst for this transformation, we were able to reproduce the reported results (93-96% ee). In most cases, we could observe variable amounts of benzaldehyde, but this by-product formation was low compared to polymer-supported versions of the catalyst.

An α,β-unsaturated aliphatic aldehyde was also tested in this transformation (**Scheme IV.22**). Notably, the reaction of *trans*-2-hexenal proceeded without the generation of butanal, although longer reaction times were required (11 h) and moderate enantioselectivity was observed (81% ee, measured after reduction and benzylation of the corresponding aldehyde).

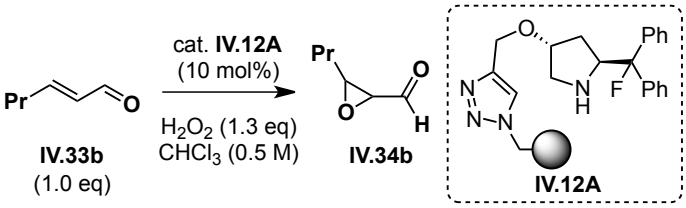

Scheme IV.22. Epoxidation of α,β-unsaturated aldehyde with an alkyl side chain.

Therefore, we conclude that the presence of the substituent at C-4 on the pyrrolidine ring (**IV.12**) can have an effect on the enantioselectivity of this transformation in comparison with β-fluoroamine **IV.11**, developed by Gilmour *et al.*

The second and more important issue in this transformation is the by-product formation, that takes place with α,β-unsaturated aromatic aldehydes and is more significant with polymer-supported organocatalysts. Other nucleophilic oxidants such as ^{t}BuOOH give rise to lower amounts of by-product during this transformation, probably because of the bulky substituent. However low enantioselectivity and prolonged reaction times are observed.

After preparation of catalyst **IV.13** (see **chapter III**) in order to determine the influence of the substituent at C-4 position, the epoxidation of cinnamaldehyde with hydrogen peroxide was screened again (**Scheme IV.23**).

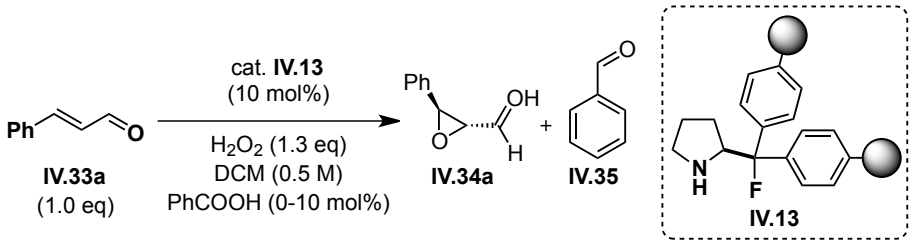

Scheme IV.23. Epoxidation of cinnamaldehyde with catalyst **IV.13**.

Unfortunately, either with or without benzoic acid, after 1.5 h the major compound in this transformation was benzaldehyde (17-29% yield), along with traces of the desired compound (3-10% yield).

In conclusion, currently we are considering alternative designs for the supported aminocatalyst to improve the enantioselectivity of this transformation, while minimizing the by-product formation.

After the results obtained for epoxidation, we aimed for testing the polymer-supported β-fluoroamines in other transformation involving the iminium ion activation mode. To this end, we selected the preparation of aziridines from α,β-unsaturated aldehydes.

Chapter IV

4.7. Preliminary results and discussion of aziridination of α,β-unsaturated aldehydes.

In order to optimize the conditions of the aziridination of *trans*-2-hexenal (1 eq), BocNHOTs (1.2 eq) was selected as the "nitrogen" source. Different catalyst loadings showed that in the presence of 10 mol% of catalyst we could reach full conversion and high enantioselectivity within 1 h. Unfortunately, decreasing this loading provided low conversion and extending the reaction time did not improve this result,[231] although the enantioselectivity remained the same (**Table IV.5**).

Table IV.5. Screening of the catalyst loading in the aziridination reaction.[a]

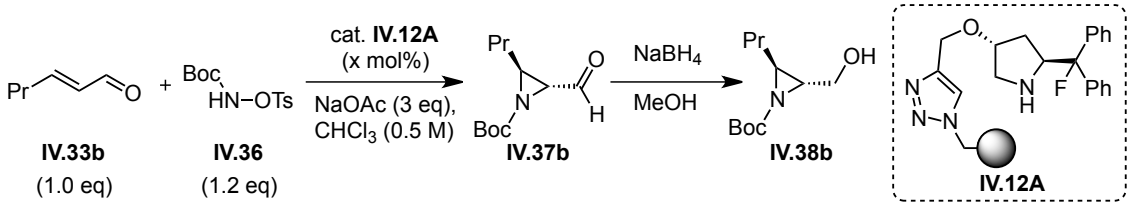

IV.33b (1.0 eq) + **IV.36** (1.2 eq) → **IV.37b** → **IV.38b**

entry	catalyst loading, %	time (h)	IV.37b, % ($dr_{trans/cis}$)[b]	IV.37b %, conv[b]	IV.38b, %, ee[c]
1	20[d]	1	88:12	full	96
2	10	1	89:11	full	96
3	5	1.5	90:10	78	95

[a] Conditions: a mixture of BocNHOTs (38.3 mg, 0.133 mmol), *trans*-2-hexenal (13 µl, 0.112 mmol), NaOAc (0.33 mmol, 27.4 mg), and catalyst (5-20 mol%, *f* = 0.454 mmol/g) in $CHCl_3$ (220 µl, 0.5 M) was stirred for the time shown in the table; [b] Determined by ^1H NMR of the crude product; [c] Determined by chiral GC after reduction with $NaBH_4$; [d] 0.25 M was used (because of the swelling of the catalytic resin)

The presence of a base is essential for this transformation; likewise, the reaction does not proceed without organocatalyst. In the initial screening of commonly used bases (**Table IV.6**), NaOAc (3 eq) was identified as the optimal choice for aziridination; even with 1.5 eq of NaOAc (**entry 2**) the reaction was completed within 4 h. Interestingly, the use of other bases led to significantly longer reaction times (**entries 4-6**).

Employing sodium benzoate led to results comparable to these obtained with NaOAc (**entry 7**). On the other hand, 2,6-lutidine showed moderate activity in this transformation (**entry 8**), since the reaction is not completed even after 3 h.

[231] For the **entry 3**: after 2.5 h only 80% conversion was observed.

Surprisingly, in the presence of tetrabutylammonium acetate (TBAA) or bis(trimethylsilyl)acetamide (BSA) the reaction does not take place (**entries 9-10**).

Table IV.6. Base screening in the aziridination reaction.[a]

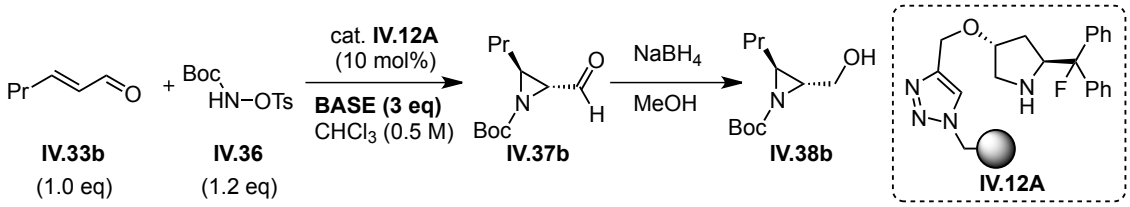

IV.33b (1.0 eq) + **IV.36** (1.2 eq) → **IV.37b** → **IV.38b**; **IV.12A**

entry	base	time (h)	IV.37b, % ($dr_{trans/cis}$)[b]	IV.37b %, conv[b]	IV.38b, %, ee[c]
1	-	4	-	3	-
2	NaOAc[d]	4	87:13	full	96
3	NaOAc	1	89:11	full	96
4	KOAc	1 (2)	91:9	56	96
5	Na_2CO_3	1.5	88:12	47	-
6	K_2CO_3	1.5	87:13	75	-
7	PhCOONa	2	88:12	full	95
8	2,6-lutidine	1 (3)	88:12	70	-
9	BSA	2	-	5	-
10	TBAA	2	-	0	-

[a] Conditions: a mixture of BocNHOTs (38.3 mg, 0.133 mmol), *trans*-2-hexenal (13 µl, 0.112 mmol), base (0.33 mmol), and catalyst (24.5 mg, 10 mol%, *f* = 0.454 mmol/g) in $CHCl_3$ (220 µl, 0.5 M) was stirred for the time shown in the table; [b] Determined by ^1H NMR of the crude product; [c] Determined by chiral GC after reduction with $NaBH_4$; [d] 1.5 eq of NaOAc was used.

When the reaction was performed in different solvents (**Table IV.7**) we found the chlorinated ones to be the best choice (**entry 1 or 2**). In the presence of toluene (**entry 3**) the reaction time was extended, probably due to the lower solubility of the starting material. Also, the scale up of the reaction under the same time provided low conversion. However, the reaction in CH_2Cl_2 presented a similar behaviour even after scale up (**entry 9-10**).

We next evaluated the effect of reagents concentration on the reaction course, finding no significant change in reactivity and selectivity with chlorinated solvents, while for toluene longer reaction times were required (**entry 11-12**).

Chapter IV

Table IV.7. Screening of the solvents in the aziridination reaction.[a]

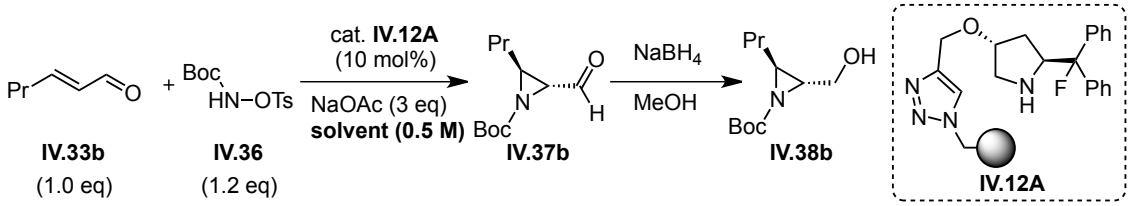

entry	solvent	time (h)	IV.37b, % ($dr_{trans/cis}$)[b]	IV.37b %, conv[b]	IV.38b, %, ee[c]	IV.37b, %[d]
1	$CHCl_3$	1	88:12	full	96	84
2	DCM	1	87:13	full	96	80
3	Toluene	3	91:9	full	98	81
4	THF	7	88:12	43	-	-
5	MeCN	8	87:13	39	-	-
6	$CHCl_3$	1	89:11	full	96	82
7	Toluene	3	87:13	full	98	78
8	Toluene:$CHCl_3$	2	89:11	full	96	65[e]
9	Toluene[f]	3	86:14	90	97	70
10	DCM[f]	1	87:13	full	97	82
11	Toluene[g]	4	89:11	97	98	78
12	CH_2Cl_2[g]	1	89:11	full	96	82

[a] Conditions: a mixture of BocNHOTs (38.3 mg, 0.133 mmol), *trans*-2-hexenal (13 µl, 0.112 mmol), NaOAc (0.33 mmol, 27.4 mg), and catalyst (24.5 mg, 10 mol%, *f* = 0.454 mmol/g) in solvent (220 µl, 0.5 M) was stirred for the time shown in the table; [b] Determined by ^{1}H NMR of the crude product; [c] Determined by chiral GC after reduction with $NaBH_4$; [d] Isolated yield (2-formylaziridines are not stable during column chromatography on silica gel); [e] Silica gel with Et_3N (2 mol%) was used for purification; [f] scale up to 0.36 mmol of BocNHOTs (103 mg), 0.3 mmol of *trans*-2-hexenal (35 µl), 0.9 mmol of NaOAc (74 mg), and catalyst (66.0 mg, 10 mol%, *f* = 0.454 mmol/g) in solvent (600 µl, 0.5 M); [g] Reaction carried out at 0.25 M.

Next, our attention was turned to the reaction of cinnamaldehyde with BocNHOTs, using the above optimized conditions (**Table IV.8**). We could observe formation of α-amino-α,β-unsaturated aldehyde (**IV.39**) as a by-product.[232] However, performing this aminocatalytic reaction at a lower temperature (0 °C) provided the desired compound and supressed the formation of this by-product. Isolation of the corresponding aziridine was not possible due to the sensitivity of the desired compound to silica gel.

[232] Formation of this by-product with α,β-unsaturated aromatic aldehydes was observed by the group of Córdova in 2011. The mechanism of formation is discussed in ref. **227b**.

Table IV.8. Effect of the temperature on the reaction between cinnamaldehyde and BocNHOTs in the presence of catalyst **IV.12A**.[a]

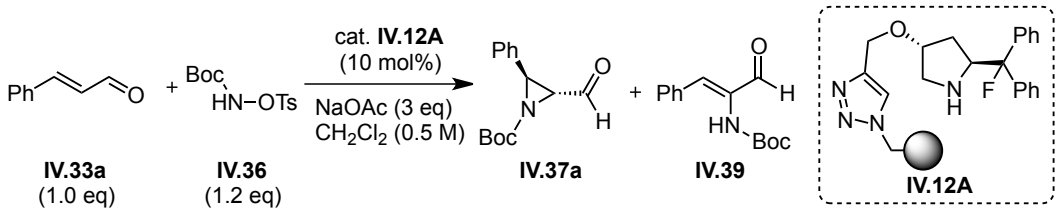

entry	condition	time (h)	IV.37a, % ($dr_{trans/cis}$)[b]	IV39, %[b]	% starting material[b]
1	rt	0.5	82 (98:2)	15	4
2	0 °C	1	81 (91:9)	2	17

[a] Conditions: 0.11 mmol of aldehyde, 0.13 mmol of BocNHOTs, 0.33 mmol of base, 24.5 mg of catalyst (10 mol%); [b] Determined by ^{1}H NMR of the crude product; [c] Determined by chiral GC after reduction with $NaBH_4$.

A recycling experiment was also conducted with the solid-supported fluorinated catalyst **IV.12A**. However, under optimal conditions the catalyst activity was lost in the second run (14% conversion was observed). After several attempts with different bases (NaOAc, 2,6-lutidine, PhCOONa) as well as increasing the amount of aldehyde in this transformation, we were not able to recycle the polymer-supported catalyst properly. The catalyst seems to deactivate relatively fast under the reaction conditions, probably due to an interaction between the catalyst and one of the reagents.

Postulating that perhaps the excess aminating reagent was responsible for catalyst deactivation we decided to revert the stoichiometry. Thus, using 2 equiv of enal, the result in the second run was improved to a 74% yield (**Table IV.9**).

Table IV.9. Recycling tests.[a]

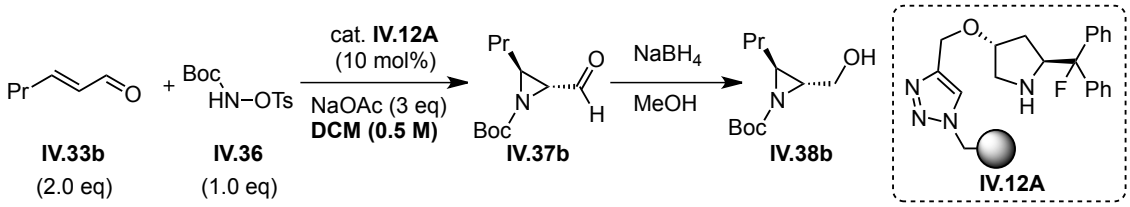

entry	time (h)	IV.37b, % ($dr_{trans/cis}$)[b]	IV.37b %, conv[b]	IV.38b, %, ee[c]	IV.37b, %[d]
1	0.5	87:13	full	96	96
2	1(2)	86:14	74	96	-

[a] Conditions: a mixture of BocNHOTs (38.3 mg, 0.133 mmol), *trans*-2-hexenal (26 µl, 0.224 mmol), NaOAc (0.33 mmol, 27.4 mg), and catalyst (24.5 mg, 10 mol%, *f* = 0.454 mmol/g) in DCM (220 µl, 0.5 M) was stirred for the time shown in the table; [b] Determined by ^{1}H NMR of the crude product; [c] Determined by chiral GC after reduction with $NaBH_4$.

Chapter IV

During the screening of conditions for recycling, we found that the use of an excess of aldehyde (2 eq) accelerates the reaction, leading to full conversions within 30 min (**Table IV.9, run 1**). A 96% yield of pure compound could be obtained without purification and in high enantioselectivity.

From these optimization studies it became apparent that the best reaction conditions were 10 mol% of the catalyst in combination with NaOAc (3 eq) and excess of aldehyde (2 eq) in DCM (**Table IV.10**).

It should be noted that in the case of aromatic α,β-unsaturated aldehydes full conversion was observed, but the compound decomposed after work up.

Table IV.10. Scope of α,β-unsaturated aldehydes.

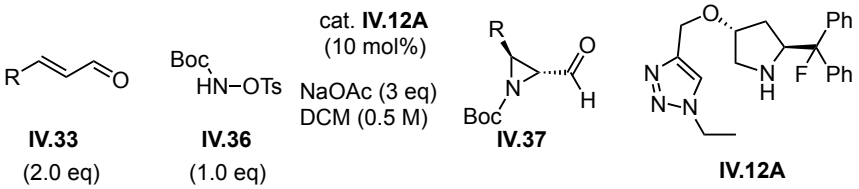

IV.33 (2.0 eq) **IV.36** (1.0 eq) **IV.37** **IV.12A**

entry	R	time (h)	product, ($dr_{trans/cis}$)[b]	%, conv[b]	%, ee[c]	yield, %[d]
1	**IV.37b**, Pr	30 min	87:13	full	97[c]	96
2	**IV.37c**, Me	1 h (-5 °C)	86:14	full	-	96
3	**IV.37a**, Ph	1 h (-5 °C)	86:14	full	-	-[e]

[a] Conditions: a mixture of BocNHOTs (51.8 mg, 0.18 mmol), aldehyde (0.36 mmol), NaOAc (0.54 mmol, 44.5 mg), and catalyst (39.4 mg, 10 mol %, *f* = 0.457 mmol/g) in 360 µl of DCM was stirred for the time and the temperature shown in the table; [b] Determined by ^{1}H NMR of the crude product; [c] Determined by chiral GC after reduction with $NaBH_4$; [d] Isolated yield; [e] During the work up procedure was decomposed (as well as after reduction with $NaBH_4$ final compound was decomposed on silica gel).

Later, we found that we were able improve the recycling ability by avoiding washing the catalyst with water between cycles. In this manner, we were able to run at least 4 cycles without addition of base, 60% conversion being observed in the fourth cycle (**Table IV.11**).

Table IV.11. Recycling tests.[a]

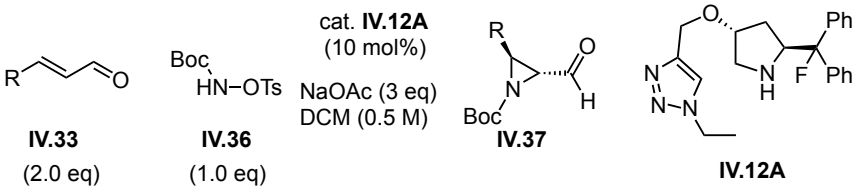

IV.33 (2.0 eq) **IV.36** (1.0 eq) **IV.37** **IV.12A**

entry	time (h)	product, ($dr_{trans/cis}$)[b]	%, conv[b]
1	0.5	87:13	full[c]
2	1	86:14	full[c]
3	1	90:10	full[c]
4	2.5	88:12	60[c]
5[d]	1	89:11	29

[a] Conditions: a mixture of BocNHOTs (38.3 mg, 0.133 mmol), *trans*-2-hexenal (26 µl, 0.224 mmol), NaOAc (0.33 mmol, 27.4 mg), and catalyst (24.5 mg, 10 mol%, *f* = 0.454 mmol/g) in DCM (220 µl, 0.5 M) was stirred for the time shown in the table; [b] Determined by ^{1}H NMR of the crude product; [c] after reaction, the catalyst was washed only with DCM (without extra addition of base); [d] 3 eq of NaOAc was added.

When the aziridination was carried out inside the glovebox under the same conditions, the conversion decreased in the second cycle (**Table IV.12**). In the last cycle the reaction was performed outside the glovebox, and the conversion was higher than in the previous run, which seems to point out to a crucial role of water in the reaction.

Table IV.12. Recycling tests in the glovebox.

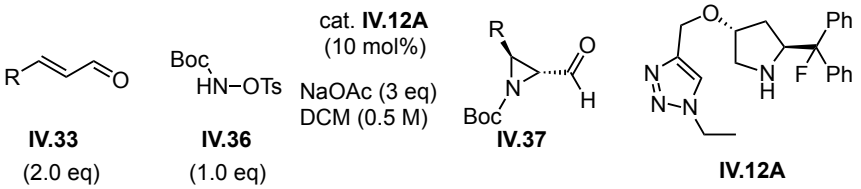

IV.33 (2.0 eq) **IV.36** (1.0 eq) **IV.37** **IV.12A**

entry	time (h)	product, ($dr_{trans/cis}$)[b]	%, conv[b]
1	0.5	86:14	full[c]
2	1.5	90:10	66[c]
3	1.5	84:16	18[c]
4[d]	1.5	86:14	38[c]

[a] Conditions: a mixture of BocNHOTs (38.3 mg, 0.133 mmol), *trans*-2-hexenal (26 µl, 0.224 mmol), NaOAc (0.33 mmol, 27.4 mg), and catalyst (24.5 mg, 10 mol%, *f* = 0.454 mmol/g) in DCM (220 µl, 0.5 M) was stirred for the time shown in the table; [b] Determined by ^{1}H NMR of the crude product; [c] After the reaction, the catalyst was washed only with DCM (without extra addition of base); [d] Reaction performed under the normal conditions outside the glovebox.

In the case of catalyst **IV.12B** or **IV.12C** (results quite similar to the catalyst **IV.12A**), the presence of the 1,2,3-triazole unit in the substituent at C-4 on the pyrrolidine ring provides high reactivity for reactions proceeding via the iminium ion activation mode. In turn, catalyst **IV.13** (prepared by co-polymerization) shows low

activity in these processes (53% conversion after 17 h).[233] Indeed, catalyst **IV.13** seems to deactivate during the first cycle, which can be due to the structure of the polymeric matrix. Since the reaction proceeds in 23% conversion during the first 2 hours, it is possible that some interaction of the catalyst with a reagent or an intermediate gives rise to unreactive catalytic species.

Monomeric catalyst **IV.12C** was also synthesized for a better understanding of the effect of the triazole linker on catalyst deactivation in the aziridination. We found that this catalyst reacted with BocNHOTs in 20 min (40 min – work up) in the absence of aldehyde, whereas the catalyst developed by Gilmour proved much more stable in the same conditions (16 h). However, the structure of this by-product has not been elucidated yet (**Scheme IV.24**).

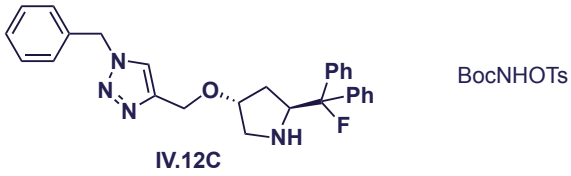

Scheme IV.24. Monomeric catalyst **IV.12C** with BocNHOTs.

We next screened different substituents on the *O* atom and *N*-protected hydroxylamines using our organocatalysts. Different nitrogen sources such as TsNHOTs, BocNHOAc and CbzNHOAc were prepared [234] and applied to this transformation (**Table IV.13** and **Table IV.14**).

In the case of TsONHTs, the reaction was performed in short reaction times under the initial conditions for BocNHOTs, but low enantioselectivities were observed, even though recycling tests showed promising results.

Table IV.13. Recycling tests in the reaction between TsNHOTs and *trans*-2-hexenal catalyzed by **IV.12A**.[a]

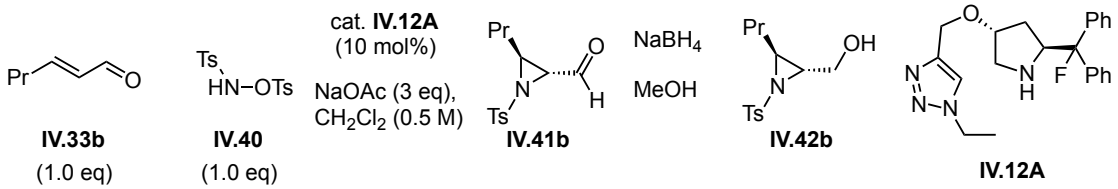

[233] **Note:** 23% conversion was observed after 2 h in this transformation. It appears as if the catalyst got deactivated during the course of the reaction.
[234] Starting materials were synthesized according to the following literature procedures: a) Albrecht, Ł.; Jiang, H.; Dickmeiss, G.; Gschwend, B.; Hansen, S. G.; Jørgensen, K. A. *J. Am. Chem. Soc*. **2010**, *132*, 9188-9196; b) Lajiness, J. P.; Robertson, W. M.; Dunwiddie, I.; Broward, M. A.; Vielhauer, G. A.; Weir, S. J.; Boger, D. L. *J. Med. Chem.* **2010**, *53*, 7731-7738; c) Katritzky, A. R.; Avan, I.; Tala, S. R. *J. Org. Chem.* **2009**, *74*, 8690-8694.

run	time (min)	product, ($dr_{trans/cis}$)[b]	conv[b]	ee[c]	yield[d]
1	15 (40)	83:17	full	82	90
2	40	86:14	full	82	60
3	40	86:14	full	82	98
4	40	88:12	70	-	-

[a] Conditions: a mixture of TsNHOTs (38.3 mg, 0.112 mmol), *trans*-2-hexenal (13 µl, 0.112 mmol), NaOAc (0.34 mmol, 27.6 mg), and catalyst (24.5 mg, 10 mol%, *f* = 0.454 mmol/g) in DCM (220 µl, 0.5 M) was stirred for the time shown in the table; [b] Determined by ^{1}H NMR of the crude product; [c] Determined by chiral HPLC after reduction with $NaBH_4$; [d] Isolated yield (2-formylaziridines are instable and volatile).

Regarding the last two nitrogen sources we considered that acylated *N*-protected hydroxylamines were beneficial since the leaving group is basic enough to keep the reaction going without an external base. In addition to being more atom-economic and environmentally friendly, this would have importance for a hypothetic flow process.

With these reagents we found that the reaction proceeds mostly to give the intermediate β-amino aldehyde (proposed according to NMR and nominal mass), which has not been observed with the Jørgensen-Hayashi catalyst (**Table IV.14**).[226,227] But the same kind of transformation can be observed in the reaction of *N*-silyloxycarbamates as the nucleophilic component in this type of reaction (**Scheme IV.14**).[225] In fact, release of the acetate group does not happen in our case, whereas in the presence of the Jørgensen-Hayashi catalyst this behaviour was observed by Córdova *et al.* They found that the acetate compound also could act in the cycle as the internal base (**Scheme IV.16**).[226,227b]

An additional attempt to isolate this compound was not successful, even after reduction with $NaBH_4$.

Table IV.14. Reaction between *N*-acyl hydroxylamine and *trans*-2-hexenal catalyzed by **IV.12A**.[a]

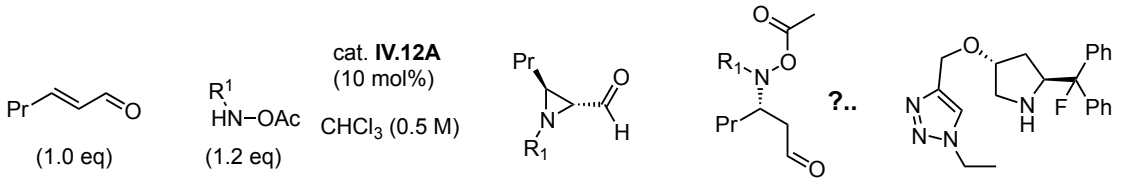

IV.33b

IV.43, R^1 = Boc
IV.44, R^1 = Cbz

IV.37b, R^1 = Boc
IV.45b, R^1 = Cbz

IV.46b, R^1 = Boc
IV.47b, R^1 = Cbz

IV.12A

entry	R_1	conditions	time (h)	aziridine, % ($dr_{trans/cis}$)[b]	IV.46b or IV.47b %, conv.[b]
1	Cbz	rt	2	12	69
2	Cbz	40 ºC	1(2)	6 (18)	72 (64)
3	Cbz	1.5 eq NaOAc	1 (2)	9 (9)	64 (69)
4	Boc	rt	1 (4)	7 (8)	68 (69)

[a] Conditions: a mixture of acylated *N*-protected hydroxylamine (0.197 mmol), *trans*-2-hexenal (19 µl, 0.164 mmol), and catalyst (35.8 mg, 10 mol%, *f* = 0.454 mmol/g) in DCM or $CHCl_3$ (328 µl, 0.5 M) was stirred for the time shown in the table; [b] Determined by ^{1}H NMR of the crude product.

In summary, we have developed an aziridination reaction promoted by an immobilized catalyst. Important features of this reaction are the high yields and enantioselectivities obtained in the presence of 10 mol% catalyst in short times. Unfortunately, efficient reusing of the catalyst remains elusive. However, in comparison with the loading reported in the literature (20-30 mol%) this result is still promising and deserves further optimization.

Interesting β-amino aldehydes can also be obtained, albeit the isolation protocol has to be optimized.

4.8. Conclusions and Outlook.

Continuous flow enantioselective aziridination could not be realized during the course of this Thesis. However, new types of fluorinated catalysts were developed and the role of the triazole function was evaluated, showing negative effect in both transformations.

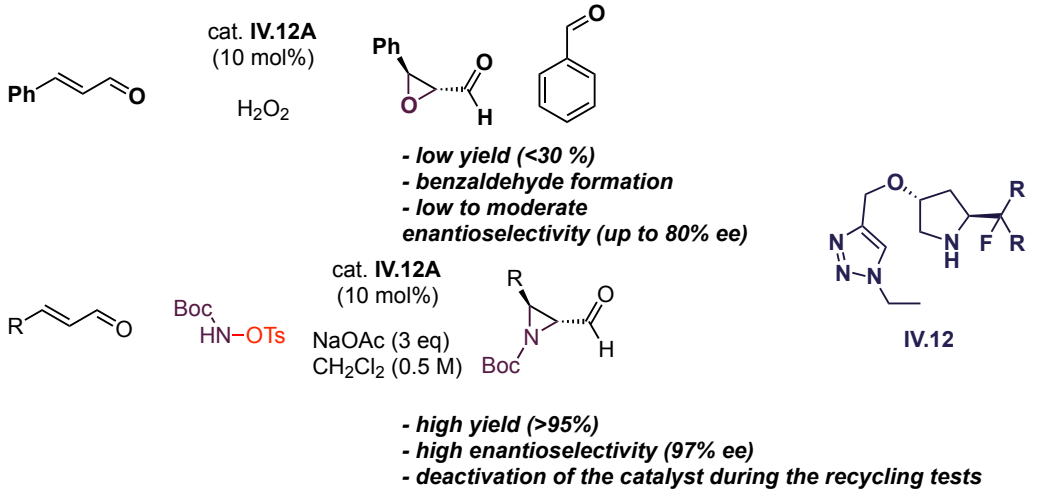

Before the project can be considered finished, a few issues deserve further exploration. In the epoxidation of α,β-unsaturated aldehydes, an optimal immobilized derivative has to be identified in order to avoid the by-product formation. This is generated via decomposition of the *trans*-epoxide during the course of reaction. Therefore, new design of catalysts is needed to develop more selective process for this transformation.

In the aziridination of α,β-unsaturated aldehydes we have been able to demonstrate the high yield and enantioselectivity of this transformation. Unfortunately, efficient reusing of the catalyst remains challenging, although 4 cycles can be run. Deactivation of the catalyst can be due to the triazole linker, since that this kind of material reacts with nitrogen sources in the absence of aldehyde. Studies to solve the deactivation problem are needed in order to create a more robust organocatalyst and avoid decomposition pathways. In addition, optimization of the conditions to generate β-amino aldehydes can also provide an interesting new application of this type of catalyst.

In general, this type of catalyst has proved to be reactive in iminium ion mode of activation, despite the several drawbacks mentioned above. Alternative designs containing the β-fluoroamine motif can provide improvement in these transformations, as well as in alternative reactions that may lead to continuous flow applications.

UNIVERSITAT ROVIRA I VIRGILI
NEW APPROACHES TO CATALYST DESIGN AND IMMOBILIZATION
Irina Sagamanova

4.9. Experimental part.

General remarks

Unless otherwise stated, all commercial reagents were used as received and all reactions were carried out directly under open air. Flash chromatography separations were carried out using 60-mesh silica gel and dry-packed columns. Thin layer chromatography was carried out using Merck TLC Silicagel 60 F254 aluminium sheets. Components were visualized by UV light (λ = 254 nm) or by staining with phosphomolybdic acid (PMA) solution. NMR spectra were registered in a Bruker Advance Ultrashield machines in $CDCl_3$ at room temperature, operating at 400 or 500 MHz for ^{1}H, 101 or 126 MHz for $^{13}C\{1H\}$ and 136 MHz for ^{19}F. TMS was used as internal standard for ^{1}H NMR and $CDCl_3$ for ^{13}C NMR. IR spectra were recorded on a Bruker Tensor 27 FT-IR spectrometer. FAB mass spectra were obtained on a FisonsV6 Quattro instrument, ESI mass spectra were obtained on a Waters LCT Premier instrument and CI and EI spectra were obtained on a Waters GCT spectrometer.

Elemental analyses CHN of the PS-resins were performed on a Thermo FlashEA 1112 elemental analyzer and F on the Metrohm761 Compact Ion Chromatograph (IC) at Medac Ltd, United Kingdom. High performance liquid chromatography (HPLC) was performed on an Agilent Technologies chromatograph (1100 Series), using the specified Daicel chiral column and guard columns. Racemic standard products were prepared using pyrrolidine as catalyst according to reported procedures in order to establish HPLC or GC conditions. The absolute configuration of the reaction products was confirmed by HPLC or GC, by comparison with reported data.

Merrifield resin (1% DVB, *f* = 0.53 mmol Cl/g resin) was obtained from Novabiochem. Aldehydes were distilled before use. *N*-Boc-*trans*-4-hydroxy-L-proline methyl ester, [235] azidomethyl polystyrene,[71g] nitrogen sources such as BocNHOTs,[234b] TsNHOTs,[234a] BocNHOAc[234a,] and CbzNHOAc[234c] were synthesized according to literature procedures.

Calculation of the functionalization of the polystyrene-supported catalyst was done on the basis of nitrogen elemental analysis.[236]

Synthesis and characterization of compounds.

(2*S*,4*R*)-1-*tert*-Butyl 2-methyl-4-(prop-2-ynyloxy)pyrrolidine-1,2-dicarboxylate.[71g]

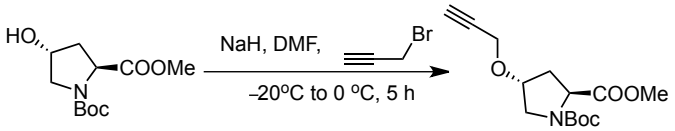

IV.28 **IV.29**

[235] Biel, M.; Deck, P.; Giannis, A.; Waldmann, H. *Chem Eur. J.* **2006**,12, 4121-4143.
[236] Vidal-Ferran, A.; Bampos, N.; Moyano, A.; Pericàs, M. A.; Riera, A.; Sanders, L. K. M. *J. Org. Chem*. **1998**, *63*, 6309-6318.

Experimental part

A 250 mL round bottom flask was charged with NaH (60% in oil; 345 mg, 8.6 mmol), flushed with argon and dry DMF was added (20 mL). A solution of *N*-Boc-*trans*-4-hydroxy-L-proline methyl ester (1.9 g, 8.22 mmol) in 14 ml DMF was slowly added to the first suspension at −20 °C. After complete addition, the solution was stirred for 20 minutes at −20 °C before propargyl bromide (80 w% in toluene; 1 mL, 8.6 mmol) was slowly added via syringe. The reaction was stirred at −20 °C for 30 min, then it was slowly warmed to 0 °C and stirred during 5 h. After the reaction was complete, NH_4Cl (10 mL) and water (50 mL) were added and the mixture was extracted with CH_2Cl_2 (3 × 40 mL). The combined organic layers were washed with brine (40 mL), dried over anhydrous $MgSO_4$, filtered and concentrated in vacuo. The residue was purified by flash column chromatography (SiO_2 with 2.5% Et_3N; cyclohexane/EtOAc 9:1 to 3:1) to obtain the product **IV.29** as a colourless oil (2.05 g, 7.23 mmol, 88%).

^{1}H NMR (500 MHz, $CDCl_3$): δ 4.45−4.26 (m, 2H), 4.21−4.07 (m, 2H), 3.75−3.70 (m, 3H), 3.68−3.50 (m, 2H), 2.44 (t, *J* = 2.4 Hz, 1H), 2.43−2.31 (m, 1H), 2.08 (ddd, *J* = 5.1, 7.5, 13.4, 1H), 1.45/1.40 (two s, 9H combined; rotamers).

^{13}C NMR (126 MHz, $CDCl_3$): mixture of rotamers: δ 173.7, 173.4, 154.4, 153.8, 80.40, 80.36, 79.41, 79.38, 76.6, 75.9, 74.97, 74.94, 58.0, 57.6, 56.55, 56.51, 52.4, 52.2, 51.8, 51.2, 36.7, 35.5, 28.5 (×3), 28.4 (×3).

(2*S*,4*R*)-*tert*-Butyl-2-(hydroxydiphenylmethyl)-4-(prop-2-ynyloxy)-pyrrolidine-1-carboxylate.[71g]

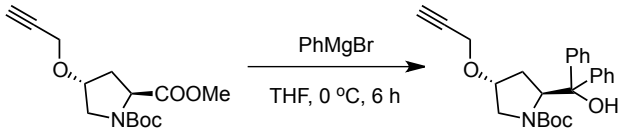

IV.29 **IV.30A**

A 250 mL round bottom flask was charged with **IV.29** (5.92 g, 20.9 mmol), flushed with argon and dry THF was added (90 mL). After cooling the solution to 0 °C, a solution of phenyl magnesium bromide (2 M in THF; 52.3 mL, 104.4 mmol) was added dropwise via addition funnel over a period of 20 min to the flask. After the addition, the reaction mixture was stirred for 6 h at 0 °C. Then, it was quenched upon addition of a saturated aqueous solution of NH_4Cl (until all the white precipitate dissolved) and further diluted with Et_2O (200 mL). The aqueous phase was back-extracted with Et_2O (3 × 50 mL). The combined organic layers were washed with a saturated aqueous solution of NH_4Cl (100 mL), dried over anhydrous $MgSO_4$, filtered and concentrated in vacuo. The crude oil was purified by flash column chromatography (SiO_2 with 2.5% Et_3N; cyclohexane/EtOAc 4:1), yielding the desired product **IV.30A** as a colourless oil (7.43 g, 18.2 mmol, 87%).

^{1}H NMR (500 MHz, $CDCl_3$): δ 7.42−7.40 (m, 2H), 7.38−7.35 (m, 2H), 7.34−7.22 (m, 6H), 5.02 (t, *J* = 7.2 Hz, 1H), 3.97 (d, *J* = 2.4 Hz, 2H), 3.56 (bs, 2H), 2.91 bs, 1H), 2.35 (t, *J* =2.4 Hz, 1H), 2.16−2.12 (m, 2H), 1.38 (s, 9H).

^{13}C NMR (126 MHz, $CDCl_3$): δ 145.7 (×2), 143.5, 129.7, 128.1 (×3), 128.0, 127.8, 127.7, 127.57, 127.4, 127.3, 81.8, 80.9, 79.5, 76.4, 74.6, 65.3, 56.2, 52.9, 36.3, 28.4 (×3).

(2*S*,4*R*)-*tert*-Butyl-2-(hydroxydi(naphthylen-2-yl)-methyl)-4-(prop-2-ynyloxy)pyrrolidine-1-carboxylate.

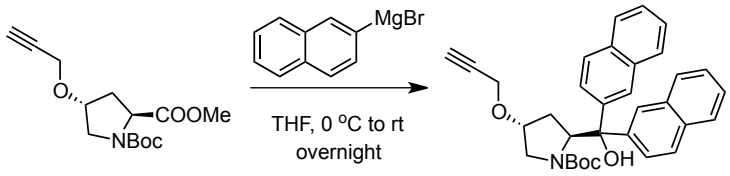

IV.29 **IV.30B**

Magnesium turnings (775 mg, 31.9 mmol) and a spatula tip of I_2 were added to a dry, 100-mL two-necked round-bottom flask fitted with a reflux condenser and it was flame dried under nitrogen. After that, a solution of 2-bromonapthalene (6.0 g, 29 mmol) in 25 mL of THF was added dropwise during 15 min. Once the addition was complete, the mixture was stirred for 40 min. Then it was cooled to −5 °C and a solution of **IV.29** (1.39 g, 4.9 mmol) in 15 mL of THF was added. The reaction mixture was stirred at room temperature overnight. Then, it was quenched upon addition of a saturated aqueous solution of NH_4Cl (until all the white precipitate dissolved) and further extracted with Et_2O (3 × 60 mL). The combined organic layers were washed with a saturated aqueous solution of NH_4Cl (50 mL), dried over anhydrous $MgSO_4$, filtered and concentrated in vacuo. After solvent removal, the crude product was purified by silica gel column chromatography (SiO_2 with 2.5% Et_3N; cyclohexane/EtOAc 9:1). Finally, crystallization (EtOAc/cyclohexane at 0 °C) provided the desired product **IV.30A** as a white solid (1.92 g, 3.78 mmol, 77%).

$[\alpha]_D^{25}$ (CH_2Cl_2, *c* 0.1) −100.2.

mp = 192-194 °C.

^{1}H NMR (500 MHz, $CDCl_3$): δ 7.94−7.91 (m, 1H), 7.88−7.84 (m, 2H), 7.84−7.75 (m, 5H), 7.60 (dd, *J* = 1.9, 8.6 Hz, 1H), 7.54 (dd, *J* = 1.9, 8.6 Hz, 1H), 7.51−7.44 (m, 4H), 5.24 (dd, *J* = 6.4, 8.1 Hz, 1H), 3.99−3.86 (m, 2H), 3.56 (bs, 2H), 2.91 (bs, 1H), 2.35−2.26 (m, 2H), 2.20 (bs, 1H), 1.37 (bs, 9H).

^{13}C NMR (126 MHz, $CDCl_3$): δ 143.0 (×2), 140.9, 133.0, 132.9, 132.77, 132.75, 128.6, 128.5, 128.0, 127.59, 127.55, 127.3, 126.9, 126.3 (×2), 126.18, 126.15 (×2), 125.13, 125.6, 82.1, 81.1, 79.2, 76.1, 74.6, 65.3, 56.2, 52.8, 36.4, 28.3 (×3).

Deprotection of the Boc-group (General Procedure A).

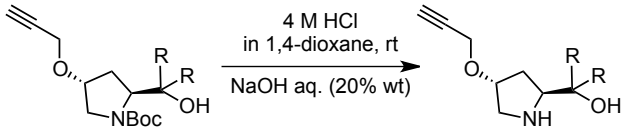

IV.30A, R = Ph
IV.30B, R = 2-naphthyl

IV.31A, R = Ph
IV.31B, R = 2-naphthyl

The Boc-protected amino alcohol was dissolved in a 4 M HCl solution of 1,4-dioxane (0.05 M) and the solution was stirred at room temperature for 40 min. Then, the reaction mixture was cooled to −5 °C and the pH value was adjusted slowly to 8.0 using NaOH solution (20 Wt %). The mixture was extracted with ethyl acetate (×3) and the combined organic phase

Experimental part

were washed with brine and dried over $MgSO_4$. Solvent removal under reduced pressure afforded the desired product.

Diphenyl [(2*S*,4*R*)-4-(prop-2-ynyloxy)pyrrolidin-2-yl]methanol.[71o]

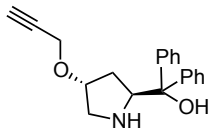

IV.31A

The reaction was carried out following the **General Procedure A**. The title compound **IV.31A** was obtained starting from compound **IV.30A** (2.85 g, 7.0 mmol) as a yellow solid (2.04 g, 6.65 mmol, 95% yield).

$[\alpha]_D^{25}$ (CH_2Cl_2, *c* 0.1) −125.4.

mp = 91-92 °C.

^{1}H NMR (500 MHz, CDCl3): δ 7.61−7.55 (m, 2H), 7.50−7.55 (m, 2H), 7.33−7.24 (m, 4H), 7.21−7.13 (m, 2H), 4.55 (dd, *J* = 6.5, 9.9 Hz, 1H), 4.18−4.13 (m, 1H), 4.10 (dd, *J* = 2.4, 15.7 Hz, 1H), 4.06 (dd, *J* = 2.4, 15.7 Hz, 1H), 3.16 (dd, *J* = 4.5, 11.5 Hz, 1H), 3.11 (dd, *J* = 1.5, 2.4, 11.5 Hz, 1H), 2.40 (t, *J* = 2.4 Hz, 1H), 1.78 (ddd, *J* = 5.3, 9.8, 13.9 Hz, 1H), 1.63 (ddt, *J* = 1.6, 6.5, 13.9, 1H).

^{13}C NMR (126 MHz, $CDCl_3$): δ 147.8, 145.0, 128.5 (×2), 128.2 (×2), 126.8, 126.6, 126.1 (×2), 125.5 (×2), 80.0, 79.7, 77.0, 74.3, 63.5, 56.2, 52.5, 32.9.

Di(naphthylen-2-yl)-[(2*S*,4*R*)-4-(prop-2-ynyloxy)pyrrolidin-2-yl]methanol.

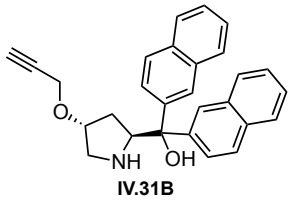

IV.31B

The reaction was carried out following the **General Procedure A**. The title compound **IV.31B** was obtained starting from compound **IV.30B** (1.2 g, 2.36 mmol) as a yellow oil (946 mg, 2.32 mmol, 98% yield).

^{1}H NMR (400 MHz, CDCl3): δ 8.13−8.08 (m, 2H), 7.88 (d, *J* = 8.1 Hz, 1H), 7.84 (d, *J* = 8.1 Hz, 1H), 7.78−7.67 (m, 5H), 7.53 (dd, *J* = 1.8, 8.7 Hz, 1H), 7.50−7.39 (m, 4H), 4.82 (dd, *J* = 6.4, 10.0 Hz, 1H), 4.18−4.14 (m, 1H), 4.11−4.04 (m, 2H), 3.15 (bs, 1H), 2.41 (t, *J* = 2.4 Hz, 1H), 1.87 (ddd, *J* = 5.3, 10.0, 14.0 Hz, 1H), 1.67 (dd, *J* = 6.5, 14.0 Hz, 1H).

^{13}C NMR (126 MHz, $CDCl_3$): δ 144.8, 142.2, 133.3, 133.2, 132.5, 132.4, 128.4 (×3), 127.9, 127.6 (×2), 126.2, 126.1, 126.0, 125.8, 125.6, 124.3, 124.0, 123.9, 80.0, 77.4, 79.6, 74.4, 63.0, 56.2, 52.5, 33.3.

Treatment with diethylaminosulfur trifluoride (Et_2NSF_3) (General Procedure B).

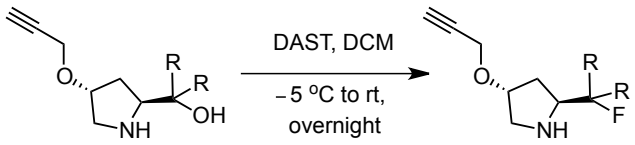

IV.31A, R = Ph
IV.31B, R = 2-naphthyl

IV.32A, R = Ph
IV.32B, R = 2-naphthyl

CAREFUL! DAST is a very dangerous reagent, because it generates HF in contact with water. Care should be taken and excess DAST must be destroyed with sat. aq. $NaHCO_3$.

A round-bottom flask was charged with the corresponding diarylprolinol (1 eq), purged with nitrogen and dry CH_2Cl_2 (0.1 M) was added. The solution was cooled to −5 °C and DAST (2 eq) was added dropwise. The reaction mixture was gradually warmed to rt over a period of 10 h and quenched with sat. aq. $NaHCO_3$. The layers were separated and the aqueous phase was back-extracted with CH_2Cl_2 (3 × 20 mL). The combined organic phases were dried under $MgSO_4$ and concentrated in vacuum. The residue was purified by silica gel column chromatography (SiO_2 with 2.5% Et_3N; eluent from DCM to DCM/MeOH 95:5) to afford the desired fluorinated compound.

(2*S*,4*R*)-2-(Fluorodiphenylmethyl)-4-(prop-2-yn-1-yloxy)pyrrolidine.

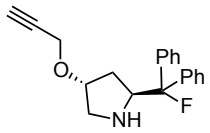

IV.32A

The reaction was carried out following the **General Procedure B**. The title compound **IV.32A** was obtained starting from the compound **IV.31A** (1.12 g, 3.64 mmol) as a yellow brown oil (800 mg, 2.59 mmol, 71 %yield).

$[\alpha]_D^{25}$ (CH_2Cl_2, *c* 0.1) −49.5.

^{1}H NMR (500 MHz, $CDCl_3$): δ 7.55−7.48 (m, 2H); 7.44−7.37 (m, 2H), 7.38−7.27 (m. 4H), 7.28−7.20 (m, 2H), 4.42 (ddd, *J* = 7.2, 8.7, 27.6 Hz, 1H), 4.22 (ddt, J = 2.2, 4.5, 6.5 Hz, 1H), 4.13−4.04 (m, 2H), 3.15 (dd, *J* = 4.6, 11.9 Hz, 1H), 3.03 (ddt, *J* = 1.3, 2.6, 12.0 Hz, 1H), 2.39 (t, *J* = 2.4 Hz, 1H), 1.93 (ddd, *J* = 5.8, 8.7, 14.2 Hz, 1H), 1.84−1.77 (m, 2H).

^{13}C NMR (126 MHz, $CDCl_3$): δ 142.9 (d, *J* = 23.5 Hz), 142.5 (d, *J* = 24.2 Hz), 128.6 (d, *J* = 0.8 Hz, 2C), 128.5 (d, *J* = 1.3 Hz, 2C), 127.7 (d, *J* = 1.3 Hz), 127.6 (d, *J* = 1.2 Hz), 125.7 (d, *J* = 9.1 Hz, 2C), 125.0 (d, *J* = 9.3 Hz, 2C), 100.1 (d, *J* = 182.7 Hz), 80.1, 79.9, 74.2, 63.3 (d, *J* = 21.8 Hz), 56.3, 52.8, 33.3 (d, *J* = 3.6 Hz).

^{19}F NMR (376 MHz, $CDCl_3$): δ = −170.6 (d, *J* = 27.6 Hz).

HRMS (ESI+) Calculated mass for $C_{20}H_{21}FNO$ $[M+H]^+$ 310.1602, found 310.1610.

Elemental analysis for $C_{20}H_{20}FNO$ (theory): %C, 77.64; % H, 6.52; % N, 4.53; %F, 6.14. Found: %C, 77.37; % H, 6.58; % N, 4.24; %F, 5.77.

(2*S*,4*R*)-2-(Fluoro-di(naphthylen-2-yl)methyl)-4-(prop-2-yn-1-yloxy)pyrrolidine.

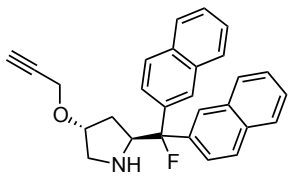

IV.32B

The reaction was carried out following the **General Procedure B**. The title compound **IV.32B** was obtained starting from the compound **IV.31B** (864 mg, 2.12 mmol) as a yellow brown oil (695 mg, 1.7 mmol, 80 % yield).

^{1}H NMR (500 MHz, $CDCl_3$): δ 8.16-8.12 (m, 1H); 8.04−8.01 (m, 1H), 7.91−7.85 (m, 2H), 7.83−7.76 (m, 4H), 7.63 (dd, *J* = 1.9, 8.7 Hz, 1H), 7.54−7.44 (m, 5H), 4.71 (ddd, *J* = 7.1, 8.6, 27.1 Hz, 1H), 4.26 (ddt, *J* = 2.0, 4.3, 6.3 Hz, 1H), 4.13 (dd, *J* = 2.4, 15.8 Hz, 1H), 4.11 (dd, *J* = 2.4, 15.8 Hz, 1H), 3.2 (dd, *J* = 4.5, 11.9 Hz, 1H), 3.09 (dt, *J* = 1.0, 11.9 Hz, 1H), 2.4 (t, *J* = 2.39 Hz, 1H), 2.06 (ddd, *J* = 5.7, 8.7, 14.1 Hz, 1H), 2.03 (bs, 1H), 1.91 (dd, *J* = 7.1, 14.1 Hz, 1H).

^{13}C NMR (126 MHz, $CDCl_3$): δ 140.0 (d, *J* = 23.4 Hz), 139.6 (d, *J* = 24.0 Hz), 133.1,

Experimental part

133.0 (dd, *J* = 0.9 Hz), 132.8 (d, *J* = 0.9 Hz), 132.7 (d, *J* = 0.9 Hz), 128.5 (d, *J* = 13.6 Hz, 2C), 128.4 (d, *J* =4.3 Hz, 2C), 127.7 (d, *J* =0.9 Hz, 2C), 126.5 (d, *J* =7.4 Hz, 2C), 126.4 (d, *J* =2.8 Hz, 2C), 124.7 (d, *J* = 9.6 Hz), 124.1 (d, *J* = 7.8 Hz), 123.8 (d, *J* = 10.1 Hz), 123.4 (d, *J* = 8.1 Hz), 100.6 (d, *J* = 182.9 Hz), 80.1, 79.9, 74.3, 63.0 (d, *J* = 21.9 Hz), 56.3, 52.8, 33.5 (d, *J* = 3.4 Hz).

^{19}F NMR (376 MHz, $CDCl_3$): δ = −168.4 (d, *J* = 27.0 Hz).

During the propargylation step the final compound **IV.29** was isolated as a mixture of diastereomers (GC analysis provides ratio of diastereomers).

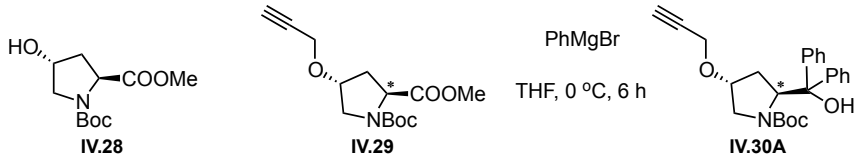

An alternative route to the synthesis of β-fluoroamines is described in this part, together with the Deprotection of the *cis*-diastereomer of the β-fluoroamine.

Preparation of (2*R*,4*R*)-2-(Fluorodiphenylmethyl)-4-(prop-2-yn-1-yloxy)pyrrolidine (IV.32A').

(2*S*,4*R*) or (2*R*,4*R*)-2-(Diphenyl(trimethylsilyxo)methyl-4-(prop-2-ynyloxy)pyrrolidine.

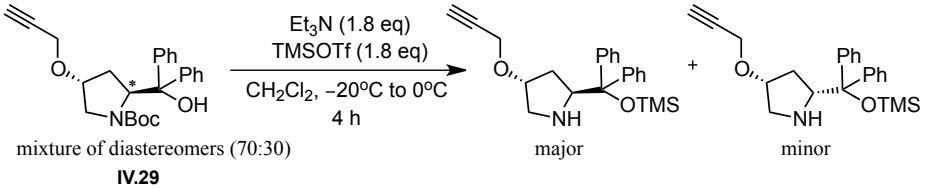

A round-bottom flask was charged with the corresponding diarylprolinol **IV.29** (1.5 g, 3.68 mmol), flushed with argon and CH_2Cl_2 were added (80 mL). The solution was cooled to −20 °C and triethylamine (0.9 ml, 6.6 mmol) was added, followed by trimethylsilyl trifluoromethanesulfonate (1.2 mL, 6.6 mmol). The reaction was gradually warmed to 0 °C over a period of 4 h and quenched with water (20 mL). The layers were separated and the aqueous phase was back-extracted with CH_2Cl_2 (3 × 20 mL). The combined organic layers were dried over anhydrous $MgSO_4$. After solvent removal, the crude product was purified by silica gel column chromatography (SiO_2 with 2.5% Et_3N; cyclohexane/EtOAc 20:1 to 9:1), providing two diastereomers in 79% overall yield.

(2*S*,4*R*)-2-(Diphenyl(trimethylsilyxo)methyl-4-(prop-2-ynyloxy)pyrrolidine.

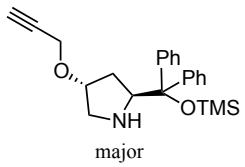

The corresponding compound was isolated as a yellow oil (908 mg, 2.39 mmol, 65% yield).

$[\alpha]_D^{25}$ (CH_2Cl_2, *c* 0.1) −95.0.

^{1}H NMR (500 MHz, $CDCl_3$): δ 7.48−7.45 (m, 2H), 7.35−7.32 (m, 2H), 7.29−7.18 (m, 6H), 4.32 (t, *J* = 7.9 Hz, 1H), 4.09−4.01 (m, 2H), 3.93 (td, *J* = 2.4, 4.6, 1H), 2.96 (dd, J = 2.4, 11.8, 1H), 2.80 (dd. *J* = 4.8, 11.8 Hz, 1H), 2.36 (t, *J* = 2.4 Hz, 1H), 1.82 (bs, 1H), 1.71-1.67 (m, 2H), −0.10 (s, 9H).

^{13}C NMR (126 MHz, $CDCl_3$): δ 146.8, 145.5, 128.6 (×2), 127.8 (×2), 127.7 (×2), 127.6 (×2), 127.1, 127.0, 83.0, 80.2, 79.4, 74.1, 63.7, 56.2, 52.8, 34.2, 2.3 (×3).

(2*R*,4*R*)-2-(diphenyl(trimethylsilyxo)methyl-4-(prop-2-ynyloxy)pyrrolidine.

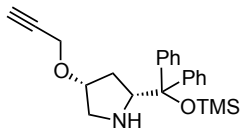

minor

The corresponding compound was isolated as a yellow oil (197 mg, 0.52 mmol, 14 %yield).

$[\alpha]_D^{25}$ (CH_2Cl_2, *c* 0.1) +54.2.

^{1}H NMR (500 MHz, $CDCl_3$): δ 7.51−7.47 (m, 2H), 7.36−7.32 (m, 2H), 7.30−7.19 (m, 6H), 4.1 (dtd, *J* = 3.1, 5.3, 6.7 Hz, 1H), 4.01−3.88 (m, 3H), 3.01 (dd, = 2.8, 12.0 Hz, 1H), 2.94 (dd, *J* = 5.6, 12.0 Hz, 1H), 2.34 (t, *J* = 2.4 Hz, 1H), 1.79−1.71 (bs, 1H), 1.75 (dt, *J* = 6.9, 13.6 Hz 1H), 1.62−1.55 (m, 1H), −0.08 (s, 9H).

^{13}C NMR (126 MHz, $CDCl_3$): δ 146.9, 145.4, 128.8 (×2), 127.83 (×2), 127.75 (×2), 127.4 (×2), 127.3, 127.0, 82.6, 80.2, 78.7, 74.0, 65.9, 55.9, 53.4, 34.7, 2.24 (×3).

HRMS (ESI+) Calculated mass for $C_{23}H_{30}NO_2Si$ $[M+H]^+$ 380.2040, found 380.2036.

Deprotection of TMS group using TBAF (General Procedure C).

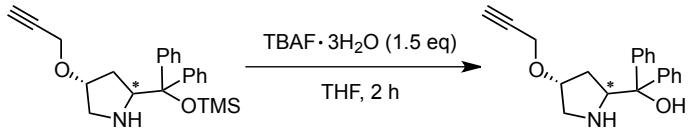

IV.31A or IV.31A'

The TMS-protected amine (1 eq) was dissolved in THF (0.5 M) and TBAF•$3H_2O$ (1.5 eq) was added. The reaction mixture was stirred at room temperature for 1.5 h. Then, water was added to the mixture, followed by extraction with Et_2O (×3) and the combined organic phase was washed with brine and dried over $MgSO_4$. Solvent removal under reduced pressure afforded the desired amino alcohol.

Diphenyl [(2*S*,4*R*)-4-(prop-2-ynyloxy)pyrrolidin-2-yl]methanol.

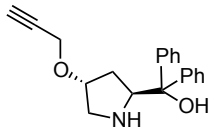

IV.31A

The reaction was carried out following the **General Procedure C**. The title compound **IV.31A** was obtained starting from compound **IV.30A** (1.08 g, 2.85 mmol) as a yellow solid (857 mg, 2.79 mmol, 98% yield).

For characterization, see this compound in General procedure A.

Experimental part

Diphenyl [(2*R*,4*R*)-4-(prop-2-ynyloxy)pyrrolidin-2-yl]methanol.

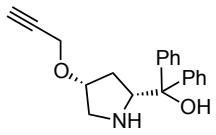

IV.31A'

The reaction was carried out following the **General Procedure C**. The title compound **IV.31A'** was obtained starting from compound **IV.30A'** (259 mg, 0.682 mmol) as a yellow oil (203 mg, 0.66 mmol, 97% yield).

$[\alpha]_D^{25}$ (CH_2Cl_2, *c* 0.1) +36.5.

^{1}H NMR (500 MHz, $CDCl_3$): δ 7.59−7.55 (m, 2H), 7.50−7.47 (m, 2H), 7.31−7.24 (m, 4H), 7.19−7.14 (m, 2H), 4.34 (dd, *J* = 7.0, 8.3 Hz, 1H), 4.23 (dddd, *J* = 2.3, 3.6, 5.1, 6.1 Hz, 1H), 4.14 (dd, *J* = 2.4, 15.9 Hz, 1H), 4.08 (dd, *J* = 2.4, 15.9 Hz, 1H), 3.16 (dt, *J* = 1.8, 10.9 Hz, 1H), 3.03 (dd, *J* = 5.1, 10.9 Hz, 1H), 2.38 (t, *J* = 2.4 Hz, 1H), 1.90 (ddd, *J* = 6.3, 8.3, 14.4 Hz, 1H), 1.80 (dddd, *J* = 1.4, 3.6, 7.1, 14.2 Hz, 1H).

^{13}C NMR (126 MHz, $CDCl_3$): δ 147.2, 145.6, 128.4 (×2), 128.2 (×2), 126.8, 126.7, 126.1 (×2), 125.7 (×2), 79.8, 77.7, 77.0, 74.4, 64.0, 56.0, 52.0, 32.8.

HRMS (ESI+) Calculated mass for $C_{20}H_{22}NO_2$ $[M+H]^+$ 308.1645, found 308.1647.

(2*R*,4*R*)-2-(Fluorodiphenylmethyl)-4-(prop-2-yn-1-yloxy)pyrrolidine (IV.32A').

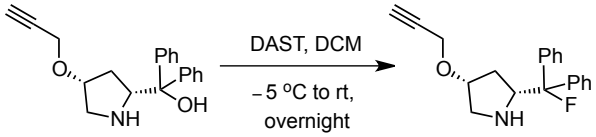

IV.31A' **IV.32A'**

The reaction was carried out following the **General Procedure B**. The title compound **IV.32A'** was obtained starting from compound **IV.31A'** (201 mg, 0.654 mmol) as a yellow brown oil (150 mg, 0.484 mmol, 74% yield).

$[\alpha]_D^{25}$ (CH_2Cl_2, *c* 0.1) −24.7

^{1}H NMR (500 MHz, $CDCl_3$): δ 7.59−7.55 (m, 2H), 7.52−7.48 (m, 2H), 7.32−7.25 (m, 4H), 7.20−7.14 (m, 2H), 4.33 (t, *J* = 7.7 Hz, 1H), 4.26-4.21 (m, 1H), 4.15 (dd, *J* = 2.4, 16.0 Hz, 1H), 4.09 (dd, *J* = 2.4, 16.0 Hz, 1H), 3.17 (dt, *J* = 1.5, 10.9 Hz, 1H), 3.04 (dd, *J* = 5.2, 10.9 Hz, 1H), 2.38 (t, *J* = 2.4 Hz, 1H), 1.90 (ddd, *J* = 6.3, 8.2, 14.1 Hz, 1H), 1.80 (dddd, *J* = 1.4, 3.6, 7.1, 14.0 Hz, 1H), 1.70-1.62 (m, 1H).

^{13}C NMR (126 MHz, $CDCl_3$): δ 142.5 (d, *J* = 23.5 Hz), 142.0 (d, *J* = 24.4 Hz), 128.53 (2C), 128.50 (d, *J* = 1.2 Hz, 2C), 128.8 (d, *J* = 1.3 Hz), 128.7 (d, *J* = 1.0 Hz), 125.5 (d, *J* = 9.0 Hz, 2C), 124.8 (d, *J* = 9.3 Hz, 2C), 99.1 (*J* = 183.0 Hz), 80.0, 79.0, 74.3, 64.4 (d, *J* = 22.5 Hz), 56.3, 53.0, 33.4.

^{19}F NMR (376 MHz, $CDCl_3$): δ = −170.6 (*J* = 27.2 Hz).

Preparation of the polymer-supported pyrrolidine IV.12A and IV.12B.

The cycloaddition of azidomethyl polystyrene to monomer (General Procedure D).

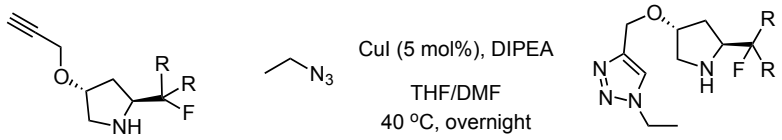

IV.32A, R = Ph
IV.32B, R = 2-naphthyl

IV.12A, R = Ph
IV.12B, R = 2-naphthyl

Alkyne (0.87 mmol), DIPEA (1.2 mL, 6.9 mmol) and CuI (6.1 mg. 0.03 mmol) were added to suspension of azidomethyl polystyrene (1.2 g, 0.666 mmol, f = 0.55 mmol g^{-1}, 2 % of DVB) in a THF/DMF (1:1, 7 mL) and the mixture was shaken at 40 °C for 10 h. The reaction progress was monitored by FT−IR spectroscopy. When the IR band of the azide (2092−2093 cm^{-1}) had completely disappeared, the reaction was filtered off and the resin was washed with THF with 2 mol% Et_3N (100 ml), H_2O (100 ml, until neutral pH), H_2O/MeOH (1:1), MeOH, MeOH/THF (1:1, 100 ml), THF (50 ml), and DCM (50 ml). The solid was dried in vacuo at 40 °C for 24 h.

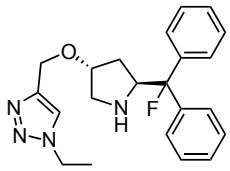

IV.12A

The polystyrene-supported derivative **IV.12A** was prepared according to the **General Procedure D** with **IV.32A** (269 mg).

IR (ATR): 3081.7, 3058.9, 2920.0, 2849.2, 1600.2, 1582.7, 1492.0, 1450.0, 1360.3, 1044.1, 905.1, 753.4, 694.6, 537.2 cm^{-1}

Elemental analysis (%) = %C. 87.94; %H, 7.88; %N, 2.30; %F, 0.59; f = 0.41 mmol g^{-1} (f_{max} = 0.44 mmol g^{-1}).

^{19}F NMR (376 MHz, $CDCl_3$): δ = −170.3 (bs)

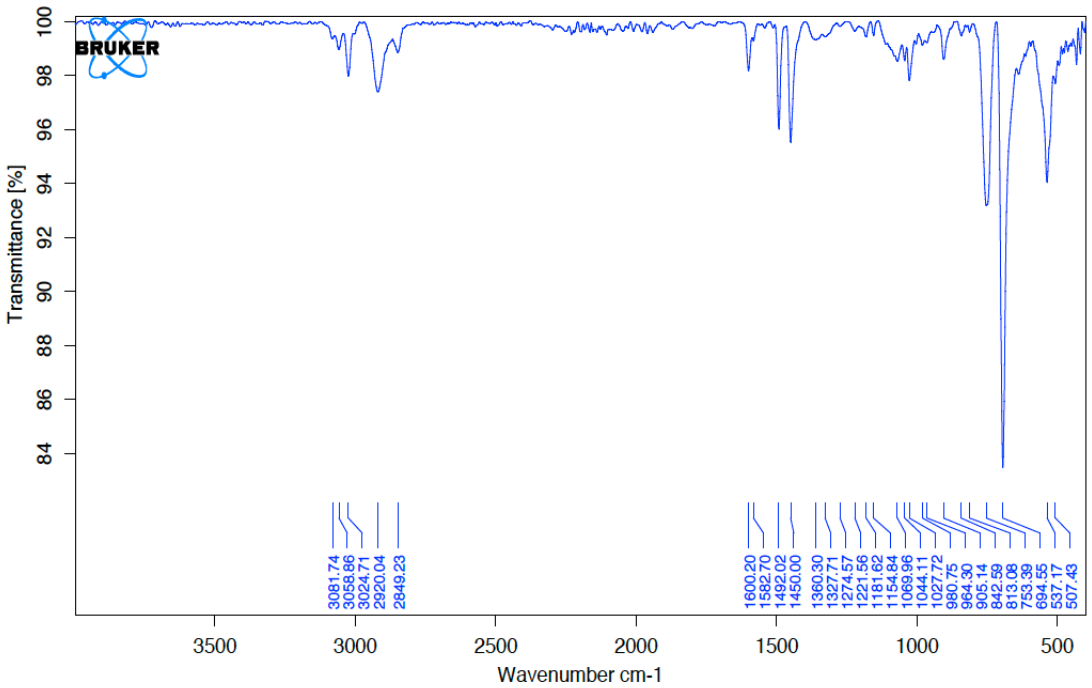

Experimental part

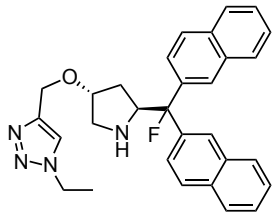

IV.12B

The polystyrene-supported derivative **IV.12B** was prepared according to the **General Procedure D** with **IV.32B** (357 mg).

IR (ATR): 3081.3, 3058.4, 3024.7, 2919.8, 2920.1, 1600.2, 1583.2, 1491.9, 1449.8, 1358.6, 1069.0, 904.9, 749.8, 694.5, 537.0 cm^{-1}

Elemental analysis (%) = %C. 87.19; %H, 7.74; %N, 2.49; %F, 0.75; *f* = 0.44 mmol g^{-1} (f_{max} = 0.44 mmol g^{-1}).

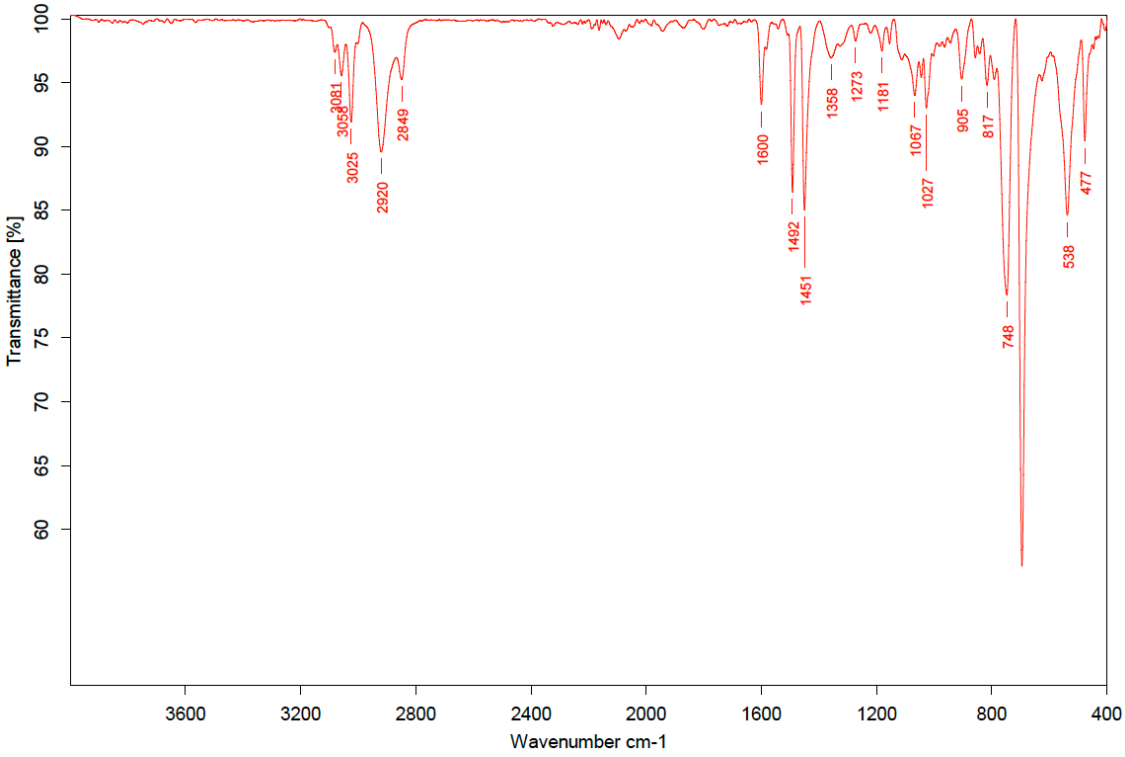

Preparation of the monomeric analogue of catalyst IV.12A.

1-Benzyl-4-((((3*R*,5*S*)-5(fluorodiphenylmethyl)pyrrolidin-3-yl)oxy)methyl)-1H 1,2,3-triazole.

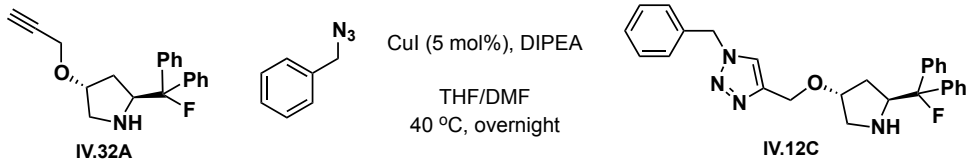

IV.32A IV.12C

A mixture of benzyl azide (55 µl, 0.44 mmol), (2*S*,4*R*)-2-(fluorodiphenylmethyl)-4-(prop-2-yn-1-yloxy)pyrrolidine (90 mg, 0.29 mmol), CuCl (2.8 mg, 0.015 mmol), and DIPEA (506 µl, 2.90 mmol) in THF/DMF)(1:1, 1.5 ml) were placed in a flask and the mixture was stirred at 40 °C for 10 h under nitrogen. The residue was purified by silica gel column chromatography (SiO_2 with 2% Et_3N; eluent from 4:1 to 1:4 hexane:EtOAc) to afford **IV.12C** as a white solid (114 mg, 0.258 mmol, 89 % yield).

$[\alpha]_D^{25}$ (CH_2Cl_2, *c* 0.1) +10.0.

mp = 90-92 °C.

^{1}H NMR (500 MHz, $CDCl_3$): δ 7.51−7.48 (m, 2H), 7.41 (s, 1H), 7.40−7.19 (m, 13H), 5.48 (s, 2H), 4.53 (d, *J* = 2.0 Hz, 2H), 4.40 (dt, *J* = 8.0, 27.6 Hz, 1H), 4.15−4.11 (m, 1H), 3.13

(dd, *J* = 4.6, 11.7 Hz, 1H), 3.00 (dt, *J* = 1.1, 11.7 Hz, 1H), 1.98-1.89 (m, 2H), 1.80 (dd, *J* = 7.3, 13.9 Hz 1H).

^{13}C NMR (126 MHz, $CDCl_3$): δ 145.8, 142.89 (d, *J* = 23.4 Hz), 142.4 (*J* = 24.2 Hz), 134.6, 129.2 (×2), 128.9, 128.5 (×2), 128.4 (d, *J* = 1.1 Hz, ×2), 128.3 (×2), 127.6 (*J* = 1.1 Hz), 127.52 (d, *J* = 1.1 Hz), 125.6 (d, *J* = 9.0 Hz, ×2), 124.9 (d, *J* = 9.3 Hz, ×2), 122.4, 100.1 (d, *J* = 182.7 Hz), 80.3, 63.3 (d, *J* = 21.9 Hz), 62.6, 54.3, 52.9, 33.3 (d, *J* = 3.4 Hz).

^{19}F NMR (376 MHz, $CDCl_3$): δ = −170.5 (d, *J* = 27.3 Hz).

Experimental part

Epoxidation of α,β-unsaturated aldehydes (General Procedure E).

To a suspension of the catalyst (10 mol%) in 0.5 M CH_2Cl_2 was added the corresponding α,β-unsaturated aldehyde (1.0 eq) at r.t. The reaction mixture was stirred for 3 min before hydrogen peroxide (30% in H_2O, 1.3 eq) was added via syringe. It was stirred for the specified time (monitored by TLC/NMR). Then it was filtered, and rinsed with CH_2Cl_2. After that, the filtrate was quenched by addition of a saturated aqueous solution of $Na_2S_2O_3$ followed by extraction of the aqueous phase with Et_2O. The combined organic layers were dried over anhydrous Na_2SO_4 and concentrated in vacuo. The crude product was purified by flash column chromatography (Et_2O: *n*-pentane, 4:1) and the solvents were removed in vacuo to yield the desired product.

Different additives were screened. However, with most polymer-supported catalysts the isolated yield did not reach 30% because of benzaldehyde formation. This by-product was identified and isolated.

(2*S*,3*R*)-3-Phenyloxirane-2-carbaldehyde and (2*R*,3*R*)-3-phenyloxirane-2-carbaldehyde.

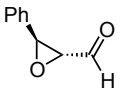

IV.34a

The reaction was carried out following the **General Procedure E** with the catalyst **IV.12A** and benzoic acid (10 mol%) as additive for 3 h. The title compound **IV.34A** was obtained as a yellow oil (8.6 mg, 0.06 mmol, 29% yield, dr 66:34, 73% ee).

The ee was determined by GC analysis using a β-DEX 120 column (120 °C isotherm): (2*S*,3*S*) t_R = 26.1 min; (2*R*,3*R*) t_R = 26.5 min; (2*S*,3*R*) t_R = 29.0 min; (2*R*,3*S*) t_R = 29.8 min.

^{1}H NMR (400 MHz, $CDCl_3$): (mixture of diastereomers) δ 9.20 (d, *J* = 6.1 Hz, 1H), 9.08 (d, *J* = 6.0 Hz, 1H*), 7.47−7.28 (m, 5H and 5H*), 4.40 (d, J = 4.6 Hz, 1H*), 4.18 (d, *J* = 1.8 Hz, 1H), 3.55 (dd, *J* = 4.5, 6.0 Hz, 1H*), 3.46 (dd, *J* = 1.8, 6.1 Hz, 1H).

All the spectroscopic data of the product match with those reported in the literature.[163]

Aziridination of α,β-unsaturated aldehydes (General Procedure F).

To a stirred solution of the catalyst (10 mol%, 0.018 mmol), NaOAc (44.4 mg, 0.54 mmol, 3 eq), and BocNHOTs (52 mg, 0.18 mmol, 1.0 eq) in 0.5 M CH_2Cl_2 (360 µl) at rt was added an α,β-unsaturated aldehyde (0.36 mmol, 2.0 eq). The reaction was stirred at rt for the specified time (TLC/NMR monitoring); mixture was filtered and rinsed with CH_2Cl_2, water and dried. The crude product was isolated without purification in some cases; otherwise, it was purified by silica gel column chromatography.

***trans*-2-Formyl-3-propyl-1-*t*-butoxycarbonyl aziridine.**

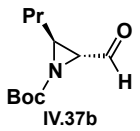

IV.37b

The reaction was carried out following the **General Procedure F** with catalyst **IV.12A**. The title compound **IV.37b** was obtained as a yellow oil (37 mg, 0.173 mmol, 96% yield, dr 87:13, 97% ee) without purification.

The ee was determined (after reduction with $NaBH_4$) by GC analysis using a β-DEX 120 column (100 °C isotherm): (2*R*,3*S*) t_R minor = 85.2 min; (2*S*,3*R*) t_R major = 88.9 min; (2*S*,3*S*) and (2R,3R) t_R =111.0 min.

^{1}H NMR (500 MHz, $CDCl_3$): δ 9.1 (d, *J* = 5.2 Hz, 1H), 2.91 (dd, *J* = 2.6, 5.2 Hz, 1H); 2.83-2.79 (m, 1H); 1.58−1.48 (m, 4H); 1.46 (s, 9H), 0.98 (t, *J* = 7.1 Hz, 3H).

^{13}C (126 MHz, $CDCl_3$): δ 195.6, 158,7, 82.3, 46.9, 43.4, 32.8, 27.8 (×3), 20.01, 13.4.

All the spectroscopic data of the product match with those reported in the literature.[227b]

***trans*-2-Formyl-3-methyl-1-*t*-butoxycarbonyl aziridine.**

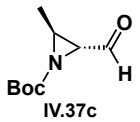

IV.37c

The reaction was carried out following the **General Procedure F** with catalyst **IV.12A**. The title compound **IV.37c** was obtained as a yellow oil (32.3 mg, 0.175 mmol, 97% yield, dr 86:14) without purification.

^{1}H NMR (500 MHz, $CDCl_3$): δ 9.08 (d, *J* = 5.1 Hz, 1H), 2.89−2.83 (m, 2H), 1.47 (s, 9H), 1.38 (d, *J* = 5.1 Hz, 3H).

All the spectroscopic data of the product match with those reported in the literature.[227b]

Reactions with different nitrogen sources were performed according to the **General Procedure F**, the data shown in **Table IV.13** and **IV.14** (during the discussion).

UNIVERSITAT ROVIRA I VIRGILI
NEW APPROACHES TO CATALYST DESIGN AND IMMOBILIZATION
Irina Sagamanova

CHAPTER V

*Palladium Catalyzed Diaryl Sulfoxide Generation from Aryl Benzyl Sulfoxides and Aryl Chlorides**

** Work described in this chapter was carried out during a research stage in the laboratory of Prof. Patrick J. Walsh at Penn University, in the framework of a collaboration between the Walsh and Pericàs laboratories.*

This part of the work was supervised by Prof. Patrick J. Walsh, and developed in collaboration with Tiezheng Jia, Mengnan Zhang, and Carol Y. Wang.

UNIVERSITAT ROVIRA I VIRGILI
NEW APPROACHES TO CATALYST DESIGN AND IMMOBILIZATION
Irina Sagamanova

Palladium Catalyzed Diaryl Sulfoxide Generation from Aryl Benzyl Sulfoxides and Aryl Chlorides

5.1. Introduction.

Palladium catalyzed cross-coupling reactions have been widely used for the formation of C-C bonds.[237] In contrast to the direct α-arylation of carbonyls (via in situ generated enolates),[238] the α-functionalization of sulfonyl and sulfinyl derivatives has been scarcely explored. For instance, Buchwald and Hartwig have developed the Suzuki-Miyaura-type reactions for the arylation of carbonyl compounds at the α-position (see more details about α-arylation in **Chapter I**).[103,107-108]

A similar approach was described by Beletskaya *et al*. in 2002[112] in what was the first direct palladium-catalyzed monoarylation of sulfones containing an additional electron-withdrawing α-substituent. However, the scope of the method is limited to the arylation of strongly CH-acidic sulfones, and cannot be extended to simple sulfones.

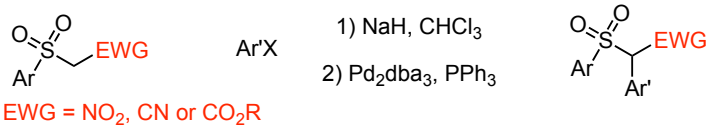

Scheme V.1. α-Arylation of prefunctionalized sulfones.

There is an alternative precedent that benzyl phenyl sulfoxides can also be accessed by a Pd-catalyzed Suzuki cross-coupling between simple α-bromosulfoxides and aryl boronic acids (**Scheme V.2**),[239] but direct arylation of methyl sulfoxides has not been reported yet.

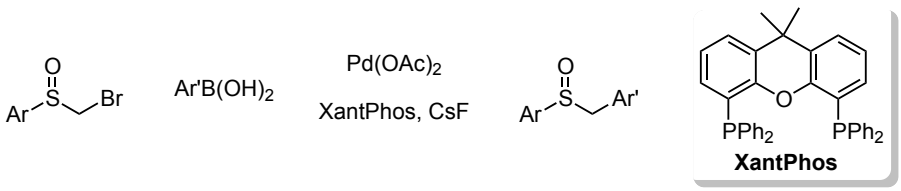

Scheme V.2. Suzuki coupling of α-bromosulfoxides and arylboronic acids.

---

[237] Littke, A. F.; Fu, G. C. *Angew. Chem. Int. Ed.* **2002**, *41*, 4176-4211.
[238] Muci, A. R.; Buchwald, S. L. *Cross-coupling reactions* (Ed.: Miyaura, N.), Springer, Berlin, Heidelberg, **2002**, *Ch. 5*, 131-209.
[239] Mollar, C.; Besora, M.; Maseras, F.; Asensio, G.; Medio-Simon, M. *Chem. Eur. J.* **2010**, *16*, 13390-13397.

Chapter V

Cross-coupling reactions are a powerful method to form C-S bonds,[240] and offer an alternative access to aryl sulfoxides. The first diaryl sulfoxide synthesis via palladium-catalyzed *S*-arylation between sulfenate anions and aryl iodides was reported the group of Madec and Poli.[241] In this report, sulfenate anions were generated in situ via retro-Michael reaction of β-sulfinyl esters (**Scheme V.3**).

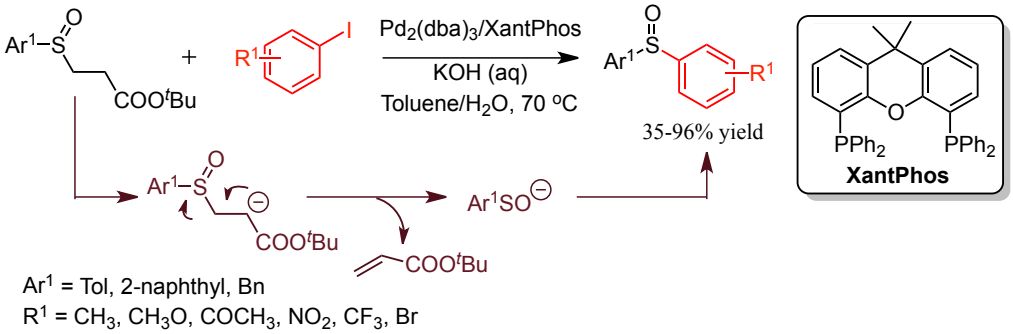

Scheme V.3. Palladium-catalyzed aromatic sulfenylation.

Later in 2010, the same group discovered that diaryl sulfoxides can be generated via arylation of sulfenate anions, which are generated in situ via [2,3]-sigmatropic rearrangement (called Mislow-Braverman-Evans rearrangement) of allylic sulfoxides (**Scheme V.4**).[120b] However more available aryl chloride substrates do not react under under these conditions.

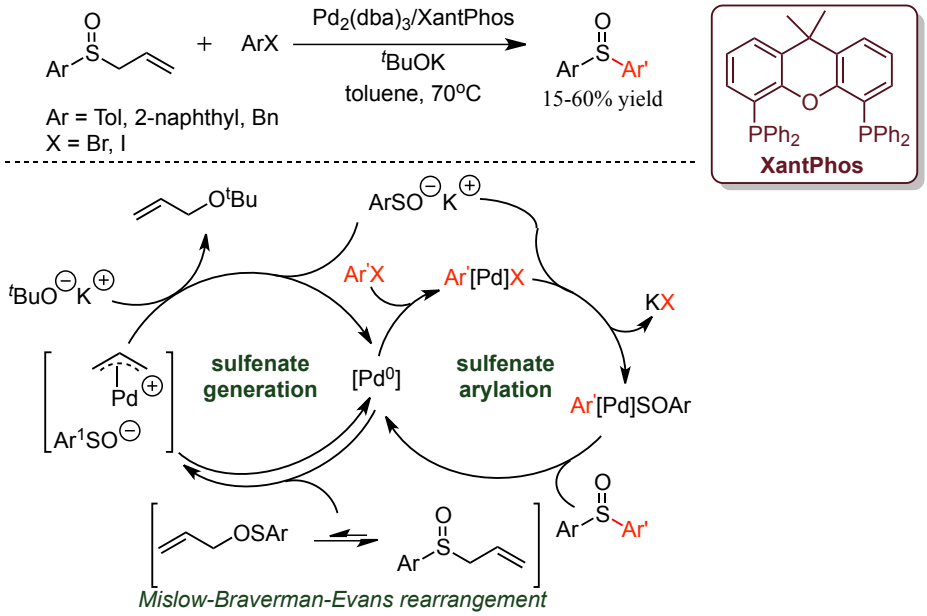

Scheme IV.4. Aromatic sulfenylation from allyl sulfoxides.

[240] For reviews, see: a) Shen, C.; Zhang, P.; Sun, Q.; Bai, S.; Andy Hor, T. S.; Liu, X. *Chem. Soc. Rev.* **2015**, *44*, 291-314; b) Modha, S. G.; Mehta, V. P.; Van der Eycken, E. V. *Chem. Soc. Rev.* **2013**, *42*, 5042-5044; c) Eichman, C. C.; Stambuli, J. P. *Molecules* **2011**, *16*, 590-608

[241] Maitro, G.; Vogel, S.; Prestat, G.; Madec, D.; Poli, G. *Org. Lett.* **2006**, *8*, 5951-5954.

In 2013 Walsh *et al.* reported the first palladium-catalyzed direct α-arylation of methyl sulfoxides with aryl halides (**Scheme V.5**).[113]

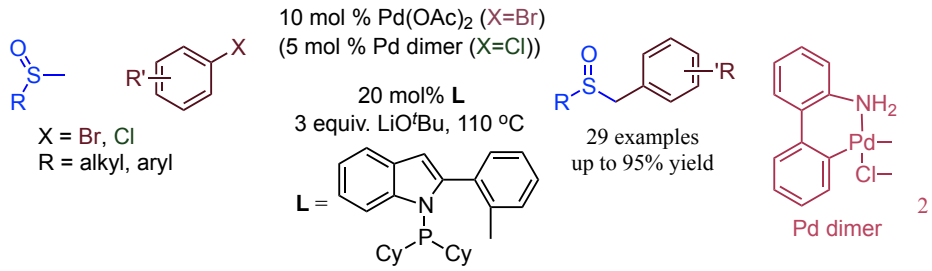

Scheme V.5. Direct α-arylation of methyl sulfoxides.

In the same year, the Nolan group described the direct *S*-arylation of unactivated arylsulfoxides, promoted by an *N*-heterocyclic carbene-based palladium catalyst (**Scheme V.6**).[242] Despite the fact that the reaction worked with aryl bromides and chlorides, only 4-chloroanisole was employed in this transformation, providing much lower yield in comparison with 4-bromoanisole. However, other activated halides, such as 1-bromo-4-nitrobenzene, 1-bromo-4-(trifluoromethyl)benzene, and 1-chloro-4-fluorobenzene failed to give the desired products.

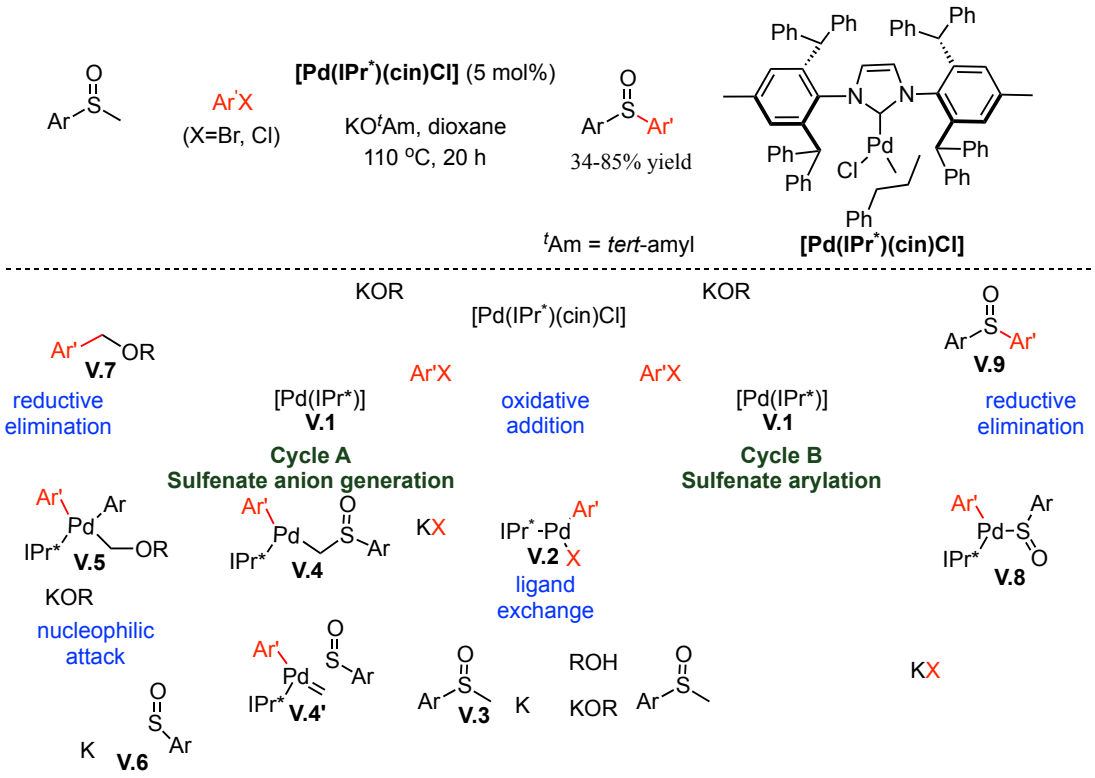

Scheme V.6. *S*-arylation of activated and unactivated arylsulfoxides via the generation of sulfenate anions.

[242] Izquierdo, F.; Chartoire, A.; Nolan, S. P. *ACS Catal.* **2013**, *3*, 2190-2193.

Chapter V

The proposed mechanism involves two different cycles: sulfenate anion generation (Cycle A) and sulfenate arylation (Cycle B) (**Scheme V.5**). The Pd^0 (**V.1**) active species is formed *in situ* by activation of the precatalyst in the presence of the base, followed by oxidative addition; this provides formation of the complex **V.2**. α-Sulfinyl anion **V.3** is afforded by reversible deprotonation of the weakly acidic α-protons of the arylmethylsulfoxide by KOR.[113] Complex **V.4** is formed after ligand exchange (X for V.3) and it is in equilibrium with the ionized carbonic form **V.4'**. Then, nucleophilic attack of the base on the carbon provides complex **V.5** and sulfenate anion **V.6**. This reacts with complex **V.2** in cycle B in order to form **V.8**. Reductive elimination provides the diarylsulfoxide derivative **V.9** and the Pd^0 species is regenerated. During the course of this reaction, by-product **V.7** is formed in the first cycle. These two cycles can explain why 2 equiv. of halide are required for the reaction.

Simultaneously, Walsh *et al.* reported diaryl sulfoxide formation from aryl benzyl sulfoxides and aryl bromides using a palladium catalyst based on van Leuween's NiXantPhos ligand [243] (**Scheme V.7**).[114] Different type of aryl methyl sulfoxides, dibenzyl sulfoxides and DMSO could be employed to generate diaryl sulfoxides.

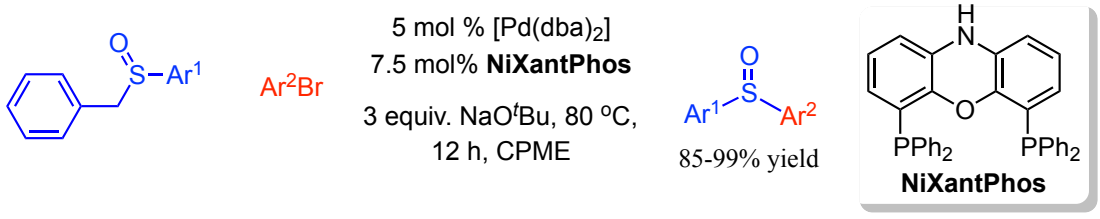

Scheme V.7. Palladium catalyzed diaryl sulfoxides formation from aryl benzyl sulfoxides and aryl bromides.

Moreover, this transformation was applied to the generation of chiral diaryl sulfoxides. After screening several mono- or bidentate chiral ligands by High-Throughput Experimentation, the JosiPhos family was found to be the best option, both in terms of yield and enantioselectivity (**Scheme V.8**).[244]

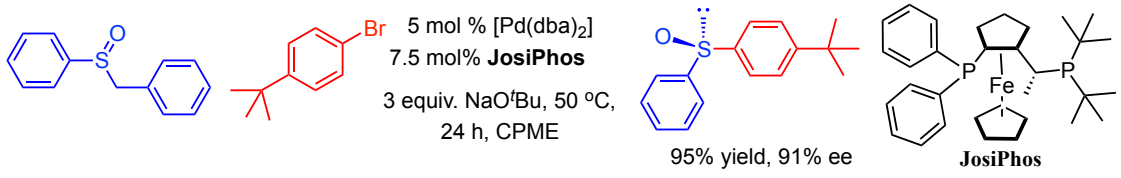

Scheme V.8. Palladium catalyzed enantioselective synthesis of diaryl sulfoxides.

---

[243] van der Veen, L. A.; Keeven, P. H.; Schoemaker, G. C.; Reek, J. N. H.; Kamer, P. C. J.; van Leeuwen, P. W. N. M.; Lutz, M.; Spek, A. L. *Organometallics* **2000**, *19*, 872-883.
[244] Jia, T. "Palladium-Catalyzed C-C Bond and C-S Bond Reactions of Sulfoxides" **2015**. *Publicly Accessible Penn Dissertations*. Paper 1069.

However, only aryl bromides or iodides were employed in all these processes. Therefore, many challenges remain in the generation of sulfoxides with alternative coupling partners. The use of aryl chlorides would provide several advantages due to their availability and lower cost in comparison to aryl bromides and iodides.

5.2. Mechanistic study of palladium catalyzed diaryl sulfoxide formation.

The mechanism of formation of diaryl sulfoxides has been described by the Walsh group.[114] Based on experiments, it was proposed that Pd/NiXantPhos promoted three transformations to generate the diaryl sulfoxides (**Scheme V.9**), including α-arylation of benzyl sulfoxides (**Cycle A**), benzylative substitution of diarylmethyl sulfoxides (**Cycle B**), and *S*-arylation of sulfenate anions (**Cycle C**).

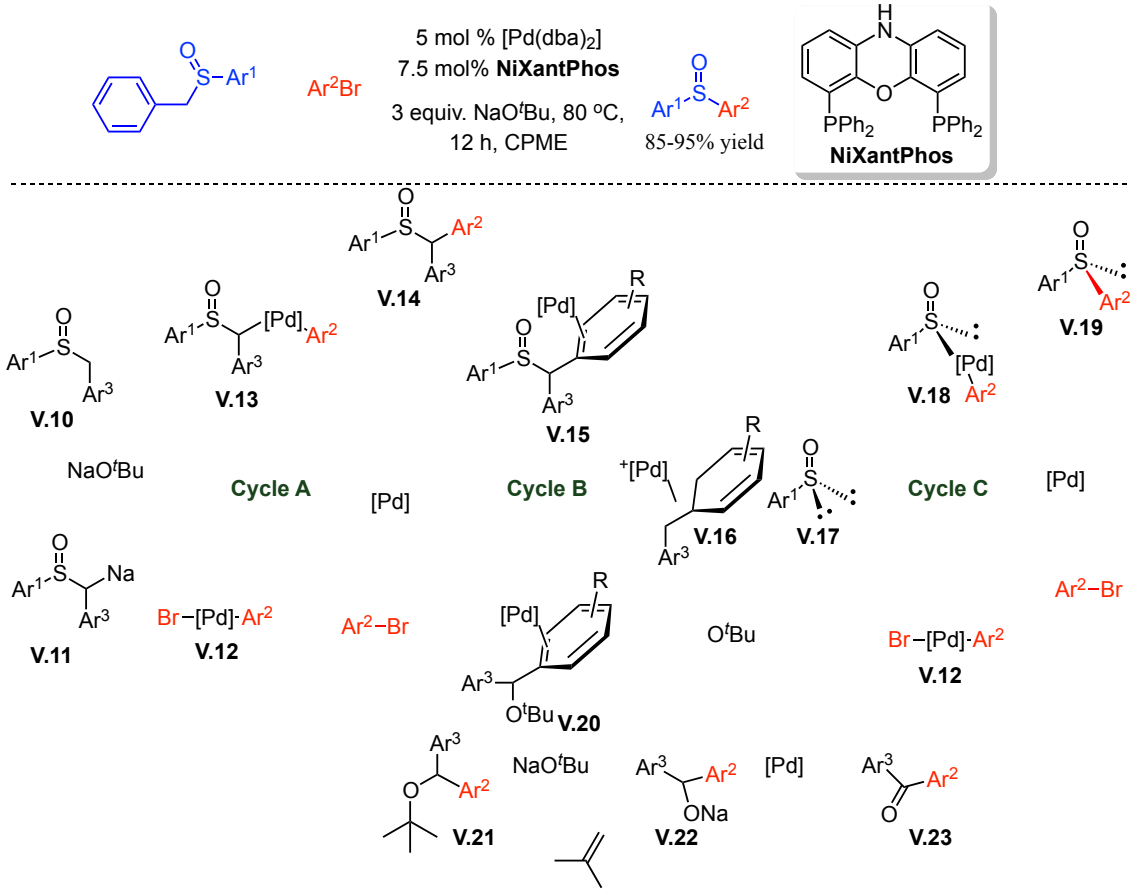

Scheme V.9. Mechanism of the Pd-catalyzed diaryl sulfoxide generation.

α-Arylation was proposed for the first cycle in this transformation, according to the previous reported catalytic arylation of methyl phenyl sulfoxides (**Scheme V.10**).[113]

Chapter V

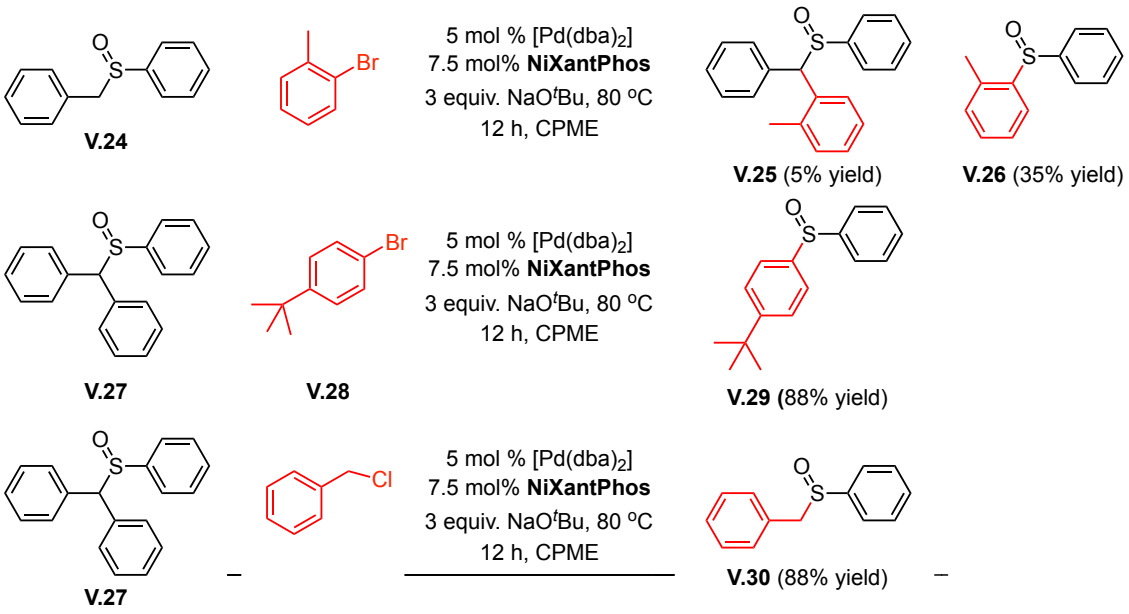

Scheme V.10. Generation of **V.25** and α-arylation and benzylation of **V.27a**.

Cleavage of the C-S bond occurs in the catalytic **cycle B**. Palladium coordinates to the arene moiety of **V.14**, followed by formation of π-benzyl intermediate **V.16** and expulsion of aryl sulfenate **V.17**. Generation of diarylmethyl *tert*-butyl ether (**V.21**) takes place by attack of the base.

Further studies demonstrated that the elimination of **V.21** gives rise to **V.22**, which is oxidized by palladium in the catalytic **cycle D** (**Scheme V.11**), providing diaryl ketone **V.23**. However, in the presence of 2 equiv of the aryl bromide, diaryl ketone could not be generated completely; therefore diaryl methyl *tert*-butyl ether **V.21** could be observed.

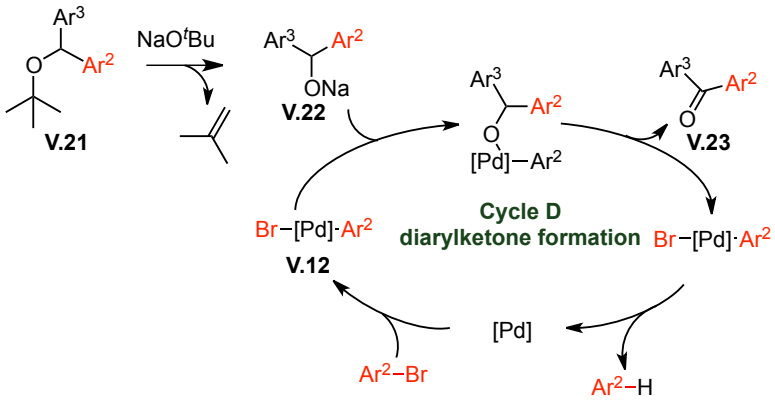

Scheme V.11. Cycle D: diaryl ketone formation.

The aryl bromide and the sulfenate anion generated in **cycle B** undergo palladium catalyzed cross-coupling in **cycle C** to produce the diaryl sulfoxide.

5.3. Aim of the project.

Given the existing literature for the synthesis of aryl sulfoxides at the beginning of this project, we considered that aryl chlorides can be interesting substrates for this transformation due to their availability and reduced cost.

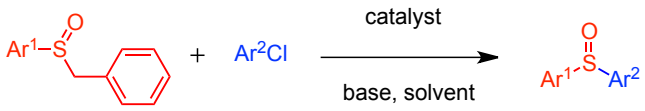

However, additional studies were needed to adapt this process to aryl chlorides. Since the C-Br bond is weaker than C-Cl (290 or 346 kJ mol^{-1} respectively), less energy is needed to break the former, and the reaction is much faster or proceeds at lower temperatures when compared to aryl chlorides.

In addition, this would provide an extension of the methodology reported in 2014 for formation of aryl sulfoxides from benzyl sulfoxides and aryl bromides,[114] which involves three catalytic cycles: the α-arylation, C-S cleavage and *S*-arylation of sulfenate anions.

UNIVERSITAT ROVIRA I VIRGILI
NEW APPROACHES TO CATALYST DESIGN AND IMMOBILIZATION
Irina Sagamanova

Organic LETTERS
Letter
pubs.acs.org/OrgLett

Palladium Catalyzed Diaryl Sulfoxide Generation from Aryl Benzyl Sulfoxides and Aryl Chlorides

Tiezheng Jia,[†] Mengnan Zhang,[†] Irina K. Sagamanova,[†,‡] Carol Y. Wang,[†] and Patrick J. Walsh*[,†]

[†]Roy and Diana Vagelos Laboratories, Department of Chemistry, University of Pennsylvania, 231 South 34th Street, Philadelphia, Pennsylvania 19104-6323, United States

[‡]Institute of Chemical Research of Catalonia (ICIQ), Av. Països Catalans 16, 43007 Tarragona, Spain

Supporting Information

ABSTRACT: Diaryl sulfoxides are synthesized from aryl benzyl sulfoxides and aryl chlorides via three sequential catalytic cycles all promoted by a NiXantPhos-based palladium catalyst. The key step is *S*-arylation of a sulfenate anion. An air- and moisture-stable precatalyst derived from NiXantPhos efficiently facilitates the transformation. Various functional groups, including those with acidic protons, were tolerated. This method can also be extended to methyl and dibenzyl sulfoxides substrates.

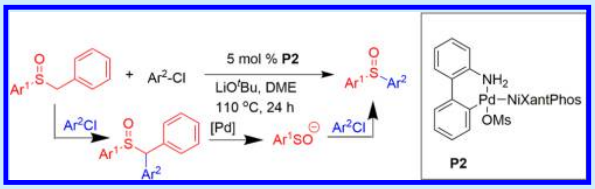

Downloaded by UNIV ROVIRA I VIRGILI on September 4, 2015 | http://pubs.acs.org
Publication Date (Web): February 16, 2015 | doi: 10.1021/acs.orglett.5b00092

Aryl sulfoxides are important structural motifs in bioactive compounds[1] and marketed therapeutics.[2] They are also widely used as ligands in transition-metal catalysis.[3] Significant effort, therefore, has been devoted to their preparation. The most popular methods for the synthesis of sulfoxides are oxidation of sulfides and nucleophilic substitution of sulfinamides or sulfinate esters.[4]

Transition-metal catalyzed cross-coupling reactions are powerful methods to form C–S bonds[5] and offer an alternative approach to construct aryl sulfoxides. In 2007, Poli and Madec reported the first diaryl sulfoxide generation via palladium-catalyzed *S*-arylation between sulfenate anions[6] and aryl bromides and iodides.[7] Sulfenate anions were generated in situ via retro-Michael reaction (Scheme 1A). The same team subsequently employed the Mislow–Braverman–Evans rearrangement of allylic sulfoxides and generated sulfenate anions that were arylated in situ to provide diaryl sulfoxides (Scheme 1B).[8] Aryl chloride substrates were noticeably absent from these reports.

Very recently, the Nolan group reported an *N*-heterocyclic carbene-based palladium catalyst for the conversion of methyl sulfoxides to diaryl sulfoxides via a proposed Pd-carbene intermediate (Scheme 1C).[9] Although the reaction worked with aryl bromides and chlorides, the only functionalized aryl chloride employed was 4-chloro anisole.

Simultaneously, we communicated[10] diaryl sulfoxide formation from aryl benzyl sulfoxides and *aryl bromides* using a palladium catalyst based on van Lewueen's NiXantPhos ligand[11] (Scheme 1D). A systematic study revealed that this single palladium catalyst promoted three distinct transformations to generate diaryl sulfoxides (Figure 1), including α-arylation of benzyl sulfoxides (Cycle A), sulfenate anion generation (Cycle B), and *S*-arylation of sulfenate anions (Cycle C). Various diaryl sulfoxides and heteroaryl aryl sulfoxides were prepared from aryl bromides in good to excellent yields. Given the scarcity of aryl chlorides that have been successfully employed in the sulfenate anion arylation, and the reduced costs and greater abundance of aryl chlorides relative to aryl bromides, we viewed the inclusion of aryl chlorides in this reaction as important. Herein, we report a palladium-catalyzed diaryl sulfoxide formation from aryl benzyl sulfoxides and aryl chlorides (Scheme 1E).

Scheme 1. Aryl sulfoxides synthesis via palladium catalyzed C–S bond formation

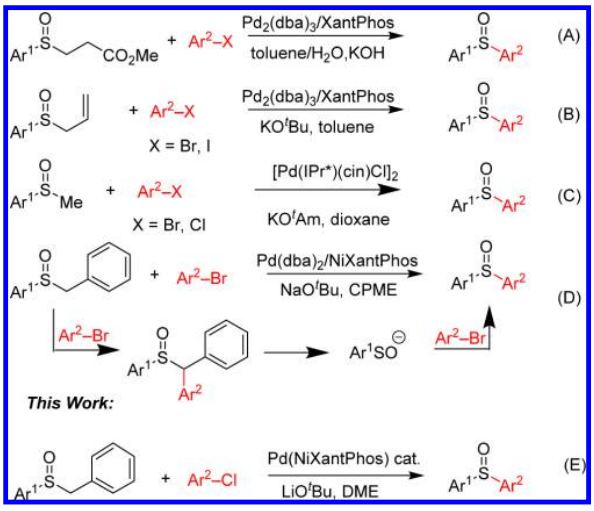

Received: January 12, 2015
Published: February 16, 2015

 © 2015 American Chemical Society

DOI: 10.1021/acs.orglett.5b00092
Org. Lett. 2015, 17, 1168–1171

Chapter V

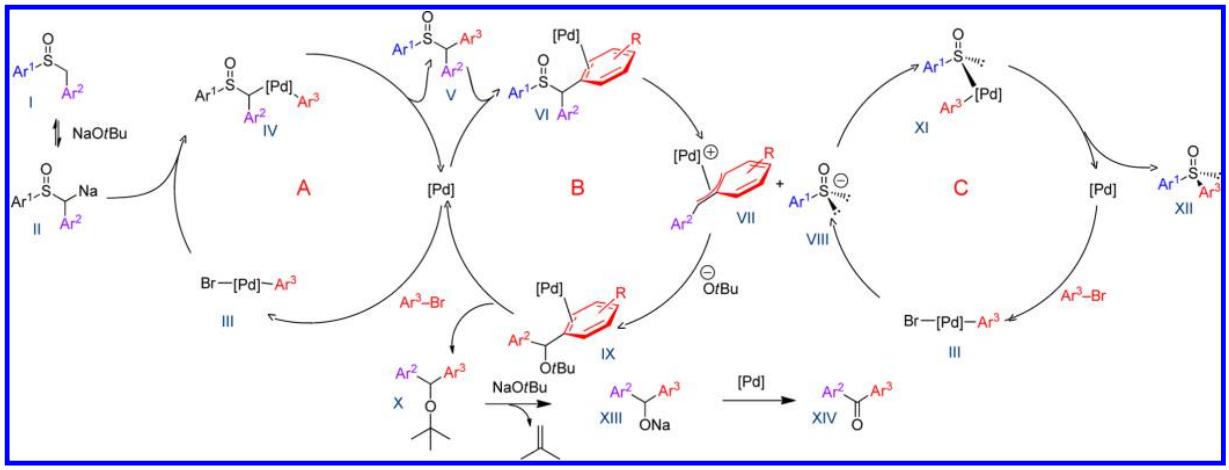

Figure 1. Palladium catalyzed diaryl sulfoxides formation from aryl benzyl sulfoxides and aryl bromides via a triple relay mechanism.

We employed coupling partners benzyl phenyl sulfoxide (**1a**) and 4-*tert*-butyl chlorobenzene (**2a**) as the model substrates to identify reaction conditions. The optimized conditions for coupling sulfoxide **1a** with *aryl bromides*, which involved 5 mol % $Pd(dba)_2$/7.5 mol % NiXantPhos ligand (Figure 2) and 3

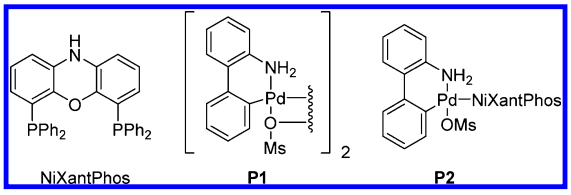

Figure 2. Structures of NiXantPhos and palladacyclic precursors **P1** and **P2**.

equiv of NaO^{t}Bu in CPME at 80 °C, were initially examined (Table 1, entry 1).[10] The desired diaryl sulfoxide product (**3a**) was formed in less than 5% assay yield. We were concerned that catalyst generation was an issue, so we used Buchwald's palladacyclic precatalysts,[12] which proved to be effective in the oxidative addition of aryl chlorides with NiXantPhos.[13] Two precatalysts (**P1** and **P2**, Figure 2) were prepared according to reported procedures[12f,13] and used under the conditions of the coupling reaction. When **P1** was used with NiXantPhos, the yield of **3a** improved to 15%. The yield of **3a** increased to 34% when the precatalyst bearing NiXantPhos (**P2**) was utilized. These low yields inspired us to screen bases that had been successfully applied to other deprotonative cross-coupling processes (DCCP). Thus, LiO^{t}Bu, KO^{t}Bu, $LiN(SiMe_3)_2$, $NaN(SiMe_3)_2$, and $KN(SiMe_3)_2$ were investigated. In this screen, LiO^{t}Bu gave the most promising result (43%, Table 1, entry 5 vs entries 3 and 6–9). Three additional ethereal solvents [DME (dimethoxyethane), dioxane, and THF) were surveyed with DME giving a better yield (51%, Table 1, entry 10 vs entries 5, 11 and 12). Increasing the temperature of the reaction from 80 to 110 °C led to a 61% yield of **3a** (Table 1, entry 13). Finally, doubling the reaction time to 24 h resulted in **3a** in 74% assay yield (^{1}H NMR) and 70% isolated yield (Table 1, entry 14). Further optimization did not lead to increased yields. Thus, the optimized conditions were 5 mol % palladacyclic **P2**, sulfoxide **1a** as the limiting reagent, 2 equiv

Table 1. Optimization of the Palladium-Catalyzed Diaryl Sulfoxide Formation[a]

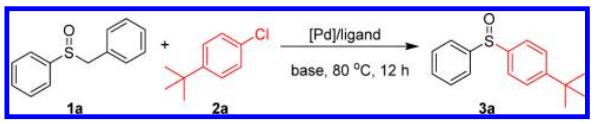

entry	Pd/mol %	base	sol	assay yield[b] (%)
1[c]	$Pd(dba)_2$/5	NaO^{t}Bu	CPME	<5
2[c]	**P1**/2.5	NaO^{t}Bu	CPME	15
3	**P2**/5	NaO^{t}Bu	CPME	34
4[c]	**P2**/5	NaO^{t}Bu	CPME	29
5	**P2**/5	LiO^{t}Bu	CPME	43
6	**P2**/5	KO^{t}Bu	CPME	27
7	**P2**/5	$LiN(SiMe_3)_2$	CPME	11
8	**P2**/5	$NaN(SiMe_3)_2$	CPME	0
9	**P2**/5	$KN(SiMe_3)_2$	CPME	0
10	**P2**/5	LiO^{t}Bu	DME	51
11	**P2**/5	LiO^{t}Bu	dioxane	37
12	**P2**/5	LiO^{t}Bu	THF	28
13[d]	**P2**/5	LiO^{t}Bu	DME	61
14[e]	**P2**/5	LiO^{t}Bu	DME	74 (70[f])

[a]1 equiv of **1a**, 2 equiv of **2a**, and 3 equiv of base at 80 °C on 0.1 mmol scale for 12 h. [b]Assay yield determined by ^{1}H NMR by using 0.1 mmol of CH_2Br_2 as an internal standard. [c]7.5 mol % NiXantPhos used. [d]110 °C. [e]24 h. [f]Isolated yield.

of aryl chloride, and 3 equiv of LiO^{t}Bu in DME at 110 °C for 24 h.

With the optimized conditions for the palladium-catalyzed cross-coupling reaction of **1a** and **2a**, the substrate scope of aryl chlorides was investigated (Scheme 2). The parent diphenyl sulfoxide (**3b**) was generated from chlorobenzene (**2b**) in 72% yield. Aryl chlorides bearing electron-withdrawing groups, such as 4-F (**2c**) and 4-CN (**2d**), afforded the products in 85% and 63% yields, respectively. Both 1-chloronaphthalene (**2e**) and 3-chloroanisole (**2f**) were suitable cross-coupling partners, furnishing **3e** and **3f** in 70% and 87% yield, respectively. 4-Chlorobenzophenone was successfully coupled, delivering **3g** in 72% yield. Surprisingly, under the optimized conditions, acetamide **2h** and piperidine **2i** afforded products **3h** and **3i** both in 73% yield. Thus, the NiXantPhos ligated catalyst successfully promoted both C–C and C–S bond formations

DOI: 10.1021/acs.orglett.5b00092
Org. Lett. 2015, 17, 1168–1171

Downloaded by UNIV ROVIRA I VIRGILI on September 4, 2015 | http://pubs.acs.org
Publication Date (Web): February 16, 2015 | doi: 10.1021/acs.orglett.5b00092

UNIVERSITAT ROVIRA I VIRGILI
NEW APPROACHES TO CATALYST DESIGN AND IMMOBILIZATION
Irina Sagamanova

Scheme 2. Substrate Scope of Aryl Chlorides in Palladium-Catalyzed Diaryl Sulfoxides Synthesis with 1a

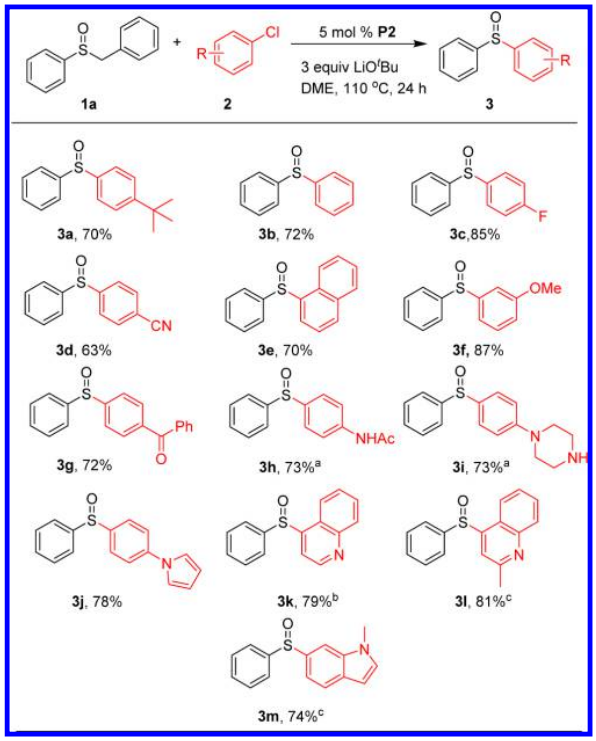

[a]5equiv LiO^{t}Bu used. [b] 10 mol % **P2** used. [c] 48 h.

(Figure 2) faster than C–N bond formation (Buchwald–Hartwig coupling[14]), leaving the N–H's intact. Heterocyclic sulfoxides, which often exhibit bioactivities,[1] could also be prepared. Thus, 4-pyrrolephenyl phenyl sulfoxide (**3j**), 4-quinoline phenyl sulfoxide (**3k**), 2-methyl 4-quinoline phenyl sulfoxide (**3l**), and (*N*-methyl)-6-indolyl phenyl sulfoxide (**3m**) were generated in 74–81% yields. However, sterically hindered aryl chlorides, such as mesityl chloride, and some heteroaryl chlorides, such as 3-chloropyridine and 3-chlorothiophene, could not be coupled under our conditions.

A variety of aryl benzyl sulfoxides were next explored in the presence of 5 mol % NiXantPhos ligated precatalyst **P2** (Scheme 3). Aryl benzyl sulfoxides bearing electron-donating groups furnished diaryl sulfoxides **3n**–**3p** in 78–83% yields. For reasons that remain unclear, 1-(benzylsulfinyl)-4-methoxybenzene (**1o**) was not a viable substrate in our initial study.[10] In contrast, in the present case 4-chloroanisole afforded **1o** in 83% yield. Diaryl sulfoxides bearing electron-withdrawing 4-F or 3-CF_3 groups generated products in 77–78% yields. Sulfoxides bearing larger substituents, such as 1-naphthyl (**1e**) and 2-tolyl (**1q**), were also viable coupling partners, providing **3e** and **3q** in 80–81% yield. Alkyl benzyl sulfoxides are more challenging substrates, because their α-C–H's are less acidic than aryl benzyl sulfoxides.[15] Nonetheless, cyclohexyl benzyl sulfoxide reacted with chlorobenzene to generate cyclohexyl phenyl sulfoxide (**3s**) in 72% yield. Heteroaryl benzyl sulfoxides are potentially useful coupling partners. The quinoline benzyl sulfoxide underwent coupling to provide the heteroaryl aryl sulfoxide **3k** in 67% yield with 10 mol % catalyst.

Scheme 3. Substrate Scope of Aryl Benzyl Sulfoxides in Palladium-Catalyzed Diaryl Sulfoxides Formation with 2b

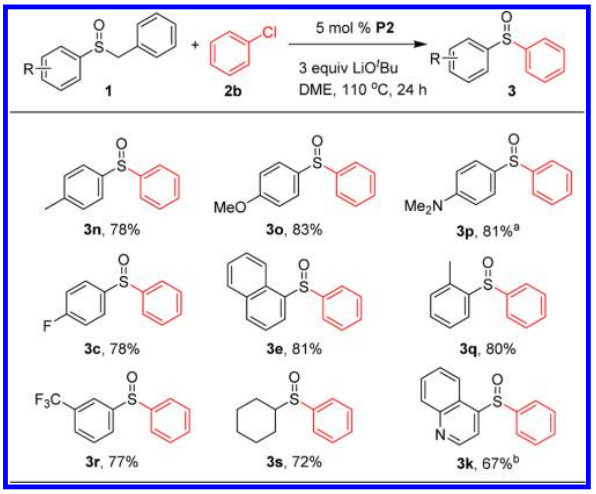

[a]3 equiv PhCl used. [b] 10 mol % **P2** used.

To demonstrate the potential utility of our method, we conducted a gram scale reaction with a heterocyclic aryl chloride (Scheme 4). Thus, phenyl benzyl sulfoxide (5 mmol, 1.08 g) was coupled with 4-chloro-2-methylquinoline (**2l**) in 80% yield (1.07 g).

Scheme 4. Gram Scale Synthesis of 3l via Palladium Catalyzed Diaryl Sulfoxide Generation

We next set out to evaluate different types of sulfoxides as precursors to diaryl sulfoxides. We previously demonstrated the arylation of aryl methyl sulfoxides to generate aryl benzyl sulfoxides,[12h] which are the substrates in the current study. Combining these two methods, we treated phenyl methyl sulfoxide with chlorobenzene under our standard conditions, giving diphenyl sulfoxide (**3b**) in 77% yield (Scheme 5A). Likewise, dibenzyl sulfoxide (**1u**) and chlorobenzene (**2b**) could also be converted to diphenyl sulfoxide in 57% yield (Scheme 5B). Considering four C(sp^2)–Cl bonds have to be

Scheme 5. Preparation of Diphenyl Sulfoxide (3b) from Methyl Phenyl Sulfoxide (1t) or Dibenzyl Sulfoxide (1u) and Chlorobenzene (2b)

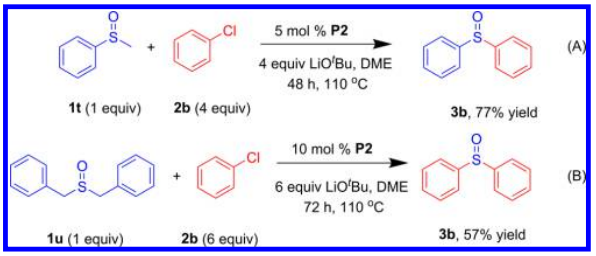

DOI: 10.1021/acs.orglett.5b00092
Org. Lett. 2015, 17, 1168–1171

Downloaded by UNIV ROVIRA I VIRGILI on September 4, 2015 | http://pubs.acs.org
Publication Date (Web): February 16, 2015 | doi: 10.1021/acs.orglett.5b00092

UNIVERSITAT ROVIRA I VIRGILI
NEW APPROACHES TO CATALYST DESIGN AND IMMOBILIZATION
Irina Sagamanova

Chapter V

broken to generate each equivalent of **3b**, the moderate yield is reasonable.

In summary, aryl chlorides have been utilized as electrophiles in the cross-coupling reactions with aryl benzyl sulfoxides to produce diaryl sulfoxides. A variety of functional groups, including those which might be expected to participate in related coupling reactions (Buchwald–Hartwig) or undergo addition reactions (C=O, CN), were well tolerated. According to the proposed mechanism, two C(sp^2)–Cl bonds have to be cleaved to generate one molecule of product. In order to do so, an air and moisture stable NiXantPhos-derived palladacyclic precatalyst was employed.

■ ASSOCIATED CONTENT

Supporting Information

Procedures, characterization data for all new compounds. This material is available free of charge via the Internet at http://pubs.acs.org.

■ AUTHOR INFORMATION

Corresponding Author

*E-mail: pwalsh@sas.upenn.edu.

Notes

The authors declare no competing financial interest.

■ ACKNOWLEDGMENTS

We thank the National Science Foundation [CHE-1152488] for financial support. I.K.S. thanks the Spanish MINECO (Grant CTQ2012-38594-C02-01) and the Institute of Chemical Research of Catalonia (ICIQ) Foundation for financial support. C.Y.W. thanks the Vagelos Integrated Program in Energy Research for financial support.

■ REFERENCES

(1) (a) Rinehart, K. L.; Sakai, R. Patent: US2004/59112 A1, 2004. (b) Amira Pharmaceuticals, Inc. Patent: US/2010/4331 A1, 2010. (c) Amira Pharmaceuticals, Inc.; Hutchinson, J. H.; Seiders, T. J.; Arruda, J. M.; Roppe, J. R. Patent: WO2010/42652 A2, 2010. (d) Combinatorx (Singapore) Pte. Ltd. Patent: US2010/9970 A1, 2010. (e) ACHAOGEN, Inc. Patent: WO2009/137130A2, 2009.

(2) (a) Astra Aktiebolag Patent: US5877192 A, 1998. (b) Laboratoire L. Lafon Patent: US4927855A, 1990.

(3) For review, see: (a) Mellah, M.; Voituriez, A.; Schulz, E. *Chem. Rev.* **2007**, *107*, 5133 and references therein. Some recent examples: (b) Jiang, C.; Covell, D. J.; Stepan, A. F.; Plummer, M. S.; White, M. C. *Org. Lett.* **2012**, *14*, 1386. (c) Stang, E. M.; White, M. C. *J. Am. Chem. Soc.* **2011**, *133*, 14892. (d) Dornan, P. K.; Leung, P. L.; Dong, V. M. *Tetrahedron* **2011**, *67*, 4378. (e) Chen, J.; Chen, J.; Lang, F.; Zhang, X.; Cun, L.; Zhu, J.; Deng, J.; Liao, J. *J. Am. Chem. Soc.* **2010**, *132*, 4552. (f) Mariz, R.; Luan, X.; Gatti, M.; Linden, A.; Dorta, R. *J. Am. Chem. Soc.* **2008**, *130*, 2172.

(4) (a) Wojaczyńska, E.; Wojaczyński, J. *Chem. Rev.* **2010**, *110*, 4303. (b) O'Mahony, G. E.; Kelly, P.; Lawrence, S. E.; Maguire, A. R. *ARKIVOC* **2011**, *1*, 1. (c) Bolm, C. *Coord. Chem. Rev.* **2003**, *237*, 245.

(5) (a) Beletskaya, I. P.; Ananikov, V. P. *Chem. Rev.* **2011**, *111*, 1596. (b) Beletskaya, I. P.; Cheprakov, A. V. *Coord. Chem. Rev.* **2004**, *248*, 2337. (c) Carril, M.; SanMartin, R.; Dominguez, E. *Chem. Soc. Rev.* **2008**, *37*, 639. (d) Eichman, C. C.; Stambuli, J. P. *Molecules* **2011**, *16*, 590.

(6) O'Donnell, J. S.; Schwan, A. L. *J. Sulfur Chem.* **2004**, *25*, 183.

(7) Maitro, G.; Vogel, S.; Prestat, G.; Madec, D.; Poli, G. *Org. Lett.* **2006**, *8*, 5951.

(8) Bernoud, E.; Le Duc, G.; Bantreil, X.; Prestat, G.; Madec, D.; Poli, G. *Org. Lett.* **2010**, *12*, 320.

(9) Izquierdo, F.; Chartoire, A.; Nolan, S. P. *ACS Catal.* **2013**, *3*, 2190.

(10) Jia, T.; Bellomo, A.; Montel, S.; Zhang, M.; El Baina, K.; Zheng, B.; Walsh, P. J. *Angew. Chem., Int. Ed.* **2014**, *53*, 260.

(11) (a) van der Veen, L. A.; Keeven, P. H.; Schoemaker, G. C.; Reek, J. N. H.; Kamer, P. C. J.; van Leeuwen, P. W. N. M.; Lutz, M.; Spek, A. L. *Organometallics* **2000**, *19*, 872. (b) Kamer, P. C. J.; van Leeuwen, P. W. N. M.; Reek, J. N. H. *Acc. Chem. Res.* **2001**, *34*, 895.

(12) For leading works, see: (a) Herrmann, W. A.; Brossmer, C.; Ofele, K.; Reisinger, C.-P.; Priermeier, T.; Beller, M.; Fischer, H. *Angew. Chem., Int. Ed. Engl.* **1995**, *34*, 1844. (b) Schnyder, A.; Indolese, A. F.; Studer, M.; Blaser, H.-U. *Angew. Chem., Int. Ed.* **2002**, *41*, 3668. (c) Biscoe, M. R.; Fors, B. P.; Buchwald, S. L. *J. Am. Chem. Soc.* **2008**, *130*, 6686. (d) Kinzel, T.; Zhang, Y.; Buchwald, S. L. *J. Am. Chem. Soc.* **2010**, *132*, 14073. (e) Albert, J.; Granell, J.; Zafrilla, J.; Font-Bardia, M.; Solans, X. *J. Organomet. Chem.* **2005**, *690*, 422. For recent examples, see: (f) Bruno, N. C.; Tudge, M. T.; Buchwald, S. L. *Chem. Sci.* **2013**, *4*, 916. (g) Bruno, N. C.; Tudge, M. T.; Buchwald, S. L. *Org. Lett.* **2013**, *15*, 2876. (h) Jia, T.; Bellomo, A.; El Baina, K.; Dreher, S. D.; Walsh, P. J. *J. Am. Chem. Soc.* **2013**, *135*, 3740. (i) Zheng, B.; Jia, T.; Walsh, P. J. *Org. Lett.* **2013**, *15*, 4190. (j) Zheng, B.; Jia, T.; Walsh, P. J. *Adv. Synth. Catal.* **2014**, *356*, 165. (k) Bruno, C. N.; Niljianskul, N.; Buchwald, S. L. *J. Org. Chem.* **2014**, *79*, 4161. (l) Smith, K. B.; Logan, K. M.; You, W.; Brown, M. K. *Chem.—Eur. J.* **2014**, *20*, 12032.

(13) Zhang, J.; Bellomo, A.; Trongsiriwat, N.; Jia, T.; Carroll, P. J.; Dreher, S. D.; Tudge, M. T.; Yin, H.; Robinson, J. R.; Schelter, E. J.; Walsh, P. J. *J. Am. Chem. Soc.* **2014**, *136*, 6276.

(14) (a) Surry, D. S.; Buchwald, S. L. *Chem. Sci.* **2010**, *1*, 13. (b) Surry, D. S.; Buchwald, S. L. *Chem. Sci.* **2011**, *2*, 27. (c) Hartwig, J. F. *Acc. Chem. Res.* **2008**, *41*, 1534. (d) Evano, G.; Blanchard, N.; Toumi, M. *Chem. Rev.* **2008**, *108*, 3054.

(15) Bordwell, F. G. *Acc. Chem. Res.* **1988**, *21*, 456.

Downloaded by UNIV ROVIRA I VIRGILI on September 4, 2015 | http://pubs.acs.org
Publication Date (Web): February 16, 2015 | doi: 10.1021/acs.orglett.5b00092

DOI: 10.1021/acs.orglett.5b00092
Org. Lett. 2015, 17, 1168–1171

5.4. Conclusions and Outlook.

We have been able to demonstrate the synthesis of diaryl sulfoxides from aryl benzyl sulfoxides and aryl chlorides with a NiXantPhos-based palladium catalyst. This air- and moisture-stable precatalyst efficiently enables this transformation.

Various functional groups, including those with acidic protons, have been produced in good to excellent yields. In addition, this method was extended to methyl and dibenzyl sulfoxide substrates.

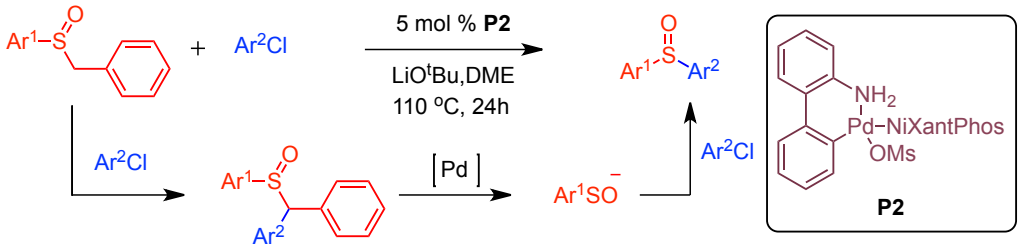

Diaryl sulfoxides have been synthesized via three sequential catalytic cycles promoted by a single catalyst, where the key step is the *S*-arylation of a sulfenate anion.

UNIVERSITAT ROVIRA I VIRGILI
NEW APPROACHES TO CATALYST DESIGN AND IMMOBILIZATION
Irina Sagamanova

SUPPORTING INFORMATION

Palladium Catalyzed Diaryl Sulfoxide Generation from Aryl Benzyl Sulfoxides and Aryl Chlorides

Tiezheng Jia,[†] Mengnan Zhang,[†] Irina K. Sagamanova,[†,‡] Carol Y. Wang, Patrick J. Walsh[*,†]*

[†] *Roy and Diana Vagelos Laboratories, Penn/Merck Laboratory for High-Throughput Experimentation, Department of Chemistry, University of Pennsylvania, 231 South 34th Street, Philadelphia, Pennsylvania 19104-6323, United States.* [‡] *Institute of Chemical Research of Catalonia (ICIQ), Av. Pasos Catalans 16, 43007 Tarragona, Spain.*

pwalsh@sas.upenn.edu

TABLE OF CONTENTS

Chapter V

General Methods: All reactions were carried out under dry nitrogen. Anhydrous CPME, dioxane, and dimethoxyethane (DME) were purchased from Sigma-Aldrich and directly used without further purification. THF was dried through activated alumina columns. Unless otherwise stated, reagents were commercially available and used as purchased without further purification. Chemicals were purchased from Sigma-Aldrich, Acros, Alfa Aesar, TCI or Matrix Scientific, and solvents were purchased from Fisher Scientific. The progress of the reactions was monitored by thin-layer chromatography using Whatman Partisil K6F 250 μm precoated 60 Å silica gel plates and visualized by short-wave ultraviolet light as well as by treatment with iodine. Flash chromatography was performed with silica gel (230–400 mesh, Silicycle). The NMR spectra were obtained using a Brüker 500 MHz Fourier-transform NMR spectrometer. Chemical shifts are reported in units of parts per million (ppm) downfield from tetramethylsilane (TMS), and all coupling constants are reported in hertz. The infrared spectra were taken with KBr plates with a Perkin-Elmer Spectrum 1600 Series spectrometer. High resolution mass spectrometry (HRMS) data were obtained on a Waters LC-TOF mass spectrometer (model LCT-XE Premier) using chemical ionization (CI) or electrospray ionization (ESI) in positive or negative mode, depending on the analyte. Melting points were determined on a Mel-Temp melting point apparatus and were uncorrected.

Preparation of Aryl Benzyl Sulfoxide: Sulfoxides were prepared according to the literature procedures.[1,2]

Preparation of Palladacyclic Precursors: Palladacyclic precursors were prepared according to the literature procedures.[3,4]

Procedure and Characterization for the Palladium Catalyzed Generation of Diaryl Sulfoxides.

General Procedure for catalysis: To an oven-dried microwave vial equipped with a stir bar was added precatalyst P2 (9.3 mg, 0.01 mmol), LiO^tBu (48.3 mg, 0.60 mmol, 3 equiv), and benzyl phenyl sulfoxide (43.2 mg, 0.20 mmol, 1 equiv) under nitrogen atmosphere in a glove box. DME (2.0 mL) was added to

the vial by syringe. The microwave vial was sealed and removed from the glove box. Then, 4-*tert*-butyl chlorobenzene (67.3 µL, 0.40 mmol, 2.0 equiv) was added by syringe under nitrogen atmosphere. Note that solid aryl chlorides were added to the reaction vial prior to LiO^tBu. The reaction mixture was heated to 110 °C in an oil bath and stirred for 24 h. Upon completion, the sealed vial was cooled to room temperature and open to air. The reaction mixture was passed through a short pad of silica gel and rinsed with 5.0 mL EtOAc. The solvent was removed under reduced pressure to yield a colorless solid. The residue was purified by flash chromatography as outlined below.

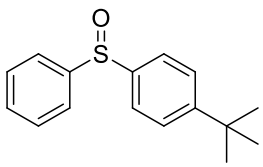

1-(*tert*-Butyl)-4-(phenylsulfinyl)benzene (3a): The reaction was performed following the General Procedure with P2 (9.3 mg, 0.01 mmol), 1a (43.2 mg, 0.20 mmol), LiO^tBu (48.0 mg, 0.60 mmol) in 2.0 mL DME, and 4-*tert*-butyl chlorobenzene (2a) (67.3 µL, 0.40 mmol) at 110 °C for 24 h. The crude product was purified by flash chromatography on silica gel (eluted with EtOAc:hexanes = 1:4) to give the product (36.2 mg, 70% yield) as a white solid. R_f = 0.4 (hexanes:EtOAc = 2:1). The spectroscopic data match the previously reported data.[5]

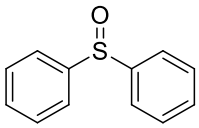

Diphenyl sulfoxide (3b): The reaction was performed following the General Procedure with P2 (9.3 mg, 0.01 mmol), 1a (43.2 mg, 0.20 mmol), LiO^tBu (48.0 mg, 0.60 mmol) in 2.0 mL DME, and chlorobenzene (2b) (40.6 µL, 0.40 mmol) at 110 °C for 24 h. The crude product was purified by flash chromatography on silica gel (eluted with EtOAc:hexanes = 1:4) to give the product (29.1 mg, 72% yield) as a white solid. R_f = 0.4 (hexanes:EtOAc = 2:1). The spectroscopic data match the previously reported data.[6]

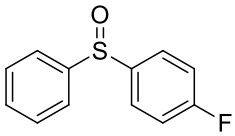

1-Fluoro-4-(phenylsulfinyl)benzene (3c): The reaction was performed following the General Procedure with P2 (9.3 mg, 0.01 mmol), 1a (43.2 mg, 0.20 mmol), LiO^tBu (48.0 mg, 0.60 mmol) in 2.0 mL DME, and 1-chloro-4-fluorobenzene (2c) (42.6 µL, 0.40 mmol) at 110 °C for 24 h. The crude product was purified by flash

Chapter V

chromatography on silica gel (eluted with EtOAc:hexanes = 1:4) to give the product (37.4 mg, 85% yield) as a white solid. R_f = 0.4 (hexanes:EtOAc = 2:1). The spectroscopic data match the previously reported data.[6]

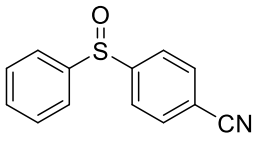

4-(Phenylsulfinyl)benzonitrile (3d): The reaction was performed following the General Procedure with P2 (9.3 mg, 0.01 mmol), 1a (43.2 mg, 0.20 mmol), LiO^tBu (48.0 mg, 0.60 mmol) in 2.0 mL DME, and 4-chlorobenzonitrile (2d) (55.0 mg, 0.40 mmol) at 110 °C for 24 h. The crude product was purified by flash chromatography on silica gel (eluted with EtOAc:hexanes = 1:4) to give the product (28.6 mg, 63% yield) as a white solid. R_f = 0.4 (hexanes:EtOAc = 2:1). The spectroscopic data match the previously reported data.[7]

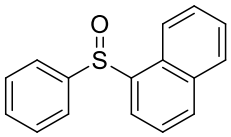

1-(Phenylsulfinyl)naphthalene (3e): The reaction was performed following the General Procedure with P2 (9.3 mg, 0.01 mmol), 1a (43.2 mg, 0.20 mmol), LiO^tBu (48.0 mg, 0.60 mmol) in 2.0 mL DME, and 1-chloronaphthlaene (2e) (54.5 µL, 0.40 mmol) at 110 °C for 24 h. The crude product was purified by flash chromatography on silica gel (eluted with EtOAc:hexanes = 1:5) to give the product (35.3 mg, 70% yield) as a white solid. R_f = 0.5 (hexanes:EtOAc = 4:1). The spectroscopic data match the previously reported data.[5]

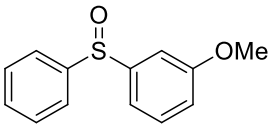

1-Methoxy-3-(phenylsulfinyl)benzene (3f): The reaction was performed following the General Procedure with P2 (9.3 mg, 0.01 mmol), 1a (43.2 mg, 0.20 mmol), LiO^tBu (48.0 mg, 0.60 mmol) in 2.0 mL DME, and 3-chloroanisole (2f) (49.0 µL, 0.40 mmol) at 110 °C for 24 h. The crude product was purified by flash chromatography on silica gel (eluted with EtOAc:hexanes = 1:4) to give the product (40.4 mg, 87% yield) as a white solid. R_f = 0.3 (hexanes:EtOAc = 2:1). The spectroscopic data match the previously reported data.[6]

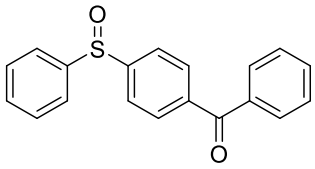

Phenyl(4-(phenylsulfinyl)phenyl)methanone (3g): The reaction was performed following the General Procedure with P2 (9.3 mg, 0.01 mmol), 1a (43.2 mg, 0.20 mmol), LiO^{t}Bu (48.0 mg, 0.60 mmol) in 2.0 mL DME, and 4-chlorobenzophenone (2g) (86.7 mg, 0.40 mmol) at 110 °C for 24 h. The crude product was purified by flash chromatography on silica gel (eluted with EtOAc:hexanes = 1:10) to give the product (44.1 mg, 72% yield) as a white solid. R_f = 0.5 (hexanes:EtOAc = 2:1); m.p. = 77–79 °C; ^{1}H NMR (500 MHz, $CDCl_3$): δ 7.84 (d, *J* = 8 Hz, 2H), 7.74 (d, *J* = 8 Hz, 4H), 7.68 – 7.66 (m, 2H), 7.58 (t, *J* = 7.5 Hz, 1H), 7.47 – 7.44 (m, 5H) ppm; ^{13}C{^{1}H} NMR (125 MHz, $CDCl_3$): δ 195.5, 149.9, 145.1, 139.8, 136.8, 132.9, 131.5, 130.7, 130.0, 129.6, 128.5, 124.9, 124.4 ppm; IR (thin film): 1660, 1590, 1441, 1394, 1317, 1305, 1276, 1090, 1048, 924, 700, 660 cm^{-1}; HRMS calculated for $C_{19}H_{15}O_2S$ 307.0793, found 307.0786 $[M+H]^+$.

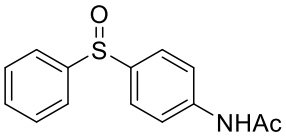

N-(4-(phenylsulfinyl)phenyl)acetamide (3h): The reaction was performed following the General Procedure with P2 (9.3 mg, 0.01 mmol), 1a (43.2 mg, 0.20 mmol), LiO^{t}Bu (80.0 mg, 1.00 mmol) in 2.0 mL DME, and 4'-chloroacetanilide (2h) (67.8 mg, 0.40 mmol) at 110 °C for 24 h. The crude product was purified by flash chromatography on silica gel (eluted with EtOAc:hexanes = 1:1) to give the product (37.8 mg, 73% yield) as a white solid. R_f = 0.2 (hexanes:EtOAc = 1:1). ^{1}H NMR (500 MHz, $CDCl_3$): δ 8.70 (s, 1H), 7.61 (d, *J* = 8.5 Hz, 2H), 7.57 – 7.55 (m, 2H), 7.48 (d, *J* = 8.5 Hz, 2H), 7.44 – 7.41 (m, 3H), 2.10 (s, 3H) ppm; ^{13}C{^{1}H} NMR (125 MHz, $CDCl_3$): δ 169.2, 144.9, 141.4, 139.2, 131.1, 129.3, 126.2, 124.6, 120.3, 24.4 ppm; IR (thin film): 3265, 1696, 1678, 1590, 1533, 1398, 1314, 1260, 1089, 1032, 833, 749cm^{-1}; HRMS calculated for $C_{14}H_{14}O_2SN$ 260.0745, found 260.0743 $[M+H]^+$. Melting point was previously reported.[8]

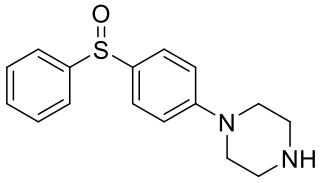

1-(4-(Phenylsulfinyl)phenyl)piperazine (3i): The reaction was performed following the General Procedure with P2 (9.3 mg, 0.01 mmol), 1a (43.2 mg, 0.20 mmol), LiO^{t}Bu (80.0 mg, 1.00 mmol) in 2.0 mL DME, and 4'-

chloroacetanilide (2i) (67.8 mg, 0.40 mmol) at 110 °C for 24 h. The crude product was purified by flash chromatography on silica gel (eluted with EtOAc:hexanes = 1:4) to give the product (37.8 mg, 73% yield) as a white solid. m.p. = 80–82 °C; R_f = 0.4 (hexanes:EtOAc = 4:1). ^{1}H NMR (500 MHz, $CDCl_3$): δ 7.68 (d, *J* = 6 Hz, 2H), 7.53 –7.50 (m, 3H), 7.31 (d, *J* = 9 Hz, 2H), 6.74 (d, *J* = 9 Hz, 2H), 3.31 –3.12 (m, 8H), ppm; ^{13}C{^{1}H} NMR (125 MHz, $CDCl_3$): δ 150.0, 142.6, 131.9, 131.1, 128.9, 126.2, 118.2, 112.6, 49.6, 45.6 ppm; IR (thin film): 2920, 2451, 1498, 1455, 1349, 1254, 1149, 810, 752, 699 cm^{-1}; HRMS calculated for $C_{16}H_{19}OSN_2$ 287.1218, found 287.1424 $[M+H]^+$.

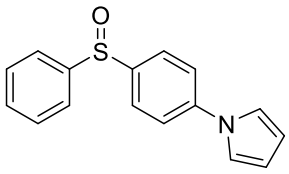

1-(4-(Phenylsulfinyl)phenyl)-1H-pyrrole (3j): The reaction was performed following the General Procedure with P2 (9.3 mg, 0.01 mmol), 1a (43.2 mg, 0.20 mmol), Li*O*^{t}Bu (48.0 mg, 0.60 mmol) in 2.0 mL DME, and 1-(4-chlorophenyl)-1H-pyrrole (2j) (67.8 mg, 0.40 mmol) at 110 °C for 24 h. The crude product was purified by flash chromatography on silica gel (eluted with EtOAc:hexanes = 1:4) to give the product (41.7 mg, 78% yield) as a white solid. R_f = 0.4 (hexanes:EtOAc = 4:1). m.p. = 104–106 °C; ^{1}H NMR (500 MHz, $CDCl_3$): δ 7.68 – 7.64 (m, 4H), 7.49 – 7.44 (m, 5H), 7.06 (d, *J* = 4.5 Hz, 2H), 6.34 (d, *J* = 4.5 Hz, 2H) ppm; ^{13}C{^{1}H} NMR (125 MHz, $CDCl_3$): δ 145.4, 142.8, 142.1, 131.2, 129.4, 126.5, 124.7, 120.7, 119.1, 111.4 ppm; IR (thin film): 1596, 1510, 1331, 1089, 1047, 919, 824, 726 cm^{-1}; HRMS calculated for $C_{16}H_{14}OSN$ 268.0796, found 268.0793 $[M+H]^+$.

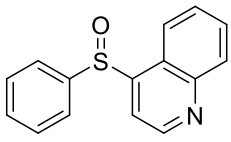

4-(Phenylsulfinyl)quinoline (3k): The reaction was performed following the General Procedure with P2 (18.6 mg, 0.02 mmol), 1a (43.2 mg, 0.20 mmol), Li*O*^{t}Bu (48.0 mg, 0.60 mmol) in 2.0 mL DME, and 4-chloroquinoline (2k) (65.4 mg, 0.40 mmol) at 110 °C for 24 h. The crude product was purified by flash chromatography on silica gel (eluted with EtOAc:hexanes = 1:4) to give the product (40.0 mg, 79% yield) as a white solid. R_f = 0.4 (hexanes:EtOAc = 4:1). m.p. = 88–90 °C; ^{1}H NMR (500 MHz, $CDCl_3$): δ 8.88 (d, *J* = 2.0 Hz, 1H), 8.61 (d, *J* = 2.0 Hz, 1H), 8.13 (d, *J* = 8.5 Hz, 1H), 7.94 (d, *J* = 8.5 Hz, 1H), 7.81 (dt, *J* = 7.8, 1.5 Hz, 1H), 7.74 – 7.72 (m, 2H), 7.65 (dt, , *J* = 7.8, 1.5 Hz, 1H), 7.51 – 7.48 (m, 3H); ^{13}C{^{1}H} NMR (125 MHz, $CDCl_3$): δ

148.8, 145.9, 144.5, 138.9, 133.0, 131.7, 131.4, 129.7, 129.6, 128.5, 128.0, 127.3, 125.0 ppm; IR (thin film): 3057, 1581, 1565, 1494, 1443, 1358, 1086, 1048, 786, 749, 689 cm^{-1}; HRMS calculated for $C_{15}H_{12}OSN$ 254.0640, found 254.0639 $[M+H]^+$.

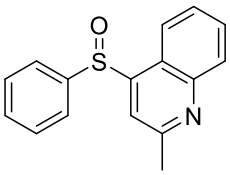

2-Methyl-4-(phenylsulfinyl)quinoline (3l): The reaction was performed following the General Procedure with P2 (9.3 mg, 0.01 mmol), 1a (43.2 mg, 0.20 mmol), Li*O*^{t}Bu (48.0 mg, 0.60 mmol) in 2.0 mL DME, and 4-chloro-2-methyl quinoline (2l) (71.1 mg, 0.40 mmol) at 110 °C for 48 h. The crude product was purified by flash chromatography on silica gel (eluted with EtOAc:hexanes = 1:4) to give the product (43.3 mg, 81% yield) as a white solid. R_f = 0.4 (hexanes:EtOAc = 4:1). m.p. = 139–141 °C; ^{1}H NMR (500 MHz, $CDCl_3$): δ 8.05 (d, *J* = 8.5 Hz, 1H), 8.02 (s, 1H), 7.94 (d, *J* = 8.0 Hz, 1H), 7.70 – 7.67(m, 3H), 7.48 (t, *J* = 8.0 Hz, 1H), 7.41 – 7.39 (m, 3H), 2.82 (s, 3H) ppm; ^{13}C{^{1}H} NMR (125 MHz, $CDCl_3$): δ 159.4, 151.4, 148.0, 143.8, 131.8, 130.1, 129.7, 129.6, 126.7, 125.7, 122.1, 121.9, 117.1, 25.7 ppm; IR (thin film): 2922, 1587, 1555, 1497, 1442, 1401, 1080, 1052, 756, 690 cm^{-1}; HRMS calculated for $C_{16}H_{14}OSN$ 268.0796, found 268.0814 $[M+H]^+$.

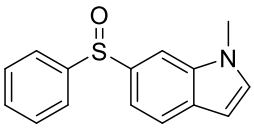

1-Methyl-6-(phenylsulfinyl)-1*H*-indole (3m): The reaction was performed following the General Procedure with P2 (9.3 mg, 0.01 mmol), 1a (43.2 mg, 0.20 mmol), Li*O*^{t}Bu (48.0 mg, 0.60 mmol) in 2.0 mL DME, and 6-chloro-1-methyl-1*H*-indole (2m) (66.2 mg, 0.40 mmol) at 110 °C for 48 h. The crude product was purified by flash chromatography on silica gel (eluted with EtOAc:hexanes = 1:4) to give the product (37.7 mg, 74% yield) as a colorless vicious oil. R_f = 0.4 (hexanes:EtOAc = 4:1). ^{1}H NMR (500 MHz, $CDCl_3$): δ 7.81 (s, 1H), 7.65 – 7.61 (m, 3H), 7.43 – 7.38 (m, 3H), 7.17 (dd, *J* = 8.0, 1.0 Hz, 1H), 7.14 (d, *J* = 3.0 Hz, 1H), 6.48 (d, *J* = 3.0 Hz, 1H), 3.82 (s, 3H) ppm; ^{13}C{^{1}H} NMR (125 MHz, $CDCl_3$): δ 146.4, 138.0, 136.3, 131.3, 130.7, 130.6, 129.1, 124.8, 121.7, 115.9, 106.7, 101.5, 33.1 ppm; IR (thin film): 2925, 1506, 1473, 1442, 1339, 1302, 1081, 1039, 809, 748, 733, 689 cm^{-1}; HRMS calculated for $C_{15}H_{14}OSN$ 256.0796, found 256.0788 $[M+H]^+$.

Chapter V

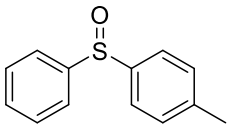

1-Methyl-4-(phenylsulfinyl)benzene (3n): The reaction was performed following the General Procedure with P2 (9.3 mg, 0.01 mmol), 1n (46.1 mg, 0.20 mmol), LiO^{t}Bu (48.0 mg, 0.60 mmol) in 2.0 mL DME, and chlorobenzene (2b) (40.6 μL, 0.40 mmol) at 110 °C for 24 h. The crude product was purified by flash chromatography on silica gel (eluted with EtOAc:hexanes = 1:4) to give the product (33.7 mg, 78% yield) as a white solid. R_f = 0.4 (hexanes:EtOAc = 2:1). The spectroscopic data match the previously reported data.[6]

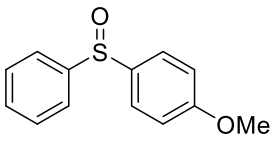

1-Methoxyl-4-(phenylsulfinyl)benzene (3o): The reaction was performed following the General Procedure with P2 (9.3 mg, 0.01 mmol), 1o (49.2 mg, 0.20 mmol), LiO^{t}Bu (48.0 mg, 0.60 mmol) in 2.0 mL DME, and chlorobenzene (2b) (40.6 μL, 0.40 mmol) at 110 °C for 24 h. The crude product was purified by flash chromatography on silica gel (eluted with EtOAc:hexanes = 1:2) to give the product (38.5 mg, 83% yield) as a white solid. R_f = 0.2 (hexanes:EtOAc = 2:1). The spectroscopic data match the previously reported data.[9]

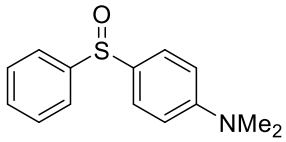

N,*N*-dimethyl-4-(phenylsulfinyl)aniline (3p): The reaction was performed following the General Procedure with P2 (9.3 mg, 0.01 mmol), 1p (51.8 mg, 0.20 mmol), LiO^{t}Bu (48.0 mg, 0.60 mmol) in 2.0 mL DME, and chlorobenzene (2b) (60.9 μL, 0.60 mmol) at 110 °C for 24 h. The crude product was purified by flash chromatography on silica gel (eluted with EtOAc:hexanes = 1:1) to give the product (39.7 mg, 81% yield) as a white solid. R_f = 0.2 (hexanes:EtOAc = 1:1). The spectroscopic data match the previously reported data.[5]

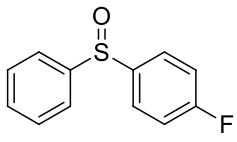

1-Fluoro-4-(phenylsulfinyl)benzene (3c) (from 1-(benzylsulfinyl)-4-fluorobenzene): The reaction was performed following the General Procedure with P2 (9.3 mg, 0.01 mmol), 1c (46.8 mg, 0.20 mmol), LiO^{t}Bu (48.0 mg, 0.60 mmol) in 2.0 mL DME, and chlorobenzene (2b) (40.6 μL, 0.40 mmol) at 110 °C for 24 h. The crude

product was purified by flash chromatography on silica gel (eluted with EtOAc:hexanes = 1:4) to give the product (34.3 mg, 78% yield) as a white solid. R_f = 0.4 (hexanes:EtOAc = 2:1). The spectroscopic data match the previously reported data.[6]

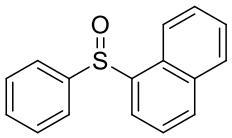

1-(Phenylsulfinyl)naphthalene (3e) (from1-(benzylsulfinyl)naphthalene): The reaction was performed following the General Procedure with P2 (9.3 mg, 0.01 mmol), 1-(benzylsulfinyl)naphthalene (1e) (53.2 mg, 0.20 mmol), LiO^{t}Bu (48.0 mg, 0.60 mmol) in 2.0 mL DME, and chlorobenzene (2b) (40.6 µL, 0.40 mmol) at 110 °C for 24 h. The crude product was purified by flash chromatography on silica gel (eluted with EtOAc:hexanes = 1:4) to give the product (41.3 mg, 81% yield) as a white solid. R_f = 0.5 (hexanes:EtOAc = 2:1). The spectroscopic data match the previously reported data.[5]

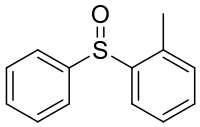

1-Methyl-2-(phenylsulfinyl)benzene (3q): The reaction was performed following the General Procedure with P2 (9.3 mg, 0.01 mmol), 1-(benzylsulfinyl)-2-methylbenzene (1q) (46.0 mg, 0.20 mmol), LiO^{t}Bu (48.0 mg, 0.60 mmol) in 2.0 mL DME, and chlorobenzene (2b) (40.6 µL, 0.40 mmol) at 110 °C for 24 h. The crude product was purified by flash chromatography on silica gel (eluted with EtOAc:hexanes = 1:4) to give the product (34.6 mg, 80% yield) as a white solid. R_f = 0.4 (hexanes:EtOAc = 2:1). The spectroscopic data match the previously reported data.[6]

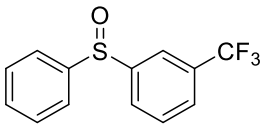

1-(Phenylsulfinyl)-3-(trifluoromethyl)benzene (3r): The reaction was performed following the General Procedure with P2 (9.3 mg, 0.01 mmol), 1-(benzylsulfinyl)-3-(trifluoromethyl)benzene (1r) (56.8 mg, 0.20 mmol), LiO^{t}Bu (48.0 mg, 0.60 mmol) in 2.0 mL DME, and chlorobenzene (2b) (40.6 µL, 0.40 mmol) at 110 °C for 24 h. The crude product was purified by flash chromatography on silica gel (eluted with EtOAc:hexanes = 1:4) to give the product (41.6 mg, 77% yield) as a white solid. R_f = 0.4 (hexanes:EtOAc = 2:1). ^{1}H NMR (500 MHz, $CDCl_3$): δ 7.93 (s, 1H), 7.77 (d, J = 7.5 Hz, 1H), 7.64 – 7.63 (m, 3H), 7.55 (t, J = 7.5 Hz, 1H), 7.47

– 7.44 (m, 3H) ppm; $^{13}C\{^{1}H\}$ NMR (125 MHz, $CDCl_3$): δ 147.2, 144.8, 132.1(q, J = 33.3 Hz), 131.6, 129.9, 129.6, 127.8, 127.6 (q, J = 4.8 Hz), 124.7, 123.3 (q, J = 271.5 Hz), 121.4 (q, J = 3.8 Hz) ppm; IR (thin film): 3055, 2924, 1580, 1476, 1443, 1090, 1045, 1021, 997, 742, 694 cm^{-1}; HRMS calculated for $C_{13}H_{10}OSF_3$ 271.0404, found 271.0406 $[M+H]^+$. Melting point was previously reported.[10]

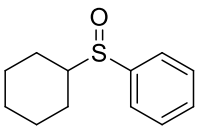

(Cyclohexylsulfinyl)benzene (3s): The reaction was performed following the General Procedure with P2 (9.3 mg, 0.01 mmol), ((cyclohexylsulfinyl)methyl)benzene (1s) (44.4 mg, 0.20 mmol), LiO^{t}Bu (48.0 mg, 0.60 mmol) in 2.0 mL DME, and chlorobenzene (2b) (40.6 μL, 0.40 mmol) at 110 °C for 24 h. The crude product was purified by flash chromatography on silica gel (eluted with EtOAc:hexanes = 1:2) to give the product (37.2 mg, 72% yield) as a pale yellow solid. R_f = 0.1 (hexanes:EtOAc = 2:1). The spectroscopic data match the previously reported data.[6]

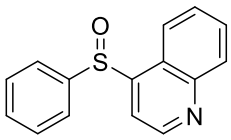

4-(Phenylsulfinyl)quinoline (3k) (from 4-(benzylsulfinyl)quinoline)): The reaction was performed following the General Procedure with P2 (18.6 mg, 0.02 mmol), 4-(benzylsulfinyl)quinoline (1k) (53.5 mg, 0.20 mmol), LiO^{t}Bu (48.0 mg, 0.60 mmol) in 2.0 mL DME, and chlorobenzene (2b) (40.6 μL, 0.40 mmol) at 110 °C for 24 h. The crude product was purified by flash chromatography on silica gel (eluted with EtOAc:hexanes = 1:4) to give the product (33.9 mg, 67% yield) as a white solid. R_f = 0.4 (hexanes:EtOAc = 4:1).

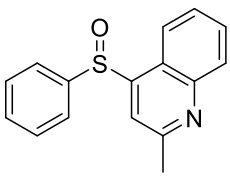

2-Methyl-4-(phenylsulfinyl)quinoline (3l) (5 mmol scale): To an oven-dried Schlenk flask equipped with a stir bar was added P2 (231.5 mg, 0.5 mmol), LiO^{t}Bu (1.2 g, 15.0 mmol, 3 equiv), benzyl phenyl sulfoxide (1.08 g, 5.0 mmol, 1 equiv), 4-chloro-2-methyl quinoline (2l) (1.78 g, 10.0 mmol, 2 equiv) at 110 °C for 24 h under nitrogen atmosphere in a glove box. DME (50.0 mL) was added to the Schlenk flask by syringe. The Schlenk flask was sealed by septa, and removed from the glove box. Under a flow of nitrogen, it was equipped with a condenser and purged. The reaction mixture was heated to 110 °C with an oil bath and stirred for

24 h. Upon completion, the Schlenk flask was cooled to room temperature and open to air. The reaction mixture was passed through a short pad of silica gel, and rinsed with EtOAc. The solvent was removed under reduced pressure to yield a colorless solid. R_f = 0.4 (hexanes:EtOAc = 4:1).

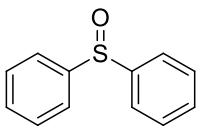

Diphenyl sulfoxide (3b) (from methyl phenyl sulfoxide): The reaction was performed following the General Procedure with P2 (9.3 mg, 0.01 mmol), methyl phenyl sulfoxide (1t) (28.0 mg, 0.20 mmol), LiO^{t}Bu (64.0 mg, 0.80 mmol, 4 equiv) in 2.0 mL DME, and chlorobenzene (2b) (81.2 μL, 0.80 mmol, 4 equiv) at 110 °C for 48 h. The crude product was purified by flash chromatography on silica gel (eluted with EtOAc:hexanes = 1:4) to give the product (31.1 mg, 77% yield) as a white solid. R_f = 0.4 (hexanes:EtOAc = 2:1). The spectroscopic data match the previously reported data.[6]

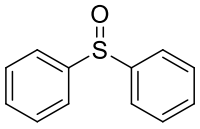

Diphenyl sulfoxide (3b) (from dibenzyl sulfoxide): The reaction was performed following the General Procedure with P2 (18.6 mg, 0.02 mmol), diphenyl sulfoxide (1u) (46.0 mg, 0.20 mmol), LiO^{t}Bu (96.0 mg, 1.20 mmol, 6 equiv) in 2.0 mL DME, and chlorobenzene (2b) (121.8 μL, 1.20 mmol, 6 equiv) at 110 °C for 72 h. The crude product was purified by flash chromatography on silica gel (eluted with EtOAc:hexanes = 1:4) to give the product (23.0 mg, 57% yield) as a white solid. R_f = 0.4 (hexanes:EtOAc = 2:1). The spectroscopic data match the previously reported data.[6]

Chapter V

References:

1. Renaud, P.; Bourquard, T.; Carrupt, P.-A.; Gerster, M. *Helv. Chim. Acta* 1998, *81*, 1048.
2. Holland, H. L.; Turner, C. D.; Andreana, P. R.; Nguyen, D. *Can. J. Chem.* 1999, *77*, 463.
3. Bruno, N. C.; Tudge, M. T.; Buchwald, S. L. *Chem. Sci.* 2013, *4*, 916.
4. Zhang, J.; Bellomo, A.; Trongsiriwat, N.; Jia, T.; Carroll, P. J.; Dreher, S. D.; Tudge, M. T.; Yin, H.; Robinson, J. R.; Schelter, E. J.; Walsh, P. J. *J. Am. Chem. Soc.* 2014, *136*, 6276.
5. Jia, T.; Bellomo, A.; Montel, S.; Zhang, M.; El Baina, K.; Zheng, B.; Walsh, P. J. *Angew. Chem., Int. Ed.* 2014, *53*, 260.
6. Xu, H.-J.; Lin, Y.-C.; Wan, X.; Yang, C.-Y.; Feng, Y.-S. *Tetrahedron* 2010, *66*, 8823.
7. Das, R.; Chakraborty, D. *Tetrahedron Lett.* 2010, *51*, 6255.
8. Szmant, H. H.; McIntosh, J. J. *J. Am. Chem. Soc.* 1951, *73*, 4356.
9. Bernoud, E.; Le Duc, G.; Bantreil, X.; Prestat, G.; Madec, D.; Poli, G. *Org. Lett.* 2010, *12*, 320.
10. Monsanto Co. Patent: NL286724, 1962.

NMR Spectra

1-(*tert*-Butyl)-4-(phenylsulfinyl)benzene (3a)

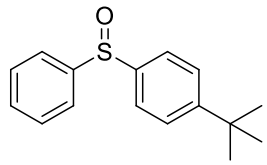

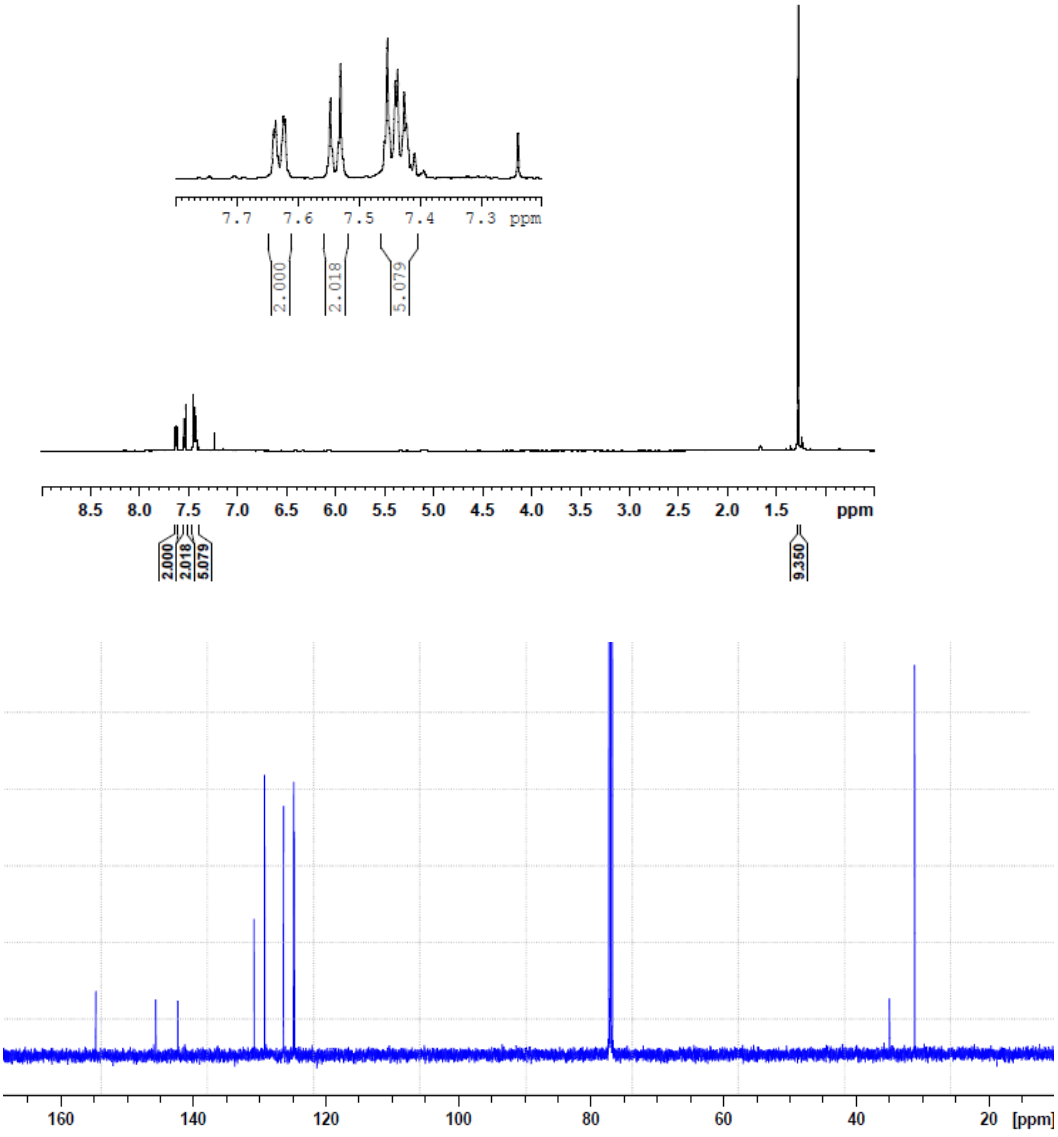

Figure S1. ^{1}H (500 MHz) and ^{13}C $\{^{1}H\}$ (125 MHz) NMR spectra of 3a in $CDCl_3$.

Chapter V

Diphenyl sulfoxide (3b)

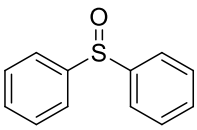

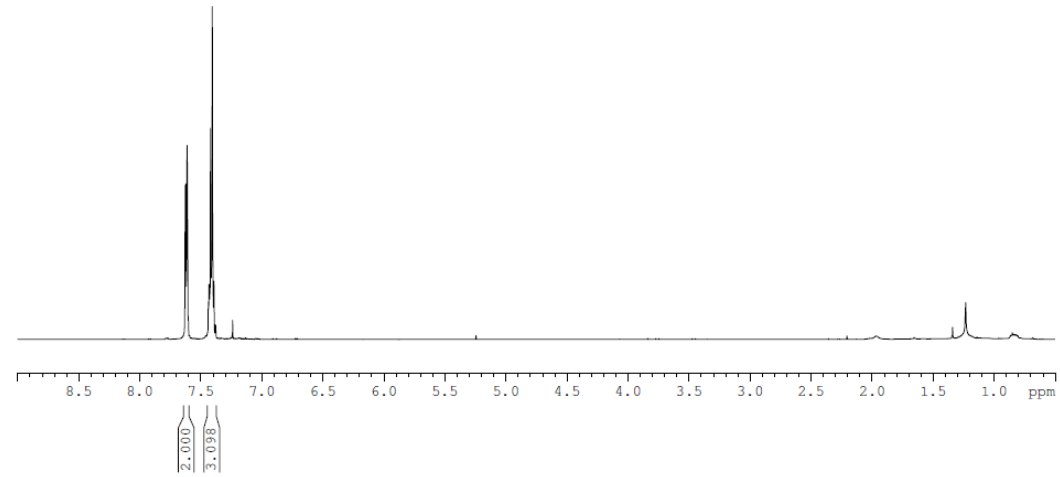

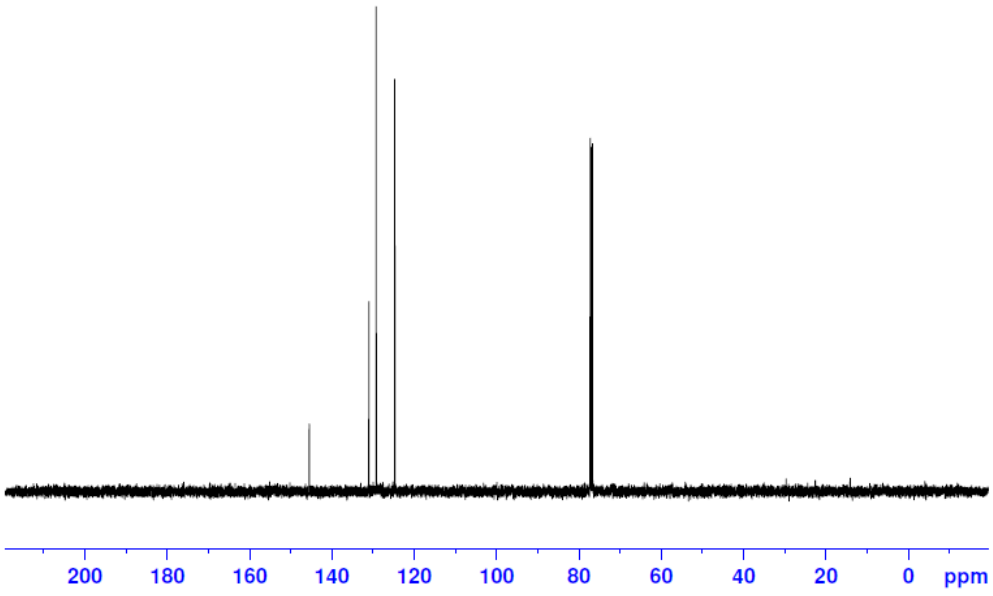

Figure S2. ^{1}H (500 MHz) and ^{13}C $\{^{1}H\}$ (125 MHz) NMR spectra of 3b in $CDCl_3$.

1-Fluoro-4-(phenylsulfinyl)benzene (3c)

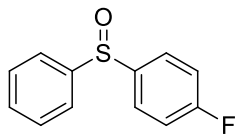

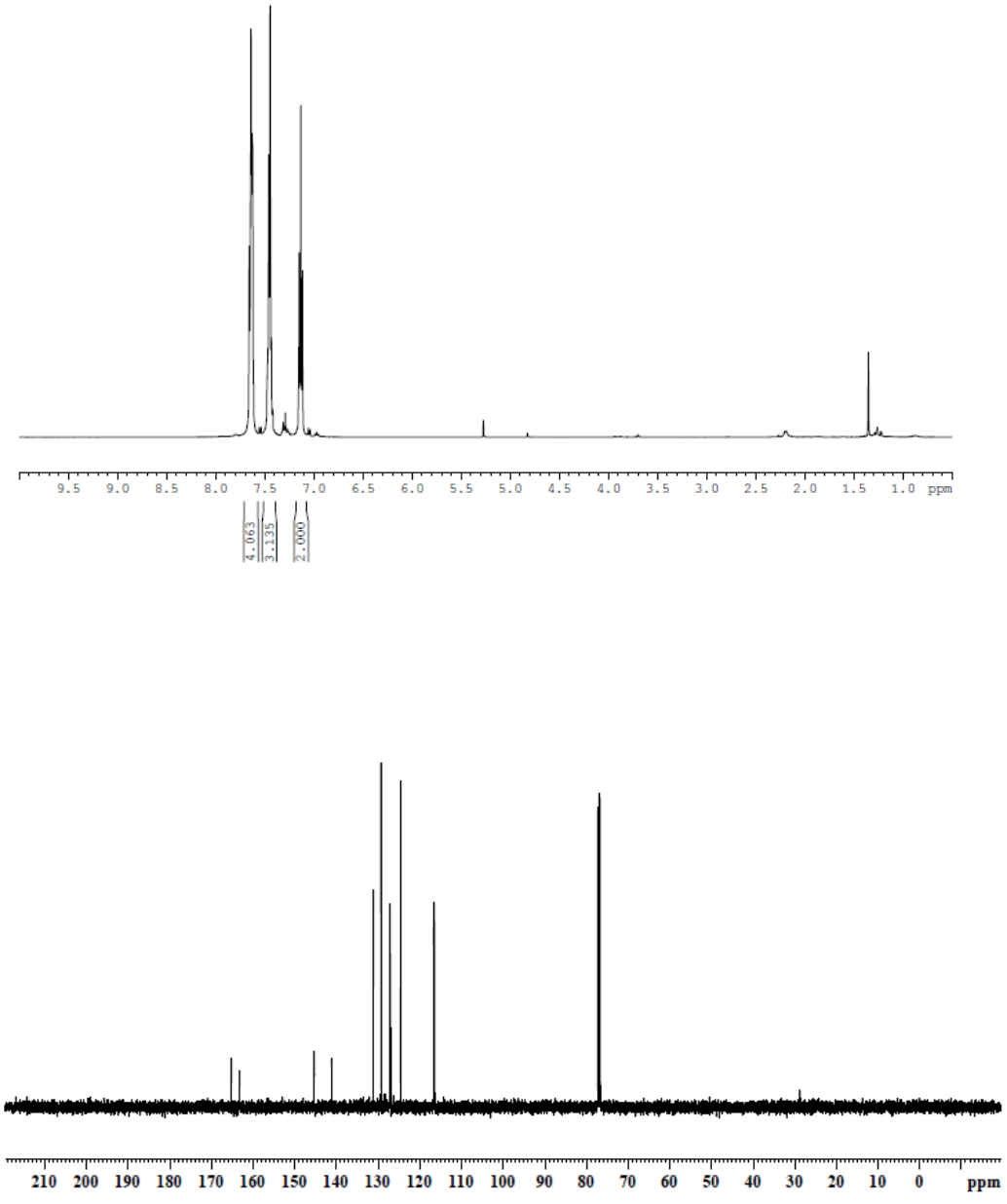

Figure S3. ^{1}H (500 MHz) and ^{13}C $\{^{1}H\}$ (125 MHz) NMR spectra of 3c in $CDCl_3$.

Chapter V

4-(Phenylsulfinyl)benzonitrile (3d)

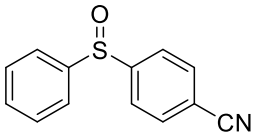

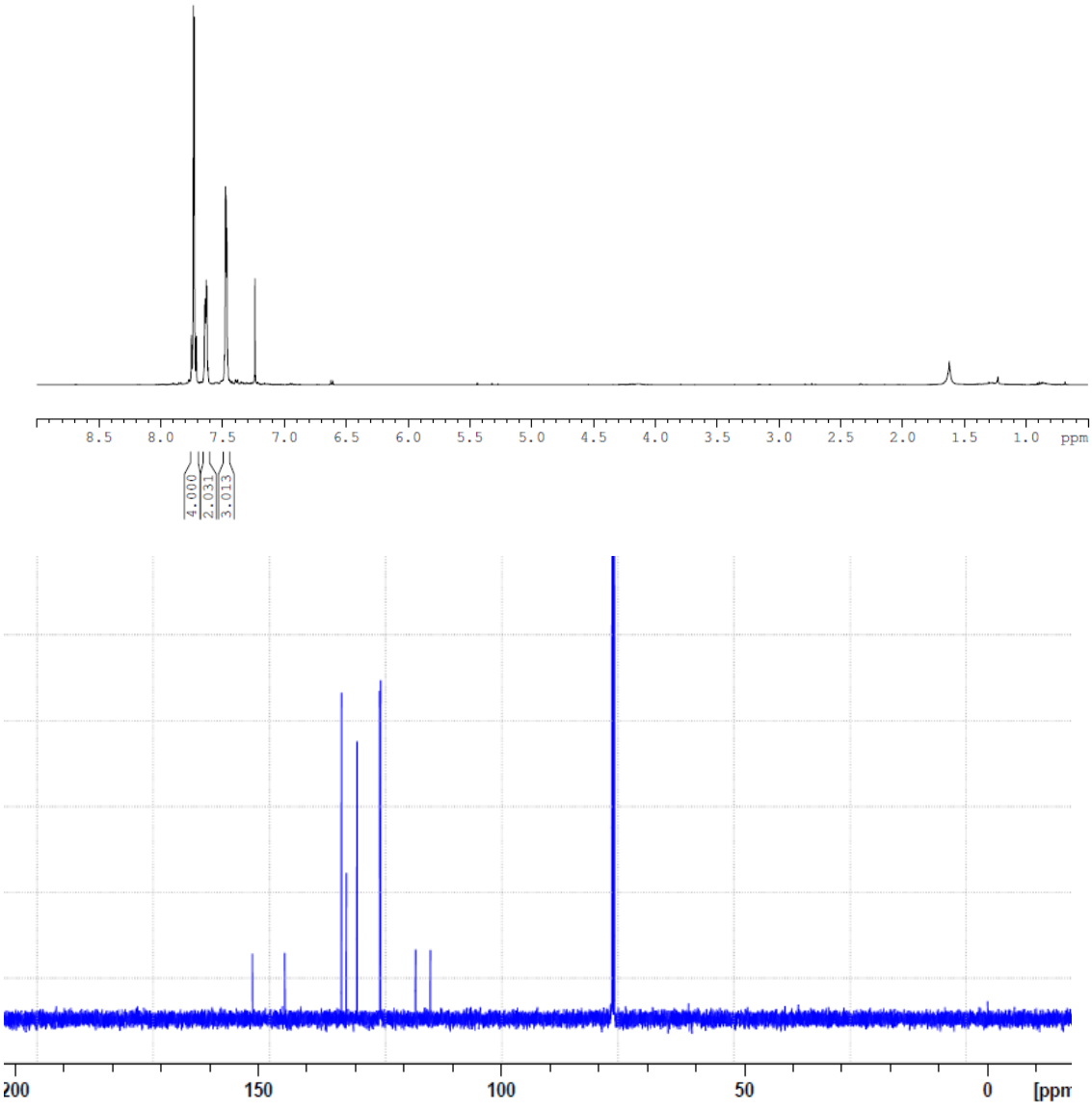

Figure S4. ^{1}H (500 MHz) and $^{13}C\{^{1}H\}$ (125 MHz) NMR spectra of 3d in $CDCl_3$.

1-(Phenylsulfinyl)naphthalene (3e)

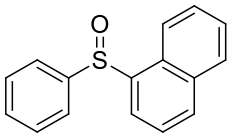

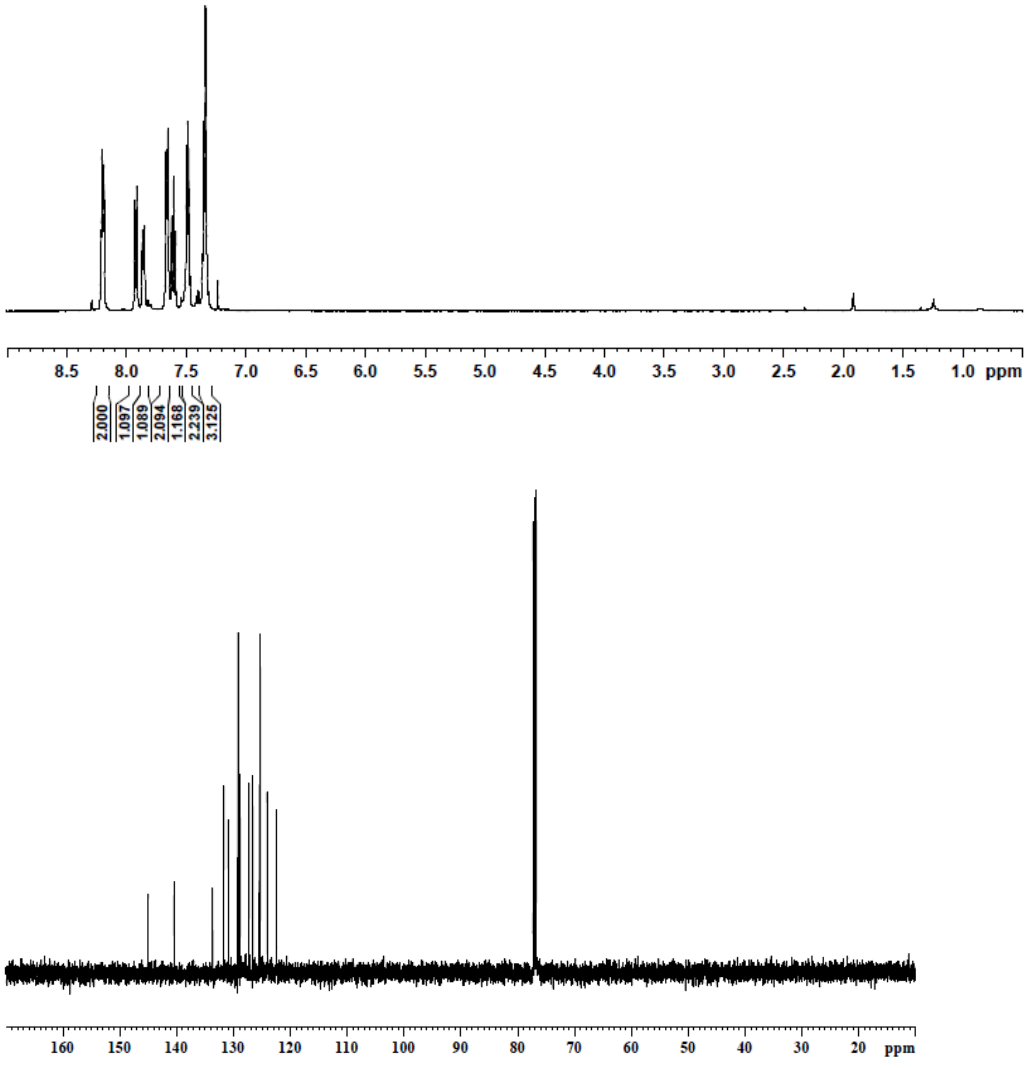

Figure S5. ^{1}H (500 MHz) and ^{13}C $\{^{1}H\}$ (125 MHz) NMR spectra of 3e in $CDCl_3$.

Chapter V

1-Methoxy-3-(phenylsulfinyl)benzene (3f)

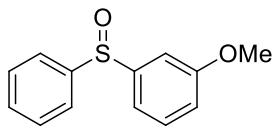

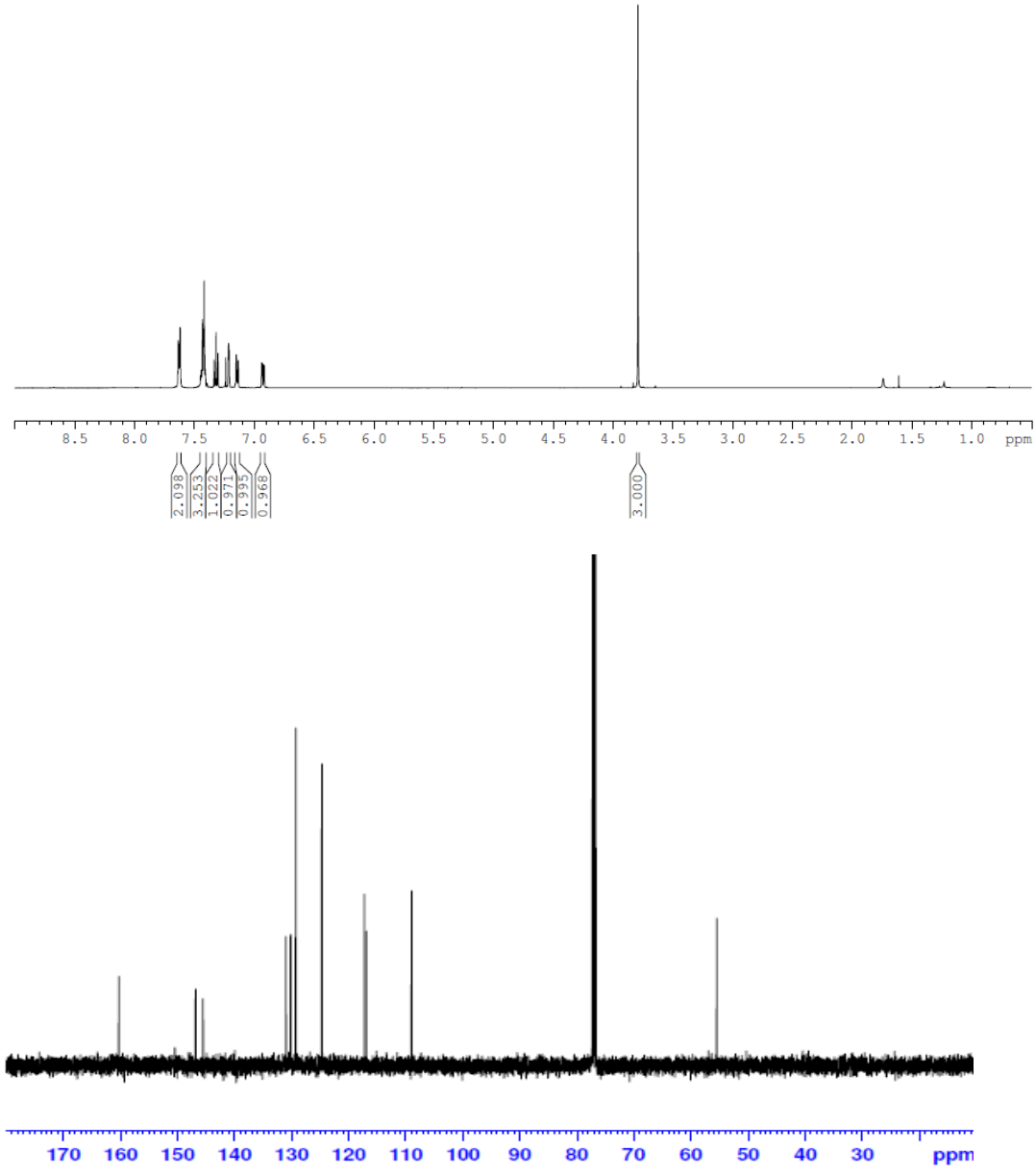

Figure S6. ^{1}H (500 MHz) and $^{13}C\{^{1}H\}$ (125 MHz) NMR spectra of 3f in $CDCl_3$.

Phenyl(4-(phenylsulfinyl)phenyl)methanone (3g)

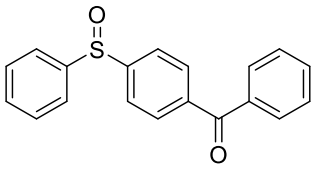

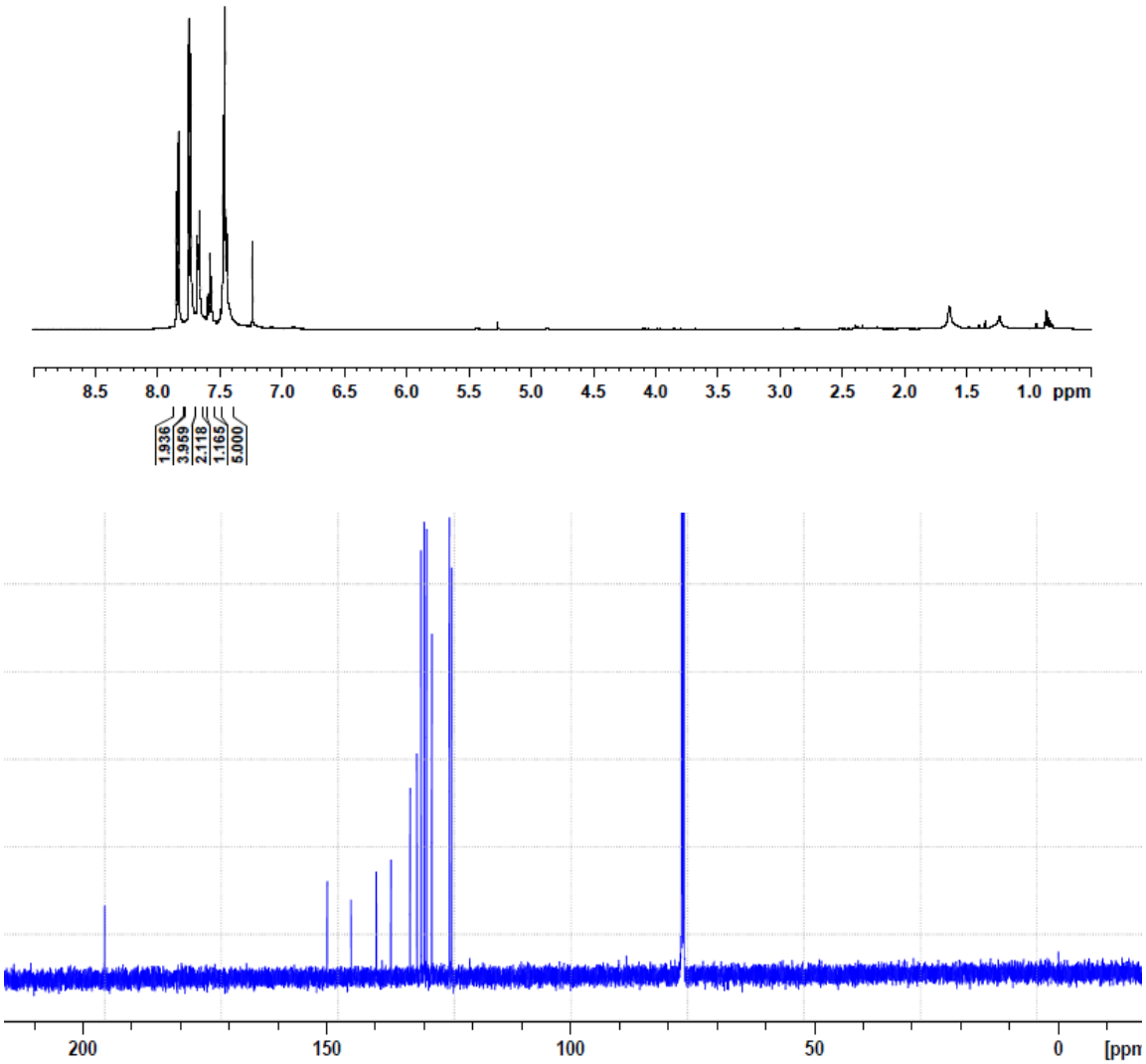

Figure S7. ^{1}H (500 MHz) and ^{13}C $\{^{1}H\}$ (125 MHz) NMR spectra of 3g in $CDCl_3$.

Chapter V

N-(4-(phenylsulfinyl)phenyl)acetamide (3h)

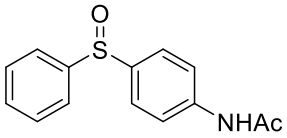

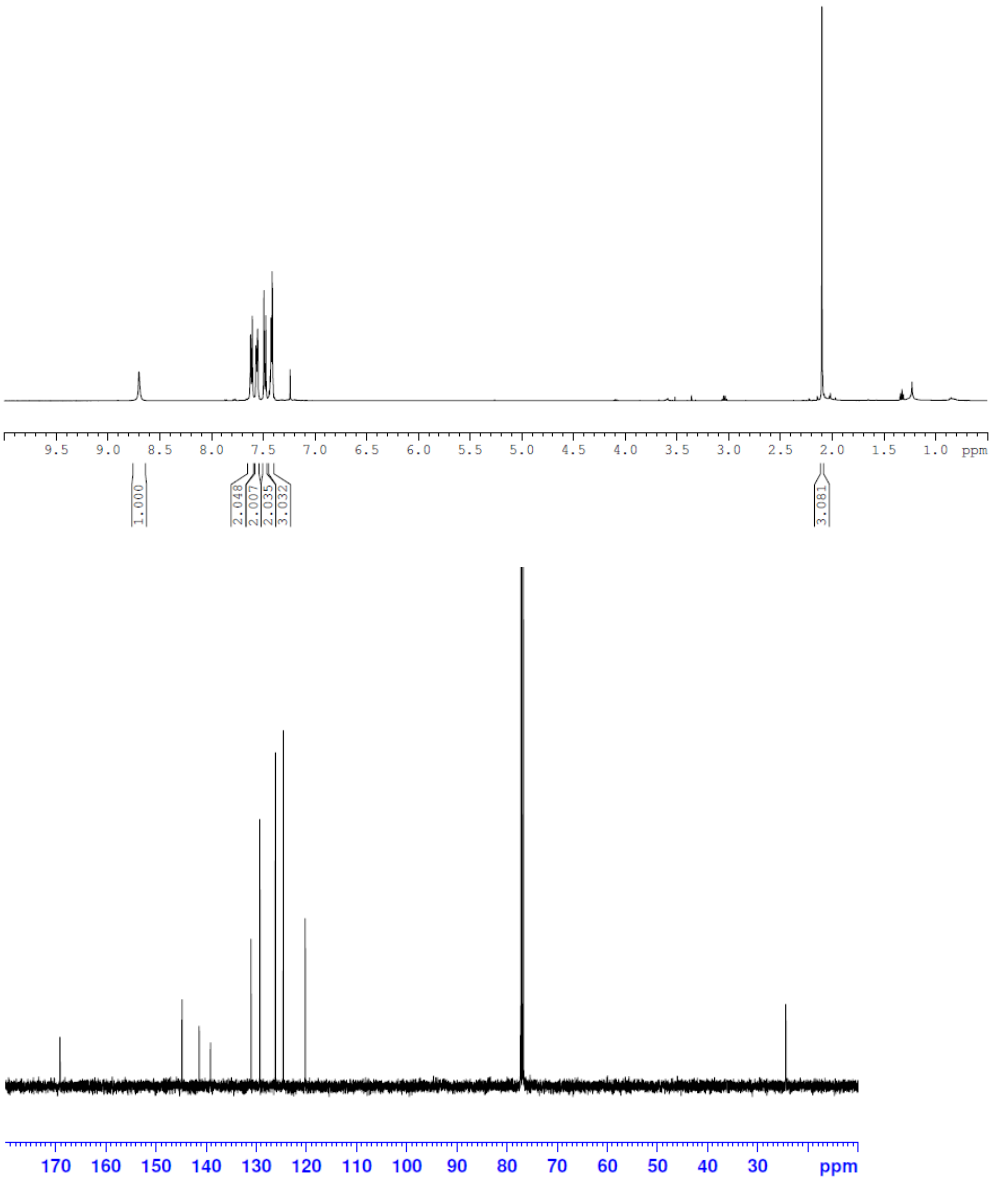

Figure S8. ^{1}H (500 MHz) and ^{13}C $\{^{1}H\}$ (125 MHz) NMR spectra of 3h in $CDCl_3$.

1-(4-(Phenylsulfinyl)phenyl)piperazine (3i)

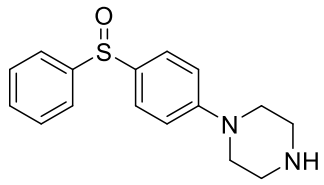

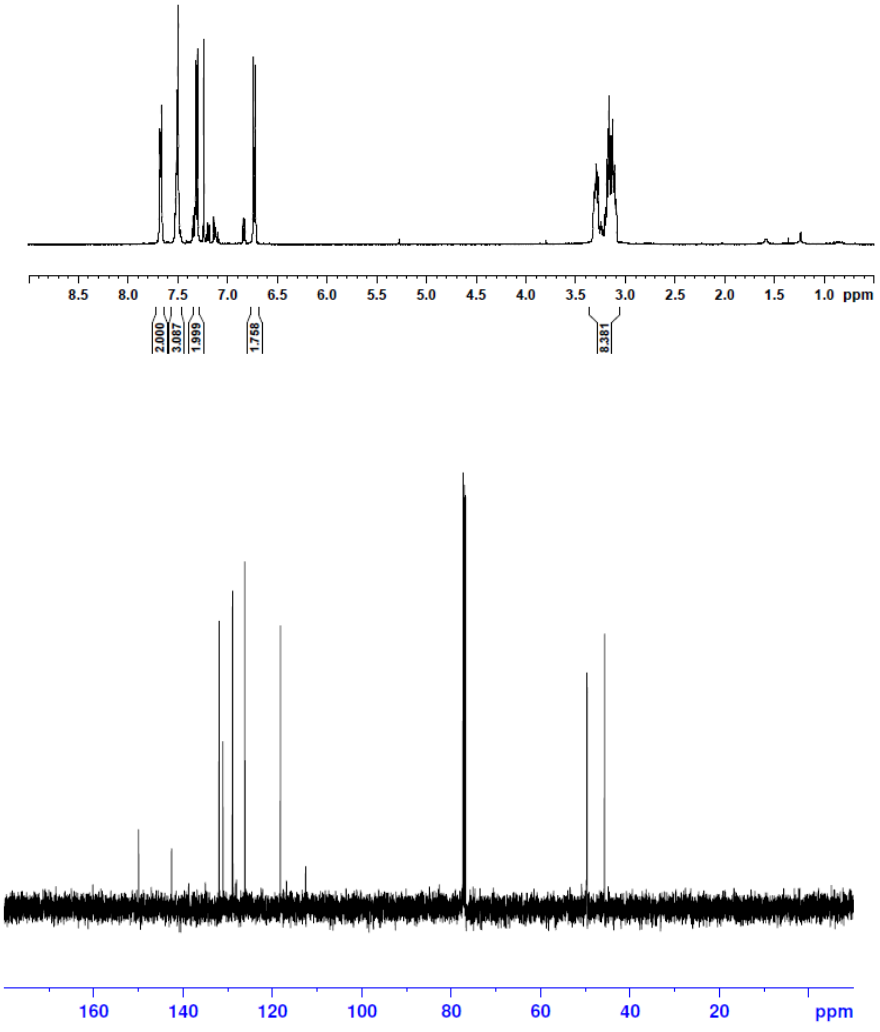

Figure S9. ^{1}H (500 MHz) and $^{13}C\{^{1}H\}$ (125 MHz) NMR spectra of 3i in $CDCl_3$.

Chapter V

1-(4-(Phenylsulfinyl)phenyl)-1H-pyrrole (3j)

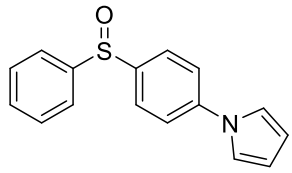

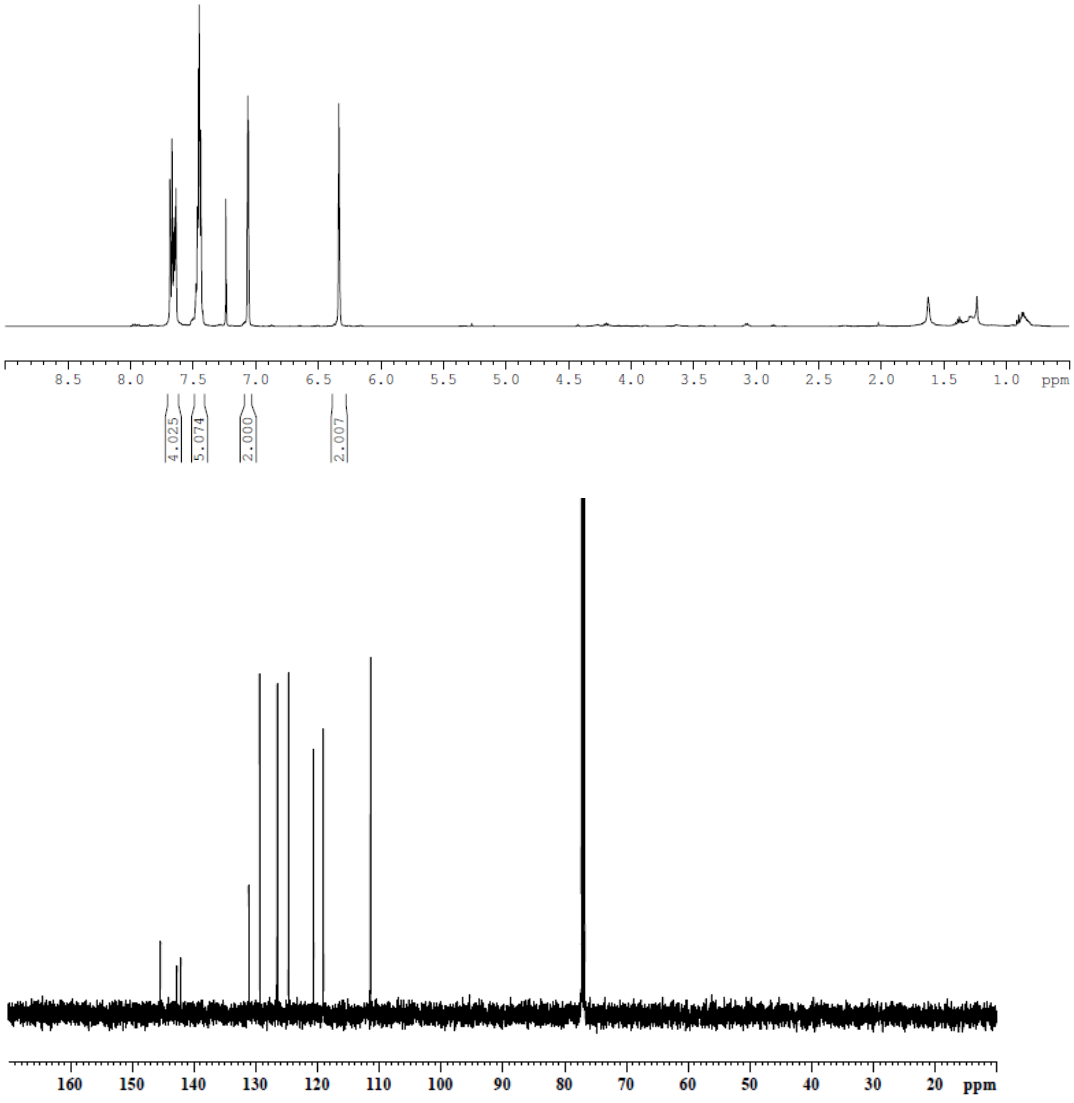

Figure S10. ^{1}H (500 MHz) and $^{13}C\{^{1}H\}$ (125 MHz) NMR spectra of 3j in $CDCl_3$.

4-(Phenylsulfinyl)quinoline (3k)

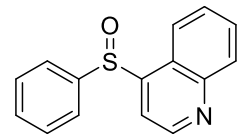

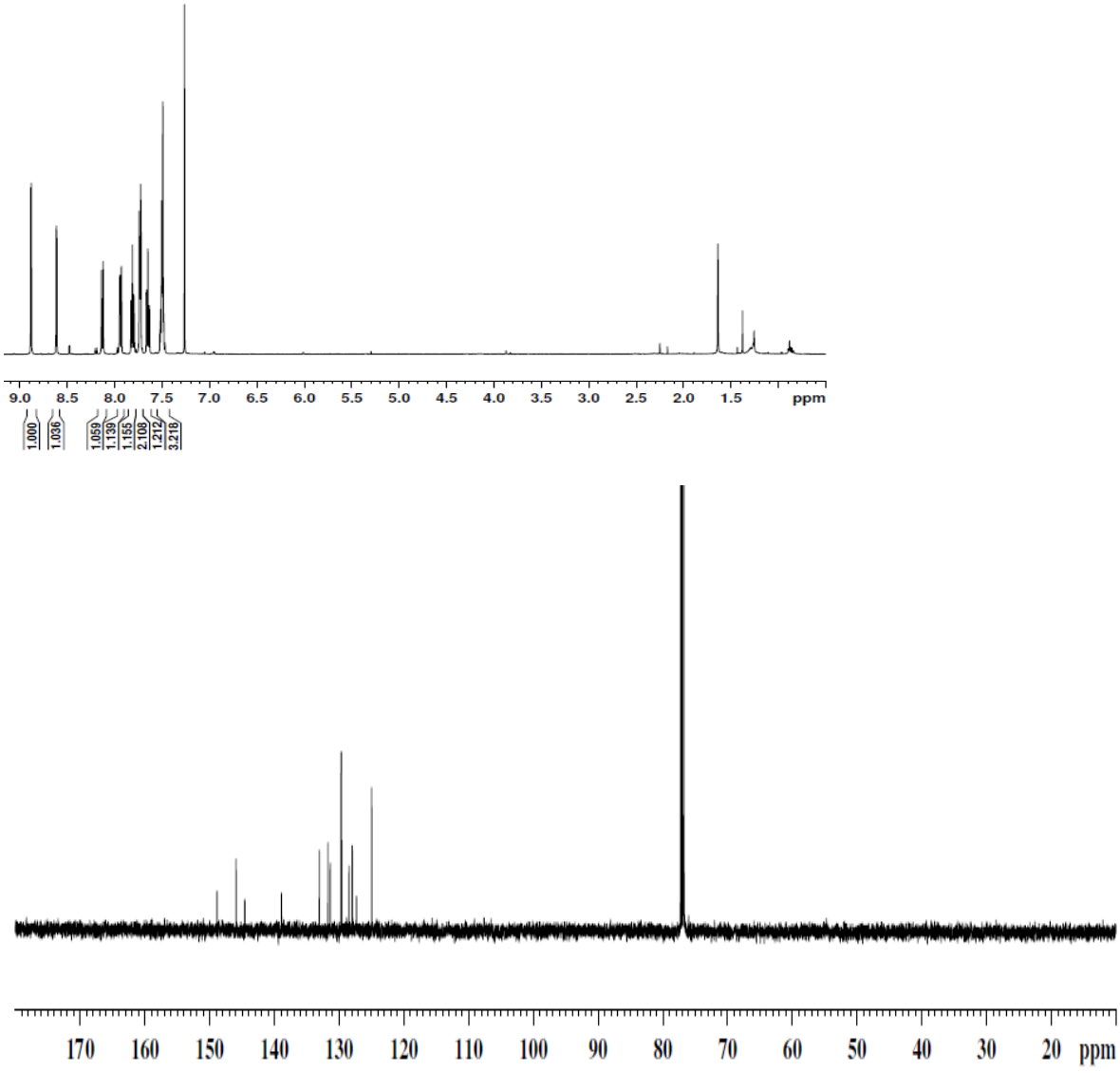

Figure S11. ^{1}H (500 MHz) and $^{13}C\{^{1}H\}$ (125 MHz) NMR spectra of 3k in $CDCl_3$.

Chapter V

2-Methyl-4-(phenylsulfinyl)quinoline (3l)

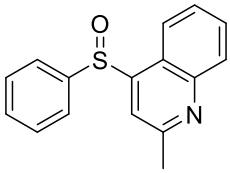

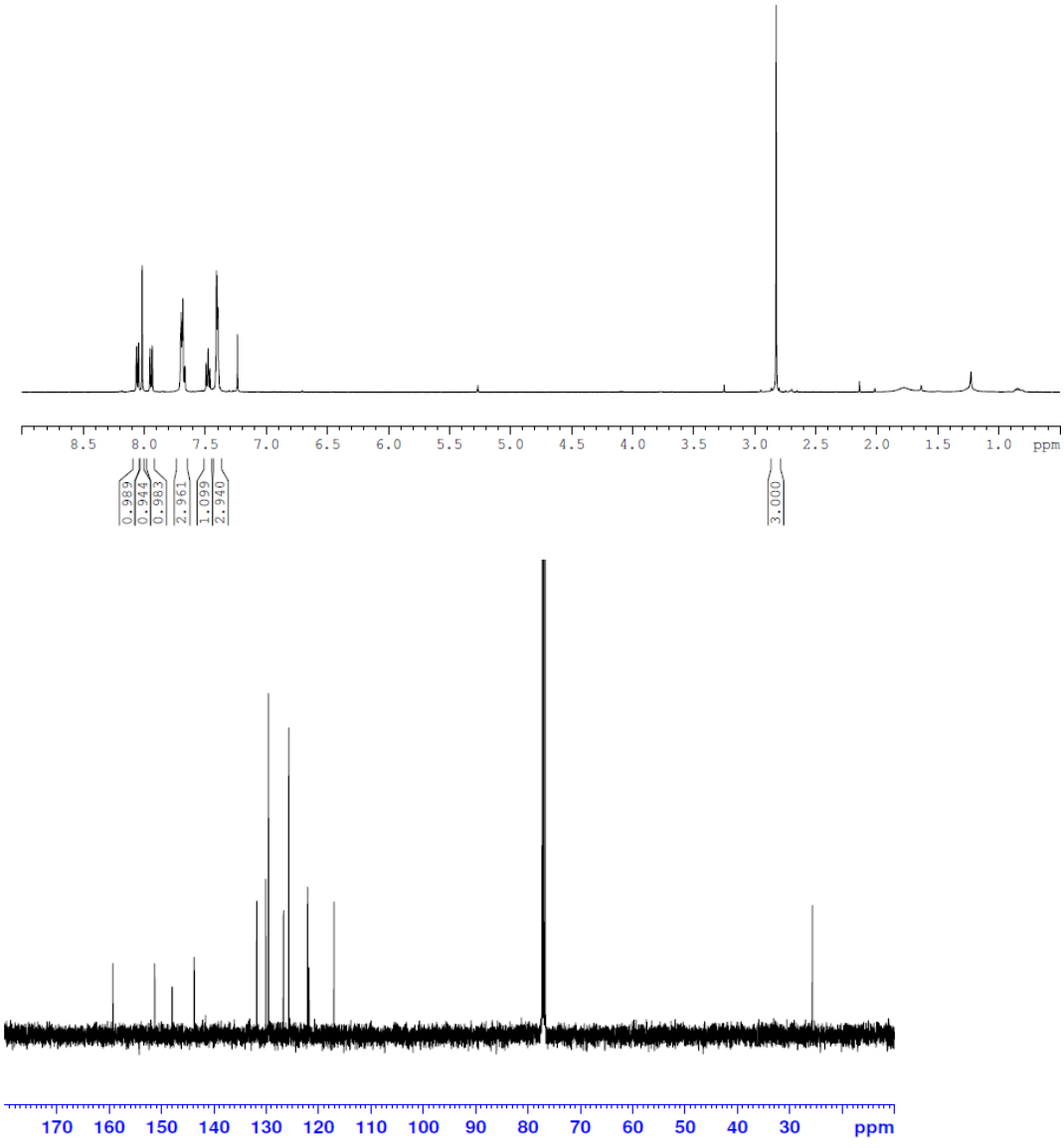

Figure S12. ^{1}H (500 MHz) and $^{13}C\{^{1}H\}$ (125 MHz) NMR spectra of 3l in $CDCl_3$.

1-Methyl-6-(phenylsulfinyl)-1*H*-indole (3m)

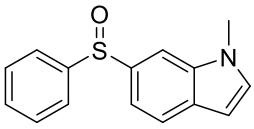

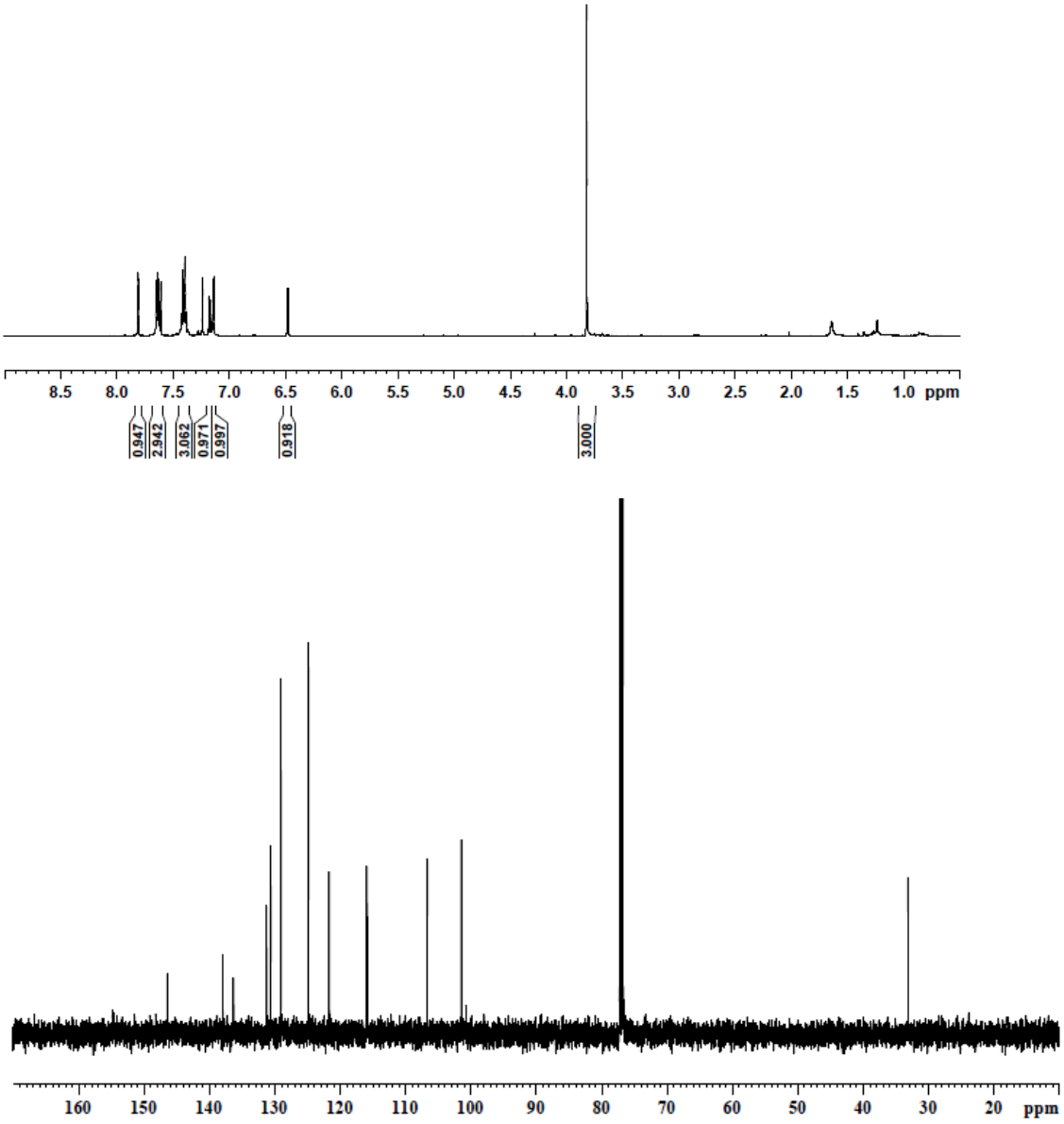

Figure S13. ^{1}H (500 MHz) and $^{13}C\{^{1}H\}$ (125 MHz) NMR spectra of 3m in $CDCl_3$.

Chapter V

1-Methyl-4-(phenylsulfinyl)benzene (3n)

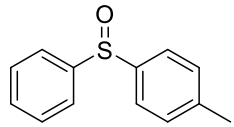

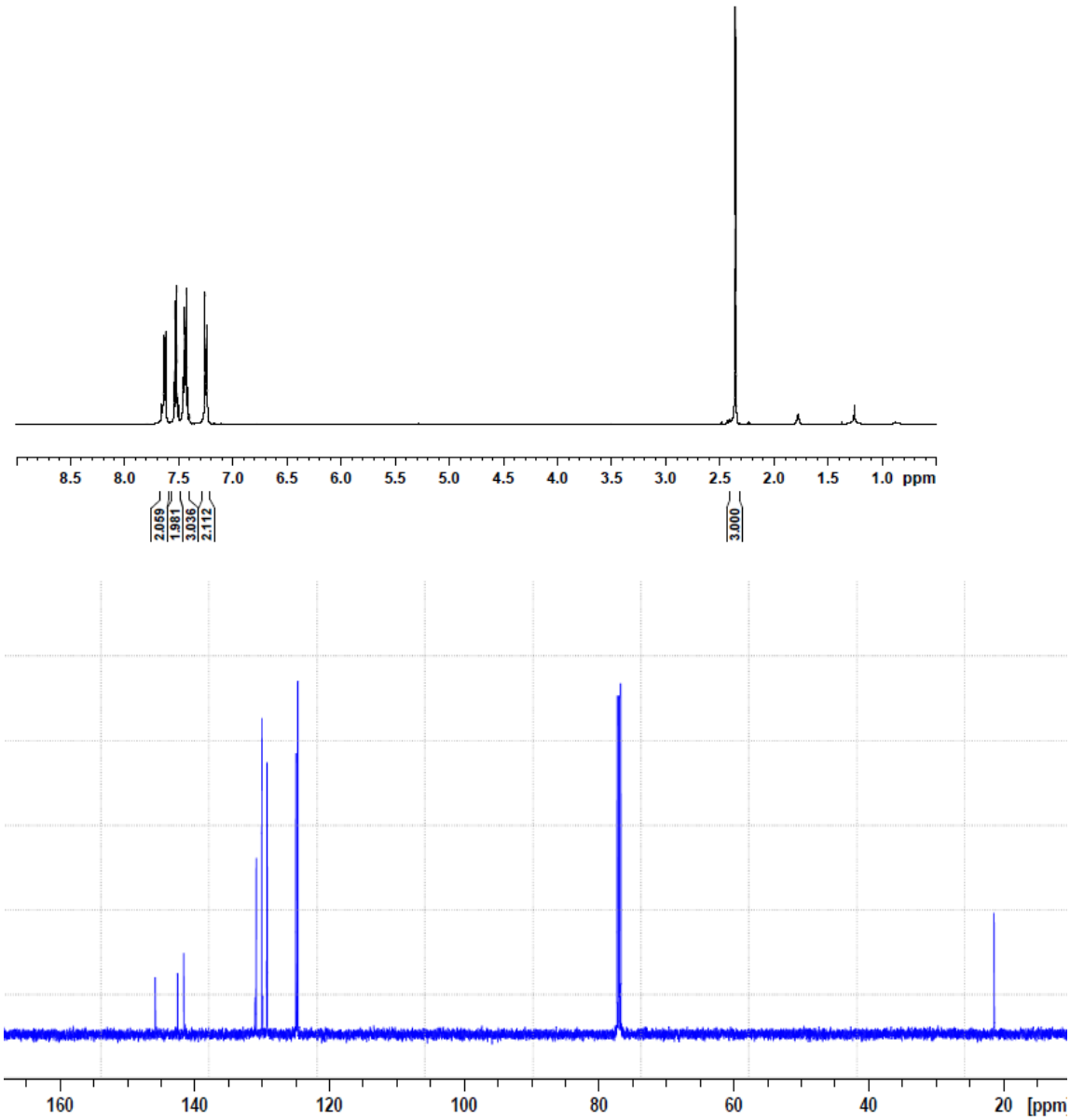

Figure S14. ^{1}H (500 MHz) and $^{13}C\{^{1}H\}$ (125 MHz) NMR spectra of 3n in $CDCl_3$.

1-Methoxyl-4-(phenylsulfinyl)benzene (3o)

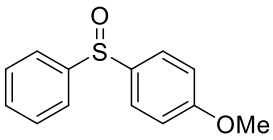

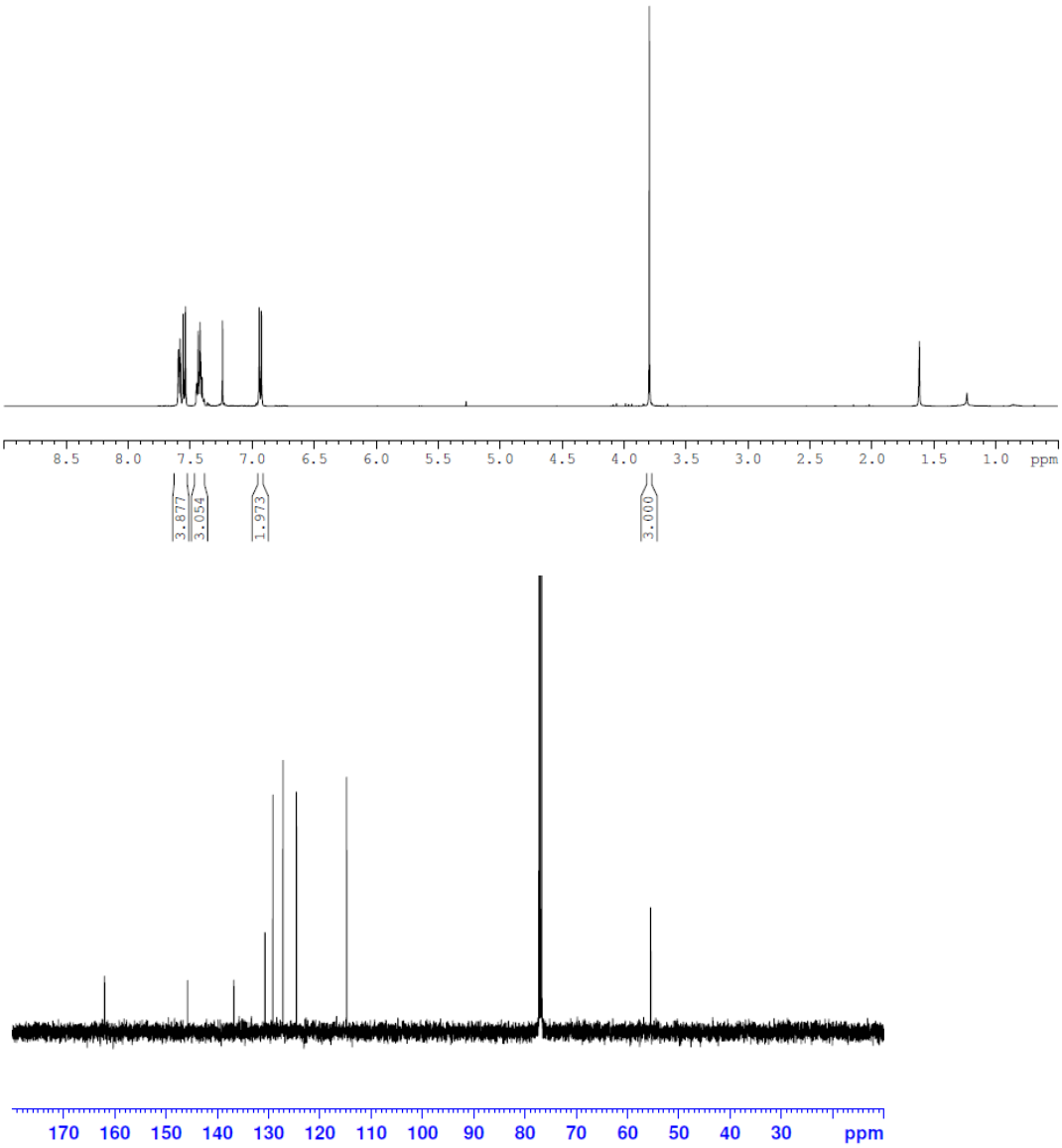

Figure S15. ^{1}H (500 MHz) and $^{13}C\{^{1}H\}$ (125 MHz) NMR spectra of 3o in $CDCl_3$.

Chapter V

N,N-dimethyl-4-(phenylsulfinyl)aniline (3p)

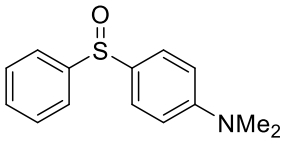

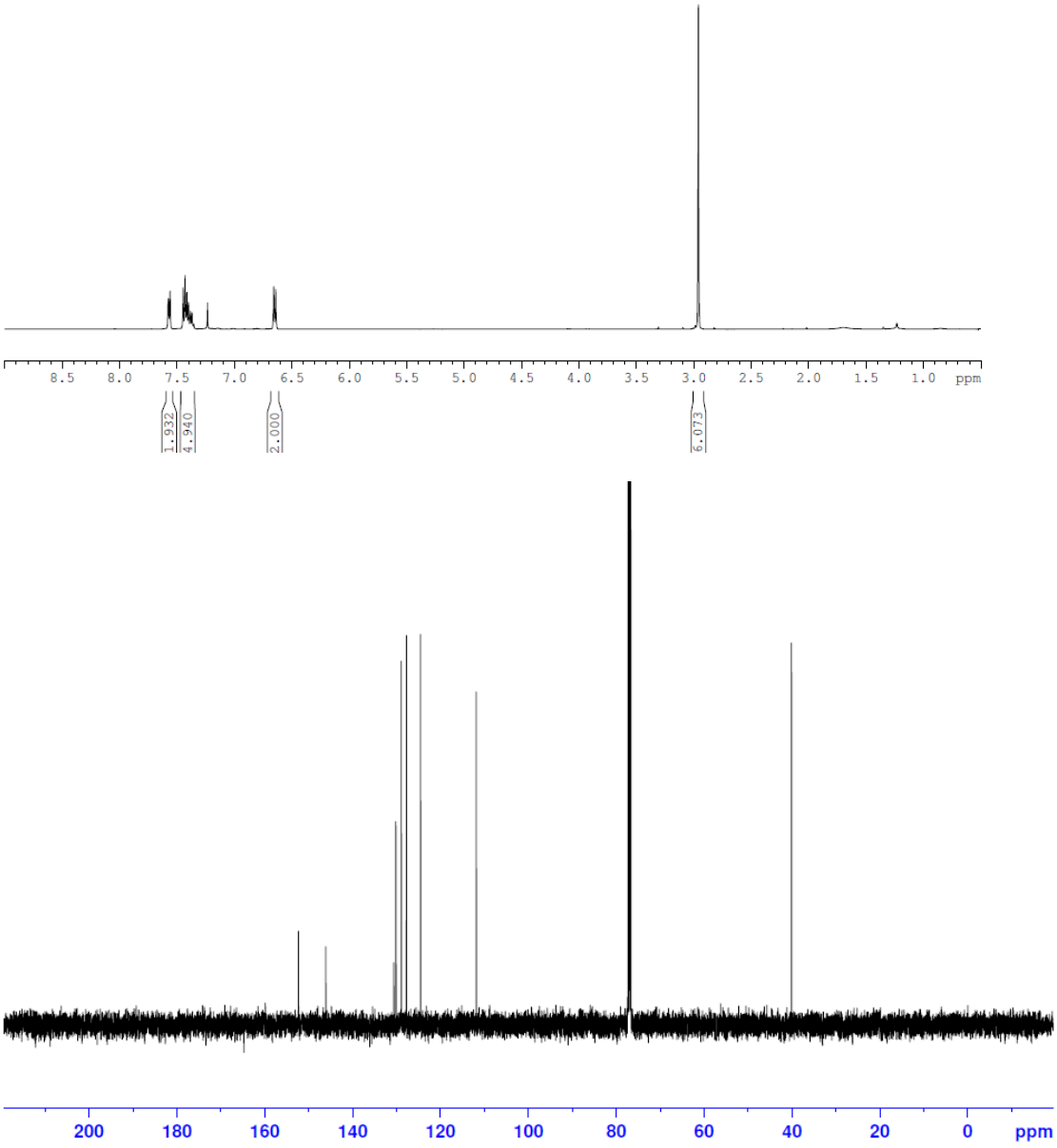

Figure S16. ^{1}H (500 MHz) and $^{13}C\{^{1}H\}$ (125 MHz) NMR spectra of 3p in $CDCl_3$.

1-Methyl-2-(phenylsulfinyl)benzene (3q)

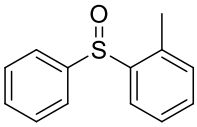

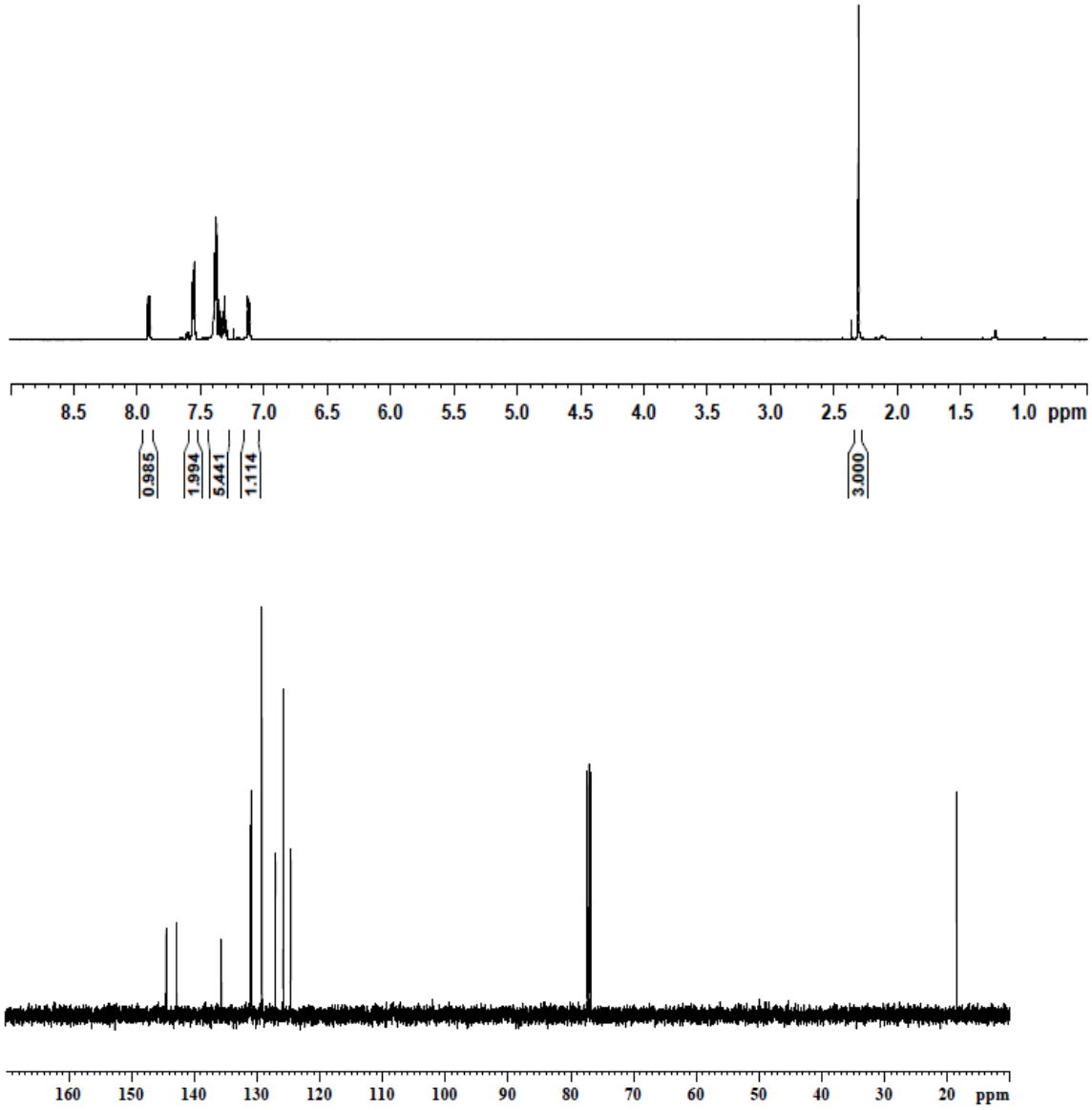

Figure S17. ^{1}H (500 MHz) and ^{13}C $\{^{1}H\}$ (125 MHz) NMR spectra of 3q in $CDCl_3$.

Chapter V

1-(Phenylsulfinyl)-3-(trifluoromethyl)benzene (3r)

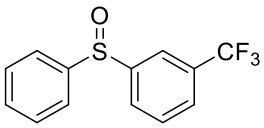

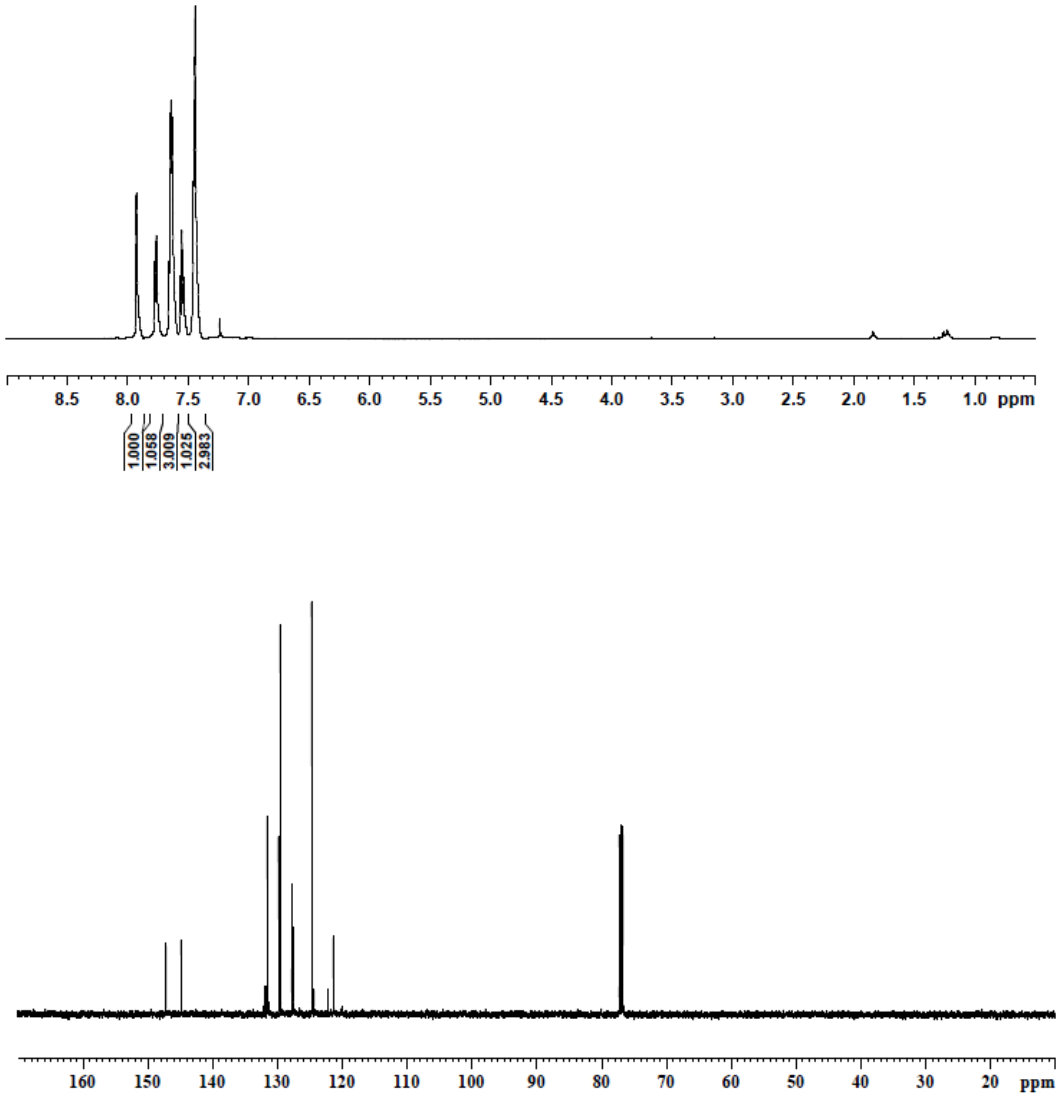

Figure S18. ^{1}H (500 MHz) and $^{13}C\{^{1}H\}$ (125 MHz) NMR spectra of 3r in $CDCl_3$.

(Cyclohexylsulfinyl)benzene (3s)

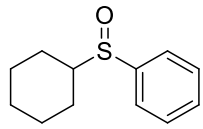

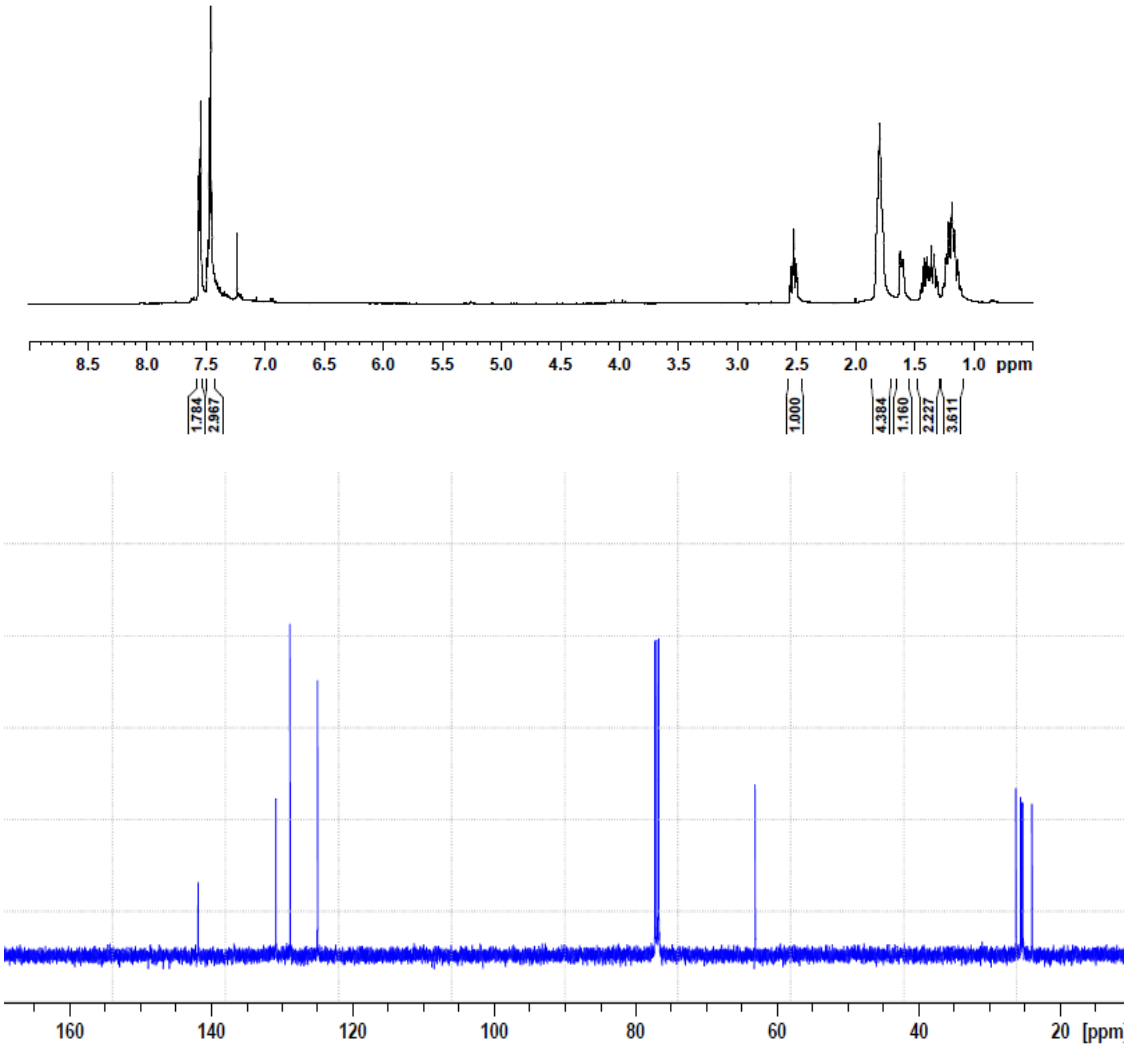

Figure S19. ^{1}H (500 MHz) and $^{13}C\{^{1}H\}$ (125 MHz) NMR spectra of 3r in $CDCl_3$.

UNIVERSITAT ROVIRA I VIRGILI
NEW APPROACHES TO CATALYST DESIGN AND IMMOBILIZATION
Irina Sagamanova

CHAPTER VI

tert-Butyl Phenyl Sulfoxide: a Traceless Sulfenate Anion Precatalyst*

** Work described in this chapter was carried out during a research stage in the laboratory of Prof. Patrick J. Walsh at Penn University, in the framework of a collaboration between the Walsh and Pericàs laboratories.*

This part of the work was supervised by Prof. Patrick J. Walsh, and developed in collaboration with Mengnan Zhang and Tiezheng Jia.

UNIVERSITAT ROVIRA I VIRGILI
NEW APPROACHES TO CATALYST DESIGN AND IMMOBILIZATION
Irina Sagamanova

tert-Butyl Phenyl Sulfoxide: a Traceless Sulfenate Anion Precatalyst

6.1. Introduction.

Stilbenes are relatively small molecules that are widespread in nature; for instance, several compounds with this scaffold have been isolated from different plant species (see examples provided in **Figure VI.1**). There are two isomeric forms of 1,2-diphenylethylene: (*E*)-stilbene (*trans*-stilbene) and (*Z*)-stilbene (*cis*-stilbene). *Cis*-stilbene is sterically hindered, because of the destabilizing interaction of the aromatic rings out-of-plane, and therefore less stable than the *trans*-isomer. They have attracted attention in biological applications[245] and in the manufacture of dyes and optical brighteners, phosphor and other materials.[246] Moreover, the chemistry and photochemistry of stilbenes has been extensively investigated in the last decades.[247]

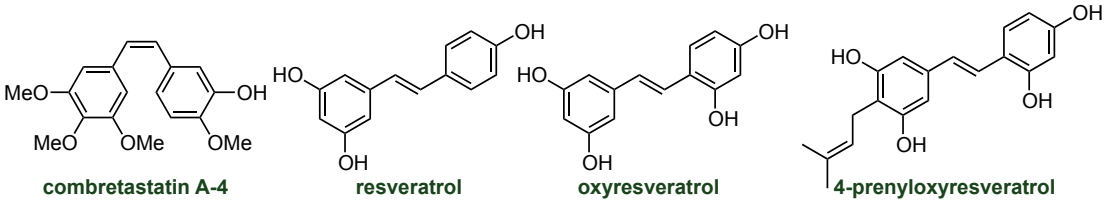

Figure VI.1. Some important stilbenes.

Many reactions have been discovered for the formation of the stilbene type double bonds. A few classical methods for the formation of this scaffold are presented in **Figure VI.2**.

---

[245] a) Tron, G. C.; Pirali, T.; Sorba, G.; Pagliai, F.; Busacca, S.; Genazzani, A. A. *J. Med. Chem.* **2006**, *49*, 3033-3044; b) Chaudnary, A.; Pandeya, S. N.; Kumar, P.; Sharma, P. P.; Gupta, S.; Soni, N.; Verma, K. K.; Bhardwaj, G. Mini Rev. Med. Chem. 2007, 17, 11-1205; c) Jeandet, P.; Delaunois, B.; Conreux, A.; Donnez, D.; Nuzzo, V.; Cordelier, S.; Clément, C.; Courot, E. *BioFactors* **2010**, *36*, 331-341.
[246] a) Meier, H. *Angew. Chem. Int. Ed.* **1992**, *31*, 1399-1420; b) Siegrist, A. E., Eckhardt, C., Kaschig, J.; Schmidt, E. *Optical Brighteners. Ullmann's Encyclopedia of Industrial Chemistry* **2003**; c) Smith, R. E. *Stilbene Dyes. Kirk-Othmer Encyclopedia of Chemical Technology* **2009**.
[247] For reviews on the methods, see: a) Becker, K. B. *Synthesis* **1983**, 341-368; b) Likhtenstein, G. I. *Stilbenes: Application in Chemistry, Life Sciences and Material Science* **2009**, Wiley-VCH, Weinheim, Germany, *Vol. 2*, 43-66.

Chapter VI

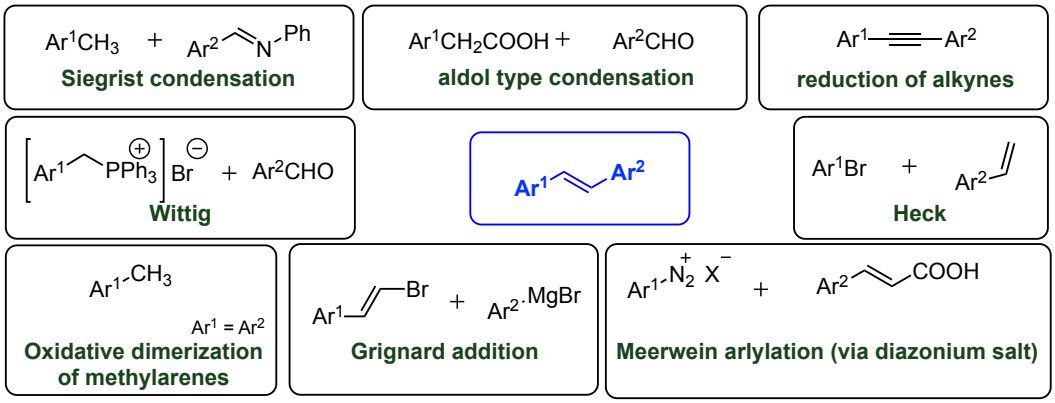

Figure VI.2. Classical methods for the synthesis of stilbene derivatives.

A classical example of the synthesis of (*E*)-stilbenes is an aldol-type condensation, using, for instance, H_2SO_4 as a catalyst (**Scheme VI.1.A**).[248] Siegrist reported some modification of the aldol-type reaction,[249] demonstrating a base catalyzed exchange-condensation of aromatic methyl compounds with benzalaniline (**Scheme VI.1.B**).[249c]

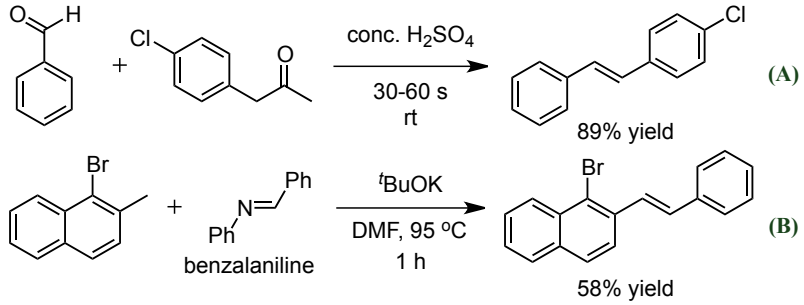

Scheme VI.1. Acid and base catalyzed condensations to form stilbenes.

Another alternative pathway to stilbene derivatives is the Wittig reaction, in which case the reaction takes place between an aldehyde or ketone and triphenyl phosphonium ylide (**Scheme VI.2A**).[250] However, this reaction has its own drawbacks belong such as the formation of a mixture of *E*/*Z*-stilbenes and the sometimes difficult separation of the product from triphenylphosphine oxide. In 1958, Horner *et al.* reported a modified Wittig reaction using phosphonate-stabilized carbanions.[251] Lately,

---

[248] a) Narender, T.; Reddy, O. P.; Madhur, G. *Synthesis* **2009**, *22*, 3791-3796; b) Narender, T.; Reddy, O. P.; Tiwari, S. *Synth. Commun.* **2011**, *41*, 1572-1583.
[249] a) Siegrist, A. E. *Helv. Chim. Acta* **1967**, *50*, 906-957; b) Siegrist, A. E.; Liechti, P.; Meyer, H. R.; Weber, K. *Helv. Chim. Acta* **1969**, *52*, 2521-2554; c) Newman, M. S.; Dhawan, B.; Kumar, S. *J. Org. Chem.* **1978**, *43*, 524-525.
[250] a) Wittig, G.; Schöllkopf, U. *Chem. Ber.* **1954**, *87*, 1381-1330; b) Wittig, G.; Haag, W. *Chem. Ber.* **1955**, *88*, 1654-1660; c) Taber, D. F.; Nelson, *J. Org. Chem.* **2006**, *71*, 8973-8974.
[251] a) Horner, L.; Hoffmann, H. M. R.; Wippel, H. G. *Chem. Ber.* **1958**, *91*, 61-63; b) Wadsworth, W. S.; Emmons, W. D. *J. Am. Chem. Soc.* **1961**, *83*, 1733-1739; c) Ianni, A.; Waldvogel, S. R. *Synthesis* **2006**, *2103-2112.*

a more convenient procedure for the optimized reaction, called the Horner-Wadsworth-Emmons (HWE), was reported[251c] (**Scheme VI.2B**).

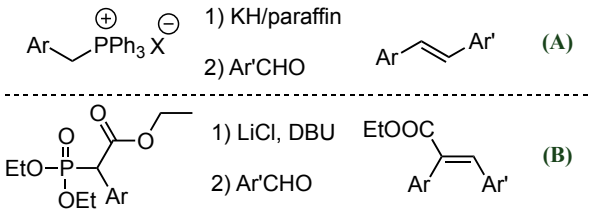

Scheme VI.2. Wittig and Horner-Wadsworth-Emmons (HWE) reactions.

Alkynes are useful intermediates for the synthesis of different types of alkenes with *cis-trans* configurations. Hydrogenation of alkynes, employing the Lindlar catalyst is the most common and facile method to obtain *Z*-alkenes.[252] Other significant results have been achieved by a variety of catalytic systems, using transition metal precatalysts in combination with hydrogen gas or transfer hydrogenation agents (for instance, silanes or formic acid).[253]

On the other hand, catalytic alkyne hydrogenation leading to *E*-alkenes is less established in comparison with *Z*-alkenes; this reaction is usually stoichiometric. For instance, common protocols include the Birch-type reduction of alkynes by alkali metals (Li, Na) in liquid ammonia, [254] or the use of chromium reagents.[255]

Metal-catalyzed processes mostly require more expensive metals like Rh, Ru, Pd, and Ir, although Ni and Fe-catalyzed processes have also been developed.[256]

An alternative to the classical protocols for the synthesis of stilbene derivatives came from the reaction between substituted alkenes and aryldiazonium salts, catalyzed by copper (I) or copper (II) chloride.[257] The initial product of this reaction is a substituted alkyl halide, which can be dehydrohalogenated under basic conditions. In the cases of electron-withdrawing substituent, contained acids, the final compound is accompanied by the decarboxylation product.[257b] In general, low to moderate yields are

---

[252] Lindlar, H.; Dubuis, R. *Org. Synth.* **1966**, *46*, 89-91.
[253] For a comprehensive review, see: Oger, C.; Balas, L.; Durand, T.; Galano, J.-M. *Chem. Rev.* **2013**, *113*, 1313-1350.
[254] Pasto, D. J. In *Comprehensive Organic Synthesis* (Eds.: Trost, B. M.; Fleming, I.), Pergamon, Oxford, **1991**, *Vol. 8*, 471-488.
[255] Castro, C. E.; Stephens, R. D. *J. Am. Chem. Soc.* **1964**, *86*, 4358-1463.
[256] For metal-catalyzed *E*-selective reduction, see examples: a) Abley, P.; McQuillin, F. J. *J. Chem. Soc. D* **1969**, 1503-1504; b) Burch, R. R.; Muetterties, E. L.; Teller, R. G.; Williams, J. M. *J. Am. Chem. Soc.* **1982**, *104*, 4257-4258; c) Radkowski, K.; Sundararaju, B.; Fürstner, A. *Angew. Chem. Int. Ed.* **2013**, *52*, 355-360; d) Srimani, D.; Diskin-Posner, Y.; Ben-David, Y.; Milstein, D. *Angew. Chem. Int. Ed.* **2013**, *52*, 14131-14134; e) Chen, T.; Xiao, J.; Zhou, Y.; Yin, S.; Han, L.-B. *J. Organomet. Chem.* **2014**, *749*, 51-54; f) Liu, Y.; Hu, L.; Chen, H.; Du, H. *Chem. Eur. J.* **2015**, *21*, 3495-3501.
[257] a) Meerwein. H.; Büchner, E.; Emster. K.; *J. Prakt. Chem.* **1939**, *152*, 237-266; b) Rondestvedt, C. S. *Org. React.* **1976**, *24*, 225-259; c) Doyle, M. P.; Siegfried, B.; Elliott, R. C.; Dellaria, J. F. *J. Org. Chem.* **1977**, *42*, 2431-2436; d) *Comprehensive Name Reactions and Reagents*, John Wiley & Sons Inc., **2010**, *419*, 1866-1870.

obtained because of competing reactions such as aryl halide formation, polymerization or hydrogen abstraction by the intermediate aryl radicals (**Scheme VI.3**).

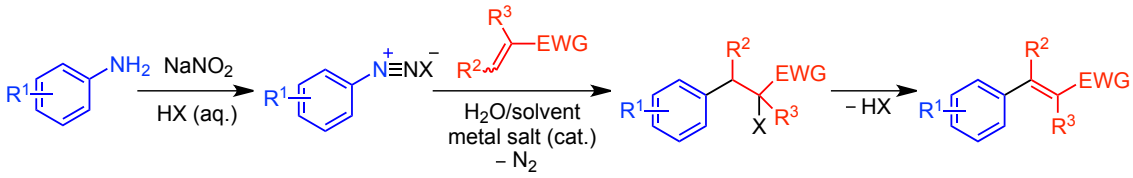

Scheme VI.3. General view of Meerwein arylation.

Palladium-catalyzed reactions have also been explored for the generation of functionalized stilbene derivatives; classical reactions such as Heck, Suzuki-Miyaura, Stille, Negishi or Hiyama can be used.[258] As a first example, the Heck reaction takes place between an unsaturated halide (or a triflate) and an alkene in the presence of strong base and palladium catalyst (**Scheme V.I.4**). Alternative transition metals such as nickel, copper, titanium and cobalt can also be employed for the cross-coupling reactions.[259]

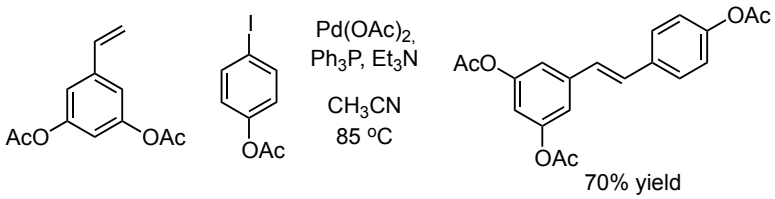

Scheme VI.4. Heck reaction in the synthesis of stilbenes.

In any case, alternative pathways completely avoiding the use of metals are also desirable for the synthesis of stilbenes.

6.2. Sulfenate anions as a new class of organocatalysts.

Sulfenate anions represent an important class of sulfur nucleophiles, which have shown high potential for the development of valuable sulfoxide derivatives.[115] Recent advances involving sulfenates have facilitated access to challenging targets, and also modern developments in the sulfenate chemistry have provided alternative

[258] a) Guiso, M.; Marra, C.; Farina, A. *Tetrahedron Lett.* **2002**, *43*, 597-598; b) Tudose, A.; Delaude, L.; André, B.; Demonceau, A. *Tetrahedron Lett.* **2006**, *47*, 8529-8533; c) Kabir, M. S.; Monte, A.; Cook, J. M. *Tetrahedron Lett.* **2007**, *48*, 7269-7273; d) Saiyed, A. S.; Bedekar, A. V. *Tetrahedron Lett.* **2010**, *51*, 6227-6231.

[259] For examples, see: a) Iyer, S.; Ramesh, C.; Sarkar, A.; Wadgaonkar, P. P. *Tetrahedron Lett.* **1997**, *38*, 8113-8116; b) Iyer, S.; Ramesh, C.; Ramani, A. *Tetrahedron Lett.* **1997**, *38*, 8533-81536; c) Ferré-Filmon, K.; Delaude, L.; Demonceau, A.; Noels, A. F. *Eur. J. Org. Chem.* **2005**, *15*, 3319-3325; d) Hilt, G.; Hengst, C. *J. Org. Chem.* **2007**, *72*, 7337-7342.

tools for the synthesis of sulfoxides, using *S*-arylation as a key step in different types of reactions.[260]

Taking into consideration early studies in this area, it became clear that sulfenate species were acting as nucleophiles and as the leaving group in some palladium-catalyzed processes. For example, the successful development of palladium-catalyzed formation of diaryl sulfoxides via aryl benzyl sulfoxides and aryl bromides can be cited.[114] This involves three distinct catalytic cycles (**Figure VI.3**), where the sulfenate anion ($ArSO^-$) is generated as leaving group in **cycle B** and undergoes arylation in **cycle C**.

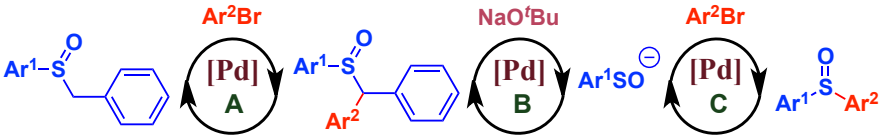

Figure VI.3. Palladium catalyzed formation of diaryl sulfoxides.

From this point, additional consideration was paid to the use of these highly reacting sulfenate species in organocatalysis. As proof-of-concept, Walsh *et al.* presented the coupling of benzyl halides as the first general protocol for the use of this kind of species as organocatalysts (**Scheme VI.5**).[121]

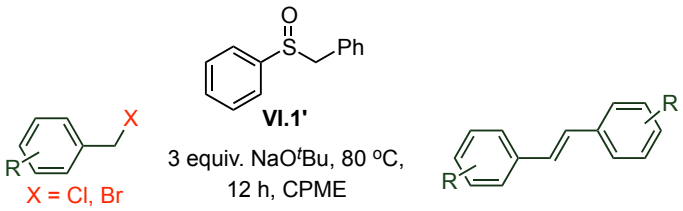

Scheme VI.5 Conversion of halides to *trans*-stilbenes.

In the proposed catalytic cycle (**Scheme VI.6**), benzylic sulfoxides are deprotonated at the α-position under basic conditions. Then, the benzyl halide reacts with sulfoxide anion **VI.2**, followed by deprotonation at the β-position of **VI.4**. In the next step, E_2 elimination generates *trans*-stilbene and sulfenate anion catalyst **VI.6**, which is the active form of the organocatalyst for this transformation.

In the first cycle, benzyl phenyl sulfoxide (**VI.1'**) acts as pre-catalyst, which generates the sulfenate anion catalyst **VI.6** and an unsymmetrical stilbene as a by-product in the cases where the aryl halide does not match the aromatic moiety of the pre-catalyst.

This is the first example of the use of sulfenate anions in metal-free catalysis, which was also highlighted by Schwan.[261]

---

[260] Schwan, A. L.; Söderman, C. *Phosphorus, Sulfur, and Silicon* **2013**, *188*, 275-286.

Chapter VI

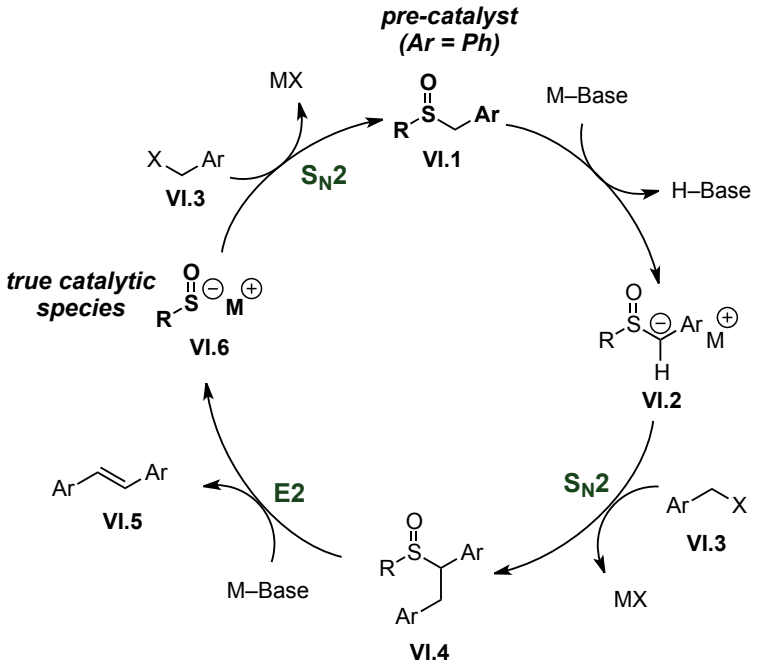

Scheme VI.6. Catalytic cycle for the sulfenate-mediated conversion of benzyl halides to *trans*-stilbenes.

However, there are still challenges regarding the nature of this catalyst, and alternative organocatalysts are needed in order to avoid the contamination of symmetric *trans*-stilbenes if aryl groups different from the first generated organocatalyst are used (**Scheme VI.7**).

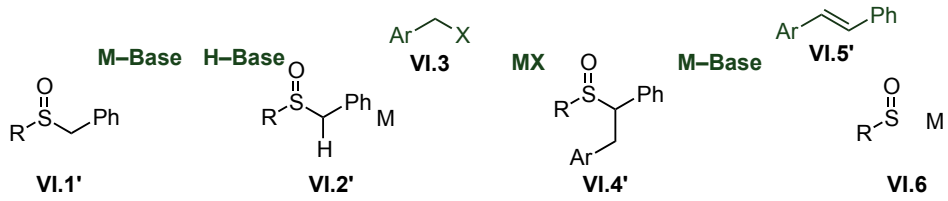

Scheme VI.7. First catalytic cycle in generation of sulfenate anions **VI.6**.

Nevertheless, this sulfenate species has shown high potential for future transformations as a new type of organocatalyst. Indeed, the same group has recently published a new type of transformation employing this type of catalyst for the generation of different alkynes (**Scheme VI.8**).[262]

[261] Schwan, A. L. *ChemCatChem* **2015**, *7*, 226-227.
[262] Zhang, M.; Jia, T.; Wang, C. Y.; Walsh, P. J. *J. Am. Chem. Soc.* **2015**, *137*, 10346-10350.

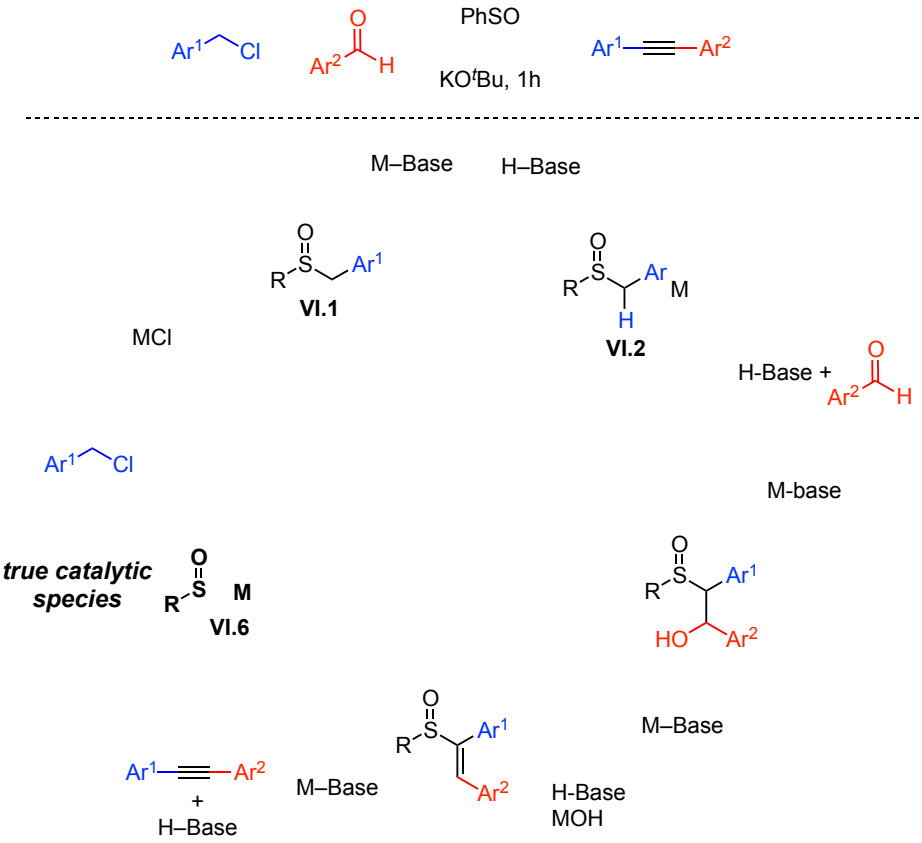

Scheme VI.8. Sulfenate anion-catalyzed synthesis of alkynes.

Chapter VI

6.3. Aim of the project.

The objective of this research is to develop a second generation pre-catalyst for the condensation of organic halides to generate *trans*-stilbenes.

Even if very low loadings were used in the sulfenate anion-catalyzed formation of stilbenes,[121] the final compounds were contaminated with small amounts of by-product. This is due to the reaction of elimination by the generated species **VI.4** in the first cycle, which can be a problem if the organic halide and the benzylic pre-catalyst have a different aromatic moiety. The final unsymmetrical substrate (**VI.5'**, PhCH=CHAr) is difficult to separate from the desired symmetrical stilbenes (**VI.5**, ArCH=CHAr).

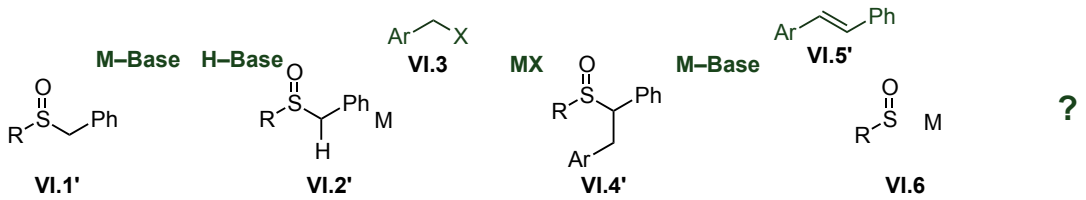

Therefore, it is important to develop a new type of traceless organocatalyst, which can be more effective in this transformation, providing alternative options to generate sulfenate species **VI.6**. In order to develop a second generation pre-catalyst additional studies are needed to optimize conditions for aryl halide coupling.

Organic LETTERS
Letter
pubs.acs.org/OrgLett

tert-Butyl Phenyl Sulfoxide: A Traceless Sulfenate Anion Precatalyst

Mengnan Zhang,[†] Tiezheng Jia,[†] Irina K. Sagamanova,[‡] Miquel A. Pericás,[‡,§] and Patrick J. Walsh*,[†]

[†]Roy and Diana Vagelos Laboratories, Department of Chemistry, University of Pennsylvania, 231 South 34th Street, Philadelphia, Pennsylvania 19104-6323, United States

[‡]Institute of Chemical Research of Catalonia (ICIQ), Av. Països Catalans 16, 43007 Tarragona, Spain

[§]Departament de Química Organica, Universitat de Barcelona (UB), 08028 Barcelona, Spain

Supporting Information

ABSTRACT: *tert*-Butyl phenyl sulfoxide is employed as a traceless precatalyst for the generation of sulfenate anions under basic conditions and has been used to catalyze the coupling of benzyl halides to *trans*-stilbenes. The advantage of this precatalyst over previous precatalysts is that the byproduct generated on catalyst formation is a gas, facilitating product isolation in high purity. Using this second generation catalyst, a variety of *trans*-stilbenes were generated in 39−98% isolated yield.

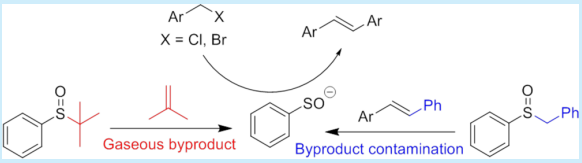

Sulfenate anions and their conjugate acids, sulfenic acids (Figure 1), are highly reactive intermediates in biochemistry[1] and organic synthesis.[2] In organic chemistry, sulfenate anions can be trapped with alkyl halides to afford sulfoxides. We,[3] and others,[4] have recently developed methods to arylate sulfenate anions with aryl halides under palladium catalysis to afford aryl sulfoxides. Our approach (Scheme 1) begins with aryl benzyl sulfoxides, which undergo an initial α-arylation under basic conditions to generate diarylmethyl aryl sulfoxides. The palladium catalyst next promotes the cleavage of the C−S bond to liberate the sulfenate anion, which is arylated in the third catalytic cycle. In this process the sulfenate anion behaves as a leaving group in the second cycle and as a nucleophile in the third cycle.[3] Inspired by the ability of sulfenate anions to behave as both leaving groups and nucleophiles in the tricatalytic cycle in Scheme 1, we recognized their potential to act as organocatalysts. No examples of sulfenate anion catalysts were previously known.

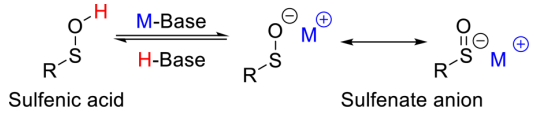

Figure 1. Sulfenic acid and its conjugate base, sulfenate anion.

Scheme 1. Palladium Promotes the Tricatalytic Cycle with Sulfenate Anion as the Leaving Group in the Second Cycle and Nucleophile in the Third Cycle

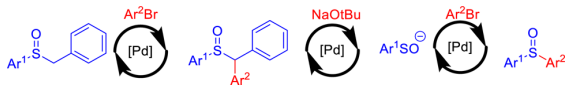

As proof of concept, benzyl phenyl sulfoxide was applied as a precatalyst in coupling of benzyl halides to form symmetrical *trans*-stilbenes under basic conditions (Scheme 2).[5] In this process, a variety of *trans*-stilbenes could be prepared in good to excellent yields with catalyst loadings as low as 2 mol %.

The proposed mechanism for the sulfenate anion-catalyzed coupling of benzyl halides is illustrated in Scheme 2. Beginning with benzyl phenyl sulfoxide (**A**), deprotonation by KO^{t}Bu generates the anion (**B**), which was demonstrated to be the catalyst resting state. The anion **B** undergoes nucleophilic substitution with benzyl halide (**C**) to form

Scheme 2. Proposed Mechanism for Sulfenate Anion Catalyzed *trans*-Stilbene Formation from Benzyl Halides

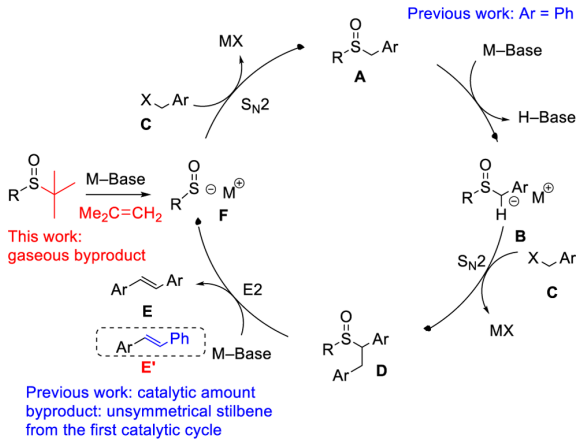

Received: January 13, 2015

ACS Publications © XXXX American Chemical Society

DOI: 10.1021/acs.orglett.5b00117
Org. Lett. XXXX, XXX, XXX−XXX

Chapter VI

sulfoxide **D**. Deprotonation of the β-position of **D** is followed by elimination to generate the double bond in **E** with very high trans selectivity and the sulfenate anion **F**. A rather serious limitation to use of benzyl phenyl sulfoxide (**A**) as precatalyst is that the first turnover installs a phenyl group on the *trans*-stilbene. In cases where the benzylic halide (**C**) is other than benzyl chloride or bromide, the first cycle forms an unsymmetrical stilbene (PhCH═CHAr, **E′**) that is usually difficult to separate from the desired symmetric *trans*-stilbene, ArCH═CHAr (**E**). To make the sulfenate anion catalyzed synthesis of *trans*-stilbenes more attractive, we envisioned entry into the catalytic cycle at the sulfenate anion, **F**.

Herein, we report a second-generation sulfenate anion catalyst that avoids contamination of the first cycle. The precatalyst, *tert*-butyl phenyl sulfoxide, undergoes base promoted elimination to generate phenyl sulfenate anion and isobutylene as a gaseous byproduct (Scheme 2).

To explore the use of *tert*-butyl phenyl sulfoxide as precatalyst, we initially employed conditions for our catalytic coupling of benzyl chlorides using KO^{t}Bu and benzyl phenyl sulfoxide precatalyst at 80 °C for 12 h. Under these conditions, *tert*-butyl phenyl sulfoxide (2.5 mol %) afforded only 33% assay yield of *trans*-stilbene (Table 1, entry 1). The

Table 1. Optimization of Sulfenate Anion Catalyzed *trans*-Stilbene (2a) Formation from Benzyl Chloride (1a)[a]

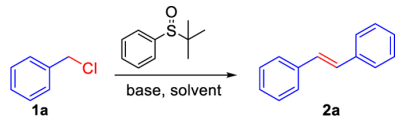

1a 2a

entry	KO^{t}Bu (equiv)	catalyst (mol %)	temperature (°C)	time (h)	yield[b] (%)
1	3.0	2.5	80	12	33
2	3.0	2.5	80[c]	12	43
3[d]	3.0	2.5	110 → 80	12	97
4[d]	3.0	1.0	110 → 80	12	69
5[d]	3.0	2.5	110 → 50	12	94
6[d]	2.0	2.5	110 → 50	12	96
7[d,e]	2.0	2.5	110 → 50	12	90
8[d]	2.0	2.5	110 → 50	6	96 (94[f])
9[d]	2.0	2.5	110 → 50	4	88

[a]Reactions performed using 1.0 equiv of **1a** on a 0.2 mmol scale in CPME. [b]Crude yield determined by ^{1}H NMR using 0.1 mmol of CH_2Br_2 as internal standard. [c]Before benzyl chloride was added, base and precatalyst were preheated at 80 °C for 30 min. [d]Before benzyl chloride was added, base and precatalyst were preheated at 110 °C for 30 min. [e]0.4 mmol of **1a**. [f]Isolated yield.

low yield was due to the reaction of benzyl chloride with KO^{t}Bu via a S_N2 process to generate benzyl *tert*-butyl ether.[6] We hypothesized that the low conversion to the desired stilbene was due to the slower E2 elimination of *tert*-butyl phenyl sulfoxide. To address this issue, we conducted the reaction in two stages. First, the precatalyst *tert*-butyl phenyl sulfoxide was heated with 3 equiv of KO^{t}Bu in CPME at 80 °C for 30 min before addition of benzyl chloride for the coupling. The assay yield of *trans*-stilbene (**2a**) increased to 43% (entry 2). Elevating the preheating temperature to 110 °C followed by cooling the reaction mixture, addition of benzyl chloride and heating to 80 °C for the coupling led to 97% assay yield of *trans*-stilbene (entry 3). Decreasing the catalyst loading to 1 mol % under otherwise identical conditions yielded 69% *trans*-stilbene (entry 4). Lowering the coupling temperature to 50 °C resulted in formation of the product with 94% assay yield (entry 5). Finally, we found that lowering the base loading to 2.0 equiv provided a slightly higher yield (96%) of *trans*-stillbene under more economical conditions (entry 6). Unfortunately, attempts to increase the reaction concentration from 0.1 to 0.2 M led to increased *tert*-butyl phenyl ether (entry 7). The assay yield remained at 96% when the coupling time was cut to 6 h (entry 8 vs 6). Further decreasing the coupling time to 4 h caused a drop in the assay yield to 88% (entry 9). Therefore, the optimized reaction conditions for *tert*-butyl phenyl sulfoxide catalyzed *trans*-stilbene formation from benzyl halides is 2.5 mol % precatalyst and 2.0 equiv of KO^{t}Bu in CPME preheated at 110 °C for 30 min, followed by addition of benzyl chloride and heating at 50 °C for 6 h.

The most surprising finding during the optimization process is that the sulfenate anion, generated at 110 °C, seems to be stable under these conditions in the absence of trapping reagents, at least for short periods of time.[7]

With the optimized conditions in hand, we set out to explore the substrate scope. In general, benzyl chloride derivatives are better substrates than benzyl bromides because the latter undergo more rapid S_N2 reactions with the base to generate benzyl *tert*-butyl ethers. To compensate for the increased reactivity of benzyl bromide derivatives, 5 mol % precatalyst loading was employed with these substrates. Benzyl chloride and bromide gave *trans*-stilbene (**2a**) in 94% and 76% yield, respectively. Benzyl chlorides with substituents at para position (**2b**, **2d**, **2e**, and **2f**) were found to give higher yields at 80 °C and in some cases with 3.0 equiv of base (**1b** and **1d**) (Scheme 3). Electron-donating groups increased the pK_a of the benzylic protons of intermediates **A** and **D** (Scheme 2) making them more difficult substrates. For example, only 71% of **2b** was obtained. Substrates bearing electron withdrawing groups were better coupling partners. For example, 4,4′-difluorostilbene (**2d**), 4,4′-dichlorostilbene (**2e**), and 4,4′-dibromostilbene (**2f**) were produced in 60–97% yield. Compounds **2e** and **2f** could be easily elaborated by standard cross-coupling methods. More sterically hindered substrates, such as 2-methyl benzyl chloride (**1h**) and 1-(chloromethyl)naphthalene (**1i**), afforded **2h** and **2i** in 86% and 85% yields, respectively. Diortho-substituted 2,6-dichlorobenzyl chloride was an excellent substrate, leading to *trans*-stilbene **2j** in 98% yield. Benzyl halides substituted at the meta position with Me, F, or CF_3 group were good substrates, giving **2k**, **2l**, and **2m** in 89%, 89% and 84% yield, respectively. Heterocycle-containing stilbenes usually exhibit interesting photochemistry properties, but are more challenging to synthesize.[8] Heterocyclic 2-(chloromethyl)pyridine did not couple under our optimized conditions. Using non-nucleophilic KH, however, generated the product **2n**, but only in 39% yield.

To demonstrate the potential utility of this approach, we performed the coupling of 1-(chloromethyl)naphthalene (**1i**, 8.4 mmol, 1.48 g) to the *trans*-stilbene (**2i**) in 88% yield (Scheme 4), suggesting the reaction is scalable.

In summary, *trans*-stilbenes are widely used as industrial dyes, laser-dyes, and optoelectronic materials,[9] and significant effort has been devoted to their synthesis.[10−14] We have developed an organocatalytic method for their preparation that addresses a deficiency in our prior precatalyst, wherein a catalytic amount of an inseparable impurity was generated in

DOI: 10.1021/acs.orglett.5b00117
Org. Lett. XXXX, XXX, XXX−XXX

Scheme 3. Substrate Scope of Stilbene Formation from Benzyl Halides Catalyzed by Sulfenate Anions

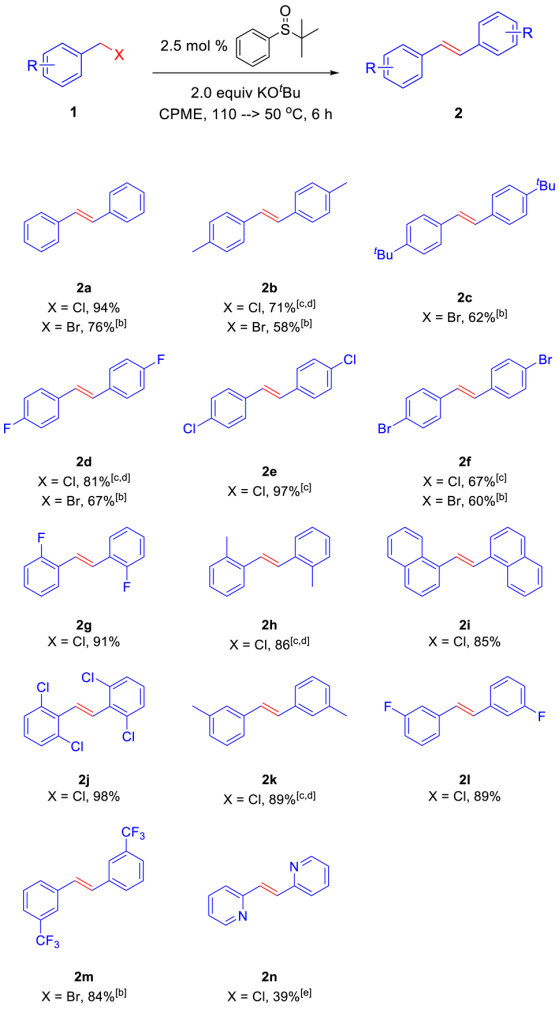

[a]Reactions were performed using 1.0 equiv of **1** and 2.0 equiv of base on a 0.2 mmol scale. [b]5 mol % precatalyst loading. [c]80 °C. [d]3.0 equiv of KO^{t}Bu used. [e]KH used as base and reaction run for 24 h at 110 °C.

Scheme 4. *trans*-1,2-Di(α-naphthyl)ethylene Formation on Gram Scale

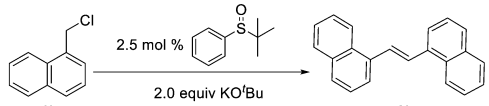

the first catalytic cycle. The precatalyst introduced herein, *tert*-butyl phenyl sulfoxide, undergoes base promoted E2 elimination to generate the sulfenate anion catalyst and a gaseous byproduct. Interestingly, the sulfenate anion generated under these conditions appears to survive the 110 °C precatalyst activation stage,[7] as judged by its ability to generate *trans*-stilbenes in up to 98% yield. Current efforts are focused on the application of sulfenate anion catalysts to other reactions.

■ ASSOCIATED CONTENT

Supporting Information

Procedures and characterization data for all new compounds. This material is available free of charge via the Internet at http://pubs.acs.org.

■ AUTHOR INFORMATION

Corresponding Author

*E-mail: pwalsh@sas.upenn.edu.

Notes

The authors declare no competing financial interest.

■ ACKNOWLEDGMENTS

We thank the National Science Foundation [CHE-1152488] and National Institutes of Health (NIGMS 104349). I.K.S. and M.A.P. thank the Spanish MINECO (grant CTQ2012-38594-C02-01) and the Institute of Chemical Research of Catalonia (ICIQ) Foundation for financial support.

■ REFERENCES

(1) (a) Hall, A.; Karplus, P. A.; Poole, L. B. *FEBS J.* **2009**, *276*, 2469. (b) Paulsen, C. E.; Carroll, K. S. *ACS Chem. Biol.* **2010**, *5*, 47. (c) Poole, L. B.; Nelson, K. J. *Curr. Opin. Chem. Biol.* **2008**, *12*, 18. (d) Griffiths, S. W.; King, J.; Cooney, C. L. *J. Biol. Chem.* **2002**, *277*, 25486.

(2) (a) Goto, K.; Holler, M.; Okazaki, R. *J. Am. Chem. Soc.* **1997**, *119*, 1460. (b) Goto, K.; Tokitoh, N.; Okazaki, R. *Angew. Chem., Int. Ed.* **1995**, *34*, 1124. (c) Davis, F. A.; Jenkins, L. A.; Billmers, R. L. *J. Org. Chem.* **1986**, *51*, 1033.

(3) (a) Jia, T.; Bellomo, A.; Montel, S.; Zhang, M.; El Baina, K.; Zheng, B.; Walsh, P. J. *Angew. Chem., Int. Ed.* **2014**, *53*, 260. (b) Jia, T.; Bellomo, A.; ELBaina, K.; Dreher, S. D.; Walsh, P. J. *J. Am. Chem. Soc.* **2013**, *135*, 3740−3743. See also: (c) Jia, T.; Zhang, M.; Sagamanova, I. K.; Wang, C. Y.; Walsh, P. J. *Org. Lett.* **2015**, DOI: 10.1021/acs.orglett.5b00092.

(4) For reviews, see: (a) O'Donnell, J. S.; Schwan, A. L. *J. Sulfur Chem.* **2004**, *25*, 183. (b) Maitro, G.; Prestat, G.; Madec, D.; Poli, G. *Tetrahedron: Asymmetry* **2010**, *21*, 1075. (c) Schwan, A. L.; Söderman, S. C. *Phosphorus, Sulfur Silicon, Relat. Elem.* **2013**, *188*, 275. For recent examples, see: (d) Maitro, G.; Vogel, S.; Sadaoui, M.; Prestat, G.; Madec, D.; Poli, G. *Org. Lett.* **2007**, *9*, 5493. (e) Bernoud, E.; Le Duc, G.; Bantreil, X.; Prestat, G.; Madec, D.; Poli, G. *Org. Lett.* **2010**, *12*, 320. (f) Singh, S. P.; O'Donnell, I. S.; Schwan, A. L. *Org. Biomol. Chem.* **2010**, *8*, 1712. (g) Söderman, S. C.; Schwan, A. L. *J. Org. Chem.* **2013**, *78*, 1638. (h) Zong, L.; Ban, X.; Kee, C. W.; Tan, C.-H. *Angew. Chem., Int. Ed.* **2014**, *53*, 11849. For a related reaction see: (i) Izquierdo, F.; Chartoire, A.; Nolan, S. P. *ACS Catalysis* **2013**, 2190−2193.

(5) (a) Zhang, M.; Jia, T.; Yin, H.; Carroll, P. J.; Schelter, E. J.; Walsh, P. J. *Angew. Chem., Int. Ed.* **2014**, *53*, 10755. (b) Schwan, A. L. *ChemCatChem* **2015**, *7*, 226.

(6) Mayeda, E. A.; Miller, L. L.; Wolf, J. F. *J. Am. Chem. Soc.* **1972**, *94*, 6812.

(7) (a) Refvik, M. D.; Schwan, A. L. *Can. J. Chem.* **1998**, *76*, 213. (b) Söderman, S. C.; Schwan, A. L. *Org. Lett.* **2011**, *13*, 4192.

(8) Ciorba, S.; Bartocci, G.; Galiazzo, G.; Mazzucato, U.; Spalletti, A. *J. Photochem. Photobiol. A* **2008**, *195*, 301.

(9) (a) Ciardelli, F.; Ruggeri, G.; Pucci, A. *Chem. Soc. Rev.* **2013**, *42*, 857. (b) Coe, B. J.; Foxon, S. P.; Harper, E. C.; Harris, J. A.; Helliwell, M.; Raftery, J.; Asselberghs, I.; Clays, K.; Franz, E.; Brunschwig, B. S.; Fitch, A. G. *Dyes Pigments* **2009**, *82*, 171.

(10) Ferre-Filmon, K.; Delaude, L.; Demonceau, A.; Noels, A. F. *Coord. Chem. Rev.* **2004**, *248*, 2323.

DOI: 10.1021/acs.orglett.5b00117
Org. Lett. XXXX, XXX, XXX−XXX

Chapter VI

(11) (a) McMurry, J. E.; Fleming, M. P. *J. Am. Chem. Soc.* **1974**, *96*, 4708. (b) McMurry, J. E. *Chem. Rev.* **1989**, *89*, 1513. (c) Idriss, H.; Pierce, K. G.; Barteau, M. A. *J. Am. Chem. Soc.* **1994**, *116*, 3063.
(12) (a) Wittig, G.; Schollkopf, U. *Chem. Ber.* **1954**, *87*, 1318. (b) Bellucci, G.; Chiappe, C.; Moro, G. L. *Tetrahedron Lett.* **1996**, *37*, 4225. (c) Shi, M.; Xu, B. *J. Org. Chem.* **2002**, *67*, 294. (d) Palacios, F.; Alonso, C.; Aparicio, D.; Rubiales, G.; de los Santos, J. M. *Tetrahedron* **2007**, *63*, 523.
(13) (a) Reitter, B. E.; Sachdeva, Y. P.; Wolfe, J. F. *Abstr. Pap. Am. Chem. Soc.* **1981**, *181*, 15. (b) Hauser, C. R.; Brasen, W. R.; Skell, P. S.; Kantor, S. W.; Brodhag, A. E. *J. Am. Chem. Soc.* **1956**, *78*, 1653.
(14) Zhao, F.; Luo, J.; Tan, Q.; Liao, Y.; Peng, S.; Deng, G. *Adv. Synth. Catal.* **2012**, *354*, 1914.

DOI: 10.1021/acs.orglett.5b00117
Org. Lett. XXXX, XXX, XXX−XXX

6.4. Conclusions and Outlook.

A second generation pre-catalyst has been developed, showing high potential in the transformation of benzylic halides to *trans*-stilbenes. The desired compounds are generated without contamination thanks to the formation of a gaseous-by-product during the first cycle.[263]

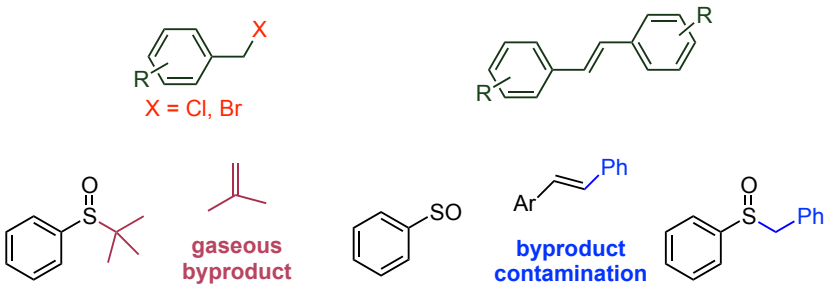

Using *tert*-butyl phenyl sulfoxide as organocatalyst, a variety of *trans*-stilbenes has been generated with 39-98% isolated yield, some of them with improved yield from the previous report. Also, challenging substrates such as those bearing *ortho* substituents and heteroaromatics can be used with this new approach.

With respect to the excellent results obtained, further studies should be devoted to the development of other sulfenate-catalyzed reactions. Recent research by Walsh *et al.* proved this potential in the transformation of aldehydes into alkynes, providing an additional example of the use these reactive sulfenate anion species in organocatalysis. [262]

[263] This work was highlighted in a recent report: Ooi, T. *ACS Catal.* **2015**, *5*, 6980-6988.

UNIVERSITAT ROVIRA I VIRGILI
NEW APPROACHES TO CATALYST DESIGN AND IMMOBILIZATION
Irina Sagamanova

SUPPORTING INFORMATION

tert-Butyl Phenyl Sulfoxide: a Traceless Sulfenate Anion Precatalyst

Mengnan Zhang,[a] Tiezheng Jia,[a] Irina K. Sagamanova,[b,c] Miquel A. Pericás,[b,c] Patrick J. Walsh*,[a]

[a]Roy and Diana Vagelos Laboratories, Department of Chemistry, University of Pennsylvania, 231 South 34th Street, Philadelphia, Pennsylvania 19104-6323, United States

[b]Institute of Chemical Research of Catalonia (ICIQ), Av. Països Catalans 16, 43007 Tarragona, Spain

[c]Departament de Química Organica, Universitat de Barcelona (UB), 08028 Barcelona, Spain

TABLE OF CONTENTS

Chapter VI

General Methods: All reactions were carried out under dry nitrogen. Anhydrous cyclopentyl methyl ether (CPME) was purchased from Sigma-Aldrich and directly used without further purification. Unless otherwise stated, reagents were commercially available and used as purchased without further purification. Chemicals were purchased from Sigma-Aldrich, Acros, Alfa Aesar or Matrix Scientific, and solvents were purchased from Fisher Scientific. The progress of the reactions was monitored by thin-layer chromatography using Whatman Partisil K6F 250 μm precoated 60 Å silica gel plates and visualized by short-wave ultraviolet light as well as by treatment with iodine. Flash chromatography was performed with silica gel (230–400 mesh, Silicycle). The NMR spectra were obtained using a Brüker 500 MHz Fourier-transform NMR spectrometer. Chemical shifts are reported in units of parts per million (ppm) downfield from tetramethylsilane (TMS), and all coupling constants are reported in hertz. Reactions were conducted in 2–5 mL microwave vials that were purchased from VWR International.

Preparation of sulfoxides: Sulfoxides were prepared according to the literature procedures.[1]

General Procedure for catalysis: To an oven-dried microwave vial equipped with a stir bar was added phenyl *tert*-butyl sulfoxide (0.91 mg, 0.005 mmol) and KO^{t}Bu (44.8 mg, 0.40 mmol, 2.0 equiv), under nitrogen atmosphere followed by 2.0 mL dry CPME. The microwave vial was sealed and heated to 110 ^{o}C for 30 min. When the solution turned to pale yellow, benzyl chloride (24 µL, 0.20 mmol) was added by syringe under nitrogen atmosphere under room temperature. Note that if the benzylic halide is a solid, it was dissolved in 0.5 mL CPME and added as a solution under nitrogen atmosphere. The reaction mixture was heated to 50 °C by oil bath and stirred for 6 h. The sealed vial was cooled to room temperature, opened to air, and the reaction mixture was passed through a short pad of silica gel. The pad was then rinsed with 10 mL ethyl acetate and the solvent was removed under reduced pressure. The crude product

was purified by flash chromatography on silica gel (eluted with Hexanes) to give the product (16.9 mg, 94% yield) as a white solid. The spectroscopic data match the previously reported data.[2]

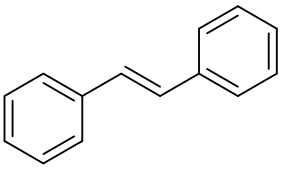

(*E*)-Stilbene (2a): The reaction was performed following the General Procedure with phenyl *tert*-butyl sulfoxide (0.91 mg, 0.005 mmol, from a stock solution), benzyl chloride (1a) (24 μL, 0.20 mmol) and KO^{t}Bu (44.8 mg, 0.40 mmol). The crude product was purified by flash chromatography on silica gel (eluted with Hexanes) to give the product (16.9 mg, 94% yield) as a white solid. The spectroscopic data match the previously reported data.[2]

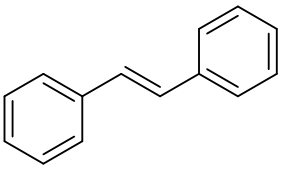

(*E*)-Stilbene (2a) (from benzyl bromide): The reaction was performed following the General Procedure with phenyl *tert*-butyl sulfoxide (1.82 mg, 0.010 mmol, from a stock solution), benzyl bromide (1a')(24.0 μL, 0.20 mmol) and KO^{t}Bu (44.8 mg, 0.40 mmol). The crude product was purified by flash chromatography on silica gel (eluted with Hexanes) to give the product (13.7 mg, 76% yield) as a white solid. The spectroscopic data match the previously reported data.[2]

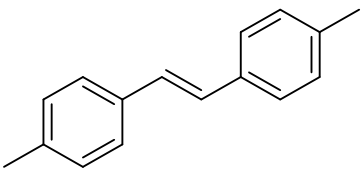

(*E*)-4,4'-Dimethylstilbene (2b): The reaction was performed following the General Procedure with phenyl *tert*-butyl sulfoxide (0.91 mg, 0.005 mmol, from a stock solution), 4-methylbenzyl chloride (1b) (27 μL, 0.20 mmol) and KO^{t}Bu (67.2 mg, 0.60 mmol). The crude product was purified by flash chromatography on silica gel (eluted with Hexanes) to give the product (14.8 mg, 71% yield) as a white solid. The spectroscopic data match the previously reported data.[2]

Chapter VI

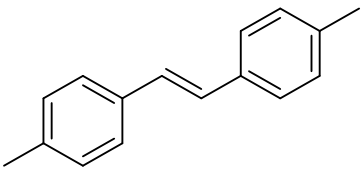

(*E*)-4,4'-Dimethylstilbene (2b) (from 4-methylbenzyl bromide): The reaction was performed following the General Procedure with phenyl *tert*-butyl sulfoxide (1.81 mg, 0.010 mmol, from a stock solution), 4-methylbenzyl bromide (1b') (37.0 mg, 0.20 mmol) and KO^{t}Bu (44.8 mg, 0.40 mmol). The crude product was purified by flash chromatography on silica gel (eluted with Hexanes) to give the product (12.1 mg, 58% yield) as a white solid. The spectroscopic data match the previously reported data.[2]

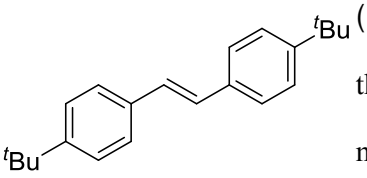

(*E*)-4,4'-Di(*tert*-butyl)stilbene (2c): The reaction was performed following the General Procedure with phenyl *tert*-butyl sulfoxide (1.82 mg, 0.010 mmol, from a stock solution), 4-*tert*-butylbenzyl bromide (1c) (37 μL, 0.20 mmol) and KO^{t}Bu (44.8 mg, 0.40 mmol). The crude product was purified by flash chromatography on silica gel (eluted with Hexanes) to give the product (18.1 mg, 62% yield) as a white solid. The spectroscopic data match the previously reported data.[3]

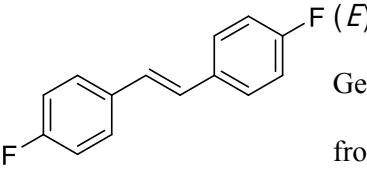

(*E*)-4,4'-Difluorostilbene (2d): The reaction was performed following the General Procedure with phenyl *tert*-butyl sulfoxide (0.91 mg, 0.005 mmol, from a stock solution), 4-fluorobenzyl chloride (1e) (24 μL, 0.20 mmol) and KO^{t}Bu (67.2 mg, 0.60 mmol). The crude product was purified by flash chromatography on silica gel (eluted with Hexanes) to give the product (17.5 mg, 81% yield) as a white solid. The spectroscopic data match the previously reported data.[2]

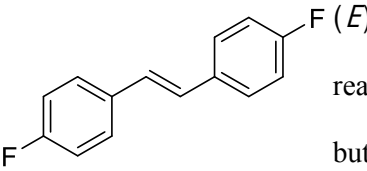

(*E*)-4,4'-Difluorostilbene (2d) (from 4-fluorobenzyl bromide): The reaction was performed following the General Procedure with phenyl *tert*-butyl sulfoxide (1.82 mg, 0.010 mmol, from a stock solution), 4-fluorobenzyl bromide (1e') (25 μL, 0.20 mmol) and KO^{t}Bu (44.8 mg, 0.40 mmol). The crude product was purified by flash chromatography on silica gel (eluted with Hexanes) to give the

product (14.5 mg, 67% yield) as a white solid. The spectroscopic data match the previously reported data.[2]

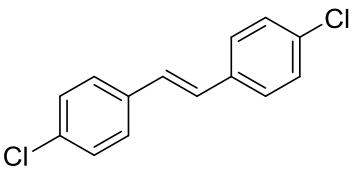

(*E*)-4,4'-Dichlorostilbene (2e): The reaction was performed following the General Procedure with phenyl *tert*-butyl sulfoxide (0.91 mg, 0.005 mmol, from a stock solution), 4-chlorobenzyl chloride (1f) (32.2 mg, 0.20 mmol) and KO^{t}Bu (44.8 mg, 0.40 mmol). The crude product was purified by flash chromatography on silica gel (eluted with Hexanes) to give the product (24.2 mg, 97% yield) as a white solid. The spectroscopic data match the previously reported data.[2]

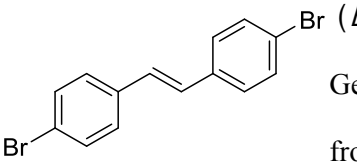

(*E*)-4,4'-Dibromostilbene (2f): The reaction was performed following the General Procedure with phenyl *tert*-butyl sulfoxide (0.91 mg, 0.005 mmol, from a stock solution), 4-bromobenzyl chloride (1e) (41.1 mg, 0.20 mmol) and KO^{t}Bu (44.8 mg, 0.40 mmol). The crude product was purified by flash chromatography on silica gel (eluted with Hexanes) to give the product (22.6 mg, 67% yield) as a white solid. The spectroscopic data match the previously reported data.[4]

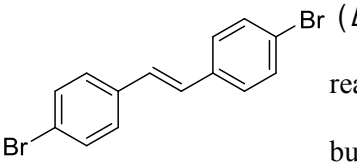

(*E*)-4,4'-Dibromostilbene (2f) (from 4-bromobenzyl bromide): The reaction was performed following the General Procedure with phenyl *tert*-butyl sulfoxide (1.82 mg, 0.010 mmol, from a stock solution), 4-bromobenzyl bromide (1e') (50 mg, 0.20 mmol) and KO^{t}Bu (44.8 mg, 0.40 mmol). The crude product was purified by flash chromatography on silica gel (eluted with Hexanes) to give the product (20.1 mg, 60% yield) as a white solid. The spectroscopic data match the previously reported data.[4]

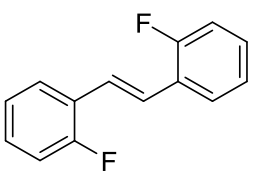

(*E*)-2,2'-Difluorostilbene (2g): The reaction was performed following the General Procedure with phenyl *tert*-butyl sulfoxide (0.91 mg, 0.005 mmol, from a stock solution), 2-fluorobenzyl chloride (1g) (24.0 μL, 0.20 mmol) and KO^{t}Bu (44.8 mg, 0.40 mmol). The crude product was purified by flash chromatography on silica gel

(eluted with Hexanes) to give the product (19.7 mg, 91% yield) as a white solid. The spectroscopic data match the previously reported data.[2]

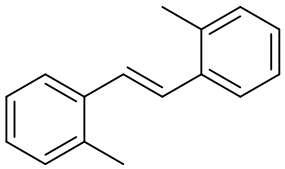

(*E*)-2,2'-Dimethylstilbene (2h): The reaction was performed following the General Procedure with phenyl *tert*-butyl sulfoxide (0.91 mg, 0.005 mmol, from a stock solution), 2-methylbenzyl chloride (1h) (27.0 μL, 0.20 mmol) and KO^{t}Bu (67.2 mg, 0.60 mmol). The crude product was purified by flash chromatography on silica gel (eluted with Hexanes) to give the product (17.9 mg, 86% yield) as a white solid. The spectroscopic data match the previously reported data. [2]

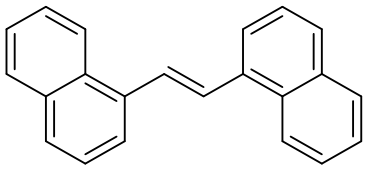

(*E*)-1,2-Di(1-naphthyl)ethylene (2i): The reaction was performed following the General Procedure with phenyl *tert*-butyl sulfoxide (0.91 mg, 0.005 mmol, from a stock solution), 1-(chloromethyl)naphthalene (1i) (35.4 mg, 0.20 mmol) and KO^{t}Bu (44.8 mg, 0.40 mmol). The crude product was purified by flash chromatography on silica gel (eluted with Hexanes) to give the product (23.8 mg, 85% yield) as a white solid. The spectroscopic data match the previously reported data.[2]

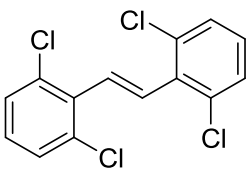

(*E*)-2,2',6,6'-Tetrachlorostilbene (2j): The reaction was performed following the General Procedure with phenyl *tert*-butyl sulfoxide (0.91 mg, 0.005 mmol, from a stock solution), 2,6-dichlorobenzyl chloride (1j) (39.2 mg, 0.20 mmol) and KO^{t}Bu (44.8 mg, 0.40 mmol). The crude product was purified by flash chromatography on silica gel (eluted with Hexanes) to give the product (31.2 mg, 98% yield) as a white solid. The spectroscopic data match the previously reported data.[2]

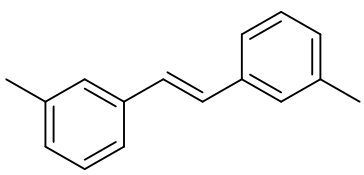

(*E*)-3,3'-Dimethylstilbene (2k): The reaction was performed following the General Procedure with phenyl *tert*-butyl sulfoxide (0.91 mg, 0.005 mmol, from a stock solution), 3-methylbenzyl chloride (1k) (27.0 μL, 0.20 mmol) and KO^{t}Bu (67.2 mg, 0.60 mmol). The crude product was purified

by flash chromatography on silica gel (eluted with Hexanes) to give the product (18.5 mg, 89% yield) as a white solid. The spectroscopic data match the previously reported data.[2]

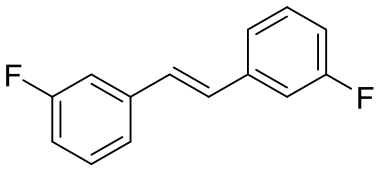

(*E*)-3,3'-Difluorostilbene (2l): The reaction was performed following the General Procedure with phenyl *tert*-butyl sulfoxide (0.91 mg, 0.005 mmol, from a stock solution), 3-fluorobenzyl chloride (1l) (24.0 μL, 0.20 mmol) and KO^{t}Bu (44.8 mg, 0.40 mmol). The crude product was purified by flash chromatography on silica gel (eluted with Hexanes) to give the product (19.2 mg, 89% yield) as a white solid. The spectroscopic data match the previously reported data.[4]

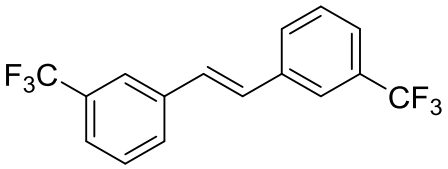

(*E*)-3,3'-Ditrifluoromethylstilbene (3m): The reaction was performed following the General Procedure with phenyl *tert*-butyl sulfoxide (1.82 mg, 0.010 mmol, from a stock solution), 3-trifluoromethylbenzyl bromide (1m) (31.0 μL, 0.20 mmol) and KO^{t}Bu (44.8 mg, 0.40 mmol). The crude product was purified by flash chromatography on silica gel (eluted with Hexanes) to give the product (26.6 mg, 84% yield) as a white solid. The spectroscopic data match the previously reported data.[5]

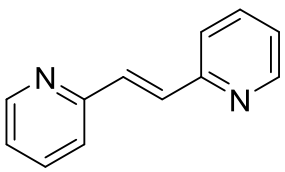

1,2-*trans*-Bis(2-pyridyl)ethylene (2n): To an oven-dried microwave vial equipped with a stir bar was added phenyl *tert*-butyl sulfoxide (0.91 mg, 0.005 mmol, from a stock solution), 2-(chloromethyl)pyridine hydrochloride (1n) (32.8 mg, 0.20 mmol) and KH (32 mg, 0.80 mmol, 4.0 equiv) in a nitrogen filled dry box followed by 2.0 mL dry CPME. The microwave vial was sealed with a vial cap with a rubber insert and the sealed vial removed from the dry box. The reaction mixture was heated to 110 °C in an oil bath and stirred for 24 h. The sealed vial was cooled to room temperature, opened to air, and the reaction mixture was passed through a short pad of silica gel. The pad was then rinsed with 20 mL ethyl acetate. The volatile materials were removed under reduced pressure. The crude product was purified by flash

chromatography on silica gel (eluted with Hexanes:EtOAc = 1:1) to give the product (7.1 mg, 39% yield) as a white solid. The spectroscopic data match the previously reported data.[6]

Gram scale reaction.

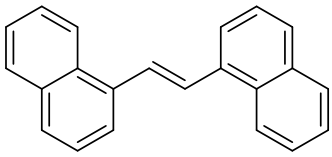

(*E*)-1,2-Di(1-naphthyl)ethylene (2i): To a three-necked round bottom flask equipped with a condenser under a nitrogen atmosphere was added phenyl *tert*-butyl sulfoxide (38.3 mg, 0.18 mmol), KO^{t}Bu (1.89 g, 16.8 mmol) and the flask was subjected to 3 cycles of vacuum/back fill with nitrogen. Two other necks were sealed with rubber septa Then 50 mL dry CPME were added via a syringe through the rubber septum. The rubber septa were replaced with greased glass stoppers. The reaction mixture was heated to 110 °C and stirred for 30 min under nitrogen. The flask was then transferred to a 50 ^{o}C oil bath and 1.48 g 1-(chloromethyl)naphthalene dissolved in 34 mL of CPME was added via a syringe with nitrogen protection. The reaction mixture was heated at 50 ^{o}C for 6 h then passed through a short pad of silica gel, and eluted with 150 mL ethyl acetate. The volatile materials were removed under reduced pressure and the residue was purified by flash chromatography on silica gel (eluted with Hexanes) to give the product (1.04 g, 88% yield) as a white solid. The spectroscopic data match the reported data.[2]

Reference

1. (a) Iwao, M.; Iihama, T.; Mahalanabis, K. K.; Perrier, H.; Snieckus, V. *J. Org. Chem.* 1989, *54*, 24. (b) Holland, H. L.; Turner, C. D.; Andreana, P. R.; Nguyen, D. *Can. J. Chem.* 1999, *77*, 463.

2. Zhao, F.; Luo, J.; Tan, Q.; Liao, Y.; Peng, S.; Deng, G. *Adv. Synth. Catal.* 2012, *354*, 1914.

3. Gelalcha, F. G.; Anilkumar, G.; Tse, M. K.; Bruckner, A.; Beller, M. *Chem. Eur. J.* 2008, *14*,7687.

4. Saiye, A. S.; Patel, K. N.; Kamath, B. V.; Bedekar, A. V. *Tetrahedron Lett.* 2012, *53*, 4692.

5. Shi, M.; Xu, B. *J. Org. Chem.* 2002, *67*, 294.

6. Annapurna, M.; Reddy, P. V.; Singh, S. P.; Kantam, M. L. *Tetrahedron* 2013, *69*,10940.

NMR Spectra

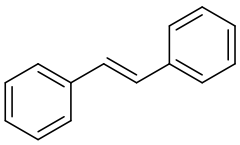

2a

Chapter VI

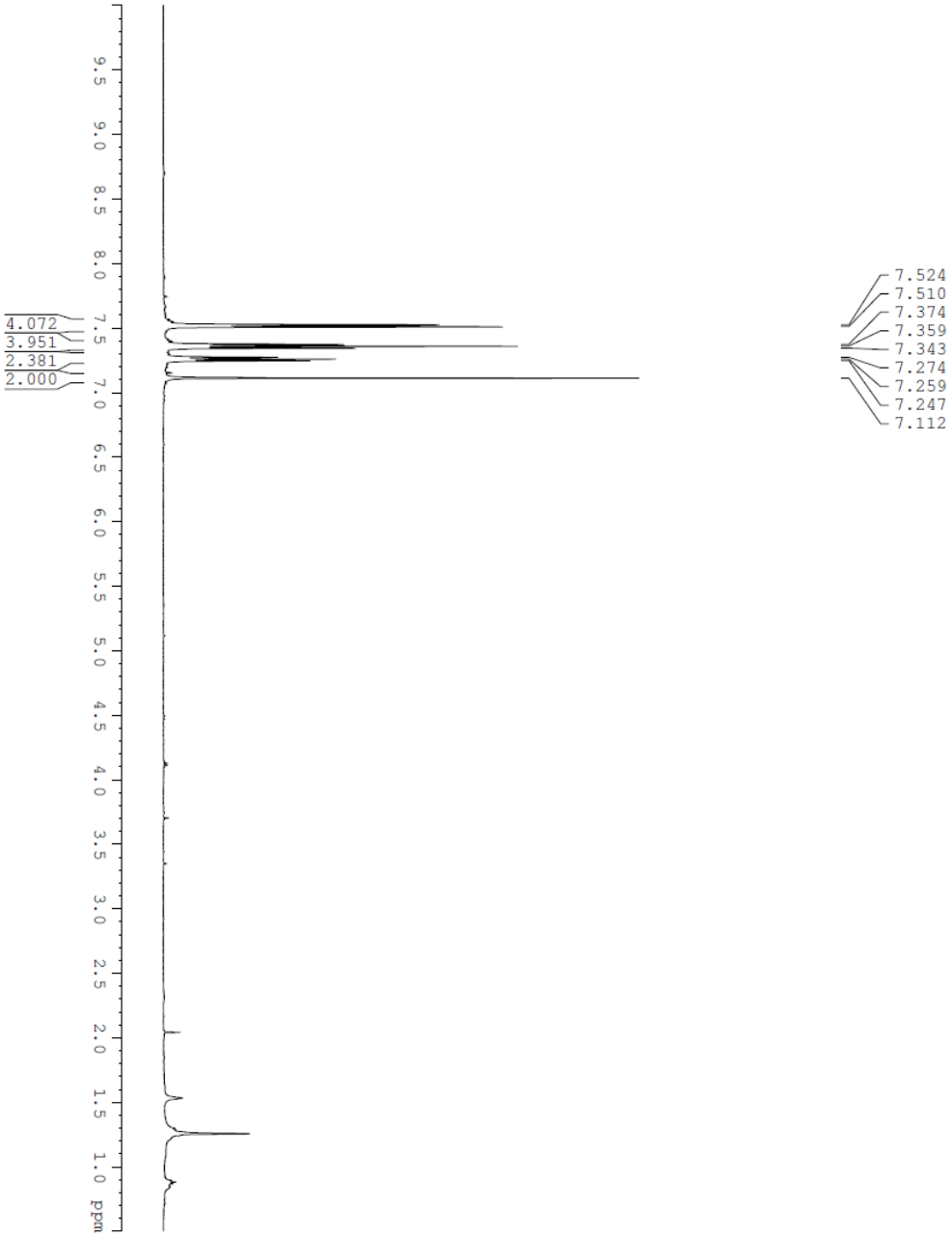

Figure S1. ^{1}H (500 MHz) NMR spectrum of 2a in $CDCl_3$.

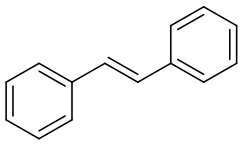

2a in $CDCl_3$

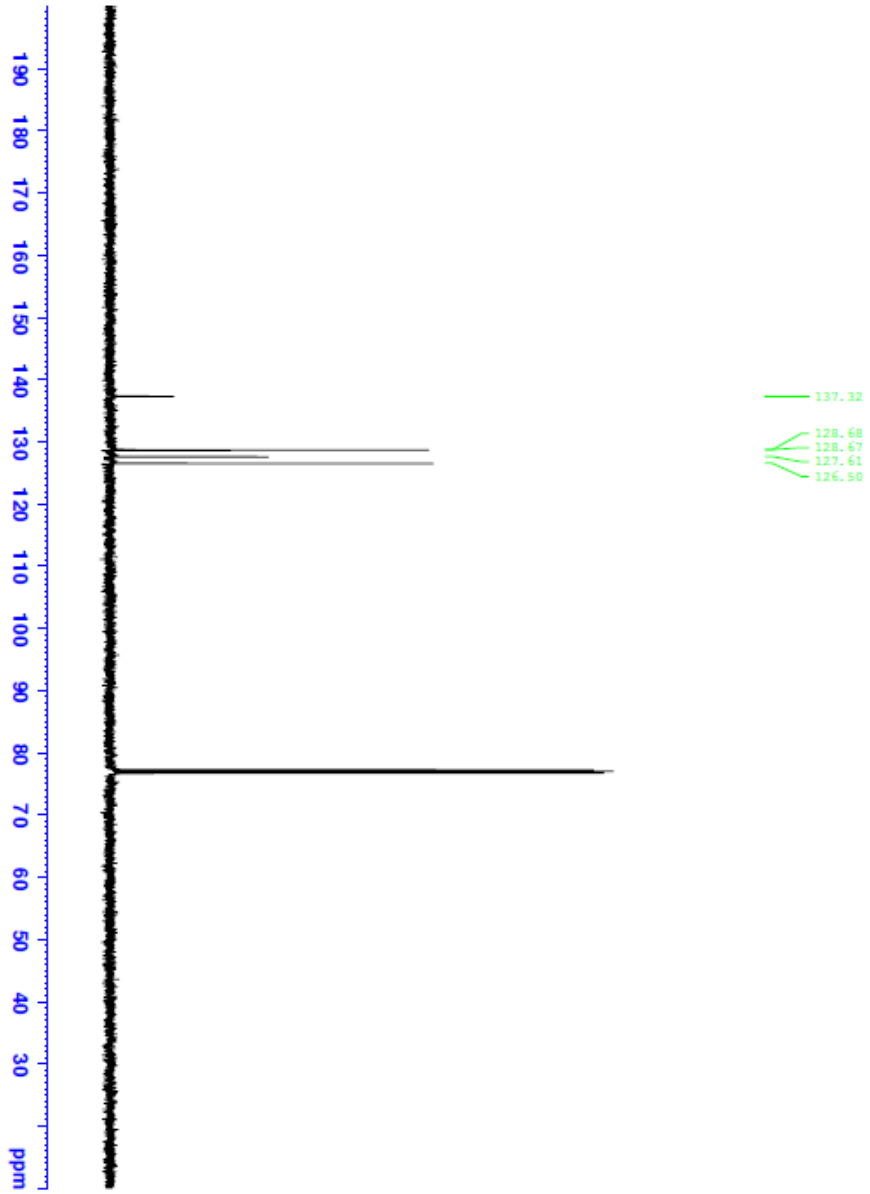

Figure S2. $^{13}C\ \{^{1}H\}$ (125 MHz) NMR spectrum of 2a in $CDCl_3$.

Chapter VI

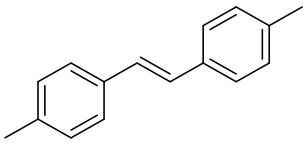

2b in $CDCl_3$

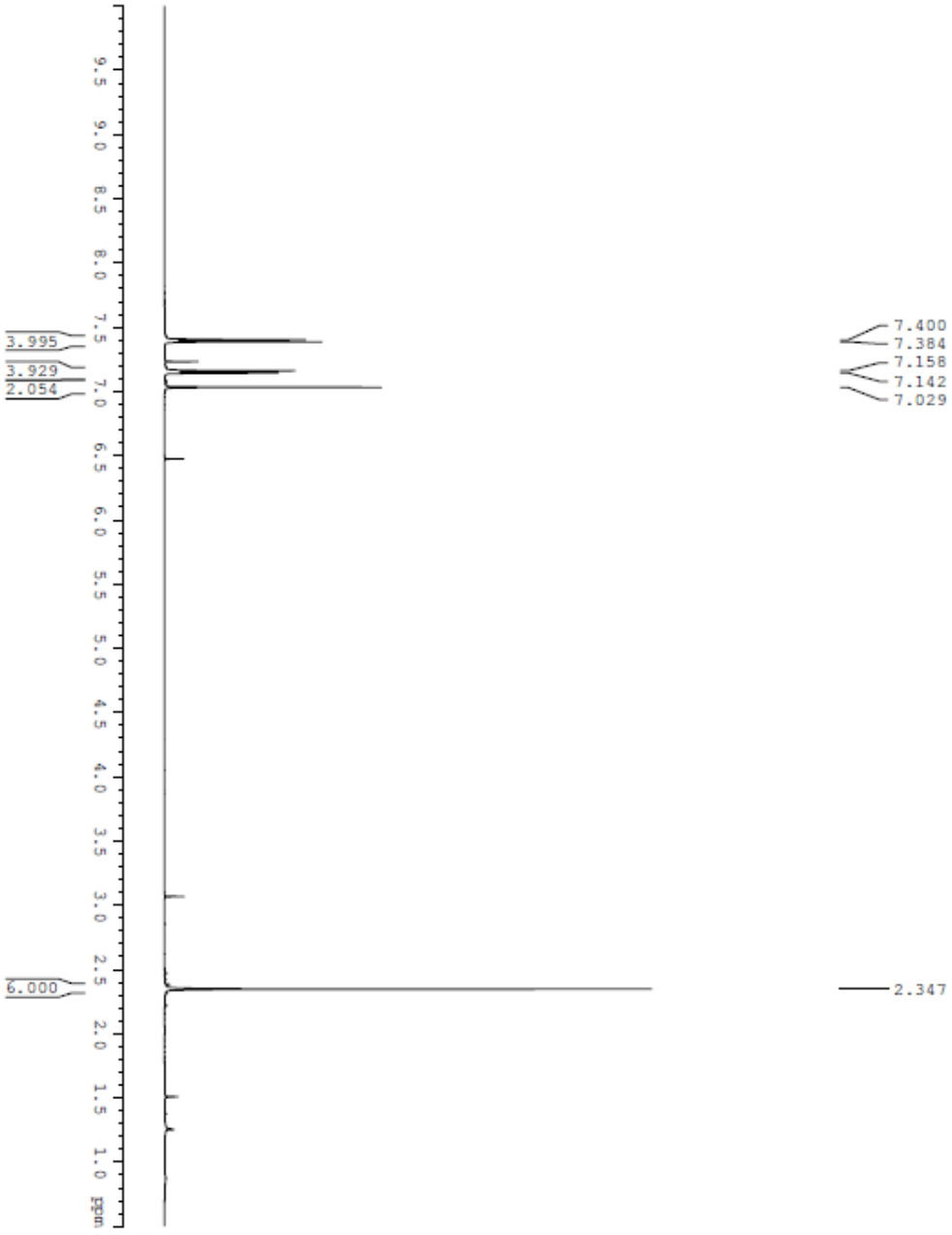

Figure S3. ^1H (500 MHz) NMR spectrum of 2b in $CDCl_3$.

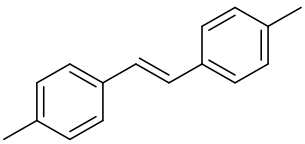

2b in $CDCl_3$

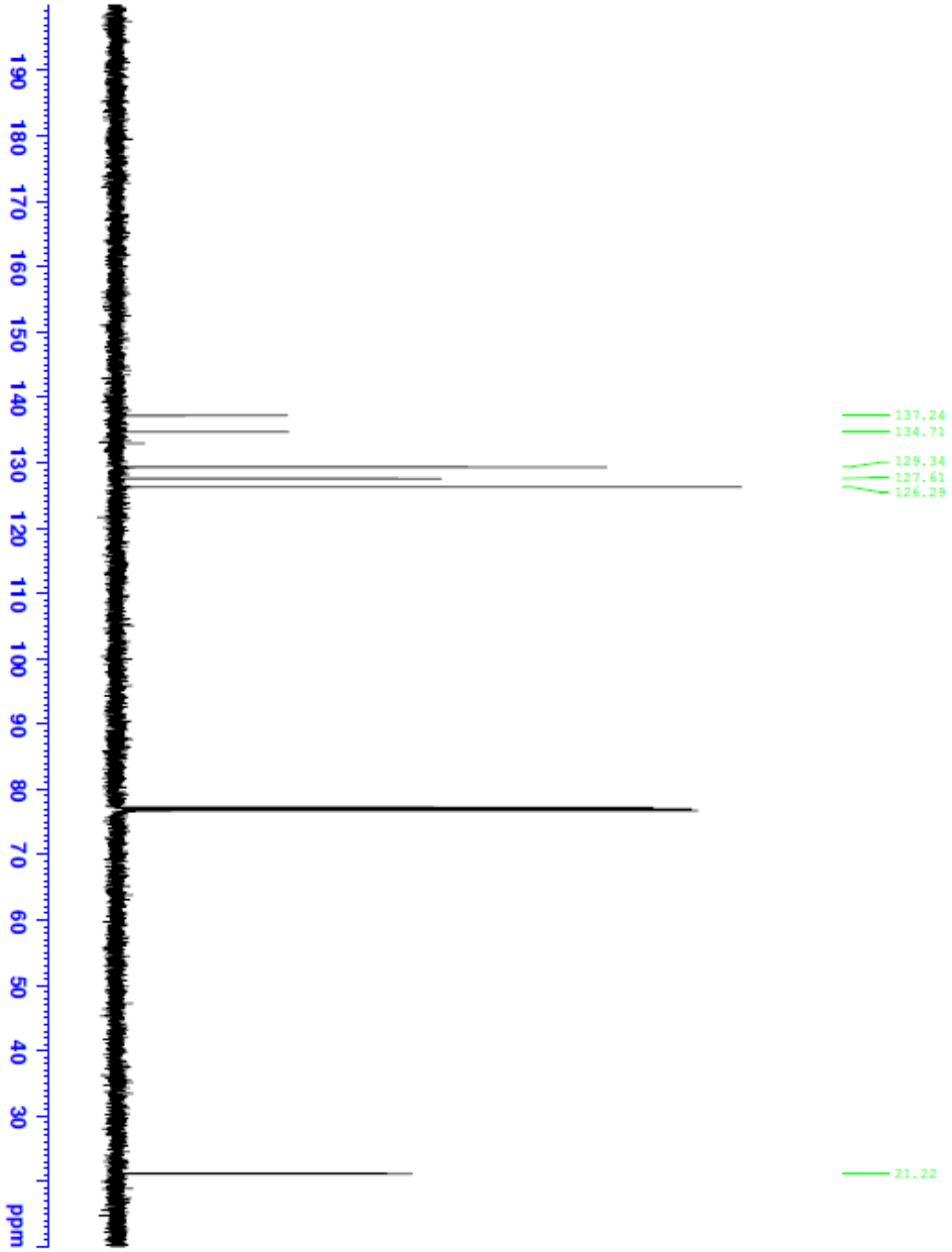

Figure S4. $^{13}C\{^{1}H\}$ (125 MHz) NMR spectrum of 2b in $CDCl_3$.

Chapter VI

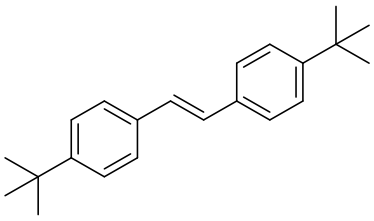

2c in $CDCl_3$

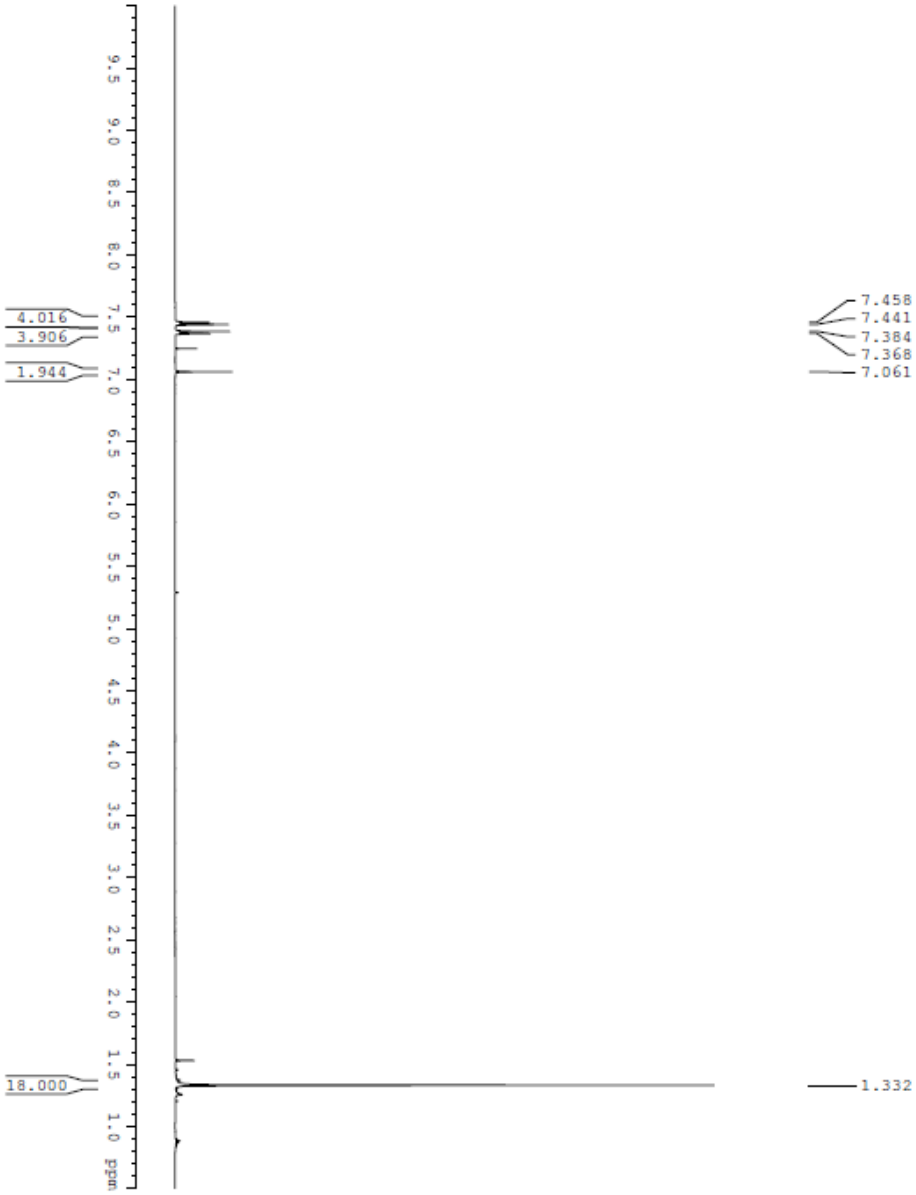

Figure S5. ^1H (500 MHz) NMR spectrum of 2c in $CDCl_3$.

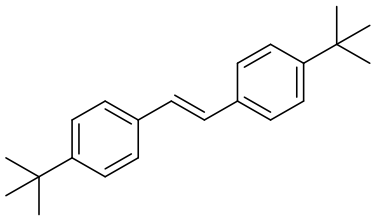

2c in $CDCl_3$

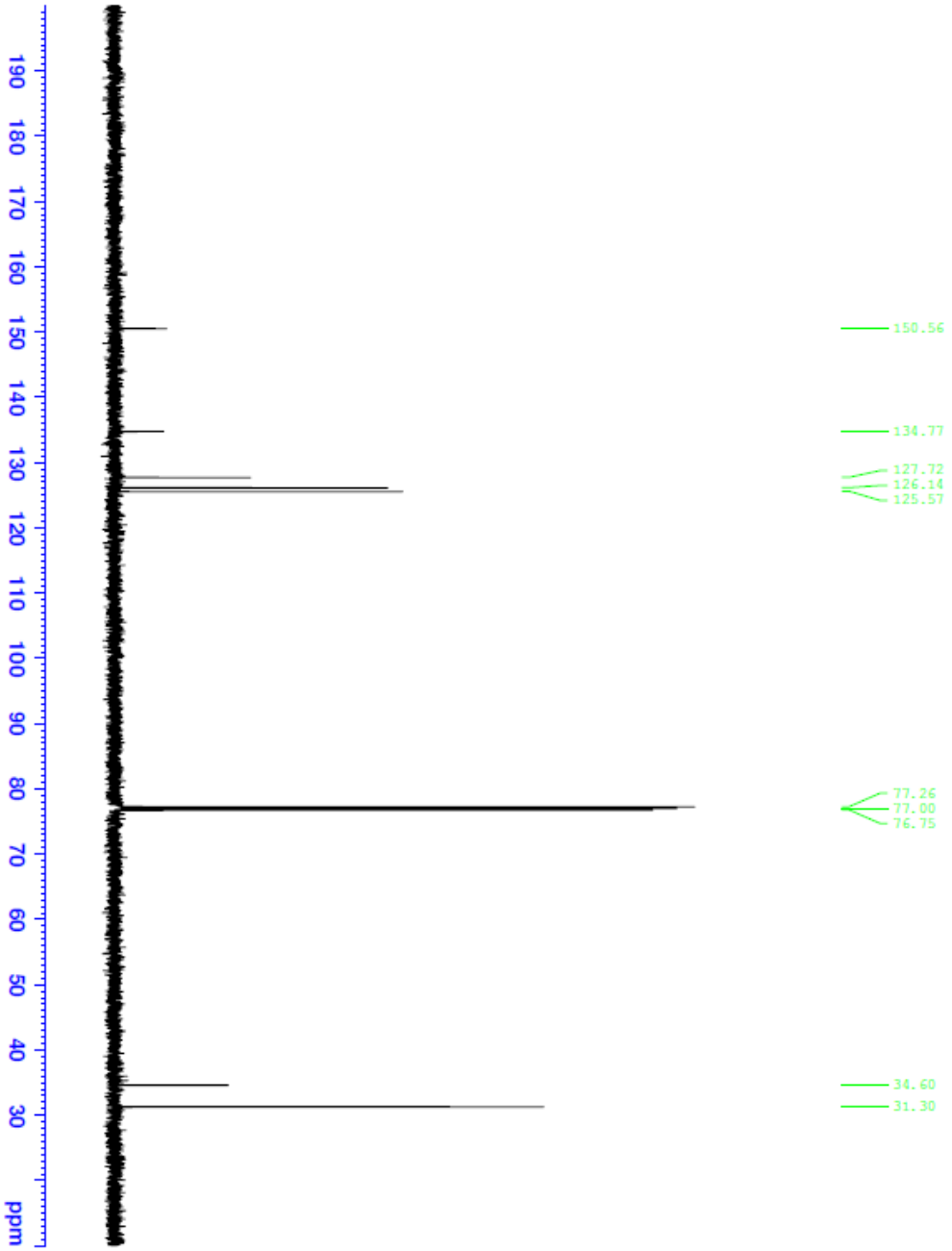

Figure S6. $^{13}C\{^{1}H\}$ (125 MHz) NMR spectrum of 2c in $CDCl_3$.

Chapter VI

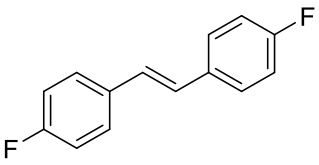

2d in $CDCl_3$

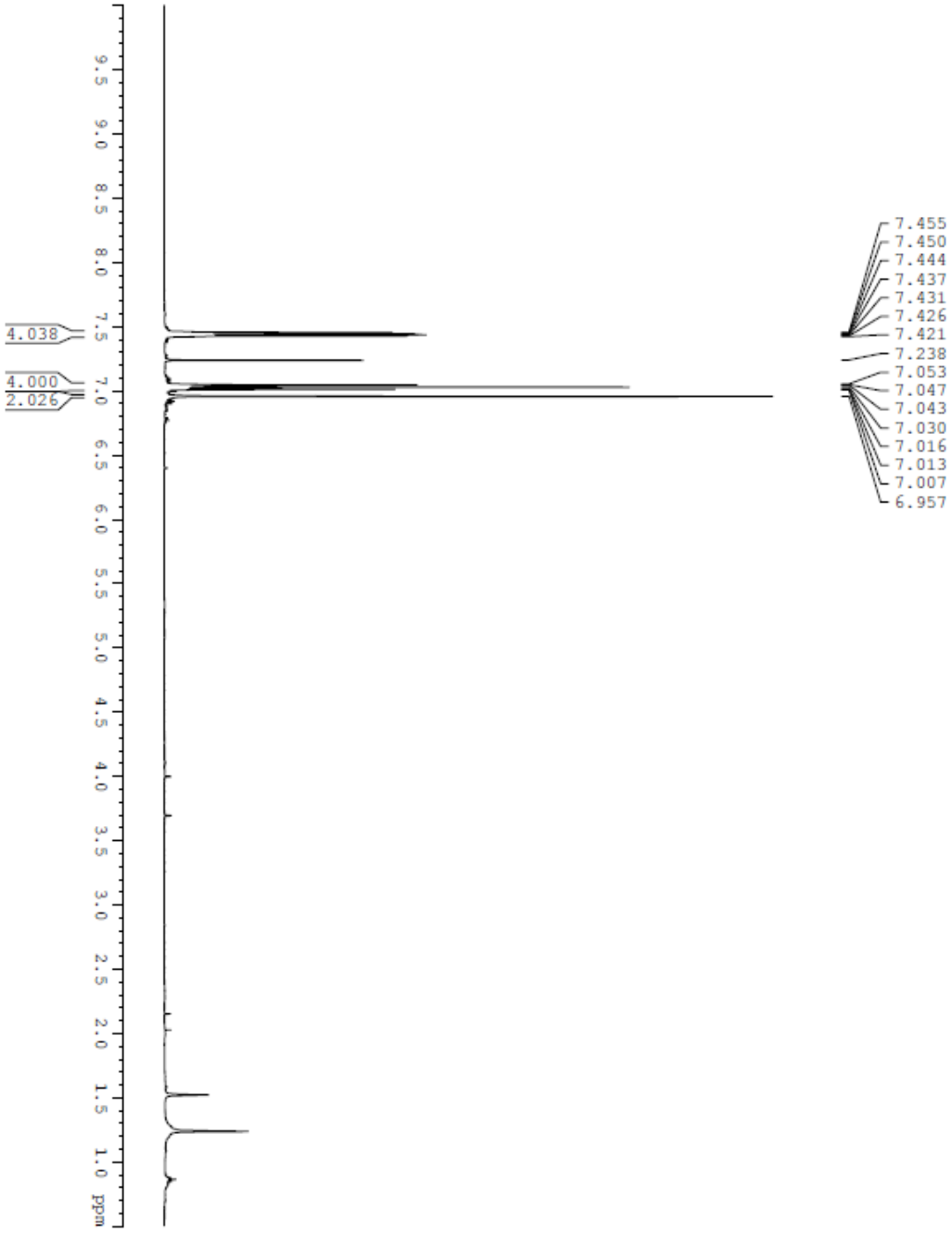

Figure S7. ^{1}H (500 MHz) NMR spectrum of 2d in $CDCl_3$.

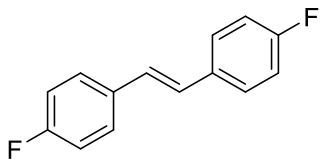

2d in $CDCl_3$

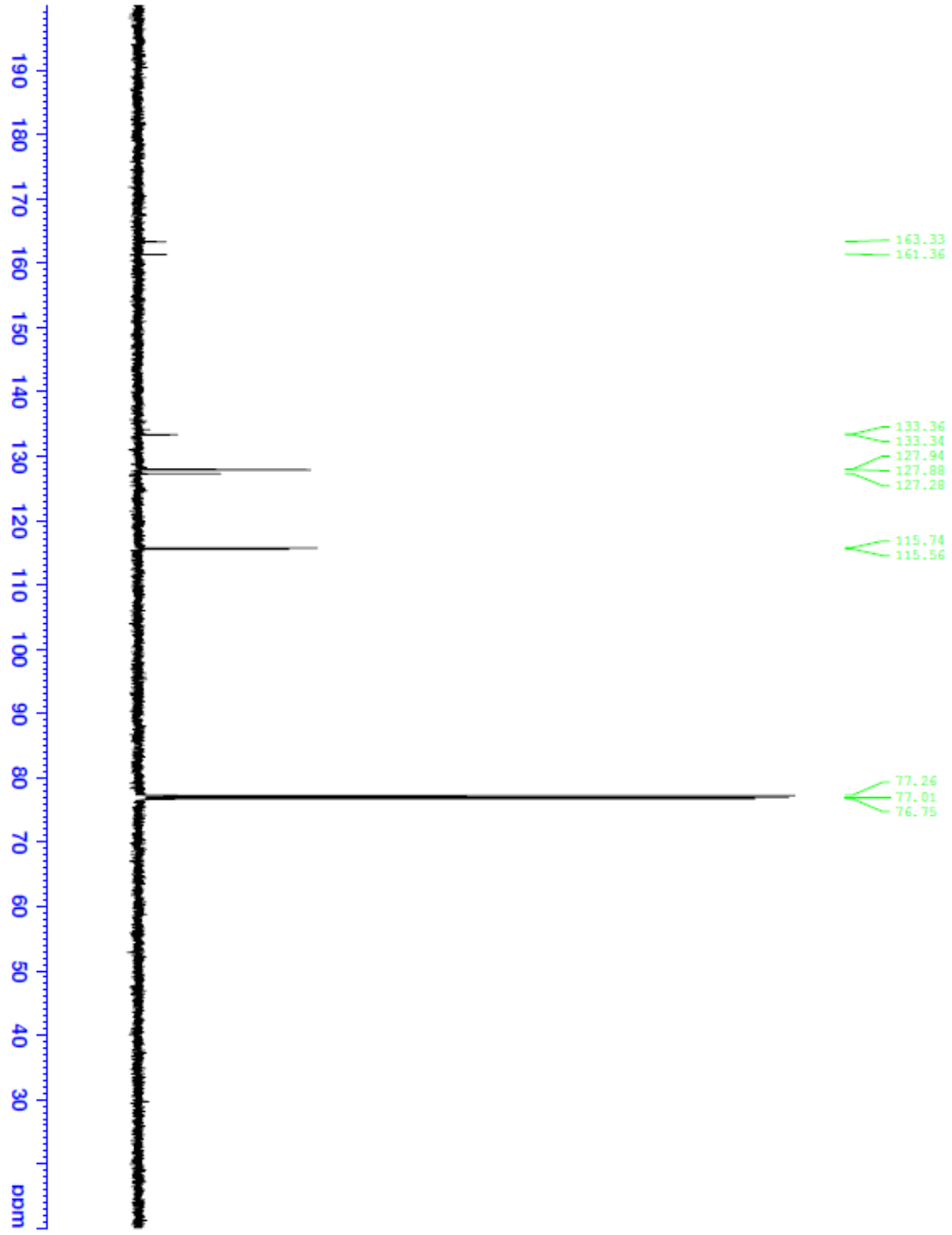

Figure S8. $^{13}C\ \{^{1}H\}$ (125 MHz) NMR spectrum of 2d in $CDCl_3$.

Chapter VI

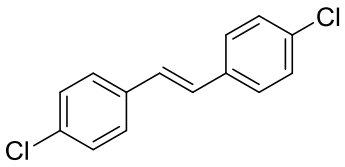

2e in $CDCl_3$

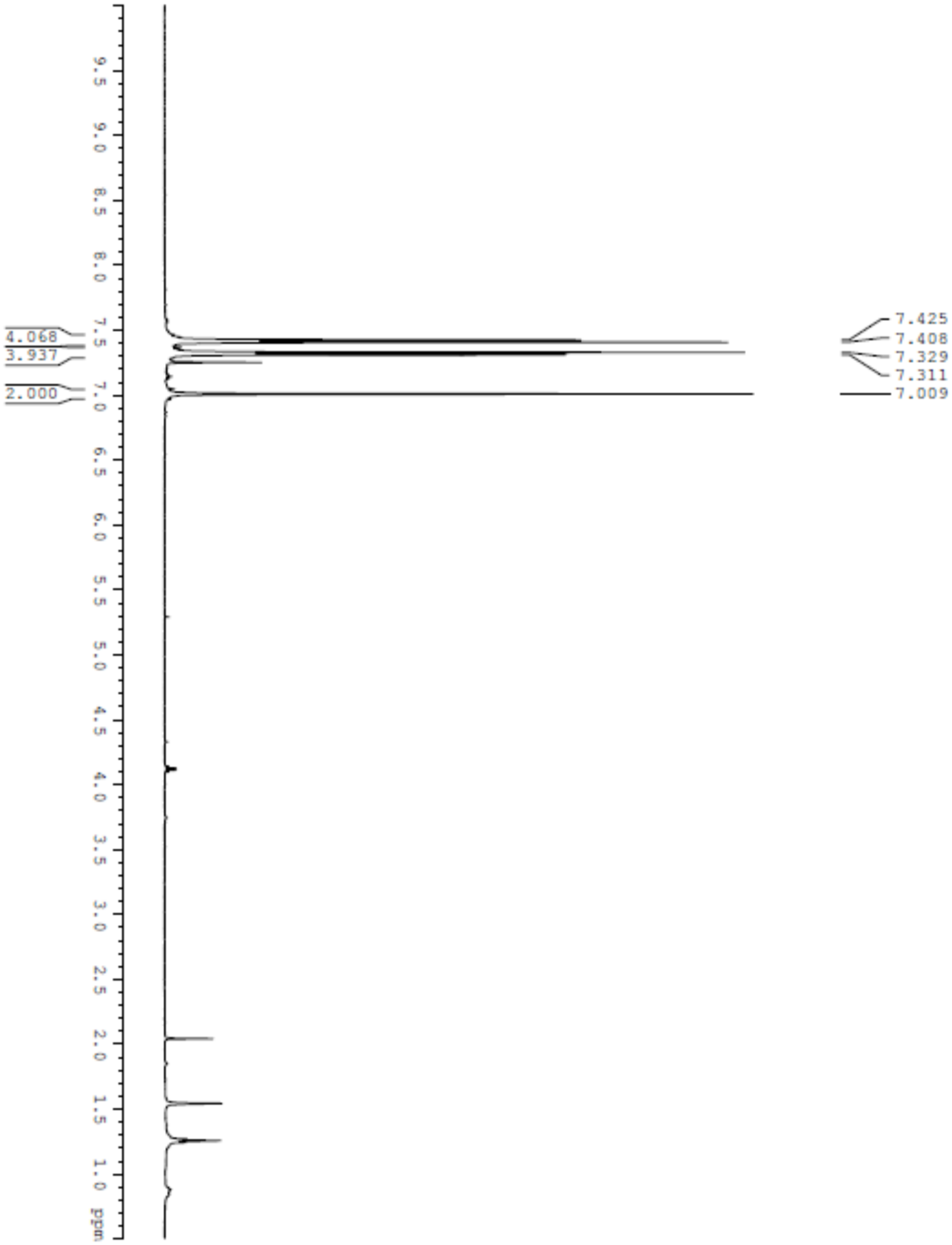

Figure S9. ^1H (500 MHz) NMR spectrum of 2e in $CDCl_3$.

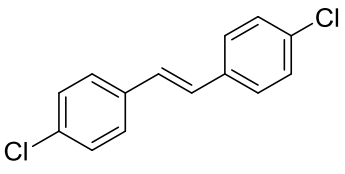

2e in $CDCl_3$

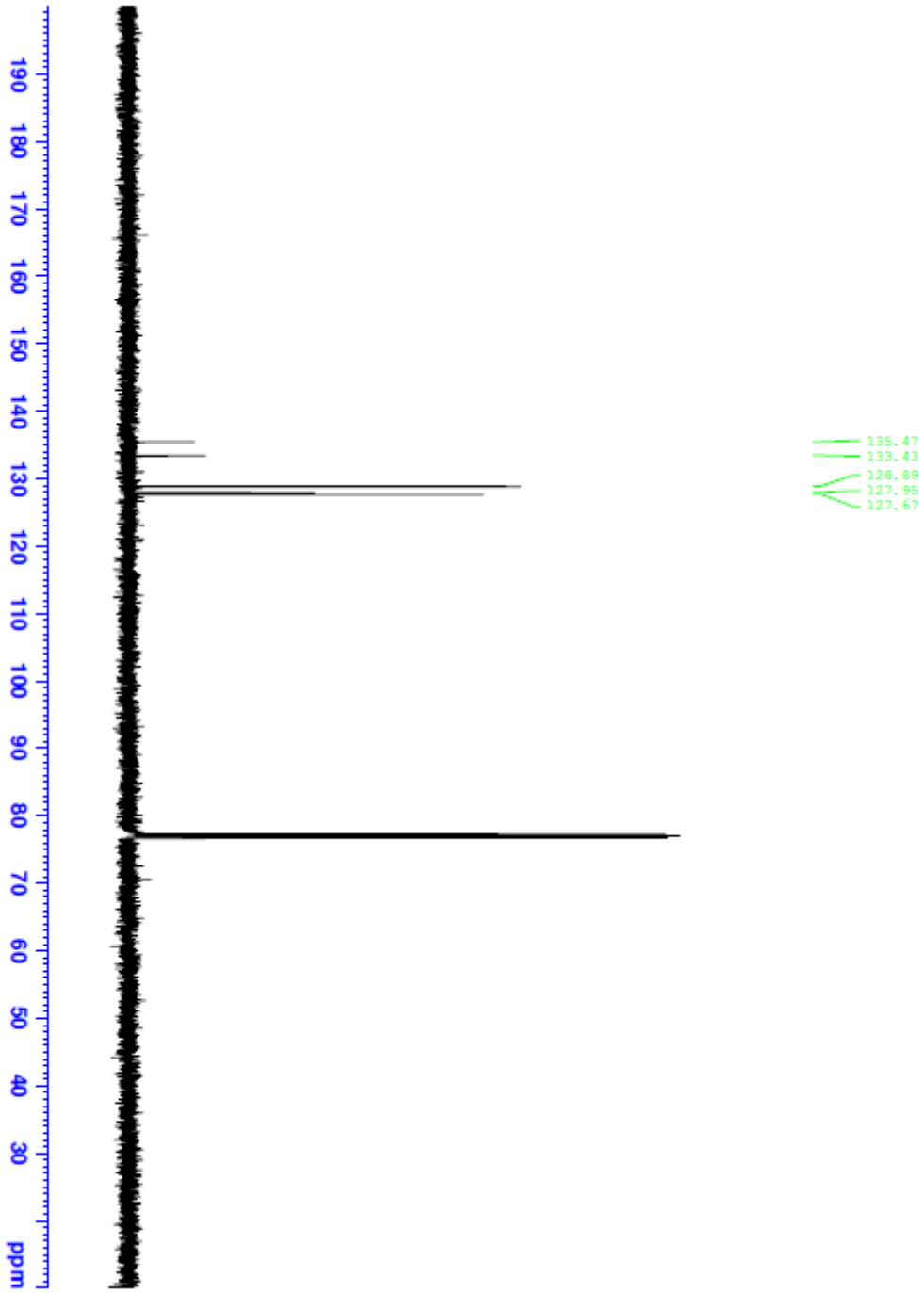

Figure S10. $^{13}C\{^{1}H\}$ (125 MHz) NMR spectrum of 2e in $CDCl_3$.

Chapter VI

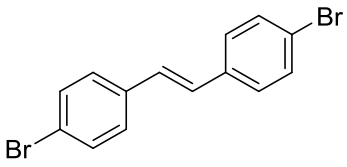

2f in THF-d_8

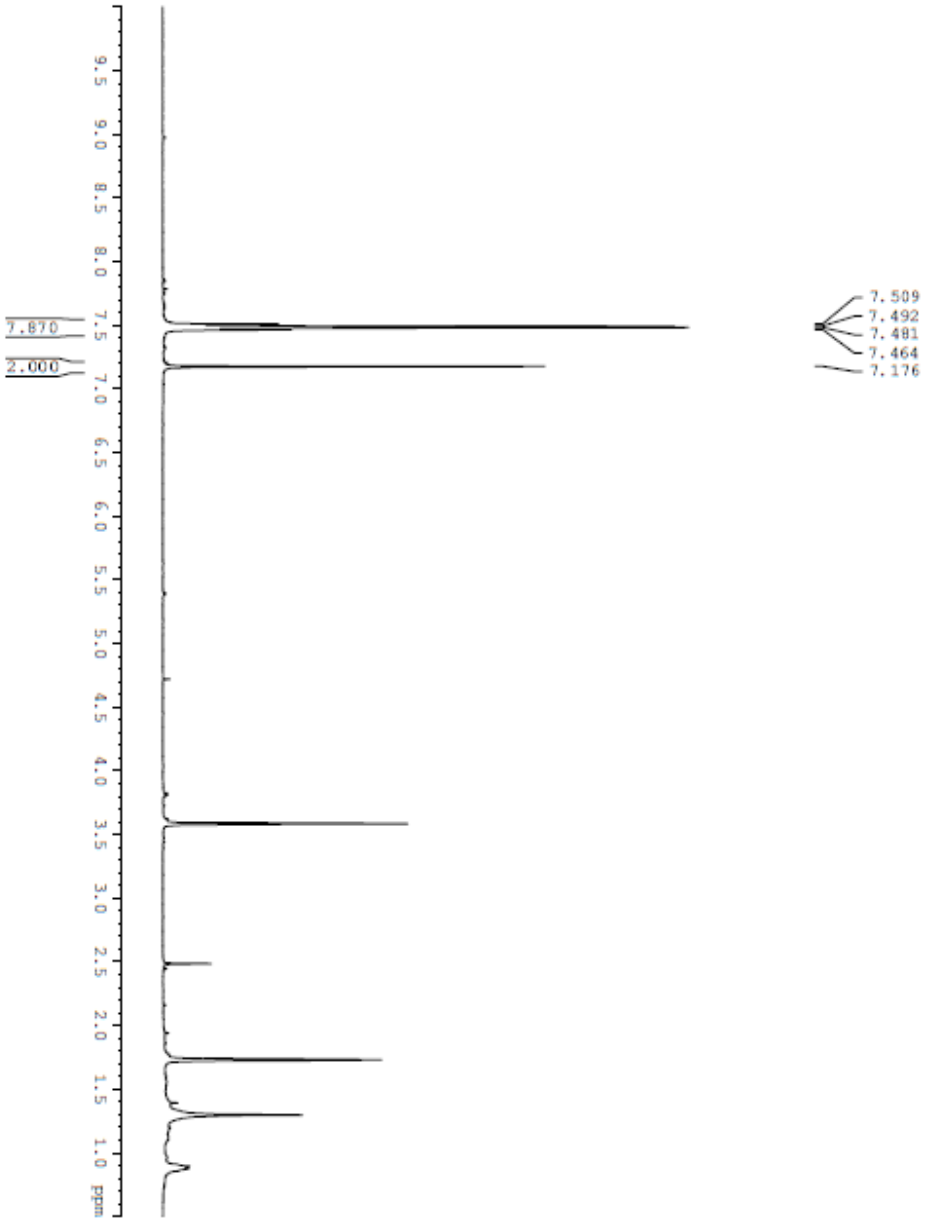

Figure S11. ^{1}H (500 MHz) NMR spectrum of 2f in THF-d_8.

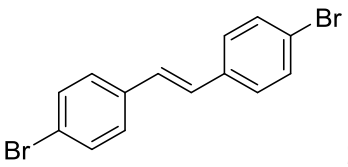

2f in THF-d_8

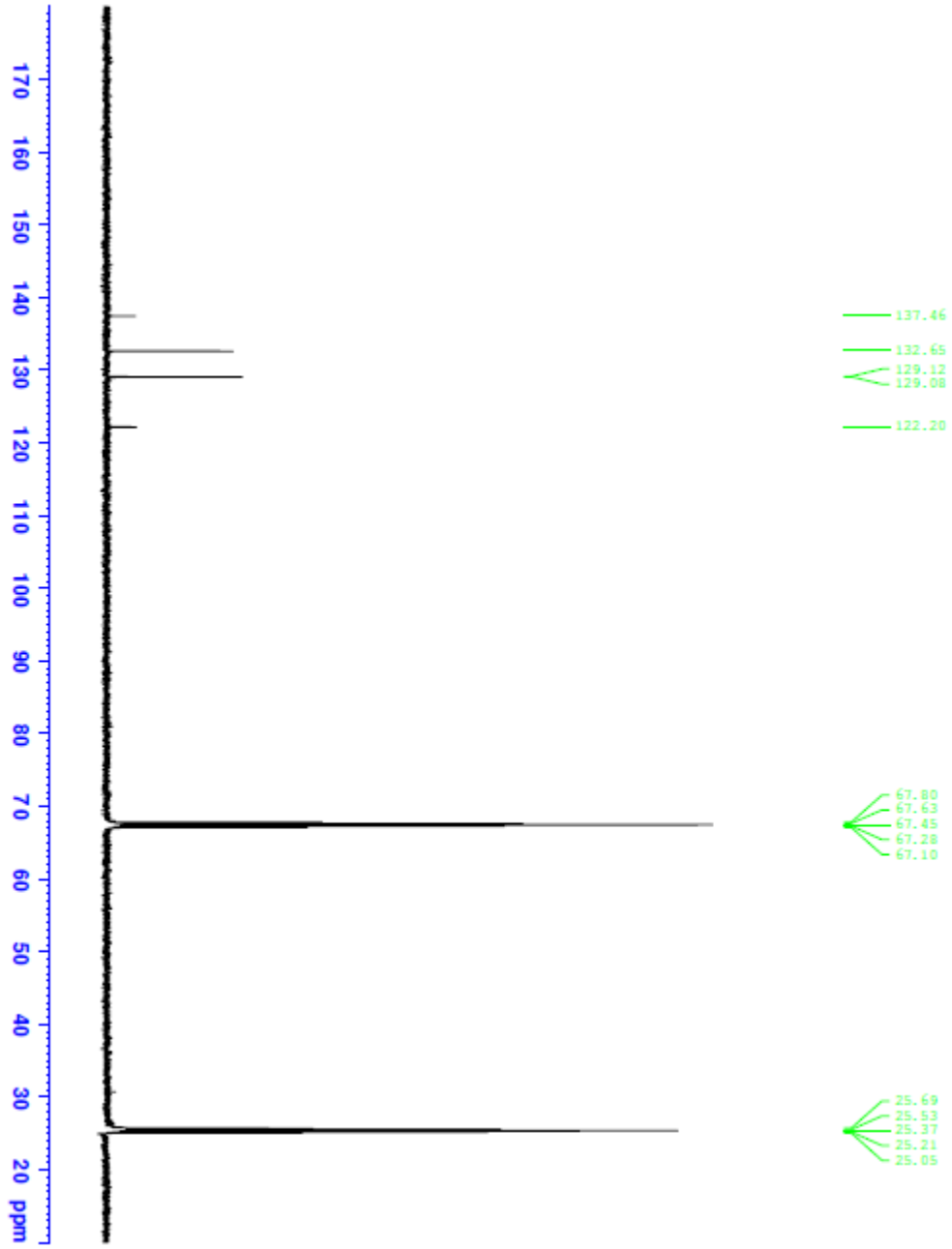

Figure S12. $^{13}C\{^1H\}$ (125 MHz) NMR spectrum of 2f in THF-d_8.

Chapter VI

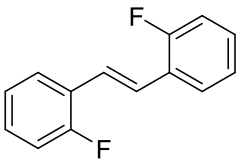

2g in $CDCl_3$

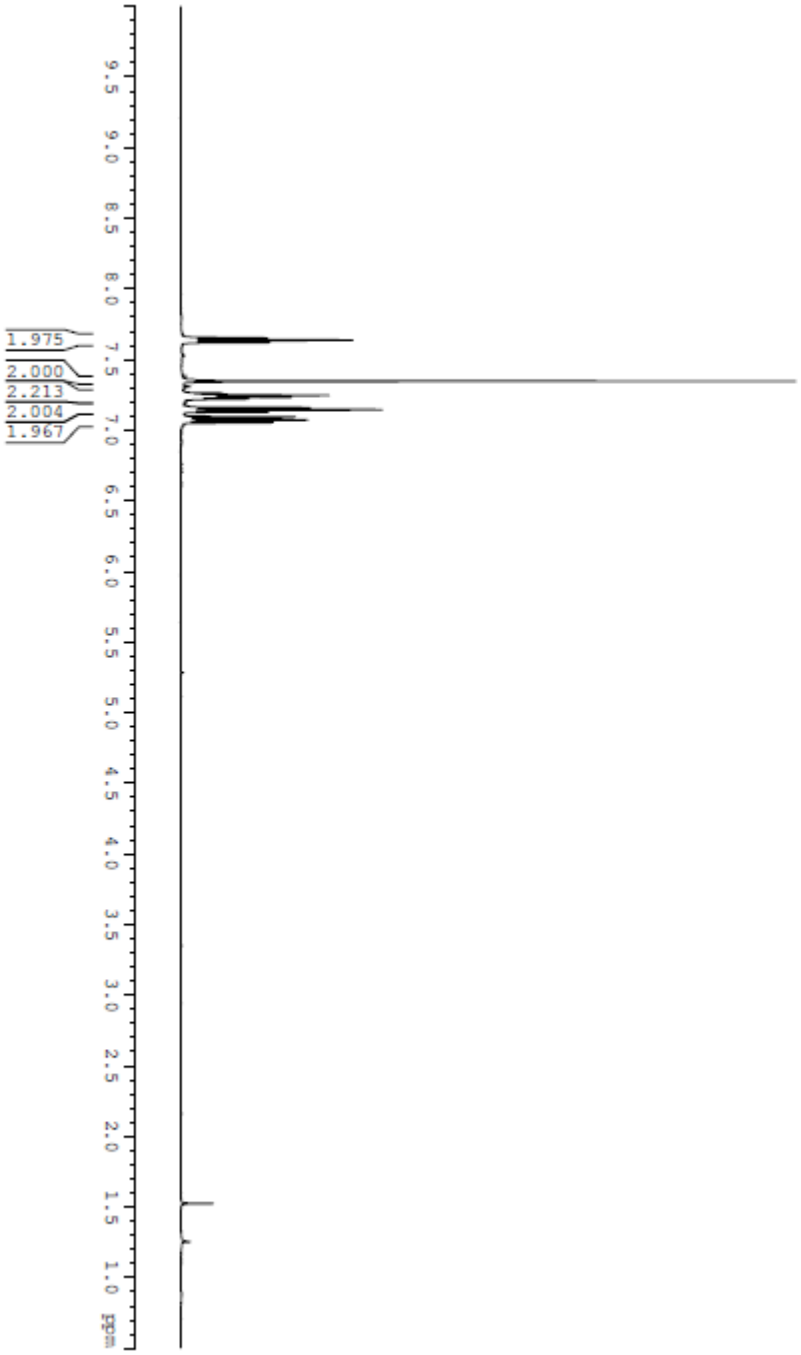

Figure S13. ^{1}H (500 MHz) NMR spectrum of 2g in $CDCl_3$.

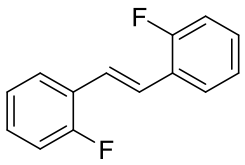

2g in $CDCl_3$

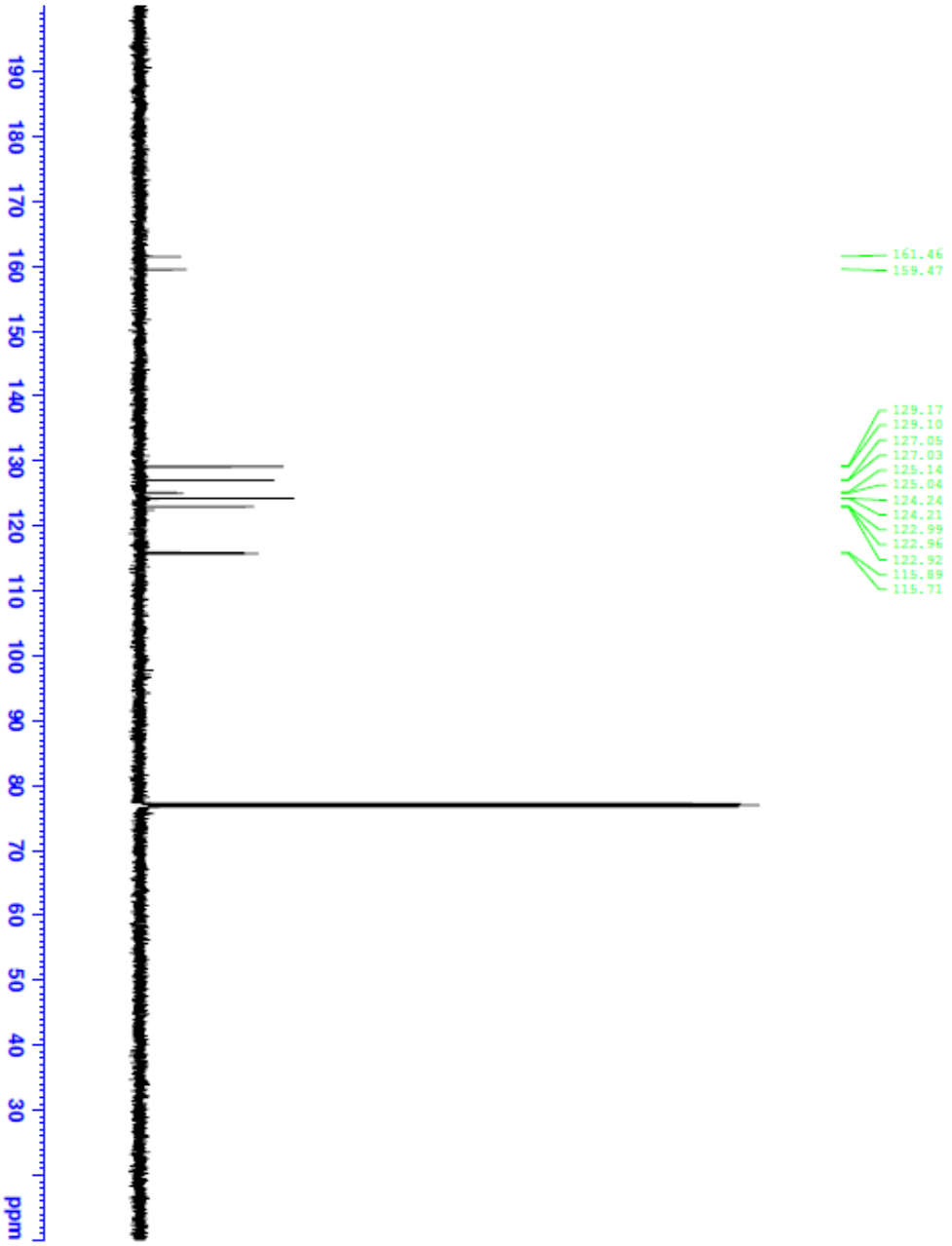

Figure S14. $^{13}C\{^{1}H\}$ (125 MHz) NMR spectrum of 2g in $CDCl_3$.

Chapter VI

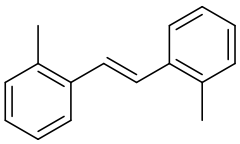

2h in $CDCl_3$

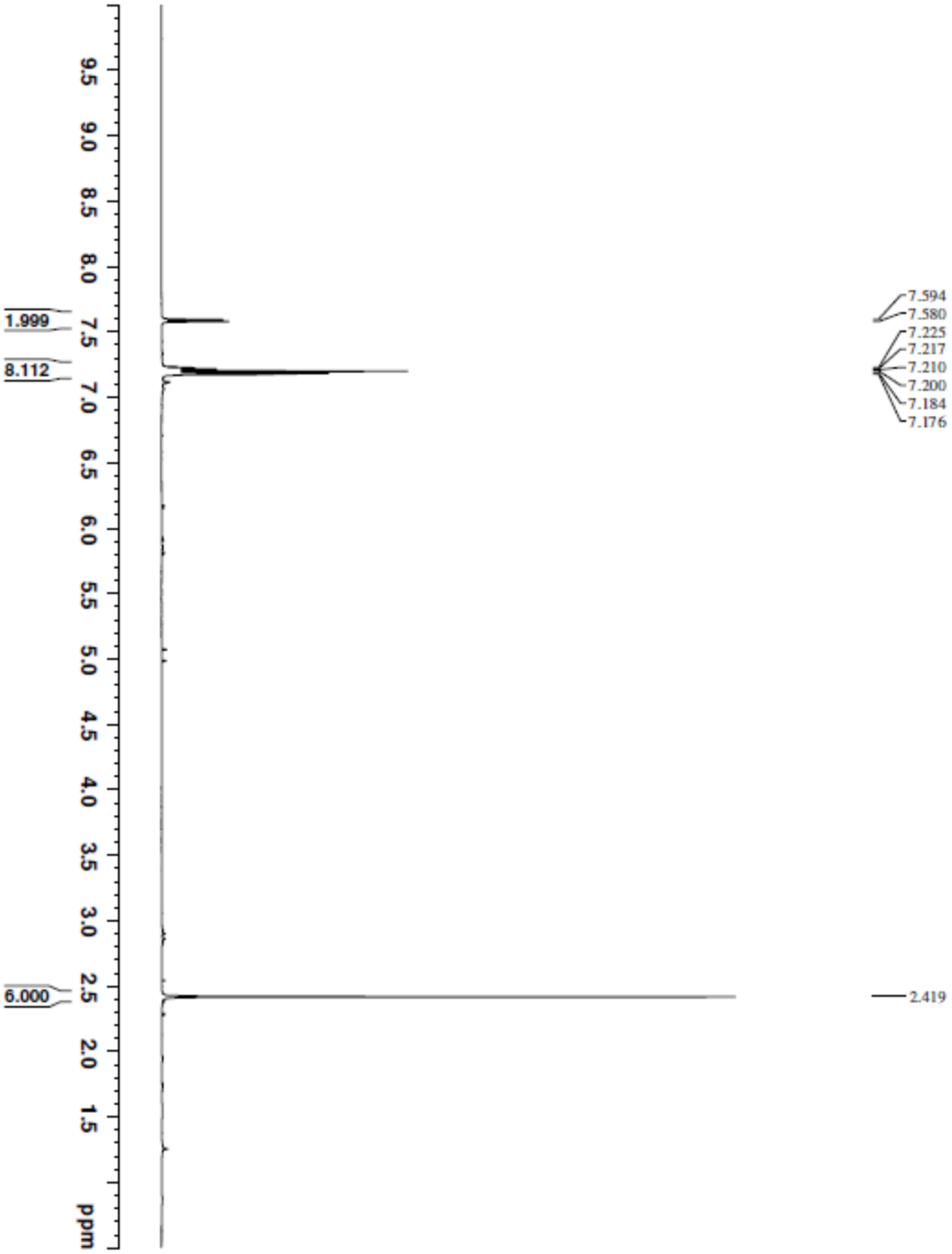

Figure S15. ^1H (500 MHz) NMR spectrum of 2h in $CDCl_3$.

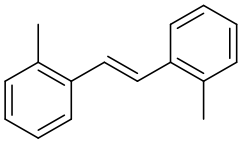

2h in $CDCl_3$

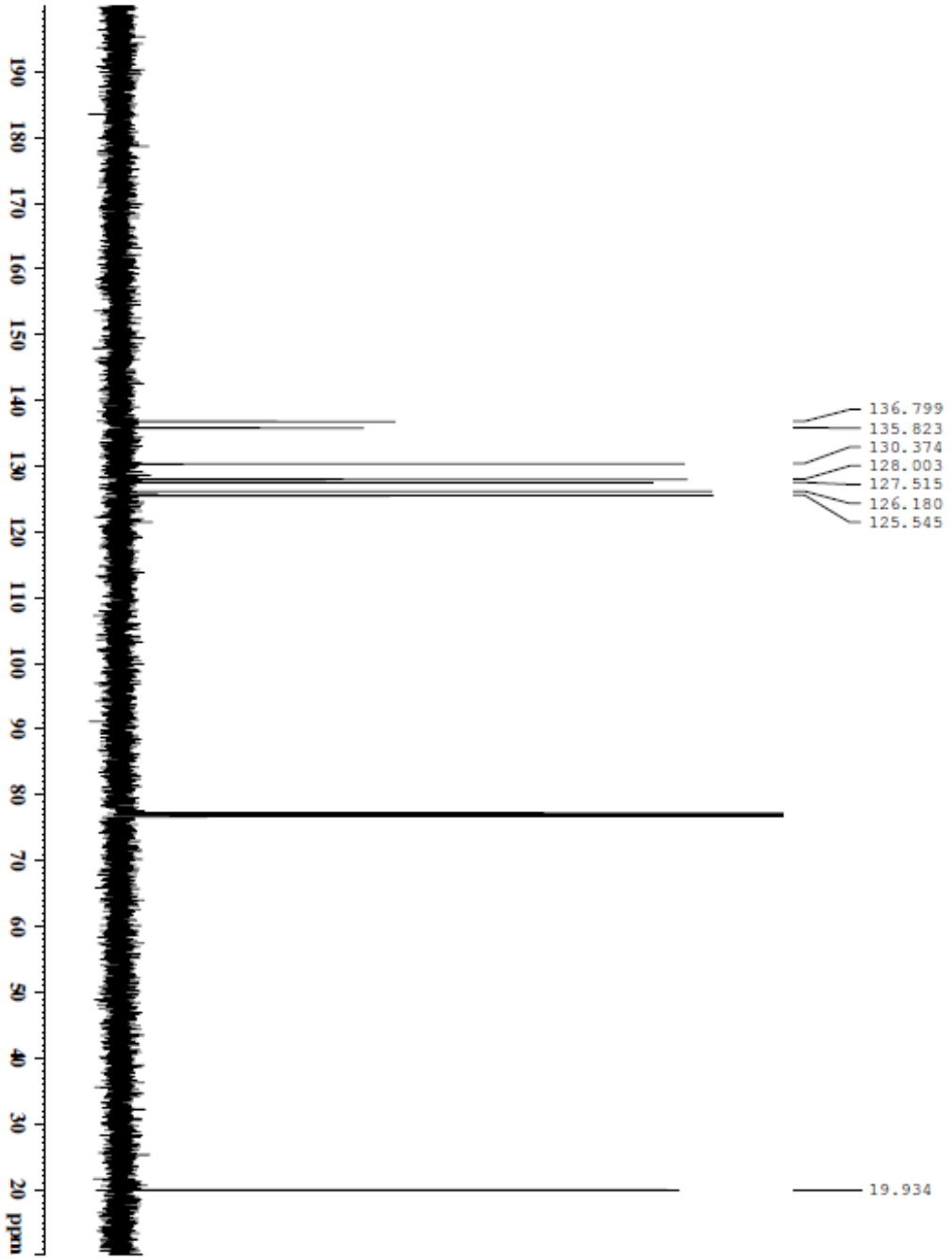

Figure S16. $^{13}C\{^{1}H\}$ (125 MHz) NMR spectrum of 2h in $CDCl_3$.

Chapter VI

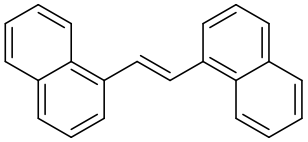

2i in $CDCl_3$

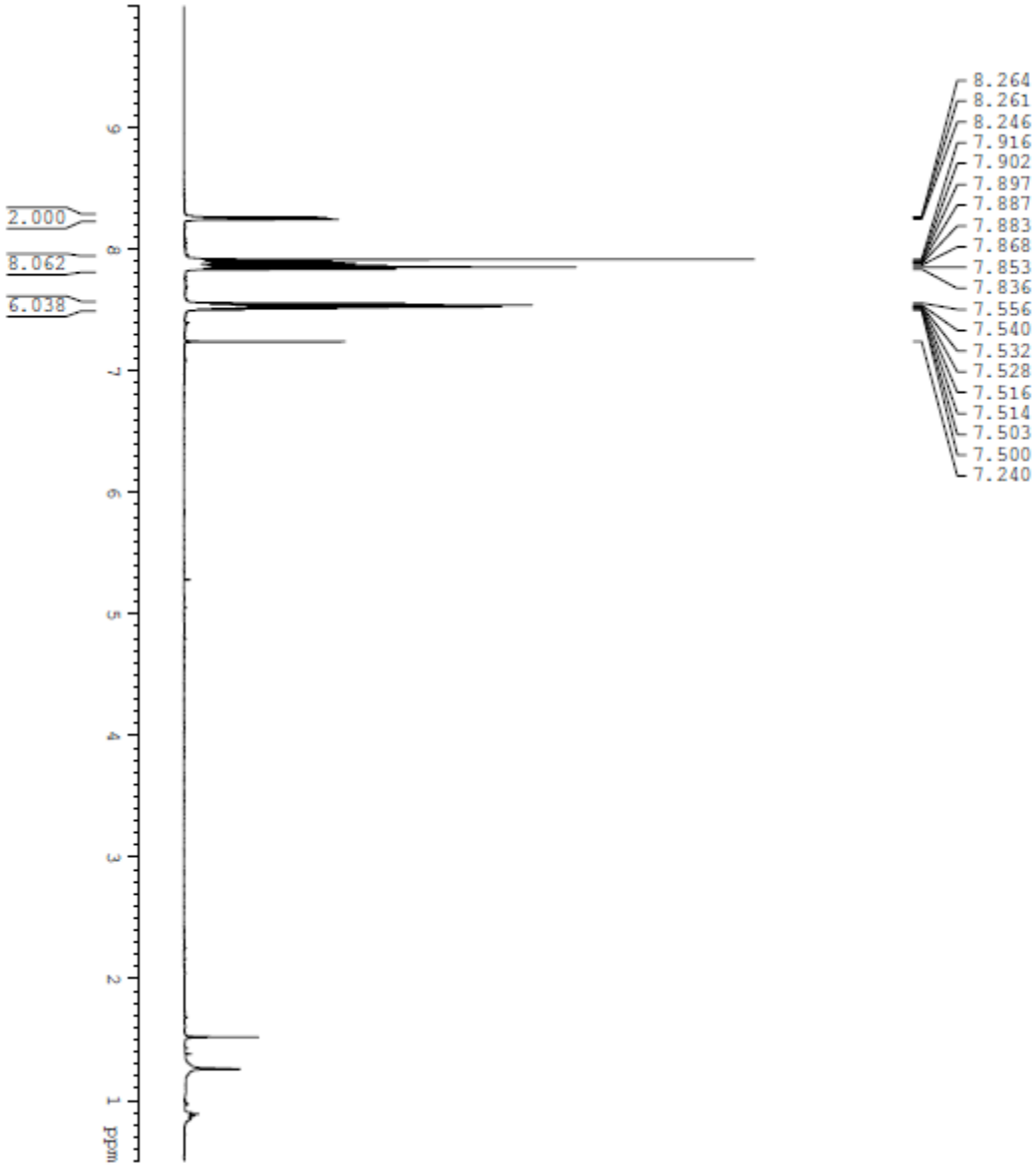

Figure S17. ^{1}H (500 MHz) NMR spectrum of 2i in $CDCl_3$.

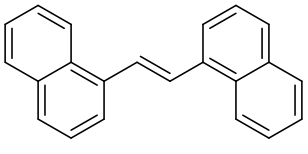

2i in $CDCl_3$

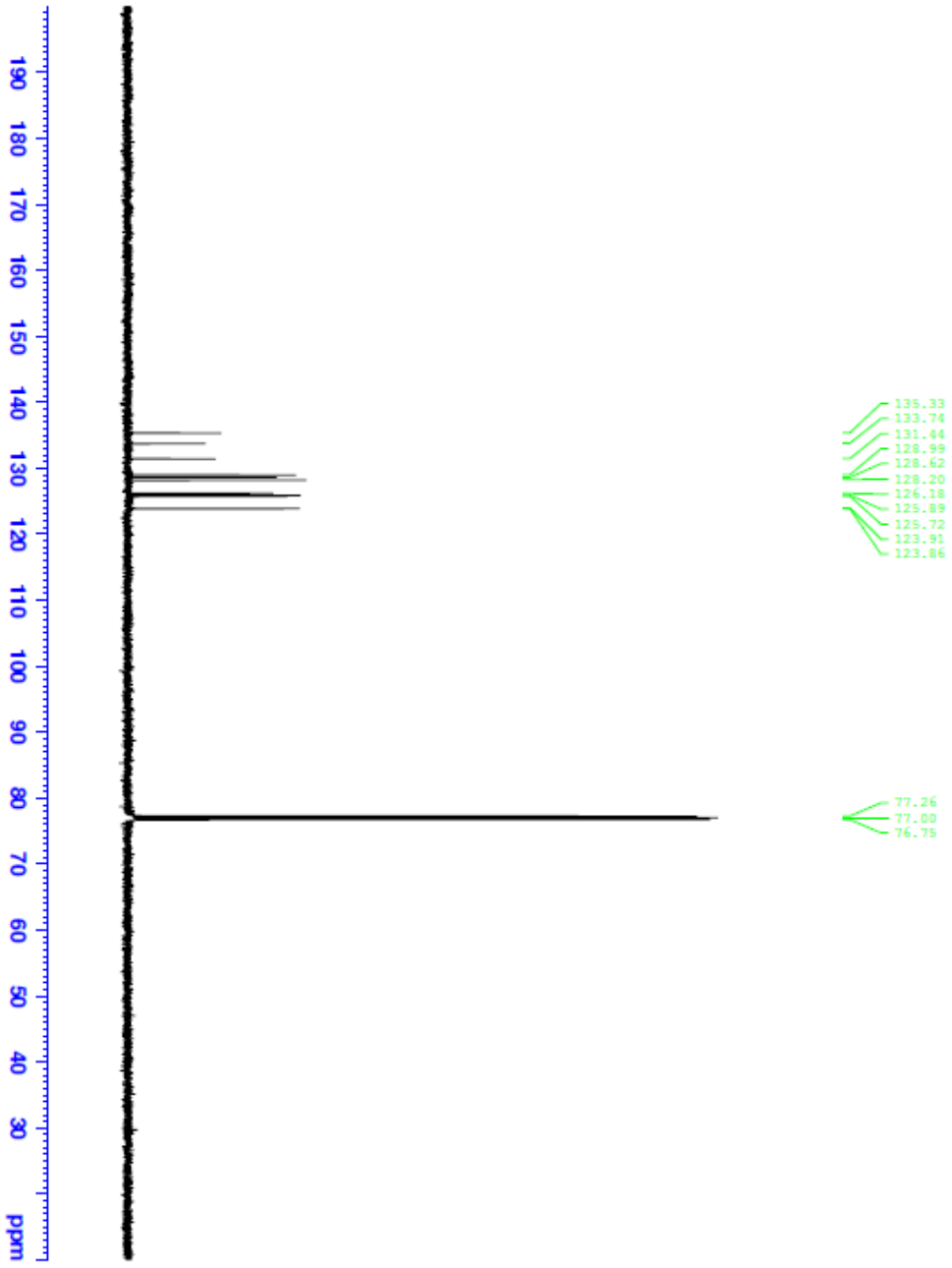

Figure S18. $^{13}C\ \{^{1}H\}$ (125 MHz) NMR spectrum of 2i in $CDCl_3$.

Chapter VI

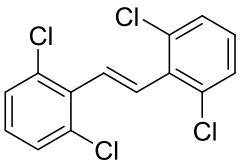

2j in $CDCl_3$

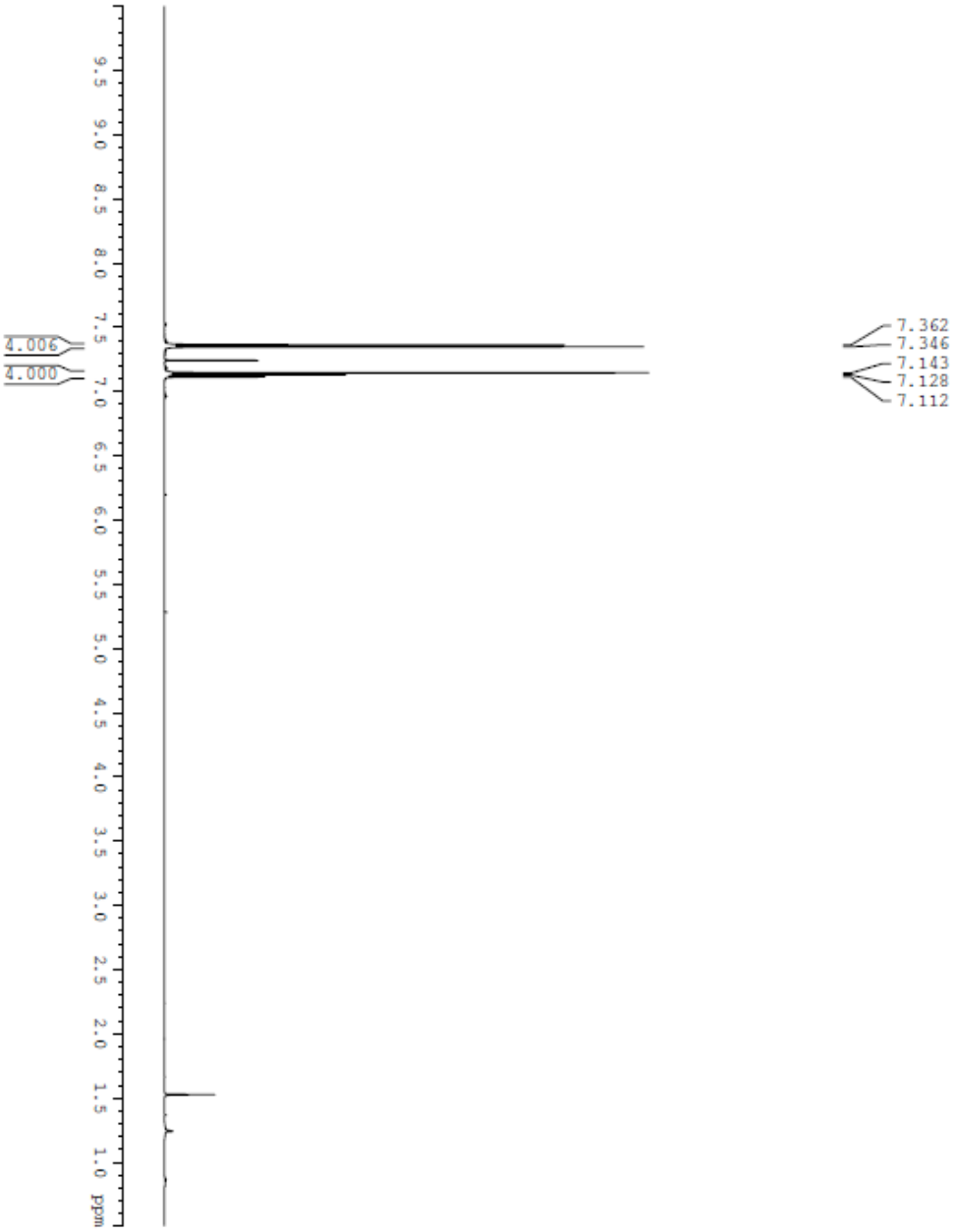

Figure S19. ^1H (500 MHz) NMR spectrum of 2j in $CDCl_3$.

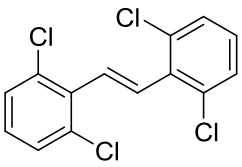

2j in $CDCl_3$

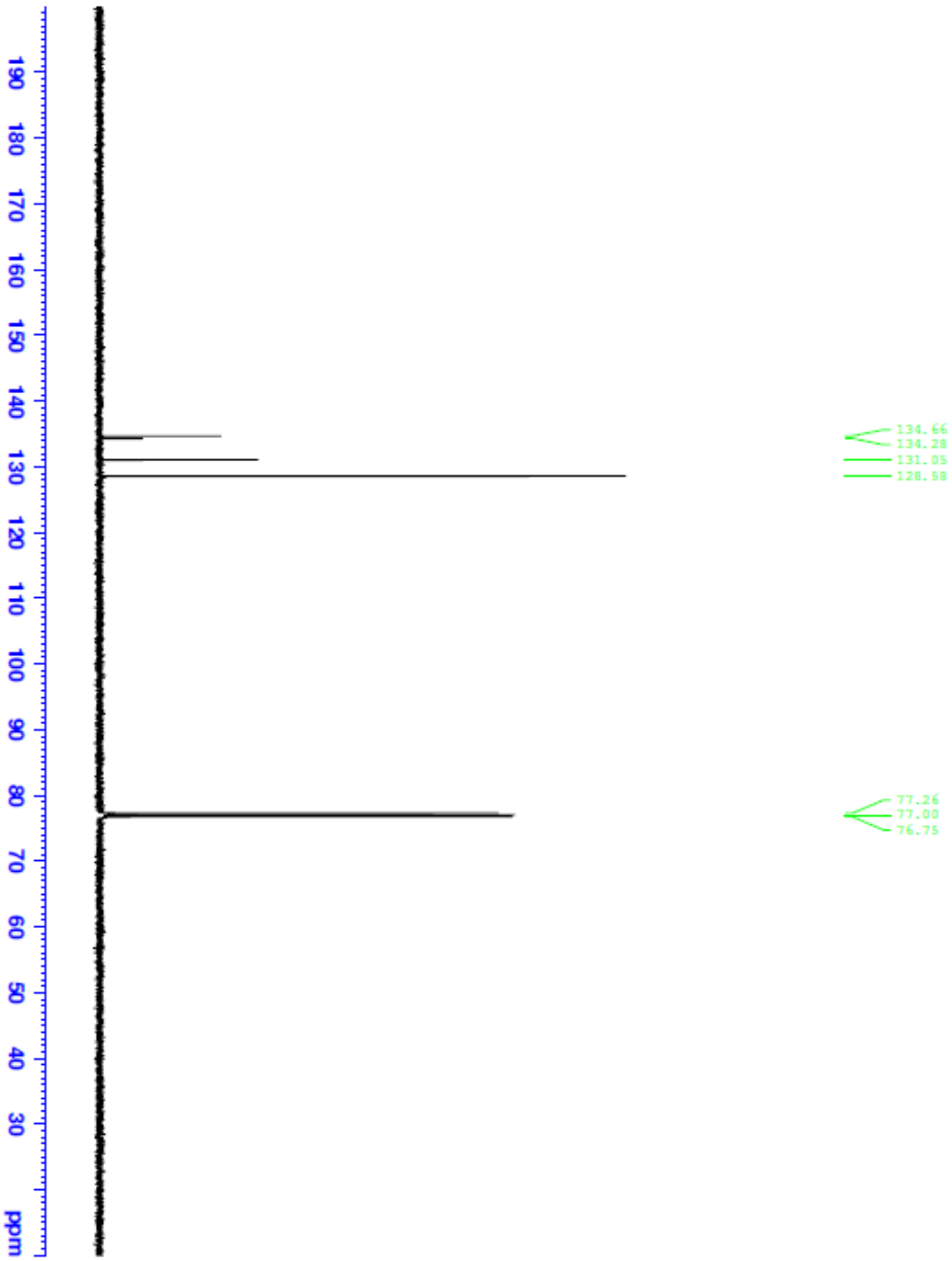

Figure S20. $^{13}C\ \{^{1}H\}$ (125 MHz) NMR spectrum of 2j in $CDCl_3$.

Chapter VI

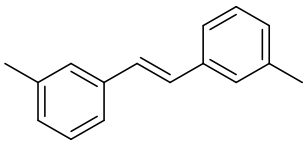

2k in $CDCl_3$

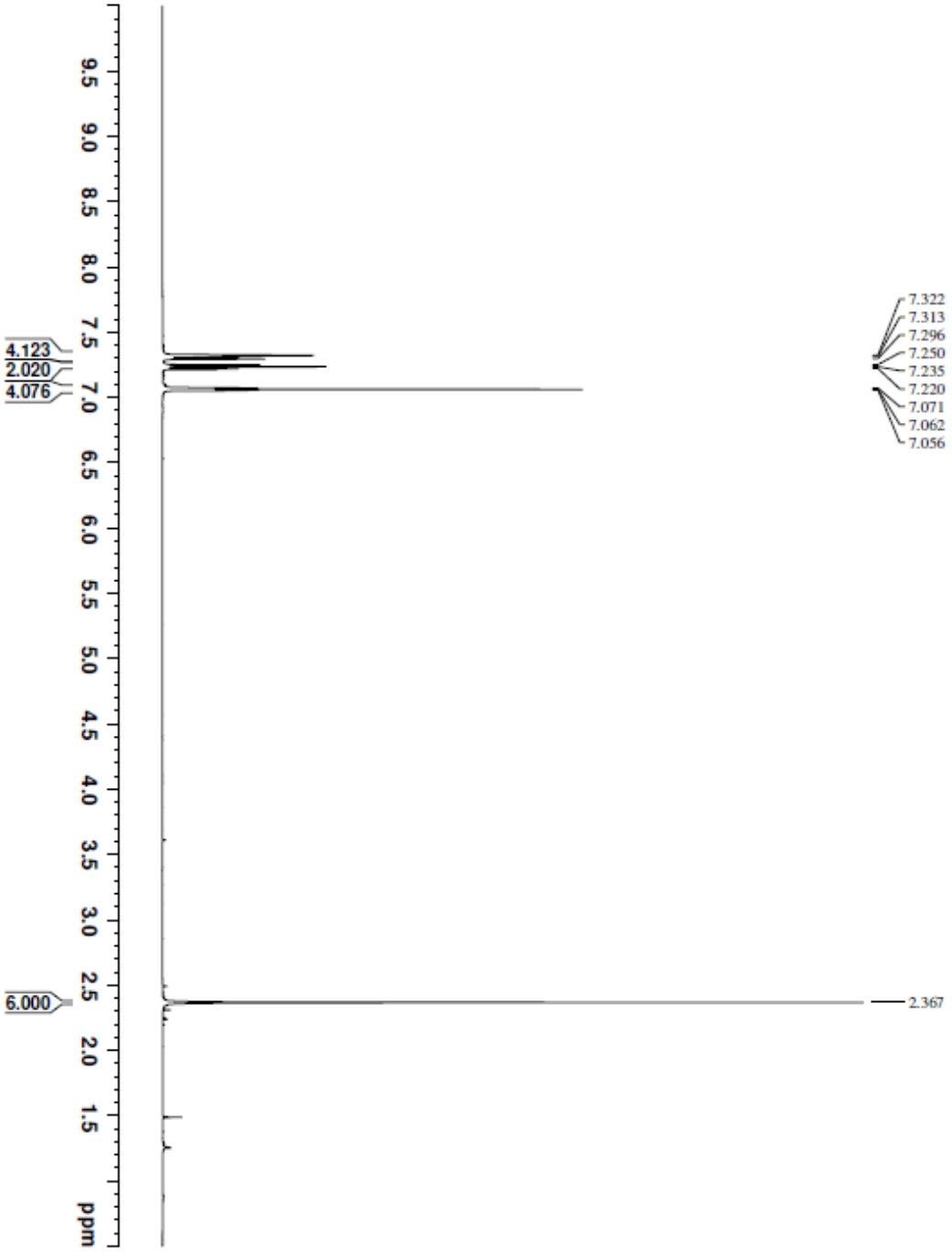

Figure S21. ^{1}H (500 MHz) NMR spectrum of 2k in $CDCl_3$.

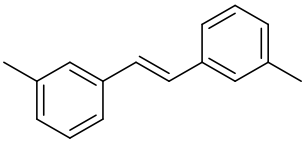

2k in $CDCl_3$

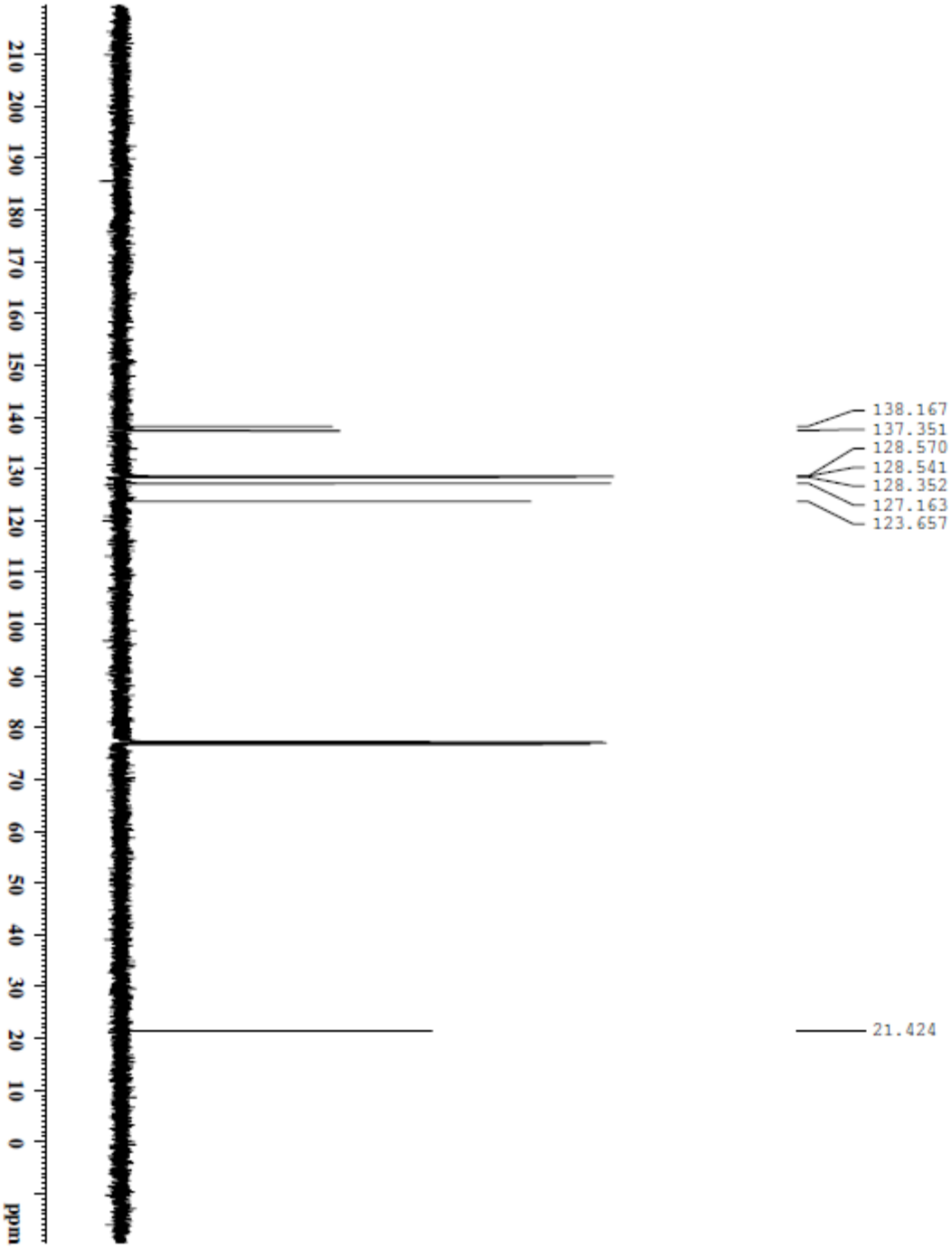

Figure S22. ^{13}C {^{1}H} (125 MHz) NMR spectrum of 2k in $CDCl_3$.

Chapter VI

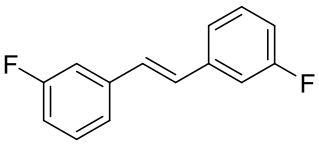

2l in $CDCl_3$

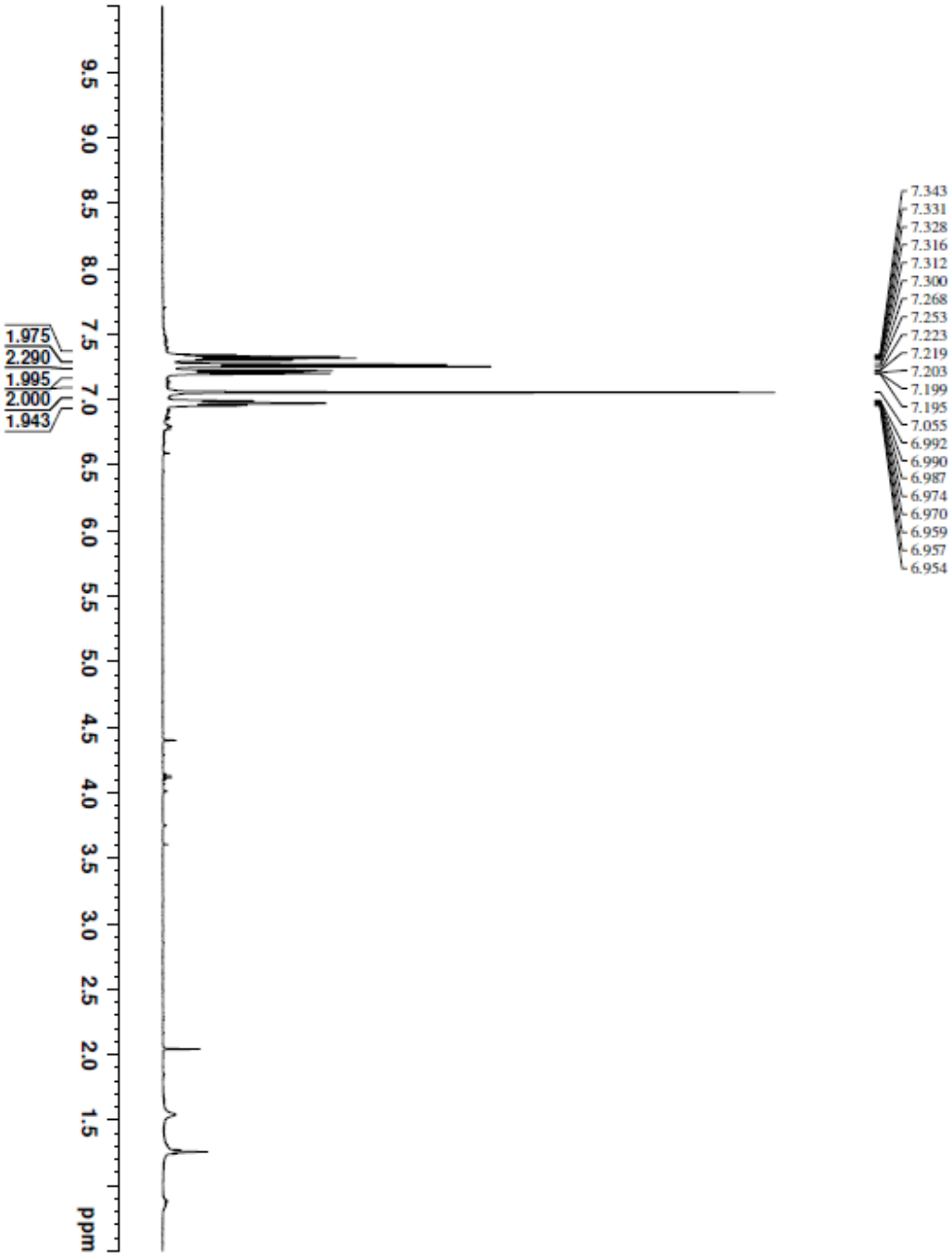

Figure S23. ^{1}H (500 MHz) NMR spectrum of 2l in $CDCl_3$.

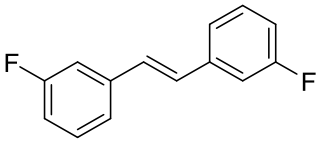

2l in $CDCl_3$

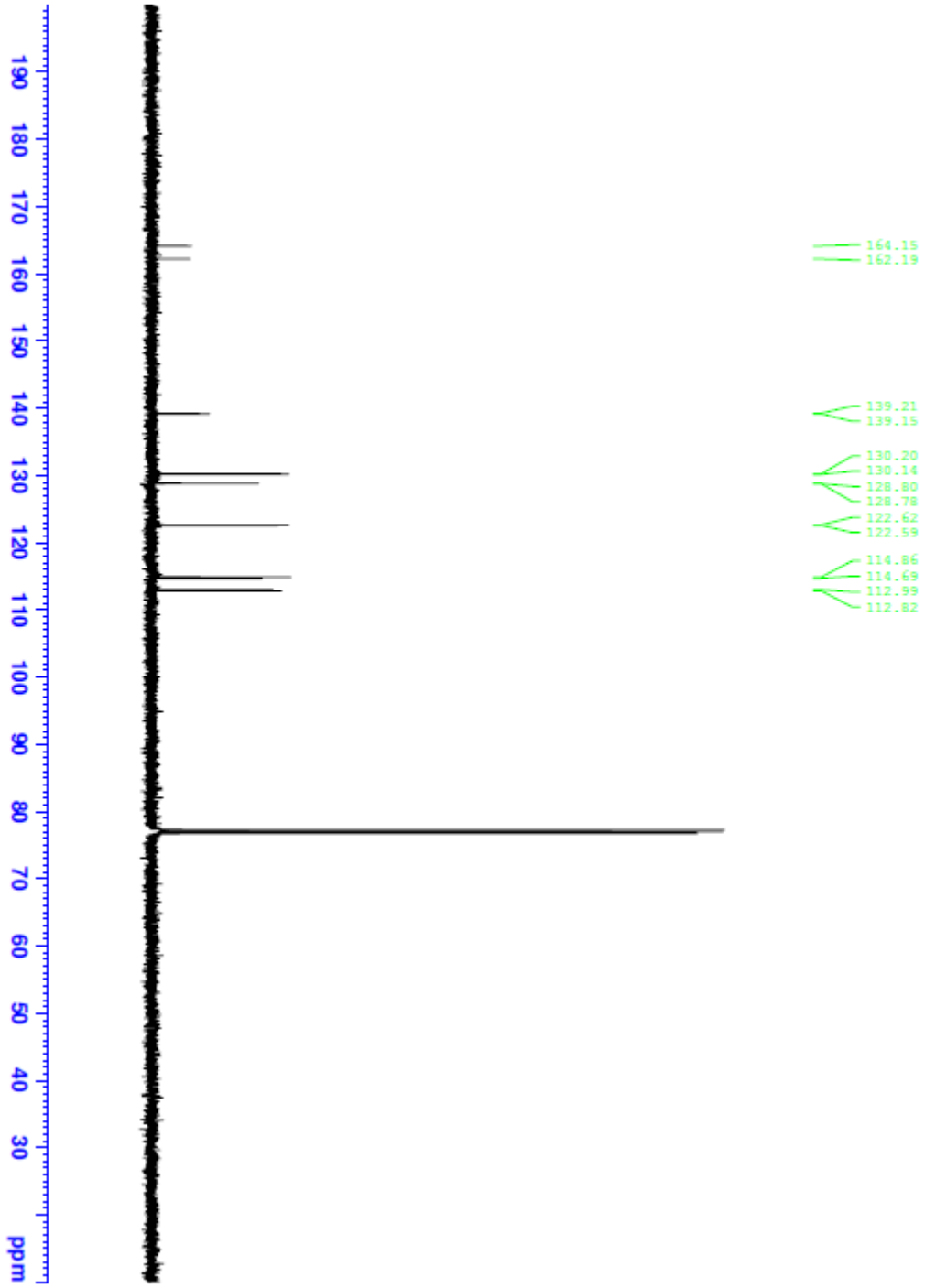

Figure S24. $^{13}C\ \{^{1}H\}$ (125 MHz) NMR spectrum of 2l in $CDCl_3$.

Chapter VI

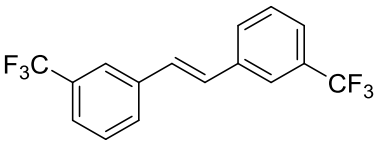

2m in $CDCl_3$

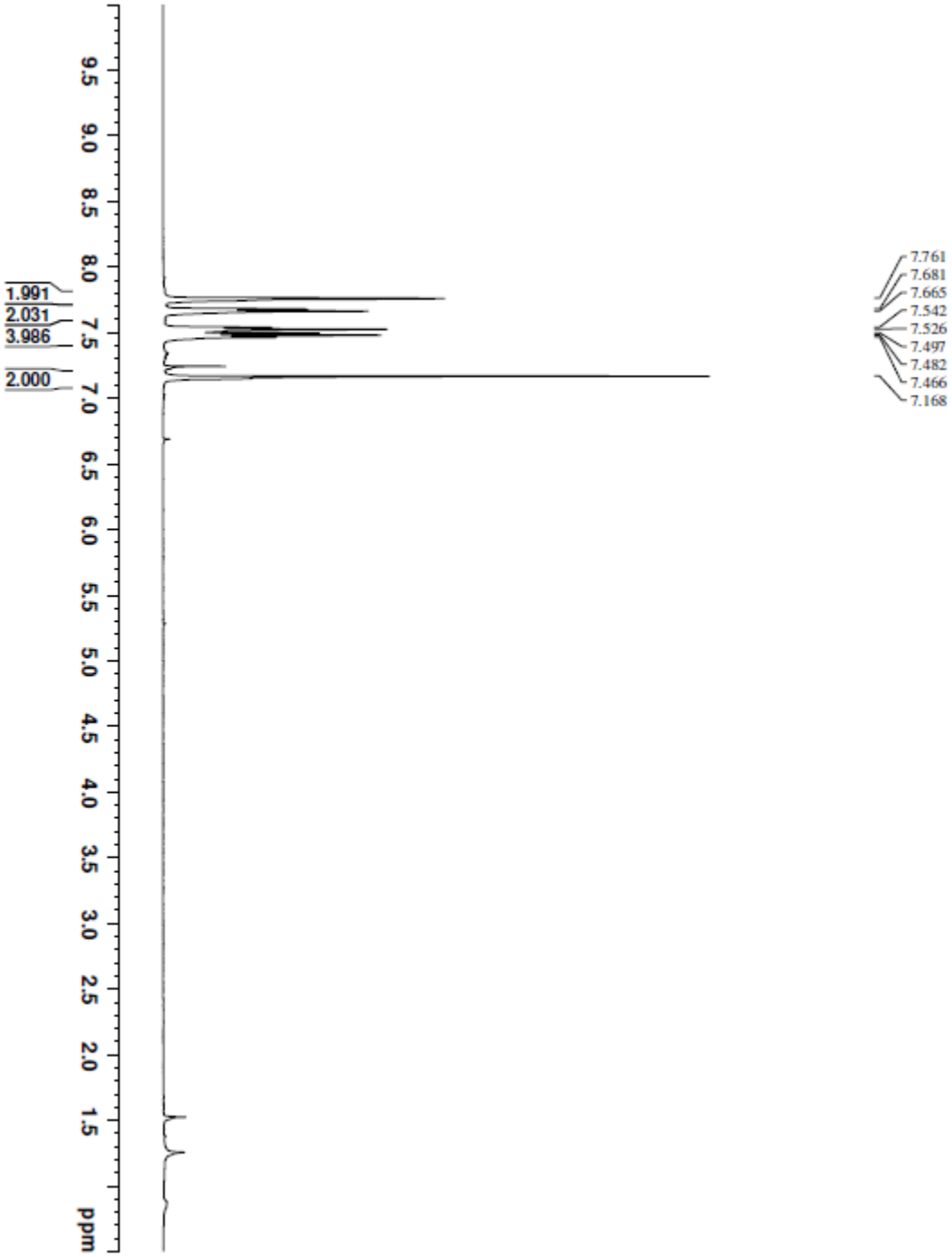

Figure S25. ^{1}H (500 MHz) NMR spectrum of 2m in $CDCl_3$.

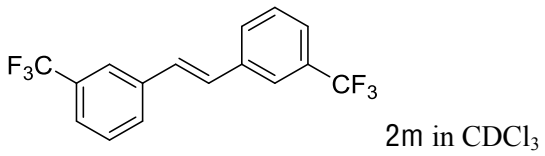

2m in $CDCl_3$

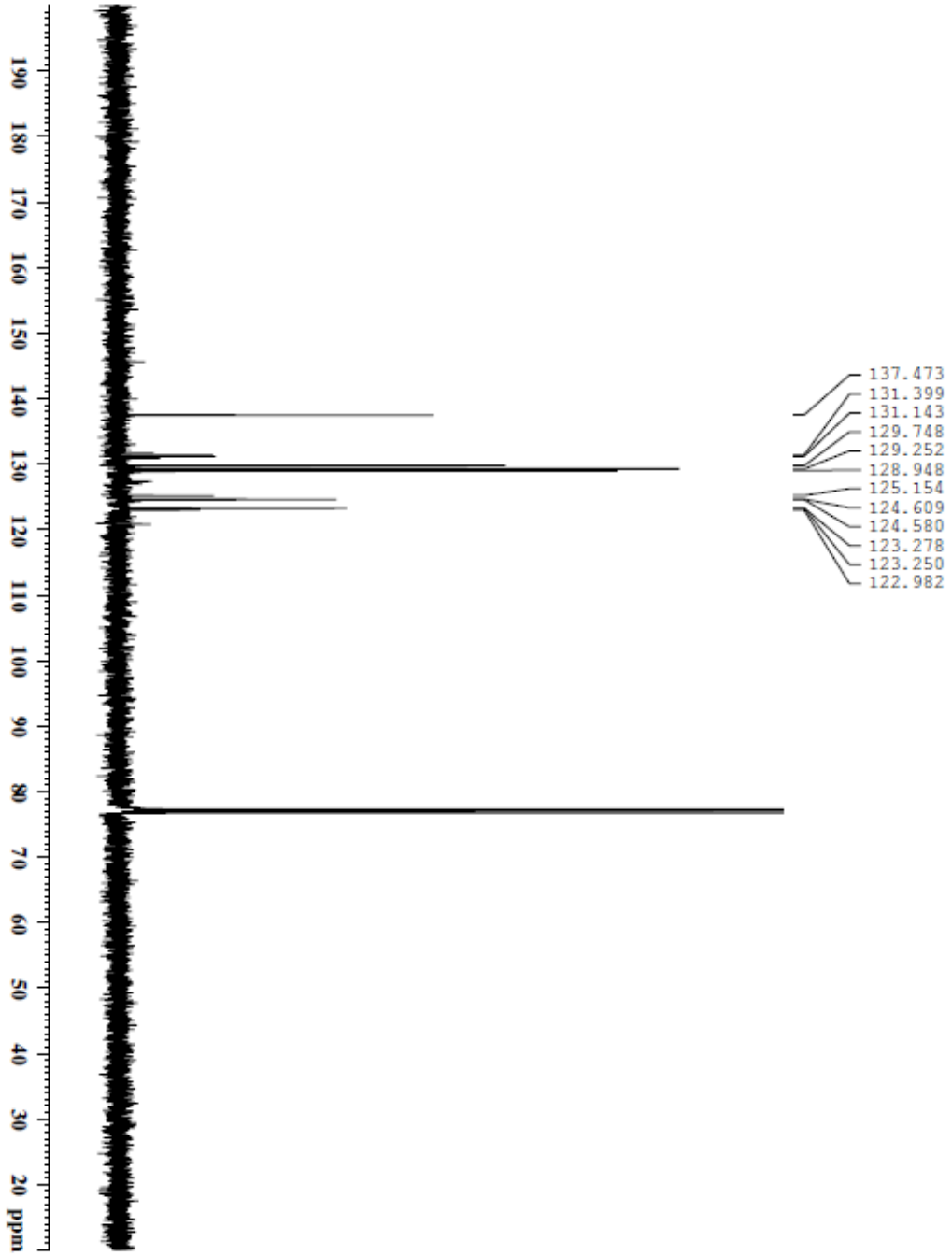

Figure S26. $^{13}C\ \{^{1}H\}$ (125 MHz) NMR spectrum of 2m in $CDCl_3$.

Chapter VI

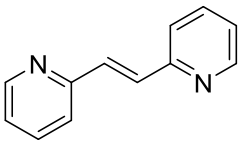

2n in $CDCl_3$

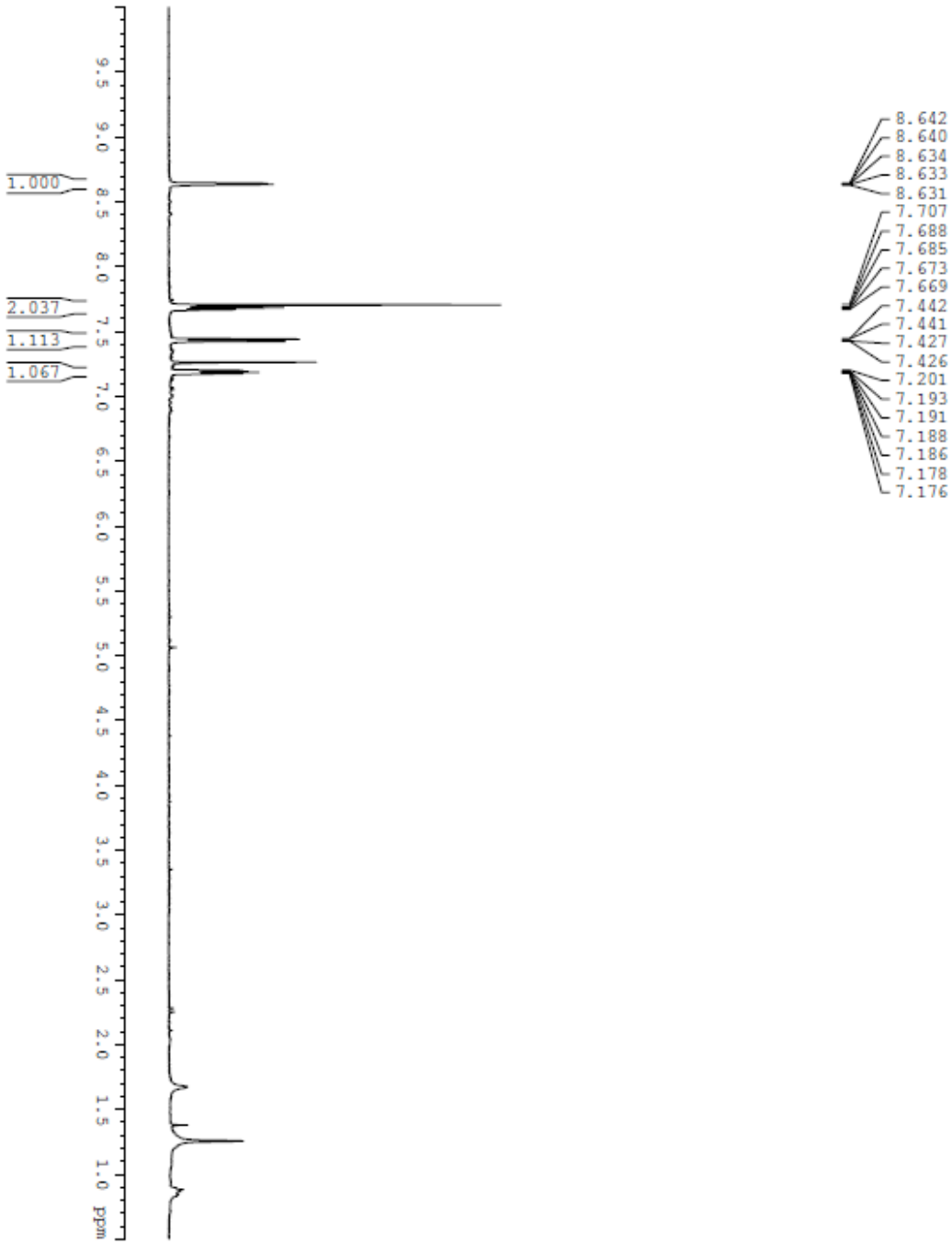

Figure S27. ^1H (500 MHz) NMR spectrum of 2n in $CDCl_3$.

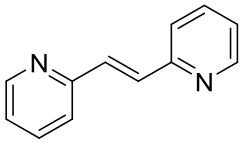

2n in $CDCl_3$

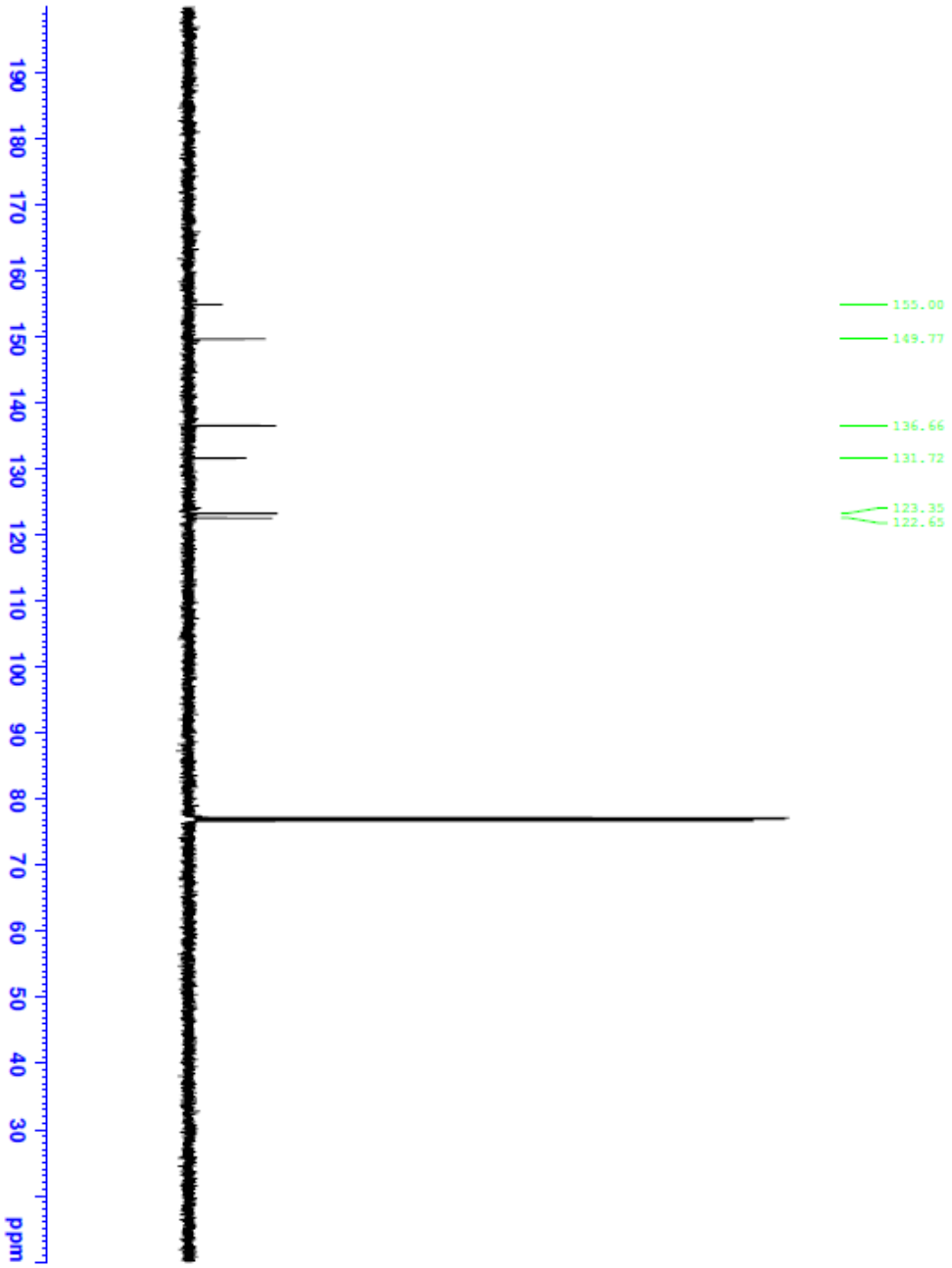

Figure S28. $^{13}C\ \{^{1}H\}$ (125 MHz) NMR spectrum of 2n in $CDCl_3$.

UNIVERSITAT ROVIRA I VIRGILI
NEW APPROACHES TO CATALYST DESIGN AND IMMOBILIZATION
Irina Sagamanova

CONCLUSIONS

Conclusions

UNIVERSITAT ROVIRA I VIRGILI
NEW APPROACHES TO CATALYST DESIGN AND IMMOBILIZATION
Irina Sagamanova

Conclusions

This Thesis embraces two main sections: (a) studies towards the synthesis of polymer-supported organocatalysts and their application in enantioselective transformations; and (b) homogenous catalysis involving application of sulfenate anions to different types of transformations such as palladium-catalyzed reactions or a new organocatalytic synthesis of stilbene derivatives.

For the efficient production of enantiopure compounds, it is important to take into consideration the design and development of robust organocatalysts. In these projects, we are developing a series of polymer-supported organocatalysts exhibiting multiple catalytic functions that promote enantioselective carbon-carbon and carbon-heteroatom bond forming reactions with perfect atom economy. Up to two adjacent stereogenic centers can be constructed simultaneously using aldol and Michael-type reactions, making them highly valuable for organic synthesis. In addition, the advantages of solid supported catalysts such as the possibility to be recycled, and implementation of continuous flow applications have been demonstrated with success for different examples.

In the iminium ion activation mode, new types of organocatalysts have been developed. Some of them show promising results in the aziridination reaction, but additional studies in catalyst design are required in order to make a fully recyclable organocatalyst.

The general summary of the Thesis by chapters is the following:

Chapter II describes the synthesis and development of a new type of immobilized catalyst, supported on polynorbornene, and the subsequent application in a symmetric transformations, particularly aldol reactions in aqueous media (**Article A**).

conclusions

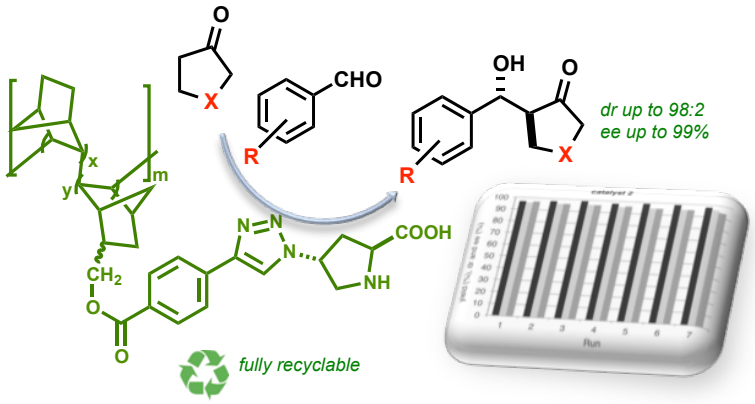

Figure 1. Graphical abstract of the article A (Chapter II)

Chapter III discusses the development of a rapid and enantioselective Michael reaction promoted by a β-fluoroamine polymer-supported catalyst (**Article B**).

A new catalyst design has been developed and evaluated in the reaction of aldehydes with nitroolefins via enamine activation. Moreover, the advantages of solid supported catalysts such as recycling and continuous flow application in Michael addition have been demonstrated with success on different examples. To demonstrate the synthetic utility of the process, the Michael adducts have been further derivatized to the corresponding 3,4-disubstituted pyrrolidines.

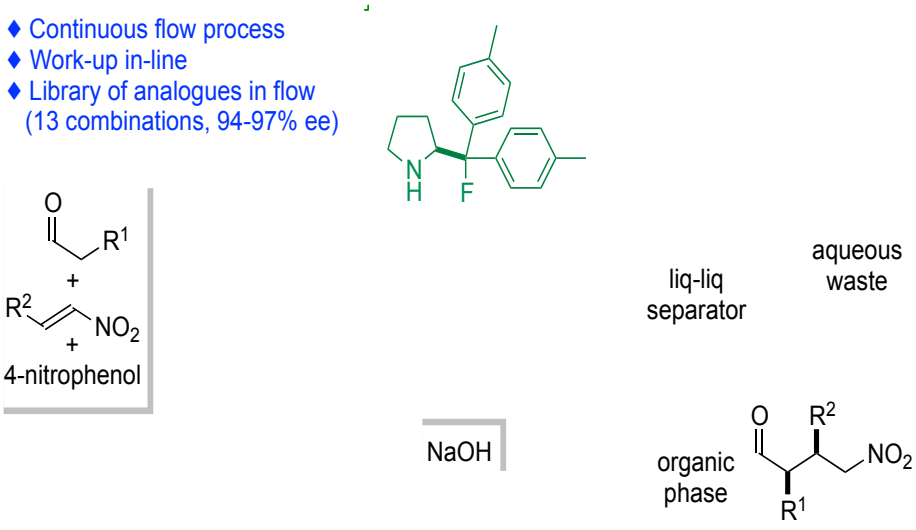

Figure 2. Graphical abstract of the article B (Chapter III).

Chapter IV reports advancements towards the design and synthesis of new β-fluoroamine polymer-supported catalysts and their use in enantioselective catalysis via the iminium ion activation mode, particularly in asymmetric aziridination and

epoxidation. Additional studies are required to optimize reaction conditions and improve the recyclability of these catalysts.

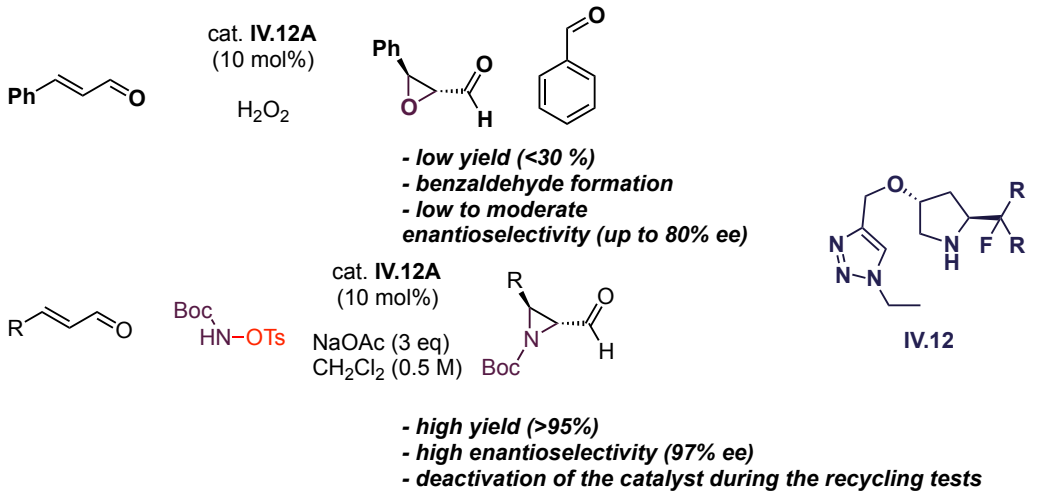

Figure 3. Graphical abstract of the results in Chapter IV.

Chapter V investigates the generation of diaryl sulfoxides from aryl benzyl sulfoxides and aryl chlorides via three sequential catalytic cycles, promoted by a NiXantPhos palladium catalyst (**Article C**).

The key step of this reaction is the *S*-arylation of a sulfenate anion. This work is an extension of previous studies towards the transformation of aryl benzyl sulfoxides into diaryl sulfoxides in the presence of aryl bromides. The main advance outlined in this work is the use of aryl chlorides, which is notable due to the reduced cost relative to aryl bromides and their greater availability.

The substrate scope of aryl chlorides and also benzyl sulfoxides was investigated, allowing the formation of various diaryl sulfoxides bearing a variety of functional groups, including secondary amines, which could participate in related coupling reactions such as Buchwald-Hartwig.

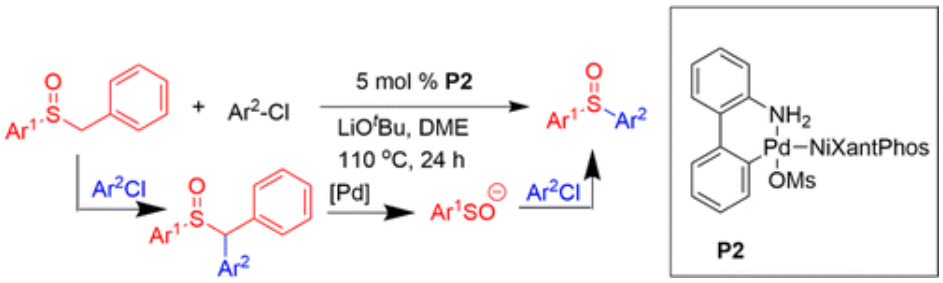

Figure 4. Graphical abstract of the article C (Chapter V).

conclusions

Chapter VI reports advancements towards the use of sulfenate anions as organocatalysts. The Walsh group has recently introduced this concept, and in their previous work using aryl benzyl sulfoxides as catalysts, the authors had observed the formation of undesired unsymmetrical stilbenes in an amount equal to the catalyst loading.

Herein, *tert*-butyl phenyl sulfoxide is employed as a traceless precatalyst for the generation of sulfenate anions under basic conditions for coupling of benzyl halides to form symmetric stilbenes (**Article D**). The advantage of this alternative source over previous precatalysts is that the byproduct generated on catalyst formation is a gas. This precatalyst has been used to promote the coupling of benzyl halides to generate symmetrical *trans*-stilbenes, providing the desired product in high purity. Using this second generation catalyst, a variety of *trans*-stilbenes were generated in 39-98% isolated yield. Many of the stilbene yields are improved from the previous report. Also, challenging substrates such as those bearing *ortho* substituents and heteroaromatics can be used with this new approach.

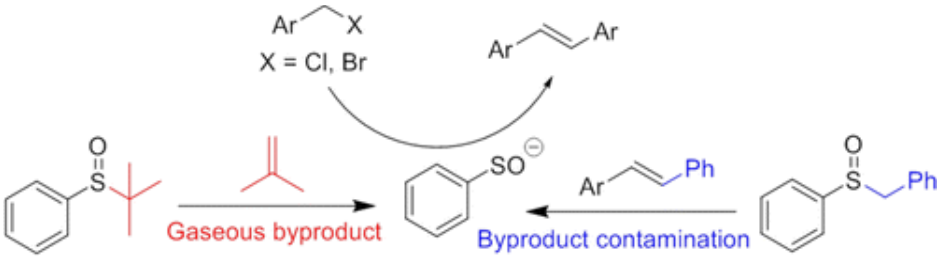

Figure 5. Graphical abstract of the article D (Chapter VI).

LIST OF PUBLICATIONS

This PhD Thesis is based on the following publications:

1. "Asymmetric Organocatalysts Supported on Vinyl Addition Polynorbornenes for Work in Aqueous Media"
Sagamanova, I. K.; Sayalero, S.; Marinez-Arranz, S.; Albeniz, A. C.; Pericàs, M. A. *Catal. Sci. Tech.,* 2015, 5, 754-764.

2. "*tert*-Butyl Phenyl Sulfoxide: a Traceless Sulfenate Anion Precatalyst"
Zhang, M.; Jia, T.; **Sagamanova, I. K.**; Pericàs, M. A.; Walsh, P. J. *Org. Lett.* **2015**, *17*, 1164-1167.

3. "Palladium Catalyzed Diaryl Sulfoxide Generation from Aryl Benzyl Sulfoxides and Aryl Chlorides"
Jia, T.; Zhang, M.; **Sagamanova, I. K.**; Wang, C. Y.; Walsh, P. J. *Org. Lett.* **2015**, *17*, 1168-1171.

4. "Polymer Supported Fluorinated Organocatalyst"
Pericàs, M. A.; **Sagamanova, I.**; Sayalero, S.; Rodríguez-Escrich, C*. Eur. Pat. Appl.* **2015**, PCT/EP2015/065866.

5. "Translating the Enantioselective Michael Reaction to a Continuous Flow Paradigm with an Immobilized, Fluorinated Organocatalyst"
Sagamanova, I.; Rodríguez-Escrich, C.; Molnar, I. G.; Sayalero, S.; Gilmour, R.; Pericàs, M. A. *ACS Catal.* **2015**, *5*, 6241-6248.